Poster Session B

PB 02 | Renal, Epithelia & Membrane Transport Physiology

B 02-01

Genistein Alleviates Vascularand Kidney Alterations via Suppressing of Renin-Angiotensin System in Renovascular Hypertensive Rats

A. Poasakate[1], P. Maneesai[1], P. Potue[1], S. Bunbupha[2], T. Tong-Un[1], W. Settheetham-Ishida[1], J. Khamseekaew[1], P. Pakdeechote[1]

[1] *Khon Kaen University, Physiology, Khon Kaen, Thailand*

[2] *Mahasarakham University, Faculty of Medicine, Mahasarakham, Thailand*

This study was supported by Invitation Research Fund (IN65101), Faculty of Medicine, Khon Kaen University. Anuson Poasakate received a scholarship from Development and Promotion of Science and Technology Talents project (DPST), Thailand.

IntroductionThe author previously demonstrated that genistein has cardioprotective effect [1]. In addition, genistein alleviated renal damage and dysfunction in rat models of ischemic acute kidney injury (Gholampour, Mohammadi, Karimi, & Owji, 2020). However, vascular-renal effects of genistein in two-kidney, one-clipped (2K1C) hypertensive rats is undiscovered. This study evaluated the effects of genistein on sympathetic activation, vascular function, renal alteration and investigated the mechanism underlying in 2K1C hypertensive rats.

MethodsMale Sprague-Dawley rats 180-220 g were used in this study. The renovascular hypertensive model was produced and modified as previously described [2]. Fourth weeks after operation, the 2K1C rats were received vehicle, genistein at dose 40 or 80 mg/kg or losartan 10 mg/kg for the last 3 weeks by oral gavage. On the other hand, sham operated rats (Sham) were treated with vehicle. At the end of experiment, heir water and food intakes were measured, and their 24 h urine samples were collected to monitor metabolic function, electrolyte balance and glomerular filtration rate (GFR). After 7 weeks, we evaluated direct blood pressure, tyrosine hydroxylase (TH) in mesenteric artery and plasma norepinephrine (NE) by immunofluorescence [3] and HPLC [4]. Vascular (Potue et al., 2019).and renal functions, oxidative stress markers, renin angiotensin system activity, apoptosis and fibrosis related proteins in both sides of kidney were determined.

ResultsGenistein reduced blood pressure, serum angiotensin converting enzyme activity and plasma angiotensin II and alleviated oxidative stress markers in 2K1C rats. Increases in sympathetic nerve-mediated contractile response, endothelial dysfunction in the mesenteric vascular beds and aorta, intensity of tyrosine hydroxylase in the mesentery and plasma norepinephrine in 2K1C rats were alleviated in the genistein-treated group. Genistein also improved renal dysfunction, atrophy of the clipped kidney (CK) (Figure 1)and hypertrophy of the non-clipped kidney (NCK) (Figure 2) in 2K1C rats. Upregulation of angiotensin II receptor type I (AT_1R), nicotinamide adenine dinucleotide phosphate oxidase subunit 4 (Nox4) and Bcl2-associated X protein (BAX) and downregulation of B-cell lymphoma 2 (Bcl2) protein found in CK were restored by genistein. It also suppressed theoverexpression of AT_1R, transforming growth factor beta I (TGF-β1), smad2/3 and p-smad3 in NCK.

ConclusionIn conclusion, genistein suppressed renin-angiotensin system-mediated sympathetic activation and oxidative stress in 2K1C rats. It alleviated renal atrophy in CK via modulation of AT_1R/Nox4/Bcl-2/BAX pathways and hypertrophy in NCK via AT_1R/TGF-β1/smad-dependent signalling pathways.

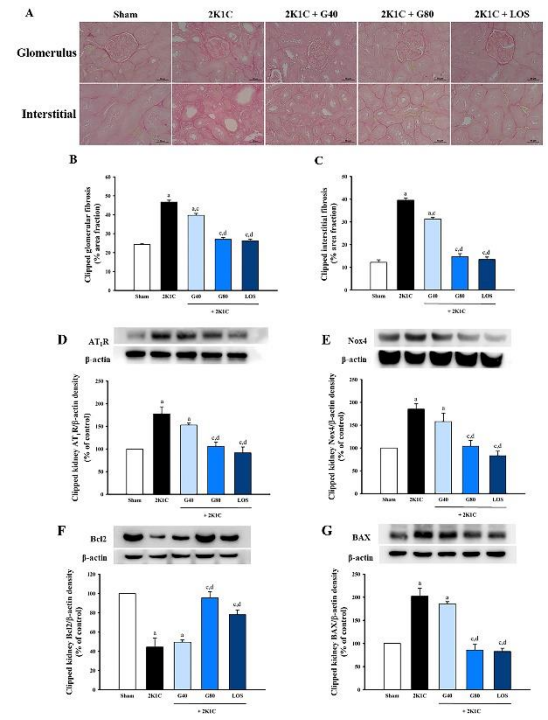

Effect of genistein on renal alterations and apoptotic protein expression in CK
Representative images of renal sections stained with picrosirius red under light microscope (**A**). Quantitative data for glomerular fibrosis (**B**) and interstitial fibrosis (**C**). Protein expression of AT_1R (**D**), Nox4 (**E**), Bcl2 (**F**) and BAX (**G**) (*n*= 8/group). Data are presented as mean ± SEM. $^{a}p < 0.05$ vs. Sham, $^{c}p < 0.05$ vs. 2K1C, $^{d}p < 0.05$ vs. 2K1C + G40

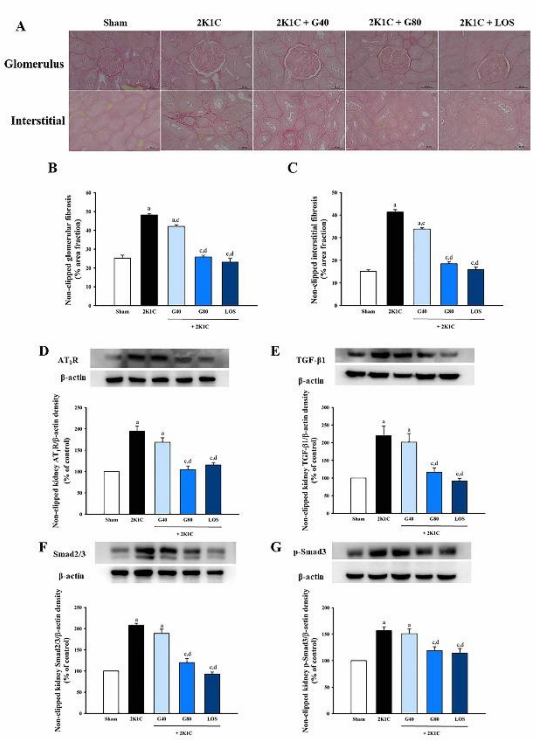

Effect of genistein on renal alterations and fibrotic protein expression in NCK

Representative images of renal sections stained with picrosirius red under light microscope (**A**). Quantitative data for glomerular fibrosis (**B**) and interstitial fibrosis (**C**). Protein expression of AT_1R (**D**), TGF-β1 (**E**), smad2/3 (**F**) and p-smad3 (**G**) (n = 8/group). Data are presented as mean ± SEM. $^{a}p < 0.05$ vs. Sham, $^{c}p < 0.05$ vs. 2K1C, $^{d}p < 0.05$ vs. 2K1C + G40

References

[2] Goldblatt, H, Lynch, J, Hanzal, RF, Summerville, WW 1934, 'STUDIES ON EXPERIMENTAL HYPERTENSION : I. THE PRODUCTION OF PERSISTENT ELEVATION OF SYSTOLIC BLOOD PRESSURE BY MEANS OF RENAL ISCHEMIA', *J Exp Med, 59*(3), 347-379.

[1] Poasakate, A, Maneesai, P, Rattanakanokchai, S, Bunbupha, S, Tong-Un, T, Pakdeechote, P 2021, 'Genistein Prevents Nitric Oxide Deficiency-Induced Cardiac Dysfunction and Remodeling in Rats', *Antioxidants (Basel), 10*(2).

[3] Tangsucharit, P, Takatori, S, Sun, P, Zamami, Y, Goda, M, Pakdeechote, P, et al 2012, 'Do cholinergic nerves innervating rat mesenteric arteries regulate vascular tone?', *Am J Physiol Regul Integr Comp Physiol, 303*(11), R1147-1156.

[4] Wunpathe, C, Potue, P, Maneesai, P, Bunbupha, S, Prachaney, P, Kukongviriyapan, U, et al 2018, 'Hesperidin Suppresses Renin-Angiotensin System Mediated NOX2 Over-Expression and Sympathoexcitation in 2K-1C Hypertensive Rats', *Am J Chin Med, 46*(4), 751-767.

[5] Potue, P, Wunpathe, C, Maneesai, P, Kukongviriyapan, U, Prachaney, P, Pakdeechote, P 2019, 'Nobiletin alleviates vascular alterations through modulation of Nrf-2/HO-1 and MMP pathways in l-NAME induced hypertensive rats', *Food Funct, 10*(4), 1880-1892.

B 02-02

Defining the role of a novel myeloid subset in driving fibrosis in models of kidney disease

R. M.B. Bell, B. R. Conway, C. Bénézech, L. Denby

University of Edinburgh, BHF/University Centre for Cardiovascular Science, Edinburgh, UK

Kidney disease is a global health burden associated with high morbidity and premature mortality and is increasing in prevalence. The common pathway in all progressive kidney disease, regardless of initiating aetiology, is fibrosis. Myeloid cells are a major cellular compartment of the immune system; they are found in the healthy kidney and in increased numbers in the damaged and/or diseased kidney, where they may act as key players in the development of fibrosis. Proinflammatory monocytes recruited to the injured kidney can exacerbate tissue damage through the release of proinflammatory factors and by activating myofibroblasts. Tissue macrophages possess enormous plasticity and heterogeneity, adopting different phenotypic and functional characteristics in response to stimuli in the local milieu. Hence, they can be injurious or may mediate repair by scavenging cell debris, degrading excess extracellular matrix and by secreting factors that may promote regeneration of injured tissue. Recently, using single-cell RNA sequencing we have identifed novel myeloid subsets in murine reversible, unilateral ureteric obstruction (UUO), an acute non-functional model of kidney fibrosis and repair[1]. Amongst the subsets, a population of cells was identified exclusively in acute injury (2 days post-UUO); they transcriptomically align to monocytes but express *Arg1*, and a large number of pro-inflammatory and pro-fibrotic genes. However, the function of this population in kidney disease has not yet been elucidated.

In these studies, we aim address the hypothesis that the Arg1+ myeloid cells play a role in the development of renal fibrosis. Kidney injury was induced in mice by UUO surgery (n=4-8) or ischemia reperfusion injury (IRI) before being culled at different timepoints over 7 or 14-days post-surgery, respectively, with kidneys harvested for analyses. Markers of kidney injury and fibrosis development were increased in injured kidneys compared to shams, as measured by histological analysis and gene expression. Analysis of intra-renal inflammation revealed persistent recruitment of $Ly6C^{hi}$ monocytes transitioning to pro-fibrotic inflammatory macrophages in injured kidneys in both models. There was an increase in the $CD45^{+}CD11b^{+}Arg1^{+}$ population at later timepoints. At early timepoints this population were F4/80lo whereas at later timepoints they are $F4/80^{hi}$ $MHCII^{+}$ $CD206^{+}$. Kidney tissue was also analysed by immunofluorescence for spatial analysis of where the $Arg1^{+}$ cells sit within the tissue.

In conclusion, $Arg1^{+}$ cells increase across the timecourse however display different markers depending on the point in the injury process. Determining their role in this and other clinically relevant models of kidney disease has the potential to lead to the development of novel therapeutics to limit

fibrosis or enhance repair to halt progression of disease. As fibrosis is a pathological process that can affect any organ, findings may be applied to other diseases.

References
[1] Conway et al., JASN, 2020; 31.

B 02-04

Renal outer medullary K^+ channel ROMK is regulated independently by WNK4 and c-Src kinases

C. K.H. Skands
University of Southern Denmark, Department of Molecular Medicine, Cardiovascular and Renal Research, 5000, Denmark

I would like to express my graditude to my supervisor Per Svenningen for great support and guidance. Thanks to Mohammed Abdullahi Ahmed for excellent technical assistance. The study was funded by the Independent Reseach Fund Denmark and the Augustinus foundation

Introduction The nephrotic syndrome is characterized by massive proteinuria and oedema formation due to an aberrantly activation of Epithelial sodium channels (ENaC) in the renal collecting ducts. High ENaC activity in this tubular segment is predicted to increase potassium secretion; however, nephrotic patients often display normal or elevated plasma potassium concentrations. The mechanisms causing the renal retention of potassium by the nephrotic kidney are unknown. Renal outer medullary K^+ (ROMK) channels are essential for renal excretion of potassium, and evidence indicates dysregulation of ROMK trafficking in nephrotic animal models. ROMK trafficking is regulated through a series of kinases such as With-no-lysine kinase 4 (WNK4), Proto-oncogene tyrosine-protein kinase (c-Src), and extracellular regulated kinase (ERK) but it is unknown whether the kinases' effects on ROMK are additive or independent of each other. This study aimed to determine how the collecting duct expressed kinases WNK4, c-Src, Sgk1, and ERK affected ROMK trafficking in HEK293T cells.
Methods HEK293T cells were transiently transfected with different combinations of plasmids (ROMK and two different combinations of kinases, e.g., WNK4 and c-Src). Surface localized proteins were biotinylated before lysing the cells and isolated through neutravidin-precipitation. Western blotting was used to determine how the kinases affected the surface expression of ROMK (see figure 1).
Results ROMK was expressed as a 44 kDa protein and was abundantly present in the plasma membrane when expressed without kinases. ROMK was also abundantly expressed as a 44 kDa band when co-expressed with c-Src or WNK4, but the expression fraction of ROMK in the plasma membrane was significantly decreased by c-Src and WNK4. Co-expression of ROMK, WNK4, and c-Src did not cause a further reduction in plasma membrane abundance of ROMK (see figure 2).
Conclusion WNK4 and c-Src cause decreased surface expression of ROMK through independent mechanisms, implying that increased WNK4 and c-Src activity may play a role in the renal potassium retention in the nephrotic syndrome.

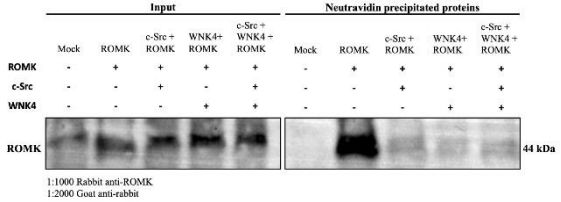

Figure 2: WNK4 and c-Src kinases regulatory effects on ROMK surface expression *Western blot showing the regulatory effects of WNK4 and c-Src kinases on the surface expression of ROMK in transfected HEK293T cells. ROMK is expressed as a 44kDa protein found in the whole cell lysate of all five experimental groups. The ROMK channel is found in abundance in the plasma membrane when expressed without kinases. When co-expressed with either WNK4 or c-Src, the presence of ROMK in the plasma membrane is significantly reduced. Co-expression of ROMK, WNK4 and c-Src does not cause further reduction in the membrane bound ROMK.*

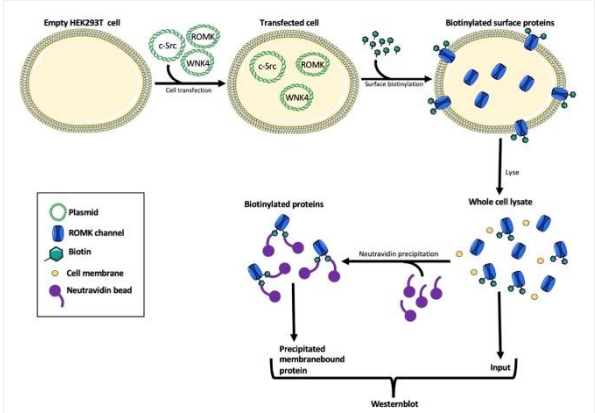

Figure 1: The experimental procedure used to isolate surface proteins from transfected HEK293T *HEK293T cells are transfected with different combinations of plasmids. Successfully transfected cells will start expressing the genes encoded by the plasmid, here illustrated with the ROMK protein product. Surface proteins are biotinylated prior to cell lysis. The whole cell lysate is sampled and kept as input for expression control. Biotinylated surface proteins are isolated through neutravidin precipitation using neutravidin beads. Precipitated membrane bound proteins and input samples can then be used in western blot analysis.*

B 02-05

Effects of a postbiotic consisting of heat-treated lactobacilli fermentate on mouse small intestinal ion transport and motility *ex-vivo*

F. Uhlig[1,3], A. Warda[3], C. M. Hueston[3], L. Draper[2,3], G. Chauvière[4], E. Eckhardt[4], C. Hill[2,3], N. Hyland[1,3]

[1] *University College Cork, Department of Physiology, Cork, Ireland*
[2] *University College Cork, School of Microbiology, Cork, Ireland*
[3] *APC Microbiome Ireland, Cork, Ireland*
[4] *Adare Pharmaceuticals SAS, Houdan, France*

FU is in receipt of an APEX postdoctoral fellowship through a Marie Skłodowska-Curie Action (MSCA) COFUND programme under Marie Skłodowska-Curie grant agreement No 754535. APC Microbiome Ireland is a research institute funded by Science Foundation Ireland (SFI) 12/RC/2273_P2, through the Irish Government's National Development Plan.

A postbiotic is defined as a "preparation of inanimate microorganisms and/or their components that confers a health benefit on the host" (1). Lactobacillus LB is a heat-treated preparation of cellular biomass and a fermentate generated by Limosilactobacillus fermentum and Lactobacillus delbrueckii ssp. delbrueckii which has been demonstrated to alleviate acute diarrhoea (2) and ameliorate the symptoms of irritable bowel syndrome (3) in human studies. However, the mechanisms underlying these beneficial effects are unknown. Here, we investigated whether modulation of intestinal ion transport and motility underpins the beneficial effects of this postbiotic observed clinically.

We used Ussing chambers and organ baths to assess the effects of a low-lactose postbiotic preparation (5%, low-lactose LB) on naïve intestinal tissue from male and female C57Bl/6 mice. Ussing chamber studies were carried out as previously described (4) but using small intestinal mucosa-submucosa preparations. Low-lactose LB was applied to the apical chamber. The neurotoxin, tetrodotoxin (TTx; 300 nM) and the Na-K-2Cl co-transporter inhibitor, furosemide (fur, 100 µM) were added to the basolateral chamber. Organ bath experiments were performed in a vertical setup using full-thickness preparations of 2-3 cm distal small intestine. Carbachol (CCh, 100 µM) was added to induce contractions pre- and post-treatment with 5% low-lactose LB (5). Statistical analysis was performed using a Mann-Whitney U test between treatment and control groups.

Ussing chamber data are presented as change in short-circuit current (ΔISC) in µA/cm2. Luminal addition of low-lactose LB (5%) significantly increased baseline ISC compared to Krebs-control (low-lactose LB, 51.2 [37.6 – 64] versus Krebs, -2.4 [-9.6 – 6.4], N = 6, $p < 0.05$, median [Interquartile range]). This effect was insensitive to pre-treatment with TTx (vehicle (veh) + low-lactose LB, 40 [31.2 – 52] versus TTx + low-lactose LB, 34.4 [25.6 – 60.8] or fur (veh + low-lactose LB, 50.4 [28.8 – 66.4] versus fur + low-lactose LB, 36.8 [24 – 64.8], N = 10-13, $p > 0.05$), suggesting that the effects of low-lactose LB may be epithelial in nature and independent of basolateral Cl- co-transport. In the organ bath, 5% low-lactose LB significantly decreased tension indicative of relaxation (Δweight in g; low-lactose LB, -0.15 [-0.19 – -0.11] versus Krebs 0.01 [0 – 0.02], N = 9-10, $p < 0.05$). After incubation with low-lactose LB (5%) for 30 min, the CCh-induced contractile response was significantly increased relative to the initial CCh-induced contraction (fold change; low-lactose LB, 1.62 [1.3 – 1.9] versus Krebs, 1.15 [1 – 1.2], N = 8-9, $p < 0.05$).

Lactobacillus LB significantly influences both intestinal secreto-motor function and intestinal motility ex vivo. These effects combined could contribute to the clinical efficacy of this postbiotic. Further characterisation is now warranted to better understand the molecular mechanisms.

References

(1) Salminen S, Collado MC, Endo A, Hill C, Lebeer S, Quigley EMM, et al. (2021) The International Scientific Association of Probiotics and Prebiotics (ISAPP) consensus statement on the definition and scope of postbiotics. *Nat Rev Gastroenterol Hepatol*. 18(9):649-67.

(2) Salazar-Lindo E, Figueroa-Quintanilla D, Caciano MI, Reto-Valiente V, Chauviere G, Colin P (2007) Effectiveness and safety of lactobacillus LB in the treatment of mild acute diarrhea in children. *Journal of Pediatric Gastroenterology and Nutrition*. 44(5):571-6

(3) Tarrerias AL, Costil V, Vicari F, Létard JC, Adenis-Lamarre P, Aisène A, et al. (2011) The effect of inactivated lactobacillus LB fermented culture medium on symptom severity: Observational investigation in 297 patients with diarrhea-predominant irritable bowel syndrome. *Digestive Diseases*. 29(6):588-91
(4) Lomasney KW, Cryan JF, Hyland NP (2014) Converging effects of a Bifidobacterium and Lactobacillus probiotic strain on mouse intestinal physiology. *American Journal of Physiology - Gastrointestinal and Liver Physiology*. 307(2):241-7
(5) Unno T, Matsuyama H, Sakamoto T, Uchiyama M, Izumi Y, Okamoto H, et al. (2005) M(2) and M(3) muscarinic receptor-mediated contractions in longitudinal smooth muscle of the ileum studied with receptor knockout mice. *Br J Pharmacol*. 2005;146(1):98-108

B 02-06

Effects of the epithelial sodium channel blocker amiloride in kidney transplant recipients with- or without albuminuria

G. R. Hinrichs[1,2], J. R. Nielsen[2], H. Birn[3,4], C. Bistrup[2,5], B. L. Jensen[1]
[1] *University of Southern Denmark, Department of Molecular Medicine, Cardiovascular and Renal Research, 5000, Denmark*
[2] *Odense University Hospital, Department of Nephrology, 5000, Denmark*
[3] *Aarhus University Hospital, Department of Renal Medicine, 8000, Denmark*
[4] *Aarhus University, Department of Biomedicine, 8000, Denmark*
[5] *University of Southern Denmark, Clinical Research, 5000, Denmark*

Background
Albuminuria in kidney transplant recipients (KTRs) is associated with hypertension and increased extracellular volume associated with Na^+ retention. This may be caused by aberrant glomerular filtration of serine proteases including plasmin that may proteolytically activate the epithelial sodium channel (ENaC). The study tests the hypothesis that one day of amiloride reduces blood pressure and increases sodium excretion and renin-angiotensin-aldosterone significantly more in albuminuric compared to normoalbuminuric KTRs.
Methods
In an open-label pharmacodynamic intervention study, KTRs with albuminuria (albumin/creatinine-ratio > 300mg/g, n=7) or without albuminuria (albumin/creatinine-ratio < 300mg/g, n=7) received a fixed sodium diet (150mmol/d) for five days. On the last day, oral amiloride 10mg x 2 was administered. Ambulatory blood pressure, 24h urine and blood samples were collected. Body water content and weight was monitored before and after treatment. Electrolyte excretion and renin-ANGII-aldosterone were measured.
Results
At baseline, the mean 24-h urinary protein excretion was 0.99g/24h and 0.11g/24h in the albuminuric and non-albuminuric KTRs, respectively (p =0.001). There were no significant differences between baseline p-creatinine (136.3 µmol/L vs. 130.1 µmol/L); urine creatinine clearance (66.6 ml/min. vs. 80.9 ml/min) or plasma electrolytes. Both groups were fluid overloaded (1.12 and 0.39 L/1,73m2 in albuminuric vs non-albuminuric KTRs, respectively. One day of amiloride treatment resulted in a significant decrease in body weight in both groups (-0.4 kg and -0.9 kg in albuminuric and non-albuminuric KTRs, respectively) consistent with an increased 24h urinary output in both groups, with statistical significance in the control group. 24h-urinary Na^+ excretion increased significantly in both groups (52.5 mmol and 85.3mmol) as well as 24h-urinary Na^+/K^+ ratio (3.89 and 4.45) in the albuminuric and non-albuminuric KTRs, respectively). P-aldosterone, renin and ANGII did not change significantly in response to amiloride. Plasma potassium increased significantly only in non-albuminuric KTRs (0.31 vs 0.37mmol/l). Amiloride reduced mean systolic and diastolic blood pressures in both groups. The decrease in night systolic blood pressure was significant in albuminuric KTRs only when compared to non-albuminuric (-5,16 mmHg, *p* 0.022 vs. 3.89mmHg, *p* 0.30).
Conclusion
Despite antihypertensive treatment targeting the renin-angiotensin-aldosterone system (ACEi/ARBs), ENaC contributes to sodium and water retention and blood pressure in kidney transplant recipients with clinical albuminuria and overt proteinuria. ENaC may be a relevant target in the diuretic- or antihypertensive treatment. Larger and long-term studies are needed to evaluate weather this effect is more pronounced in KTRs with proteinuria compared to KTRs with normoalbuminuria.

B 02-07

Accelerated Lysine Metabolism Conveys Kidney Protection in Hypertensive Kidney Disease

M. Rinschen[1,3], O. Palygin[4], J. Jaegers[1], F. Demir[1], G. Siuzdak[2], A. Staruschenko[5]
[1] *Aarhus University, Department of Biomedicine, Aarhus, Denmark*
[2] *Scripps Research, Department of Chemistry, San Diego, USA*
[3] *University Hospital Hamburg-Eppendorf (UKE), Department of Internal Medicine III, Hamburg, Germany*
[4] *MUSC, Department of Nephrology and Hypertension, Charleston, USA*
[5] *USF, College of Medicine Molecular Pharmacology & Physiology, Tampa, USA*

Funding is acknowledged from the Novo Nordisk Foundation, Carlsberg Foundation and the DFG.

Introduction: Hypertension and kidney disease have been repeatedly associated with genomic variants and alterations of lysine metabolism.
Methods: Here, we coupled dietary stable isotope labeling with untargeted metabolomics to investigate lysine's metabolic fate *in vivo*. Metabolic trajectories of $^{13}C_6$ labeled lysine were tracked to lysine metabolites across all major organs in hypertension. Functional studies of lysine's bioactivity and fate were performed in rat models of hypertension and kidney disease, as well as humans at risk for hypertensive kidney disease.
Results: Globally, lysine reacts rapidly with molecules of the central carbon metabolism, but incorporates slowly into proteins and acylcarnitines. Lysine metabolism is accelerated in a rat model of hypertension and kidney damage, chiefly through N-*alpha*-mediated degradation. Lysine administration diminished development of hypertension and kidney injury. Protective mechanisms include diuresis, further acceleration of lysine conjugate formation, and inhibition of tubular albumin uptake. Lysine also conjugates with malonyl-CoA to form a novel metabolite Ne-malonyl-lysine to deplete malonyl-CoA from fatty acid synthesis. Through conjugate formation and excretion as fructoselysine, saccharopine, and Ne-acetyllysine, lysine lead to depletion of central carbon metabolites from the organism and kidney. Consistently, lysine administration to patients at risk for hypertension and kidney disease inhibited tubular albumin uptake, increased lysine conjugate

formation, and reduced tricarboxylic acid (TCA) cycle metabolites, compared to kidney-healthy volunteers.
Conclusion: Lysine isotope tracing mapped an accelerated kidney metabolism in hypertension, and lysine's bioactivity could protect kidneys in hypertensive kidney disease.

B 02-08
ATP signaling in pancreatic cancer: the P2X7 receptor
L. Magni[1], R. Bouazzi[1], N. Christensen[1], M. Tozzi[1], M. Poulsen[2], J. Johansen[3], S. Pless[2], I. Novak[1]
[1] *University of Copenhagen, Biology/Cell Biology and Physiology, Copenhagen, Denmark*
[2] *University of Copenhagen, Department of Drug Design and Pharmacology, Copenhagen, Denmark*
[3] *Herlev and Gentofte Hospital, Department of Oncology, Herlev, Denmark*

Funding: *This research was funded by the Danish Council for Independent Research Medical Sciences, grant number 8020-00254B, Marie Skłodowska-Curie COFUND Doctoral Programme TALENT, grant number H2020-MSCA-COFUND-2017-801199.*

Studies of human blood samples was approved by the local ethical committees.

Introduction
Pancreatic ductal adenocarcinoma (PDAC) is a lethal disease. The PDAC tumor microenvironment (TME) is a highly fibrotic, composed of cellular and non-cellular elements, including extracellular ATP (eATP), cytokines and collagen. In particular, eATP is considered to be high in the TME and this leads to the activation of the low sensitive purinergic receptor P2X7 (P2X7R). P2X7R is encoded by a highly polymorphic gene resulting in several splice variants and SNPs, some of which are associated with several diseases, including some cancers [1], but no information is available for PDAC. There is a cross-talk between pancreatic cancer and stellate cells (PSCs), involving cytokines such as IL-6, but the role of P2X7R that is expressed in these cells is unknown [2,3]. The aim of this study was to elucidate the role of P2X7R in PDAC.
Methods
Release of IL-6 and collagen from PSCs were detected with ELISA kits. PSCs were treated with agonists/antagonists of P2X7R and the conditioned media with/without Tocilizumab (IL-6 receptor specific monoclonal antibody) was tested on PDAC cell line (PANC-1) and pSTAT3 levels quantified using western blot. ATP released from PANC-1 and PSCs was measured with luminescence ATP kit. Association analysis was performed between P2X7R mutations detected in human blood samples from PDAC and control patients. Ca^{2+} signals and pore formation were studied using fluorophores Fura-2 and YO-PRO in PANC-1 and PSCs expressing P2X7R variants. PANC-1 migration was analyzed by time-lapse microscopy.
Results
PSCs and PANC-1 released ATP following mechanical, metabolic and osmotic stimulation. Activation of P2X7R with BzATP in PSCs caused release of collagen and IL-6. Conditioned media from P2X7R-activated PSCs stimulated STAT3 pathway in PANC-1 and treatment with Tocilizumab reduced pSTAT3 to the basal conditions. P2X7R mutations analysis carried out in DNA extracted from PDAC patient blood samples showed that two missense mutations (rs28360447 and rs7958316) leading to Gly150Arg and Arg276His, which are associated with different risk of developing PDAC, one protective and one promoting (OR=0.490 and 1.791), respectively. The expression of the receptor variants in PSCs and PANC-1 revealed different cellular behavior. Gly150Arg receptor showed lower Ca^{2+} signals and pore formation than WT, indicating loss of function phenotype. Arg276His showed diverse effects compared to WT: Ca^{2+} signals were similar, pore formation was reduced but cancer cell migration was increased.
Conclusion
In conclusion, we give first evidence of the P2X7R-IL-6-STAT3 cross-talk between PSCs and cancer cells, which may be potential therapeutic targets. Moreover, we provide the first risk-association between P2X7R SNPs and PDAC and functional studies of phenotypes that may help us to understand PDAC.

References
[1] Pegoraro, A.; De Marchi, E.; Adinolfi, E. *P2X7 Variants in Oncogenesis.* Cells 2021, 10, doi:10.3390/cells10010189
[2] Giannuzzo, A.; Pedersen, S.F.; Novak, I. *The P2X7 receptor regulates cell survival, migration and invasion of pancreatic ductal adenocarcinoma cells.* Mol Cancer 2015, 14, 203, doi:10.1186/s12943-015-0472-4
[3] Haanes, K.A.; Schwab, A.; Novak, I. *The P2X7 receptor supports both life and death in fibrogenic pancreatic stellate cells.* PLoS One 2012, 7, e51164, doi:10.1371/journal.pone.0051164.

B 02-09
The role of LRRC8 in the hypotonic stress response of human keratinocytes
M. G. Rotordam[1], A. Horvath[1], T. Fauth[2], C. Buerger[3], D.-D. Scheub[4], O. Rauh[4], N. Fertig[1], A. Obergrussberger[1]
[1] *Nanion Technologies GmbH, Munich, Germany*
[2] *BRAIN Biotech AG, Zwingenberg, Germany*
[3] *Clinic of the Goethe-University, Frankfurt am Main, Germany*
[4] *Technische Universität Darmstadt, Darmstadt, Germany*

Introduction
The human skin is constantly exposed to various stress factors such as temperature changes, mechanical stress, different humidity levels, air pollution or radiation. These factors can have a tremendous impact on the skin and can contribute to barrier disruption and inflammation, dry and fragile skin as well as premature ageing[1]. Recent advances in different research areas point to an impor-tant role of LRRC8 volume regulated anion channels (VRACs) in a plethora of different physiological processes[2]. The function of LRRC8 has been characterized in human keratinocytes and in the native human epidermis[3] and the LRRC8 ion channel has been proposed to be a novel molecular target to modulate keratinocyte differ-entiation. LRRC8A (also named SWELL1) has been identified as the first essential component of VRACs in various cell types[4,5]. LRRC8A is composed of four transmembrane domains and a C-terminal domain containing up to 17 leucine-rich repeats. Together with four additional LRRC8 family members (LRRC8B-E) it assembles into hetero-hexameric complexes[4,5]. The LRRC8 subunit composi-tion differs between cell types and influences VRAC prop-erties such as inactivation kinetics, voltage-dependence and selectivity of the transported osmolyte. The gen-eration of $LRRC8A^{-/-}$ knockout HaCaT keratinocytes has provided evidence for the essential function of LRRC8A in hypotonic stress response of human keratinocytes[3].

Methods
We used automated patch clamp devices to record LRRC8-mediated currents from WT and LRRC8A$^{-/-}$ knockout keratinocytes activated by hypotonic solution. We also measured LRRC8 activity, as well as cell volume changes, indirectly using the fluorescent halide-sensitive YFP and the volume-sensitive calcein-AM dye.

Results
LRRC8 was activated in wild type (WT) HaCaT keratinocytes by hypotonic solution and blocked by DIDS or NPPB. In contrast, no activation by hypotonic solution was observed in the LRRC8A$^{-/-}$ knockout HaCaT keratinocytes. LRRC8 currents recorded from WT HaCaT keratinocytes showed current at both negative and positive potentials, with currents showing prominent inactivation at voltages above 100 mV.

Conclusion
Keratinocytes coupled with automated patch clamp provide a tool to investigate the roles of VRAC channels in hypotonic stress.

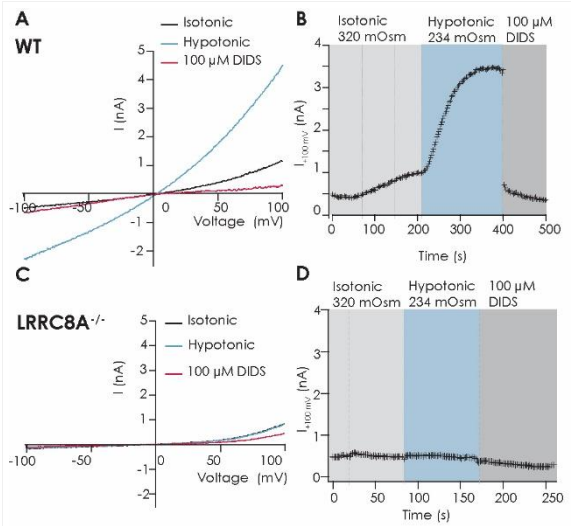

Automated patch clamp recordings from WT and LRRC8A-/- KO HaCaT keratinocytes using a ramp protocol.
A LRRC8 current was recorded using a voltage ramp protocol from -100 mV to +100 mV over 200 ms and activated using hypotonic solution (osmolarity: 234 mOsm). **B** Timecourse of the experiment shown in A, after addition of hypotonic solution, there was a large increase in current at both +100 mV and -100 mV (not shown). The LRRC8 current was blocked by DIDS. **C** There was no activation of LRRC8 current in the LRRC8A$^{-/-}$ knockout keratinocytes recorded on the Patchliner using a voltage ramp protocol. **D** Corresponding timecourse of the experiment, there was no activation by hypotonic solution.

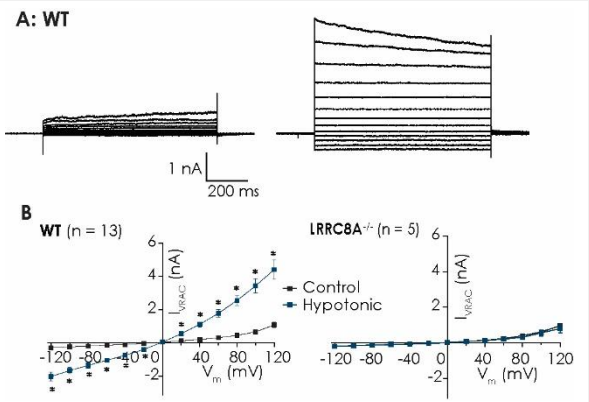

Effect of hypotonic solution on WT and LRRC8A-/- HaCaT keratinocytes using a voltage step protocol
A Traces from a representative WT cell in isotonic (left) and hypotonic (right) conditions. **B** Current voltage-plot for an average of 13 WT cells (left) and 5 LRRC8A$^{-/-}$ cells (right).

References

[1] Rosso, JD, Zeichner, J, Alexis, A, Cohen, D, Berson, D, 2016, 'Understanding the Epidermal Barrier in Healthy and Compromised Skin: Clinically Relevant Information for the Dermatology Practitioner: Proceedings of an Expert Panel Roundtable Meeting', J. Clin. Aesthet. Dermatol. 9(4 Suppl 1) S2-S8.

[2] Chen, L, Konig, B, Liu, T, Pervaiz, S, Razzaque, YS, Stauber, T, 2019, 'More than just a pressure relief valve: physiological roles of volume-regulated LRRC8 anion channels', Biol Chem 400(11) 1481-1496.

[3] Trothe, J, Ritzmann, D, Lang, V, Scholz, P, Pul, U, Kaufmann, R, Buerger, C, Ertongur-Fauth T. 2018 'Hypotonic stress response of human keratinocytes involves LRRC8A as component of volume-regulated anion channels', Exp. Dermatol. 27(12), 1352-1360

[4] Qiu, Z, Dubin, A.E, Mathur, J,Tu, B, Reddy, K, Miraglia, L.J, Reinhardt, J, Orth, A.P Patapoutian, A, 2014, 'SWELL1, a plasma membrane protein, is an essential component of volume-regulated anion channel', Cell 157(2), 447-58.

[5] Voss, FK, Ullrich, F, Munch, J, Lazarow, K, Lutter, D, Mah, N, Andrade-Navarro,MA, von Kries, JP, Stauber, T, Jentsch,TJ, 2014, 'Identification of LRRC8 heteromers as an essential component of the volume-regulated anion channel VRAC', Science, 344(6184), 634-8.

B 02-10

TWIK-1 - a heterodimer-forming subunit that controls K2P-channel trafficking?

M. Prüser, M. Musinszki, S. Cordeiro, T. Baukrowitz
Christian-Albrechts-University Kiel, Institute of Physiology, Kiel, Germany

Heteromerisation, i.e. the formation of channels by different subunits, is a frequently employed method by which cells increase ion channel diversity. In recent years, a number of examples of heteromerisation in the K2P-channel family, in which two subunits form functional channels, have been identified. In the present study, we intend to analyse the ability of TWIK-1 to form heterodimeric channels with other members of the TWIK-subgroup (i.e. intragroup heterodimers), as well as other K2P-channel family subgroups (i.e. intergroup heterodimers).

In order to study the interaction between TWIK-1 and other members of the K2P-channel family, we, first, created dominant-negative pore mutants and co-expressed them with wildtype channels at different RNA-concentration ratios in *Xenopus* oocytes. Currents were measured using the two-electrode voltage clamp method.

Interestingly, our data indicate that the TWIK-1 current is depressed in a concentration dependent manner by pore mutants of every K2P channel subgroup. Moreover, the dominant negative pore mutant of TWIK-1 also inhibited the currents of all the WT K2P channels we tested, but not of the BK-, Kv1.5 and Kir2.1 channels. This suggests that TWIK-1 is able to form heterodimeric channels with members of every K2P-channel subgroup.The homodimeric TWIK-1 channel differs from other members of the K2P channel family in that it only generates small currents, likely due to retrieval from the membrane through clathrin-mediated endocytosis and storage in the endo-lysosomal compartment[1]. It was previously shown that mutation of a di-isoleucine-based motif in the C-terminal region stabilises TWIK-1 at the membrane.

Surprisingly, when we used the unmutated TWIK-1 channel in co-expression studies with other WT K2P channels, we observed a reduction in current that was similar to that of a dominant-negative pore mutant, suggesting that the di-isoleucine retrieval motif may also have a dominant negative effect by promoting endocytosis of heterodimeric channels.

Next, in order to further study the functional properties of TWIK-1 containing heterodimeric channels, we created concatenated tandem channels in which the TWIK-1 subunit is covalently linked to a subunit of a different K2P-channel family member. Two-electrode voltage clamp studies in *Xenopus* oocytes revealed markedly reduced currents in tandem channels in which the di-isoleucine motif of TWIK-1 is intact, suggesting that the heterodimeric channels, too, are re-targeted to the endo-lysosomal compartment. Mutation of the retrieval motif led to a significant increase in current, allowing functional characterisation of these heterodimeric K2P-channels.

[1] Feliciangeli S, Tardy MP, Sandoz G, Chatelain FC, Warth R, Barhanin J, Bendahhou S, Lesage F. Potassium channel silencing by constitutive endocytosis and intracellular sequestration. J Biol Chem. 2010 Feb 12;285(7):4798-805. doi: 10.1074/jbc.M109.078535. Epub 2009 Dec 3. PMID: 19959478; PMCID: PMC2836085.

References

[1] [1] Feliciangeli S, Tardy MP, Sandoz G, Chatelain FC, Warth R, Barhanin J, Bendahhou S, Lesage F. Potassium channel silencing by constitutive endocytosis and intracellular sequestration. J Biol Chem. 2010 Feb 12;285(7):4798-805. doi: 10.1074/jbc.M109.078535. Epub 2009 Dec 3. PMID: 19959478; PMCID: PMC2836085.

B 02-11

Bayesian Hidden Markov modeling of ensemble data of chemical reaction networks exemplified on ion channels

J. L. Muench, R. Schmauder, K. Benndorf
Friedrich Schiller University Jena, Universitätsklinikum, Physiologie 2, Jena, Germany

Introduction

Inferring adequate kinetic schemes for ion channel gating from ensemble currents is a daunting task due to limited information in the data. Based on the rate equation approach by Milescu et al. [1] and the Kalman filter by Moffat [2], we developed a parallelized Bayesian filter (continuous state hidden Markov model) by defining a likelihood that correctly models the *first-order Markov* property of each single molecule within an ensemble signal. The crucial first step compared to the work of [2] was to find a solution to a generalized *noise model* which is beyond the classical Kalman filter. Our solution is exact for the first two statistical moments, no matter which signal distribution is modeled. This means it can be adapted to different measuring modalities as patch-clamp currents, conventional fluorescence detection or photon counting. In a second step, our algorithm samples the Bayesian posterior distribution of the parameters.

Results

Our generalized Bayesian filter outperforms both a classical Kalman filter and a rate equation approach when applied to patch-clamp data exhibiting realistic open-channel noise. For data sets, for which the Rate equation samples an improper posterior leading to unidentified parameters, our Bayesian filter delivers a fully identified rate matrix. When including orthogonal fluorescence data, estimates are further improved, which allowed us to identify previously unidentifiable parameters and which increased the accuracy of the parameter estimates by an order of magnitude.

The central advantage of Bayesian statistics is an accurate uncertainty quantification of the parameter inference. By using Bayesian highest credibility volumes, we showed that the likelihood derived through our approach yields a realistic uncertainty quantification. In contrast, deterministic rate equation approaches show unrealistically small Bayesian or non Bayesian error-estimates, leading to biases or potentially even misleading parameter estimates. These results also demonstrate the power of assessing the validity of algorithms by Bayesian credibility volumes in general, thereby addressing the question whether or not the predicted uncertainty of the inference matches the true uncertainty of the inference.

Finally, we demonstrate examples for which the Bayesian framework with a minimal informative prior Jaynes [3] and Jeffreys [4] expands the range of parameter identifiability by more than two orders of magnitude compared to naive Bayesian approaches with uniform priors or even maximum likelihood. Using a uniform prior explicitly or implicitly (maximum likelihood) may render the parameter inference unidentified.

Our algorithm is not limited to ion channels, but can be applied to any kind of time series that originate from an at least pseudo-monocular chemical reaction network obeying the 1st-order Markov property.

References
[1] Milescu, Lorin S., Gustav Akk, and Frederick Sachs. "Maximum likelihood estimation of ion channel kinetics from macroscopic currents." *Biophysical journal* 88.4 (2005): 2494-2515.
[2] Moffatt, Luciano. "Estimation of ion channel kinetics from fluctuations of macroscopic currents." *Biophysical journal* 93.1 (2007): 74-91.
[3] Jaynes, Edwin T. "Prior probabilities." *IEEE Transactions on systems science and cybernetics* 4.3 (1968): 227-241.
[4] Jeffreys, Harold. "An invariant form for the prior probability in estimation problems." *Proceedings of the Royal Society of London. Series A. Mathematical and Physical Sciences* 186.1007 (1946): 453-461.N YYYY, 'Article', *Journal*, Edition, Page, Place of publication: publishers

---

B 02-12

Claudin-19 localizes to the thick ascending limb where its expression is required for junctional Claudin-16 localization

H. Dimke[1,2], C. Griveau[3,4], W.-M.E. Ling[3,4], G. Brideau[3,4], L. Cheval[3,4], P. Houillier[3,4], C. Prot-Bertoye[3,4]
[1] *University of Southern Denmark, Department of Cardiovascular and Renal Research, Odense, Denmark*
[2] *Odense University Hospital, Department of Nephrology, Odense, Denmark*
[3] *Université Paris Cité, Centre de Recherche des Cordeliers, INSERM, Sorbonne Université, Paris, France*
[4] *CNRS ERL 8228, Laboratoire de Physiologie Rénale et Tubulopathies, Paris, France*
[5] *Assistance Publique-Hôpitaux de Paris, Hôpital Européen Georges Pompidou, Service de Physiologie, Paris, France*
[6] *Centre de Référence des Maladies Rénales Héréditaires de l'Enfant et de l'Adulte (MARHEA), Paris, France*
[7] *Centre de Référence des Maladies Rares du Calcium et du Phosphate, Paris, France*

Introduction

The kidneys play a critical role in maintaining mineral homeostasis. Calcium and magnesium reabsorption in the renal thick ascending limb (TAL) involves CLDN16 and CLDN19 and pathogenic variants in either gene lead to Familial Hypomagnesemia with Hypercalciuria and Nephrocalcinosis (FHHNC) with severe calcium and magnesium wasting. While both CLDN16 and CLDN19 localizes to the TAL, varying expression patterns in the renal tubule has been reported using different antibodies and it remains untested whether CLDN19 influence CLND16 *in vivo*.

Methods

We therefore determined the localization of CLDN19 in frozen and paraffin-embedded kidney sections from wild-type and *Cldn19* deficient mice using three different antibodies directed against the protein. Furthermore, we examined the role of *Cldn19* deletion on CLDN16 and CLDN10 localization in kidney.

Results

We find that CLDN19 localizes to basolateral membrane domains of the medullary and cortical TAL but only to the tight junction of TALs in the outer stripe of outer medulla and cortex, where it colocalizes with CLDN16. Furthermore, in TALs from *Cldn19* deficient mice, CLDN16 is expressed in basolateral membrane domains but not at the tight junction. In contrast, *Cldn19* ablation does not change CLDN10 localization.

Conclusion

In vivo, the CLDN19 protein is required for the proper CLDN16 expression at the tight junction.

These findings implicate directly CLDN19 in regulating permeability in the TAL, by allowing junctional insertion of CLDN16 and may explain the shared renal phenotypic characteristics in FHHNC patients.

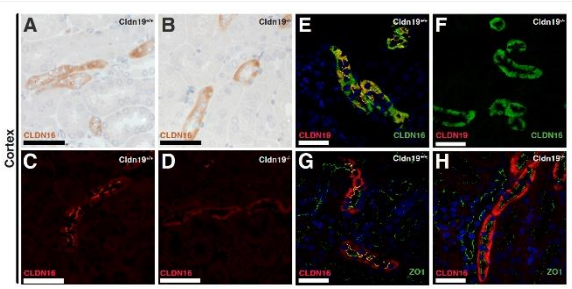

CLDN16 labelling in kidney of Cldn19 deficient animals
CLDN16 is expressed in both the tight junction and basolateral membrane domains in a mosaic pattern. Following *Cldn19* ablation, immunohistochemical staining revealed that while CLDN16 localized in basolateral membrane domains it was absent from the junction (Figure 4A-D). CLDN16 was found to colocalize with CLDN19 (Figure 4E-F) and the tight junctional marker ZO1 (Figure 4G-H) in the tight junction in a mosaic pattern, while tight junction localization was completely absent at the tight junction in the kidney of *Cldn19* deficient animals.

B 02-13

Phd inhibition reduces anemia and capillary rarefaction in the setting of Cyclosporine-A induced nephrotoxicity.

R. Labes[1], L. Brinkmann[1], V. A. Kulow[2], K. Rögner[1], S. Mathia[1,2], B. Balcerek[1], P. Persson[1], C. Rosenberger[2], M. Fähling[1]

[1] Charité - Universitätsmedizin Berlin, corporate member of Freie Universität Berlin and Humboldt-Universität zu Berlin, Institute for Translational Physiology, Berlin, Germany

[2] Charité - Universitätsmedizin Berlin, corporate member of Freie Universität Berlin and Humboldt-Universität zu Berlin, Medizinische Klinik m.S. Nephrologie und Internistische Intensivmedizin, Berlin, Germany

The Else Kröner-Fresenius-Stiftung has funded this work (grant: 2016_A207 to M. Fähling).

Introduction

Cyclosporine-A (CsA) is widely used in organ transplantation and various autoimmune diseases for its immunosuppressive effects. Unfortunately, CsA treatment is associated with side effects such as nephrotoxicity and anemia. The mechanisms behind CsA mediated kidney injury are incompletely understood. Through inhibition of the phosphatase calcineurin, CsA is supposed to change protein phosphorylation, however, a systematic phospho-proteomic analysis has not been performed so far. The prolyl hydroxylase inhibitor daprodustat is designed for treatment of renal anemia. Having a special focus on the phospho-proteome, we investigated the impact of daprpodustat on CsA mediated renal toxicity and anemia.

Methods

Mice received daily oral gavage with CsA (80 mg/kg BW) and/or daprodustat (10 mg/kg BW) for up to 8 weeks. Blood samples served for evaluation of kidney function and anemia. qPCR and immunofluorescence were used to access kidney injury markers. Kidney homogenates served for large scale phospho-proteomic analysis and data were analyzed by gene set enrichment analysis. Examination of capillary density was performed by immunofluorescence staining of kidney slices for the endothelial marker CD31 followed by quantification of the stained area.

Results

Treatment with CsA for 8 weeks resulted in anemia and elevated kidney injury markers Kim-1, Ngal, Dkk3 and vimentin. However, unchanged serum creatinine levels indicate a subclinical stage. Combined treatment with daprodustat ameliorated anemia, but renal injury markers remained unaffected. Analysis of the phospho-proteome of CsA treated animals compared to control mice showed a differential expression of 79 proteins and a change in phosphorylation level of 86 proteins. Combination of CsA with daprodustat resulted in alteration of 95 proteins at expression and only 6 at phosphorylation level. On its own, daprodustat showed only marginal effects. As shown by gene set enrichment analysis, angiogenesis-related pathways were among the top enriched candidates under CsA and daprodustat/CsA treatment. A loss of peritubular vessels by CsA was shown by immunofluorescence staining of CD31. Combined treatment of daprodustat/CsA prevented CsA mediated capillary rarefaction.

Conclusion

This study provides a detailed renal phospho-proteomic map of the renal response to CsA, daprodustat, and the combination of both. We demonstrate that nephrotoxicity through chronic CsA treatment involves capillary rarefaction and anemia. We show that daprodustat on top of CsA prevents CsA induced effects on microcirculation and Hb. Data suggest that the protective action of daprodustat involves changes in the renal phospho-proteome, which results from long-term CsA treatment.

B 02-14

Complications and Treatment of Hypercalciuria in Familial Hyperkalaemic Hypertension (FHHt)

V. D'Ambrosio, K. Siew, **S. Walsh**
UCL, Department of Renal Medicine, London, UK

Introduction

Hypertension is frequently associated with hypercalciuria, nephrolithiasis and low bone mineral density. Familial Hyperkalaemic Hypertension (FHHt) causes hypercalciuria, although complications of this are not reported.

Methods

We examined a cohort of 9 patients with genetically confirmed FHHt. Biochemical, radiological, and clinical data was obtained in patients before and after thiazide treatment. All patients gave informed consent. The study had ethics committee approval (REC 05/Q0508/6). Data were compared using paired t tests or Wilcoxon paired rank tests.

Results

5 of the 9 patients were female (median age 41.7 years). The genetic diagnosis was confirmed in all patients, 5 patients had variants in KLHL3, 3 patients had variants of WNK4, and one had a variant of WNK1.

Pre-treatment potassium was high (median 5.6 IQR 5.2-6.2 mmol/L). Pre-treatment calcium was in the normal range (2.34 IQR 2.29-2.38 mmol/L). There was significant hypercalciuria with a raised urinary calcium/creatinine ratio (0.69 IQR 0.41-1.13). However, PTH (4 IQR 3.95-4.35 pmol/L), phosphate (1.15 IQR 1.25mmol/L) and alkaline phosphatase (57 IQR 45-84 mmol/L) were all in the normal range.

Thiazide treatment significantly reduced hypercalciuria (calcium/creatinine ratio 0.15 IQR 0.05-0.29 p=0.04) as well as the serum potassium (3.9 IQR 3.5-4.4 mmol/L p=0.0167).

Patients also developed complications of hypercalciuria. 3 patients had kidney stones demonstrated on cross-sectional imaging. One of these patients (male, 30 years old) had DXA criteria for osteoporosis (T score Femoral neck -1.5, lumbar spine -2.4).

Conclusion

This is the first case series to demonstrate complications of hypercalciuria (i.e. kidney stones) in patients with FHHt. We demonstrate that thiazide treatment normalises urinary calcium excretion. Thiazide treatment may have clinical utility in FHHt even if hypertension or hyperkalaemia are not problematic in order to avoid the complications of hypercalciuria.

B 02-15

Role of SLC26A2 in the kidney

I. Lukianova, U. Scholl
Berlin Institute of Health (BIH), Institute of Functional Genomics, Berlin, Germany

Introduction

Chondrodysplasias are hereditary disorders, some of which are caused by mutations in a transmembrane protein, called SLC26A2, or DTDST. Mutations often result in loss of activity or low expression levels of the protein. In cartilage, SLC26A2 acts as a sulfate transporter, and clinical severity of patients with diastrophic chondrodysplasia, one of the mild forms of the disorder, is related to the residual activity of SLC26A2 and the sulfation state of proteoglycans in the extracellular matrix (Rossi et al. 1998). So far, SLC26A2 research has focused on the investigation of its role in bone and cartilage, although it is expressed in various organs. Interestingly, SLC26A2 is found in the proximal tubule of the kidney, a site of sulfate reabsorption (Chapman and Karniski 2010). The aim of this study is to investigate the role of SLC26A2 in the kidney, its regulation and function.

Methods and Results

Opossum kidney cells (OK cells) are a common *in vitro* model of the proximal tubule. Using CRISPR/Cas9-based genome editing, we generated *SLC26A2* knock-out OK cell lines along with wildtype control lines. Preliminary data showed decreased uptake of radioactive sulfate by knock-out cells compared to the wildtype controls. Using qPCR, we identified potential additional sulfate transporters in OK cells that might contribute to sulfate uptake and release in these cells.

We also aim at generation of an *in vivo* mouse model of renal *Slc26a2* deficiency through conditional knock out of *Slc26a2* in the proximal tubule employing the Cre/lox-system. After the generation of the model, we will grossly phenotype the mice, isolate brush border membrane vesicles and perform sulfate transport assays. All experiments and animal care will be performed in accordance with the current EU legislation.

For quantitative analysis of membrane targeting and trafficking and to distinguish between the surface fraction and intracellular fraction of the protein, we inserted an AviTag in an extracellular loop. Further, we generated constructs with depleted glycosylation sites and deleted C-terminal domains using site-directed mutagenesis. Protein with either one or two mutated glycosylation sites successfully trafficked to the cell membrane. However, the stability and functionality of the protein are still to be tested. Contrarily, deletion of the STAS domain, an intracellular C-terminal domain that contributes to dimer formation, led to intracellular localization of the mutant protein.

Conclusion

Understanding the role of SLC26A2 in the kidney could provide better insight on the pathology of chondrodysplasias and help characterize mechanisms of sulfate homeostasis in the body.

References

[1] Chapman, J.M. and Karniski, L.P. (2010). Protein localization of SLC26A2 (DTDST) in rat kidney. *Histochemistry and Cell Biology*, 133(5), pp.541–547. doi:10.1007/s00418-010-0694-x.

[2] Rossi, A., Kaitila, I., Wilcox, W.R., Rimoin, D.L., Steinmann, B., Cetta, G. and Superti-Furga, A. (1998). Proteoglycan sulfation in cartilage and cell cultures from patients with sulfate transporter chondrodysplasias: Relationship to clinical severity and indications on the role of intracellular sulfate production. *Matrix Biology*, 17(5), pp.361–369. doi:10.1016/s0945-053x(98)90088-9.

B 02-16

Functional expression of calcium homeostasis modulator 2 (calhm2) as slowly activating outwardly rectifying current in mouse B cells.

S.W. Choi[1], K.S. Park[2], S.J. Kim[1]

[1] *Seoul National University, College of Medicine, Seoul, South Korea*

[2] *Wide River Institute of Immunology, College of Medicine, Hongcheon, South Korea*

This work was supported by the National Research Foundation of Korea (NRF-2018R1A5A2025964). Also, it was partly supported by the 2022 Support from Seoul National University Hospital to Dr. SJ Kim.

Previously, we found very slowly activating voltage-dependent current (I_{VSAC}) in mouse B lymphocytes, which showed significant thermosensitivity and inhibited by Gd^{3+} or ruthenium red (RuR) [1]. Calcium homeostasis modulator 1(c*alhm1*) is a newly identified membrane protein forms nonselective ion channel with large pore structure, activated by membrane depolarization, blocked by Gd^{3+} and RuR. The voltage-dependent activation of calhm1 is facilitated by lowering extracellular Ca^{2+} concentration and by physiological temperature [2]. Based on the electrophysiological properties similar with calhm1, we explored the molecular nature of I_{VSAC}. RT-PCR analysis revealed the mRNAs of calhm2 and 6, while not calhm1, are expressed in the primary B cells and B cell lymphoma lines (WEHI-231 and BAL-17) of mice. Using the conventional whole-cell patch clamp with CsCl or NMDG-Cl pipette solution, the thermosensitivity of I_{VSAC} was confirmed in the mouse B cells along with the facilitation by lowering $[Ca^{2+}]_{ext}$. The overexpressed calhm2 in N2A cell also showed similarly slow activation by sustained depolarization at 35 – 37 °C. However, calhm6 overexpression did not show noticeable I_{VSAC} even at 37 °C. Also, coexpression of calhm2 and 6 did not show significant augmentation of I_{VSAC}. A knockdown of calhm2 by transfection with the anti-calhm2 siRNA showed smaller amplitude of I_{VSAC} in BAL-17. Interestingly, no I_{VSAC} was recorded in the human primary B cells and cell lines despite the consistent expression of the mRNA for CALHM2. Based on the above results, we suggest that calhm2 is the molecular nature of I_{VSAC} in mouse B lymphocytes. In mice, calhm2 has been suggested as an ATP-releasing mechanism in astrocytes and microglia [3]. Further investigation of the physiological role of calhm2 in B lymphocytes is necessary.

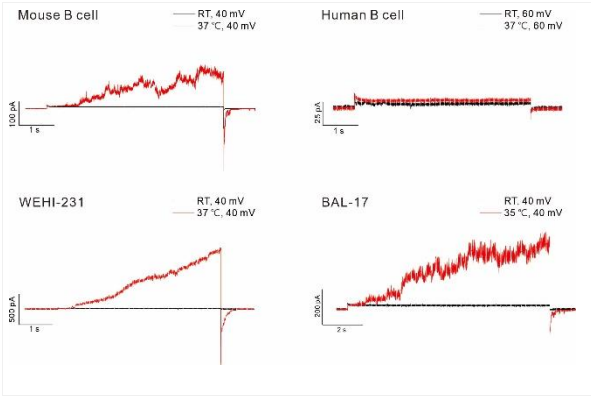

Calhm channel in mouse and human B cells.
Calhm current showed in mouse B cells but not showed in human B cells.

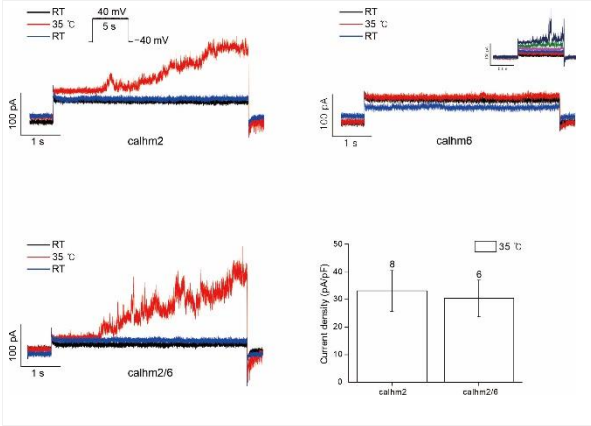

Calhm2 channel is important in mouse B cells.
Using patch-clamp technique, investigated the relationship between calhm2 and calhm6. Calhm6 channel function is smaller than calhm2 in Neuro-2A cells. Current density of calhm2 and calhm2/6 are not significant.

References

[1] Joo Hyun Nam, Hai Feng Zheng, Ki Hyun Earm, Jae Hong Ko, Ik-Jae Lee, Tong Mook Kang, Tae Jin Kim, Yung E Earm, Sung Joon Kim, Voltage-dependent slowly activating anion current regulated by temperature and extracellular pH in mouse B cells, 2006, *Pflugers Arch - Eur J Physiol*, 452, 707–717, Springer-Verlag

[2] Young Keul Jeon, Si Won Choi, Jae Won Kwon, Joohan Woo, Seong Woo Choi, Sang Jeong Kim, Sung Joon Kim, Thermosensitivity of the voltage-dependent activation of calcium homeostasis modulator 1 (calhm1) ion channel, 2021, *Biochemical and Biophysical Research Communications*, 534, 590-596, ELSEVIER

[3] M Jun, Q Xiaolong, Y Chaojuan, , P Ruiyuan, W Shukun, W Junbing, H Li, C Hong, C Jinbo, W Rong, L Yajin, M Lanqun, W Fengchao, W Zhiying, A Jianxiong, W Yun, Z Xia, Z Chen and Y Zengqiang, Calhm2 governs astrocytic ATP releasing in the development of depression-like behaviors, 2018, *Molecular Psychiatry*, 23, 883-891, Springer Nature

---

B 02-17

Characterization of a thick ascending limb-specific Cre/loxP inducible system generated by insertion of the CreERT2 sequence in the 3'UTR of the SLC12a1 gene

L. Bourqui, D. Loffing, J. Loffing

University of Zurich, Institute of Anatomy and Institute for Experimental Immunology and Imaging, Zurich, Switzerland

The thick ascending limb (TAL) plays a pivotal role for the renal control of fluid and ion homeostasis. The function of the TAL depends on the activity of the furosemide-sensitive Na-K-2Cl co-transporter NKCC2, which is highly abundant in the luminal membrane of TAL cells. The TAL function is regulated by various hormonal and non-hormonal factors. However, many of the underlying signal transduction pathways remain elusive.
Here, we describe the development and characterization of a novel gene-modified mouse model for an inducible and specific deletion of regulatory and other genes expressed in the TAL. In these mice, a tamoxifen-dependent Cre (CreERT2) was inserted into the 3' UTR of the Slc12a1 gene, which encodes NKCC2 (NKCC2-Cre). Although this gene-modification strategy reduced endogenous NKCC2 expression at the mRNA and protein level, the lowered NKCC2 abundance was not associated with an altered urinary fluid and ion excretion. Likewise, the renal response to loop-diuretics or water restriction was similar in wildtype and in NKCC2-Cre mice. Immunohistochemistry on kidneys from NKCC2-cre mice revealed strong Cre expression exclusively in TAL cells but not in any other nephron portion. Cross-breeding of these mice with the mT/mG reporter mouse line showed a very low recombination rate (0.22%) at baseline, but a complete recombination (100%) after repeated tamoxifen administration. The achieved recombination encompassed the entire TAL and included also the macula densa. Thus, the new NKCC2-Cre mouse line allows an inducible and very efficient gene-targeting in the TAL and hence promises to be a powerful tool to advance our understanding of the regulation of TAL function.

Key words: NKCC2, TAL, Cre/Lox P system, CreERT2 inducibility

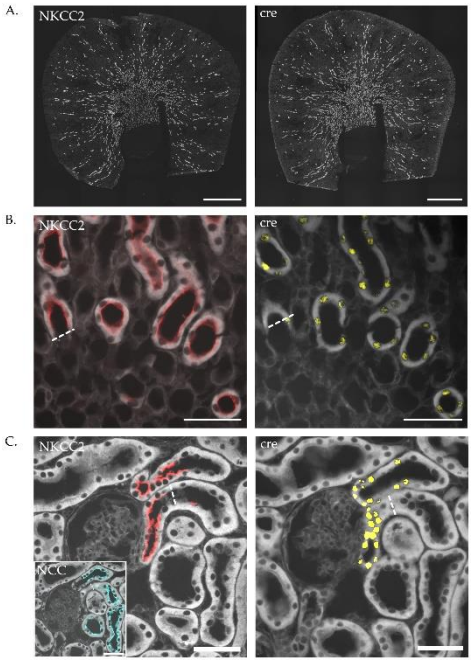

Cre expression is restricted to TAL
The cre recombinase signal is mainly located in the cortex and in the outer medulla and shares an identical distribution pattern as the NKCC2 signal. Higher magnification reveals that the expression of Cre recombinase is limited to the cells stained with NKCC2 and stops abruptly at the thin limbs to TAL and TAL to DCT transitions.

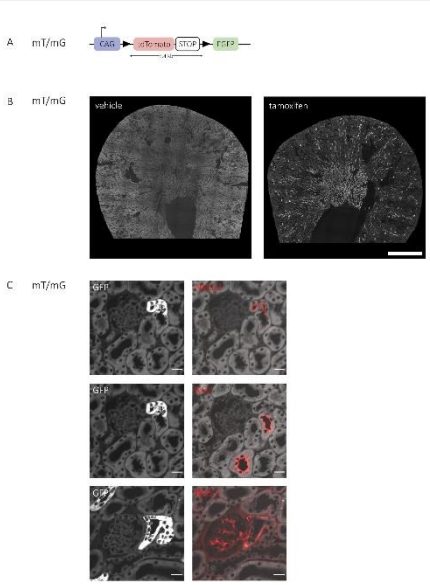

The system is high inducible with a low tamoxifen-independent recombination rate
Slc12a1CreERT2 mice were crosbred with mt/mg reporter mice. On kidney overviews we detected a strong EGFP signal in the TALs of tamoxifen-induced mice, while this signal was restricted at discrete locations in the kidneys of control mice. Higher magnifications confirmed that EGFP was strictly and continuously available in TAL, importantly the signal encompassed the macula densa. A tamoxifen independent recombination rate was calculated at 0.22%.

References

[1] C. Schnoz, S. Moser, D. V. Kratschmar, A. Odermatt, D. Loffing-Cueni, and J. Loffing, "Deletion of the transcription factor Prox-1 specifically in the renal distal convoluted tubule causes hypomagnesemia via reduced expression of TRPM6 and NCC," *Pflugers Arch - Eur J Physiol*, vol. 473, no. 1, pp. 79–93, Jan. 2021, doi: 10.1007/s00424-020-02491-1.

[2] R. J. Cornelius *et al.*, "A novel distal convoluted tubule-specific Cre-recombinase driven by the NaCl cotransporter gene," *American Journal of Physiology-Renal Physiology*, vol. 319, no. 3, pp. F423–F435, Sep. 2020, doi: 10.1152/ajprenal.00101.2020.

[3] A. Álvarez-Aznar, I. Martínez-Corral, N. Daubel, C. Betsholtz, T. Mäkinen, and K. Gaengel, "Tamoxifen-independent recombination of reporter genes limits lineage tracing and mosaic analysis using CreERT2 lines," *Transgenic Res*, vol. 29, no. 1, pp. 53–68, Feb. 2020, doi: 10.1007/s11248-019-00177-8.

B 02-18

The Ca^{2+} channel TRPV6 modulates pancreatic cancer cell aggressiveness

G. Mesquita[1,3], A. Haustrate[1,2], B. Soret[1,3], I. Azzam[4], V. Lehen'kyi[1,2], A. Schwab[3]

[1] *University of Lille, Laboratory of Cell Physiology, Department of Biology, Villeneuve d'Ascq, France*

[2] *INSERM U1003, PHYCELL-Laboratoire de Physiologie Cellulaire, Villeneuve d'Ascq, France*

[3] *University of Münster, Institut für Physiologie II, Münster, Germany*

[4] *University of Münster, Institut für Immunologie, Münster, Germany*

Introduction

Pancreatic ductal adenocarcinoma (PDAC) is a major cause of cancer-associated mortality in Western countries. Prevention is exceedingly difficult since patients rarely exhibit symptoms and currently no specific tumor markers are available for early diagnosis at a curable stage. Furthermore, the current treatments have failed to provide an answer to the aggressiveness of this cancer. PDAC is inherently linked to the unique physiology and microenvironment of the exocrine pancreas such as pH, mechanical stress, and hypoxia. On the other hand, Ca^{2+} signals are emerging to be particularly relevant in cancer. They mediate interactions between tumor cells and the tumor microenvironment to drive different aspects of cancer progression. The control and modulation of these Ca^{2+}-dependent processes revolve around TRP channels. Increasing evidence suggests that the overexpression of the Ca^{2+} channel TRPV6 is a common event in cancers of epithelial origin. Thus, our work aims at studying the role of TRPV6 channel in PDAC cell lines.

Methods

After analyzing the channel expression in several PDAC cell lines, we prepared a stable clone model from Panc-1 cells. These clones either under- or overexpress TRPV6. Our work seeks to elucidate the potential role of TRPV6 in cell viability, proliferation and cell cycle progression, both at basal conditions and treated with common drugs used in PDAC: gemcitabine, cisplatin, and 5-fluorouracil (one of the compounds used in the FOLFIRINOX regime).

Results

We demonstrate that cancer cells deficient in TRPV6 have a less aggressive phenotype which is characterized by reduced cell proliferation and intracellular ATP levels. They are also more prone to exhibit a pro-apoptotic phenotype, which was studied using cell cycle assay with focus on the cell cycle arrest in the sub-G1 phase. Contrasting with these results, overexpression of the TRPV6 channel leads to increased cell proliferation and cell metabolism, measured by MTS assay. Using both ATP assay and cell cycle assay, we can also verify the higher vulnerability to the common chemo-treatments demonstrated by cells deficient in TRPV6.

Conclusion

Overall, our results suggest that TRPV6 plays a role in the modulation of PDAC cell phenotype on proliferation, cell survival and chemotherapy resistance.

B 02-19

Podocyte-derived urinary extracellular vesicles mirror podocyte proteostasis

K. Lahme[1], K. Deheshwar[1], G. Gloede[1], O. Kretz[2], S. Zielinski[1], T. B. Huber[2], S. Liu[2], F. Braun[2], W. Sachs[1], D. Loreth[1], C. Meyer-Schwesinger[1]

[1] University Medical Center Hamburg-Eppendorf, Institut of Cellular and Integrative physiology, Hamburg, Germany

[2] University Medical Center Hamburg-Eppendorf, III Department of Medicine, Hamburg, Germany

Introduction

Upregulation of the ubiquitin-proteasome system (UPS) within podocytes occurs upon injury and correlates with disease progression in rodent models. During progressive podocyte injury, the proteasome system becomes impaired resulting in the accumulation of non-degraded proteins. Here we tested whether the abundance of urinary extracellular vesicles (EVs) and their content on UPS proteins displays the proteostatic condition of glomerular podocytes.

Methods

During terminal organ extraction, mice were treated with buprenorphin (0,1 mg/kg bodyweight subcutaneously, 30 minutes before surgery) and isoflurane (3.5 %, inhaled). EVs were isolated from mT/mG and BALB/c mice, and from human urine by differential ultracentrifugation. Isolation of podocyte-derived EVs from human urine was established and validated. Mouse urine was collected prior to and on different days after disease induction (THSD7A-associated membranous nephropathy (MN), adriamycin nephritis (AN) and diabetic nephropathy (DN)). The abundance and proteostatic content of EVs was analysed by immunoblotting and compared to the proteostatic situation in podocytes. Podocyte-specific urinary EVs from nephrotic patients were investigated for differences in EV amount and abundance of UPS components.

Results

The amount of podocyte-derived EVs increases differentially in murine podocyte injury models. The abundance increases in a dose- and time-dependent manner in THSD7A MN, but not in AN und DN. Both human and murine urinary EVs contain UPS components. The proteostatic content changes in a disease-dependent manner, mirroring the proteostatic situation of podocytes. Human podocyte-specific EVs differentiate in size from total urinary EVs. In nephrotic patients the amount of podocyte-specific EVs differs depending on the underlying podocyte injury.

Conclusion

Analysis of podocyte-specific EVs has the potential to give insight into the proteostatic status of podocytes.

B 02-20

Increased Activity of Cx26 Hemichannel in Epithelial Cells of the Respiratory Airways in Response to Lipopolysaccharide

A. Dierks[1], T. Lehrich[1], S. Tamm[2,3], P. Braubach[4,3], F. Stanke[2,3], A. Ngezahayo[5]

[1] Leibniz University Hannover, Dept. Cell physiology and Biophysics/ Institute of Cell Biology and Biophysics, Hannover, Germany

[2] Hannover Mediacl School, Department of Pediatric Pneumology/ Neonatology and Allergology, Hannover, Germany

[3] Hannover Mediacl School, German Center for Lung Research (DZL), Biomedical Research in Endstage and Obstructive Lung Disease Hannover (BREATH), Hannover, Germany

[4] Hannover Mediacl School, Institute for Pathology, Hannover, Germany

[5] University of Veterinary Medicine Hannover Foundation, Center for Systems Neuroscience (ZNS), Hannover, Germany

Introduction

The most recognized function of connexins (Cx) is the formation of cell-to-cell gap junction channels that connect the intracellular spaces of adjacent cells in tissue. Cx also form hemichannels in single cells and recent results show that the activity of Cx hemichannels is involved in response of a tissue to pathological stress.**Methods**

We analysed how lipopolysaccharide (LPS) affect Cx hemichannels of the epithelial cells of the respiratory airways. As model we used the Calu-3 epithelial cells and human primary bronchial epithelial cells (PBECs) expanded from donor lung tissue from explanted lungs. Dye uptake experiment was used to evaluate the activity of Cx hemichannels in the cells.

Results

We observed an enhanced rate of dye uptake in PBECs and Calu-3 cells that were cultivated with LPS compared to respective cells cultivated without LPS. The LPS related enhancement of the rate of dye uptake was antagonised by inhibition of the TLR-4 receptors. Moreover inhibitors of Cx channels like carbenoxolone or La^{3+} inhibited the dye uptake, suggesting that dye uptake and its LPS-induced enhancement were related to the activity of Cx hemichannels. Correspondingly, Cx26 but not Cx43 specific siRNA suppressed the LPS-related enhanced rate of dye uptake. Concerning the concentration and time dependency, a significant enhancement of the rate of dye uptake was observed at a concentration of about 0.75 ng/ml after an application time of at least 3 h and achieved a maximum of more than doubling the rate of the dye uptake at about 1.25 ng/ml. Further increase of the LPS concentration did not increased the maximal rate of dye uptake, but reduced the application time necessary to achieve the maximal effect. With 100 ng/ml LPS the maximal increase was achieved after an application time of 1 h. The LPS related enhancement of dye uptake was accompanied by an increase of the resting cytosolic Ca^{2+} and was suppressed in cells preloaded with the Ca^{2+}-chelator BAPTA. Furthermore, pharmacological inhibition of the TNF-α secretion or the TNF-α receptor antagonized the LPS-related enhancement of the rate of dye uptake. Correspondingly TNF-α, like LPS, induced an enhancement of the rate of the dye uptake which was avoided by repression of Cx26 using specific siRNA. Additionally specific siRNA of the purinergic receptor P2X4 reduced the LPS related enhanced dye uptake rate.

Conclusion

The results showed that LPS, by stimulating the TLR-4 receptor, induced an enhancement of the activity of the Cx26 hemichannels in the bronchial epithelial cells, by inducing release of TNF-α in a mechanism that involved P2X4 receptors and Ca^{2+}. Since increased activity of Cx hemichannels

may increase the leakage of intracellular metabolites serving as injury signals, the data suggest a participation of Cx26 hemichannels in the induction of inflammatory reactions in the bronchial epithelium.

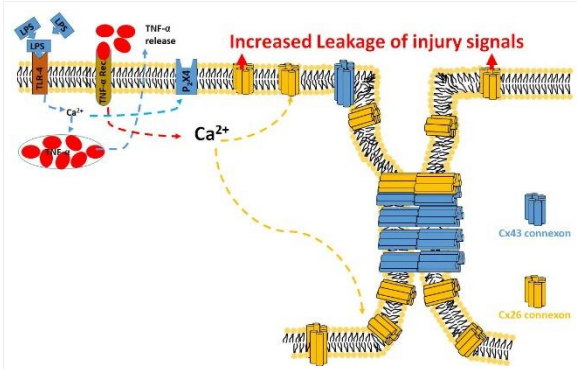

LPS induced enhancement of the activity of Cx26 hemichannels.
The binding LPS onto TLR-4 recepto is followed by an increase of the cytosolic Ca^{2+} conctration and the release of TNF-α. TNF-α binds to its receptor and induces an reinforcement of the cytosolic Ca^{2+} by a mechanism that involes P2X4 receptor. The Ca^{2+} in turn induces a remodelling of the cell-to-cell contact region, liberating threby Cx26 hemichannels in the membrane of single cells. The increased activity of Cx hemichannels in the cell membrane may lead to an increased leakage of intracellular metabolites that may act as injury signals

---

B 02-21

pHe-sensitive Store-Operated Ca^{2+} signals contribute to tumor acidic microenvironment-induced PDAC cells' selection to more aggressive phenotypes

M. Audero[1,2], K. Kondratska[1], F.A. Ruffinatti[2], L. Munaron[2], A. Fiorio Pla[1,2], N. Prevarskaya[2]
[1] *Université de Lille, PHYCELL-Laboratoire de Physiologie Cellulaire INSERM U1003, Villeneuve d'Ascq, France*
[2] *Università degli Studi di Torino, Department of Life Sciences and Systems Biology,Laboratory of Cellular and Molecular Angiogenesis, Torino, Italy*

We acknowledge the Marie Skłodowska Curie Innovative Training Network (#GA 813834 pHioniC-H2020-MSCA-ITN-2018 and PRIN-2017 "Lioness" project (#GA 754345) from Italian Ministry for Education, University and Research (MIUR) for financial support.

Introduction
Pancreatic ductal adenocarcinoma (PDAC) is a deadly disease characterized by a particular acidic microenvironment (TME), which promotes its aggressiveness[1]. Deregulated Ca^{2+}-permeable channels, such as Store-Operated Ca^{2+} channels (SOCs), regulate cancer hallmarks[2] and their pHe-sensitivity allow them to transduce TME signals to activate intracellular downstream pathways linked to PDAC progression, acting as drivers of its aggressiveness[3]. Although the roles of tumor acidosis and Ca^{2+} signaling in cancer progression are well established, the hypothesis of acidic TME employing Ca^{2+} signaling as preferential route for sustaining tumor progression has not yet been sufficiently explored. Here we evaluated how tumor acidosis modulates Ca^{2+} signals and phenotypes in two PDAC cell lines, with a particular focus on Ca^{2+} oscillations and Store-Operated Ca^{2+} entry (SOCE).
Methods
The effect of low pHe was evaluated in PANC1 and MIA PaCa-2 CT cells (pH 7.4), 4 days pHe 6.6 cells (early low pHe selection stage), 1-month pHe 6.6 cells and cells exposed for 1 month in pHe 6.6 and recovered to pHe 7.4 for 2 weeks (pHe-selected). Cell proliferation was assessed by EdU staining assay, cell adhesion by washing assay, migration and invasion by transwell system, Ca^{2+}-permeable channels expression by qPCR and Western Blot, intracellular Ca^{2+} signals by Ca^{2+} imaging. ORAI1 was selectively inhibited by Synta66 and by siRNA targeting.
Results
During the first days of selection (4 days pHe 6.6), pHe acts as a stressor factor, reducing cells' proliferation, adhesion, migration and invasion, promoting the selection of cancer cells with limited proliferation rate but enhanced invasive and migratory abilities (1-month pHe 6.6). Recovery to pHe 7.4 further boost cancer cells aggressive phenotype, also enhancing the invadopodia activity. Concerning Ca^{2+} signals, PANC1 Ca^{2+} oscillations are SOCE-dependent in all models, as ORAI1 blockade with Synta66 and siORAI1 result in impaired Ca^{2+} oscillations' initiation and maintenance. While 4 days pHe 6.6 cells show slower Ca^{2+} oscillations respect to CT and a tendency of ORAI1 SOC channel downregulation, 1-month pHe 6.6 and pHe-selected cells present a recover of faster Ca^{2+} oscillations, with overexpression of ORAI1.These data correlate with SOCE, which is decreased during early stages of selection in PANC1 cells and increased in pHe -selected cells in both cell lines. ORAI1-mediated Ca2+ entry might be involved in the increased migration and invasion of all the cell models exposed to acidic pHe, as Synta66 treatment and siORAI1 didn't affect control cells' invasion and migration.
Conclusion
Tumor acidosis promotes the selection of more aggressive PDAC cells, characterized by increased proliferation, adhesion, migration and invasion and upregulation of SOCE, required for the generation of fast Ca^{2+} oscillations which may trigger Ca^{2+}-dependent signaling pathways involved in PDAC progression.

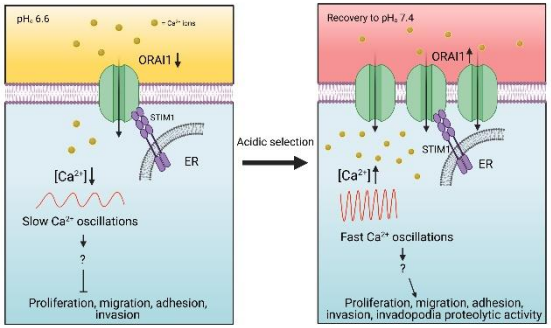

Schematic representation of the effect of acidic PDAC microenvironment on Ca2+ signals in PDAC cells Initial phase of selection is characterized by PANC1 and Mia PaCa-2 low proliferation, adhesion, migration and invasion, in which decrease of SOCE, probably due to the pH_e-induced downregulation of SOCs, promote low frequency Ca^{2+} oscillations in PANC1 cells (left). At the end of selection process and recovery to pHe 7.4, both cell lines show increase of SOCE and recover of fast Ca^{2+} oscillations in PANC1, which might induce a more aggressive cell phenotype, boosting PDAC progression (right).

References

[1] Pedersen, S. F., Novak, I., Alves, F., Schwab, A., & Pardo, L. A. (2017). Alternating pH landscapes shape epithelial cancer initiation and progression: Focus on pancreatic cancer. *BioEssays : news and reviews in molecular, cellular and developmental biology*, *39*(6), 10.1002/bies.201600253. https://doi.org/10.1002/bies.201600253

[2] Monteith, G. R., Prevarskaya, N., & Roberts-Thomson, S. J. (2017). The calcium-cancer signalling nexus. *Nature reviews. Cancer*, *17*(6), 367–380. https://doi.org/10.1038/nrc.2017.18

[3] Hofschröer, V., Najder, K., Rugi, M., Bouazzi, R., Cozzolino, M., Arcangeli, A., Panyi, G., & Schwab, A. (2021). Ion Channels Orchestrate Pancreatic Ductal Adenocarcinoma Progression and Therapy. *Frontiers in pharmacology*, *11*, 586599. https://doi.org/10.3389/fphar.2020.586599

B 02-22

mRNA transfection via chitosan-based nanocapsules restores CFTR function

V. Mete[1,2], A. K. Kolonko[1], L. Schnüttgen[1], H. Omran[2], J. Große-Onnebrink[2], W.-M. Weber[1]

[1] *University of Muenster, Department of Animal Physiology, Institute of Biology, Münster, Germany*

[2] *University Hospital Muenster, Department of General Paediatrics, Münster, Germany*

We acknowledg financial support from "Deutsche Förderungsgesellschaft zur Mukoviszidoseforschung e.V.".

Introduction

Cystic fibrosis (CF) is caused by the malfunction of the chloride channel cystic fibrosis transmembrane conductance regulator (CFTR). It is the most common genetic disorder in the Caucasian population. Decreased CFTR function leads to an imbalance in homeostasis of ion and water transport in secretory epithelia. Particularly in the lung, this defect impairs mucociliary clearance leading to the common clinical picture.

Methods

Here we tested a state-of-the-art Ussing chamber named Multi Transepithelial Current Clamp (MTECC) for its suitability to record changes in conductance via CFTR. Primary cell samples were collected by nasal brushings. The epithelial cells were cultured at an air-liquid interface and CFTR activity was evaluated after cAMP application.

Results

This culturing system proved to be resilient enough for multiple measurements of the same material. Transmembrane resistance reminded constant over three month. In a first attempt CF cell were transfected with wtCFTR-mRNA via the commercially available Lipofectamine™. No significant improvement of the CFTR activation was recorded in the MTECC Ussing chamber. However, when chitosan-based nanocapsules were used to introduce the nucleic acid to the cells cAMP-induced activity of CFTR measured as transepithelial conductance was drastically improved (from -0,03 ± 0,26 to 0,93 ± 0,45 mS/cm^2). The effect could be observed over a period of more than 48 h after transfection ($p \leq 0.0001$).

Conclusion

These results distinguish the chitosan-based nanocapsules as a new and more efficient way for mRNA transfections. A future use in drug delivery seems very feasible.

B 02-23

Role of TMEM16J in chronic kidney disease

K. Talbi, **R. Schreiber**, J. Ousingsawat, K. Kunzelmann

Universität Regensburg, Physiology department, Regensburg, Germany

TMEM16J is a member of the TMEM16 family and acts as a putative calcium-activated ion channel or phospholipid scramblase. TMEM16J is expressed predominantly in intracellular membranes and less in the plasma membrane. As shown before SIGIRR (single immunoglobulin IL-1 related receptor), PKP3 (plakophilin 3), and TMEM16J control immune response and the extend of inflammation. Variants of SIGIRR/PKP3/TMEM16AJ lead to severe inflammatory diseases such as pneumonia, enterocolitis and kidney graft rejection. Meta-analysis of genome-wide association studies identified TMEM16J-T604A as a strong promotor for chronic kidney disease (CKD), but the disease mechanism and function of TMEM16J remains unknown. In kidneys of CKD patients

TMEM16J is not only expressed in tubular epithelial cells but also in infiltrated CD45 positive immune cells and in activated fibroblast which are positive for smooth muscle actin. Immunocytological staining and measurements of intracellular calcium concentration demonstrate TMEM16J as calcium-activated calcium permeable leak channel in the endoplasmic reticulum (ER). TMEM16J controls intracellular distribution of calcium, receptor mediated intracellular Ca^{2+} signals and transcription of pro inflammatory cytokines. Renal epithelial cells that express the variant TMEM16J-T604A show enhanced calcium signals and interleukin release. Whole cell patch clamp recordings in HEK293T cells expressing plasma membrane targeted TMEM16J T604A CAAX show no current activation by ATP compared to the wtTMEM16J suggesting impaired ATP induced conductance for chloride by the amino acid exchange T604A. This study identifies TMEM16J as a major regulator of intracellular Ca^{2+} signaling, ion channel activity and inflammation, and suggests a pronounced impact of TMEM16J in the immune response in CKD.

B 02-24

Identification of K_{Ca}3.1 channels in mitochondria of non-small lung cancer cells.

E. Bulk[1], L.M. Todesca[1], M. Bachmann[2], I. Szabo[2], M. Rieke[1], A. Schwab[1]
[1] *University of Muenster, Physiological Institute II, Muenster, Germany*
[2] *University of Padova, Padua, Italy, Department of Biology, Padua, Italy*

Introduction
Non-small cell lung cancer (NSCLC) is one of the leading causes of cancer-related deaths worldwide. Recently, we identified the Ca^{2+}-activated potassium channel K_{Ca}3.1 that contributes to the progression of NSCLC. As some other ion channels, K_{Ca}3.1 channels were also found in the inner membrane of mitochondria in different cancer cells as melanoma, glioblastoma or pancreatic ductal adenocarnoma (PDAC). Here, we investigated whether K_{Ca}3.1 channels are functionally expressed in mitochondria of NSCLC cells and if so, whether pharmacological inhibition of K_{Ca}3.1 impacts the mitochondrial function in those cells.
Methods
To detect K_{Ca}3.1 expression in mitochondria western blot and immunoflurescence experiments were performed. The mitochondrial function was investigated with mitochondrial membrane potential measurements using the cationic fluorescent dye Tetramethylrhodamine Methyl Ester (TMRM). The release of reactive oxygene species (ROS) was verified by using the mitochondrial superoxide indicator MitoSOX™ Red.
Results
Via Western blotting, we detected K_{Ca}3.1 expression in lysates of isolated mitochondria from different NSCLC cells. Using immunofluorescence, a co-localization of K_{Ca}3.1 channels with mitochondria of NSCLC cancer cells was found. Pharmacological inhibition of K_{Ca}3.1 using senicapoc results in a hyperpolarization of the mitochondrial membrane potential in NSCLC cells. This hyperpolarization is accompanied by an increase in the generation of reactive oxygene species (ROS) in NSCLC cells exposed to senicapoc or its analog TRAM-34.
Conclusion
Our results give clear evidence for the functional expression of K_{Ca}3.1 channels in mitochondria of NSCLC cells.

B 02-25

Sexual dimorphism and role of the cGAS-STING pathway in the progression of diabetic kidney disease

S. Khedr[3], O. Palygin[4], **A. Staruschenko**[1,2]
[1] *University of South Florida, Molecular Pharmacology and Physiology, Tampa, USA*
[2] *James A. Haley Veterans' Hospital, Tampa, USA*
[3] *Ain Shams University, Physiology, Faculty of Medicine, Cairo, Egypt*
[4] *Medical University of South Carolina, Medicine, Charleston, USA*

National Institutes of Health grants R35 HL135749 and Department of Veterans Affairs grant I01 BX004024. We also thank Drs. Romica Kerketta, Angela Mathison, and Raul Urrutia from MCW Mellowes Center for Genomic Sciences and Precision Medicine for help with RNA-Seq analysis.

Introduction
Diabetic kidney disease (DKD) is the leading cause of chronic renal pathology. Understanding the molecular underpinnings of DKD is critical to designing tailored therapeutic approaches. We have demonstrated previously that T2DN rats develop renal and physiological abnormalities similar to clinical observations in humans with DKD, indicating these rats are an excellent model for studying the progression of renal injury in type 2 DKD (Palygin et al., 2019). Furthermore, our recent studies revealed sexual dimorphism in this model, indicating that while both male and female T2DN rats developed non-obese DKD phenotype, females had significant protection from the development of severe forms of glomerular and tubular damage (Spires et al., 2021). Here we focused on sex differences in DKD and the contribution of aging to the progression of DKD.
Methods
To explore the sexual dimorphisms in the development of DKD, we utilized young (12-week-old) and aged (>48 weeks old) type 2 diabetic nephropathy (T2DN) rats. All animal use and welfare adhered to the NIH Guide for the Care and Use of Laboratory Animals. To delineate transcriptional changes, RNA-Seq analysis was performed in the kidney cortex of T2DN rats of both sexes at a younger and older age. Western blotting, immunohistochemistry, and flow cytometry analyses were further used to identify specific pathways contributing to sexual dimorphism in T2DN rats.
Results
We have revealed that the cyclic GMP-AMP synthase (cGAS) / Stimulator of interferon genes (STING) signaling pathway is upregulated in T2DN rats compared to non-diabetic Wistar rats and in type 2 diabetic human kidneys. The expression of key proteins in the cGAS-STING pathway was significantly different between male and female T2DN rats and following the progression of DKD. Proinflammatory genes were also upregulated in male T2DN rats compared to female rats of the same age, and their levels were further elevated in aged rats. The transcriptional analysis revealed a number of critical molecules including genes in the cGAS-STING pathway.
Conclusion
Our study provides critical insights into the sexual dimorphism and progression of DKD and identifies the cGAS-STING pathway as an essential contributor to disease development.

References
[1] PALYGIN, O., SPIRES, D., LEVCHENKO, V., BOHOVYK, R., FEDORIUK, M., KLEMENS, C. A., SYKES, O., BUKOWY, J. D., COWLEY, A. W., JR., LAZAR, J., ILATOVSKAYA, D. V. & STARUSCHENKO, A. 2019. Progression of diabetic kidney disease in T2DN rats. *Am J Physiol Renal Physiol,* 317, F1450-F1461.

[2] SPIRES, D. R., PALYGIN, O., LEVCHENKO, V., ISAEVA, E., KLEMENS, C. A., KHEDR, S., NIKOLAIENKO, O., KRIEGEL, A., CHENG, X., YEO, J. Y., JOE, B. & STARUSCHENKO, A. 2021. Sexual dimorphism in the progression of type 2 diabetic kidney disease in T2DN rats. *Physiol Genomics,* 53, 223-234.

B 02-26

Negative charges in the S2-S3 linker are involved in voltage-dependent gating of HCN channels

I. Saß, C. Sattler, K. Benndorf, J. Kusch

University Hospital Jena, Friedrich Schiller University Jena, Institute for Physiology II, Jena, Germany

Hyperpolarization-activated cyclic nucleotide-modulated (HCN) channels are key regulators of rhythmic electrical activity in the nervous system and heart. Channel opening requires membrane hyperpolarization and is further enhanced by the binding of intracellular cyclic nucleotides.
Each channel is formed by four subunits as a homo- or heterotetramer. The subunits comprise defined structural domains: An intracellular HCN domain in the N-terminal region, followed by the membrane-spanning voltage-sensing domain (VSD, including helices S1 to S4), and the pore-domain including helices S5 and S6. The helical C-linker domain connects the S6 helix to the cyclic nucleotide-binding domain.
The HCN domain is in close contact with the C-linker of the opposite subunit and is thought to play a crucial role in integrating voltage- and ligand-dependent gating mechanisms. A flexible region connecting helices S2 and S3 is positioned in close proximity. This S2-S3 linker includes a series of highly conserved negative charges, that are not fully resolved in the available cryo-EM structures of hHCN1 (Lee and MacKinnon, 2017). Recent structures of the cAMP-bound and unbound rabbit HCN4 channel show the S2-S3-linker positioned near the end of the main voltage-sensing helix S4 (Saponaro et al., 2021).
The combination of the conserved negative charges and the structural proximity to the contact site of the HCN domain and opposite subunit C-linker as well as to the S4-helix, suggests a role of these negative charges in voltage-dependent activation.
To study the effects of both charge neutralization and reversion at positions E243, D244 and E247 of the S2-S3 linker, mutated mHCN2 channels were heterologously expressed in *X. laevis* oocytes and characterized by electrophysiological methods. The constructs showed a systematic shift of voltage-dependent activation towards hyperpolarizing potentials, which was essentially more pronounced in cAMP-free than in cAMP-saturating conditions. Furthermore, a reduction of the apparent gating charge was observed in all charge reversal mutants.
Considering these results, the loss of negative charges inside the S2-S3 linker seems to further stabilize the autoinhibited state of the unliganded mutant channels, shifting channel opening to very low hyperpolarized potentials. At the same time, cAMP binding is able to fully relieve autoinhibition and re-establish wildtype-like gating behaviour.
Our data contribute to a better understanding of the complex gating behaviour of HCN pacemaker channels.

References

[1] Lee, C. H., and MacKinnon, R. 2017, 'Structures of the Human HCN1 Hyperpolarization-Activated Channel', *Cell*, 168(1-2), 111–120.e11

[2] Saponaro, A., Bauer, D., Giese, M. H., ..., Thiel, G., Santoro, B., Moroni, A. 2021, 'Gating movements and ion permeation in HCN4 pacemaker channels', *Molecular Cell,* 81(14), 2929–2943.e6

B 02-27

Role of the calcium-activated K^+ channel $K_{Ca}3.1$ in the progression of pancreatic ductal adenocarcinoma

B. Soret[1,3], Z. Pethö[3], V. Lehen'kyi[1,2], A. Schwab[3]

[1] *University of Lille, Laboratory of Cell Physiology, Department of Biology, Villeneuve d'Ascq, France*
[2] *INSERM U1003, PHYCELL-Laboratoire de Physiologie Cellulaire, Villeneuve d'Ascq, France*
[3] *University of Münster, Institut für Physiologie II, Münster, Germany*

Introduction

Pancreatic ductal adenocarcinoma (PDAC) is the fourth most frequent cause of cancer-related deaths in Western countries. The molecular mechanisms that give rise to PDAC are far from being clear and have not yet delivered targeted therapies. PDAC is linked to the physiology and microenvironment of the exocrine pancreas. Ca^{2+} signals are emerging to be particularly relevant in cancer. The cellular "Ca^{2+} toolkit" includes ion channels that indirectly affect Ca^{2+} signaling such as the Ca^{2+}-dependent K^+ channel $K_{Ca}3.1$. In PDAC, its elevated expression indicates a poor prognosis. While there is already some *in vitro* information on the role of $K_{Ca}3.1$ channels on individual cell types of the PDAC cancer tissue, its role is still poorly characterized, and *in vivo* data are missing. The current project is aimed at reducing this gap of knowledge.

Methods

In vivo experiments were performed by using $^{KrasLSL-G12D/+}Trp53^{fl/fl}Pdx1^{Cre/+}$ (KPfC) mice, a PDAC model. They were treated at the age of 20 weeks for four weeks with vehicle, the standard treatment gemcitabine, the $K_{Ca}3.1$ inhibitor TRAM-34 or a combination of gemcitabine and TRAM-34. Pancreas weights, volumes and metastatic status were determined. Tissue samples were stained (sirius red, hematoxylin/eosin) and analyzed in order to assess the extent of fibrosis, the size of the tumors as well as the infiltration of immune cells into the tumor tissue. Western blot analysis of protein lysates from tumor samples complemented the analysis. The therapeutic potential of $K_{Ca}3.1$ channels and the impact of the channel on migration/invasion was assessed in spheroids model of PDAC composed of pancreatic tumor cells and pancreatic stellate cells.

Results

While there are no significant differences between control mice and TRAM-34 treated mice, the inhibition of the $K_{Ca}3.1$ channels in combination with gemcitabine leads to a moderate decrease in tumor size and an increase in the extent of fibrosis in tumors. This change of fibrosis is similar to the one observed in mice treated with only gemcitabine. These results could be explained by a combined effect of the two treatments leading to a change in cell type within the tumor tissue towards a more fibroblastic phenotype. This could cause a decreased expression of $K_{Ca}3.1$ and thus an inhibition of tumor growth. In mixed spheroids containing pancreatic cancer cells and pancreatic stellate cells treatment with TRAM-34 increases the invasive potential of the cells. This is not observed in the combination treatment, gemcitabine seemingly negating this anomalous effect of TRAM-34.

Conclusion

Collectively these results point to a function of $K_{Ca}3.1$ channels in complex tumor models that goes beyond the well described roles of the channels in individual cells types from the tumor microenvironment.

B 02-28

Pharmacology and Gating Properties of „silent“ TWIK K2P Channels

M. Musinszki, S. Cordeiro, T. Baukrowitz

Christian-Albrechts-University Kiel, Institute of Physiology, Kiel, Germany

Two-Pore Domain Potassium (K2P) channels are regulators of cellular excitability and involved in diverse physiological processes like sleep, secretion, and pain. They are modulated by diverse intra- and extracellular stimuli as temperature and pH and respond to cellular signaling lipids and phosphorylation. K2P channels comprise 15 members in 6 subfamilies, most of which can be characterized by electrophysiological methods. However, the TWIK channel subfamily is poorly understood because they lack functional expression in heterologous systems.

It has been proposed that TWIK-1 acts as regulatory subunit that controls the activity of heterodimeric K2P channels at the plasma membrane, and TWIK-2 has been found in lysosomes and in macrophages, where it is involved in inflammasome activation.

If the selectivity filter comprises the gate in TWIK channels is still under discussion. In contrast to most other K2P channels, TWIK channels are not activated by depolarization in the physiological range and it has been considered that their particularly small open probability is related to selectivity filter instability (1). A cryo-EM study proposed a closure of the ion permeation pathway by rearrangement of the extracellular domain, but also a collapse of the selectivity filter (2). Further, MD simulations suggested a hydrophobic barrier in the pore of TWIK-1 that impairs ion permeation (3), implying that these channels may not be gated at the selectivity filter.

To gain insight into the regulation properties and gating mechanisms of TWIK channels, we investigated wildtype and mutant channels in cultured HEK293 cells and *Xenopus* oocytes by pharmacological means. TWIK channel mutants in which a retrieval motif was removed were used to increase plasma membrane expression. To further enhance current amplitudes, we utilized the activation of currents by intracellular as well as extracellular Rb^+ ions that is known for TWIK-1 channels and we corroborate this activation also for the TWIK-2 channel.

We first applied several known K2P channel activators and inhibitors and found that TWIK-1 and TWIK-2 channels share a common pharmacology. They are also sensitive to cellular signaling lipids and established pharmacological modulators of components of G-protein coupled receptor pathways, e.g. PLC and PKA/PKC.

We then determined the mechanism of action of several inhibitors by TPA competition assays and found that TWIK channels are inhibited by substances acting consistent with a pore blocking mechanism, e.g. BL-1249, as well as allosteric inhibitors, i.e. 2-APB.

Interestingly, inhibition of TWIK channels by TPA, 2-APB, BL-1249 and the DAG analogue DiC8 was strongly reduced in a mutant which disrupts the hydrophobic barrier, irrespective of their mechanism of action. Therefore, these hydrophobic barrier residues located in TM2 and TM4 may be critically involved in transduction of allosteric stimuli to the selectivity filter gate of TWIK channels.

References

[1] Nematian-Ardestani, E., Abd-Wahab, F., Chatelain, F.C., Sun, H., Schewe, M., Baukrowitz, T., Tucker, S.J., 2020. Selectivity filter instability dominates the low intrinsic activity of the TWIK-1 K2P K+ channel. J. Biol. Chem. 295, 610–618. https://doi.org/10.1074/jbc.RA119.010612

[2] Turney, T.S., Li, V., Brohawn, S.G., 2021. Structural Basis for pH-Gating of the K+ Channel TWIK1 at the Selectivity Filter 2021.11.09.467928. https://doi.org/10.1101/2021.11.09.467928

[3] Aryal, P., Abd-Wahab, F., Bucci, G., Sansom, M.S.P., Tucker, S.J., 2014. A hydrophobic barrier deep within the inner pore of the TWIK-1 K2P potassium channel. Nature Communications 5, 1–9. https://doi.org/10.1038/ncomms5377

B 02-29

Knockout of Renal BPGM Leads to Acute Kidney Injury.

V. A. Kulow[1], K. Rögner[2], R. Labes[2], P. B. Persson[2], C. Rosenberger[1], M. Fähling[2]

[1] *Charité – Universitätsmedizin Berlin, corporate member of Freie Universität Berlin and Humboldt-Universität zu Berlin, Medizinische Klinik m.S. Nephrologie und Internistische Intensivmedizin, Berlin, Germany*

[2] *Charité – Universitätsmedizin Berlin, corporate member of Freie Universität Berlin and Humboldt-Universität zu Berlin, Institut für Translationale Physiologie, Berlin, Germany*

Introduction

In erythrocytes, 2,3-bisphosphoglycerate mutase (BPGM) produces 2,3-bisphosphoglycerate (2,3-BPG) which decreases oxygen binding to hemoglobin, and hence, improves oxygen delivery to tissues. We have recently shown that BPGM is constitutively expressed in the kidney, mainly in the distal nephron, and up-regulated upon acute kidney injury (AKI). Here we search for a potential role of kidney BPGM with help of an inducible, nephron-specific BPGM knockout in mice.

Methods

In adult mice, nephron specific *Bpgm* knockout (Pax8CreBPGM$^{fl/fl}$) was induced with help of a single dose of doxycycline, and kidneys were harvested 4 d later. The extent of kidney injury was assessed by serum creatinine, routine histology and molecular markers (qPCR, immunofluorescence): KIM-1, NGAL. Immunofluorescent double staining with Megalin, vimentin, Ki-67, CD-3 (T-cells), Ly-6G (neutrophils) and F4/80 (macrophages) served to assign injury to nephron segments and to assess tissue responses, respectively.

Results

BPGM knockout per se led to AKI, as demonstrated by an increase in serum creatinine and proximal tubular injury, evident both on routine histology and by increased KIM-1 and NGAL expression. In the proximal tubule, segments with overt injury alternated with apparently normal portions. Two mutually exclusive types of injury were detected: first, a more subtle injury within the S1 segment, with preserved routine histology and brush border Megalin, but NGAL positivity; second, a more severe injury within the S3 segment, with disruption of tubular architecture on routine histology, loss of brush border Megalin and KIM-1 positivity. In the latter, tubular cells also exhibited vimentin and Ki-67, suggesting proliferation and epithelial to mesenchymal trans-differentiation. Moreover, KIM-1 positive tubules were surrounded by F4/80 positive macrophages.

Conclusion
BPGM, constitutively expressed in the distal nephron, appears to sustain proximal nephron well-being, since a BPGM deficit in distal tubules rapidly leads to remote injury to proximal tubules. The mechanisms responsible for such inter-tubular crosstalk remain elusive.

B 02-30

Involvement of potassium channels in alveolar cells response to oxidative stress

R. Canella[1], M. Benedusi[1], A. Vallese[2], G. Valacchi[3,2]
[1] *University of Ferrara, Department of Neuroscience and Rehabilitation, Ferrara, Italy*
[2] *University of Ferrara, Department of Environmental Sciences and Prevention, Ferrara, Italy*
[3] *North Carolina State University, Department of Animal Science, Kannapolis, USA*
[4] *Kyung Hee University, Department of Food and Nutrition, Seoul, South Korea*

Introduction
The lung tissue is one of the main targets of oxidative stress due to external pollutants and respiratory activity. Biological and electrophysiological techniques were applied to study the action of ozone, one of the most noxious pollutants present in the troposphere, on K currents in A549 cells, which simulates the first barrier encountered by oxidants **(1)**.
Exposure of human lung epithelial cells to ozone alters cell membrane currents inducing its decrease with respect to the control, when the cell undergoes to a voltage-clamp protocol ranging from -90 to +70mV. The membrane potential of these cells is mainly maintained by the interplay of potassium and chloride currents. Our previous studies indicated an increase of chloride current by oxidative stress due to ORCC channels activation **(2)**.
In this study our aim wastounderstand the role of potassium current during oxidative stress and try to identify which potassium channel is mainly related to the effect of O_3, addressing our analyses first to BK channel an ubiquitarian K channel characterized by big conductance (up to 300pS) **(3)**.
Methods
The A549 cells were cultured in DMEM and kept in an incubator at 37° degrees temperature with 95% air and 5% CO2.
The cells were exposed to 0.1 ppm ozone for 30 minutes and were analyzed by patch clamp technique immediately after exposure.
Western blot analysis was applied to quantify the BK channel before and after ozone treatment.
Patch clamp technique in whole cell configuration was applied to measure membrane current.
Results
After measuring the total membrane current using an intracellular solution containing or not potassium ions, we obtained the contribution of potassium to the overall membrane current in control condition by a mathematical approach. In similar experimental conditions after ozone treatment, we observed a significant decrease of IK with respect to the control.
By Western blot analysis before and after ozone exposure we observed a decrease of the BK channel after ozone treatment that was recovered in about one hour. Adding Iberiotoxin (IbTx), a specific inhibitor of BK channel, to the bath we also verified the functionality of BK channels in control condition.
On the contrary, administrating of 4-Aminopyridine (an inhibitor of voltage dependent K channels but not BK channels) before and after ozone treatment the decrease of the total current is almost equal to that observed in control condition. This last finding is a strong indication that BK channel is the target of oxidative stress.

Conclusion
We suggest that ozone inhibits potassium current and that the main involved channel could be BK. We need further studies to clarify its role and its interplay with the other membrane channels under oxidative stress conditions. These findings can contribute to identify the biomolecular pathway induced by ozone allowing a possible pharmacological intervention against oxidative stress in alveolar tissue.

References

[1] Arbex MA, Santos UP, Martins LC, Saldiva PHN, Pereira LAA, Braga ALF, 2012, Air pollution and the respiratory system. *J Bras Pneumol* 38: 643–655, . doi:10.1590/S1806-37132012000500015.
[2] Canella, R., Benedusi, M., Martini, M., Guiotto, A., Cervellati, F., & Valacchi, G, 2021, The role of pulmonary ORCC and CLC-2 channels in the response to oxidative stress. Molecular & Cellular Toxicology, 1-10.
[3] Hermann A, Sitdikova GF, Weiger TM, 2015, Oxidative Stress and Maxi Calcium-Activated Potassium (BK) Channels. Biomolecules, 5(3):1870-91 doi: 10.3390/biom5031870.

B 02-31

The Na^+/H^+ exchanger NHE3 inhibitor tenapanor prevents intestinal obstructions in CFTR-deleted mice

X. Tan, A. Kini, D. Römermann, U. Seidler
Hannover Medical School, Department of Gastroenterology, Hannover, Germany

We acknowledge the help of all members of the institute for animal research of the Hannover Medical School.
This project was funded by Cystic Fibrosis Trust SRC 011 and the Deutsche Forschungsgemeinschaft grants Se460/19-1 and For5046 Se460/22-1.

Introduction
Mutations in the CFTR chloride channel result in meconium ileus in newborns and distal intestinal obstructive episodes (DIOS) in adults and in CFTR null (*cftr*$^{-/-}$) animal models. This study aims to explore the effect of tenapanor, a gut selective NHE3 inhibitor, on reducing the frequency of obstructive episodes in the *cftr*$^{-/-}$ mice, and study the underlying molecular mechanisms.
Methods
Age (9-13 weeks old) and sex matched *cftr*$^{+/+}$ and *cftr*$^{-/-}$(FVB/N-CFTRtm1CAM) mice were intragastrically gavaged with tenapanor (30mg/kg) or vehicle, twice daily for a period of 21 days. Body weight and stool water content was assessed daily while gastrointestinal transit time (GTT) was measured weekly once. Stool pH was assessed pre and 3 hours post gavage with tenapanor. The mice were either euthanized with a suspected intestinal obstruction, or after 21 days. The intestinal tissues were collected for further analysis including RT-PCR, histology and immunohistochemistry.
Results
While tenapanor did not result in an overall decrease in body weight, it resulted in a significant and consistent increase in stool water content in the *cftr*$^{-/-}$mice, compared to the vehicle group (vehicle- n ≥ 7/timepoint, tenapanor- n ≥11/timepoint; Day 21- vehicle: 58.757 ± 2.201 vs tenapanor: 72.514

± 1.577%, t-test, p<0.0001). A significant increase in stool alkalinity was observed in the *cftr*$^{-/-}$ mice 3 hours post tenapanor gavage (n=5 pairs, pH 6.517±0.117 vs 7.266±0.120, t-test, p<0.05). Overall, tenapanor treatment resulted in a significant decrease in GTT in the *cftr*$^{-/-}$ mice (vehicle- n ≥ 7/timepoint, tenapanor- n ≥ 9/timepoint; t-test, p<0.05). Importantly, tenapanor significantly reduced obstructive episodes to 8% (1/12 mice) compared to observed 46% (6/13 mice) in vehicle treated *cftr*$^{-/-}$mice and resulted in a considerable decrease in cryptal hyper-proliferation (vehicle unobstructed: n=7, tenapanor unobstructed: n=11; t test, p<0.005) and mucus accumulation (n=5 pairs, t-test, p<0.05) in the ileum and proximal colon. Tenapanor also prevented mucosal inflammation, as evidenced by lack of neutrophil infiltration and cytokine elevation in comparison to control tissue. In contrast, mucosal inflammation was obvious in obstructed intestine in the intestinal segments that contained the accumulated fecal material (vehicle/tenapanor unobstructed: n≥ 5, vehicle obstructed: n=5; t-test, p<0.05).

Conclusion

3 week oral tenapanor application increased stool water content and alkalinity, normalized gastrointestinal transit time, and reduced obstructive episodes. It also reversed crypt-villus elongation, reduced mucus accumulation and prevented intestinal inflammation. These findings suggest that tenapanor could be a safe and affordable adjunctive therapy for cystic fibrosis patients to alleviate constipation and prevent recurrent DIOS.

B 02-32

Transcriptional profiling of transport mechanisms and regulatory pathways in rat choroid plexus

S. N. Andreassen[1], T. L. Toft-Bertelsen[1], J. H. Wardman[1], R. Villadsen[2], N. MacAulay[1]

[1] *University of Copenhagen, Faculty of Health Sciences, Department of Neuroscience, Copenhagen, Denmark*

[2] *University of Copenhagen, Faculty of Health Sciences, Department of Cellular and Molecular Medicine, Copenhagen, Denmark*

We are grateful for the technical assistance from Trine Lind Devantier and Dagne Barbuskaite and for the valuable input on transcriptomics from Tune H Pers, Novo Nordic Center for Basic Metabolic Research, University of Copenhagen.

Introduction

Dysregulation of brain fluid homeostasis associates with brain pathologies in which fluid accumulation leads to elevated intracranial pressure. Surgical intervention remains standard care, since specific and efficient pharmacological treatment options are limited for pathologies with disturbed brain fluid homeostasis. Such lack of therapeutic targets originates, in part, from the incomplete map of the molecular mechanisms underlying cerebrospinal fluid (CSF) secretion by the choroid plexus.

Methods

The transcriptomic profile of 9-week-old Sprague Dawley rat choroid plexus was generated by RNA Sequencing (RNAseq) of whole tissue and epithelial cells captured by fluorescence-activated cell sorting (FACS), and compared to proximal tubules. The bioinformatic analysis comprised mapping to reference genome followed by filtering for type, location, and association with alias and protein function. The transporters and associated regulatory modules were arranged in discovery tables according to their transcriptional abundance and tied together in association network analysis.

Results

The transcriptomic profile of choroid plexus displays high similarity between sex and species (human, rat, and mouse) and lesser similarity to another high-capacity fluid-transporting epithelium, the proximal tubules. The discovery tables provide lists of transport mechanisms that could participate in CSF secretion and suggest regulatory candidates.

Conclusion

With quantification of the transport protein transcript abundance in choroid plexus and their potentially linked regulatory modules, we envision a molecular tool to devise rational hypotheses regarding future delineation of choroidal transport proteins involved in CSF secretion and their regulation. Our vision is to obtain future pharmaceutical targets towards modulation of CSF production in pathologies involving disturbed brain water dynamics.

B 02-33

Renal NADPH oxidase 4 maintains systemic redox homeostasis by controlling sulphur amino acids metabolism

F. Rezende[1], L. Hannibal[2], R.P. Brandes[1]

[1] *Goethe University Frankfurt, Institute for Cardiovascular Physiology, 60590, Germany*

[2] *University of Freiburg, Freiburg, Germany*

The NADPH oxidase 4 (Nox4) produces H_2O_2 and is highly expressed in the kidney. Its expression is reduced in diabetic and chronic renal disease, suggesting its role in normal renal function which is still unknown and was studied here. In situ hybridization (RNAscope) combined with immunofluorescence showed that Nox4 is selectively expressed in the proximal tubule, a part of the kidney responsible for mass transport. To study this function, WT (wild type) and Nox4-/- (tamoxifen-inducible, global Nox4 knockout mice) were put on protein-free diet, with low sodium (130 mg/kg chow) and low micronutrients. Urine samples (day 0, 3, 14), renal cortex and plasma (day 14) were analyzed by global untargeted LC/MS for metabolites. Genome scale metabolic reconstruction using fastcore showed a significant downregulation of extracellular and mitochondrial transport; metabolism of nucleotides, inositol phosphate and folate in response to the deletion of Nox4. Importantly, Sulphur metabolites (cystine, cysteine and homocysteine) were reduced in Nox4-/- mice as compared to WT. Moreover, human single nucleotide polymorphisms (SNPs) in Nox4 gene reduced cystine and homocysteine. The results indicate that the physiological function of Nox4 in the kidney is to control reabsorption and metabolism of sulphur amino acids and folate which are important for redox homeostasis.

B 02-34

The Ubiquitin C-Terminal Hydrolase L1 (UCH-L1) in THSD7A-associated membranous nephropathy

S. Frömbling, D. Loreth, J. Brand, C. Meyer-Schwesinger
University Medical Center Hamburg-Eppendorf, Institute for Cellular and Integrative Physiology, Hamburg, Germany

Introduction

Membranous nephropathy (MN) is an autoimmune disease, induced by autoantibodies directed against the podocyte foot process antigens PLA_2R1 or THSD7A. Following autoantibody binding, podocyte proteostasis is challenged by oxidative stress and by a dysregulation of degradation systems. The deubiquitinating enzyme UCH-L1 is one of the highest upregulated proteins of the ubiquitin proteasome system (UPS) in MN. Its main role is the stabilization of the intracellular monoubiquitin pool. Additionally, to PLA_2R1 and THSD7A, autoantibodies against UCH-L1 are found in sera of MN patients, which show preferential reactivity to dysfunctional (oxidative modified) UCH-L1. The aim of this study is to analyze the functional integrity and turnover of UCH-L1 in an *in vitro* THSD7A MN model, to display a possible route of autoantibody formation against this intracellular protein and to assess, whether autoantibodies to UCH-L1 have a pathophysiological significance in MN.

Methods

To measure the expression and enzymatic activity of UCH-L1, THSD7A overexpressing human podocytes were treated with rabbit anti-THSD7A-antibodies (abs) or control abs for 0, 1, 6, 24, 48 hours. To analyze the turnover of UCH-L1, degradation systems were additionally inhibited *via* Bafilomycin A1 (autophagosomal-lysosomal inhibitor) or epoxomicin (proteasomal inhibitor). The localization of UCH-L1 in aggregates was assessed by super-resolution microscopy.

Results

Treatment of human podocytes with THSD7A-abs induces a slight increase in UCH-L1 protein abundance and activity and UCH-L1 localizes to THSD7A aggregates. UCH-L1 is highly abundant in podocyte-derived microvesicles isolated from the cell culture medium. Inhibition of protein degradation systems, especially of the lysosomal system leads to higher levels of active UCH-L1 protein.

Conclusion

UCH-L1 activity is altered in THSD7A MN, especially when protein degrading systems are additionally disrupted. Further, UCH-L1 is abundant in podocyte-derived microvesicles.

B 02-35

Hypoxia inducible factors during the onset of colitis: an *in vitro* analysis

K. Herbrich, L. Deckers, J. Schiefer, C. Padberg, J. Fandrey, **S. Winning**
University of Duisburg-Essen, Institute of Physiology, Essen, Germany

Introduction

Inflammatory bowel diseases such as Morbus Crohn or Colitis Ulcerosa affect more than 400.000 people in Germany – with steadily increasing numbers of initial diagnoses each year, which highlights the urgent need for a better understanding of the onset of these diseases.

The colon is special with regard to the organ oxygenation as it exhibits physiologically hypoxic epithelial tips in its mucosa. Disruption of the epithelial layer initiates a spreading of the hypoxic areas towards deeper layers and leads to the stabilization and activation of hypoxia inducible factors (HIFs). The experimental onset of murine colitis includes (amongst others) models that administrate chemical substances such as i) dextran sodium sulfate (DSS), which directly destroys the epithelial cell integrity, or ii) TNBS (2,4,6-Trinitrobenzenesulfonic acid), which is known to induce immunogenic reactions in the colon wall, most likely induced by $CD4^+$ T cells.

Methods

Only little is known so far about the interplay of innate immune cells such as macrophages and dendritic cells and colon epithelial cells during the onset of colitis although these cells are in the first line of immunological defense. Thus, we elucidated the effects of DSS and TNBS on colon epithelial cells (murine MC38 cell line) and innate immune cells (murine bone marrow derived dendritic cells and macrophages with and without *Hif1a knockout*; human THP-1 cell line) under normoxic and hypoxic conditions. The cells were either treated with DSS and TNBS directly or they received the medium of the treated respective other cell type. We then analyzed the HIF1α protein expression and the expression of *Hif1a* mRNA and HIF1 target genes. In addition, we analyzed the partial oxygen pressure in these cultures and the viability of the cells. Finally, we examined the cellular localization of the NF-κB subunit p65 within dendritic cells.

Results

Whereas DSS did not affect the expression of HIFs and HIF target genes in any of the cell lines, TNBS reduced the HIF-1α protein and mRNA expression significantly in all examined cells in a dose dependent manner. This reduction was accompanied by a diminished nuclear abundancy of the nuclear factor (NF)-κB subunit p65, a known regulator of *Hif1a/HIF1A* mRNA expression under conserved cellular viability.

Conclusion

An activation of HIF-1 in colon epithelial cells has been shown to increase the epithelial barrier integrity in murine models of colitis. These findings might therefore extend the current knowledge about the mechanism how TNBS favors the onset of acute colitis by the reduction of intestinal barrier integrity and altered immune cell functions due to a loss of HIF-1 activity.

B 02-36

Cashew seed supplemented in diet exacerbates experimental gastrointestinal dysmotility in male Wistar rats

O. A. Odukanmi, A. A. Aderibigbe, A. J. Adeagbo, S. B. Olaleye
University of Ibadan, Department of Physiology, Ibadan, Nigeria

Introduction

Many parts of the cashew plant have been reported for its anti-motility effect on the gastrointestinal tract, but the possibility of the inherent anti-motility property is not yet researched in the cashew seed. This study investigates the possible effect of cashew seed diet supplementation (CSDS) on intestinal motility and secretion in experimentally induced gastrointestinal dysmotility in male Wistar rats.

Methods

Four experiments were carried out using male Wistar rats which were randomly separated into 4 (n=5 rats/ group/experiment) groups- Control, 6% CSDS, 12 % CSDS, and Loperamide/Atropine group, depending on the experiment. The CSDS feeding was initiated 4 weeks before the start of the procedures. The control and Loperamide/Atropine groups had normal rat feed throughout. Experiment 1 assessed intestinal transit with a charcoal meal, and experiments 2 and 3 assessed enteropooling and diarrhea which was induced using 2 ml castor oil per rat. Colonic

motility was determined using the bead load test. Colon tissue was excised for histology and stained with hematoxylin and eosin. Colon histomorphometry was assessed with Motic Images Plus 2.0 ML. All the animals were given an overdose of ketamine (200 mg/kg, ip) to terminate the experiment and collect tissues and data for the protocol except for the colonic motility experiment. Data was collated and expressed as Mean ± SEM. Analysis was done by one-way ANOVA using GraphPad Prism software, version 7.0®. Results within p≤0.05 were considered significant

Results

There was no significant change in the transit time. CSDS increase significantly in the luminal fluid content of animals and a decrease in % change in luminal fluid content in 6% CSDS (63.5%) and 12% CSDS (27.0%) when compared with the control. The onset of diarrhea was observed to be significant in 12% CSDS (39.6 ± 1.9 min) when compared with the control (61.4 ± 1.2 min). There was a significant decrease in colonic motility time in the 6% CSDS (297±27.26 sec.) and 12% CSDS (167±32.35 sec.) compared with the control (1064±43 sec). A significant reduction was observed in the crypt height and mucosa width in the colon of the experimental groups when compared to the control

Conclusion

In conclusion, these results showed that CSDS possesses prosecretory and –motility properties and caution should be applied when consumed

---

B 02-37

Ion permeation in non-selective cation channels studied by molecular dynamics simulations

H. Sun

Leibniz Forschungsinstitut für Molekulare Pharmakologie, Chemical Biology, Berlin, Germany

Computational electrophysiology is an atomistic molecular dynamics (MD) based approach for simulating ion permeation through ion channels under realistic ion gradient and the resulting transmembrane potential. Using this theoretical method, we simulated ion permeation of a number of non-selective cation channels, such as (i) prokaryotic NaK channel, (ii) vertebrate AMPA receptor and (iii) CNGA1 channel. We could show that for NaK channel structural plasticity within the selectivity filter and the selection of these conformations by different ions are key molecular determinants for highly efficient conduction of different cations. In contrast, for AMPA and CNG channels, monovalent ions permeate at similar rates through the open channel pore by exploiting different binding sites and hydration states, and not by ion-dependent structural accommodations. Comparison of ion permeation in these different channels clearly revealed that the ion conduction mechanism in non-selective cation channels is more diverse and complex than previously thought. Finally, a combined MD and quantum mechanics/molecular mechanics (QM/MM) study will be presented to show the calcium permeation across the AMPA receptor channel.

B 02-38

Contribution of Oxidized lipoprotein to poor outcomes in critically ill patients

Y. Prado[1,2], F. Marchant[1,2], F. Simon[1,2]

[1] *Universidad andrés bello, Ciencias de la Vida, Santiago, Chile*

[2] *Instituto Mileno en Inmunologia e Inmunoterapia, Santiago, Chile*

Fondecyt Regular 1201039, Instituto Milenio de Inmunología e Inmunoterapia ICN09_016/ICN 2021_045, ANID scholarship 21220694.

Introduction

High-density lipoprotein (HDL), an abundant lipoprotein in the bloodstream, is widely recognized for its contribution in cardiovascular health, being associated to low risk for the development of arterial and coronary diseases. During inflammatory diseases such as sepsis or COVID-19, the pro-oxidative environment promotes oxidative modifications to several macromolecules, including HDL. Unlike native HDL, oxidized HDL (oxHDL) exhibits high pro-inflammatory activity, and whether oxHDL contributes to poor outcomes in critically ill patients has not been explored yet.

Aim

To evaluate the contribution of oxHDL to poor outcomes in critically ill patients

Methods

36 patients admitted to the intensive care unit (ICU) at Hospital Clínico Metropolitano La Florida and Hospital Clínico de la Fuerza Aérea, both located in Santiago, Chile, were enrolled under signed informed consent form. Furthermore, 38 healthy volunteers were registered as controls. Blood samples were taken within 24 hours after admission (ICU patients) and throughout the study in healthy controls and underwent analysis of oxHDL levels, coagulation and renal function markers. 28-days mortality and length of ICU stay were also analyzed. This study was approved by the local institutional Ethics and Bioethics Review Board and outlined in the Declaration of Helsinki. All results are presented as mean ± SD or mean ± 95% confidence interval (CI) for the relative risk. Differences were considered significant at $p < 0.05$. Statistical differences were assessed by student's t-test (Mann-Whitney). Survival curves were compared by Log-rank (Mantel-Cox) test and Gehan-Breslow-Wilcoxon test to determine survival rates. Contingency analyses with Fisher's exact test were used to assess the relative risk of death.

Results

Patients admitted at intensive care unit (ICU) showed increased levels of oxHDL compared to healthy volunteers and interestingly, non-survivor ICU patients showed increased oxHDL levels in comparison with survivor ICU patients. ICU patients showed increased creatinine and BUN that directly correlates with oxHDL levels. We also found decreased levels GFR and increased BUN/Creatinine ratio, that correlated with oxHDL levels, depicting a strong association between circulating oxHDL level and kidney failure parameters. We also found increased TF, tPA and D-dimer levels that correlated with oxHDL levels and kidney failure markers. Remarkably, plasma oxHDL levels strongly correlates with days of permanence at ICU for non-survival patients, 28-days mortality, showing an association between elevated plasma oxHDL levels and bad prognosis.

Conclusion

High OxHDL level is associated to poor outcomes in ICU patients promoting renal failure, coagulation alterations, increased length of ICU stay and mortality. Results suggest that oxHDL could be considered as target to improve the diagnosis and treatment of patients with inflammatory diseases, to reduce poor outcomes.

B 02-39

An „out of the box“ look at the role of TRPV3 in epithelia

F. Stumpff[1,2], F. Liebe[2], H. Liebe[2], D. Manneck[1,2]
[1] *Health and Medical University Potsdam, Department of Physiology, Potsdam, Germany*
[2] *Freie Universität Berlin, Institute for veterinary Physiology, Berlin, Germany*

Funding by the Deutsche Forschungsgemeinschaft DFG Stu-258/7-1, by Akademie für Tiergesundheit and by the Sonnenfeldstiftung is gratefully acknowledged.

Introduction

TRP channels have emerged as important sensors for stimuli ranging from light in drosophila to temperature or pain in humans. Thus, TRPV3 is activated by temperatures > 33°C, suggesting a role in thermosensation. However, unlike other thermosensors in skin, it is not expressed by peripheral neurons but by keratinocytes and hair follicles [1]. Instead, gain of function mutations of TRPV3 in humans typically do not affect thermal sensation [2], but lead to palmoplantar hyperkeratosis that can be mutilating, suggesting pathways with impact on keratin formation. Furthermore, epithelial cells of the gastrointestinal tract also amply express TRPV3, despite a relatively constant temperature around 37°C [3-5].

Methods

Using the results of various studies, we developed an „out of the box“ model for the possible role of TRPV3 in epithelia. In these studies, the porcine gastrointestinal tract, rumen from cattle and human skin constructs were investigated for expression of TRPV3 using qPCR and immunoblotting. Confocal laser microscopy was used for channel localization. Ussing chamber experiments were performed to study function in native epithelia, while the permeability was studied in overexpressing HEK-293 cells.

Results

Expression of full-length TRPV3 could be shown both via qPCR and immunoblotting in the porcine caecum and colon and in the rumen of cattle, with shorter bands visible in the remaining segments of the porcine gastrointestinal tract, possibly reflecting TRPV3 splice variants previously described in mice and ruminants. In the monolayered epithelia of the gastrointestinal tract, staining for TRPV3 was visible in the apical membrane of the epithelium, with very little staining of the cytosol or subepithelial space. Likewise, the apical membrane of the stratum granulosum of human skin constructs or native bovine rumen showed intense staining for TRPV3, with little staining of the cytosol. However, in stratified squamous epithelia (skin & rumen), cytosolic staining was visible in the lower layers of the functional syncytium, possibly reflecting generation of TRPV3 subunits in the endoplasmic reticulum. The subepithelial space again showed no staining. In transporting epithelia, Ussing chamber experiments demonstrate transport of Ca^{2+} and ofmonovalent cations such as Na^+ and NH_4^+ via pathways sensitive to TRPV3 channel agonists. Whole cell and single channel patch clamp experiments confirm the permeability of TRPV3 to NH_4^+.

Conclusion

We propose that TRPV3 may play a role not just in signalling but also in the bulk transport of cations across epithelia. In the gut, influx of urea with microbial degradation to $NH_3$and efflux of the protonated form, NH_4^+, via TRPV3 may contribute to luminal buffering. Likewise, relatively large amounts of NH_3 are generated from urea by the microbial flora of the skin. Reuptake as NH_4^+ via TRPV3 should enhance formation of glutamate from glutamine, with consequences for the keratinization process.

References

[1] Nilius, B, Biro, T, and Owsianik, G, 2014, 'TRPV3: time to decipher a poorly understood family member!',*J Physiol*.592 (Pt 2), 295-304.

[2] Lin, Z, Chen, Q, Lee, M, Cao, X, Zhang, J, Ma, D, Chen, L, Hu, X, Wang, H, Wang, X, Zhang, P, Liu, X, Guan, L, Tang, Y, Yang, H, Tu, P, Bu, D, Zhu, X, Wang, K, Li, R, and Yang, Y, 2012, 'Exome sequencing reveals mutations in TRPV3 as a cause of Olmsted syndrome',*Am J Hum Genet*.90 (3), 558-64.

[3] Ueda, T, Yamada, T, Ugawa, S, Ishida, Y, and Shimada, S, 2009, 'TRPV3, a thermosensitive channel is expressed in mouse distal colon epithelium',*Biochem Biophys Res Commun*.383 (1), 130-4.

[4] Manneck, D, Braun, HS, Schrapers, KT, and Stumpff, F, 2021, 'TRPV3 and TRPV4 as candidate proteins for intestinal ammonium absorption',*Acta Physiol (Oxf)*.e13694.

[5] Liebe, F, Liebe, H, Sponder, G, Mergler, S, and Stumpff, F, 2022, 'Effects of butyrate(-) on ruminal Ca(2+) transport: evidence for the involvement of apically expressed TRPV3 and TRPV4 channels',*Pflugers Arch*.474 (3), 315-342.

B 02-40

Synergism of epidermal growth factor (EGFR) and angiotensin II (AT1R) receptor activation alters gene expression regulation via SRF.

B. Schreier, V. Dubourg, S. Hübschmann, S. Rabe, S. Mildenberger, M. Gekle
Martin Luther University Halle-Wittenberg, Julius-Bernstein-Institute of Physiology, Halle (Saale), Germany

Introduction

The EGFR, a receptor tyrosine kinase, and the AT1R induce essential cellular responses, partially via receptor crosstalk. Although AT1R-EGFR interaction with regard to proximal signalling in the reno-cardiovascular system is well studied, our understanding of the results in terms of information transfer to the nucleus, transcription regulation and at last the transcriptome remains limited. It is not clear whether AT1R-EGFR transactivation results in (i) a linear, EGFR-triggered, nuclear signalling or whether transactivation induces (ii) parallel AT1R and EGFR signalling leading to (iii) synergistic effects, comparable to separate but simultaneous activation by external ligands (EGF and AII). Therefore, we investigated the potential interaction of EGFR and AT1R with relation to transcriptional regulation, underlying signalling pathways and also the response mode at the single cells level, concentrating on the serum response factor (SRF), AP1 and EGR.

Methods

EGFR & AT1R interaction was estimated by proximity labelling. To assess SRF-mediated gene expression, single cell digital high content microscopy, immunofluorescence and quantitative realtime PCR were performed with or without stimulation by EGF, angiotensin II or both. Next generation sequencing analysis was performed on human kidney cells (HK-2 and HEK293 cells) either transiently or permanently transfected with AT1R followed by differential expression analysis and gene ontology enrichment analysis.

Results

AT1R and EGFR synergistically activate SRF via the ERK1/2-TCF and actin-MRTF pathways. Synergism converges on the transcription factors AP1 and EGR, leading to synergistic transcriptome alterations, in qualitative (over-additive number of genes), quantitative (over-additive

expression changes of individual genes) and temporal (more late onset and prolonged expressed genes) terms. Gene ontology and IPA® pathway analysis indicate prolonged cell stress (e.g. hypoxia-like) and dysregulated vascular biology. Synergism occurs during separate but simultaneous activation of both receptors and during AT1R-induced EGFR transactivation.

Conclusion

Both receptors elicit an impact of their own, yet when activated simultaneously, the resulting effect is significantly larger than the sum of the individual effects. The effects of both receptors converge on the SRF pathway. Both of the SRF activation pathways at least partially mediate this synergy, resulting in qualitative, quantitative and temporal differences in gene expression regulation. SRF is a transcription factor of key importance for the activity of many immediate early genes and thereby participates in cell cycle regulation, apoptosis, cell growth, and cell differentiation, alterations of its activity might have a large influence, especially for cells of the reno-cardiovascular system. Now, the precise nature of this impact in vivo needs to be addressed in future studies.

References

[1] Schreier B, Dubourg V, Hübschmann S, Rabe S, Mildenberger S, Gekle M (2022), Synergy of epidermal growth factor (EGFR) and angiotensin II (AT1R) receptor determines composition and temporal pattern of transcriptome variation, Cell Mol Life Sci 79:57, Basel : Springer

---

B 02-41

Effect of interleukin-1 cytokines on NADPH oxidase (Nox)-derived superoxide production and ATP release from bladder urothelium

A. Gurpinar[1], M. Roberts[1], L. Meira[1], P. Camelliti[1], M. R.S. Ruggieri[2], C. Wu[1]

[1] *University of Surrey, Biochemistry, Surrey, UK*

[2] *Temple University, Philadelphia, USA*

Funding bodies:

BBSRC (BB/P004695/1/BB)

NIH (NIA1R01AG049321-01A1/AG)

Bladder disorders are highly prevalent with overactive bladder syndrome (OAB) alone affecting 16% of the Western population but their pathogenesis is poorly understood [1,2]. Urothelium - the inner epithelial layer of the bladder, has been recognised as a new sensory structure and its dysfunction may underlie the bladder disorders such as OAB[3]. Inflammation is a key pathogenic mechanism in many chronic diseases and inflammatory oxidative damage contributes to cell injury. Amongst all enzymatic sources of reactive oxygen species (ROS), NADPH oxidase (Nox) enzymes are the only drug-targetable molecules without effect on physiological oxidation. Recent investigation on OAB patient biopsies shows chronic inflammation in the urothelium[4] and our pilot study has also identified Nox system in this tissue[5]. This study aimed to examine the effect of the key pro-inflammatory factors Interlekin-1alpha (IL-1α) and Interleukin-1beta (IL-1β) on ROS generation and release of the sensory mediator ATP in the urothelium.

Young adult male (3-6 months) C57BL/6J mice were used in accordance with UK /EU regulations. Bladder mucosa, smooth muscle and full thickness tissue strips were isolated by microdissection. Nox-derived superoxide was determined by lucigenin-enhanced chemiluminescence in live tissue, with NADPH as a cofactor and verified by the superoxide scavenger Tiron. Longitudinal full thickness strips were mounted in a perfusion trough and urothelial ATP release was determined by measuring ATP concentration in the superfusate in the vicinity of the urothelium using luciferin-luciferase assay. Data are expressed as median±interquartile range and the difference between an intervention and control was tested by Wilcoxon's test (nonparametric).

Interlekin-1alpha (IL-1α, 1ng/ml) and Interleukin-1beta (IL-1β, 5ng/ml) caused significant increase in superoxide release from the mucosa with no effect on the smooth muscle (%change, IL1α[n=8]: mucosa [control: 99[76,123], treated: 117[96,166], p≤0.01], smooth muscle [control: 91[74,132], treated: 86[45,113], p>0.05], IL1β[n=8]: mucosa [control: 95[63,132], treated: 120[79,180], p≤0.01], smooth muscle [control: 87[49,138], treated: 79[49,112], p>0.05]). IL-1α was chosen to test the ability to release ATP from the urothelium. IL-1α application significantly enhanced urothelial ATP release (%change, IL1α [n=18]: control 62[31,167], and treated: 81[37,240], p≤0.01).

These data provide the first evidence that Interlekin-1α and Interleukin-1β can enhance Nox-derived ROS production from the urothelium, suggesting their ability to elicit inflammatory oxidative damage; these proinflammatory factors can also directly influence the urothelial function by releasing the sensory mediator ATP, contributing to heightened sensation. These findings suggest a key role of these pro-inflammatory cytokines in urothelial function and pathogenesis, whereby Nox-mediated oxidative stress amplifies inflammatory tissue damage.

References

[1] Irwin, D. E., Milsom, I., Hunskaar, S., Reilly, K., Kopp, Z., Herschorn, S., et al. (2006). Population-based survey of urinary incontinence, overactive bladder, and other lower urinary tract symptoms in five countries: results of the EPIC study. *Eur. Urol.* 50, 1306–1314; discussion 1314–1315.

[2] Peyronnet B, Mironska E, Chapple C, Cardozo L, Oelke M, Dmochowski R, Amarenco G, Gamé X, Kirby R, Van Der Aa F, Cornu JN. A Comprehensive Review of Overactive Bladder Pathophysiology: On the Way to Tailored Treatment. Eur Urol. 2019 Jun;75(6):988-1000.

[3] Birder, L., Andersson, K.-E., 2013. Urothelial signalling. Physiol. Rev. 93, pp.653–80.

[4] Apostolidis A, Jacques TS, Freeman A, Freeman A, Kalsi V, et al. (2008) Histological changes in the urothelium and suburothelium of human overactive bladder following intradetrusor injections of botulinum neurotoxin type A for the treatment of neurogenic or idiopathic detrusor overactivity. Eur Urol 53: 1245–1253.

[5] Roberts M, Amosah J, Sui G, Wu R, Archer S, Ruggieri M, and Wu C (2018). Identification of NADPH oxidases: implication for urothelial and bladder function. Journal of Urology, 199, 4S PD55-11.

B 02-42

The Na^+/Ca^{2+} exchanger impairs the migration of pancreatic stellate cells in the tumor microenvironment

T. Loeck, M. Rugi, Z. Pethö, A. Schwab
University of Münster, Institute of Physiology II, Münster, Germany

The authors gratefully acknowledge funding by the Deutsche Forschungsgemeinschaft (GRK 2515/1, Chembion and SCHW407/22-1).

Introduction
Thepancreatic ductal adenocarcinoma (PDAC) is the most frequent pancreatic cancer and it is a serve, malignant disease. Cancer cells communicate with cancer associated fibroblasts (CAFs). Pancreatic stellate cells (PSCs) belong to CAFs and are involved in the remodeling of the tumor microenvironment (TME) by producing large amounts of extracellular matrix. They are responsible for producing the fibrotic microenvironment typically found in PDAC. Moreover, PSCs are able to migrate so that they co-metastasis with pancreatic cancer cells. The Na^+/Ca^{2+} exchanger (NCX) is an important Ca^{2+} regulatory transport protein. The aim of this study was to understand weather migration of PSCs is regulated by the NCX in the different physico-chemical properties of the TME.
Methods
Migration of murine PSCs was monitored with 2D live-cell imaging experiments that recapitulated some of the conditions of the TME. Cells were treated with hypoxia, pressure, acidic pH and platelet derived growth factor (PDGF). Moreover, ionic imaging experiments of Ca^{2+}, Na^+ and membrane potential were performed to analyze the NCX activity under acidic conditions.
Results
The blockade of the NCX in the conditions of the tumor microenvironment resulted in a differential impact on the migration behavior of PSCs. Under forward and reverse mode inhibition of the NCX in physiological microenvironment conditions, the PSCs migrated faster. Translocation increased upon NCX inhibition when PSCs were pressurized or treated with PDGF. The inhibition of the NCX had no effect under hypoxia. Under acidic conditions, the NCX inhibition leads to a reduced migration.
Conclusion
The migration of PSCs depends on cues from the TME. The Na^+/Ca^{2+} exchanger plays a differential role in translating these cues into an altered migratory behavior.

B 02-43

Dysregulation of the polyamine system in favour of its catabolism is a common mechanism after kidney injury

T. Sieckmann[1], N. Ögel[1], S. Kelterborn[1], F. Boivin[4], G. Schley[5], M. Fähling[1], M. I. Ashraf[3], M. Reichel[2], E. Vigolo[4], A. Hartner[6], F. Knauf[2], C. Rosenberger[2], F. Aigner[7], K. Schmidt-Ott[2,4], H. Scholz[1], **K. M. Kirschner**[1]
[1] Charité-Universitätsmedizin Berlin, corporate member of Freie Universität Berlin, Humboldt-Universität zu Berlin, and Berlin Institute of Health, Institute of Translational Physiology, Berlin, Germany
[2] Charité-Universitätsmedizin Berlin, corporate member of Freie Universität Berlin, Humboldt-Universität zu Berlin, and Berlin Institute of Health, Department of Nephrology and Medical Intensive Care, Berlin, Germany
[3] Charité-Universitätsmedizin Berlin, corporate member of Freie Universität Berlin, Humboldt-Universität zu Berlin, and Berlin Institute of Health, Department of Surgery, Berlin, Germany
[4] Max Delbrück Center for Molecular Medicine in the Helmholtz Association, Molecular and Translational Kidney Research, Berlin, Germany
[5] Friedrich-Alexander University Erlangen-Nürnberg (FAU) and University Hospital Erlangen, Department of Nephrology and Hypertension, Erlangen, Germany
[6] Friedrich-Alexander University Erlangen-Nürnberg (FAU) and University Hospital Erlangen, Department of Pediatrics and Adolescent Medicine, Erlangen, Germany
[7] St. John of God Hospital Graz, Department of Surgery, Graz, Austria

This study was funded by the Deutsche Forschungsgemeinschaft (DFG, German Research Foundation) – Project-ID 394046635 – SFB 1365 Renoprotection. T.S. received support from the Wilhelm Sander-Stiftung (grant no. 2018.015.1).

The polyamines putrescine, spermidine and spermine are organic polycations that regulate fundamental cell functions including proliferation and differentiation. It is known that certain genes of the polyamine system are dysregulated after kidney ischemia reperfusion injury. We hypothesise that different forms of acute and chronic kidney injury lead to similar changes in the expression patterns of the polyamine system.
In different models of acute and chronic kidney injury expression of genes involved in polyamine homeostasis was analyzed by RT-qPCR and RNAScope. Interestingly, the expression of catabolic enzymes (*Aoc1* and *Sat1*) was upregulated, while the anabolic enzymes (*Odc1*, *Sms*) were downregulated. The same trend is observed in RNA sequencing data sets of transplanted donor kidneys in humans. The putrescine-degrading enzyme AOC1 exhibits the most striking changes. The detected increase of *Aoc1* can be located to injured but regenerating proximal tubules. We used mouse embryonic kidney explants to screen for stimuli modulating *Aoc1* expression, and observed *Aoc1* expression is induced under hyperosmotic conditions. Using reporter gene and RNA-stability assays, we could show that the increase in *Aoc1* expression is based on mRNA-stabilization and transcriptional activation via NFAT5. Notably, the *Aoc1* splice variant that is regulated by NFAT5 contains an additional set of 22 amino acids N-terminally that lead to an altered subcellular localization and increased secretion. Overexpression of *Aoc1* led to elevated autophagy activity.
In conclusion, different models of kidney injury exhibit a similar pattern of dysregulation of the polyamine system with the most striking change being the upregulation of *Aoc1* in proximal tubules. Using hyperosmolarity as a stimulus, we established a model to study polyamine function and provide first insights into the regulation of *Aoc1* under damaging conditions.

B 02-44

Phenotypic characterisation of novel immortalised human distal convoluted tubule cells

C. Zhong, K. Siew, S. Walsh
UCL, Department of Renal Medicine, London, UK

Introduction

The distal convoluted tubule (DCT) is responsible for fine-tuning the final excretion of sodium, potassium, calcium and magnesium in the urine. The study of rare monogenic diseases (namely Gordon and Gitelman syndromes) have highlighted the physiological importance of the DCT in blood pressure control. However, the most commonly used cellular models of this segment are either not truly kidney cells (e.g. studies have shown HEK293 are more likely of neuronal lineage) or of murine origin, and thus there is need for advanced human DCT (hDCT) models. Recently, 4 immortalised hDCT models isolated from human urine have been created by Dr Tetsuro Kusaba, but have not been biochemically or functionally characterized.

Methods

Four immortalised hDCT cell lines gifted from Dr Kusaba (Kyoto Prefectural University of Medicine, Japan) were cultured as previously described (Ikeda et al., 2020. DOI: 10.1159/000509419). hDCT cells were used for analysis at 80-90% confluency and lysed either with TRI reagent for high quality RNA or in the presence phosphatase and protease inhibitors for protein extraction. Western blot analysis and qPCR analysis was performed for NCC, TRPM6 and parvalbumin.

Results

Western blot analysis on total cellular lysates by using NCC antibody detected three different states of NCC in all four hDCT cell lines. qPCR detected the presence of NCC mRNA at Cq 29.57-32.18 across all four samples (Human kidney positive control Cq 27, and HEK293 negative control Cq 45).

Conclusion

The preliminary western blot and qPCR results confirmed NCC expression in all four hDCT cell lines and the position of bands agreed with previous studies (de Jong et al., 2003; DOI 10.1074/jbc.M303101200. Zhang et al., 2015. doi: 10.1093/hmg/ddv185.). Further experiments will be performed using other key markers expressed in DCT, including TRPM6 and parvalbumin, Calbindin, KS-WNK1, WNK4, human isoforms of SPAK and NCC. These cell lines could be the first validated hDCT cellular models which reflect the human DCT physiology and can be adapted to 3D cell culture system for functional experiments

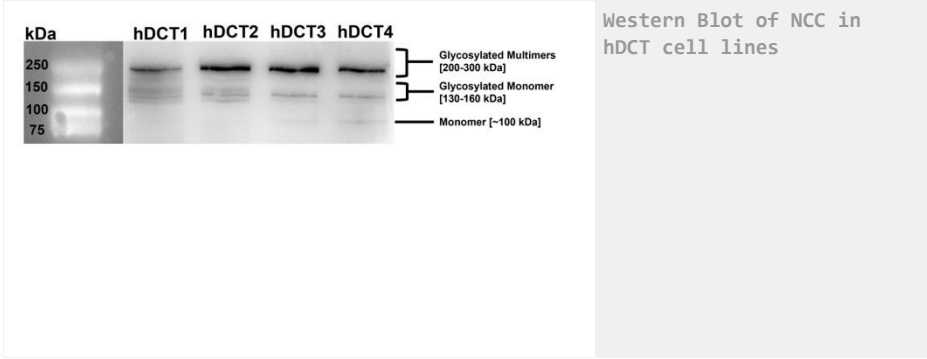

Western Blot of NCC in hDCT cell lines

B 02-45

Mechanoactivation of a membrane reservoir is activated by Piezo and TMEM16F

C. Deisl[1,4], R. Syeda[2], D. Hilgemann[1], **M. Fine**[1,3]
[1] *University of Texas Southwestern Medical Center, Physiology, Dallas, USA*
[2] *University of Texas Southwestern Medical Center, Neuroscience, Dallas, USA*
[3] *University of Texas Southwestern Medical Center, Molecular Genetics, Dallas, USA*
[4] *Johannes Kepler Universität, Physiologie und Pathophysiologie, Linz, Austria*

Introduction

This work addresses the unique properties of biological membranes and the ability of cell surfaces to sense changes and adjust to changes in membrane tension by regulating membrane reserves. The understanding of how cells respond to membrane stress and how activation of the membrane reserve facilitates change in cellular morphology, differentiation, cell signaling, and cell migration will have significant impact on a myriad of biological pathways. Recently we described a novel *in vitro* mechanism for the rapid mechanically activated regulation of the PM. This involves the regulation of charged lipid movement across the membrane through the action of the phospholipid scramblase, TMEM16F. This scramblase is activated by elevated cytoplasmic Ca and can mediate profound changes in cellular morphology. These processes rely on the natural gradient of anionic lipids enriched in the inner leaflet of the PM such as phosphatidylserine, phosphatidic acid and the phosphoinositides. Loss of this gradient through activation of TMEM16F releases a sequestered membrane reserve which alleviates membrane tension in a localized manner through loss of membrane associated adapter proteins such as Dynamin. We now propose that this membrane reservoir can be activated by mechanosensitive channels and the lipid scramblase TMEM16F.

Methods

All experiments were performed on immortalized cell lines which were genetically modified as needed. We employed whole-cell patch-clamp techniques to obtain real-time capacitance measurements with simultaneous confocal microscopy as well as life cell imaging and standard confocal microscopy techniques.

Results

We describe potential physiological implications of activation of this membrane reserve using pharmacological modulators, control of the extracellular matrix and osmotic stimulation of mechanical stress.

Conclusion

Our data suggests that membrane stress signaling through Piezo1 mechanotransduction leads to activation of a novel membrane reserve, expansion of the cell surface area in a rapid and potentially tunable manner. These processes may provide insight into how these cells can rapidly respond to environmental cues and long-term alterations in physiological and pathophysiological function.

B 02-46

Involvement of Aquaporin-1 in brain water homeostasis

D. B. Jensen, D. Barbuskaite, N. MacAulay

University of Copenhagen, Department of Neuroscience, Copenhagen, Denmark

Introduction

The majority of cerebrospinal fluid (CSF) is produced by the choroid plexus, a highly specialized tissue consisting of an epithelial monolayer surrounding fenestrated capillaries. The choroid plexus epithelial cells express a multitude of membrane transporters and channels, and their transepithelial ion movement has been proposed to drive CSF secretion by osmotically obliged water movement through aquaporin-1 (AQP1) localized to the luminal membrane. However, CSF production occurs in the absence of a transchoroidal osmotic gradient, and can even take place against an experimentally-induced unfavorable osmotic gradient, questioning the exact role of AQP1 in CSF production. This ongoing project aims to determine the contribution of AQP1 in CSF secretion and brain water homeostasis by using mouse models deficient in AQP1.

Methods

MRI were performed on wild type (WT) and global AQP1$^{-/-}$ mice to study the size of the lateral ventricles. Additionally, the total brain water content was determined by dehydrating the brains.

Results

The initial study with the AQP1$^{-/-}$ mouse model revealed brain water content and lateral ventricle size similar to those of WT mice.

Conclusion

These results indicate that AQP1 may play a minor role in brain water homeostasis. Future studies will determine the intracranial pressure and rate of CSF production in the two strains, which are aimed to extend into differentiation between a direct effect of AQP1 deficiency in choroid plexus versus the indirect effects on brain water homeostasis anticipated to arise following the altered systemic water homeostasis and lower central venous blood pressure in the global AQP1$^{-/-}$ mouse.

B 02-47

MCU and MICOS control melanoma cell biology

C. S. Gibhardt[1], I. Stejerean-Todoran[1], N. G. Kirpal[1], K. Zimmermann[2], A. M. Vultur[1,3], C. Ickes[1], B. Shannan[3,4], Z. Bonilla del Rio[1], S. Cappello[1], H.-M. Sung[1], M. Shumanska[1], X. Zhang[1], A. Wölling[5], M. S. Nanadikar[6], F. Lange[7], A. Wittek[7], M.U. Latif[8], A. Waters[3], P. Brafford[3], D. Riedel[9], J. Wilting[10], H. Urlaub[11,12], S. Jakobs[7], V. Ellenrieder[8], D. M. Katschinski[6], P. Rehling[13], C. Lenz[11,12], A. Roesch[4], M. P. Schön[5], M. Herlyn[3], H. Stanisz[5], I. Bogeski[1]

[1] *University Medical Center Göttingen, Georg-August-University, Molecular Physiology, Institute of Cardiovascular Physiology, Göttingen, Germany*

[2] *Saarland University, Biophysics, CIPMM, Homburg, Germany*

[3] *The Wistar Institute, Melanoma Research Center, Philadelphia, USA*

[4] *University Hospital Essen, Department of Dermatology, Essen, Germany*

[5] *University Medical Center Göttingen, Georg-August-University, Department of Dermatology, Venereology and Allergology, Göttingen, Germany*

[6] *University Medical Center Göttingen, Georg-August-University, Institute for Cardiovascular Physiology, Göttingen, Germany*

[7] *Max Planck Institute for Biophysical Chemistry, Department of NanoBiophotonics, Göttingen, Germany*

[8] *University Medical Center Göttingen, Georg-August-University, Department of Gastroenterology, Gastrointestinal Oncology and Endocrinology, Göttingen, Germany*

[9] *Max Planck Institute for Biophysical Chemistry, Laboratory of Electron Microscopy, Göttingen, Germany*

[10] *University Medical Center Göttingen, Georg-August-University, Institute of Anatomy and Cell Biology, Göttingen, Germany*

[11] *Max Planck Institute for Biophysical Chemistry, Bioanalytical Mass Spectrometry Group, Göttingen, Germany*

[12] *University Medical Center Göttingen, Georg-August-University, Bioanalytics, Institute of Clinical Chemistry, Göttingen, Germany*

[13] *University Medical Center Göttingen, Georg-August-University, Department of Cellular Biochemistry, Göttingen, Germany*

Mitochondria are powerhouses of cells and their proper function is indispensable for normal cell function. In melanoma, however, mitochondria control therapeutic sensitivity and invasive properties. Here, we examine how mitochondrial calcium homeostasis (via MCUa) and mitochondrial inner organization (via Mic60) affect melanoma cell biology.

Downregulation of MCUa, a pore forming subunit of the mitochondrial calcium uniporter (MCU) complex, strongly inhibited mitochondrial calcium uptake and affected metabolic and redox regulation of melanoma cells. Moreover, MCUa downregulation suppressed melanoma cell growth, but promoted migration and invasion. Furthermore, MCUa expression strongly correlated with melanoma patient survival.

Mic60, as a core subunit of the mitochondrial contact site and cristae organizing system (MICOS), is essential for mitochondrial function. Hence, Mic60 downregulation disturbed cristae formation and affected the inner mitochondrial organization. This impacted mitochondrial function and therapy resistance in melanoma cells.

In summary, our study indicates that MCUa and Mic60 control mitochondrial calcium and redox signaling as well as bioenergetic output in melanoma cells. We also demonstrate that both the MCU

and the MICOS complexes regulate melanoma cell invasive behavior and have influence on patient survival.

B 02-48

On Viral Infections: Pathophysiological Factors ofe.g. SARS-CoV-2 (ACE-2-Virus-Complex)

E. Neu[1], M. C. Michailov[1], A. Srivastava-Werner[1,2], H. Grindler-Greimel[1], D. Martin[1], G. Iyengar[1,3], G. Govil[1,4], G. Weber[1,5]

[1] Inst. Umweltmedizin (IUM) c/o ICSD/IAS e.V., POB 340316, 80100 M. (Int.CouncilSci.Develop./ Int.Acad.Sci. Berlin-Innsbruck-Muenchen-NewDelhi-Paris-Sofia-Vienna), Muenchen, Germany

[2] Sana Klinikum, Kl. Gyn. & Geb.hilfe, Offenbach, Germany

[3] IAEA (Ex-Dir.), New York &, Vienna, Austria

[4] Indian Nat. Sci. Acad. (Inst.-Dir.), New Delhi, India

[5] Univ. Luxembourg & Vienna, Fac. Psychology (Dean), Vienna, Austria

Introduction

General principles for regulation of electro-&motor activity in urogenital tract are described in vesical myocytes as mechanosensitive ionic channels [1]: Ionic dependence can be clarified by new kind of electro-physiological reactions [2], also in pyeloureter [3]. High sensitivity of animal&human renal vascular preparations to angiotensin-2 is reported conc idiopathic&renal hypertension [1b,2,4]. Actually is considered importance of stretch ionic channels (A), renin-angiotensin-aldosteron-system (RAAS) (B) for infections on example of ACE-2-virus complex of SARS-CoV-2C for pathogenesis (C).

Methods

Motor&electrical (intracellular recording) activities of vascular&vesical preparations (ref).

Results

Present conception.

A. MECHANO-SENSITIVE IONIC-CHANNELS (n=367,p<0.01): Experiments about electrical spikes/S, bursts/B, burst-plateaus/BP of vesical detrusor/D-myocytes (guinea-pig&human/surgical-tissue) described stretch-channels in 1989-93 [1a,2]. Contractions to neural (nCES: 10&100Hz,0.3ms,3-5V)&muscular electrostimulation (mCES: 10Hz,40ms,3-5V) are strongly increased after stretch (>100%). D generates spontaneous-phasic (SPC: 4.0+0.7/min), trigone slow-tonic contractions (STC: 0.28+0.15/min).

B. RENIN-ANGIOTENSIN-ALDOSTERON SYSTEM (RAAS) (n=120,p<0.01): Isolated human renal&uterine-vessels, rat-aorta generate SPC&STC. Angiotensin-2 (0.01-0.1ng/ml) induces contractions in human-renal-veins. Vasopressin (0.02-1mU/ml)&prostaglandin F2alpha induces STC in human renal arteries&rat aorta.

C. On SARS-CoV-2 (ACE-2-virus complex): Angiotensin-converting-enzyme-2 (ACE-2)/metalcarboxypeptidase is essential factor for RAAS, also for SARS-CoV-2-receptor. It is suggested that these mechano-sensitive ionic channels are responsible for interaction between ACE-2&virus!

Conclusion

Physiological interdisciplinary research incl. biophysics-pharmacology-pathology,etc. is necessary to clarify importance of **ions** (Na+,K+,Ca++,Mg++), **hormonal-receptors -** nicotinic nACH alpha4_2, beta 2_3, alpha-/ß-adrenergic, VPR1a-1b/5-HT1a-f/5-HT2a-c/5-HT7,etc and **mesomorphic-states** (nematic-smectic-cholesteric) and ferro-piezo-pyrro-electricity resp. for **electrical&dielectrical phenomena** conc genesis of ACE-2-virus complex & possible prevention.

Project about corona pandemic supported by Eur.&int. societies for physiology-biophysics-pathology,etc. conc A-C could be essential factor counteracting viral infections on example of SARS-CoV-2 in context of UNO-Agenda21 for better health-education-ecology-economy on global level.
Further Ref./DEDICATION for Nobel Laureates: *see Neu et al this congress*

REFERENCES:

[1a] EurJ*Physiol*. Vol420/S 1992 R19; 419/S 1991 p124; [1b] 402,1984 R15.
[2] IntCongr*Physiol*: IUPS2022-Peking, Abs-Book:918,919,934,935; IUPS1989-Helsinki: ProcXVII, p529.
[3] ESP2019-Nice, Eur.J.*Pathol*.475/Suppl1: E-PS-03-023, 17-032&033, 25-066&067;
[4] GTPS-2022-Bonn, Arch*Pharmacol* 396/S1:S11,S73-74,S75;
IUPHAR2018-Kyoto. Abs-Book 22093,22127,22330,22335

B 02-49

Analysis of Klotho function in the choroid plexusAnalysis of Klotho function in the choroid plexus

Z. Fanaei-kahrani, C. Kaether

Leibniz Institut für Alternsforschung-Fritz Lipmann Institut, jena, Germany

Introduction

α-Klotho is an “aging suppressor” that declines gradually with age. Hypomorphic klotho mice show phenotypes resembling human premature aging after 3-4 weeks of age. On the other hand, overexpression of this protein in mice increases lifespan [1, 2].

The Klotho protein exists in three distinct forms including transmembrane Klotho, shed Klotho and secreted Klotho. The membrane-bound Klotho is subject to posttranslational modifications such as ectodomain shedding, giving rise to the shed Klotho [3, 4]. People with the heterozygous polymorph variant of Klotho named Klotho-VS polymorphism, have significantly higher soluble Klotho compared to noncarriers. Interestingly, higher level of soluble Klotho in the serum is related to higher cognition in these patients. Therefore, finding the regulators of shedding process could be beneficial for future cognition drug discoveries [5].

Methods

Klotho is mainly expressed in the kidney and choroid plexus of the brain. While the role of Klotho in the kidney is well established, its function in choroid plexus remains unclear [4]. The first aim of this study is to find out the role of this protein in choroid plexus using genetically engineered mice. To this purpose, Klotho$^{fl/fl}$ Oatp1c1-CreER^{T2} mice were used in which Klotho is specifically deleted in the choroid plexus after the injection of Tamoxifen. After the Tamoxifen injection, structural and physiological features of choroid plexus were analyzed using immunofluorescence staining of brain sections containing choroid plexus.

Results

Using using immunofluorescence staining, we showed that the basic structure and function of choroid plexus does not change after the deletion of Klotho in this tissue.

Furthermore, to study the regulators of Klotho transport to the membrane and its subsequent shedding, cellular high-throughput screens were performed and the possible hits are being analyzed.

References
[1] Kuro-o, M.; Matsumura, Y.; Aizawa, H.; Kawaguchi, H.; Suga, T.; Utsugi, T.; Ohyama, Y.; Kurabayashi, M.; Kaname, T.; Kume, E. Mutation of the mouse klotho gene leads to a syndrome resembling ageing. *nature* **1997**, *390*, 45-51.
[2] Kurosu, H.; Yamamoto, M.; Clark, J.D.; Pastor, J.V.; Nandi, A.; Gurnani, P.; McGuinness, O.P.; Chikuda, H.; Yamaguchi, M.; Kawaguchi, H. Suppression of aging in mice by the hormone Klotho. *Science* **2005**, *309*, 1829-1833.
[3] Kuro-o, M. Klotho and aging. *Biochimica et Biophysica Acta (BBA)-General Subjects* **2009**, *1790*, 1049-1058.
[4] Xu, Y.; Sun, Z. Molecular basis of Klotho: from gene to function in aging. *Endocrine reviews* **2015**, *36*, 174-193.
[5] Almeida, O.P.; Morar, B.; Hankey, G.J.; Yeap, B.B.; Golledge, J.; Jablensky, A.; Flicker, L. Longevity Klotho gene polymorphism and the risk of dementia in older men. *Maturitas* **2017**, *101*, 1-5

PB 03 | Human & Exercise & Skeletal Muscle Physiology

B 03-01

Ischemic Pre-Conditioning counteracts fatigue development in intermittent isometric elbow flexions

R. Allois[1], P. Pagliaro[2], R. Silvestro[3]
[1] *University of Torino, Department of Neuroscience, Torino, Italy*
[2] *University of Torino, Department of Biomedical and Clinical Sciences, Torino, Italy*
[3] *University of Torino, Department of Neuroscience, Torino, Italy*

Introduction
Ischemic Pre-Conditioning (IPC) is a non-invasive maneuverer that alternates short periods of occlusion and reperfusion of muscle blood flow. IPC has been reported to increase muscle blood flow, mitochondrial activation, and maximal oxygen consumption. While most studies investigated the effect on global performance, only a few investigated local IPC-induced changes in the exposed muscles. This study aimed to assess local IPC effects, in exposed muscles in terms of tissue oxygenation and fatigue.
Methods
Twenty-two subjects were enrolled in one of the two groups IPC and SHAM. A weightlifting bench was modified to implement isometric contractions of the right biceps muscle. A fatiguing contraction protocol, consisting of unilateral intermittent isometric elbow flexions (3 s ON, 3 s OFF, at 80% of the maximum voluntary contraction) and continuing until exhaustion, was performed before and 30 min after IPC/SHAM treatment. Implemented through a pneumatic cuff positioned proximally to the right biceps muscle, the IPC treatment consisted of a sequence of 3 ischemic cuff inflations (200 mmHg) of 5-min duration) and separated by 5-min rest; SHAM consisted of the same treatment but with cuff pressure of 20 mmHg. Electromyography (EMG) and near-infrared spectroscopy (NIRS) were continuously recorded from the right biceps muscle.
Results
While the number of exercise bouts was not affected by IPC (pre: 7.3 ± 2.7; post: 7.1 ± 4.3) it decreased in the SHAM group (pre: 6.4 ± 2.8; post 4.1±1.7, $p<0.01$). Analysis over single exercise bouts revealed no significant effects of time (from the beginning of the exercise) and treatment for EMG power, but a significant reduction of the EMG mean frequency with time and IPC treatment. Tissue oxygenation during exercise was also affected by time, with significant interaction with treatment in the IPC group. A progressive slowing of NIRS responses to the subsequent ischemic stimuli was observed in the IPC group (initial TOI slope decreasing from 1.1 ± 0.6 %/s in IPC1; to 0.3 ± 0.2 %/s in IPC3, $p<0.01$) as well as in TOI values during the reactive hyperemia (from 81.5 ± 6.1 % after IPC1 to 74.1 ± 8.4 % after IPC3, $p<0.05$).
Conclusion
The results indicate that IPC counteracts the development of fatigue in the intermittent isometric contraction exercise, compared to the SHAM treatment. An IPC-induced reduction in the oxygen consumption rate as revealed by NIRS both at rest and during the exercise could account for the observed anti-fatigue effect.

References
[1] Barbosa TC, Machado AC, Braz ID, et al. Remote ischemic preconditioning delays fatigue development during handgrip exercise. Scand J Med Sci Sports. 2015;25(3):356–64.
[2] Marocolo M, Willardson JM, Marocolo IC, da Mota GR, Simão R, Maior AS. Ischemic Preconditioning and Placebo Intervention Improves Resistance Exercise Performance. J Strength Cond Res. 2016 May;30(5):1462-9.
[3] Paradis-Deschênes P, Joanisse DR, Billaut F. Ischemic preconditioning increases muscle perfusion, oxygen uptake, and force in strength-trained athletes. Appl Physiol Nutr Metab. 2016 Sep;41(9):938-44.
[4] Paradis-Deschênes P, Joanisse DR, Billaut F. Sex-Specific Impact of Ischemic Preconditioning on Tissue Oxygenation and Maximal Concentric Force. Front Physiol. 2017 Jan 5;7:674.

B 03-02

The combined effect of outdoor exercise and ambient air pollution on parameters of pulmonary and immune function in asthmatics and non-asthmatics: a systematic review

S. Moloney, J. Black, N. Bury, G. Devereux
University of Suffolk, School of Health and Sport Sciences, Ipswich, UK

Introduction
The benefits of habitual exercise are promoted with emphasis on prevention of non-communicable diseases. However, air pollution is a potent environmental cause of global mortality[1].Respiratory adaptations during exercise amplify the volume of inhaled pollutants, leading to airway dysfunction by initiating systemic oxidative stress & stimulating pro-inflammatory mediators. Subsequent bronchoconstriction may lead to declines in pulmonary function, especially in asthmatics. In attempt to evaluate the benefit to risk ratio of outdoor exercise, risk of cardiopulmonary & immune dysfunction was associated with air pollution exposure during exercise[2]. Yet, parameters determining risk (exercise intensity & duration) were not clear. Also, extrapolation of findings from exercise in environmental chambers to outdoors lack ecological validity[3].
Thus, this review aims to better understand the combined effect of ambient air pollution & outdoor exercise on pulmonary & immune function in asthmatic & non-asthmatics.

Methods

The review adhered to the PRISMA guidelines[4]. A search was conducted on 3 databases(Oct 2021) using a population, intervention, comparison & outcome approach. A narrative synthesis was used as a meta-analysis was not appropriate due to heterogeneity of samples, and variance in study designs & exercise protocols. The methodological strength of included studies was then assessed[5]

Results

Eleven studies were identified (3 with asthmatics). All studies used walking, running, or cycling, but duration & intensity varied. All studies measured ambient air pollution; particulate matter was consistently reported. Most studies compared responses to exercise in a high & low traffic environment. Spirometry & fractional exhaled nitric oxide (FeNO) were mostly used to indicate pulmonary & immune function, respectively. Of the 9 studies that measured pulmonary function, 5 reported a decline ($p<0.05$) in at least one spirometry measurement & 2 reported an increase ($p<0.05$) following exercise in a high traffic environment. Further, 2 studies found an increase in FeNO ($p<0.05$), others reported a decrease or no change ($p>0.05$). Most studies reported no differences ($p>0.05$) in any measure after exercise in low traffic environments.

Conclusion

A key finding is pulmonary & immune function were often adversely impacted by exercise in high but not low traffic environments. Alongside air pollution exposure, exercise intensity appears to modulate these responses to exercise & air pollution. In non-asthmatics, higher intensity exercise (75-90%HRmax) was associated with negative effects on pulmonary & immune function, yet lower intensity exercise (50-60%HRmax) was associated with an increase in pulmonary function despite a longer exercise duration. Although based on few studies, pulmonary function declines were greatest in asthmatics despite exercise intensity being lower (walking); the exacerbated response is likely due to their hypersensitive predisposition.

References

[1] Landrigan PJ, Fuller R, Acosta NJR, Adeyi O, Arnold R, Basu N, et al., 2018 'The Lancet Commission on pollution and health', *Lancet,* 391(10119), 462–512

[2] Qin, F, Yang, Y, Wang S, Dong Y, Xu M, Wang Z, et al., 2019, 'Exercise and air pollutants exposure: A systematic review and meta-analysis', *Life Sciences,* 218, 153–64

[3] Carlisle, AJ 2001, 'Exercise and outdoor ambient air pollution', *British Journal of Sports Medicine,* 35(4), 214–22

[4] Moher, D, Liberati, A, Tetzlaff, J, Altman, DG 2009, 'Preferred reporting items for systematic reviews and meta-analyses: the PRISMA statement', *Physical Therapy,* 89(9), 873–80.

[5] National Heart, Lung and Blood Institute, Quality assessment tool for before-after (pre-post) studies with no control group 2014, Available from: https://www.nhlbi.nih.gov/health-topics/study-quality-assessment-tools

B 03-03

Investigation of inflammatory and muscle damage responses of downhill running in different menstrual cycle phases.

H. Çakır-Atabek, B. Dokumacı

Eskişehir Technical University, Department of Coaching Education Faculty of Sports Science, Eskişehir, Turkey

Introduction

Downhill running (DR) is a whole-body exercise model used to investigate the physiological responses of eccentric muscle actions and/or exercise-induced muscle damage (EIMD) [1], which is accompanied by inflammation. In line with the findings that the estrogen hormone reduces EIMD responses, in the current study the inflammatory and muscle damage responses were investigated in the follicular (FP) and luteal phase (LP) following DR.

Methods

Recreationally physically active women (n=13; age: 20±2.0 years; height: 163.8±7.0 cm; menstrual cycle days: 27.9±2.4 days; VO_2max: 40.6±4.7 $mL.kg^{-1}.min^{-1}$) participated in the study. Using any hormone preparations or antioxidants were main exclusion criteria. The tests and measurements were performed in random either in FP (6-13 days) and LP (17-24 days), regardless of phase order. The periods were confirmed by hormone analysis. On the first visit of the laboratory, following the anthropometric measurements, maximum voluntary isometric contraction ($MVIC10^0$) for knee joint, and then VO_2max test was performed. 48h after the VO_2max test, DR with –10% slope was performed at a speed coincide to 75% of their VO_2max (mean running speed=8.6±0.9 $km.h^{-1}$) for 30 min. Blood samples were obtained at rest (PRE) and immediately (POST), POST24h, POST48h, POST72h, and POST96h after the DR. Interleukin (IL)-6, C-reactive protein (CRP), myoglobin (Mb), and lipid hydroperoxide (LHP) were analyzed.

Results

No significant phase x measurement interaction, phase differences and time-dependent alterations were observed for $MVIC10^0$ ($N.m^{-1}$). No significant time-dependent changes in both FP and LP were observed for IL-6 and CRP activities ($p>0.05$; Friedman two-way variance). On the other hand, Mb concentration increased from 20.99±0.0 to 34.10±14.0 ng/mL in FP, and from 20.99±0.0 to 33.5±13.9 ng/mL in LP, but only the increment in LP was significant ($p<0.05$; Friedman). Phase x measurements time interaction wasn't significant for LHP ($p>0.05$; ANOVA results), no significant differences were observed between phases ($p>0.05$), however, LHP significantly increased and reached peak level at POST measurement time in both phases (from 1.66±0.4 to 1.92±0.5 in FP vs. from 1.86±0.4 to 2.28±1.0 in LP; $p<0.05$). When the amount of changes calculated according to the PRE-level are examined; the %Δ of IL-6 didn't significantly changed either over the time or between phases ($p>0.05$), furthermore, the %Δ of $MVIC10^0$, %Δ of Mb, and %Δ of LHP significantly changed over the time ($p<0.05$), but didn't differ between phases ($p>0.05$). The results of correlation analysis show that there is no significant relationship between estrogen and examined variables in FP and LP. Moderate correlation was observed only between %Δ of Mb and %Δ of LHP (POST72h-PRE; $r=0.58$; $p=0.03$).

Conclusion

Even though the applied DR protocol did not cause serious muscle damage, inflammation and oxidative stress are related and estrogen does not affect this process.

References
[1] Bontemps, B., et al., *Downhill running: What are the effects and how can we adapt? A Narrative Review.* Sports Medicine, 2020. **50**(12): p. 2083-2110

B 03-04

Effects Of Melatonin Supplementation And Different Exercise Models On Cognitive Function In Long-Term Exposure To Constant Light In Rats

G. Erol[1], B. E. Dinçer[2], H. N. Çalık[2], H. Öksüz[2], S. Yıldırım[2], D. Şener[3], B. Aydın[4], O. Kasımay[1]
[1] *Marmara University, Department of Physiology / Faculty of Medicine, İstanbul, Turkey*
[2] *Marmara University, School of Medicine, İstanbul, Turkey*
[3] *Bahçeşehir University, Department of Histology and Embriology/Faculty of Medicine, İstanbul, Turkey*
[4] *Marmara University, Faculty of Medicine, Department of Biophysics, İstanbul, Turkey*

Introduction
Long-term exposure to constant light causes circadian arrhythmia, affects cognition adversely. Positive effects of exercise are well-known on cognition, however, effects of different types of exercise models are objects of interest. Our aim is to investigate the possible effects of continuous moderate-intensity training (CMT), high-intensity intermittent training (HIIT) and exogenous melatonin supplementation on cognition in rats with circadian arrhythmia caused by long-term constant light exposure.

Methods
Rats, including control group, were divided into seven groups (n=8/group) such as; sedentary (SED), moderate-intensity continuous exercise (CMT), high-intensity intermittent exercise (HIIT) groups and melatonin (MEL) added groups. Control group was housed in light/dark cycle (LD); other animals were housed in light/light cycle (LL). Exercises were performed on treadmill 5 days/week for 6 weeks, constant light protocol was applied for last 3 weeks. During light exposure, respective rats received daily intraperitoneal (ip) injections of melatonin (10 mg/kg).Cognition was evaluated with object recognition test, spatial memory was measured with Y-Maze. Anxiety level was evaluated via hole-board and plus-maze tests. Biochemical, histological evaluations were made in brain tissues.

Results
Neuron cytoplasms of control group had normal lines, while SED had pycnotic nuclei; these degenerative effects were reduced in MEL. Dentat girus region of exercise and melatonin groups was found to be similar to control, an increase in neurogenesis was observed. Neurogenesis in CA3 region was significantly increased in HIIT. While cognitive function was suppressed in SED with continuous light exposure, it returned back withmelatonin administration and/or exercise ($p<0.05$). Melatonin administration and/or exercise recovered the spatial memory which was declined in SED with continuous light exposure. ($p<0.05$-0.001). Anxiety level decreased with both exercises ($p<0.05$-0.01). MPO activity increased with circadian arrhythmia, was suppressed by melatonin and exercise ($p<0.05$-0.001).

Conclusion
MEL reduced degenerative effects on neurons; while HIIT and CMT increased neurogenesis, HIIT significantly increased angiogenesis and neurogenesis. Our results reported the improvement of suppressed cognition levels andspatial memorywith circadian arrhythmia via melatonin and exercise applications, and recovery in neurodegenerative damage.

B 03-05

Training Impulse (TRIMP) Evaluation in Healthy Young and Older Adult Master Cyclists.

E. Newton[1], E. Milbourn[1], A. Fathi[1], T. Francis[1], N. Duggal[2], J. Lord[2], N. Lazarus[1], R. Pollock[1], S. Harridge[1]
[1] *King's College London, Centre for Human and Applied Physiological Sciences, London, UK*
[2] *University of Birmingham, Centre for Musculoskeletal Ageing Research & Institute of Inflammation and Ageing, Birmingham, UK*

Acknowledgment
Nadace Ageing Biology Foundation EU

Introduction
Ageing is typically associated with a decline in general physiological function and aerobic power, even in exercisers (Pollock et al., 2015). Aerobic power is particularly sensitive to training load, therefore, in addition to age, it is important to understand any differences in training load between young and older exercisers. The aim of the present study was to investigate the relative training loads of both young and old amateur cyclists during representative training rides.

Methods
Ten young cyclists (30±3 years; 6 males, 4 females) and 19 master cyclists (73±6 years; 17 males, 2 females) all categorised as healthy (Greig et al., 1994) recorded two self-selected training rides on the road (100km for males, 60km for females) within a 2-week period. These rides were tracked using Garmin Forerunner 45 Plus watch and Polar H10 heart rate sensor to assess cycling speed (kph), ascent (metres), distance (km) and heart rate (bpm). Laboratory testing determined individuals maximum heart rate (MHR) and maximal aerobic power (VO_{2max}) during an incremental exercise test on a cycle ergometer. Cycling intensity during the two qualifying rides was quantified as training impulse (TRIMP) using the method of Banister (1992). Percentage of time spent in 5 pre-determined HR zones corresponding to individuals MHR was also determined (Zone 1 = 50-59%, Zone 2 = 60-69%, Zone 3 = 70-79%, Zone 4 = 80-89%, Zone 5 = 90-100%). The average of the two rides were used for analysis. Self-reported cycling volume (km/month) was also collected. Depending on normality, independent samples t-tests or Mann-Whitney U tests were used to compare age groups. Data is presented as mean±SD.

Results
VO_{2max} was significantly lower in the master cyclists compared to the young cyclists (38±5 vs. 55.2±6.7 $ml.kg.min^{-1}$; $p<0.001$) as was MHR (158±14 vs. 190±5 bpm; $p<0.001$). There was no significant difference in time spent in HR zone 1 (4.2±7.0 vs. 4.8±4.4 %), 2 (11.7±9.8 vs. 18.5±8.9 %), 3 (30.6±12.0 vs. 36.7±4.9 %) and 4 (30.9±14.9 vs. 33.0±13.4 %) ($p>0.05$) while the percentage of time spent in HR zone 5 was significantly higher in the master cyclists (18.3±18.7 vs. 5.1±3.6 %; $p<0.001$). Average cycling speed was significantly lower in the master cyclists (18.5±4.8 vs. 25.6±3.3 kph; $p<0.001$). There was no significant difference in ascent (621.5±207.8 vs. 707.0±225.9 metres), TRIMP (330.3±123.2 vs 314.5± 50.3) or self-reported cycling volume (433.5±288.9 vs. 540.0± 365.0 km/month) ($p>0.05$). There was no significant effect of sex on any variable ($p>0.05$).

Conclusion
Except for the time spent at the higher training intensities (Zone 5), which was greater in the older cyclists, and the speed of cycling, which was lower, the data show remarkable similarity between the training loads of the young and older cyclists. This suggests that, in the present study, changes in indices such as VO_{2max} are not due to an age-related change in training load.

References
[1] Banister, E. (1991). "Modeling elite athletic performance," in *Modeling Elite Athletic Performance*, eds H. Green, J. McDougal, and H. Wenger (Champaign, IL: Human Kinetics), 403–424.
[2] Greig, C. A., Young, A., Skelton, D. A., Pippet, E., Butler, F. M. M., & Mahmud, S. M. (1994). Exercise studies with elderly volunteers. Age and ageing, 23(3), 185-189.
[3] Pollock, R.D., Carter, S., Velloso, C.P., Duggal, N.A., Lord, J.M., Lazarus, N.R. and Harridge, S.D. (2015). An investigation into the relationship between age and physiological function in highly active older adults. *The Journal of physiology*, *593*(3), pp.657-680.

B 03-06

Reliability and repeatability of ultrasound Doppler for assessment of blood flow during one legged knee-extensor exercise – preliminary results.

J. P. Hartmann[1,2], S. B. Nymand[1,3], L. Gliemann[4], R. M.G. Berg[2,5], U. W. Iepsen[1,6]

[1] *Rigshospitalet, Centre for Physical Activity Research, Copenhagen, Denmark*
[2] *Rigshospitalet, Department of Clinical Physiology and Nuclear Medicine, Copenhagen, Denmark*
[3] *Copenhagen University, Department of Biomedical Sciences, Copenhagen, Denmark*
[4] *University of Copenhagen, Department of Nutrition, Exercise and Sports, Copenhagen, Denmark*
[5] *University of South Wales, Neurovascular Research Laboratory, Pontypridd, Denmark*
[6] *Bispebjerg hospital, Department of Anaesthesiology and Intensive Care, Copenhagen, Denmark*

Introduction

Ultrasound Doppler is frequently used to estimate femoral blood flow during rest and exercise and is known to be a valid and accurate measurement. We wanted to investigate the reliability and repeatability of this measurement during rest and during incremental workloads in a single legged knee-extensor exercise (KEE) model.

Methods

Common femoral artery blood flow was measured by the same sonographer using Doppler ultrasound (Logic E9, GE Healthcare, Milwaukee, WI, USA) equipped with a linear probe (9 MHz). The site of the blood flow measurements was below the inguinal ligament but well above the bifurcation of the artery and recordings were obtained at the lowest possible insonation angle and always below 60˚. The sample volume was maximized according to the width of the vessel and kept clear of the walls. Arterial diameter was measured during systole from resting arterial B-mode images with the transducer parallel to the vessel. Doppler tracings were averaged over eight heart cycles. 6/40 participants have been included. Blood flow is measured at rest, during KEE at 0, 6, 12 and 18 watts. Two measurements were obtained at each intensity and all measurements were repeated with an interval of 7 days to obtain repeated measurement for calculation. The between-day coefficient of variation (CV) and intraclass correlation coefficient (ICC) were determined. CV <5% was considered acceptable, and an ICC > 0.90 was interpreted as excellent agreement.

Results

The femoral arterial Doppler blood flow increased linearly with added resistance. At rest the average blood flow was 284 (35) ml/min and increased to 2262 (97) ml/min during KEE at 18 watt **(figure 1)**. The CV was between 9.7 % and 16.7 % across workloads with the highest at rest and the lowest at 0 watts. The ICC ranged from 0.46-0.86 with decreasing values as the workload increased (**Table 1).**

Conclusion

Ultrasound Doppler exhibits a low to moderate degree of measurement error from rest to submaximal work. This suggests that this method should be used with caution by untrained sonographers when looking for small changes in blood flow.

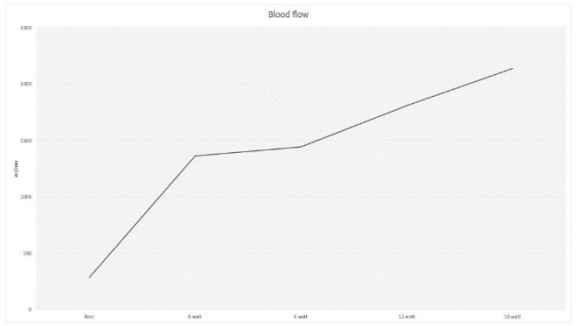

Figure 1 - Blood flow
Mean blood flow is shown during incremental single leg knee extensor exercise from rest to 18 watts.

	Coefficient of variance (%)	Intraclass correlation (ICC)
Rest	16.7	0.86
0 W	9.4	0.66
6W	10.0	0.72
12 W	10.0	0.73
18 W	14.5	0.45

Table 1
Repeatability and reliability measurement in form of CV and ICC, n=6.

B 03-07

Comparison of body composition, bone mineral content and muscle strength variables between elite taekwondo and swimming athletes

H. Çakır-Atabek, C. Aygün, B. Dokumacı
Eskişehir Technical University, Department of Coaching Education Faculty of Sports Science, Eskişehir, Turkey

This study was supported by Eskişehir Technical University Research Fund (Project number: 22ADP082).

Introduction

The strength and the body composition (BC) are very important determinants of sportive performance which can be evaluated with many different methods. Isokinetic dynamometry tests are considered as reliable and validated methods of testing athletic strength variables [1]. On the other hand skinfold testing, hydrostatic weighing, and bioelectrical impedance (BIA) are the ways to test BC. However, the most promising and practical means of testing BC is dual energy X-ray absorptiometry (DXA) [2]. Scanning athletes using a DXA machine allows practitioners to obtain a reliable estimate of three compartments of the athlete's mass; bone mineral content, lean mass and fat mass. This study aimed to investigate the effects of training on BC and strength variables, hence, the current study compared the BC, bone mineral contents, and isokinetic muscle strength variables (maximum strength and muscular endurance) between young elite taekwondo and swimming athletes.

Methods

Twelve taekwondo athletes (age 16.66±2.46 years, height 167.90±7.89 cm, body mass 57.31±5.63 kg, and BMI 20.34±1.68 kg/m^2), and 7 swimmers (age 14.00±1.00 years, height 170.95±5.97 cm, body mass 59.98±7.76 kg, and BMI 20.44±1.53 kg/m^2) volunteered to participate in this study. All athletes were well trained and engaged approximately more than 8 years to the specific training (mean training experience: 8.23 ± 1.75 years). The BC and bone mineral content were evaluated with DXA (Lunar Prodigy Pro; GE, Healthcare, Madison, WI, USA). The concentric isokinetic maximum muscle strength of the knee extensors and flexors was evaluated at angular velocity of 180^0/sec for 5 reps, and muscular endurance calculated as fatigue index [3] was evaluated at angular velocity of 180^0/sec for 30 reps using the CSMI-Humac/Norm TM–770 device. Statistical analysis was done using the Univariate-ANOVA using SPSS-23.0, and $p<0.05$ value was taken as the significance level.

Results

The findings show that the body fat (%) was significantly higher in taekwondo athletes (25.39±4.88 vs 20.14±4.47), consequently tissue lean (%) was significantly higher in swimmers (71.39±4.47 vs 76.82±4.3, respectively; $p<0.05$). The bone mineral density (g/cm^2) was recorded significantly higher in taekwondo athletes (1.15±0.71 vs. 1.02±0.10, $p<0.05$), therefore, the bone mineral content (g) and Z-score were not significantly different between groups. The comparison of maximum torque values of knee extensors and flexors were not significantly different between groups ($p>0.05$). On the other hand, the muscular endurance evaluated with the fatigue index was significantly different between groups: higher fatigue index values were calculated for taekwondo athletes ($p<0.05$; Figure 1).

Conclusion

Body composition differs according to the sport training, and this reflects to the strength variables. Considering the requirements of the sports, coaches must maintain the optimum body composition for the best performance [4].

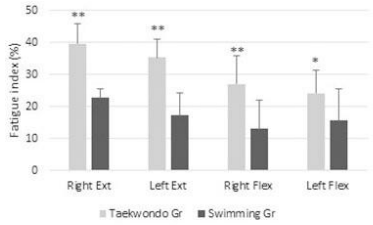

Muscular endurance performance
Figure 1: Muscular endurance performance evaluated with fatigue index. Ext: extensors; Flex: flexors; **p<0.01 and *p<0.05 significantly different.

References

[1] Jiang, C., Olson, M. W., & Li, L. (2013). Determination of biomechanical differences between elite and novice San Shou female athletes. *Journal of Exercise Science & Fitness*, *11*(1), 25-28.

[2] Borgard, C. P. (2010). Assessing Body Composition Among Male Collegiate Runners and Swimmers Using Dual-Energy X-ray Absorptiometry (DXA). *Master's Theses and Project Reports*, 250.

[3] Pincivero, D. M., Gear, W. S., & Sterner, R. L. (2001). Assessment of the reliability of high-intensity quadriceps femoris muscle fatigue. *Medicine and science in sports and exercise*, *33*(2), 334-338.

[4] Mitchell, L. J., Morris, K. S., Bolam, K. A., Pritchard-Peschek, K. R., Skinner, T. L., & Shephard, M. E. (2020). The non-linear relationship between sum of 7 skinfolds and fat and lean mass in elite swimmers. *Journal of Sports Sciences*, *38*(20), 2307-2313.

B 03-08

A regular light home-activity program might improve distal perfusion in aged, non-healthy pro-sedentary individuals

M. M. Florindo[1,2], L. M. Rodrigues[1]

[1] *Universidade Lusófona, CBIOS – Research Center for Biosciences & Health Technologies;, Lisbon, Portugal*

[2] *ESSCVP - Portuguese Red Cross Health School, Department of Physiotherapy, Lisbon, Portugal*

This work was supported by national funds from FCT grant UIDB/04567/2020 and UIDP/04567/2020.

Introduction: Throughout life, hemodynamic homeostasis ensures an efficient balanced, controlled perfusion of all organs, as needed. With age, the incidence and prevalence of peripheral arterial disease (PAD) increases dramatically and is often associated with other co-morbidities. However, there is a generalized idea that an adequate lifestyle, in particular involving regular physical activity (by opposition to sedentarism) might work as preventive for many of these pathological processes (1, 2). Our study focuses on foot perfusion a principal location for multiple circulatory – related impairments in ageing. The goal is to assess the potential impact of a 4-week pre-established and supervised light intensity home-based activity program in an older, sedentary adult cohort with different mobilities.

Methods: Five women and five men (n=10) mean age of 62.4 ± 5.6 years old completed the program. These were chosen after pre-defined selection criteria, with all suffering from different health conditions although preserving their autonomy and mobility. All participants signed an informed written consent (4). Participants were evaluated in the beginning (D0) and in the end (D30) of the study. Perfusion measurements took place distally in both feet. Laser Doppler flowmetry (LDF, Perimed 5000 SW) probes were applied in the metatarsus of the 3rd toe. Perfusion was also measured with polarized light spectroscopy (PSp) using a digital camera at a distance of 60 cm from the dorsal region of both forefeet (TiVi701 Camera; WheelsBridge, SW), quantifying the concentration of red blood cells in the region of interest (3, 4). The home-based activity program involved of a sequence of previously tested activities, namely step in place, for five minutes, isometric plantar flexion for one minute of and walking for five minutes in a comfortable rhythm chosen by the individual compared with baseline and recovery. Statistical analysis was performed and a 5% significance level applied.

ResultsNo differences could be found between participants in the baseline register (D0). Significant increases of LDF values were found in both feet for women and men at D30 compared to D0. With PSp a significant decreases were only found in women (p=0.017). LDF and PSp measure perfusion at different skin depths. Thus, our results suggest that perfusion changes consistently occurred in all individuals at deeper (LDF) structures. At D30 a decrease in arterial pressure, still within normal range, was found only in men (p=0.042) without changes in pulse rate.

Conclusion: This regular, light intensity activity program results in significant physiological changes impacting the patients' distal perfusion and lower limb hemodynamics (5). Supervision and accompaniment might to be principal for its regularity.

References

[1] Baker WB, Li Z, Schenkel SS, Chandra M, Busch DR, Englund EK, Schmitz KH, Yodh AG, Floyd TF, Mohler ER. Effects of exercise training on calf muscle oxygen extraction and blood flow in patients with peripheral artery disease. J Appl Physiol (1985). 2017 Dec 1; 123(6): 1599–1609

[2] Casillas, JM, Troisgros, O, Hannequin, A, Gremeaux, V, Ader, P, Rapin, A, Laurent, Y. Rehabilitation in patients with peripheral arterial disease. Annals of Physical and Rehabilitation Medicine 54 (2011) 443–461444. doi:10.1016/j.rehab.2011.07.001

[3] Rodrigues, L. M,. Rocha, C., Ferreira, H., Silva, H. (2019). Different lasers reveal different skin microcirculatory flowmotion – data from the wavelet transform analysis of human hindlimb perfusion. Scientific Reports 9: 16951. https://doi.org/10.1038/s41598-019-53213-2

[4] Florindo M, Rodrigues LM. The march in place activity – a view from the local concentration of red blood cells (CRBC) in the human foot dorsum. Biomed Biopharm Res. 2019; (16) 1: 62-69. DOI: 10.19277/bbr.16.1.199

[5] Elgersma KM, Brown RJL, Salisbury DL, Stigen L, Gildea L, Kirk LN, Larson K, Schorr EN, Treat-Jacobson D. Adherence and exercise mode in supervised exercise therapy for peripheral artery disease. J Vasc Nurs. 2020 September; 38(3): 108–117. doi:10.1016/j.jvn.2020.07.002

B 03-09

Effect of wearing N95 mask on temperatures inside the mask during incremental exercise

A. A. Kokkuvayil, R. Mannan, S. Kumar, G. Bade, A. Talwar, K.K. Deepak

All India Institute of Medical Sciences, New Delhi, Physiology department, New Delhi, India

Acknowledgment

Department of Physiology, All India Institute of Medical Sciences, New Delhi

Introduction

Since the onset of the COVID pandemic, there has been a wide spread usage of protective masks such as N95 masks. N95 maskss have fine pore size of less than <0.3 µm diameter that filter 95% of small particles in the air (1). It also makes a tight air seal on the face and ensures that air transmission occurs only through the pores of the mask(2). The aim of this study was to compare the temperatures inside the N95 respirator to the ambient temperature during rest and incremental exercise.

Methods

Twenty one healthy volunteer were recruited for study. They were provided disposable N95 protective face masks and a temperature probe was placed inside the mask to record the temperature changes in the microenvironment of facemask. Incremental exertion tests(IET) was done using bicycle ergometer (COSMED, Italy) at a constant speed of 60 revolutions per minute (rpm). The test began at a workload of 0 W with an increase of 10W within 1 min (as a ramp) until 80 percent of maximum heart rate was achieved. The ambient temperatures were noted throughout the study. Perception ratings related to the humidity, heat, breathing difficulty, and discomfort were also recorded.

Results

The mean ambient environmental temperature was 22.31 ± 0.06^{O}C. The mean temperatures inside N95 mask was significantly higher than the ambient temperatures both at rest (32.93 ± 0.93^{O}C) and during incremental exercise (33.16 ±0.77^{O}C during 50-60%, 32.77±1.01^{O}C during 60-70% and 32.36±0.89 ^{O}C during 70-80% of maximum achievable heart rate). But there were no significant

changes in temperature during rest and during incremental exercise. The mean scores of perception rating indicated that humidity, heat, breath resistance and fatigue were higher while using N95 mask.

Conclusion

The study results suggest that wearing of N95 respirators causes a significant increase in temperatures inside the mask as compared to the ambient environmental temperatures and is resposible for the feeling of discomfort and reduced compliance for wearing the mask. However further increase in temperatures were not noted during increasing grades of exercise or strenuous physical activity. This could be due to the initiation of thermoregulatory cooling mechanisms initiated in the body.

References

[1] Shiu EYC, Leung NHL, Cowling BJ (2019) Controversy around airborne versus droplet transmission of respiratory viruses: implication for infection prevention. Curr Opin Infect Dis 32, 372–9.

[2] Li Y, Tokura H, Guo YP, Wong AS, Wong T, Chung J, Newton E (2005) Effects of wearing N95 and surgical facemasks on heart rate, thermal stress and subjective sensations. Int Arch Occup Environ Health 78, 501–9

B 03-10

Skeletal muscle oxygen consumption and oxidative capacity in long COVID measured using Near Infrared Spectroscopy (NIRS)

A. Jamieson[1], R. Astin[2], R. Bell[3], M. Hamer[4], L. Hamill Howes[1], M. Heightman[5], T. Hillman[5], A. Hughes[1], H. Montgomery[2], L. Al Saikhan[1], M. Scully[6], T. Treibel[1], S. Jones[1]

[1] *University College London, MRC Unit for Lifelong Health and Ageing, London, UK*

[2] *University College London, Centre for Human Health and Performance, London, UK*

[3] *University College London, Hatter Cardiovascular Institure, London, UK*

[4] *University College London, Division of Surgery and Interventional Science, London, UK*

[5] *University College London Hospital, Department of Respiratory Medicine, London, UK*

[6] *University College London Hospital, Department of Haematology, London, UK*

The MEXICO study was approved by the Leicester Central Research Ethics Committee. This work is funded by the British Heart Foundation as part of a 4-year BHF Cardiovascular Biomedicine PhD Studentship at UCL (Grant No. FS/19/63/34902). BCCP received infrastructure support from the National Institute for Health Research, University College London Hospitals Biomedical Research Centre and the BHF.

Introduction

Persistent symptoms of fatigue and severe exercise intolerance have been observed in some patients following infection with CoV-2. Termed 'long COVID', these symptoms may persist for months after the acute infection has resolved. The mechanisms underlying exercise intolerance in long COVID are not fully understood and could be the result of dysfunction at any point along the transfer pathway of oxygen from atmosphere to skeletal muscle, including in the capacity for oxidative respiration locally within skeletal muscle. Near Infrared Spectroscopy (NIRS) can be applied in skeletal muscle for assessment of local skeletal muscle oxygen consumption ($musVO_2$) and oxidative capacity (τ). The objective of this study was to compare $musVO_2$ & τ in two groups of individuals living with long COVID. Group 1 included individuals with mild exercise impairment (able to achieve 85% of their predicted maximum heart rate during a cardio-pulmonary exercise testing (CPET)) versus Group 2 who had moderate-severe exercise impairment (unable to achieve 85% predicted maximum HR).

Methods

Participants were individuals with laboratory confirmed COVID-19 recruited from the University College London Hospital (UCLH) COVID-19 follow-up clinic. Cardio-respiratory fitness was measured using a sub-maximal (85% of predicted maximum heart rate) CPET performed on a semi-recumbent cycle ergometer (Ergoselect1200, Ergoline, Germany) to measure whole-body oxygen consumption by analysis of expired gases (Quark CPET, COSMED, Italy). Oxygenated and deoxygenated haemoglobin were measured from the gastrocnemius using NIRS (Portamon, Artinis, Netherlands), arterial occlusions were applied proximal to the measurement at rest to measure $musVO_2$ and following a 5-minute resistance band exercise protocol to measure the time constant for the recovery of $musVO_2$ (τ). All measurements were performed during one clinic visit to Bloomsbury Centre for Clinical Phenotyping (BCCP), UCL. Data are presented as mean±SD.

Results

Preliminary analysis is of7 adults (male 4(57%), mean age±SD 40±7 years) who completed all measurements. 4 participants achieved 85% of their predicted maximum heart rate (Group 1) and 3 participants did not achieve 85% of their predicted maximum heart rate (Group 2. Resting mean $musVO_2$ ±SD was -0.18±0.09 (μM/s) for Group 1 (85%) vs -0.16±0.10 (μM/s) for Group 2 (<85%), p=0.74. τ was 94±122 seconds for Group 1 (≥85%) vs 94±66 seconds for Group 2 (<85%), p=0.99.

Conclusion

In this preliminary analysis, there was not a significant difference in resting skeletal muscle oxygen consumption (mVO_2) or oxidative capacity (τ) between long COVID patients with mild versus moderate-severe exercise incapacity.

B 03-13

Antioxidants supplementation in a form of functional food enhances oxidative status of competitive athletes

I. Drenjančević[1,2], L. Kolar[2,3], M. Stupin[1,4], A. Stupin[1,2], P. Šušnjara[1,2], N. Kolobarić[1,2], Z. Mihaljević[1,2], I. Jukić[1,2]

[1] *Faculty of Medicine Josip Juraj Strossmayer University of Osijek, Department of Physiology and Immunology, Osijek, Croatia*

[2] *Josip Juraj Strossmayer University of Osijek, Scientific Center of Excellence for Personalized Health Care, Osijek, Croatia*

[3] *National Memorial Hospital Vukovar, Department of Internal Medicine, Vukovar, Croatia*

[4] *Osijek University Hospital, Department for Cardiovascular Disease, Osijek, Croatia*

This study was funded by the European Structural and Investment Funds to Science Centre of Excellence for Personalized Health Care, the Josip Juraj Strossmayer University of Osijek, Scientific Unit for Research, Production and Medical Testing of Functional Food, # KK.01.1.1.01.0010.

Introduction: Even though regular physical activity is known to reduce oxidative stress level, strenuous exercise and overtraining increases oxidative stress level in competitive athletes. Thus, proper nutrition which maintains proper oxidative balance is very important in athlete's performance and attaining high level achievements. Analyses of dietary habits in various athletes' groups found that a substantial proportion of the studied populations did not reach the dietary goals for many

macro- and micronutrients, including those with antioxidant properties. Thus, this study aimed to investigate the effect of antioxidant nutrient supplementation in a form of functional food on measurable biomarkers of oxidative stress and antioxidant capacity in competitive athletes.
Methods: Thirty-one young healthy competitive athletes (all men) were instructed to eat three hard boiled hen eggs per day during study protocol that lasted for 21 days (total of 63 eggs). Subjects were divided in experimental NUTRI4 group (14 subjects) which consumed n-3 polyunsaturated fatty acids (n-3 PUFAs), selenium, vitamin E and lutein enriched hen eggs (1050 mg of n-3 PUFA/day, 0.06 mg of selenium/day, 3.29 mg of vitamin E/day, and 1.85 mg of lutein/per day), and in control group (17 subjects) which consumed regular hen eggs produced on the same farm (249 mg of n-3 PUFA per day, 0.05 mg of selenium/day, 1.79 mg of vitamin E/day, and 0.33 mg of lutein/per day). Serum protein concentration of 8-iso prostaglandin F2α (8-iso-PGF2α) and hydrogen peroxide and peroxynitrite (DCF-DA) formation in peripheral blood mononuclear cells (PBMCs) were measured as a markers of oxidative stress level, while serum enzyme activity of antioxidant enzymes catalase (CAT), glutathione peroxidase (GPx), and superoxide dismutase (SOD) were measured as markers of enzymatic antioxidant defense, before and after respective diet protocol.
Results 8-iso-PGF2α serum protein concentration significantly decreased in the NUTRI4 group, while the control group remained unchanged following the respective diet protocol. Similarly, formation of hydrogen peroxide and peroxynitrite (DCF-DA) in PBMCs significantly decreased in the NUTRI4 group, and remained unchanged in controls. Serum activity of CAT, GPX and SOD did not significantly change after the diet protocol neither in control nor Nutri4 group.
Conclusion: Three-week antioxidants supplementation in a form of functional food (n-3 PUFAs, selenium, vitamin E and lutein enriched hen eggs) significantly reduced oxidative stress level in competitive athletes potentially by modifying non-enzymatic (or other enzymatic, beside measured) endogenous antioxidant pathways.

B 03-14

Recovery after passive heating compared to heart rate matched cycling in young healthy adults

I. Potočnik, P. Železnik, N. Potočnik
University of Ljubljana, Medical Faculty, Institute of Physiology, Ljubljana, Slovenia

Introduction
Passive heating (PH) has been proposed as a potential exercise mimetic strategy showing acute and chronic effects on skeletal muscle adaptation in people who are unable to perform or complete sufficient exercise. Like exercise, heating increases heart rate (HR), peripheral arterial blood flow and provoke thermoregulatory response. The aim of our study was to evaluate the cardiovascular response in recovery after PH and to compare it with the recovery after HR and duration matched cycling (HMC).
Methods
In a fixed crossover study, designed in accordance with the Declaration of Helsinki and approved by the national ethical board of the Republic of Slovenia, 9 healthy participants (23.6 ± 2.4 yr) underwent 30 min of whole body passive heating (55gradC in infrared sauna) followed by 30 min of manually load managed cycling on a separate day. Cycling load was added in steps to comply the same HR versus time profile as obtained during PH. HR (Polar) and sublingual temperature (Tsl) were measured continuously 25 minutes during recovery after PH and HMC. Values were compared at 5th and 25th minute after PH/HMC cessation. Heart rate recovery in 120 seconds after PH/HMC cessation (HRR120) was calculated.

Results
HRR120 was statistical significantly greater after HMC compared to PE (24,6 ± 2,8 and 19,7 ± 1,3, respectively, p=0,048). On the other hand, 5 and 25 minutes after PH/HMC cessation HR did not differ statistically comparing PE and HMC. Tsl did not change after PH/HMC compared to rest and did not differ during recovery comparing values after both sessions.
Conclusion
Different HR recovery after PH compared to HMC indicates that different cardiac autonomic regulation mechanisms may control the acute cardiac adaptation to heat/exercise stress nevertheless the HR at the end of stress stimuli was the same. Further investigations like heart rate variability studies are needed to find the main differences in autonomic mechanisms underlying these differences.

References
[1] Hoekstra SP, Bishop NC, Leicht CA, 2020, Elevating body termperature to reduce low-grade inflammation: a welcome strategy for those unable to exercise?, Exerc Immunol Rev.;26:42-55. PMID: 32139348.
[2] Amin SB, Hansen AB, Mugele H, Willmer F, Gross F, Reimeir B, Cornwell WK, Simpson LL, Moore JP, Romero SA, Lawley JS, 2021, Whole body passive heating versus dynamic lower body exercise: a comparison of peripheral hemodynamic profiles, J Appl Physiol (1985), 130(1):160-171. doi: 10.1152/japplphysiol.00291.2020. Epub 2020 Oct 22. PMID: 33090910.
[3] Hoekstra SP, Bishop NC, Leicht CA, 2020, Elevating body termperature to reduce low-grade inflammation: a welcome strategy for those unable to exercise? Exerc Immunol Rev., 26:42-55. PMID: 32139348.

B 03-15

How does exercising twice-a-day affect gastrointestinal hormones, energy intake, and metabolic responses after consuming a standardised breakfast and lunch respectively after each exercise bout in healthy men.

L. R. Mattin[1,2], K. Ishihara[3], V. J. McIver[4,2], A. M. Yau[2], L. J. James[5], G. H. Evans[2]
[1] *University of East Anglia, Faculty of Medicine and Health, Norwich, UK*
[2] *Manchester Metropolitan University, Department of Life Sciences, Manchester, UK*
[3] *Ryukoku University, Faculty of Agriculture, Shiga, Japan*
[4] *Northumbria University, Department of Sport, Exercise and Rehabilitation, Newcastle upon Tyne, UK*
[5] *Loughborough University, School of Sport, Exercise and Health Sciences, Loughborough, UK*

Introduction
Adaptations in markers of oxidative metabolism are routinely achieved in athletic individuals exercising twice-a-day [1, 2]. If healthy individuals don't complete enough physical activity, a natural decline in metabolic health and an increase in adipose tissue will result in chronic long-term complications [3]. The aim was to investigate, if altering when high intensity intermittent exercise (HIIE) and continuous exercise is conducted (AM and PM), would affect metabolic markers, gastrointestinal hormones, appetite, and energy intake (EI).
Methods

Twelve healthy men (Mean ± SD; BMI 24.6 ± 0.4 kg/m^2; $\dot{V}O_{2peak}$ 48 ± 10 ml/kg/min), completed two ~8-h trials in a randomised order. Exercise bout one (EX-1) commenced on a cycle ergometer for 30-min either by, 10 X 1-min at peak power output separated by 2-min rest (HIIE-AM); or a continuous cycle at 50% $\dot{V}O_{2peak}$ (HIIE-PM). A standardised breakfast (BKFST) was then provided, before recovering for 3-h. The second 30-min exercise bout (EX-2) commenced in the opposite order, ensuring both modes where accomplished. A standardised semi-solid lunch was provided, before a further 2-h recovery. Substrate utilisation was measured at baseline (BSL), post-EX bouts and every 1-h during both recoveries. Circulating levels of ghrelin, glucagon-like peptide-1 (GLP-1), peptide tyrosine tyrosine (PYY), pancreatic polypeptide (PP), insulin, glucose (GLU), cholesterol (CHOL), triglycerides (Trigs), non-esterified fatty acid (NEFA) and subjective appetite were measured at BSL, post-EX bouts, pre-BKFST, pre-lunch and every 1-h during both recoveries. Subjective wellbeing (W_{being}) was measured pre- post-EX bouts and post-24-h with nutritional intake recorded for EI.

Results

Fat oxidation was greater after AM and PM HIIE bouts (P<0.05). HIIE-PM NEFA was greater than HIIE-AM after EX-1 (0.49 ± 0.33 vs 0.24 ± 0.07mmol/L; *P* = 0.020) and held until pre-lunch (All P<0.05). HIIE-AM GLU was greater than HIIE-PM, post-EX1 (5.1 ± 0.4 vs 4.7 ± 0.2mmol/L; *P* = 0.017) and elevated at 1- and 2-h post-lunch (*P*<0.05). HIIE-PM ghrelin was greater than HIIE-AM after EX-1 (434 ± 236 vs 263 ± 211mmol/L; *P* = 0.001) and lower after EX-2 (267 ± 167 vs 584 ± 419mmol/L; *P* = 0.003). No differences between trials were seen for GLP-1, PYY, Insulin, PP, CHOL, and Trigs (P>0.05). HIIE-PM hunger was greater than HIIE-AM, post-EX-1 (72 ± 20 vs 39 ± 22mm; *P* = 0.002) and pre-BKFST (79 ± 25 vs 51 ± 26 mm; *P* = 0.016). Appetite did not change between trials once all participants consumed the BKFST or lunch meal (P>0.05). Post-24-h EI and W_{being} were greater after HIIE-PM vs HIIE-AM (3510 ± 879 vs 2829 ± 613 Kcal; *P* = 0.007) and (13 ± 3 vs 10 ± 2 Total; *P* = 0.043).

Conclusion

A twice-a-day approach using health individuals, caused variations in ghrelin, GLU, and hunger directly after exercise, and elevated 24-h EI and W_{being} after completing HIIE in the afternoon. This might have critical long-term consequences for weight management in men.

References

[1] Hulston CJ, Venables MC, Mann CH, Martin C, Philp A, Baar K, Jeukendrup AE, 2010, Training with low muscle glycogen enhances fat metabolism in well-trained cyclists, Med Sci Sports Exerc, 42(11).

[2] Ghiarone T, Andrade-Souza VA, Learsi SK, Tomazini F, Ataide-Silva T, Sansonio A, Fernandes MP, Saraiva KL, Figueiredo RCBQ, Tourneur Y, Kuang J, Lima-Silva AE, Bishop DJ, 2019, Twice-a-day training improves mitochondrial efficiency, but not mitochondrial biogenesis, compared with once-daily training. J Appl Physiol, 127.

[3] Bray GA, Heisel WE, Afshin A et al, 2018, The Science of Obesity Management: An Endocrine Society Scientific Statement. Endocr Rev, 39.

B 03-16

Effect of Postactivation Performance Enchangement (PAPE) on Inter-Limb Unipedal Static Balance Asymmetry in Physically Active Individuals

C. Kacoglu

Eskişehir Technical University, Sport Sciences Faculty, Eskişehir, Turkey

Introduction

Lower extremity strength is a factor that contributes to the ability to control postural balance (Lapszo et al., 2012). It is stated that vibration training increases the balance due to neuromuscular mechanisms (Schlee et al., 2012). Vibration produces a Postactivation performance enhancement (PAPE) effect (Cochrane et al., 2010). Acute WBV increases lower extremity muscular strength and flexibility (Jacobs et al., 2009). In addition, although lower extremity injuries are a multifactorial process, whole body vibration (WBV) studies are effective as a warm-up strategy in athletes with low balance ability (Cloack et al., 2006). The aim of this study is to investigate the effect of PAPE with WBV application on unipedal static balance asymmetry.

Methods

Twenty-seven physically healthy and active individuals (25.3±2.6 years, 174±6.8 cm, 72.4±10.1 kg) voluntarily participated in this study. In the study, which was designed as a Pretest Posttest in depended groups, balance measurements were made after standard warming up, PAPE which 2 sets of vibration were applied for one minute after the balance measurements, and a 1 minute passive rest interval was given between sets. Balance measurements were made before and after PAPE. Participants stood on the platform without shoes and in a static squat position (120^0 knee flexion) during vibration (30Hz, 2mm). After the vibration period was completed, a passive rest of 3 minutes was taken. Afterwards, in unipedal static balance measurements, the subjects' arms are crossed, their hands were crossed on the shoulders, the other leg is 90^0 (not touching the side where the balance is measured), the eyes are open, and the cursor is focused on the measuring device (Sportkat 4000, Berg inc. USA) screen and this cursor is placed. They tried not to error from the center point for 30 seconds. For the determination of asymmetry values, Zifchock et al. (2008)'s symmetry angle formula was used.

Results

The PAPE vibration application didn't elicited a statistically significant mean difference in inter-limb unipepdal static balance values compared to pre-PAPE condition according to paired-samples t-test . It was observed that there was no statistically significant difference between the static balance symmetry angle values of the right and left single leg (p>0.05) (Table 1).

Conclusion

It can be concluded that PAPE conditioning has no significant effect on unipedal static balance asymmetry. It also shows that vibration does not have a negative effect on balance asymmetry, as it causes less destabilizing movements and improved balance ability by suppressing spinal reflex excitability such as muscle stretch reflex during stance (Hrysomallis, 2011).

Balance Assessment	Before	After	*t*	*p*	*d*
Medial	-6,3±21,7	0,5±21,3	-1,359	0,185	0,25
Lateral	6,6±23,1	9,0±19,4	-0,463	0,647	0,08
Front	-0,2±14,4	5,2±17,4	-1,350	0,188	0,25
Back	4,1±23,5	-3,0±22,4	1,278	0,212	0,23

Table 1. Symmetry angles (θ_sym) means (±SD) of inter-limb unipedal static balance

B 03-17

Adherence to a remotely monitored exercise intervention using wearable technology

B. J. Pena Carrillo[1], S. Philip[2], F. Thies[1], D. Blana[3], **B. Gabriel**[1,4]

[1] University of Aberdeen, The Rowett Institute, Aberdeen, UK

[2] Aberdeen Royal Infirmary, Grampian Diabetes Research Unit, Diabetes Centre, Aberdeen, UK

[3] University of Aberdeen, Centre for Health Data Science, Institute of Applied Health Sciences, Aberdeen, UK

[4] Karolinska Institutet, Department of Physiology and Pharmacology, Integrative Physiology, Stockholm, Sweden

Introduction

Type 2 Diabetes is one of the important challenges to healthcare and remains an area of current research. Exercise is beneficial for several organ systems in the body and increases insulin sensitivity (Gabriel & Zierath, 2017). However, previous evidence suggests that exercise at different times of the day in people with Type 2 Diabetes may have opposing outcomes on glycaemia during the day of exercise (Savikj et al., 2018). This may be particularly relevant in people also being prescribed metformin (Gabriel & Zierath, 2021). We hypothesise that evening exercise is more efficacious than morning exercise at lowering glycaemia in people who are also being prescribed metformin. In order to test this hypothesis, we have conducted a remote crossover exercise intervention using wearable technology. Within this exercise intervention we aimed to monitor adherence and compliance to the exercise protocol.

Methods

We recruited 22 people with Type 2 Diabetes on metformin to a non-invasive randomised crossover trial with 2-week baseline recording, six weeks randomly assigned to a morning exercise (7-10am) or afternoon/evening exercise (4-7pm), 2-week wash-out period and another six weeks of the opposing arm of the exercise intervention. To monitor trial adherence, we assessed step count per day and heart rate. Data was monitored using the Garmin Vivosmart 4 watch (Garmin International Inc., Kansas, USA) throughout the entirety of the trial. Participants were asked to perform 30 minutes of running or walking at 70% of their estimated maximum heart rate (220-age≈maximum heart rate) every second day. Adherence was not considered to have been met when participants missed >4 exercise windows within two weeks or a heart rate discrepancy during exercise of >20%.

Results

Seven participants were excluded from the study. Fifteen participants (7 male, 8 female, aged 50-75 year) completed the trial. The mean 70% of maximum heart rate was 112.2±4.9 bpm. Participants reached an average exercising heart rate during the morning intervention of 112.5±8.9 bpm and 111.3±10.7 bpm during the evening intervention. No significative differences in average heart rate were observed between morning or evening exercise ($p>0.05$). During walking days participants completed an average of 10463±2399 steps during the morning intervention and 9764±1870 steps during the evening intervention. No significant difference was observed between morning and evening exercise ($p>0.05$) in the active days. During the resting days participants walked and average of 6426±1802 steps in the morning intervention and 6508±2156 steps in the evening intervention. No significant differences in number of steps were observed between morning and evening exercise ($p>0.05$) during resting days.

Conclusion

Participants with type 2 diabetes had good adherence to a remote, crossover exercise intervention whilst using wearable technology.

References

[1] Gabriel BM & Zierath JR (2021). Zeitgebers of skeletal muscle and implications for metabolic health. The Journal of Physiology; 600(5):1027-1036.

[2] Gabriel, B. M., & Zierath, J. R. (2017). The Limits of Exercise Physiology: From Performance to Health. Cell metabolism, 25(5), 1000–1011.

[3] Savikj, M., Gabriel, B. M., Alm, P. S., Smith, J., Caidahl, K., Björnholm, M., Fritz, T., Krook, A., Zierath, J. R., & Wallberg-Henriksson, H. (2019). Afternoon exercise is more efficacious than morning exercise at improving blood glucose levels in individuals with type 2 diabetes: a randomised crossover trial. Diabetologia, 62(2), 233–237.

B 03-18

MPO Serum Concentration: a potential biomarker to access the impact of a supervised physical exercise program in Breast Cancer survivors?

V. Geraldes[1,2], A. I. Duarte[2], F. Machado[1,2], Â. A. Leal[1,2], I. Rocha[1,2], A. Góis[5], A. Amarelo[3,6], A. Alves[4,6], S. Viamonte[3,6], L. Helguero[5], A. Joaquim[3,6]

[1] Instituto de Fisiologia, Faculdade de Medicina da Universidade de Lisboa, Lisboa, Portugal

[2] Centro Cardiovascular da Universidade de Lisboa, Lisboa, Portugal

[3] Centro Hospitalar de Vila Nova de Gaia/Espinho (CHVNG/E), Vila Nova de Gaia, Portugal

[4] Centro de Investigação em Desporto, Saúde e Desenvolvimento Humano e Instituto Universitário da Maia (CIDESD-ISMAI), Maia, Portugal

[5] Institute of Biomedicine - iBiMED, Department of Medical Sciences, University of Aveiro, Aveiro, Portugal., Aveiro, Portugal

[6] Associação de Investigação de Cuidados de Suporte em Oncologia (AICSO), Vila Nova de Gaia, Portugal

The authors gratefully acknowledge the financial support of Fundação para a Ciência e Tecnologia (FCT), through the TRACKING3C project (Ref: PTDC/MEC-CAR/31626/2017) and UID/BIM/04501/2020. Also to Programa Operacional Regional do Centro (CENTRO-01-0246-FEDER-000018) and Bolsa Dr. Rocha Alves (LPCCNRC). Vera Geraldes acknowledge the post-doctoral fellowship given by the Fundação para a Ciência e Tecnologia (FCT) (Ref: SFRH/BPD/119315/2016) and Ana I. Afonso for her PhD scholarship (2020.09352.BD).

Introduction: Myeloperoxidase (MPO) and growth differentiation factor-15 (GDF-15) are recognized biomarkers of inflammation released in high quantities by infiltrating immune cells in breast cancer and are associated with cardiovascular disease. Anthracyclines are the most commonly prescribed antineoplastic drugs, although they have adverse effects on the heart, leading to progressive cardiomyopathy and heart failure. Antiestrogen treatment, the gold standard in hormone-receptor positive treatment also impacts cardiovascular health and inflammation. Exercise training has been reported to reduce chronic inflammation in various diseases and is safe for most breast cancer (BC) survivors, improving physiological, psychological, and functional parameters. Therefore, in the present work, we sought to investigate the benefits of aerobic and resistance training in BC survivors by measuring leucocytes, MPO, and GDF-15 in serum.

Methods: In a prospective pilot study of 16 BC survivors treated with anthracyclines and/or hormone therapy were recruited at Gaia Hospital (Portugal), in 2018 and 2019, and entered a community-based supervised physical exercise program with a duration of 16-weeks with 3 sessions/week.

Blood samples are collected before (MC1) and at 8 weeks after starting the program (ME1). Serum samples were analyzed by protein multiplex to quantify MPO and GDF-15 levels. Leucocytes were evaluated by flow cytometry. A control (CTL) group matching age and sex was used.
Results: All BC survivors (female, n=13, aged 61±2 and BMC 30±1.2) follow the program and CTL subjects (female, n=13; aged 57±2 and BMC 26±1.2) were sedentary. MOP and GDF-15 serum levels were lower in BC survivors than in CTL before the initiation of the exercise program (CTL: 155860±13690, MC1: 78884±8435 pg/ml and CTL: 291,9± 57,93, MC1: 192,0± 27,99 pg/ml, p<0.0001, respectively). At the end of the training program, MPO (65568± 9393 pg/ml, p<0.05), GDF-15 (170,8± 25,31 pg/ml, p=0.0535), Neutrophiles (MC1: 3423 $x10^3$ cells/µL and ME1: 2929 $x10^3$ cells/µL, p<0.05) and Neutrophiles/Leucocyte (MC1: 0.62 and ME1: 0.58, p<0.05) levels were decreased. No significant changes were observed in Eosinophils, Basophils, Monocytes, or Lymphocytes.
Conclusion: These preliminary results show that a combined aerobic and strength exercise at moderate to vigorous intensity is capable of decreasing MPO and GDF-15 serum levels in BC survivors which is in agreement with reduced levels of Neutrophils and Neutrophil/Lymphocyte ratio, suggesting an improvement in endothelial dysfunction due to a decrease in inflammation and oxidative stress. The impact of neutrophil reduction on innate immunity must be further evaluated. The present data also highlights the putative role of MPO as a reliable biomarker of the efficacy of physical exercise in decreasing inflammation and ameliorating cardiac dysfunction evoked by cardiac aggressors such as anthracyclines, radiotherapy and/or hormonotherapy.

B 03-19

Reliability and correlations of a single-frequency tetrapolar BIA device with DEXA in male university students

H. Moya Amaya[2], A. Molina López[2], A. Portolan[3], D. Rojano Ortega[1], A.J. Berral Aguilar[1], J. Naranjo Orellana[1], F.J. Berral de la Rosa[1]
[1] *University Pablo de Olavide, Sevilla, Spain*
[2] *Udinese Calcio, Udine, Italy*
[3] *Unifarco, Barcelona, Spain*

Introduction
Body composition assessment is a valuable tool for assessing health, nutritional and fitness status (1,2). The main techniques most commonly used to determine body composition are Bioelectrical impedance (BIA), dual energy X-ray absorptiometry (DEXA) and anthropometry. The BIA is mainly used in epidemiological settings, and DEXA in clinical settings to evaluate the body composition (3,4) and both techniques are interchangeable at a population level (5). Most studies focus on high-cost multi-frequency devices (6), although some single-frequency ones have proven useful in the determination of some parameters in healthy (7) or sick subjects (8). Both techniques, BIA and DEXA, have certain limitations (9,10), but the main target of this study whether is determinate is the BIA device could be used in a similar way to determine body composition as DEXA.
The main objective of this study is to investigate the reliability a device that is less invasive than DEXA, and to see the correlations between both devices in order to be able to use it BIA more frequently and efficiently for the healthcare professional.
Methods
The total sample of this study was 18 male university students (age 21,53 ± 2,47 years). Subjects were assessed using an Akern Telelab single-frequency tetrapolar BIA device and a DEXA Hologic. We have studied the normality of the samples through Kolmogorov-Smirnov and Shapiro-Wilk test. For the reliability of this device, correlation analysis as Pearson correlation and Rho de Spearman were carried out with DEXA and BIA values. Moreover, Intraclass Correlation Coefficient (ICC) and Coefficient of Variation (CV) were studied to investigate about the reproducibility of measuring devices using BIA.
Results
BIA shows a high correlation with DEXA in parameters related with muscle mass Free Fat Mass (FFM) (r = 0.931, p<0.01), a moderate correlation with DEXA in Fat Mass (FM) (r = 0.568, p<0.01). and a high correlation with DEXA in Skeletal Muscle Mass (SMM) (r = 0.901, p<0.01).
The ICC results for FM, FFM, Appendicular Skeletal Muscle Mass, Total Body Water, Extracellular Body Water and Intracellular Body Water show an excellent reliability. In the case of SMM and Cellular Mass, the ICC shows a good reliability (Table).
Conclusion
Telelab BIA is a device that presents sufficient reliability to be used in the monitoring of young healthy subjects and could be an interesting option as an alternative to DEXA, due to the good correlations in body composition parameters, reducing risks such as radiation exposure, time and cost and assuming the limitations of this BIA. Future studies should determine the validity of this device versus DEXA in populations of different genders and ages.

Bioimpedance parameters

Bioimpedance Parameters	ICC	CV
Fat Mass	0,966	9,74
Free Fat Mass	0,993	1,52
Skeletal Muscle Mass	0,897	4,87
Appendicular Skeletal Muscle Mass	0,932	4,25
Total Body Water	0,960	3,66
Extracellular Body Water	0,967	3,97
Intracellular Body Water	0,928	3,89
Cellular Mass	0,867	6,33

References

[1] Marra M, Sammarco R, De Lorenzo A, Iellamo F, Siervo M, Pietrobelli A, Donini LM, Santarpia L, Cataldi M, Pasanisi F, Contaldo F. Assessment of Body Composition in Health and Disease Using Bioelectrical Impedance Analysis (BIA) and Dual Energy X-Ray Absorptiometry (DXA): A Critical Overview. Contrast Media Mol Imaging. 2019;2019:3548284.
[2] Thibault R, Genton L, Pichard C. Body composition: why, when and for who? Clin Nutr. 2012;31(4):435-47.
[3] Grover I, Singh N, Gunjan D, Pandey RM, Chandra Sati H, Saraya A. Comparison of Anthropometry, Bioelectrical Impedance, and Dual-energy X-ray Absorptiometry for Body Composition in Cirrhosis. J Clin Exp Hepatol. 2022;12(2):467-474.
[4] Achamrah N, Colange G, Delay J, Rimbert A, Folope V, Petit A, Grigioni S, Déchelotte P, Coëffier M. Comparison of body composition assessment by DXA and BIA according to the body mass index: A retrospective study on 3655 measures. PLoS One. 2018;13(7):e0200465.

[5] Nickerson BS. Agreement between single-frequency bioimpedance analysis and dual energy x-ray absorptiometry varies based on sex and segmental mass. Nutr Res. 2018;54:33-39.

B 03-20

Effect of Sprint Interval Training on Yo-Yo Intermittent Recovery Test Scores in Cricket Players: Randomised Controlled Trial

I. H. Mohammad, K. M. Badaam

Government Medical College, Aurangabad, Department of Physiology, Aurangabad, India

We acknowledge the support from Dr. Syeda Afroz, Professor and Head, Department of Physiology, Dr Nanda Somwanshi, Professor, Department of Physiology, Faculty from Physiology department and the Dean of our Institute.

Introduction

Cricket involves mainly bat and ball and has complex rules requiring physical fitness and skill, although the technique has a predominant role. The fitness demands of competitive cricket have increased manifold. [1-2] Yo-Yo intermittent recovery (IR) test is a validated test for assessing the ability of a person to undergo repeated intense exercise. It is a simple test to assess the aerobic capacity and the change in fitness levels to carry out repeated, intense exercise [3]. Sprint interval training (SIT) has been found to enhance the Yo-Yo intermittent recovery test (YYIT) scores in athletes playing team sports like soccer and hockey [4-5]. The present study was undertaken to assess the effect of SIT on the YYIT scores in club level cricket players.

Methods

The Randomised Controlled Trial enrolled male cricket players (18-30 years) with minimum 5 years of club level cricket experience. Sample size estimated was 7 players in each group as per apriori calculation for a single tailed hypothesis, α at 0.05 and 80% power of the study. 9 subjects in each group were enrolled to take care of loss to follow up. They were assigned to groups by computer generated randomisation process. Study was approved by Institutional Ethics Committee and informed consent was taken from partcipants. The SIT group did high intensity sprint exercise at intensity (>65% heart rate above resting heart rate) for 10 minutes a day in four cycles of 2.5 minutes each. In each cycle one minute all out running effort was made and it was followed by 1.5 minutes recovery period of slow walking. So, each cycle comprised of 2.5 minutes and such 4 cycles meant a total of 10 minutes. This protocol was done alternate day and thrice a week (Total of 30 minutes a week). This group did this additional training apart from the routine practice drills. The control group did regular cricket training which continued with their routine practice guidelines. Intervention duration of the study was 8 weeks. YYIT score was assessed before and after intervention.

Results

Mean age of the participants was 21.6 ± 2.9 years in control group (n=9) and 21 ± 3.4 years in SIT group (n=9). All players completed the study. In control group, the YYIT score changed from 14.9 ± 0.7 to 15 ± 0.6 with no significant difference (paired t test, p=0.2165). In SIT group, the YYIT score improved from 14.7 ± 0.7 to 15.6 ± 0.5 with statistically significant difference (paired t test, p= 0.0005) after the intervention of 8 weeks. The change in YYIT score was 0.1 ± 0.2 in control group and 0.9 ± 0.5 in SIT group. This between group difference was statistically significant (unpaired t test, p value- 0.0003). Thus, sprint interval training improved the YYIT score significantly as compared to the regular training.

Conclusion

SIT is an efficient mode of improving the YYIT scores and considering that the magnitude of time required is also quite less, it can gain popularity by raising awareness among the players.

Table 1: Baseline characteristics of the participants

Parameter	Regular Training	Sprint Interval Training
Age (years)	21.56 ± 2.92	21 ± 3.43
Weight (kg)	64.07 ± 5.71	65.37 ± 6.89
Height (m)	1.72 ± 0.04	1.73 ± 0.04
BMI (kg/m^2)	22.08 ± 2.75	21.83 ± 2.69

Table 2: YYIT Score in Cricket Players before and after Intervention

Parameter	Regular Training		p value	Sprint Interval Training		p value
	Before	After		Before	After	
YYIT score	14.9 ± 0.7	15 ± 0.6	0.2165	14.7 ± 0.7	15.6 ± 0.5	0.0005*
Change in YYIT score	0.1 ± 0.2			0.9 ± 0.5		0.0003*

References

[1] Pardiwala DN, Rao NN, Varshney AV. Injuries in Cricket. Sports Health. 2018 May/Jun;10(3):217-222. doi: 10.1177/1941738117732318.

[2] Orchard J, James T, Kountouris A, Portus M. Changes to injury profile (and recommended cricket injury definitions) based on the increased frequency of Twenty20 cricket matches. Open Access J Sports Med. 2010 May 19;1:63-76. doi: 10.2147/oajsm.s9671.

[3] Bangsbo J, Iaia FM, Krustrup P. The Yo-Yo intermittent recovery test: a useful tool for evaluation of physical performance in intermittent sports. Sports Med. 2008;38(1):37-51. doi: 10.2165/00007256-200838010-00004.

[4] Jones B, Hamilton DK, Cooper CE. Muscle oxygen changes following Sprint Interval Cycling training in elite field hockey players. PLoS One. 2015 Mar 25;10(3):e0120338. doi: 10.1371/journal.pone.0120338.

[5] Wahl P, Güldner M, Mester J. Effects and sustainability of a 13-day high-intensity shock microcycle in soccer. J Sports Sci Med. 2014 May 1;13(2):259-65.

B 03-21

Cardio-physiological adaptation in handball players during Bruce treadmill test

J. Pluncevic Gligoroska, B. Dejanova, V. Cao
University Ss Cyril and Methodius, Faculty of Medicine/Institute of Physiology I, Skopje, Macedonia

Introduction
Ergometrical testing in athletes is method for monitoring the cardiophysiological parameters as indicator of the cardiovascular health and the physical fitness. The ultimate product of Bruce protocol is maxymal oxygen consumption ($VO2_{max}$). A grafical presentation of the Bruce test's result is the heart rates curve which is made of mean values of heart frequency for each minute, starting with heart rate during resting period, through the ten consequent minutes of the treadmil testing, until the end of 3 minutes recovery period.
Methods
28 male HB players from two top ranking teams from R.N.Macedonia were tested ergometrically with Bruce protocol for determination of maximal oxygen consumption. Body analysis was made with bioelectrical impedance analyzer, InBody 720.
Results
Anthropometric parameters were as follows: mean height was 190.4 ± 7.8 cm and weight 96.3 ± 15.5 kg, skeletal muscle mass (SMM) = 47.11±6.69 kg; BMI = 26.38 ± 3.1; BF%=15.04 ±6.01 and WHR = 0.9 ±1.8. The result of ergometrical test produce mean VO2 max= 43.92 ml/kg/min which is 100.46% of reference value.
Conclusion
Bruce protocol heart rates curve showed succesful cardiovascular adaptation to submaximal effort in handball players from elite macedonian handball teams. The general endurance expressed with maxymal oxygen consumpiton was at level of healthy active people.

PB 05 | Metabolism & Endocrinology

B 05-01

Impact of omnivorous and vegetarian dietary patterns on body composition and metabolic markers

C. Ferreira-Pêgo, T. Fontes, S. Lopes, R. Menezes, L. M. Rodrigues
Universidade Lusófona de Humanidades e Tecnologias, CBIOS, Lisbon, Portugal

ACKNOWLEDGMENTS: *The authors acknowledge all the participants.*

Introduction: Plant-based diets are believed to benefit multiple nutrition-related metabolic outcomes. Nevertheless, evidence on these matters is often insufficient and sometimes contradictory. This study aimed to identify differences between omnivorous (OM) and vegetarian (VG) participants regarding total body composition, biochemical parameters, and food group intake.
Methods: The total body composition of 208 human individuals (132 OM, 76 VG) was assessed using dual-energy x-ray absorptiometry (DXA Lunar-GE Healthcare®). Dietary intake was assessed using a validated food frequency questionnaire. Specific biochemical parameters were obtained (LINX DUO, Menarini) from capillary blood from 92 of the participants (65 OM, 27 VG). All variables were collected by trained registered dietitians.
Results: Statistically significant differences were found only for age (mean=29.27 years), with the VG being older than OM participants (32.72 vs. 27.28 years). No differences were observed between groups for the body mass index (BMI=22.87 kg/m^2 [SD=4.39]) or any other body composition variables, including visceral and subcutaneous adipose tissue, fat mass, or lean mass. The OM group presented significantly higher levels of total cholesterol, LDL cholesterol, non-HDL cholesterol, and a higher heart rate. Total cholesterol was positively correlated with the consumption of cheese, tubers, sugar-sweetened beverages, and seafood, and negatively correlated with the intake of vegetable drinks. Similar results were found for LDL cholesterol and non-HDL cholesterol, and also when analyzed for omnivorous and vegetarians separately. Heart rate was positively correlated with the consumption of ice creams and desserts.
Conclusion: The dietary regime seems not to significantly influence body composition. However, the statistically significant differences detected in the blood lipid profile might have other repercussions (e.g., cardiovascular risk) that should be investigated.

B 05-02

***Cryptosporidium parvum* infection modulates glucose metabolism, transport and barrier function in intestinal epithelium of neonatal calves**

F. Dengler[1], C. Delling[2], W. Liermann[3], C. Helm[4], R. Ulrich[4], L. Bachmann[5], H. M. Hammon[3]
[1] *University of Veterinary Medicine, Institute of Physiology, Pathophysiology and Biophysics, Vienna, Austria*
[2] *University of Leipzig, Institute of Parasitology, Leipzig, Germany*
[3] *Leibniz Institute for Farm Animal Biology, Dummerstorf, Germany*
[4] *University of Leipzig, Institute for Veterinary Pathology, Leipzig, Germany*
[5] *University of Applied Sciences Neubrandenburg, Neubrandenburg, Germany*

Introduction
Beyond posing an immense economic problem in calf rearing, infection with *C. parvum* is a life-threatening zoonosis causing massive diarrhea especially in children and immune-deficient people. So far, there is no fully effective therapy available, which is at least partly due to lacking understanding of the pathophysiology. Previous studies in cell culture models indicated an interference of the infection with intestinal glucose uptake and metabolism. Therefore, we aimed to investigate the effects of infection with *C. parvum* in neonatal calves on the transepithelial transport and metabolism of glucose *in vivo*.
Methods
Neonatal calves were infected with $2x10^7$ *C. parvum* oocysts (INF, N=5) while a control group (CON, N=5) was administered H_2O orally. The feeding regime was identical in all animals. Clinical parameters and fecal shedding of *C. parvum* oocysts were monitored for one week. 6 days post infection (p.i.) rates of systemic glucose appearance were monitored after application of [$^{13}C_6$]- (orally) and [$^2H_2$]-labelled glucose (i.v.). On day 7 p.i. the calves were sacrificed; the isolated distal jejunum epithelium was mounted in Ussing chambers and the electrogenic glucose uptake via Na^+-linked transport (SGLT1) was evaluated. The mRNA and protein expression of genes involved in glucose transport and metabolism as well as epithelial barrier function was assessed by RT-qPCR

and Western Blot. Data were pooled for each animal and the groups were compared using a Student's t-test. Statistically significant differences were assumed at $p<0.05$.

Results

On day 4, 6 and 7 p.i. plasma glucose concentrations of INF were lower compared to CON. In line with this, the appearance rate of orally applied [$^{13}C_6$]-glucose in the circulation was significantly higher in CON compared to INF, whereas the systemic metabolism represented by [$^{2}H_2$] was not different. Ussing chamber experiments revealed a significant increase of phlorizin-sensitive electrogenic transport of glucose across the infected epithelia compared to CON, but SGLT1 expression was not changed on mRNA or protein level, whereas enzymes of glycolysis and claudins 3 and 4 were upregulated. Tissue conductance was similar in both groups.

Conclusion

Our results indicate an upregulation of glucose uptake and metabolism machinery in *C. parvum* infected jejunum epithelium at simultaneously lower systemic blood glucose levels and reduced oral glucose appearance rate in infected animals. This might indicate an increased metabolic demand of the enterocytes due to the infection and/or a nutritional competition of the parasite, diminishing the glucose supply of the host. In contrast to the prevailing view that glucose uptake is disturbed in *C. parvum* infection, the enterocytes seem to attempt to compensate and increase the transport capacities for glucose uptake. The upregulation of tight junction proteins might indicate an attempt to sustain the epithelial barrier function during infection.

B 05-03

Mitochondria energetics; diving versus non-diving mammals

S. Núñez Egido, S. Geiseler, O. J. How

UiT - The Arctic University of Norway, Cardiovascular Research Group, Tromsø, Norway

Introduction

Diving mammals rely on metabolic and physiological adjustments to sustain low oxygen levels (Ramirez et al., 2007). Little is known about such adaptations to hypoxia at the mitochondrial level. This study describes mitochondria energetics by high-resolution respirometry in the heart, kidney and liver from diving and non-diving mammals.

Methods

Fresh heart, kidney and liver tissue samples were harvested from NMRI mice (*Mus musculus,* n=7), Wister rats (*Rattus norvegicus*, n=8), reindeers (*Rangifer tarandus*, n=5) and hooded seal pups (*Cystophora cristata*, n=6). Samples were immediately placed in ice-cold A1 buffer (250mM sucrose, 0.5mM Na_2EDTA, 10mM Tris) and homogenized. High-resolution respirometry measurements were carried out, using the Oxygraph-2k high-resolution respirometer. A Substrate-Uncoupler-Inhibitor Titration (SUIT) protocol was designed to assess LEAK respiration, OXPHOS state and electron transport system (ETS) capacity with pyruvate as substrate. Outer membrane integrity was evaluated by Cytochrome C addition, and the respiratory control ratio (RCR), as OXPHOS/LEAK, calculated. MS Excel and Graphpad Prism 9 were used for statistical analyses and plotting. One-way ANOVA with *post hoc* Tukey's tests ($p < 0,05$) was performed to show individual differences in between groups.

Results

Table 1 summarizes RCR values as means ± standard deviations for all samples analysed. Statystical analyses showed significant differences in kidney efficiency in between the rodents and the reindeers and seals; with the highest values found in the larger mammals. Contrary to the kidney, higher RCR values and efficiency is reported for the liver of rodents when compared to the reindeers and seals. Heart RCR values remain quite similar in all the studied animal groups. There are no significant differences in mitochondiral efficiency in any of the organs analysed between reindeers and seals.

Table 1. Respiratory control ratio (RCR) values presented as group means ± standard deviations for the heart, kidney and liver of mice (*Mus musculus*), rats (*Rattus norvegicus*), reindeers (*Rangifer tarandus*) and hooded seals (*Cystophora cristata*) when pyruvate is used as substrate.

	Mice		Rats		Reindeers	Seals
Heart	9.16 ± 2.26	9.97 ± 0.67	10.49 ± 1.71	9.71 ± 2.56		
Kidney	4.27 ± 0.58^{a,b}	4.98 ± 0.81^{c,d}	8.66 ± 1.1^{a,c}	8.81 ± 1.65^{b,d}		
Liver	10.93 ± 2,32^{e,f}	10.21 ± 1.85^{g,h}	4.52 ± 0.62^{e,g}	3.48 ± 1.21^{f,h}		

^{a,b,c,d,e,f,g,h}denotes significant difference, i.e. a vs a, b vs b and so on

Conclusion

This study provides a mitochondrial function overview for different animal species. Mitochondrial efficiency seems to differ in the kidney and liver between the animal groups, but remains similar for the heart. More research is needed to elucidate these differences and understand the possible implications for hypoxia adaptation.

References

[1] Ramirez, JM, Folkow, LP, Blix, AS 2007, 'Hypoxia tolerance in mammals and birds: from the wilderness to the clinic', *Annual Review of Physiology, 69*, 113-143, California (USA): Annual Reviews.

B 05-04

The metabolic transition from famine to feast: pre-absorptive tissue remodeling is required for rapid postprandial skeletal muscle protein synthesis in the Burmese python

E. Rindom, K. B. Last, T. Wang

Aarhus University, Department of Biology, Aarhus, Denmark

This study was supported by the NOVO Nordisk Foundation (NNF21OC0071589) and the Danish Council for Independent Research (Det Frie Forskningsråd| Natur og Univers; 7014-00375A).

Sit-and-wait predators, such as Burmese pythons, are renowned for their ability to devour enormous meals and digestion is accompanied by a massive and rapid rise in metabolism, believed to support protein synthesis as all tissues growth as the prey is assimilated. Metabolism increases already within the first few hours after ingestion, when the ingested prey still remains intact and undigested in the stomach lumen. How can pythons support this metabolic transition? As prey-derived nutrients are unlikely to have been absorbed at this early time-point, we hypothesize that the metabolic transition from fasting to feast is fueled by breakdown of endogenous protein.

Pythons were instrumented with arterial catheters allowing for vascular injections of drugs as well as withdrawal of blood samples from undisturbed animals. All snakes ate voluntarily when presented with dead mice on the following day. Skeletal muscle protein synthesis was measured by

incorporation of exogenous puromycin into nascent peptides and plasma amino acid concentrations were measured with high-performance liquid chromatography. We measured a five-fold rise in the rate of protein synthesis already 1-3 hours after ingestion, while there was no change in plasma amino acid concentration for the first 6 hours. In a subset of snakes, chemical inhibitors of the autophagy-lysosomal and the ubiquitin-proteasomal systems, chloroquine and epoxomicin, were administered prior to feeding to prevent degradation of endogenous proteins. This treatment greatly alleviated the early stimulation of protein synthesis, as well as the early rise in oxygen consumption. These findings suggest that the initial rise in protein synthesis is dependent on breakdown of endogenous proteins and that these processes account for early rise in metabolism. In current studies, we investigate how the nutrient-independent signal is initiated, and what pools of endogenous proteins are actually degraded to support digestion?

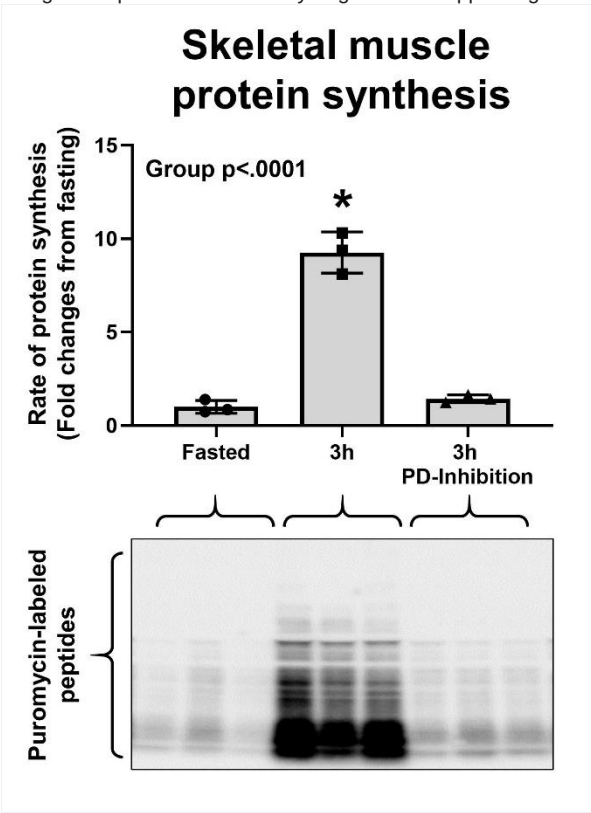

Breakdown of endogenous proteins is required for the rapid rise in postprandial protein synthesis

Puromycin-labeling was used to measure rate of postprandial protein synthesis in fasting snakes, digesting snakes at 3 hours after feeding of a standard rodent meal, and digesting snakes at 3 hours after feeding of a standard rodent meal receiving intravascular injections of Chloroquine and Epoxomycin. a One-way ANOVA was used to test for a group effect as indicated in the upper left corner and Tukey's posthoc test was used to determine differences between individual groups. *P<0.05, (n = 3 animals per group). Data is presented as Mean ± SD.

B 05-05

Association of obesity with *CD36* gene polymorphisms and hypermethylation in Senegalese women

M. Touré[1,2], A. S. Khan[2], A. Hichami[2], A. Samb[1], N. A. Khan[2]

[1] *Université Cheikh Anta Diop (UCAD), Laboratoire de Physiologie Humaine et d'Explorations Fonctionnelles, FMPOS / IRL3189 ESS « Environnement, Santé, Sociétés », CNRS, CNRST, UCAD, Dakar, Senegal*

[2] *Université de Bourgogne-Franche Comté (UBFC), Physiologie de la Nutrition & Toxicologie, INSERM U1231, 21000 Dijon AgroSup, France*

Acknowledgment

- *Participants*
- *UMI3189 ESS "Environnement, Santé, Sociétés"*
- *NuTox, Dijon 21000*

Introduction

obesity and related metabolic disorders are associated with genetic and epigenetic alterations. Here, we have examined the association between polymorphisms and methylation of the *CD36* gene promoter with obesity in Senegalese women.

Methods

the study was conducted with healthy lean control and obese women (age; 49.98 years ± 7.52 vs 50.50 years ± 8.76 and BMI; 24.19 kg/m² ± 2.74 vs 34.30 kg/m² ± 4.41). We determined three genetic polymorphisms of *CD36* i.e., rs1761667, rs1527483, and rs3211867 by real-time polymerase chain reaction (RT-PCR), and methylation of CPG islands of *CD36* was assessed by methylation-specific polymerase chain reaction (MS-PCR) in DNA isolated from peripheral blood of each participant. Plasma CD36 and DNMT3a were determined by ELISA. Biochemical parameters were analyzed from fasting serum or plasma according to the standard laboratory protocol.

Results

for rs3211867, obese subjects harboring the AA/AC genotype had significantly higher BMI (35.3 ± 5.0 & 33.3 ± 3.5; p=0.02) than obese subjects harboring the CC genotype. At the same time, for rs1527483, only the control subjects had statistically significant different parameters depending on the genotypic distribution. The control subjects harboring the GG genotype had a significantly higher BMI than the control subjects harboring the AA/AG genotype (p=0.003).

The *CD36* gene methylation was 1.36 times more associated with obesity compared to lean control (RR=1.36; p=0.04). DNMT3a levels were higher in subjects with *CD36* gene methylation than in subjects without *CD36* gene methylation in each group. In the control group, an increase in sCD36 levels would be associated with a decrease in total cholesterol and triglyceride levels (coef = -7647.56 p=0.01 and coef=-2528.50 p=0.048, respectively) would be associated with an increase in LDL cholesterol levels (coef = 11547.28 p<0.0001*). For the obese group, an increase in sCD36 levels would be associated with an increase in fasting insulin levels (coef=490.99 p=0.02) and a decrease in glycated hemoglobin levels (coef = -1196.26 p= 0.03).

The AA/AC genotype of rs3211867 polymorphism was significantly associated with *CD36* gene methylation in the control group (p=0.05; 95% CI).

Conclusion

these observations suggest that polymorphisms and epigenetic changes in *CD36* gene promoters may be implicated in the onset of obesity in Senegalese women.

B 05-06

Dietary low molar mass oat beta-glucans influence the blood hematology parameters and colon lymphocytes profile in the early stage of colorectal cancer

W. Grodzicki[1], L. Kopiasz[1], M. Gajewska[2], K. Dziendzikowska[1], J. Harasym[3], J. Gromadzka-Ostrowska[1]

[1] *Warsaw University of Life Sciences, Department of Dietetics, Institute of Human Nutrition Sciences, Warsaw, Poland*

[2] *Warsaw University of Life Sciences, Department of Physiological Sciences, Institute of Veterinary Medicine, Warsaw, Poland*

[3] *Wrocław University of Economics, Adaptive Food Systems Accelerator—Research Centre, Wrocław, Poland*

The authors acknowledge the financial support of the National Science Centre, Poland (grant no. 2018/29/B/NZ9/01060).

Introduction: Beta-glucans are a dietary fiber fraction naturally occurring in the cell walls of fungi, yeast, seaweed, and higher plants such as cereals composed of D-glucose monomers linked by β-1,3, β-1,4, or β-1,6 glycosidic bonds. Due to their specific structure, they are characterized by attractive health-promoting properties, including an anti-inflammatory effect. Therefore, this study aimed to evaluate the activity of oat beta-glucans in the early stage of colon cancer.

Methods: Forty-five male Sprague-Dawley rats were divided into two main groups: with early stage of colon cancer experimentally induced by azoxymethane intraperitoneal (i.p.) injection (CRC group, n=24) and control animals i.p. injected with 0.9% NaCl (control group, n=21). Both main groups were divided into three dietary subgroups fed AIN-93M feed with 1% w/w (subgroup BGl+1%) or 3% w/w (subgroup BGl+3%) low molar mass oat beta-glucan or AIN-93M feed without oat beta-glucan (subgroup BGl-). After 8 weeks of experiment, rats were sacrificed and blood and colons were sampled. The count of blood cells was analyzed by electrical impedance method (Coulter principle) and the profile of colon lamina propria lymphocytes (LPL) subpopulations were analyzed by flow cytometry. Results were expressed as a percentage of specific lymphocytes within LPL population and as the number of leukocytes in whole blood samples.

Results: The results showed that colon carcinogenesis significantly influenced the immune cells population both in the colon and systemic circulation. Significant differences were observed in T cells subpopulation of the colon's LPL as well as in the number of white blood cells (WBC), and lymphocytes (LYM) in blood. In CRC BGl- group populations of cytotoxic T lymphocytes (Tc: CD3+CD8+) in LPL were significantly higher, and helper T lymphocytes (Th: CD3+CD4+) were significantly lower than in the control BGl- group. Consumption of feed with 3% oat beta-glucan resulted in restoring both T lymphocyte subpopulations to the level detected in the control group. Moreover, the WBC and LYM counts were significantly lower than the control BGl- group and rats with CRC fed with feed containing beta-glucan had similar numbers of these blood cells as the control groups.

Conclusion: The early stage of colon carcinogenesis resulted in a significant increase in Tc cells and a decrease in Th cells subpopulation within the lamina propria as well as a lower number of WBC and LYM in blood. Low molar mass oat beta-glucan supplementation reversed this effect. These results indicate the potential activity of low molar mass oat beta-glucan at the early stage of colon cancerogenesis and suggest that these polysaccharides may be useful as a supporting agent in the prevention of the early stages of colon cancer.

B 05-07

Aphanizomenon flos aquae (AFA) extract intake accelerates the reversion of the metabolic dysfunctions in mice with diet-induced obesity.

A. Amato[1], S. Terzo[1], P. Calvi[2], M. Di Carlo[3], G. Gallizzi[3], F. Mulè[1]

[1] *University of Palermo, Department of Biological- Chemical- Pharmaceutical Science and Technology, Palermo, Italy*

[2] *University of Palermo, Department of Biomedicine, Neuroscience and Advanced Diagnostic, palermo, Italy*

[3] *CNR, Biomedical Research and Innovation Institute, Palermo, Italy*

This work was supported by the company Nutrigea, BorgoMaggiore, Republic of SanMarino

Several evidence indicates that an High Fat Diet (HFD) is involved in the onset of obesity and the related metabolic diseases. The consuption of foods with anti-oxidant and anti-inflammatory properties could help to lower the risk of the onset and progression of metabolic dysfunctions and could be proposed as alternative or integrative therapeutic tool to treat dysmetabolic diseases. The *Aphanizomenon flos aquae* (AFA) is a peculiar variety of microalgae considered one of the most nutrient-dense foods rich of compounds with well-known antioxidant and anti-inflammatory properties.Much evidence has shown AFA's ability to prevent the progression of chronic diseases such as cancer and colitis. However, no data are about AFA's beneficial effects on obesity and related metabolic dysfunctions. Therefore, the purpose of the present study was to analyze if the daily intake of one of the commercialized AFA extracts, KlamExtra, was able to accelerate the reversion of the obesity-related metabolic dysfunctions in a mouse model of HFD-induced obesity.

For this purpose, we investigated the effects of switching HFD fed obese mice back to a standard diet (STD), alone or in combination with KlamExtra (25 mg/die). C57BL/6J mice were divided into four groups: 1) control animals fed with a standard diet (STD) for 18 weeks; 2) obese animals fed with HFD (HFD) for 18 weeks; 3) mice fed HFD for 10 weeks followed by 8 weeks of the standard cow (HFD→STD); 4) mice fed HFD for 10 weeks followed by 8 weeks of standard cow supplemented with KalmExtra (25 mg/die) (HFD→STD+AFA). Bodyweight, food intake, lipaemia, hyperglycemia, glucose tolerance, insulin sensitivity and insulin resistance (HOMA-index), hepatic steatosis, adipocyte size, hepatic inflammation (protein expression of NfkB, TNF-α, IL-10), and hepatic gene expression of lipid metabolism factors (FAT-P, FAS, SCD1, SREBP-1c), were analyzed and compared among the different groups of animals.

The diet reversal supplemented with AFA's extract resulted in marked reductions in body weight, fasting glucose levels, insulin sensitivity, and HOMA index when compared to the obese control and obese mice fed with the only standard cow. Cholesterol plasma level was significantly ameliorated in obese mice fed STD+AFA in comparison with HFD and HFD→STD animals, while hepatic steatosis was completely normalized and adipocyte size was significantly lower in mice fed STD+AFA compared to both obese mice and obese mice fed only STD. AFA-diet was able to strongly reduce HFD-induced hepatic overexpression of FAS, SCD1, and SREBP-1c compared to HFD→STD mice. Similarly, STD plus AFA diet significantly ameliorated the hepatic expression levels of NfkB, TNF-α, and IL-10 compared to the only STD diet.

In conclusion, our data show that AFA supplementation can accelerate the STD-induced reversion of obesity-related dysfunctions by positively modulating the expression of hepatic genes linked to lipid metabolism and inflammation.

B 05-09

Omega-3 supplementation and changes in AA/EPA and AA/DHA ratios in professional football players.

A. Molina López[2], H. Moya Amaya[2], P. Estevan Navarro[2], P. Baratto[3], D. Rojano Ortega[1], F.J. Berral de la Rosa[1], J. Naranjo Orellana[1]

[1] *University Pablo de Olavide, Sevilla, Spain*

[2] *Udinese Calcio, Udine, Italy*

[3] *Unifarco, Barcelona, Spain*

Introduction

Omega-3 has been studied in the improvement of different parameters of inflammation and sports performance (1)(2)(3)(4). In the field of elite sport, this compound has become particularly important in recent years, and numerous studies have been carried out to establish an administration protocol and to obtain clearly defined biochemical effects (5). The aim of this study is to establish whether the administration of an omega-3 supplement improves the parameters of Eicosapentaenoic acid (EPA) and Docosahexaenoic acid (DHA) at blood level in professional football players (3).

Methods

The sample was divided into intervention group (n=11) and control group (n=7). Total of 18 players of the first team of Udinese Calcio, an Italian first division football team (Serie A) were assessed. During the pre-season period, subjects underwent a fasting blood test before and after a one-month retreat in Austria, where they were monitored in terms of training, nutrition and rest. Arachidonic Acid/Eicosapentaenoic Acid (AA/EPA) ratio and Arachidonic Acid/Docosahexanoic Acid (AA/DHA) ratio values were assessed in blood. The product administered daily to the intervention group was an omega-3 supplement providing a dose of 1 g EPA and 0.7 g DHA, and was delivered to the players in individualised doses prepared by the TIMEDI JV-DEN dispensing robot. The intervention group (n=11) achieved a weekly intake of more than 90% of the intakes. The control group (n=7) did not receive omega-3 supplementation.

Results

The results obtained from the players are shown in the table. Supplementation significantly improved the value of the AA/EPA ratio, as previously observed in other studies (6). In contrast, the value of the AA/DHA ratio improved but not significantly, which may be due to the fact that EPA and DHA compete with each other when administered together (7) or because the dose administered was not sufficient. On the other hand, the players in the control group did not improve their values in both parameters (AA/EPA and AA/DHA), and even worsened in the AA/EPA value.

Conclusion

Omega-3 supplementation over a controlled period of time is effective in improving biochemical AA/EPA and AA/DHA ratios in professional football players. The administration of 1g of EPA daily together with a correct diet supervised by the nutritionist is sufficient to achieve a better balance of the AA/EPA ratio. In contrast, the administration of 0.7g of DHA is not sufficient to significantly improve the AA/DHA ratio.

	Parameters	Pre-test Mean ± SD	Post-test Mean ± SD	*p-value*
Intervention group n = 11	AA/DHA	2,72 ± 1,07	2,48 ± 0,59	0,722
	AA/EPA	4,25 ± 2,47	0,75 ± 0,35	0,001**
Control group n = 7	AA/DHA	3,80 ± 1,18	3,65 ± 0,54	0,661
	AA/EPA	8,97 ± 4,44	9,57 ± 8,31	0,805

AA/DHA, Arachidonic Acid/Docosahexaenoic Acid Ratio
AA/EPA: Arachidonic Acid/Eicosapentanoic Acid Index.
*Significant differences between pre and post. * p < 0.05, ** p < 0.01.

Results of supplementation

References

[1] Goldberg RJ, Katz J. A meta-analysis of the analgesic effects of omega-3 polyunsaturated fatty acid supplementation for inflammatory joint pain. Pain. 2007;129(1–2):210–23.

[2] Shahidi F, Ambigaipalan P. Omega-3 Polyunsaturated Fatty Acids and Their Health Benefits. Annu Rev Food Sci Technol. 2018;9:345-81.

[3] Dinicolantonio JJ, O'Keefe JH. Importance of maintaining a low omega-6/omega-3 ratio for reducing inflammation. Vol. 5, Open Heart. BMJ Publishing Group; 2018.

[4] McGlory C, Calder PC, Nunes EA. The Influence of Omega-3 Fatty Acids on Skeletal Muscle Protein Turnover in Health, Disuse, and Disease. Front Nutr. 2019;6(September):1-13.

[5] Nelson JR, Raskin S. The eicosapentaenoic acid:arachidonic acid ratio and its clinical utility in cardiovascular disease. Postgrad Med [Internet]. 2019;131(4):268-77.

B 05-10

Hypoxia induces activation of Mineralocorticoid receptor.

M. M. Mohib[1], S. Rabe[1], A. Zipprich[2], M. Gekle[1], B. Schreier[1]

[1] *Martin Luther University of Halle-Wittenberg, Julius Bernstein Institute of Physiology, Medical School, Halle (Saale), Germany*

[2] *Universitätsklinikum Jena, Clinic for Internal Medicine IV, Jena, Germany*

Introduction

The mineraolcorticoid receptor (MR) belongs to the nuclear receptor family and regulates water and electrolyte homeostasis in the body. In pathophysiological situations, the MR contributes to fibrosis in various tissues. In healthy liver, the main cell types expressing MR are hepatocytes. In an experimental cirrhosis model, reduction of MR mRNA and protein expression was observed. Moreover, MR is already predominantly located in the nucleus of hepatocytes exposed to low oxygen tension under baseline conditions, indicating an increased activation of MR due to micromilieu changes. Treatment with the MR antagonist eplerenone reduced extracellular matrix deposition, spleen weight (indicator of portal hypertension), and restored liver weight. Interestingly, both the glucocorticoid receptor (GR) and MR share the same hormone response element in the

nucleus but have different effects. In our current study, we investigate the changes in the microenvironment and intracellular mechanisms involved in the activation of MR in hepatocytes.

Methods

We stimulated human hepatoma cells (HepG2) with lipopolysaccharides (1 & 10 µg/mL LPS), extracellular acidosis (pH 6.6) and hypoxia (0.2% O2) for 24 hours and analysed MR expression at protein and mRNA levels. In addition, we incubated our cells with the MR ligand aldosterone (10 nM) and the MR antagonist eplerenone (5 µM). As, MR and GR affect the expression of an overlapping set of genes, we treated the cells with Ru 486 (1 µM), an antagonist of GR. We used real-time qRT-PCR to determine the mRNA levels of various genes and Western blot to determine the expression of MR protein. HEK cells were co-transfected with reporter gene plasmids for GRE-SEAP, NF-κB-SEAP and MR-construct or with an empty vector. 24 hours after transfection, cells were exposed to normoxia (20% O2) or hypoxia (1% O2) with or without the addition of aldosterone (10 nM).

Results

To analyse the functionality of MR in HepG2 cells, the expression of several MR-responsive genes were analysed. PAI-1, SGK-1, TGF-ß, CTGF, Col1a1 are significantly upregulated upon stimulation with aldosterone. As evidence for the functionality of our interventions, we analysed the expression of TNF-α and HIF-2α. Both LPS and extracellular acidosis increased the expression of TNF-α but only Hypoxia increased HIF-2α expression. Interestingly, only under hypoxic conditions, the expression of MR mRNA as well as MR protein is reduced. Even though, MR expression was reduced, there is an up-regulation of PAI-1 and TGF-β that can be reduced by eplerenone treatment. This suggests MR activation under hypoxia. Interestingly, MR activity at the GRE element is significantly reduced, while NF-κB reporter gene activity is significantly increased under hypoxia.

Conclusion

Our results revealed that hypoxia can induce activation of the MR in hepatocytes, which might lead to a pro fibrotic phenotype in these cells.

B 05-11

Dietary patterns and their impacts on skin physiology

S. F. Andrade, T. M. Ferreira, T. Fontes, S. Lopes, R. Menezes, C. Ferreira-Pêgo, L. M. Rodrigues

Lusofona University, CBIOS/ECTS, Lisbon, Portugal

This work is funded by national funds through FCT - Foundation for Science and Technology, I.P., under the UIDB/04567/2020 and UIDP/ 04567/2020 projects. Cíntia Ferreira Pêgo is funded by Foundation for Science and Technology (FCT) Scientific Employment Stimulus contract with the reference number CEEC/CBIOS/NUT/2018.

Introduction

A growing number of studies suggest dietary patterns influence skin physiology and might affect the progression of several cutaneous diseases[1,2]. However, the effect of dietary patterns on skin health has not been sufficiently characterized. Therefore, in the present study, we compared the cutaneous physiology of vegan-vegetarian (VG) and omnivorous (OM) participants relating these to the highest impact food groups.

Methods

Our study involved 122 healthy volunteers, both sexes. These included 82 omnivores (32.0 ± 13.1 y.o.) and 40 vegetarians (34.0 ± 9.62 y.o) with similar Body Mass Indices (23.20 kg/m^2 ± 4.16 and 23.20 kg/m^2 ± 3.22, respectively). The protocol was previously approved by the institutional Ethical Commission and all procedures respected the principles of good clinical practice applied to human research. Food group intakes were assessed using a validated Food Frequency Questionnaire. The skin functionality was characterized in each participant in five anatomical sites (forehead, cheek, neck, hand, and leg) by transepidermal water loss (TEWL, Tewameter® CK electronics), hydration (Moisturemeter® DTec), and biomechanics skin (Cutometer® CK electronics) parameters The carotene skin content was determined in the hand palm by Multiple Spatially Resolved Reflection Spectroscopy (MSRRS) (Biozoom® GmbH). Statistical analysis was performed by Jamovi® Software. The dietary patterns and their impact on the skin were compared using Mann–Whitney test and correlations were investigated by the Spearman rank correlation coefficient ($p<0.05$).

Results

Regarding skin physiology, skin biomechanics and hydration were not different between the two groups. However, higher TEWL was consistently present in the VG group with significant differences in the neck and leg areas. As expected, the carotenoid content was higher in the VG group. Looking for a potential relationship between the most frequent foods consumed by these two groups of participants and skin physiology we found that vegetables, vegetable drinks, milk, yogurt, and cheese showed a significant positive relationship with epidermal water balance. On the other hand, alcoholic beverages and fast food showed a significant negative relationship with those variables. The VG group depicted a positive correlation with the carotenoid content, while red meat, viscera, alcoholic beverage, and sugar-sweetened beverage consumption typical of the OM group were negatively correlated.

Conclusion

Our results clearly suggest that dietary patterns influence and might determine skin physiology. However, these results are still exploratory. Larger sample sizes and more narrow dietary subgroupings are necessary to develop this research theme.

References

[1] Parke, M. A., Perez-Sanchez, A., Zamil, D. H., & Katta, R. (2021). Diet and Skin Barrier: The Role of Dietary Interventions on Skin Barrier Function. Dermatology Practical & Conceptual, Artigo e2021132. https://doi.org/10.5826/dpc.1101a132

[2] Hai, J., Nguyen, M., Hasan, A., Pan, A., Engel, T., & Sivamani, R. (2021). Patient perceptions about nutrition and skin health: a survey study characterizing patient opinions and information resources. Dermatology Online Journal, 27(1). https://doi.org/10.5070/d3271052020

B 05-12

Short-term fasting elevates circulating fibroblast growth factor 23 (FGF23) through ketone body β-hydroxybutyrate

M. Feger[1], J. Alber[1], A. Grund[2], M. Leifheit-Nestler[2], D. Haffner[2], M. Föller[1]

[1] *University of Hohenheim, Physiology, Stuttgart, Germany*

[2] *Medizinische Hochschule Hannover, Department of Pediatrics, Hannover, Germany*

Introduction

Phosphate and vitamin D homeostasis are controlled by fibroblast growth factor 23 (FGF23) from bone. FGF23 suppresses renal sodium-dependent phosphate transporter NaPiIIa (*Slc34a1*) and

enhances 24-hydroxylase (*Cyp24a1*), the key enzyme for inactivating $1,25(OH)_2D_3$, active vitamin D. Hyperphosphatemia and further mechanisms result in early elevation of plasma FGF23 in patients with chronic kidney disease (CKD). Plasma FGF23 correlates with cardiovascular outcomes not only in kidney disease, but also in other acute and chronic disorders. Fasting stimulates the production of ketone bodies like β-hydroxybutyrate. Given the relevance of FGF23 as a disease biomarker, we investigated whether short-term fasting (16 h) impacts on FGF23 production through ketogenesis.

Methods

Osteoblast-like UMR106 cells and isolated neonatal rat ventricular myocytes (NRVM) were treated with β-hydroxybutyrate. Wild type mice were fasted overnight or fed *ad libitum*, blood parameters were determined by enzyme-linked immunoassay (ELISA) or colorimetric methods, and gene expression by quantitative real-time polymerase chain reaction (qRT-PCR).

Results

β-hydroxybutyrate stimulated FGF23 production in UMR106 cells in a nuclear factor kappa-light-chain enhancer of activated B-cells (NFκB)-dependent manner, and in cardiomyocytes. Compared to fed animals, fasted mice exhibited higher β-hydroxybutyrate, C-terminal and intact FGF23 serum levels, cardiac *Fgf23* and renal *Cyp24a1* expression, and lower $1,25(OH)_2D_3$ serum concentration as well as renal *Slc34a1* and αKlotho (*Kl*) expression. In contrast, *Fgf23* expression in bone and serum phosphate, calcium (Ca^{2+}) and parathyroid hormone (PTH) concentration were not significantly affected by fasting.

Conclusion

Short-term fasting increased FGF23 production at least in part through ketone body β-hydroxybutyrate, an effect of high clinical relevance in view of the increasing use of FGF23 as a surrogate parameter in clinical monitoring of diseases. The fasting state of patients is therefore likely to strongly affect plasma FGF23.

B 05-13

NoxO1 and Erbin- a cooperation to control EGFR-signaling ?

M. Hebchen[1], T. Schader[1], N. Müller[1], M. Spaeth[1], C. Reschke[1], J. Graumann[2], K. Schröder[1]

[1] *Goethe University, Institue for Cardiovascular Physiology, Frankfurt, Germany*

[2] *Max-Planck-Institute for Heart and Lung Research, Biomolecular Mass Spectrometry, Bad Nauheim, Germany*

Introduction

NADPH oxidase organizer 1 (NoxO1), is a subunit of the ROS-producing Nox1 complex. NoxO1 plays a role in various cellular processes like angiogenesis and differentiation of colon epithelial cells (2, 4, 5). Based on its higher expression levels compared to the other subunits, NoxO1 could exert additional functions by interacting with other proteins than Nox1.

We recently identified and validated Erbin (ErbB2-interacting protein), a negative regulator of epidermal growth factor receptor (EGFR) signaling (1, 3), as novel interaction partner of NoxO1. Interestingly, neither the cellular consequences nor the mechanisms behind are uncovered so far. Thus, we aim to explore the impact of NoxO1 on intracellular EGFR trafficking and signaling.

Methods and Results

Overexpression of NoxO1 in HEK293 cells induces the formation of early endosomes in the resting state and on a short time course of EGF stimulation, thereby delaying EGFR-signaling. By immunofluorescence, we examined several endosomal markers from which only Rab7 and LAMP-both markers of degradative pathways- were elevated in presence of NoxO1. Furthermore, we visualized NoxO1 in proximity ligation assays where it enhanced the interaction of EGFR and (phospho) Erbin. In a Western Blot-based degradation assay, NoxO1 reduced EGFR stability in presence of the translation inhibitor cycloheximide. In order to establish a pathophysiological model system in the future, we studied NoxO1 mRNA levels via RT-qPCR and found differing expression in murine tissues and human cancer cell lines.

Conclusion

NoxO1, a novel interaction partner of Erbin, delays EGF signaling and might promote EGFR degradation via the lysosomal pathway. We conclude that NoxO1 and Erbin cooperatively regulate EGF-signal transduction and EGFR receptor turnover. The mechanism of NoxO1-mediated EGFR downregulation and its pathophysiological relevance demands for further investigation.

References

[1] Borg JP, Marchetto S, Le Bivic A, Ollendorff V, Jaulin-Bastard F, Saito H, Fournier E, Adélaïde J, Margolis B, and Birnbaum D. ERBIN: a basolateral PDZ protein that interacts with the mammalian ERBB2/HER2 receptor. *Nat Cell Biol* 2: 407–414, 2000.

[2] Brandes RP, Harenkamp S, Schürmann C, Josipovic I, Rashid B, Rezende F, Löwe O, Moll F, Epah J, Eresch J, Nayak A, Kopaliani I, Penski C, Mittelbronn M, Weissmann N, and Schröder K. The Cytosolic NADPH Oxidase Subunit NoxO1 Promotes an Endothelial Stalk Cell Phenotype. *ATVB* 36: 1558–1565, 2016.

[3] Jang H, Stevens P, Gao T, and Galperin E. The leucine-rich repeat signaling scaffolds Shoc2 and Erbin: cellular mechanism and role in disease. *FEBS J* 288: 721–739, 2021.

[4] Moll F, Walter M, Rezende F, Helfinger V, Vasconez E, Oliveira T de, Greten FR, Olesch C, Weigert A, Radeke HH, and Schröder K. NoxO1 Controls Proliferation of Colon Epithelial Cells. *Front Immunol* 9, 2018.

[5] Schader T, Reschke C, Spaeth M, Wienstroer S, Wong S, and Schröder K. NoxO1 Knockout Promotes Longevity in Mice. *Antioxidants (Basel)* 9, 2020.

B 05-14

Sex differences in long-term effects in collagen-induced arthritis in middle-aged mice

B. M. Schuh, V. Borbélyová, K. Macáková, T. Groß, P. Belvončíková, A. Feješ, J. Janko, M. Pastorek, B. Vlková, P. Celec

Comenius University in Bratislava, Faculty of Medicine, Institute of Molecular Biomedicine, Bratislava, Slovakia

This project was supported by the following grants: APVV-18-0366 and KEGA 045UK-4/2020

Introduction

Rheumatoid arthritis (RA) is a chronic inflammatory disorder with a high prevalence among women. Collagen-induced arthritis (CIA) is the most widely used animal model of RA and is usually observed for 5-7 weeks in both sexes. Sex differences and long-term effects of CIA are poorly described in the literature.

Aim

To analyze the long-term effects of CIA on the joints in mice of both sexes.

Materials and methods
CIA was induced in adult DBA/1 mice (12 females, 11 males) by immunization with bovine type II collagen and complete Freund's adjuvant. Control mice (5 females, 5 males) received saline. Arthritis score assessment, plethysmometry and thermal imaging of the joints were conducted weekly for 4 months. Locomotor activity was analyzed in the open field at the end of the experiment at the age of one year.
Results
A sex difference was proved neither in the prevalence of arthritis (10/12 females and 8/11 males) nor in its severity. Following collagen injection, symptoms of CIA developed sooner in males (day 14 vs 35) and the RA score also peaked sooner in males (day 52 vs 55). The RA scores decreased afterwards, the difference to the control group disappeared by day 70. Similar dynamics was observed in paw volume and thermal imaging analyzing different aspects of joint inflammation. There were no significant differences in locomotor activity of CIA mice in comparison to CTRL mice in any of the sexes.
Conclusion
This is the first experiment to analyze sex differences in the CIA model in the long-term. Our results indicate slight sex differences in the dynamics, but not the extent of arthritis. In contrast to previously described sex differences in this model, we have used middle-aged animals that might be clinically more relevant. However, the lack of major sex differences in the occurrence of symptoms and the limited duration of their presence suggests that the pathogenesis of the model is far from the mechanisms involved in RA in patients.

References
[1] Marinov L, Mangarov I, Nikolova I, 2021, 'Gender differences in collagen-induced arthritis (CIA) in mice', Biotechnology & Biotechnological Equipment, 35:1, 1899-1905.
[2] Holmdahl R, Jansson L, Larsson E, Rubin K, Klareskog L, 1986, 'Homologous type II collagen induces chronic and progressive arthritis in mice', Arthritis and Rheumatism, 29:1, 106-113
[3] Favalli EG, Biggioggero M, Crotti C, Becciolini A, Raimondo MG, Meroni PL 2019, 'Sex and Management of Rheumatoid Arthritis', Clinical Reviews in Allergy & Immunology, 56:3, 333-345
[4] Osthoff et. al, 2018, '2018 EULAR recommendations for physical activity in people with inflammatory arthritis and osteoarthritis' Annals of Rheumatic Disease, 77:9, 1251-1260
[5] Smolen J, Aletaha D, McInnes I, 2016, 'Rheumatoid arthritis', Lancet, 388:10055, 2023-2038.

B 05-15
Mineralocorticoid receptor regulated genes involved in energy homeostasis
Y. Gadasheva, A. Nolze, N. Straetz, K. Quarch, C. Grossmann
Martin Luther University of Halle-Wittenberg, Julius-Bernstein-Institute of Physiology, Halle (Saale), Germany

This study was supported by the Deutsche Forschungsgemeinschaft (DFG): grant GR 3415/1- 5 and RTG 2155 ProMoAge SP11.

Introduction
The renin-angiotensin-aldosterone system (RAAS) plays a pivotal role in cardiovascular physiology, mediating the regulation of blood pressure and electrolyte balance. However, pathophysiological RAAS effects can lead to inflammation and structural remodeling, thus promoting cardiac and vascular damage. One of the RAAS players is the mineralocorticoid receptor (MR), a transcription factor with aldosterone (Aldo) as an endogenous ligand. MR antagonists provide effective treatment for patients with cardiovascular diseases, reducing morbidity and mortality. We aimed to identify and characterize MR--regulated genes that play a role in cardiovascular diseases and aging.
Methods/Results
To assess MR-target genes, an inducible MR overexpression HEK cell clone was generated and used for further analysis. RNA-seq data comparing aldo and vehicle treated MR expressing cells yielded four hundred twenty four genes with a 1,5-fold induction. Among the novel MR--regulated genes we identified several genes involved in energy homeostasis of which PDK4 (pyruvate dehydrogenase kinase 4) was the most prominent one. All four known isoforms of PDK were detectable but only PDK4, mostly expressed in skeletal muscle, heart muscle, and vasculature, was differentially expressed by aldo. RNA-Seq results were validated by qRT--PCR and Western blot. Furthermore, PDK4 activity was assessed by analyzing the phosphorylation of the downstream target PDHA1. The pPDHA1/PDHA1 ratio was increased in aldo--stimulated cells compared to control, which thus correlates with high PDK4 mRNA and protein levels in HEK cells. We studied the functional consequences with enzymatic assays and Seahorse XF Analyzer and saw an increase in glucose consumption and lactate production. Additionally, we found elevated caspase and LDH levels (i.e., markers of apoptotic and necrotic cell death). We obtained similar results for PDK4 expression and activity, from a human endothelium--derived cell line, EA.hy 926.
Conclusion
Thus, activated MR can enhance PDK4 expression, inducing a metabolic shift. Reduced oxidative phosphorylation of glucose due to activated PDK4 may contribute to mitochondrial dysfunction that in turn forces cell death mostly through apoptosis. Clinical data furthermore suggest a link between upregulated PDK4 and calcification in vessels, oxidative stress, inhibited lysosomal function, and decreased autophagy, which are also associated with cardiovascular diseases and aging.

B 05-18
Assessment of Fat-Free Mass and Fat Mass: Comparison of impedance and dual-energy x-ray absorptiometry techniques
C. Ferreira-Pêgo, S. Lopes, T. Fontes, R. Tavares, R. Menezes, L. M. Rodrigues
Universidade Lusófona de Humanidades e Tecnologias, CBIOS, Lisbon, Portugal

Acknowledgments: The authors acknowledge all the participants.

Introduction: Body composition evaluation is an important method for the identification of nutritional status, requiring a precise, sensitive, and fast method for assessment. At the clinical level, bioimpedance (BIA) is the main technique used for body composition evaluation, due to its relatively lower cost and easy accessibility. However, it is important to keep in mind that BIA is an estimating device. The dual-energy x-ray absorptiometry (DXA) is a gold standard, however, its bigger size and high price can be limiting at the clinical level. The study aimed to compare BIA and DXA in body composition assessment and to analyze the differences obtained mainly in Fat-Free Mass (FFM) and Fat Mass (FM).

Methods: A descriptive observational cross-sectional study was conducted with a final sample of 121 participants, 93 women, and 28 men (28,26 years old ± 9,72), and a mean Body Mass Index of 22,68 kg/m^2. Data were collected from a BIA (Tanita TBF 300®), and DXA (Lunar Prodigy Advance by General Electric Healthcare®), by trained dietitians. A correlation was observed by paired t-test and agreement by the Bland-Altman method. Statistical significance was considered when the p-value was less than 0.05.
Results: BIA underestimated FM by 5.56% and overestimated FFM by 2.90kg. There was a positive correlation between the two types of equipment, which was higher for FFM (r=0.980) than for FM (r=0.932). Despite the positive correlation, the methods were shown not to agree ($p < 0.001$).BIA underestimated FM by 5.56% and overestimated FFM by 2.90kg. There was a positive correlation between the two types of equipment, which was higher for FFM (r=0.980) than for FM (r=0.932). Despite the positive correlation, the methods were shown not to agree ($p < 0.001$).
Conclusion: Although data obtained using DXA and BIA were correlated, they were not congruent methods. Therefore, the risk of (mis)interpretation and bias is clear with BIA, potentially impacting the nutritional planning of clinical dietitians and further results of its patients.

B 05-19

Renal proteasomal activity is impaired in a type-2 diabetes mouse model

L. Heintz[1], M. Wang[1], S. Liu[2], J. Brand[1], S. Zielinski[1], T. Huber[2], T. Wiech[3], D. Loreth[1], W. Sachs[1], C. Meyer-Schwesinger[1]
[1] *University Medical Center Hamburg-Eppendorf, Institute of Cellular and integrative Physiology, Hamburg, Germany*
[2] *University Medical Center Hamburg-Eppendorf, Department of Internal Medicine III, Hamburg, Germany*
[3] *University Medical Center Hamburg-Eppendorf, Insitute of Pathology, Hamburg, Germany*

Introduction
In contrast to the significance of the autophagosomal-lysosomal pathway (ALP) in diabetic nephropathy (DN), little is known about the involvement of the ubiquitin-proteasome system (UPS). Therefore, this study aimed at characterising important players of this degradative system in both glomeruli and total kidney tissue in a DN type 2 model (BTBR ob/ob mice) at an early (8 weeks) and a late stage (ca. 20 weeks) of disease. We focused on the assessment of proteasomal subtype composition, the actual proteolytic activity and how these relate to cell-type specific mRNA and protein levels of the corresponding proteasomal subunits.
Methods
Proteasome subtype composition and activity was quantified via in-gel activity assays and activity-based probes targeting the proteolytic subunits. Transcript and protein levels of important UPS and ALP players were assessed via RNAseq (both bulk and single cell) and Western blot analysis. The protein abundance of proteasomal proteins was correlated with the resulting catalytic activities. Immunohistochemical analyses in mice and patient biopsies with diabetic nephropathy were used to identify the renal cell-types which exhibited changes in proteasome abundance. During terminal organ extraction, mice were treated with buprenorphin (0,1 mg/kg bodyweight subcutaneously, 30 minutes before surgery) and isoflurane (3.5 %, inhaled).
Results
Using activity-based probes and in-gel activity assays, a decrease in proteasomal catalytic activity was observed in diabetic glomerular and kidney tissue, both for different proteasome subtypes and catalytic subunits, partly due to a downregulation of proteasomal components on the protein level. These effects were exacerbated with disease progression as the impairment was stronger at 20 than at 8 weeks. Interestingly, most proteasomal subunits were not regulated on the mRNA level. K48-ubiquitin, which commonly targets substrates for proteasomal degradation, showed a mild accumulation in glomeruli at 8 weeks, and a decrease in kidney at 8 and 20 weeks, especially in male mice. Immunohistochemical staining of proteasomal proteolytic subunits revealed an accumulation and aggregation in glomerular endothelial cells and podocytes, but not in mesangial cells in BTBR ob/ob mice and patient biopsies.**Conclusion**
In the BTBR ob/ob mouse model of diabetic type-2 nephropathy, renal proteasomal activity is already reduced at 8 weeks, especially in non-glomerular cells. Similarly altered glomerular cell-type expression patterns between ob/ob and patient biopsies indicate a common pathophysiologic proteasomal disturbance in diabetic nephropathy.

B 05-20

Effect of Oral Caprylic Acid Supplementation on Acyl Ghrelin, Growth, and Anxiety-Like Behavior in Rats

E. Bilge, E. Ileri Gurel
Hacettepe University, Department of Physiology /Faculty of Medicine, Ankara, Turkey

This study was supported by Scientific Research Unit of Hacettepe University (Project No: TTU-2020-18870).

Introduction
Ghrelin is an important peptide connecting physiological processes regulating food intake, body composition, and growth (1, 2). It has also been shown that ghrelin has effects on anxiety-like behavior (3-5). Attachment of a fatty acid, a rare post-translational modification (acylation), is required for activation of ghrelin. Caprylic (octanoic) acid is a medium-chain fatty acid used for ghrelin's acylation (1). Whether activation of ghrelin, hence growth, increases in response to dietary caprylic acid supplementation, is unclear. Therefore this study aimed to investigate the effect of oral caprylic acid supplementation on somatic growth, serum acyl ghrelin, growth hormone, insulin-like growth factor-1 (IGF-1), and insulin levels in rats. Anxiety-like behavior was also examined, which is the most frequent psychiatric disorder in children and adolescents.
Methods
3-week-old male Wistar albino rats (n=30) were allocated into control and two caprylic acid groups. Caprylic acid was administered orally 3 mg/kg and 6 mg/kg daily for 30 consecutive days (Figure 1). Caprylic acid was dissolved in saline and the control group received only oral saline. Body weight, tail length, and food consumption were recorded regularly. On the postpartum 54^{th} day, the anxiety-like behavior of rats was evaluated with elevated plus-maze and light/dark box tests. On the postpartum 24^{th} and 55^{th} days fasting blood glucose was measured. On the postpartum 55^{th}day, the animals were sacrificed with intraperitoneal ketamine (100 mg/kg) and xylazine (10 mg/kg) anesthesia. Somatic growth was assessed by naso-anal length, body weight, and organ weights (heart, liver, and kidney). Serum acyl ghrelin, growth hormone, IGF-1, and insulin levels were measured by ELISA.
Results
Compared with the control group (4.7±0.22 ng/mL), growth hormone levels were lower in 6 mg/kg caprylic acid group (4.01±0.14 ng/mL) ($P < 0.05$, one-way ANOVA). On the other hand blood glucose, serum acyl ghrelin, IGF-1, and insulin levels were similar between groups. No significant

difference was found between the groups in terms of somatic growth, food consumption, or anxiety-like behavior of rats.

Conclusion

These datademonstrate that oral caprylic acid supplementation does not cause an increase in acyl ghrelin levels and hence growth and anxiety-like behavior in healthy growing rats. As far as we know, this is the first study investigating whether caprylic acid stimulates growth by changing the levels of active ghrelin, growth hormone, insulin, and IGF-1 levels. More studies are needed to elucidate the interaction between caprylic acid and ghrelin hormone and its effect on growth-related hormones, somatic growth, and anxiety.

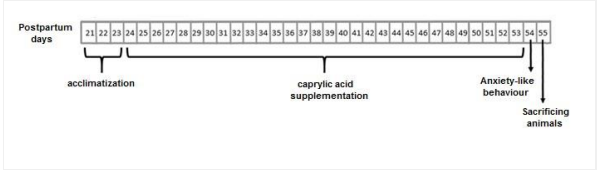

Figure 1
Experiment design

References

[1] Kojima, M, Hosoda, H, Date Y, Nakazato M, Matsuo H, Kangawa K 1999, 'Ghrelin is a growth-hormone-releasing acylated peptide from stomach' *Nature,* 402 (6762), 656-60.

[2] Delporte, C 2013, 'Structure and Physiological Actions of Ghrelin', *Scientifica*.

[3] Carlini, VP, Monzon, ME, Varas, MM, Cragnolini, AB, Schioth, HB, Scimonelli, TN, et al. 2002, 'Ghrelin increases anxiety-like behavior and memory retention in rats', *Biochem Bioph Res Co,* 299(5), 739-43.

[4] Asakawa, A, Inui, A, Kaga, T, Yuzuriha, H, Nagata, T, Fujimiya, M, et al. 2001, 'A role of ghrelin in neuroendocrine and behavioral responses to stress in mice', *Neuroendocrinology,* 74(3), 143-7.

[5] Jensen, M, Ratner, C, Rudenko, O, Christiansen, SH, Skov, LJ, Hundahl, C, et al. 2016, 'Anxiolytic-Like Effects of Increased Ghrelin Receptor Signaling in the Amygdala', *Int J Neuropsychoph,* 19(5).

B 05-21

Activation of brown adipose tissue is GC-C, gender, and phase of the estrous cycle dependent

N. Habek[1,2], M. Ratko[1], M. Kordić[3], **A. Dugandžić**[1,2]

[1] University of Zagreb, School of medicine, CIBR, Centre of Excellence for Basic, Clinical and Translational Neuroscience, Zagreb, Croatia

[2] University of Zagreb, School of medicine, Department of Physiology, Zagreb, Croatia

[3] MKP Ltd, Zagreb, Croatia

This study is financed by the Croatian science foundation research grant (IP-2018-01-7416) and co-financed by the European Union through the European Regional Development Fund, Operational Programme Competitiveness and Cohesion, grant Agreement No. KK.01.1.1.01.0007, CoRE-Neuro.

Introduction

Uroguanylin (UGN) activates guanylate cyclase C, leading to cGMP synthesis. UGN is released from the gut in plasma after a meal when activation of brown adipose tissue (BAT) occurs and leads to browning after prolonged i.c.v. application. In this study, we determined the acute activation of BAT by intranasal (i.n.) UGN application and possible mechanism of postprandial BAT activation via UGN.

Methods

In this study, male and female mice in estrus (E) and diestrus (DE) C57Bl/6NCrl (WT) were used. The activity of BAT was determined by infrared thermography (FLIR T-1020). The expression of UGN in the hypothalamus upon i.n. insulin or GLP-1 stimulation was determined by ELISA. The expression of GC-C was determined by immunohistochemistry. Membrane potential was measured by whole-cell patch-clamp and changes in intracellular ion concentrations by specific fluorescent dyes.

Results

BAT activity is activated far stronger by a five-time smaller amount of UGN applied i.n. (activation of brain GC-C) compared to activation after i.p. application. This activation was smaller in female animals in DE when compared to male mice and not present during E. Even though the depolarisation of POMC neurons by UGN was similar in all tested animal groups, the ratio of GC-C expression in POMC and dopaminergic neurons in the Arcuate nucleus of the hypothalamus was different in male and female mice in DE and in E which could explain differences in BAT activation during estrous cycle. Furthermore, UGN increased intracellular concentration of K^+ and Ca^{2+} but not Cl^-, in hypothalamic cells, which leads to depolarization. Applied i.n., GLP-1 changed BAT activity differently depending on gender and estrous cycle, similar to changes in BAT activation after a meal. GLP-1 also changed pro-UGN expression in male but not female hypothalamus which was not accompanied by similar changes in blood, suggesting the existence of brain UGN and involvement of UGN in BAT activation via GLP-1 in male mice.

Conclusion

Metabolic studies, especially ones investigating the regulation of BAT activity, should pay special attention to gender and the phase of estrous cycle. The interplay between UGN and GLP-1 is especially important when the activity of BAT is measured in diabetic patients. Since BAT activation leads to glucose expenditure[1,2], similar studies could lead to the development of new approaches involving the activation of BAT for the treatment of hyperglycaemia in diabetic patients, which will improve glucose metabolism and postpone insulin application.

References

[1] 1. Habek N, Dobrivojević Radmilović M, Kordić M, Ilić K, Grgić S, Farkaš V, Bagarić R, Škokić S, Švarc A, Dugandžić A. Activation of brown adipose tissue in diet-induced thermogenesis is GC-C dependent. Pflugers Arch. 472(3):405-417 2020

[2] Habek N, Kordić M, Jurenec F, Dugandžić A. Infrared thermography, a new method for detection brown adipose tissue activity after a meal in humans. Infrared Phys. Technol. 89: 271-276 2018

B 05-22

Regulation of Prepro-Neuropeptide W/B and its receptor in the heart of ZDF rats: An animal model of type II DM

T. Smrhova[1], **S. Pandey**[2,3], Z. Tuma[2], M. Chottova Dvorakova[1,2]

[1] Charles University, Faculty of Medicine in Pilsen, Department of Physiology, Pilsen, Czech Republic

[2] Charles University, Faculty of Medicine in Pilsen, Biomedical Center, Pilsen, Czech Republic

[3] Charles University, Faculty of Medicine in Pilsen, Department of Pharmacology and toxicology, Pilsen, Czech Republic

This work was supported by the Charles University Research Fund [Progres Q39].

Introduction

Neuropeptide B (NPB) and neuropeptide W (NPW) are neuropeptides, which constitute NPB/W signalling systems together with G-protein coupled receptors NPBWR1. The location and function of NPB/W signalling system have been predominantly detected and mapped within the CNS including its role in modulation of inflammatory pain, neuroendocrine functions and autonomic nervous system. Altered serum levels of both neuropeptides have been previously shown in patients with DM, suggesting its potential role in pathophysiology of diabetes mellitus (DM). The aim of this study is to investigate the impact of diabetes on neuropeptide B/W signalling system in different heart compartments and within intracardiac nervous system in animal model of type 2 DM.

Methods

Zucker diabetic fat (ZDF) rats were sacrificed by decapitation at week 40 of age, heart atria and ventricles, stellate ganglia and upper thoracic dorsal root ganglia were dissected. From gathered samples, total RNA or protein was isolated. In addition, samples containing coronary arteries walls from left ventricle tissues were collected via laser capture microdissection and used for RNA or protein isolation. Obtained RNA was reverse-transcripted and subsequently RT-qPCR analysis was done. Relative expression of mRNA of NPB, NPW and NPBWR1 was expressed as a ratio of target gene concentration to control gene. Data obtained by qPCR were first subjected to Shapiro-Wilk normality test and Mann-Whitney test was used for statistical evaluation. In WB analysis, the mean of all the technical replicates (n=3) or (n=2) was used to analyse the expression of protein for each analyte. The difference of expression between groups was calculated by t-test. Results were considered significantly different when $p<0.05$. Additionally, sections of tissues were examined using the methods of immunofluorescence.

Results

In RT-qPCR analysis, we observed the upregulation of mRNA for preproNPB in RV (3.0-fold, p = 0.018), for preproNPW in LA (3.2-fold, p = 0.022) and for NPBWR1 in DRG in diabetic rats. On the contrary, expression of mRNA for NPBWR1 was downregulated in the LV (0.56-fold, p = 0.029) in diabetic rats. In WB analysis, significant downregulation of NPBWR1 in LV (0.54-fold, p= 0.046) in diabetic rats was observed at proteomic level. The presence of NPBWR1 was also confirmed in dissected LCM section of cardiomyocytes. Moreover, specific NPB and NPW immunoreactivity was detected in nerve fibers innervating intracardiac ganglia, as well as nerve cell bodies of these ganglia, nerve fibers in between cardiomyocytes and smooth muscle cells of coronary vessels.

Conclusion

NPB/W signalling system is involved in regulation of heart functions and long-term diabetes leads to changes in the expression of individual members of this signalling system differently in each cardiac compartment, which is related to the different morphology and function of these cardiac chambers.

B 05-23

Postoperative treatment with caffeine supports the recovery of intestinal motility in rats: antioxidant action of caffeine

L. S. Şen[1], K. S. Mermer[1], M. M. Kahraman[1], A. E. Toraman[2], E. Tiftikçi[2], M. Harlak[2], M. S. Recai[2], Z. N. Akkurt[2], M. Yüksel[3], F. Ercan[4], B. C. Yeğen[1]

[1] Marmara University, Department of Physiology / Faculty of Medicine, Istanbul, Turkey

[2] Marmara University, School of Medicine, Istanbul, Turkey

[3] Marmara University, Vocational School of Health-Related Professions/Department of Medical Laboratory, Istanbul, Turkey

[4] Marmara University, Department of Histology and Embriology/Faculty of Medicine, Istanbul, Turkey

Introduction

Postoperative ileus (POI) is deceleration/cessation of bowel movements following abdominal surgery. Amprical clinical data have indicated that coffee consumption shortens the postoperative recovery of gastrontestinal dysmotility. Our aim was to assess the possible underlying mechanisms of the beneficial effects of caffeine on POI.

Methods

InSprague-Dawley male rats, POI model was conducted under ketamine-xylazine anesthesia by handling the small intestines smoothly for 3 minutes (n=32), while the anesthetized control rats had no surgery (n=8). Different doses of caffeine (5, 10, 25mg/kg) or physiological saline were administered twice subcutaneously at 15th minute and 21st hour following surgery. Locomotor activity and fecal pellet outputs of rats were measured. A charcoal mixture was orogastrically administered to evalaute 30-min small intestine motility and rats were decapitated at the 24th h of surgery to determine the distance of propogated charcoal. Myeloperoxidase activity (MPO), malondialdehyde and glutathione levels, luminol and lucigenin-mediated chemiluminescence (CL) levels, which indicate formation of reactive oxygen metabolites (ROM), were measured in the small intestine samples. Microscopic damage scores were assessed by hematoxylin-eosin staining. Statistical evaluations were made using one-way ANOVA.

Results

Locomotor activity and fecal output counts were not statistically different among the experimental groups. Mild handling procedure of the intestines has not resulted in any alterations in intestinal MPO, malondialdehyde and glutathione levels. Small intestinal transit index was decreased in saline-treated POI group as compared to control ($p<0.01$), while transit was facilitated in caffeine-treated groups (5 or 25 mg/kg; $p<0.05$). Both lucigenin-and luminol-enhanced CL levels in intestines were higher in saline-treated POI group ($p<0.01$-$p<0.001$), but caffeine significantly reduced lucigenin and luminol CL levels ($p<0.05$-$p<0.01$). Elevated microscopic damage score, presenting with mild blunting in villi structure in saline-treated POI group was reduced in all caffeine-treated POI groups, but a statistically significant difference was reached at 10mg/kg dose ($p<0.05$).

Conclusion

Our results demonstrated that post-operative administration of caffeine, at doses that had no impact on general motor activity, suppressed the production of ROM in small intestines, protected epithelial integrity, and improved gastrointestinal dysmotility. These results suggest that caffeine could be used as a safe therapeutic agent for its antioxidant and prokinetic effects in shortening the duration of postoperative ileus.

References
[1] Bragg, D., El-Sharkawy, A. M., Psaltis, E., et al. (2015). Postoperative ileus: Recent developments in pathophysiology and management. *Clinical nutrition (Edinburgh, Scotland)*, *34*(3), 367–376.
[2] Türler, A., Moore, B. A., Pezzone, M. A., et al. (2002). Colonic postoperative inflammatory ileus in the rat. *Annals of surgery*, *236*(1), 56–66.
[3] Yildirim, A., Arabacı Tamer, S., Sahin, D., et al. (2019). The effects of antibiotics and melatonin on hepato-intestinal inflammation and gut microbial dysbiosis induced by a short-term high-fat diet consumption in rats. *The British journal of nutrition*, *122*(8), 841–855.

B 05-24

Resveratrol attenuates vancomycin induced testicular toxicity in rats

F. S. Alshehri

Umm Al-Qura University, Pharmacology and toxicology, College of Pharmacy, Makkah, Saudi Arabia

Introduction

Cumulative reports have indicated that antibiotics may adversely affect testicular and sperm function. Vancomycin is a glycopeptide antibacterial developed as an alternative to penicillin for treating resistant Staphylococcus aureus strains [5]. Recently, few studies have suggested that vancomycin could produce testicular toxicity and apoptosis. However, the mechanism of vancomycin inducing testicular toxicity has not been investigated.

Methods

The study investigated the effect of vancomycin (200 mg/kg, i.p) for seven days on Wistar rats to induce testicular toxicity. Resveratrol (20 mg/kg, oral gavage) was concomitantly used with vancomycin. The rats were divided into three groups: the Control group(received saline i.p and oral gavage), the vancomycin group received (200 mg/kg, i.p), the vancomycin + resveratrol group received (200 mg/kg, i.p + 20 mg/kg, oral gavage).

Results

Vancomycin (200 mg/kg, i.p) treatment for seven days caused a significant reduction in testosterone levels, sperm count, and sperm motility, while treatment of resveratrol attenuated vancomycin effects and normalized testosterone levels, sperm count, and sperm motility. Vancomycin (200 mg/kg, i.p) treatment for seven days caused a significant increase in luteinizing hormone and follicular hormone, while resveratrol treatment attenuated vancomycin effects and normalized luteinizing hormone and follicular hormone. Histopathological examination showed that vancomycin (200 mg/kg, i.p) treatment for seven days thin and splitting of the basal lamina atrophied and widely separated seminiferous tubules, while treatment of resveratrol prevented the effect of vancomycin on testicular tissues and thickness of the basal lamina.

Conclusion

This study showed resveratrol's potential antioxidant and anti-inflammatory effects on attenuating vancomycin-induced testicular toxicity in Wistar rats.

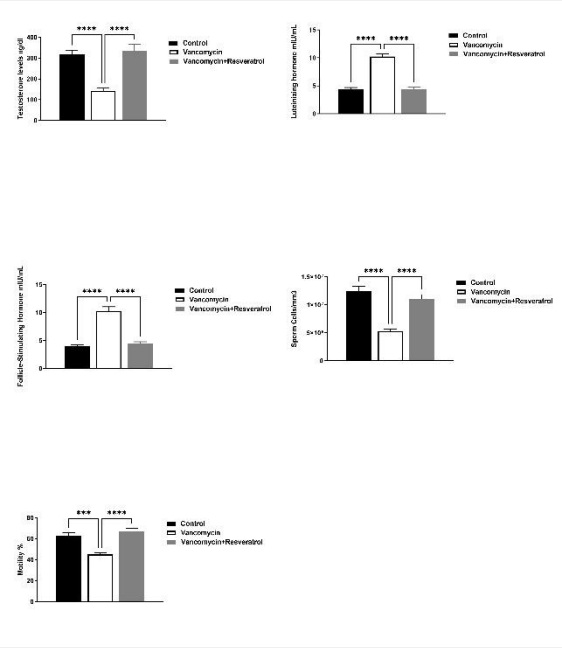

Results

References
[1] Manson, J.M., et al., *Effects of cefonicid and other cephalosporin antibiotics on male sexual development in rats*. Antimicrobial agents and chemotherapy, 1987. **31**(7): p. 991-997.
[2] Farombi, E.O., et al., *Tetracycline-induced reproductive toxicity in male rats: effects of vitamin C and N-acetylcysteine*. Experimental and Toxicologic Pathology, 2008. **60**(1): p. 77-85.
[3] Sakai, K., et al., *Effects of doxorubicin on sperm DNA methylation in mouse models of testicular toxicity*. Biochemical and biophysical research communications, 2018. **498**(3): p. 674-679.
[4] Karaman, M., H. Budak, and M. Çiftci, *Amoxicillin and gentamicin antibiotics treatment adversely influence the fertility and morphology through decreasing the Dazl gene expression level and increasing the oxidative stress*. Archives of physiology and biochemistry, 2019. **125**(5): p. 447-455.
[5] Marsot, A., et al., *Vancomycin*. Clinical pharmacokinetics, 2012. **51**(1): p. 1-13.

B 05-25

Basic biometric, biochemical and oxidative stress parameters in Zucker diabetic fatty rats during aging.

M. Kollarova[1], M. Chomova[2], D. Radosinska[3], L. Tothova[4], I. Shawkatova[3], **J. Radosinska**[1,5]

[1] *Comenius University in Bratislava, Faculty of Medicine, Institute of Physiology, Bratislava, Slovakia*

[2] *Comenius University in Bratislava, Faculty of Medicine, Institute of Medical Chemistry, Biochemistry and Clinical Biochemistry, Bratislava, Slovakia*

[3] *Comenius University in Bratislava, Faculty of Medicine, Institute of Immunology, Bratislava, Slovakia*

[4] *Comenius University in Bratislava, Faculty of Medicine, Institute of Molecular Biomedicine, Bratislava, Slovakia*

[5] *Slovak Academy of Sciences, Centre of experimental medicine, Bratislava, Slovakia*

This research was funded by the Scientific Grant Agency of the Ministry of Education, Science, Research and Sport of the Slovak Republic grant No.VEGA 1/0314/19 and VEGA 1/0193/21, and grant for young researchers of Comenius University in Bratislava UK/78/2021.

Introduction

The Zucker diabetic fatty (ZDF) rat is a common animal model for the study of type 2 diabetes. Though most experimental studies consider ZDF rats as a uniform group, there are indices regarding their growing inhomogeneity over time. The main objective of our study was monitoring biometric and biochemical parameters of ZDF rats during development to type 2 diabetes and comparing them with two control rat models - commonly used Zucker Lean and independent control - Wistar rats. Moreover, we investigated the activity of matrix metalloproteinases (MMPs) - multifunctional enzymes involved in tissue remodelling.

Methods

Males of 3 rat strains were included in the study: ZDF, Wistar (WIS) and Zucker Lean (LEAN). Body weight, blood glucose, and plasma insulin levels were recorded regularly. Between the 38^{th}–39^{th} week of life, rats were subjected to 2.5-3 % isoflurane inhalation-induced anesthesia, trunk blood was collected and plasma was separated. The heart was excised and the weight of the right and the left ventricle was registered. Markers of oxidative stress, antioxidant capacity, carbonyl stress, and MMP-2 and MMP-9 activities were analyzed both in plasma and 10% myocardial tissue homogenate in phosphate-buffered saline.

Results

According to fasting glycaemia and insulin concentration, ZDF were split into two phenotypes - obese (FAT) and diabetic (DIA). Glycaemia showed progressively rising tendency only in DIA which also exhibited higher cholesterol levels compared with FAT. In addition, FAT revealed more pronounced left ventricular hypertrophy and greater body weight, clearly differentiating them from DIA. Rats in the FAT group had lower plasma MMP-2 and MMP-9 activity compared with DIA. However, increased myocardial MMP-2 activity indicated left ventricular remodelling in both ZDF phenotypes.

Conclusion

Our study suggests that ZDF rats increase inhomogeneity in basic biochemical and biometric characteristics during aging. According to our observations, the generally accepted characteristic of ZDF rats - hyperphagia, obesity, hyperinsulinemia, and insulin resistance, applies only to a part of these animals. As diabetes in humans represents a heterogenous group of chronic metabolic disorders, the inhomogeneity of ZDF rats may be beneficial in the study of different aspects of this pathology. Our experiments may also promote a discussion regarding the suitable normoglycemic non-obese control counterparts for aged ZDF rats, especially when the experiments are focused on myocardial tissue. The greater left ventricular weight, as well as the increase in carbonyl stress in the left myocardial tissue and the increase in MMP-2 activity in both ventricles of Zucker lean rats, could indicate remodeling of their heart in comparison with Wistar rats.

B 05-26

Nerve conduction and its correlations with duration of diabetes mellitus and glycosylated haemoglobin in type 2 diabetes mellitus (T2DM)

W. S. Hamid[1], H. S. Ahmed[2], M. A. Osman[3], R. Babiker[4]

[1] *University of Medical Sciences & Technology, Medical Physiology Department, khartoum, Sudan*

[2] *International University of Africa, Medical Physiology Department, khartoum, Sudan*

[3] *University of Medical Sciences & Technology, Medical Physiology Department, khartoum, Sudan*

[4] *RAK College of Dental Sciences, RAK Medical and Health Sciences University, Medical Physiology Department, Ras Al Khaimah, United Arab Emirates*

We would like to acknowledge the efforts of all participants, Dr Asmaa, Dr Mounkeila Noma, and Prof. Eltaher Obeid, for their support and permission to conduct this research in their clinics, and for helping us throughout this research.

Introduction

Diabetic neuropathy is one of the most common microvascular complications associated with diabetes mellitus. Diabetic peripheral neuropathy (DPN) has been linked to hyperglycaemia and long duration of uncontrolled type 2 diabetes mellitus (T2DM) as measured by glycosylated haemoglobin (HbA1c). To our knowledge the estimated duration between diagnosis and developing DPN and the level of HbA1c have not yet been investigated in Sudanese patients with type 2 DM. Therefore, this study aims to investigate the relationship between the duration of diabetes and HbA1c with nerve conduction velocity (NCV) in patients with type 2 DM.

Methods

This cross-sectional study recruited 63 male and female patients with T2DM who attended the diabetic outpatient clinic of Academy Charity Teaching Hospital (ACTH) and Alzaytouna Private Hospital for Nerve Conduction Velocity (NCV) and electromyography (EMG) tests. Nerve conduction was done by using ADInstruments PowerLab series 26. SPSS was used to analyse the data and p-value < 0.05 was considered significant.

Results

The mean duration of DM was 14.7 (± SD 9.24) years and the mean age of participants was 57.71 (± SD 12.2) years. The most common symptom was numbness (50%). Pearson's correlation test revealed a significant negative correlation between HbA1c and nerve conduction velocity ($r = 0.4$, $p < 0.05$) and negative significant correlation between the duration and the amplitude ($r = 0.35$, $p < 0.05$).

Conclusion

There is a slowing of nerve conduction velocity in type 2 diabetic patients, which is accelerated by the poor glycaemic control (HbA1c). These findings support the need for tight glycaemic control to avoid drastic neuropathic complications of diabetes.

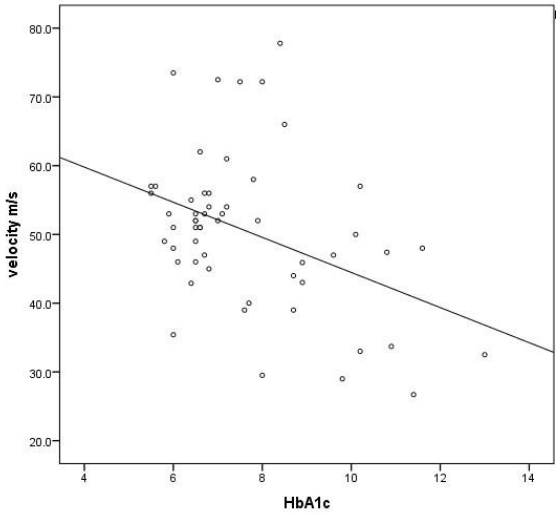

Figure 1: Correlation between HbA1c and sensory nerve conduction velocity. Shows a significant negative correlation between HbA1c and nerve conduction velocity (r = −0.4, p = 0.002).

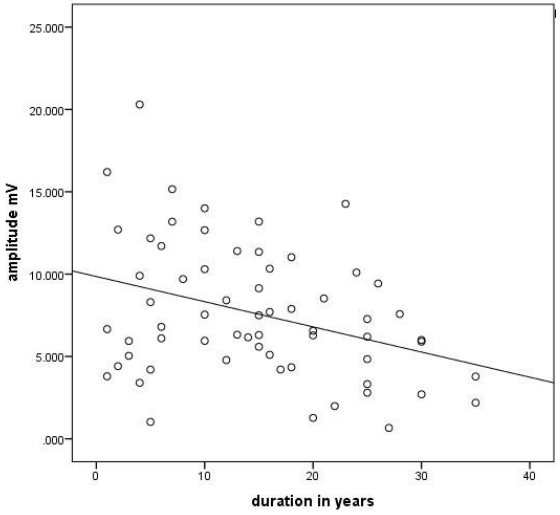

Figure 2: Correlation between duration of DM and amplitude
There was a significant negative correlation between amplitude and duration in years of Type2 DM (r = −0.3, p = 0.005)

References

[1] Awadalla H, Noor SK, Elmadhoun WM, et al. Diabetes complications in Sudanese individuals with type 2 diabetes: overlooked problems in sub-Saharan Africa? Diab Metab Syndr Clin Res Rev. 2017;11: S1047–51

[2] Qureshi MS, Iqbal M, Zahoor S, et al. Ambulatory screening of diabetic neuropathy and predictors of its severity in outpatient settings. J Endocrinol Invest. 2017;40(4):425–30.

[3] Garoushi S, Johnson MI, Tashani OA. Point prevalence of painful diabetic neuropathy in the Middle East and North Africa region: a systematic review with meta-analysis. Libyan J Med Sci. 2018 Jul 1;2 (3):85.

[4] Masood A, Rizvi SA, Siddiqi SS, et al. A study on effects of HbA1c levels on nerve conduction velocity in type 2 diabetes mellitus patients. Int J Cur Res Rev. 2019;11(03):6–8.

[5] Chethan K, Sowjanya T. A study on the effect of duration of type 2 diabetes mellitus on nerve conduction velocity. Natl J Physiol Pharm Pharmacol. 2018;8(12):1622–4

B 05-27

CADMIUM-INDUCED CHANGES IN REPRODUCTIVE ACTIVITIES OF MALE WISTAR RATS: PROTECTIVE ROLE OF PALMITIC ACID

A. O. Akinola[1], A. W. Oyeyemi[2], B. A. Adetula[1], O. D. Adeleke[1]

[1] *University of Medical Sciences, Department of Physiology, Ondo, Nigeria*

[2] *Osun State University, Department of Physiology, Osogbo, Nigeria*

Introduction

Acute exposure to Cadmium (Cd) can cause significant reproductive dysfunction via generation of free radical and increased oxidative stress leading to histological alteration and spermatological damage [1]. Palmitic acid (PA) acts as a biological antioxidant protecting tissues from the effect of free radicals. Aims: This study investigated the ameliorative effects of palmitic acid against cadmium-induced reproductive toxicity in male Wistar rats

Methods

Twenty male Wistar rats (150-170g) were randomly divided into four groups, (n=5), and treated as follows: Control (1 ml/kg normal saline), Cd (2 mg/kg), Cd+PA (2 mg/kg+200 mg/kg), PA (200 mg/kg). Palmitic acid was administered orally for 4 weeks and a single dose of 2 mg/kg of cadmium was injected intraperitoneally. The animals were then given 50 mg/kg BW of sodium thiopental, laparoscopy was done and blood was obtained by cardiac puncture. Testicular magnesium, calcium, zinc, cadmium levels were analysed by atomic absorption spectrophotometry technique.Semen parameters were evaluated as aproved by WHO [2]. Serum follicle stimulating hormone (FSH), luteinizing hormone (LH) and testosterone were measured by ELISA while testicular cytoarchitecture was done by Haematoxylin and Eosin staining. Data were analysed using ANOVA followed by *turkey's post-hoc test*, and results were expressed as mean ± SEM at p<0.05 level of significance. The study followed the Guidelines approved by the ethics committee of the University of Medical Sciences, Ondo city, Ondo state, Nigeria

Results

Cadmium significantly decreased (p<0.05) serum FSH (0.39±0.008 vs 0.45±0.011 mIU/mL), LH (0.20±0.09 vs 0.30±0.0012 mIU/mL) and testosterone (0.63±0.05 vs 0.91±0.08 ng/ml) levels, sperm motility (50±5.30 vs 82±6.04 %), viability (44±4.7 vs 77±8.0 %), counts (7.2±1.54 vs 12.8±3.09

million/ml), testicular magnesium (3.96±0.05 vs 4.95±0.037 mg/L), calcium (3.0±0.41 vs 4.30±0.47 mg/L) and zinc (0.30±0.039 vs 0.44±0.027 mg/L) compared with controls. Abnormal sperm morphology (13.7±0.33 vs 12.1±0.39 %) and testicular cadmium levels (0.0180±0.00127 vs 0.0021 mg/L) were significantly increased ($p<0.05$) in cadmium group compared with controls. Co-administration of PA (200 mg/kg) with cadmium significantly improved ($p<0.05$) serum FSH (0.53±0.017 mIU/mL), LH (0.32±0.032 mIU/mL) and testosterone (0.99±0.14 ng/ml) levels, sperm motility (69±3.4 %), viability (62±6.6 %), counts (10.6±0.98 million/ml), testicular magnesium (4.60±0.07 mg/L), calcium (3.60±0.45 mg/L), zinc (0.41±0.025 mg/L) and architecture when compared with cadmium group. Also, abnormal sperm morphology (13.6±0.15 %) and testicular cadmium (0.0140±0.0024 mg/L) levels were significantly decreased ($p<0.05$) when compared with cadmium group respectively.

Conclusion

Palmitic acid ameliorated cadmium-induced testicular cytoarchitectural damages in rats, suggesting its therapeutic efficacy in improving male reproductive functions in heavy metal toxicity.

References

[1] Akinola, O.A., Oyeyemi, A.W., Daramola, O.O. and Raji, Y. (2020). Effects of the methanol root extract of *Carpolobia lutea* on sperm indices, acrosome reaction, and sperm DNA integrity in cadmium-induced reproductive toxicity in male Wistar rats. *JBRA Assisted Reproduction*, 24(4): 454-465.

[2] World Health Organization (2010) WHO laboratory manual for the Examination and processing of human semen. 5th Ed. Geneva: WHO Press.

B 05-28

Gum Arabic Improves ovarian Antioxidant capacity and Reproductive Outcome In Cafeteria Diet Induced Obesity in Female Rats

S. M. Satti[1], L. A. Kaddam[1], E. F.A. Abdalla[3], A. M. Saeed[4]

[1] *ALNeelain University, Department of physiology /Faculty of Medicine, khartoum, Sudan*

[2] *ALNeelain University, Department of physiology /Faculty of Medicine, khartoum, Sudan*

[3] *ALNeelain University, Department of mollecular medicine /Faculty of Medicine, khartoum, Sudan*

[4] *Khartoum University, Department of physiology /Faculty of Medicine, khartoum, Sudan*

I extend my thanks to all animal house staff members in University of Khartoum, faculty of veterinary medicine for their great help and to Mr.Abdalazim Higawee,Military Hospital Central Lab for their co-operation.

Introduction

Obesity is a worldwide public health concern associated with high morbidity and mortality. Evidence of etiological links between the obesity and reproductive health problems. FDA has identified Gum Arabic (GA) as one of the safest of dietary fiber . The present research aimed to study the effects of gum Arabic on reproductive outcome in obesity induced by Western dietary model (Cafeteria Diet).

Methods

Females Westar rats' weight about 120 -130 gram were divided randomly into two groups distinguished by dietary composition, Control group (n=10), were fed only standard rodent chew diet. Obese group n=20 were fed Cafeteria diet (varying menu of sausage, cheese, snacks, peanuts, chocolate, biscuits) for 8 weeks, random selection of 10 obese rats was done and the addition of 10% Gum Arabic dissolved in tap water (100 g/l) for 4 weeks, then rats were transferred to a mating cage and cohabit with proven fertility male rats (1:1). Mating, fertility, fecundity index, the number of live pups and their body weights were recorded. In the first estrous phase rat anathatazied and dissected. Then ovaries were removed. The Catalase and nitric oxide level in the ovaries were measured. Ovary lipid peroxidation was evaluated by measuring the amount of malondialdehyde (MDA) using a spectrophotometer.

Results

The mating index was found to be 100% all groups. The fertility index and fecundity index were lower in obese rats $p<0.05$ and significantly improved in obese treated with GA. Number of live pups were altered by obesity mean (12 ± 0.97) while for mother fed standard diet (15 ±1.45) ($P< 0.05$). Pups weight was higher in fetuses from obese mothers (1.55 ± 0.05) gm than in control rats (1.31 ± 0.03) gm ($P<0.05$).Gum Arabic treated group showed no significant difference in weight and number of pups when compared to control groups

The Malondialdehyde (MDA) and Nitric Oxide (NO) concentrations significantly increased in the ovary of rats fed a CAF diet, while catalase level were decreased in ovarian tissues mean $P<0.05$, Ovarian MDA and NO significantly reduced in gum Arabic treated group ,while catalase was increased in this group . Furthermore, there is no statistically significant difference in ovarian level MDA and catalase between the GA treated group and the control group.

Conclusion

GA treatment reduced lipid peroxidation and nitric oxide level and increased the activities of ovarian antioxidant enzyme activity. Further more GA improved reproductive outcomes that have been disrupted by obesity-induced by cafeteria diet in rats,

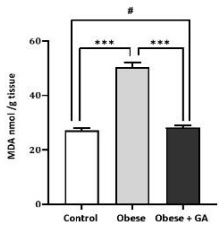

MDA level in ovarian tissues
p <0.05 ***p<.001 # no statistically significant difference

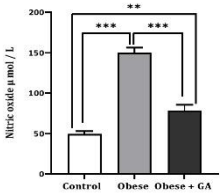

Nitric oxide level in ovarian tissue
*p <0.05 ***p<.001

B 05-29

Potential Role of Prebiotic dietary Supplementation (Acacia Senegal) on Hormonal Profile and Metabolic Markers among Polycystic Ovary Syndrome Patients

R. I. Daoud[1], L. A. Kaddam[1,3], I. M. Daoud[4]

[1] *ALNeelain University, Department of physiology /Faculty of Medicine, khartoum, Sudan*

[2] *ALNeelain University, Department of physiology /Faculty of Medicine, khartoum, Sudan*

[3] *king AbdulaAziz University, Department of physiology /Faculty of Medicine, Rabigh, Saudi Arabia*

[4] *ALNeelain University, Department of Obstetrics and Gynaecology, khartoum, Sudan*

Acknowledgement to the *working team in Bannon fertility center Khartoum Sudan for their great help and support.*

Introduction

Polycystic ovary syndrome (PCOS) is the most common endocrine disease in women of reproductive age, affects 6-20 % of women of reproductive age worldwide. PCOS associated with multiple metabolic abnormalities, it increases the risk for type 2 diabetes mellitus, cerebrovascular and cardiovascular events and one of the main causes of infertility. Pathogenesis remain unclear; but increased Gonadotrophin releasing hormone pulsitility, altered gut microbiome and oxidation stress play a major role. Gum Arabic (GA), edible, dried, gummy exudates from Acacia Senegal tree, is known for its prebiotic and antioxidant properties. GA has a been recognized as lipid lowering agent and has proven effect in reducing body weight.

In this study, we investigated the effect of oral ingested GA on the level of FSH, LH, insulin, testosterone hormones and cholesterol and HBA1C in polycystic ovary syndrome patients. . We assumed that Gum Arabic would reduce the LH/FSH ratio and improve the metabolic profile in PCOs women by reducing the insulin and cholesterol level. To the best of our knowledge, this is the first study conducted to investigate GA intake on PCOS patients.

Methods

Fifteen PCOS patients aged 20-40 years were recruited. All recruited patients met the inclusion criteria (Patients with PCOs based on Rotterdam criteria (2003), married aged from 20-40 and having primary or secondary infertility).

The patients received 30 g/day of GA for 8 weeks dissolved in 200 ml of water. Follicular stimulating hormone(FSH), luteinizing hormone(LH), total testosterone(TT) fasting insulin, cholesterol and HBA1c were measured before and after GA intake. Ethical approval from the National Medicines and Poisons Board was obtained. ClinicalTrials.gov Identifier: NCT04215380

Results

The study clarified that Gum Arabic ingestion significantly decreased in Luteinizing Hormone LH (P value 0.001) mean Follicular Stimulating Hormone (FSH) slightly reduced post intervention with no significant differences (P value =0.414), significant decreased in, FSH/ LH ratio and cholesterol pre and post intervention (P values 0.001, 0.013 and 0.007) respectively, the mean testosterone, insulin and HBA1c shows insignificant differences in pre and post intervention (p value 0.912, P value 0.555 and 0.579 (respectively).

Conclusion

Our study demonstrated that Gum Arabic ingestion for eight weeks in PCOS patients decreases the Luteinizing Hormone (LH) and LH/FSH ratio and improve the metabolic profile by lessening the cholesterol level.

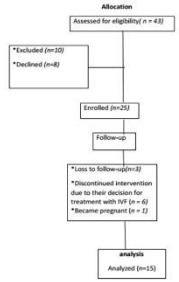

Figure 1
Patients Allocation Figure

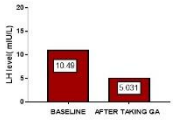

Figure 2
Effect of GA intake on LH level (p.value=.001*)

References
[1] Tremellen K, Pearce K. Dysbiosis of Gut Microbiota (DOGMA) - A novel theory for the development of Polycystic Ovarian Syndrome. Med Hypotheses [Internet]. 2012;79(1):104–12. Available from: http://dx.doi.org/10.1016/j.mehy.2012.04.016
[2] Dubey P, Reddy S, Boyd S, Bracamontes C, Sanchez S, Chattopadhyay M, et al. Effect of Nutritional Supplementation on Oxidative Stress and Hormonal and Lipid Profiles in PCOS-Affected Females. 2021;1–13.
[3] Calame W, Weseler AR, Viebke C, Flynn C, Siemensma AD. Gum arabic establishes prebiotic functionality in healthy human volunteers in a dose-dependent manner. Br J Nutr. 2008;100(6):1269–75.
[4] Babiker R, Elmusharaf K, Keogh MB, Saeed AM. Effect of Gum Arabic (Acacia Senegal) supplementation on visceral adiposity index (VAI) and blood pressure in patients with type 2 diabetes mellitus as indicators of cardiovascular disease (CVD): a randomized and placebo-controlled clinical trial. 2018;1–8.
[5] Kaddam L, Fadl-Elmula I, Eisawi OA, Abdelrazig HA, Saeed AM. Acacia senegal (Gum Arabic) supplementation modulate lipid profile and ameliorated dyslipidemia among sickle cell anemia patients. Journal of Lipids. 2019 Jun 18;2019.

B 05-30

Regular green tea supplementation increases total antioxidant status and reduces exercise-induced oxidative stress: a systematic review.

D. Rojano Ortega[1], J. Naranjo Orellana[1], A.J. Berral Aguilar[1], A. Molina López[2], H. Moya Amaya[2], P. Estevan Navarro[2], F.J. Berral de la Rosa[1]
[1] *University Pablo de Olavide, Sevilla, Spain*
[2] *Udinese Calcio, Udine, Italy*

Introduction

Strenuous muscular exercise leads to an increase in ROS production, generating oxidative stress in cell structures, which has a negative impact on exercise performance (1,2). The elimination of ROS is carried out by the body's endogenous antioxidant defense system in conjunction with exogenous antioxidants consumed through diet, which come primarily from ingestion of fruits and vegetables (3,4). There is some evidence suggesting that ROS play an important physiological role in supporting the recovery process and that antioxidant supplements may hinder the specific cellular adaptations to exercise (5). However, it should be noted that the negative impact of antioxidant supplementation on exercise training adaptation has not been reported with natural antioxidant foods (6).
Green tea is also popular among the beverages rich in polyphenol compounds (7). Its health benefits are due to the antioxidant properties of catechins, of which epigallocatechin-3-gallate, considered the most bioactive, accounts for between 50–80% of the total catechin content (8,9). The positive effects of green tea (GT) supplementation on reducing oxidative stress after exercise have been reported in animals (10,11). Therefore, the aim of this systematic review was to summarize the effects of GT supplementation on exercise-induced oxidative stress found in the existing literature to date in humans.

Methods

The studies included in this systematic review fulfilled the following inclusion criteria: (i) research conducted with human participants, (ii) original articles in peer-reviewed publications, (iii) original studies that had investigated only GT supplementation interventions on oxidative stress after a protocol to induce muscle damage, (iv) research conducted with one control/placebo group, and (v) articles published from inception to December 2020. SPORTDiscuss, PubMed, Scopus, and Web of Science were searched. The methodological quality of the articles was assessed with the PEDro scale.

Results

Eleven randomized or non-randomized placebo-controlled trials were included. (12-22). Four studies evaluated the effects of acute GT ingestion and 7 studies evaluated the effects of a regular GT ingestion. When sufficient data were provided, effect sizes (Hedges' g) for the difference between GT and PLA groups after exercise were calculated (figure).

Conclusion

GT supplementation before exercise for periods of more than 1 week, in a dose range of 400 to 800 mg of catechins per day, appears to be a good strategy to protect the cells against oxidative stress. Nevertheless, none of the studies included in this review analysed oxidative stress markers more than 24 h after exercise. Future investigations should focus on initiating GT supplementation more than seven days before exercise and completing it two or three days after, monitoring the evolution of oxidative stress markers up to 48/72 h after exercise.

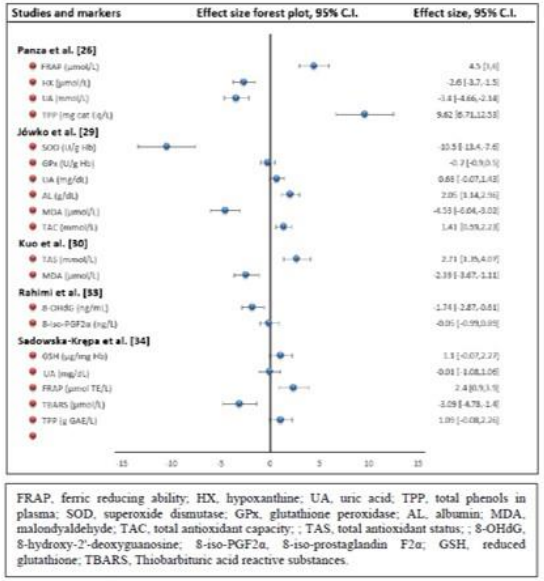

FRAP, ferric reducing ability; HX, hypoxanthine; UA, uric acid; TPP, total phenols in plasma; SOD, superoxide dismutase; GPx, glutathione peroxidase; AL, albumin; MDA, malondyaldehyde; TAC, total antioxidant capacity; ; TAS, total antioxidant status; ; 8-OHdG, 8-hydroxy-2'-deoxyguanosine; 8-iso-PGF2α, 8-iso-prostaglandin F2α; GSH, reduced glutathione; TBARS, Thiobarbituric acid reactive substances.

References
[1] Howatson G, van Someren KA. The prevention and treatment of exercise-induced muscle damage. Sports Med. 2008;38:483–503. doi:10.2165/00007256-200838060-00004
[2] Rojano D, Molina A, Moya H, Berral FJ. Tart cherry and pomegranate supplementations enhance recovery from exercise-induced muscle damage: a systematic review. Biol Sport. 2021;38:97–111. doi:10.5114/biolsport.2020.97069
[3] Bloomer RJ, Goldfarb AH. Anaerobic exercise and oxidative stress: a review. Can J Appl Physiol. 2004;29:245–63. doi:10.1139/h04-017
[4] Watson TA, Callister R, Taylor RD, Sibbritt DW, MacDonald-Wicks LK, Garg ML. Antioxidant restriction and oxidative stress in short-duration exhaustive exercise. Med Sci Sports Exer. 2005;37:63–71. doi:10.1249/01.mss.0000150016.46508.a1
[5] Gomez-Cabrera M, Borras C, Pallardo FV, Sastre J, Ji LL. Decreasing xanthine oxidase-mediated oxidative stress prevents useful cellular adaptations to exercise in rats. J Physiol. 2005;567:113–20. doi:10.1113/jphysiol.2004.080564

B 05-34

Elevated levels of CO2 alter mitochondrial gene expression and acyl carnitine production in monocytes.

D. E. Phelan[1,2], C. Mota[1,2], X. Yin[3,2], L. Brennan[3,2], D. Crean[4,2], E. P. Cummins[1,2]
[1] *University College Dublin, School of Medicine, Dublin, Ireland*
[2] *University College Dublin, Conway Institute of Biomolecular and Biomedical Science, Dublin, Ireland*
[3] *University College Dublin, School of Agriculture and Food Science, Dublin, Ireland*
[4] *University College Dublin, School of Veterinary Medicine, Dublin, Ireland*

This work was supported by a Science Foundation Ireland (SFI) Career Development Award to Eoin P. Cummins (15/CDA/3490)

Introduction

CO_2 is an ancient physiological gas produced during aerobic respiration. As a consequence all cells in the body are exposed to some level of CO_2, and under normal physiological conditions the levels of CO_2 in the blood are tightly regulated. The levels of CO_2 and O_2 are inextricably linked with regions of hypoxia co-associating with regions of elevated CO_2 [1]. In disease states, elevated CO_2 levels in the blood (hypercapnia >45mmHg) present in patients with chronic respiratory disorders e.g. Chronic Obstructive Pulmonary Disease (COPD). Hypercapnia is risk factor in COPD [2] but may be of benefit in the context of destructive inflammatory signalling [3]. The effects of CO_2 changes *per se* on cell signalling and signal transduction are poorly understood and warrant further investigation. A better understanding of how CO_2 elicits cellular signalling may be of benefit in the treatment of patients experiencing hypercapnia.

In this study we aim to elucidate how increased CO_2 influences the behaviour of immune cells, through integration of state of the art RNA-sequencing, metabolic and metabolomic approaches in monocytes.

Methods

THP-1 monocytes were incubated in environmental chambers at different CO_2 levels (5% CO_2 ~40mmHg (pH~ 7.3)/ 10% CO_2 ~ 77mmHg (pH~ 7.4)) for 4 hours, +/-LPS under pH buffered conditions. Gene expression was analysed by RNAseq and qPCR. Metabolite levels were determined by targeted LC/MS. Mitochondrial oxidant production was measured using MitoSOX and AmplexRed assays. Mitochondrial DNA content was measured by qPCR and mitochondrial protein content was measured by acridine orange 10-nonyl bromide fluorescence and western blotting. Cellular reductase activity was measured using 3-(4,5-Dimethylthiazol-2-yl)-2,5-diphenyltetrazolium bromide (MTT) conversion to formazan.

Results

In hypercapnia, RNA-seq analysis identified hundreds of differentially expressed genes under basal and LPS-stimulated conditions. Notably, transcripts relating to mitochondrial gene expression and mitochondrial-encoded electron transport were enhanced in hypercapnia in both basal and LPS-stimulated cells. Mitochondrial DNA content and protein expression did not appear to be enhanced under similar conditions however, using a metabolomic approach we identified several key metabolites to be altered in hypercapnia, particularly specific acyl-carnitines species.

Conclusion

Our results indicate that elevated levels of CO_2 elicit metabolic shifts in lipid metabolism in monocytes under pH buffered conditions. Taken together these data support the concept of CO_2 as a mild but consistent modulator of monocyte transcription that can influence immunometabolic signalling in immune cells in hypercapnia. A better understanding of how immune cells respond to elevated CO_2 on a cellular and metabolic level may be of benefit in the treatment of patients experiencing hypercapnia.

References
[1] Cummins, E.P., M.J. Strowitzki, and C.T. Taylor, *Mechanisms and Consequences of Oxygen and Carbon Dioxide Sensing in Mammals*. Physiol Rev, 2020. **100**(1): p. 463-488.
[2] Nin, N., et al., *Severe hypercapnia and outcome of mechanically ventilated patients with moderate or severe acute respiratory distress syndrome*. Intensive Care Med, 2017. **43**(2): p. 200-208.
[3] Gao, W., et al., *Effect of Therapeutic Hypercapnia on Inflammatory Responses to One-lung Ventilation in Lobectomy Patients*. Anesthesiology, 2015. **122**(6): p. 1235-52.

PB 06 | Neuroscience

B 06-01

The impact of hypoxia-inducible factors on ferroptotic cell death in the retinal pigment epithelium

U. S. Blind, J. Fandrey, **Y. Henning**
University Hospital Essen, University of Duisburg-Essen, Institute of Physiology, Essen, Germany

Introduction
Age-related macular degeneration (AMD) is the most common blinding disease in the elderly population. Although there are still many uncertainties regarding the pathophysiology of AMD, oxidative stress and hypoxia in the retinal pigment epithelium (RPE) have long been considered major risk factors leading to photoreceptor degeneration in the macula. Hypoxia leads to an accumulation of hypoxia-inducible factors (HIF), dimeric transcription factors with an oxygen-labile α-subunit and a constitutively expressed β-subunit, which enable adaptation to hypoxic conditions. Albeit protective in the short-term, chronic induction of HIF signaling is associated with the pathophysiology of many diseases.
Methods
In order to mimic AMD pathophysiology, we combined oxidative stress and HIF stabilization in a human RPE cell line (ARPE-19). We induced oxidative stress by sodium iodate (SI) and HIF accumulation by dimethyloxalylglycine (DMOG), a prolyl hydroxylase inhibitor. To separately investigate the roles of the two HIF isoforms HIF-1 and HIF-2, we conducted siRNA-mediated knockdowns of HIF-1α and HIF-2α and treated the cells with SI. Knockdown cells were treated under hypoxic conditions with 1% O_2 in a hypoxic incubator to induce HIF stabilization. Treatment effects were analyzed with cell viability assays, Western Blot and quantitative Real-Time PCR.
Results
Co-treatment of ARPE-19 cells with SI and DMOG revealed that HIF stabilization by DMOG exacerbated cell death compared to cell death induced by SI alone. By treating the cells with different cell death pathway inhibitors, we could identify ferroptosis as the major cell death mode, which is caused by iron accumulation and oxidative stress leading to lipid peroxidation. Knockdown of HIF-1α and HIF-2α revealed that SI-treated cells were rescued by HIF-1α knockdown but ferroptosis was exacerbated by HIF-2α knockdown. To find out if these effects are generally applicable to ferroptosis, we used RSL3, which induces ferroptosis by inhibiting GPX4, a major anti-ferroptosis regulator. In contrast to SI-induced ferroptosis, RSL3-induced ferroptotic cell death was decreased by knockdown of both, HIF-1α and HIF-2α. These findings suggest that HIFs play differential roles in ferroptosis regulation depending on the mode of induction. The molecular pathways responsible for these observations are currently under investigation.
Conclusion
Taken together, our findings provide important insights into the involvement of HIFs in ferroptosis regulation. Ferroptosis is associated with the pathophysiology of several diseases and is also discussed as a therapeutical strategy in cancer treatment. Hence, a better understanding of ferroptosis regulation will contribute to novel treatment approaches not only restricted to AMD in the long-term.

B 06-02

The modulation of TRPA1 ion channel by the antimalarial drug artemisinin

D. E. Hutanu[1], R. M. Babes[2], G. Oprita[1], T. Andries[1], A. Manolache[1], A. Babes[1]
[1] *University of Bucharest, Faculty of Biology, Department of Anatomy, Animal Physiology and Biophysics, Bucharest, Romania*
[2] *Carol Davila University of Medicine and Pharmacy, Department of Biophysics, Bucharest, Romania*

Introduction:
Malaria is caused by parasites of the genus *Plasmodium* and is transmitted to humans by mosquitoes of the genus *Anopheles*. The disease is found in subtropical and tropical regions, where specific conditions of temperature, humidity and precipitation are met. The symptoms are varied, may be absent, moderate or severe and, if they occur, complications can even lead to death.
Artemisinin and its derivatives comprise the most important class of drugs used in medical practice to treat malaria. When administered, it has been found that moderate side effects may occur, such as dizziness, nausea or vomiting. Based on these considerations, we investigated the possible effects of artemisinin on three ion channels: TRPM8, TRPV1 and TRPA1.
Methods:
Non-ratiometric calcium microfluorimetry experiments were performed on HEK293T cells, transiently transfected with human TRPA1 (hTRPA1), mouse TRPA1 (mTRPA1), human TRPM8 (hTRPM8) or human TRPV1 (hTRPV1), as well as primary sensory neurons from adult mice. Mice (male) were killed by inhalation of 100% CO_2 followed by decapitation. Dorsal root ganglia (DRG) were removed and DRG neurons were isolated and kept in primary culture. Cells were plated onto poly-D-lysine-coated glass coverslips and used for experiments within 24 h.
Results:
Untransfected HEK293T cells (n=363), as well as HEK293T cells expressing hTRPV1 (n=177) or hTRPM8 (n=257) showed no activation following the application of artemisinin (200 µM). However, the application of artemisinin induced an influx of Ca^{2+} into HEK293T cells transiently transfected with hTRPA1 (n=265) or mTRPA1 (n=133). The functional expression of hTRPV1, hTRPA1, mTRPA1 and hTRPM8 was demonstrated by responses to specific agonists of these ion channels: capsaicin (300 nM), AITC (50 µM) and WS-12 (5 µM). The response to artemisinin was reversibly inhibited by the specific TRPA1 antagonist A967079 (1 µM). When artemisinin was applied in calcium-free conditions (n=112), the response to artemisinin was reversibly suppressed, resulting that the source of calcium is extracellular. A subpopulation of mouse DRG neurons (97 neurons in a total of 437, ca. 22%) was also activated by artemisinin (400 µM). The viability of neurons was tested using a high concentration of KCl (50 mM).
Conclusion:
Based on our data obtained on heterologous expression systems and on primary sensory neurons from adult mice, we conclude that artemisinin acts as a TRPA1 agonist, which could explain the side effects of the drug.

B 06-03

Hypothalamic knockdown of *FAM163A* decreases the firing frequency of AgRP neurons without altering food intake in transgenic mice

C. S. Erdogan, Y. Yavuz, H. B. Ozgun, V. A. Bilgin, S. Agus, B. Yilmaz
Yeditepe University, Faculty of Medicine, Department of Physiology, İstanbul, Turkey

This study was partially supported by TUBITAK (Project # 118S245).

Introduction
Agouti-related peptide (AgRP)-expressing neurons in the arcuate nucleus (ARC) of the hypothalamus are a major orexigenic population driving the food intake [1]. FAM163A, also named neuroblastoma-derived secretory protein, is a 168 amino acid protein, with a putative signal peptide and membrane binding domain [2]. It has been reported to found both intracellularly and extracellularly, and act as an oncogene . However, functional studies on the FAM163A are scarce. In this study, we aimed to investigate the effect of FAM163A knockdown in the ARC on food intake and electrophysiology of AgRP neurons.
Methods
Male AgRP-IRES-Cre knock-in mice were infected with either control shRNA or FAM163A shRNA lentivirus together with AAV-CAG-Flex-GFP virus, which tags the AgRP neurons, intracerebroventricularly (posterior: -1.35 mm, lateral: ± 0.35 mm and vertical: 5.85 mm). Fifteen days after infection, single animals were housed in cages and food intake was monitored for 25 days. After the experimental period, electrophysiological recordings were obtained *ex vivo* from the brain slices. Hypothalamic expression profile was examined by confocal microscopy.
Results
Food intake and body weight of the animals were not affected by *FAM163A* knockdown. FAM163A is ubiquitously expressed in the hypothalamus, while a subpopulation of AgRP neurons expresses FAM163A. Firing frequency of AgRP neurons were significantly reduced by *FAM163A* knockdown.
Conclusion
Our results suggest that FAM163A may be a regulatory factor for the hypothalamic neuronal activity in the regulation of energy metabolism.

References
[1] Deem JD, Faber CL, Morton GJ. 2022, 'AgRP neurons: Regulators of feeding, energy expenditure, and behavior', *The FEBS Journal*, 289(8):2362-2381.
[2] Chen YL, Li XL, Li G, Tao YF, Zhuo R, Cao HB, Jiao WY, Li ZH, Zhu ZH, Fang F, Xie Y, Liao XM, Wu D, Wang HR, Yu JJ, Jia SQ, Yang Y, Feng CX, Yang PC, Fei XD, Wang JW, Xu YY, Qian GH, Zhang ZM, Pan J. 2022, 'BRD4 inhibitor GNE987 exerts anti-cancer effects by targeting super-enhancers in neuroblastoma', *Cell & Bioscience*, 12: 33.

B 06-04

Investigation on the Effect of Selected Autophagy/Mitophagy Modulator and Antioxidant Agents on Cell Viability of Mouse Sensory Neurons

A.K. Salihoğlu, A. Ayar
Karadeniz Technical University, Department of Physiology, Faculty of Medicine, Trabzon, Turkey

This study is supported by TUBITAK (The Scientific and Technological Research Council of Turkey), Project No: 220S863.

Introduction
Peripheral neuropathy is one of the most common diabetic complications in a chronic process in the absence of glycemic control. Mitochondrial dysfunction and autophagic dysmodulation are novel mechanisms to explain the cellular pathophysiology of many diseases, and effects of mitochondrial dysfunction and autophagy/mitophagy modulation in diabetic peripheral neuropathy (DPN) are not fully understood yet. The aim of this study was to examine the possible neuroprotective effects of selected autophagy/mitophagy modulator and antioxidant agents on sensory neurons in DPN *in vitro* mouse model.
Methods
Dorsal root ganglia -DRG- (as the cellular model of neuropathy) were cultured as primary sensory neurons from 12-week-old male C57BL/6J mice (which is a diabetic-prone, genetically modified model). Neuroprotective effects of selected mitophagy/autophagy modulators; anethole trithione (10, 30, 100 µM), urolithin A (3, 10, 30 µM), rapamycin (0.03, 0.1, 0.3 µM) (three different doses determined based on the literature) and their combination with metformin (1mM), a common antidiabetic agent, on hyperglycemic DRG cells were examined in a concentration-dependent manner, by cell viability analysis (xCELLigence real-time cell viability analysis - RTCA, ACEA Biosciences, USA) for 36th hours. Cell indices obtained by xCELLigence RTCA were compared by repeated measures ANOVA (RMA).
Results
In the hyperglycemic (HG) control groups, the cell indices of HG (only), HG+saline, and HG+dimethyl sulfoxide groups decreased from 0th to 36th hours (p=0.034, p=0.022 and p=0.022, respectively, RMA). In the HG and anethole tritione test groups, the cell indices of the low-dose and high-dose anethole trithione groups increased from 0th to 36th hours (p=0.017 and p=0.037, respectively, RMA). In the HG and urolithin A test groups, cell indices decreased from 0th to 36th hours in the low dose urolithin A group (p=0.038, RMA). In the HG and rapamycin test groups, the cell indices of the low and medium-dose rapamycin groups decreased from 0th to 36th hours (p=0.038 and p=0.031, respectively, RMA). There were no significant changes in cell indices from 0th to 36th hours in the test groups that combined with metformin and test agents separately (p>0.05, RMA).
Conclusion
Results from this *in vitro* analysis indicate that anethole trithione, an antioxidant which prevents mitochondrial dysfunction, may have neuroprotective effects on diabetic sensory neuropathy.

B 06-05

Frequency dependence of ATP generating pathways in an auditory brainstem nucleus

N. Palandt[1,2], C. Resch[3], P. Unterlechner[1], L. Voshagen[1], L. Kunz[1]

[1] *Ludwig-Maximilians University, Munich, Germany*

[2] *Graduate School of Systemic Neuroscience, Munich, Germany*

[3] *Technical University Munich, Munich, Germany*

Funding: Graduate School of Systemic Neuroscience, German Research Foundation (DFG KU 1282/9-1)

Introduction: Neurons are extremely energy demanding. Especially during firing, large amounts of ATP need to be produced in a short time. This holds particularly for neurons capable of firing at high frequencies such as those in the medial nucleus of the trapezoid body (MNTB), that have a broad range of firing frequencies up to 1000 Hz. Several metabolic pathways can supply neurons with energy. We show that the contribution of different metabolic pathways is dependent on the firing frequency.

Methods: We stimulate electrically the fibres leading to the MNTB in acute brainstem slices of the Mongolian gerbil (*Meriones unguiculatus*). Varying frequencies are used within a physiological range of 10 to 1000 Hz. By monitoring changes in the levels of NADH, FAD and O_2, we have an indirect track of ATP generation and with it a hint to which metabolic pathways are used. Additionally, we are working on a linear-kinetic dynamic flux balance analysis (LK-DFBA) to calculate the contribution of each metabolic pathway at different firing frequencies.

Results: At higher frequencies, MNTB neurons consume less oxygen compared to lower frequencies. The NADH and $FADH_2$ consumption are lowest at very low (below 100Hz) and higher frequencies when stimulating with 400 electrical impulses. An increase in the glucose concentration of the artificial cerebrospinal fluid (ACSF) in the recording chamber above physiological levels (from 2mM to 10mM) leads to a significant reduction in FAD production for all frequencies. Most likely due to a shift to glycolysis for ATP production caused by the Crabtree effect.

Conclusion: Our results indicate a metabolic switch from oxidative phosphorylation (OXPHOS) to glycolysis at higher frequencies above 200 Hz. Nevertheless, OXPHOS represents an important pathway of ATP generation also for higher frequencies, as the recordings with higher glucose concentration show. The computational model will help us to better understand our data and calculate ATP levels based on the measured changes in levels of NADH, FAD and O_2.

B 06-06

The influence of hypoxia-inducible factor-2α on synaptic architecture and function under normoxia and hypoxia

T. Quinting[1], H. Jastrow[2], J. Fandrey[1], T. Schreiber[1,3]

[1] *University of Duisburg-Essen, Institute of Physiology, Essen, Germany*

[2] *Imaging Centre Essen, Essen University Hospital, Institute of Anatomy and Institute for Experimental Immunology and Imaging, Essen, Germany*

[3] *University of Witten/Herdecke, Department of Physiology, Pathophysiology and Toxicology and Center for Biomedical Education and Research (ZBAF), Witten, Germany*

Sufficient oxygen supply is fundamental for maintaining normal brain functions and to avoid hypoxia. Prolonged hypoxia as in an ischemic stroke can lead to irreversible brain injury with symptoms like epilepsy, speech and language deficits or even paralysis. In acute hypoxia, neuronal cells adapt in different ways to the decreased oxygen supply for protection of neurons including synaptic signaling decrease or changes in excitation and inhibition of neuronal and glial cells.

Key factors of the cellular response to low oxygen are the heterodimeric transcription factors “hypoxia-inducible factors” (HIF-1, HIF-2 and HIF-3). HIFs are heterodimers composed of an oxygen-sensitive alpha-subunit and a constitutively expressed beta-subunit. Under normoxic conditions, the alpha-subunits are targeted for proteasomal degradation. HIFs alter the expression of oxygen-related genes and play an important role during brain development and neural regeneration after hypoxic events as it has been shown for HIF-1. However, the exact role of HIF-2 in the brain remains unknown.

By using brain-specific *Hif-2α* knockout (KO) mice, we showed that synaptogenesis is highly oxygen-dependent and a *Hif-2*α KO led, amongst others, to an altered expression of genes involved in synaptic transmission in the animals in vivo, as well as in an in vitro neurosphere system where cells were also challenged with hypoxic conditions [1]. Next, we addressed synaptic plasticity by performing an in vivo environmental enrichment study with a complex combination of physical and mental stimuli in the Hif-2a KO mice and wild-type littermates, followed by analysis of gene expression. Although we found differently expressed synapse-associated genes due to housing conditions, an overall effect of *Hif-2α* KO was absent. A first electron microscopy study of synapses of wild type and *Hif-2α* KO mice furthermore showed a reduced postsynaptic density length and area in *Hif-2*α KO animals indicating differences in synaptic ultrastructure, which will be further analyzed in a larger mouse cohort.

We next addressed the regulation of synaptic transmission by HIF-2α in vitro by using a co-culture system with combinations of primary wild type or *Hif-2α* KO hippocampal neurons and cortical wild type or *Hif-2α* KO astrocytes, where we can directly challenge the cells with hypoxia. Both astrocytes and hippocampal neurons showed a good response to hypoxia independent of their genotype, as seen by up-regulation of HIF target genes like *Vegf* and *Phd2*. Quantitative real-time PCR data furthermore showed differences between wild type and *Hif-2α* KO neurons on synapse-associated genes like *Synapsin* and *Neurogranin* under normoxic, but not under hypoxic conditions, indicating an effect of *Hif-2α* already under normoxic conditions.

How exactly and why HIF-2α, as an transcription factor which is normally active under low oxygen levels, influences synapses even under normoxic conditions is still under investigation so far.

References

[1] Kleszka K, Leu T, Quinting T, Jastrow H, Pechlivanis S, Fandrey J 2020, ‘Hypoxia-inducible factor-2α is crucial for proper brain development’, *Sci Rep*, 10(1):19146

B 06-07

Autophagosomal dysfunction in biallelic SPRED2 loss-of-function mouse model elicits a neurodegenerative tauopathy

S. Gredy, D. Hepbasli, A. Niedermeier, K. Schuh
University of Wuerzburg, Institute of Physiology I, Wuerzburg, Germany

Functionality of autophagy is essential for cell homeostasis and intracellular signaling pathway inactivation. An important signaling cascade controlling cell homoeostasis but also important steps of autophagy, is the ERK-MAPK pathway (1). Potent inhibitors of this ERK-MAPK pathway are SPRED proteins. Due to the suppressive effect on this cascade (2), SPREDs play a role in a variety of processes, in cardiovascular organ and brain development, hormonal homeostasis, carcinogenesis and metastasis (3). Biallelic SPRED2 KO mice show clear alterations in autophagy related processes. Further, SPRED2 interacts with the microtubule-associated LC3, thereby increasing the conversion of LC3-I to LC3-II, which in turn regulates autophagy and cell death (4). Among others, the protein Tau is phosphorylated by MAPKs and then dissociates from microtubules and forms multimeric aggregates. We hypothesize that missing inhibition of MAPK by SPRED2 leads to an increase in Tau phosphorylation, dissociation from microtubules, and accumulation within the cell, the pathogenic mechanisms of tauopathies.
We used pull down assays to check the interaction of SPERD2 with autophagy-related proteins. To clarify if lack of SPRED2 influences Kinesin or Dynein ATPase activity, we used a Dynein/Kinesin ATPase End-Point Kit. Brain morphology was investigated by MRI and histology. To analyze phosphorylated Tau aggregates in brains of SPRED2 KO mice, we did Western blot (WB) analyses and IHC.
We detected SPRED2 interaction with SQSTM1/p62, an adapter guiding ubiquitinated proteins to LC3-mediated autophagy. GST pull-downs showed that full-length SPRED2 and the SPRED2-EVH1 domain interact with p62 in brain lysates. WB analyses revealed a decreased expression of p62 in SPRED2 KO brains, indicating that SPRED2 is required for p62 recruitment and autophagy induction. We detected a reduced autophagic flux (LC3-II/LC3-I ratio) in brains of SPRED2 KO mice. The Dynein/Kinesin ATPase End-Point Kit with vesicle preparations from WT and SPRED2 KO mice revealed that lack of SPRED2 impairs Dynein activity, responsible for retrograde transport in neurons, but not Kinesin activity. MRI and histology studies revealed enlarged brain ventricles and cortex atrophy in KO brains. WB and IHC demonstrated hyperphosphorylated Tau aggregation in hippocampi of SPRED2 KO mice, a common finding in various neurodegenerative diseases.These data indicate that the autophagosomal dysfunction in SPRED2 KO mice is connected to a tauopathy. Identification of the molecular processes involved will be relevant in many areas of medical research, as a variety of diseases are triggered by disorders of intracellular transport and lack of fusion with lysosomes. In view of the fact that the first people with mutations in the SPRED2 gene have now been identified (5), the knowledge gained from this project is very important for a possible diagnosis or therapy of these surely rare diseases in humans.

References

[1] Martinez-Lopez, N, Singh, R, 2014, ATGs: Scaffolds for MAPK/ERK signaling, *Autophagy*, 10(3) (2014) 535-7
[2] Wakioka, T, Sasaki, A, Kato, R, Shouda, T, Matsumoto, A, Miyoshi, K, Tsuneoka, M, Komiya, S, Baron, R, Yoshimura, A, 2001, Spred is a Sprouty-related suppressor of Ras signalling, *Nature*, 412(6847) (2001) 647-51
[3] Bundschu, K, Walter, U, Schuh, K, 2007, Getting a first clue about SPRED functions, *Bioessays*, 29(9) (2007) 897-907
[4] Jiang, K, Liu, M, Lin, G, Mao, B, Cheng, W, Liu, H, Gal, J, Zhu, H, Yuan, Z, Deng, W, Liu, Q, Gong, P, Bi, X, Meng S, 2016, Tumor suppressor Spred2 interaction with LC3 promotes autophagosome maturation and induces autophagy-dependent cell death, *Oncotarget*, 7(18) (2016) 25652-67
[5] Motta, M, Fasano, G, Gredy, S, Brinkmann, J, Bonnard, AA, Simsek-Kiper, PO, Gulec, EY, Essaddam, L, Utine, GE, Guarnetti Prandi, I, Venditti, M, Pantaleoni, F, Radio, FC, Ciolfi, A, Petrini, S, Consoli, F, Vignal, C, Hepbasli, D, Ullrich, M, de Boer, E, Vissers, LELM, Gritli, S, Rossi, C, De Luca, A, Ben Becher, S, Gelb, BD, Dallapiccola, B, Lauri, A, Chillemi, G, Schuh, K, Cavé, H, Zenker, M, Tartaglia, M, 2021, SPRED2 loss-of-function causes a recessive Noonan syndrome-like phenotype, *Am J Hum Genet*, 108(11):2112-2129. doi: 10.1016/j.ajhg.2021.09.007

B 06-09

Asprosin Can Have a Beneficial Influence on Male Rats' Sexual Behaviour

M.R. Ozdede[1], Z.D. Oz[1], A. Ucer[2], T. Yalcin[1], S.U. Orhan[2], A. Yasar[3], E. Kacar[1], I. Serhatlioglu[2], B. Yilmaz[4], **H. Kelestimur**[1]
[1] *Firat University, Faculty of Medicine, Department of Physiology, Elazig, Turkey*
[2] *Firat University, Faculty of Medicine, Department of Biophysics, Elazig, Turkey*
[3] *Firat University, Vocational School of Health Services, Elazig, Turkey*
[4] *Yeditepe University, Faculty of Medicine, Department of Physiology, İstanbul, Turkey*

This study was supported by TUBITAK (project# 220S744).

Introduction
Asprosin is a novel adipokine that is synthesized from white adipose tissue. Asprosin can pass the blood-brain barrier, increase appetite, and improve smell on the olfactory bulbs of mice. Additionally, asprosin increases sperm motility in male mice through the OLFR-734 receptor. However, the effects of asprosin on sexual behaviour remain unknown. Therefore, the aim of the present study was to examine the impact of exogenous asprosin administration on sexual behaviour in male rats.
Methods
In this study, 24 male Sprague-Dawley rats, 21 days old and 35 ± 2 g weight, were divided into two groups (control and asprosin). The animals were administered daily intraperitoneally asprosin (500 ng/kg) for 10 weeks or saline from day 21. From the eighth week, male rats were performed sexual behaviour tests simultaneously. Sexual behaviour tests were performed individually between 8 PM and 10 PM. The recording was started after the receptive females were presented to the males. The recording was performed for 30 minutes. The variables were measured: ejaculation frequency (number of ejaculations in each copulatory series); intromission latency (time between the introduction of the female into the cage and the first intromission). At the end, the animals were decapitated, and their blood was collected. FSH, LH, Testosterone, Estradiol and AMH hormones were measured from the blood serum using the ELISA method.
Results
In the sexual behaviour experiment of the male rats, in the asprosin group, intromission latency time (10.18 ± 2.53) was observed much earlier than in the control group (38.7 ± 5.96), and it was statistically significant (p<.001). When comparing the asprosin group (2.18 ± 0.40) to the control

group (1.81 ± 0.40), it was found that the frequency of ejaculation was enhanced (p<.05). Compared to the control group, the quantity of testosterone in the blood serum of animals treated with asprosin hormone increased; nevertheless, the estradiol level decreased in the asprosin group compared to the control group. AMH levels were significantly higher in the control group than in the asprosin group. Furthermore, there was no significant difference in FSH or LH between the groups.

Conclusion

Our results show that chronic administration of asprosin increases ejaculation frequency and reduces intromission latency. Additionally, testosterone levels increase in animals treated with asprosin. Asprosin is known to improve the sense of smell in rodents. Therefore, asprosin may confirm the significance of olfaction in male sexual behaviour.

B 06-10

Characterisation of BK currents co-expressed with the putative regulatory subunits LINGO1-4.

S. Dudem, K. D. Thornbury, G. P. Sergeant, M. A. Hollywood

Dundalk Institute of Technology, Smooth Muscle Research Centre, Dundalk, Ireland

This study was funded as part of the Borders and Regions Airway Training Hub project by the European Union (EU), under the Interreg VA Programme, managed by the Special EU Programmes Body (to K.D.T., G.P.S., and M.A.H.) and funding from the Higher Education Authority via DKIT Research Office.

Large-conductance, voltage and Ca^{2+} activated potassium (BK) channels are widely expressed in both excitable and non-excitable cells. The biophysical and pharmacological properties of the pore-forming α subunits are modulated by regulatory β and γ subunits[1]. The γ1-4 subunits are single transmembrane proteins, which have an extracellular domain (containing 6 leucine rich repeat (LRR) regions) and a short intracellular tail. LINGO1 is also an LRR containing protein[2,3] and shares a number of features with the γ subunits. It has a large extracellular domain containing 12 LRR regions, a single TM helix and a short intracellular tail. Since LINGO1 is a regulatory subunit of BK channels[4], we wanted to examine if the three other LINGO proteins modulated the biophysical properties of BK currents.

HEK cells were transiently co-transfected with BKα and LINGO1-4 cDNA. Inside out patches were studied at 37^{o}C under voltage clamp using the patch clamp technique and all procedures accorded with current EU legislation. Cells transfected with BKα:LINGO4 produced currents that were indistinguishable from BKα alone (Table1). However, BKα:LINGO1-3 all produced rapidly inactivating currents that could be distinguished from each other on the basis of their biophysical properties. The half maximal activation voltage ($V_{1/2}$) of BKα:LINGO1 currents was 112±1 mV, (n=6) compared to 162±3 mV (n=6) in BKα alone, in 100 nM Ca^{2+}, as shown previously[4]. The activation $V_{1/2}$ for BKα:LINGO2 currents was 130±2mV (n=8), compared to BKα:LINGO3 which was 198±3mV (n=8, p<0.05). As shown in Table 1, the steady state half-maximal inactivation voltage (Inactivation $V_{1/2}$) of BKα:LINGO2 and BKα:LINGO3 were indistinguishable but both were shifted ~+30 mV compared to BKα:LINGO1 channels. Co-expression of LINGO1-3 with BKα increased the rate of activation ~10-fold in response to a step from -100 mV to +100 mV. The rate of inactivation was approximately 2-fold slower in BKα:LINGO2 channels (9.2±0.95ms) compared to BKα:LINGO1 or BKα:LINGO3, as measured from a single exponential fit to currents at +100 mV.

In conclusion, co-expression of LINGO1-3 proteins with BKα subunits results in inactivating BK currents in HEK cells.

	Activation $V_{1/2}$ (mV)			Inactivation $V_{1/2}$ (mV)			Kinetics (ms)			Inactivation (ms)
	100nM Ca^{2+}	1μM Ca^{2+}	10μM Ca^{2+}	100nM Ca^{2+}	1μM Ca^{2+}	10μM Ca^{2+}	$\tau_{activation/+100mV}$	$\tau_{deact/-100mV}$	$\tau_{deactivation/-100mV}$	$\tau_{recovery/+100mV}$
BKα	162±3	44±3	-35±2	N/A	N/A	N/A	4.29±0.40	N/A	0.14±0.01	N/A
BKα:LINGO1	112±1	66±2	--	9±2	-68±2	--	0.48±0.05	5.23±0.43	3.51±0.41	1.5–0.4
BKα:LINGO2	130±2	53±1	--	35±2	-39±2	--	0.60±0.07	9.17±0.95	2.84±0.35	0.8–0.1
BKα:LINGO3	198±3	68±3	-18±3	35±3	-36±3	-85±2	0.43±0.03	5.19±0.61	1.00±0.07	0.4–0.1
BKα:LINGO4	164±2	41±3	-50±2	N/A	N/A	N/A	5.21±0.89	N/A	0.16±0.01	N/A

Table 1. *Biophysical properties of BK and BK:LINGO1-4 currents recorded in excised patches from HEK cells. The data for Kinetics and Recovery from inactivation were obtained in 100 nM Ca^{2+}. Mean±SEM are shown and replicates were n=5-9.*

References

[1] Latorre, Ramon, et al. "Molecular Determinants of BK Channel Functional Diversity and Functioning." *Physiological Reviews*, vol. 97, no. 1, Jan. 2017, pp. 39–87.

[2] Mosyak, Lidia, et al. "The Structure of the Lingo-1 Ectodomain, a Module Implicated in Central Nervous System Repair Inhibition." *Journal of Biological Chemistry*, vol. 281, no. 47, Nov. 2006, pp. 36378–36390.

[3] Andrews, Jessica L., and Francesca Fernandez-Enright. "A Decade from Discovery to Therapy: Lingo-1, the Dark Horse in Neurological and Psychiatric Disorders." *Neuroscience & Biobehavioral Reviews*, vol. 56, Sept. 2015, pp. 97–114.

[4] Dudem, Srikanth, et al. "LINGO1 Is a Regulatory Subunit of Large Conductance, Ca^{2+} -Activated Potassium Channels." *Proceedings of the National Academy of Sciences*, vol. 117, no. 4, 13 Jan. 2020, pp. 2194–2200.

B 06-11

Endogenous but not sensory-driven activity controls migration, morphogenesis and survival of adult-born neurons in the mouse olfactory bulb.

Y. Kovalchuk[1], K. Li[1], K. Figarella[1], X. Su[1], J. Gorzolka[1], J. N. Neher[2,3], N. Mojtahedi[1], N. Casadei[4,5], U. B.S. Hedrich[6], O. Garaschuk[1]

[1] *University of Tübingen, Department of Neurophysiology, Tübingen, Germany*

[2] *German Center for Neurodegenerative Diseases (DZNE), Tübingen, Germany*

[3] *University of Tübingen, Hertie Institute for Clinical Brain Research, Department of Cellular Neurology, Tübingen, Germany*

[4] *University of Tübingen, Institute of Medical Genetics and Applied Genomics, Tübingen, Germany*

[5] *NGS Competence Center Tübingen, Tübingen, Germany*

[6] *University of Tübingen, Hertie Institute for Clinical Brain Research, Department of Neurology and Epileptology, Tübingen, Germany*

This work was supported by the DFG grants GA 654/14-1 to O.G, GA 654/13-1/HE8155/1-1 to O.G. and U.H.-K. The NCCT is financed by the DFG grant INST 37/1049-1.

The rodent olfactory bulb (OB) is a highly plastic brain region receiving new neurons throughout life. Cumulative evidence revealed an important role of these cells in the fine-tuning of odor perception/discrimination, facilitation of the task-dependent pattern separation, learning, and memory. Generated in the subventricular zone of the lateral ventricle, adult-born cells migrate along the rostral migratory stream into the OB and differentiate into local GABAergic interneurons: granule cells (GCs) and juxtaglomerular cells (JGCs). While adult-born GCs (abGCs) migrate straight to their final destinations, abJGCs enter the 3-4 weeks long pre-integration phase where abJGCs undergo a millimeter-long lateral migration [1]; grow and prune their dendritic trees [2, 3] and incorporate into the existent OB circuitry. This phase is unique to abJGCs and its regulating factors remain unclear.

Therefore, we have tested the role of endogenous/sensory activity in migration, morphogenesis, and survival of abJGCs. To do so, we genetically suppressed their excitability via viral overexpression of either voltage-gated Kv1.2- or inwardly rectifying Kir2.1-channels and used longitudinal *in vivo* two-photon imaging of cells labeled with the ratiometric Ca^{2+} indicator Twitch-2B to monitor cell activity and morphology. Odor deprivation via nostril suture was used to test for the role of sensory activity. To understand the molecular pathways involved, we analyzed the transcriptome of adult-born cells right after their arrival into the OB.

In line with previous publications, whole-cell patch-clamp experiments in acute OB slices assured spiking of both Kv1.2 and Kir2.1 overexpressing cells. Neither input resistance, nor the action potential (AP) threshold, amplitude, or duration differed significantly between the control and Kv1.2 overexpressing cells. A functional signature of the Kv1.2 overexpression was, however, observed in the magnitude of AP afterhyperpolarization.

The results of longitudinal *in vivo* experiments show that Kv1.2/Kir2.1 overexpression modified spontaneous Ca^{2+} signaling of abJGCs and significantly impaired their migration, morphogenesis, odor-evoked responsiveness, and survival rate. Interestingly, abJGCs in odor-deprived hemibulbs displayed normal migration and morphology, thus stressing the importance of endogenous activity for these processes. Further, our results showed that pCREB expression was down-regulated in Kv1.2/ Kir2.1 overexpressing abJGCs. In accordance with the above findings, we observed a decreased expression of pCREB-driven immediate early genes and downregulation of pathways responsible for neuronal migration, differentiation, and morphogenesis in the Kv1.2/Kir2.1 groups.

Our results demonstrate that the endogenous but not sensory-driven activity plays a key role in regulating migration, morphogenesis, integration, and early-phase survival of adult-born OB interneurons.

References

[1] [1] Liang et al., Long-term in vivo single-cell tracking reveals the switch of migration patterns in adult-born juxtaglomerular cells of the mouse olfactory bulb. Cell Res26, 805-821 (2016).

[2] Kovalchuk et al., In vivo odourant response properties of migrating adult-born neurons in the mouse olfactory bulb. Nat Commun 6, 6349 (2015).

[3] Su et al., Enhanced ongoing endogenous activity predicts elimination of adult-born neurons in the mouse olfactory bulb. bioRxiv 10.1101/2020.09.09.286591 (2020).

B 06-12

Characterization of ion channel currents endogenously expressed in Neuro2A cells using automated patch clamp

M. G. Rotordam[1], F. X. Sureda[2], N. Becker[1], A. Horvath[1], N. Fertig[1], **A. Obergrussberger**[1]

[1] *Nanion Technologies GmbH, Munich, Germany*

[2] *Universitat Rovira i Virgili, Pharmacology Unit, Department of Basic Medical Sciences, Reus, Spain*

Introduction

Neuro2A cells are a mouse neuroblastoma cell line used extensively to investigate neuronal differentiation, axonal growth and cell signalling pathways . They are also used as an expression system for studying ion channels. Neuro2A cells have been shown to endogenously express NaV channels, predominantly $Na_V1.7$ but also $Na_V1.2$, 1.3 and 1.4[1], mechanosensitive channels Piezo 1[2,3], purinergic receptors[4] and glutamate receptors[5].

Methods

We used medium and high throughput automated patch clamp devices to record different ion channels endogenously expressed in Neuro2A cells.

Results

We recorded voltage-gated sodium channels that were blocked by TTX, tetracaine and lidocaine, with an IC_{50} of 4.1 ± 0.8 nM (n = 8), 9.9 ± 1.9 µM (n = 8) and 702.9 ± 57.2 (n=14), respectively. The V_{half} of activation was -19.4 ± 0.6 mV (n = 8), although there was some variation between cells. We also recorded Piezo1-mediated responses in Neuro2A cells activated by Yoda1. In addition, we recorded a heat-activated response to external solution heated to 42°C. This heat-activated response could be attributed to TRPV3 or TRPV4 but not TRPV1 as ligand-gated responses to 2-APB and GSK1016790A were observed but no response to the TRPV1 ligand, capsaicin.

Conclusion

Neuro2A cells can be used on automated patch clamp devices with success rates of 60-80% for >1 GOhm seals and are a suitable cell type for investigating endogenous NaV currents, as well as Piezo1 and some TRP channels.

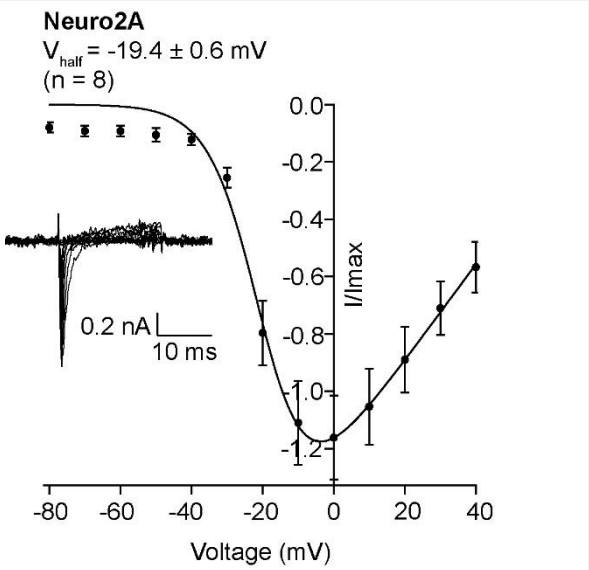

NaV recorded in Neuro2A cells

Data were fit with a Boltzmann equation revealing a V_{half} of activation = -19.4 ± 0.6 mV (n = 8).

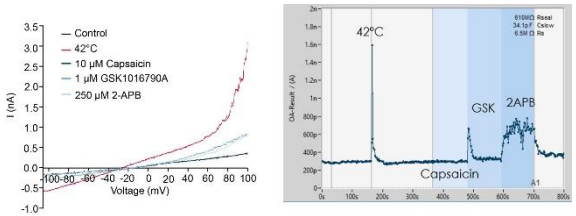

TRP channels are expressed in Neuro2A cells

TRP-mediated currents were activated first using 42°C, followed by different TRP channel activators. No activation was seen with capsaicin in 8/8 cells, whereas all cells (8/8) responded to GSK1016790A and 4/8 cells responded to 2-APB. Shown are raw current traces from an example cell (left) and the timecourse of the experiment (right).

References

[1] Lou JY, Laezza F, Gerber BR, Xiao M, Yamada KA, Hartmann H, Craig AM, Nerbonne JM & Ornitz DM 2005,. 'Fibroblast growth factor 14 is an intracellular modulator of voltage-gated sodium channels.' *J Physiol.*, 569, 179–193

[2] Coste B, Mathur J, Schmidt M, Earley TJ, Ranade S, Petrus MJ, Dubin AE & Patapoutian A 2010, 'Piezo1 and Piezo2 are essential components of distinct mechanically activated cation channels.' *Science*330, 55–60

[3] Rotordam MG, Fermo E, Becker N, Barcellini W, Brüggemann A, Fertig N, Egée S, Rapedius M, Bianchi P & Kaestner L 2019, 'A novel gain-of-function mutation of Piezo1 is functionally affirmed in red blood cells by high-throughput patch clamp.' *Haematologica,* 104, e179

[4] Vetter I & Lewis RJ 2010, 'Characterization of endogenous calcium responses in neuronal cell lines.' *Biochem. Pharmacol.,* 79, 908–920

[5] Van der Valk JBF & Vijverberg HPM 1990, 'Glutamate-induced inward current in a clonal neuroblastoma cell line.' *Eur. J. Pharmacol.* 185, 99–102

B 06-13

Multi-target modulation of ion channels underlying the analgesic effects of α-mangostin in dorsal root ganglion neurons.

S. Kim[1], M.Z. Yin[2], J.W. Roh[3], H.J. Kim[4], S.W. Choi[5], W.K. Kim[6], S.J. Kim[7], J.H. Nam[8]

[1] *Seoul National University, Department of Physiology/ College of Medicine, Seoul, South Korea*

[2] *The Second Affiliated Hospital, Zhejiang University School of Medicine, Department for Anesthesiology, Hangzhou, China*

[3] *Yonesi University, Department of Pharmacology/ College of Medicine, Seoul, South Korea*

[4] *Dongguk University, Department of Physiology/ College of Medicine, Gyeongju, South Korea*

[5] *Dongguk University, Department of Physiology/ College of Medicine, Gyeongju, South Korea*

[6] *Dongguk University, Department of Internal Medicine, Ilsan, South Korea*

[7] *Seoul National University, Department of Physiology/ College of Medicine, Seoul, South Korea*

[8] *Dongguk University, Department of Physiology/ College of Medicine, Gyeongju, South Korea*

Introduction

Pain is a critical health problem imposing significant socioeconomic burdens. So many reserchers stdudied neuromous analgesics. Despite the availability of a variety of analgesics, including opioids and non-steroidal anti-inflammatory drugs (NSAIDs), on the market, these drugs are insufficient in terms of the efficacy or tolerability required for adequate pain management. This unmet medical need has fueled significant research efforts aimed at finding more effective therapeutic strategies toward the development of new analgesics.

Garcinia mangostana Linn. (mangosteen) is a tropical tree cultivated in Southeast Asia. α-mangostin is a major xanthone derived from the pericarps of the mangosteen fruit, with multiple biological activities demonstrated, including antioxidant, pro-apoptotic, and anti-inflammatory effects. However, the precise mechanism underlying these activities of α-mangostin has not yet been elucidated. We revelated that α-mangostin exerts analgesic action by blocking both the transduction and conduction of nociceptive signals.

Methods

Using patch clamp study.

Used Cells : Isolation of DRG neruons from C57BL/6 male mice and cultured.

HEK293T stably overexpressed cells : hTRPV1, rTREK-1, rTREK-2, hTRAAK, mTRESK genes. ND7/23 cells .
Cell viability test : MTT assay.
Molecular docking model : AutoDock Vina, *In silico* ADME analysis.

Results

Under the zero-current clamp condition, α-mangostin (1–3 μM) hyperpolarized the resting membrane potential of mouse small dorsal root ganglion (DRG) neurons with increased membrane conductance, inhibited the action potential generated by current injection at 3 μM, and increased the activities of two-pore domain potassium channels TREK-1, TREK-2, and TRAAK, but not TRESK, overexpressed in HEK293T cells. Under the voltage-clamp condition, 3 μM α-mangostin inhibited the tetrodotoxin-sensitive voltage-gated Na^+ channel (Na_V) currents in small DRG neurons and ND7/23 cells by ~40% and potently inhibited capsaicin-induced but not proton-induced TRPV1 currents in TRPV1-overexpressing HEK293T cells and DRG neurons. Molecular docking simulation revealed that multiple oxygen atoms in α-mangostin form stable hydrogen bonds with TREKs, TRAAK, TRPV1, and Na_V channels. *In silico* ADME tests revealed that α-mangostin satisfies drug-likeness properties and does not penetrate the blood-brain barrier.

Conclusion

α-Mangostin stabilizes the membrane potential and inhibits AP firing by activating TREK/TRAAK as well as by inhibiting the TTX-S Na_V channel. Furthermore, α-mangostin potently inhibits TRPV1, one of the most well-known nociceptive channels, which might suppress pain transduction. Therefore, α-mangostin can be a very effective analgesic candidate targeting multiple ion channels.

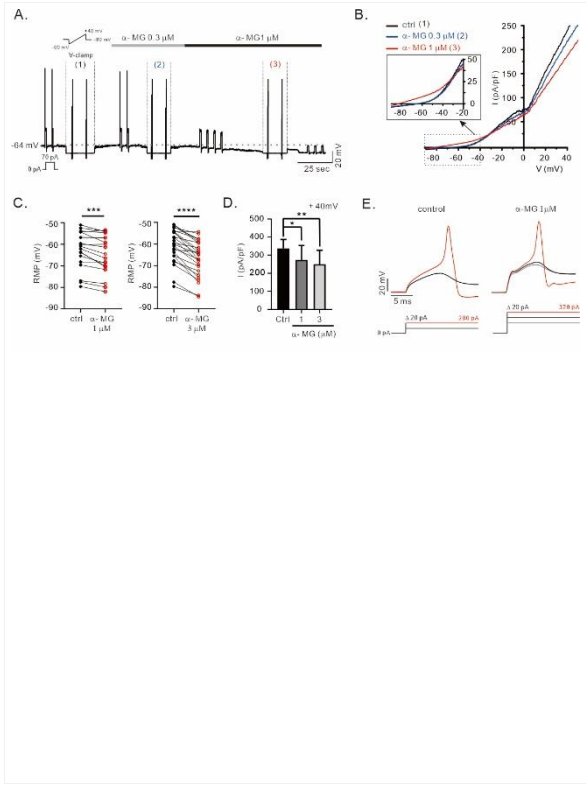

α-Mangostin hyperpolarizes the membrane potential of dorsal root ganglion (DRG) neurons and increase

(A,B) Whole-cell currents (I_K), demonstrating the generation of AP from DRG neurons with 0.3 and 1 mM α-mangostin. Black curves represent the control (1), blue (2) and red (3) curves represent currents after treatment with 0.3 mM and 1 mM α-mangostin, respectively. (C) Summary of the RMP before and after 1 mM α-mangostin and 3 mM α-mangostin treatment. (D) Summary of current density at 40 mV in the control, 1 mM α-mangostin and 3 mM α-mangostin groups. (E) APs were evoked by current injection at 280 pA in the control and at 320 pA in the 1 mM α-mangostin treatment group.

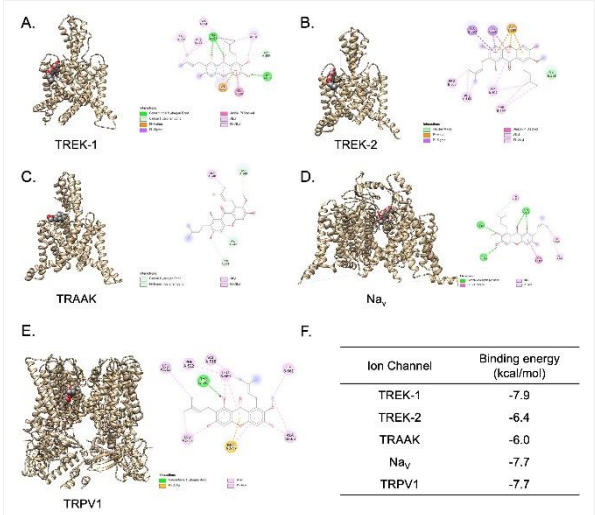

Ion Channel	Binding energy (kcal/mol)
TREK-1	-7.9
TREK-2	-6.4
TRAAK	-6.0
Na_V	-7.7
TRPV1	-7.7

Molecular docking simulation of α-mangostin to the ion channels. (A–E) Predicted binding poses and interacting residues of α-mangostin to TWIK-related K^+ channel (TREK) -1, TWIK-related K^+ channel (TREK) -2, TWIK-related arachidonic acid activated K^+ channel (TRAAK), voltage-gated Na^+ channel (Na_V), and transient receptor potential vanilloid 1 (TRPV1), respectively. (F) Calculated binding energy of α-mangostin to each ion channel.

References

[1] Mills SEE, Nicolson KP, Smith BH, Chronic pain: a review of its epidemiology and associated factors in population-based studies. Br J Anaesth. 123 (2019) 73-83. http://doi.org/10.1016/j.bja.2019.03.023.

[3] Dubin AE, Patapoutian A, Nociceptors: the sensors of the pain pathway, J Clin Invest. 120 (2010) 3760-3772. http://doi.org/10.1172/JCI42843.

[4] Chen G, Li Y, Wang W, Deng L. Bioactivity and pharmacological properties of alpha-mangostin from the mangosteen fruit: a review. Expert Opin Ther Pat. 28 (2018). 415-427. http://doi.org/ 10.1080/13543776.2018.1455829.

[5] Han SY, You BH, Kim YC, Chin YW, Choi YH, Dose-Independent ADME Properties and Tentative Identification of Metabolites of alpha-Mangostin from Garcinia mangostana in Mice by Automated Microsampling and UPLC-MS/MS Methods. PLoS One. 10 (2015). http://doi.org/ 10.1371/journal.pone.0131587.

[6] Lee J, Kim S, Kim HM, Kim HJ, Yu FH, $Na_V1.6$ and $Na_V1.7$ channels are major endogenous voltage-gated sodium channels in ND7/23 cells. PLoS One. 14 (2019). e0221156. http://doi.org/ 10.1371/journal.pone.0221156.

B 06-14

Integrated analysis of glucocorticoid-binding receptor interaction with the rat hippocampus genome reveals novel glucocorticoid-regulated physiological functions

K. R. Mifsud[1], C. L.M. Kennedy[1], E. M. Price[1], S. N. Haque[1], A. Gialeli[2], H. M. Goss[1], P. E. Panchenko[1], O. Cordero Llana[2], J. M. Reul[1]

[1] *University of Bristol, Neuroepigenetics Research Group, Bristol Medical School, Bristol, UK*

[2] *University of Bristol, Stem Cell Biology Research Group, Bristol Medical School, Bristol, UK*

Supported by the BBSRC and Wellcome Trust, UK

Introduction

Glucocorticoid hormones (GCs) are of critical importance for physiological regulation and behavioural adaptation across the circadian cycle and during stressful events. They act through mineralocorticoid (MR)- and glucocorticoid (GR) receptors in the hippocampus, which in turn translocate to the nucleus where they bind to glucocorticoid response elements (GREs) within the genome to regulate transcription[1]. Dysregulation of GCs has been associated with psychiatric disorders like major depression but much of the underlying physiology of GC action in healthy individuals was unknown. This work identified MR- and GR-regulated genes under physiological conditions (circadian variation, acute stress) that stimulate differing GC secretion patterns.

Methods

We conducted genome-wide MR and GR ChIP-seq and Ribo-Zero RNA-seq studies on hippocampal samples collected from rats killed under basal conditions across the circadian cycle or at various timepoints after exposure to an acute swim stress[2]. Subsequent bioinformatic analysis integrated these datasets. Pathway analysis was performed using software packages such as Gene Ontology (GO) and Ingenuity Pathway Analysis (IPA). Validation experiments confirmed key findings. All animal procedures accorded with current UK legislation.

Results

Both circadian and stress-induced changes in GC concentrations resulted in altered MR and/or GR to genome binding and related gene transcriptional changes in a subset of genes. MR and GR binding occurred at overlapping as well as distinct loci[2]. Pathway analysis uncovered that MR and GR regulate a substantial number of neuroplasticity-related pathways with a high level of statistical significance, such as those involved in synaptic plasticity (e.g. *Ptk2b*, *Dlgap1*, *Camk2a*, *Grin2a*) and axonogenesis (e.g. *Rtn4r*, *Slit1*, *Sema7a*, *Plxna2*). Surprisingly, we also discovered the almost exclusive MR regulation of over 50 cilium-associated genes (e.g. *Cep41*, *Ift43*, *B9d2*). This subset of genes was expressed constitutively in the hippocampus, irrespective of circulating GC levels. Subsequent studies using human foetal neuronal progenitor cells (hfNPCs) demonstrated that MR function and ciliogenesis are linked as part of the neuronal differentiation process. Moreover, the transcription factor recognition site composition within genomic MR and GR binding peaks showed marked differences depending on physiological condition. For example, MR peaks related to ciliogenesis were often devoid of GC response elements (GREs) but likely to contain regulatory factor for X box (RFX) recognition sites. Studies are ongoing to further elucidate the relationship between glucocorticoid binding receptors, transcription factor recognition sites, and molecular and cellular functions.

Conclusion

Our results show that hippocampal MRs and GRs, constitutively and dynamically, regulate genome activities that underpin the molecular basis of neuronal development, adaptation, and resilience.

References
[1] Mifsud, KR, Reul,JMHM 2016, 'Acute stress enhances heterodimerization and binding of corticosteroid receptors at glucocorticoid target genes in the hippocampus', *Proceedings of the National Academy of Sciences of the United States of America*, 113, 11336-11341
[2] Mifsud, KR, Kennedy, CLM, Salantino, S, Sharma, E, Price, EM, Haque, SM, Gialeli, A, Goss, HM, Panchenco, PE, Broxholme, J, Engledow, S, Lockstone, H, Cordero Llana, O, Reul, JMHM, 2021, 'Distinct regulation of hippocampal neuroplasticity and ciliary genes by corticosteroid receptors', *Nature Communications*, 12, 4737

B 06-15

Mutations associated with epileptic encephalopathy modify the electrophysiological properties of the EAAT2 anion channel.

P. Kovermann[1], Y. Kolobkova[2], C. Fahlke[1]
[1] *Forschungszentrum Jülich, Molekular- und Zellphysiologie, Jülich, Germany*
[2] *Medicalschool Hamburg, Human Medizin, Hamburg, Germany*

We thank the German Ministry of Education and Research (E-RARE Network, Treat-ION, BMBF 01GM1907C to ChF).

Motivation
Naturally occurring mutations in *SLC1A2* encoding the glutamate transporter EAAT2 have been associated with severe forms of epileptic encephalopathy. EAAT2 is expressed in both, glial and neuronal cells. Beside its secondary active transporter function, it also acts as an anion channel. How disease-associated mutations modify these two transport functions of EAAT2 and how such alterations cause epileptic syndromes is insufficiently understood.
Methods
We studied the functional consequences of the three disease-associated missense mutations, p.Gly82Arg, p.Leu85Pro and p.Pro289Arg, by heterologous expression in mammalian cells, biochemistry, confocal imaging, and whole-cell patch clamp recordings of EAAT2 L-glutamate transport and anion currents.
Results
G82R and L85P exchange amino acid residues that contribute to the formation of the EAAT anion pore. They enlarge the pore diameter sufficiently to permit the passage of L-glutamate and thus function as L-glutamate efflux pathways. The mutation P289R decreases L-glutamate uptake, but increases anion currents despite a lower membrane expression.
Conclusion
L-glutamate permeability of the EAAT anion pore is an important functional consequence of naturally occurring missense mutations. L-glutamate efflux through mutant EAAT2 anion channels will cause glutamate excitotoxicity and neuronal hyperexcitability in affected patients. Thus, antagonists that selectively suppress the EAAT anion channel function could serve as therapeutic agents in the future.

B 06-16

Fractional amplitude of low-frequency fluctuations in hypertensives – retrospective analysis of UK Biobank resting-state functional MRI data

O. B. Woodward[1], I. Driver[1], E. Hart[2], R. Wise[3]
[1] *Cardiff University, Cardiff University Brain Research Imaging Centre, Cardiff, UK*
[2] *University of Bristol, Bristol, UK*
[3] *Università degli Studi 'G. d'Annunzio', Chieti, Italy*

Acknowledgment
GW4 BioMed MRC Doctoral Training Partnership

Introduction
The selfish brain mechanism proposes that hypertension is a compensatory mechanism that aims to maintain cerebral blood flow (CBF) by increasing systemic blood pressure through an increase in cardiovascular sympathetic tone. There is evidence that hypertension is associated with reduced CBF and cerebrovascular reactivity (CVR)[1].
The amplitude of low frequency fluctuations (ALFF) in the resting-state functional MRI (rfMRI) signal has previously been applied as an index of cerebrovascular function[2]. The physiological basis of ALFF is multifactorial[3], but there is evidence that ALFF between 0-0.1164Hz correlates with CVR[4]. We hypothesise that ALFF in areas of central autonomic activity is different between hypertensives and normotensives.
Methods
rfMRI data was obtained from UK Biobank[5], a large biomedical database. Regional analysis minimises the contribution of thermal noise to ALFF[3]. Therefore, a targeted hypothesis-driven analysis of ALFF in selected regions involved in autonomic activity in 141 hypertensive and 141 matched normotensives was undertaken. ALFF values were normalised against frontal grey matter and are expressed as z-scores±standard deviation. A fractional correction which suppresses noise was also applied (fALFF)[2].
The results prompted a whole-brain exploratory analysis, in which a general linear model with blood pressure group as the independent variable and age, sex and BMI as covariates was applied to whole-brain fALFF maps for 2054 hypertensives and 1724 normotensives. Unpaired two-sample t-test was performed to look for significant fALFF clusters.
Results
In the initial regional analysis, a two-way ANCOVA comparing blood pressure group and brain region, with age, BMI and sex as covariates, found no significant effect of blood pressure group on fALFF (mean fALFF z-score in hypertensives = -1.25±0.84 and in normotensives = -1.24±0.93, $F(1)=1.67$, $p=0.20$, partial $\eta^2=4.8\times10^{-4}$).There was a significant regional difference in fALFF (($F(12)=569.0$, $p<2\times10^{-16}$, partial $\eta^2=0.72$). However, there was no statistically significant effect of the interaction between region and blood pressure group (figure 2, $F(12=1.36$, $p=0.17$, partial $\eta^2=0.005$). In the larger whole-brain analysis, there were no statistically significant clusters of fALFF anywhere in the brain.

Conclusion

fALFF was compared between hypertensives and normotensives in the context of the selfish brain mechanism. Of interest to our hypothesis, fALFF was lower in the brainstem than in other cortical and subcortical regions, but there were no significant differences in regional fALFF between hypertensives and normotensives. The results of this study suggest that regional changes in fALFF, which is a possible index of CVR, are not associated with hypertension. . However, fALFF contains contributions from sources other than CVR, including neuronal fluctuations and noise. Further studies using more specific measures of CVR in hypertensives are currently planned.

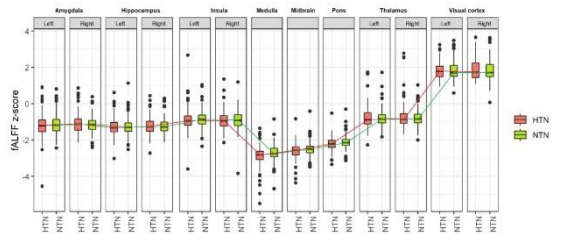

Figure 2: No significant difference in the pattern of regional fALFF variation between blood pressure group, as demonstrated by red (hypertensive) and green (normotensive) lines.

Figure 2: Regional fALFF variation according to blood pressure group

No significant difference in the pattern of regional fALFF variation between blood pressure group, as demonstrated by red (hypertensive) and green (normotensive) lines.

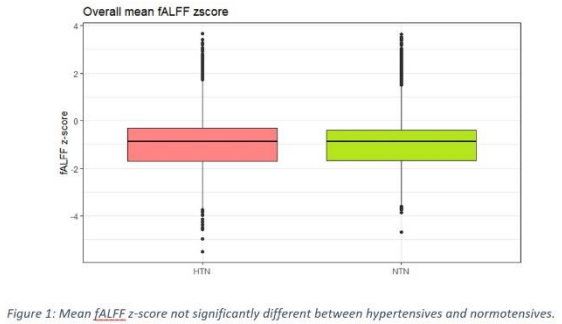

Figure 1: Mean fALFF z-score not significantly different between hypertensives and normotensives.

Figure 1: Overall mean fALFF z-score

Mean fALFF z-score not significantly different between hypertensives and normotensives.

References

1. Hart, E C et al., 2016, 'Human hypertension, sympathetic activity and the selfish brain.' *Exp Physiolo*, 1689-99.
2. Zou, Qi-Hong et al, 2008, 'An improved approach to detection of amplitude of low-frequency fluctuation (ALFF) for resting-state fMRI: Fractional ALFF.' *Journal of Neuroscience Methods*, 137-141.
3. Bianciardi, M et al., 2009, 'Sources of fMRI signal fluctuations in the human brain at rest: a 7T study.' *Magnetic Resonance Imaging*, 1019-29.
4. Liu, P et al, 2021, 'Cerebrovascular Reactivity Mapping Using Resting-State BOLD Functional MRI in Healthy Adults and Patients with Moyamoya Disease.' *Radiology*, 419-425.
5. Sudlow C, Gallacher J, Allen N, Beral V, Burton P, Danesh J, et al., 2015, 'UK Biobank: An Open Access Resource for Identifying the Causes of a Wide Range of Complex Diseases of Middle and Old Age', PLoS Med

---

B 06-18

Metabolic challenge by deep anesthesia or hypoxia as well as in the motor neuron disease ALS reduces nerve conduction velocity of spinal fibers in mice in vivo

P. Dibaj[1], E. D. Schomburg[2]

[1] *Max Planck Institute for Multidisciplinary Sciences, Göttingen, Germany*

[2] *University of Göttingen, Institute of Physiology, Göttingen, Germany*

Introduction

The conduction velocity of a nerve fiber is not absolutely constant, but can vary. We have now investigated the influence of acute metabolic changes on nerve conduction velocity (NCV) of spinal fibers in mice in vivo.

Methods

We have developed an electrophysiological setup for in vivo recording of CNS fibers in the fasciculus gracilis of the spinal dorsal column [using intravenous anesthesia and artificial ventilation; cf. P. Dibaj and E. D. Schomburg (Physiol Res. 2017; 66:545-548)] and measured NCV under different metabolic conditions: a) under low and high state of anesthesia, indicated by relatively high and low heart rate, respectively; b) under normoxia and hypoxia.

Results

The increase in the state of anesthesia, as well as the decrease in oxygen saturation in the blood, led to a decrease of NCV, which indicates an immediate influence of acute metabolic changes on the speed of signal propagation in nerve fibers. The decrease in NCV under the various systemic metabolic challenges mentioned above was rescued by the local supply of lactate, which has already been shown to be secreted by glial cells and metabolized by axons to generate ATP. In the deeply anesthetized state, a similar rescue by lactate was observed during tetanic stimulation in terms of reduction in compound action potential amplitude. The metabolic support of the axons by glial cells is impaired in the motor neuron disease ALS, which is a major contributor to the pathophysiological progression of axonal damage in the course of the disease. We confirmed the critical role of glia in metabolic support by breeding ALS mice (SOD1G93A) with inducible conditional knockout mice lacking GLUT1 (a glucose transporter) in oligodendroglia. In ALS mice lacking oligodendroglial GLUT1, disease onset was earlier and motor performance was worse. Also, they died earlier. In the case of SOD1G93A, in electrophysiological experiments similar to those mentioned above, we observed an improvement in the reduced NCV in clinically affected mice after lactate administration.

Conclusion

Local lactate energization leads to the rescue of metabolically induced changes in the NCV of spinal fibers in vivo, not only in acute systemic challenges such as deep anesthesia or hypoxia, but also in the chronic paradigm of ALS.

B 06-19

Irisin may change the monoamine levels in different regions related to the sexual behavior of the male rat brain

N. U. Ertugrul, A. Yardimci, M.R. Ozdede, A. Ozgen, G. Ozbeg, **S. Canpolat**
Firat University, Faculty of Medicine, Department of Physiology, Elazig, Turkey

This study was supported by TUBITAK-118S519.

Introduction: Irisin is an adipomyokine that is released into the circulation due to exercise. Recently, it has been revealed that irisin hormone has effects on the reproductive system, such as pubertal maturation, reproductive hormones, reproductive organs, sexual behavior, and sexual dysfunction (1-3). However, the effectiveness of irisin on the neurotransmitter system associated with the sexual behavior is precisely unknown. Given that exercise can alter the levels of dopamine, noradrenaline, and serotonin in several brain regions associated with the reproductive system (4, 5), it is hypothesized that irisin, an exercise hormone, may also affect brain monoamine levels. Based on this hypothesis, we aimed to investigate the effects of irisin on monoamine levels in the specific brain regions, including nucleus accumbens (NAc), medial preoptic area (mPOA), and medial amygdala (MeA), which are relevant to the sexual behavior in male rats.
Methods: For the experimental studies, a totally of 12 male Sprague-Dawley rats (21 days old and 35 ± 2 g weight) were used. All animals were randomly divided into two groups: the control group (n=6) and the irisin group (n=6). All rats in the irisin group were intraperitoneally injected with irisin (100 ng/kg/day) daily for 10 weeks, while the control group received an equivalent volume of deionized water. At the end of the experiment, all rats were sacrificed by decapitation and then the brains were rapidly removed and frozen on dry ice. The levels of dopamine (DA), DOPAC (a metabolite of dopamine), norepinephrine (NE), DHPG (a metabolite of norepinephrine), serotonin (5-HT), and 5-HIAA (a metabolite of serotonin) were measured in the micropunched NAc, mPOA, and MeA by high-performance liquid chromatography-electrochemical detection (HPLC-ECD) method.
Results: In the NAc,it was observed that irisin treatment significantly increased DHPG and DA levels ($p<0.05$). Depending on these changes, it was determined that dopaminergic turnover (DOPAC/DA ratio) decreased and noradrenergic turnover (DHPG/NE ratio) increased ($p<0.05$). When compared to the control group, 5-HT and 5-HIAA concentrations in the MeA were found significantly lower in the irisin group ($p<0.01$ and $p<0.05$, respectively). On the other hand, it was shown that irisin treatment did not change the monoamine levels in the mPOA.
Conclusion: Our results showed that irisin caused changes in neurotransmitter levels in specific brain regions associated with the sexual behavior in male rats. All these results suggest that irisin hormone may play an essential role in the central effects of exercise on the sexual behavior.

References

[1] Ulker, N, Yardimci, A, Kaya Tektemur, N, Bulmus, O, Ozer Kaya, S, Gulcu Bulmus, F, Turk, G, Ozcan, M, Canpolat, S 2020, 'Irisin may have a role in pubertal development and regulation of reproductive function in rats', Reproduction, 160(2), 281–292, Cambridge, England.
[2] Canpolat, S, Ulker, N, Yardimci, A, Tancan, E, Sahin, E, Yaman, SO, Bulmuş, O, Alver, A, Ozcan, M 2022, 'Irisin ameliorates male sexual dysfunction in paroxetine-treated male rats', Psychoneuroendocrinology, 136, 105597.
[3] Yardimci, A, Ulker, N, Bulmus, O, Sahin, E, Alver, A, Gungor, IH, Turk, G, Artas, G, Kaya Tektemur, N, Ozcan, M, Kelestimur, H, Canpolat, S 2022, 'Irisin improves high-fat diet-induced sexual dysfunction in obese male rats'. Neuroendocrinology, 10.1159/000523689.
[4] Lin, TW, Kuo, YM 2013, 'Exercise benefits brain function: the monoamine connection'. Brain sciences, 3(1), 39-53.
[5] Meeusen, R, De Meirleir, K 1995, 'Exercise and brain neurotransmission'. Sports medicine, 20(3), 160-188.

B 06-20

Lorcaserin requires preproglucagon neurons to reduce food intake in mice and acts additively to liraglutide-induced hypophagia

S. Wagner[1], **D. Brierley**[2], A. Leeson-Payne[1], W. Jiang[2], R. Chianese[1], B. Lam[3], G. Dowsett[3], C. Cristiano[1], D. Lyons[1], F. Reimann[3], F. Gribble[3], G. Yeo[3], S. Trapp[2], L. Heisler[1]
[1] University of Aberdeen, The Rowett Institute, Aberdeen, UK
[2] University College London, Department of Neuroscience, Physiology and Pharmacology, London, UK
[3] University of Cambridge, Welcome-MRC Institute of Metabolic Neuroscience, Cambridge, UK

Obesity is a major public health challenge, and its prevalence has reached epidemic levels. Most pharmacological approaches to target appetite-regulating brain circuitry produced underwhelming results. The most efficacious single approach to date is GLP-1 receptor agonists (GLP-1RAs) which produce widespread activation throughout the CNS. However, it is largely unclear how this activation relates to pathways engaged by other drugs producing hypophagia. Additionally, previous studies suggest that systemic GLP-1RAs and GLP-1 released from preproglucagon (PPG) neurons reduce food intake via mostly separate pathways. Here we explore the circuitry employed by the 5-HT_{2C} receptor agonist lorcaserin, the MC4 receptor agonist melanotan II (MTII), the GLP-1RA liraglutide and brain-derived GLP-1, and assess whether combination therapy might provide an effective therapeutic strategy for obesity.
We first confirmed using single nucleus RNA sequencing analysis that 5HT2c receptors are widely expressed in the mouse brainstem, including in PPG neurons and GLP-1R expressing neurons. In contrast, MC4 receptors are not expressed in PPG neurons. Additionally, lorcaserin (10 mg/kg, i.p.) increased c-fos immunoreactivity in PPG neurons. We then specifically ablated nucleus tractus solitarius (NTS) PPG neurons in Glu^{cre} mice by stereotaxically-delivered cre-dependent viral expression of diphtheria toxin subunit A (DTA). The anorexigenic effect of lorcaserin (7.5 mg/kg i.p.), but not of MT-II (3 mg/kg i.p.) was significantly attenuated in mice lacking NTS PPG neurons (n=8/group). We next used 5-$HT_{2C}R^{Cre}$ mice injected into the NTS with cre-dependent AAV encoding hM3Dq to demonstrate that selective activation of NTS $5HT_{2C}$ receptor expressing cells with CNO (2mg/kg) strongly reduces food intake, but that this effect is lost when NTS GLP-1R expression is knocked down with virally delivered GLP-1R shRNA. Collectively, this suggests that NTS PPG neurons are necessary for the anorexigenic effect of lorcaserin and may produce this effect by activation of GLP-1Rs in the NTS. We then tested whether NTS GLP-1R knockdown also prevents the hypophagic action of liraglutide, but that effect was retained, suggesting that the NTS GLP-1Rs are primarily a target for PPG neurons, but not systemic GLP-1RAs, and that lorcaserin activated circuits are separate from those activated by GLP-1RAs. Consequently, we examined the effect of liraglutide (0.1 mg/kg, s.c.) and lorcaserin (7.5 mg/kg, i.p.) in combination. As expected, a

greater reduction in food intake was observed following administration of the drug combination than either monotherapy.
We conclude that lorcaserin, unlike MTII, mediates its hypophagic effect partly through PPG neurons, and that lorcarserin can be combined with liraglutide for more effective appetite suppression. These findings support that this combination strategy has potential to improve current anti-obesity therapies.

B 06-21

Postweaning development shifts endogenous $VPAC_1$ modulation of LTP induced by theta-burst stimulation.

M. Gil[2], M. Bento[2], N. C. Rodrigues[3], A. Silva-Cruz[3], D. Cunha-Reis[1,2]
[1] Faculdade de Ciências da Universidade de Lisboa, 1Departamento de Química e Bioquímica, Lisboa, Portugal
[2] Faculdade de Ciências da Universidade de Lisboa, 2BioISI - Biosystems & Integrative Sciences Institute, Lisboa, Portugal
[3] Faculdade de Medicina da Universidade de Lisboa, 3Instituto de Medicina Molecular, Unidade de Neurociências, Lisboa, Portugal

This work was supported national and international funding managed by Fundação para a Ciência e a Tecnologia (FCT, IP), Portugal.
***Grants:** UIDB/04046/2020 and UIDP/04046/2020 centre grants (to BioISI) and research grants PTDC/SAU-NEU/103639/2008 and FCT/POCTI (PTDC/SAUPUB/28311/2017) EPIRaft grant (to DC-R).*
***Fellowships:** SFRH/BPD/34661/2007 to DCR and **Researcher contract:** Norma Transitória - DL57/2016/CP1479/CT0044 to DCR. Funding sources made no contribution to the writing, research plan and decision to publish this paper.*
***Acknowledgements:** We acknowledge the Institute of Physiology, FMUL, for animal housing facilities and Raquel Batista Dias for help with initial LTP experiments in juvenile rats.*

Long-term potentiation (LTP) induced by theta-burst stimulation (TBS) undergoes postweaning developmental adaptations, likely relying on GABAergic circuit maturation[1]. Endogenous modulation of LTP by VIP acting on $VPAC_1$ receptors involves regulation of GABAergic transmission[2]. $VPAC_1$ receptor expression is developmentally regulated during embryogenesis but little is known on the influence of postweaning development on hippocampal $VPAC_1$ expression and function. In this work we investigated the time-course of alterations in $VPAC_1$ modulation of LTP from weaning to adulthood and its relation to GABAergic circuit and synapse maturation. LTP induced by TBS (5x4) (5 bursts of 4 pulses delivered at 100Hz) was increasingly greater from weaning to adulthood. TBS delivered in the presence of the $VPAC_1$ receptor antagonist PG 97-269 (100nM) induced a much larger potentiation in juvenile (3-week-old) than in young adult (7-week-old) or adult (12-week-old) rats. This effect was not associated to a developmental decrease in $VPAC_1$ receptor expression in hippocampal membranes or synaptosomes but was linked to an increase in synaptic GABAergic markers suggesting an increase in the number of total GABAergic synaptic contacts. Conversely, endogenous $VPAC_2$ receptor activation did not significantly influence CA1 TBS-induced LTP even though a major enhancement in $VPAC_2$ receptor expression was observed during postweaning development. Given the recently reported involvement of VIP interneurons in several aspects of hippocampal-dependent learning, neurodevelopmental disorders and epilepsy[3,4], these findings could provide important insights into the role of VIP modulation of hippocampal synaptic plasticity in normal and altered brain development and in epileptogenesis.

References
[1] Rodrigues, N. C. *et al*. Hippocampal CA1 theta burst-induced LTP from weaning to adulthood: Cellular and molecular mechanisms in young male rats revisited. *Eur. J. Neurosci.***54**, 5272–5292 (2021).
[2] Caulino-Rocha, A., Rodrigues, N. C., Ribeiro, J. A. & Cunha-Reis, D. Endogenous VIP VPAC1 Receptor Activation Modulates Hippocampal Theta Burst Induced LTP: Transduction Pathways and GABAergic Mechanisms. *Biol. 2022, Vol. 11, Page 627***11**, 627 (2022).
[3] Cunha-Reis, D., Caulino-Rocha, A. & Correia-de-Sá, P. VIPergic neuroprotection in epileptogenesis: challenges and opportunities. *Pharmacol. Res.***164**, 105356 (2021).
[4] Goff, K. M. & Goldberg, E. M. A Role for Vasoactive Intestinal Peptide Interneurons in Neurodevelopmental Disorders. *Dev. Neurosci.* 1–13 (2021). doi:10.1159/000515264.

B 06-22

Chemogenetic activation of astrogliosis and microvasculature disturbance in the spinal cord induces pain hypersensitivity

R. P. Hulse
Nottingham Trent University, Department of Biosciences, Nottingham, UK

Introduction
A quarter of people living in the UK with diabetes suffer from neuropathic pain, and receive minimal pain relief as current painkillers are ineffective. Pain perception is modulated by the somatosensory nervous system that relies heavily upon not only sensory neurons, but also the interplay of a heterogenous cell population (endothelial cells, astrocytes). This heterogenic cell population encapsulates the somatosensory nervous system (including the spinal cord) with a protective vascular barrier – blood neural barrier, providing critical nutritional support and protection. We have identified in rodent models of diabetic (type 1 and type 2) neuropathic pain that this blood spinal cord barrier is damaged. Astrocytes are a fundamental modulator of nerouvs system health. Furthermore, a pathological hallmark of chronic pain is astrogliosis, a hub that acts as a potent source of inflammatory response, impacting upon vessel integrity and sensory neuronal activity. To date it remains unclear how diabetic neuropathic pain develops and how microvessels are damaged. Here we elucidate using chemogenetic activation, the role of astrogliosis in the modulation of the blood spinal cord barrier and nociception.
Methods
All rodent studies were performed in accordance with local AWERB authorisation, ASPA and ARRIVE guidelines. Male C57 bl6 (~25g) mice were intrathecally administered AAV consisting of either GFAP hMD3gq mCherry (GFAP-hMD3gq) or GFAP-mCherry (~2% oxygen isoflurane anaesthetic). Rodents were left 2 weeks before nociceptive behavioural assays (Von Frey Hair and Hargreaves Test) were performed. Baseline nociceptive behavioural values were acquired prior to delivery of either vehicle or clozapine n oxide (CNO 0.3mg/kg ip). Animals were terminally

anaesthetised (sodium pentobarbital 60mg/kg ip) and cardiac perfused with 4% paraformaldehyde, lumbar region of the spinal cord was extracted and cryosectioned for confocal microscopy.

Results

GFAP positive astrocytes were mCherry positive in the lumbar dorsal horn. CNO induced nociceptive behavioural hypersensitivity in GFAP-hMD3gq mice (Von Frey P<0.001 Two way ANOVA, n=8-14), which was accompanied by increased astrocyte number (**Mann Whitney test, n=5) and GFAP fluorescence in the dorsal horn (** Mann Whitney test, n=5). Furthermore, the volume of the microvessel (CD31) network in the dorsal horn of GFAP-hMD3gq mice was reduced versus controls (**Mann Whitney test, n=5).

Conclusion

This demonstrates astrocytes in the dorsal horn have an extensive role in modulating nociception via interactions with the blood spinal cord barrier.

B 06-23

Brain dysfunction during warming is caused by oxygen limitation in larval zebrafish

A. H. Andreassen[1], P. Hall[1], P. Khatibzadeh[1], F. Jutfelt[1], **F. Kermen**[1,2]

[1] *Norwegian University of Science and Technology, Department of Biology, Trondheim, Norway*

[2] *University of Copenhagen, Department of Neuroscience, Copenhagen, Denmark*

This work was supported by the Research Council of Norway (FRIPRO grants, FK: 262698, FJ: 262942).

Heatwaves are becoming more frequent and severe as climate change progresses, which calls for a better understanding of the physiological mechanisms enabling animals to cope with high temperatures. Central to this topic, studies have measured ectotherms' upper thermal limit (CTmax), the temperature at which locomotor function is lost and movement becomes disorganized. Yet, despite decades of research, the physiological mechanisms limiting the upper thermal tolerance of animals are currently unclear and remain hotly debated. One of the hypotheses posits that whole organism's upper thermal tolerance is limited by that of the brain, which controls coordinated movement. To test this hypothesis, we developed methods for measuring the upper thermal limit in larval zebrafish (*Danio rerio*) with simultaneous recordings of brain activity using epifluorescence imaging of the pan-neuronal calcium indicator GCaMP6s, in free-swimming or in agar-embedded fish. We discovered that during warming, CTmax measured as the loss of touch-evoked escape occurs before a slowly propagating wave of intracellular calcium indicative of a global brain depolarization. CTmax coincides with a pronounced reduction in locomotor-related neural activity in the medulla and of sensory-evoked responses in the optic tectum. Using bidirectional manipulation of water oxygen levels, we found that oxygen availability during heating affects locomotor-related and sensory-evoked neural activity, CTmax and the onset of the brain depolarization. Our results therefore suggest that the mechanism limiting the upper thermal tolerance in zebrafish larvae is reduced oxygen availability causing impaired brain function.

B 06-25

Modelling post-stroke depression: a systematic review and meta-analysis of animal studies

E. Gray[1], I.-E. Mosneag[2], S. M. Allan[2], **C. J. Cunningham**[1]

[1] *University of Aberdeen, School of Medicine, Medical Sciences and Nutrition, Aberdeen, UK*

[2] *Geoffrey Jefferson Brain Research Centre, Manchester Academic Health Science Centre, Northern Care Alliance & University of Manchester, Manchester, UK*

Background

Stroke is a global health problem affecting over 13 million people annually. While often overlooked, post-stroke depression is a common complication experienced by around one third of survivors. Post-stroke depression is associated with poorer rehabilitation outcomes, impaired quality of life and increased mortality rates. To better understand the complex pathology of post-stroke depression and develop more effective treatment strategies, robust animal models are required. Stress-based models including a chronic unpredictable mild stress paradigm and social isolation are commonly used to induce depressive-like behaviours in rodents. Several groups have used these models following cerebral ischaemia to specifically model post-stroke depression. However, there appears to be no consensus on which combination of models should be used and the methods for phenotyping depressive-like behaviours. The aim of this systematic review was therefore to explore which models and behavioural tests are most commonly used to study post-stroke depression.

Methods

We conducted a keywords literature search of PubMed and Ovid databases to identify relevant studies. Study characteristics including post-stroke depression model, species and age were extracted from the included studies. We assessed study quality and bias using a 10-point CAMARADES checklist.

Results

A total 46 studies were included in the systematic review. The vast majority used the transient middle cerebral artery occlusion (MCAO) model of stroke (n=30) and the unpredictable chronic mild stress model of depression (n=31). The sucrose preference test (n=41) followed by the forced swim test (n=19) were the most widely used tests for phenotyping depressive-like behaviours. The median score of the CAMARADES checklist was 5/10 (IQR 4-6). In particular, reporting of blinding and sample size calculations was low.

Conclusions

The unpredictable chronic mild stress model of depression and sucrose preference test, used by the majority of studies, have high validity. We recommend that these become standardised methods for modelling post-stroke depression. However, we did identify a need for improved study design and reporting in future research. An outstanding question is whether cerebral ischaemia alone induces a robust depressive-like phenotype. Our ongoing meta-analysis is investigating the effects of the addition of a depression model on depressive-like behaviours and lesion volume in stroke animals.

B 06-26

Movement initiation-related functional diversity of dopamine substantia nigra neurons in mice during open-field locomotion

D. Schenkel[1], M. Kuhn[2], N. Hammer[1], P. Vogel[1], S. Betz[1], G. Schneider[2], J. Roeper[1]

[1] *Goethe University Frankfurt, Institute of Neurophysiology, Frankfurt am Main, Germany*

[2] *Goethe University Frankfurt, Institute of Mathematics, Frankfurt am Main, Germany*

Dopamine substantia nigra (DA SN) neurons are a major target of Parkinson disease (PD) and their loss is thought to contribute to the motor impairments in PD. Da Silva et al. (2018) demonstrated that subpopulations of DA SN neurons either increased or decreased their firing rates shortly before movement initiations. However, the functional topography of this diversity among DA neurons across the SN has not been fully characterized. We performed chronic multi-electrode recordings of pharmacologically identified DA SN neurons in awake freely-moving mice, while simultaneously tracking their head and body movements. Overall, our data set of n=59 (N=16) DA SN neurons was in accordance with the results by Da Silva and colleagues (2018) with about 30% of DA SN neurons (n=17/59) transiently increasing their firing rate (baseline to maximum: +5.3 ± 4.8Hz, mean ± SD) and also about 30% of DA SN neurons (n=18/59) transiently decreasing their firing rate (baseline to minimum: -3.6 ± 1.2Hz, mean ± SD) shortly before initiation of self-paced movement in the open field. A more fine-grained topographical analysis revealed that DA neurons with transient rate reductions were predominantly found in the medial SN (n=11/22) compared to central SN (n=7/30). These responses were absent in the lateral SN (n=0/7). In contrast, the proportion of DA neurons with transient rate increases were more prominent in central SN (n=13/30) compared to medial SN (n=3/22) and lateral SN (n=1/7). In light of the functional topography of axonal projections of DA SN neurons (Farassat et al., 2019), our data suggest a differential involvement of distinct nigrostriatal projections in self-paced movement initiation. However, definitive experiments require selective molecular tagging of distinct DA SN projections.

B 06-27

Using cGMP analogues to modulate photoreceptor sensitivity: Perspectives for *Retinitis pigmentosa*.

S. Wucherpfennig[1], W. Haq[2], V. Popp[1], S. Kesh[1], F. Schwede[3], F. Paquet-Durand[4], V. Nache[1]

[1] *Friedrich Schiller University Jena, Institute of Physiology II, Jena University Hospital, Jena, Germany*

[2] *University of Tübingen, Institute for Ophthalmic Research, Tübingen, Germany*

[3] *Biolog Life Science Institute GmbH & Co. KG, Bremen, Germany*

[4] *University of Tübingen, Cell Death Mechanism Group, Institute for Ophthalmic Research, Tübingen, Germany*

For many hereditary degenerative diseases of the retina, like *retinitis pigmentosa* (RP), there is currently no approved treatment. In case of RP the primary degeneration of rod photoreceptors leads to a secondary loss of cone photoreceptors and eventually to blindness. An early, common symptom for many RP forms is the dysregulation of cGMP homeostasis. Thus, rod degeneration is thought to be triggered by an over-activation of cyclic nucleotide-gated (CNG) channels and excessive Ca^{2+} influx through these channels. Pharmacological strategies to inhibit selectively the cGMP targets were already considered, but so far with no conclusive outcome. Selective modulation of rod CNG channels without compromising cone-mediated vision has proven to be the most challenging aspect of these therapies.

Here we present a novel approach, based on a cGMP-analogues cocktail, which enables the selective modulation of either rods or cones. This strategy was first tested by means of the patch-clamp technique on retinal CNG channels, heterologously expressed in *Xenopus* oocytes and further confirmed by micro electroretinography (µERG) recordings on wild-type mouse retina.

The cGMP-analogues mixture contained a general CNG-channel inhibitor (Rp-8-Br-PET-cGMPS) and a cone-selective CNG-channel activator (8-pCPT-cGMP). While Rp-8-Br-PET-cGMPS, when applied alone, behaved as a partial agonist and inhibited both cone and rod CNG channels equally, 8-pCPT-cGMP behaved as a very potent agonist and showed a strong concentration-dependent cone selectivity. Co-application of both compounds inhibited rod CNG-channel function under RP-like conditions and preserved cone functionality under physiological and pathological cGMP levels. Next, we tested the effect of this treatment on both the kinetics of CNG-channel gating and on the photoreceptor function. While the kinetics of rod channels was not changed, we observed a slower deactivation kinetics of cone CNG channels. Surprisingly, this aspect did not affect the physiological cone responsiveness to light, indicating possible intracellular compensatory mechanisms.

In conclusion, this straightforward strategy, by delaying primary rods degeneration and protecting secondary cone survival at functional level, may successfully either postpone the onset or slow down the RP development. Beyond the treatment of retinal diseases, using cGMP analogues with desired properties may elegantly address the isoform-specificity problem in future pharmacological therapies of related diseases.

B 06-28

Irisin protects against neuroinflammation in rats induced by epileptic seizure

Z. N. Özdemir-Kumral[1], T. Akgün[1], C. Hasim[2], E. Ulusoy[2], F. Yüksel[2], M. K. Kalpakçıoğlu[2], T. Okumuş[2], Z. Uslu[3], D. Akakın[4], Z. Gören[3], M. Yüksel[5], A. Yıldırım[1], B. Yeğen[1]

[1] *Marmara University, Department of Physiology / Faculty of Medicine, Istanbul, Turkey*

[2] *Marmara University, School of Medicine, Istanbul, Turkey*

[3] *Marmara University, Department of Pharmacology / Faculty of Medicine, Istanbul, Turkey*

[4] *Marmara University, Department of Histology and Embriology/Faculty of Medicine, Istanbul, Turkey*

[5] *Marmara University, Vocational School of Health-Related Professions/Department of Medical Laboratory, Istanbul, Turkey*

Introduction

Generalized epilepsy is a chronic neurological disease characterized by recurrent seizures due to neuronal hyperexcitability, which is exacerbated by glia-mediated excitation and inflammation[1]. Irisin, a myokine and adipokine, is also found in the cerebrospinal fluid and hypothalamus[2]. Irisin levels were shown to increase after epileptic seizures[3], while anti-inflammatory effects of irisin were demonstrated in neurodegenerative disease models. The aim of the study was to investigate the possible neuroprotective effects of irisin on seizure-induced oxidative brain damage.

Methods

Under anesthesia, female Sprague Dawley rats were equipped with intracerebroventricular cannulas (n=48). Half of the rats were injected intraperitoneally with pentylenetetrazole (PTZ, 45 mg/kg) to induce epileptic seizure, while the control rats received saline. Ten minutes before PTZ or saline injection, irisin (7.5 µg/2 µl) or saline was administered intracerebroventricularly. In order

to induce the endogenous release of irisin by muscle contraction, a group of rats performed an exhaustive swimming exercise for 10 minutes (with weights on their tails) before PTZ-seizure. Seizures were evaluated using the Racine score. To evaluate memory performance, passive avoidance test was performed before and after PTZ injection. Rats were decapitated at 24th hour following seizure induction. Brain tissues were taken for histopathological examination and for evaluating oxidative damage, antioxidant capacity and the neurotransmitter levels. Data were analyzed by one-way ANOVA.

Results

Irisin reduced the average of stage scores, reduced the duration of generalized tonic-clonic seizures ($p<0.05$). Increased lipid peroxidation and decreased glutathione and catalase levels observed in the brain tissues of saline-treated PTZ rats as compared to control rats ($p<0.05$) were reversed in exercised or irisin-treated rats with seizures ($p<0.05$). Reduced GABA levels in saline-treated PTZ-rats were elevated in irisin-treated or exercised rats, while PTZ-induced elevation in glutamate was decreased ($p<0.05$). PTZ-induced memory dysfunction and microscopically observed neuronal damage were improved in rats treated with irisin ($p<0.05$).

Conclusion

Exogenous irisin or its possible release by strenuous exercise improved the severity of PTZ-induced seizures and alleviated memory dysfunction, which appear to occur by modulating neurotransmitter homeostasis and by limiting oxidative neuronal damage.

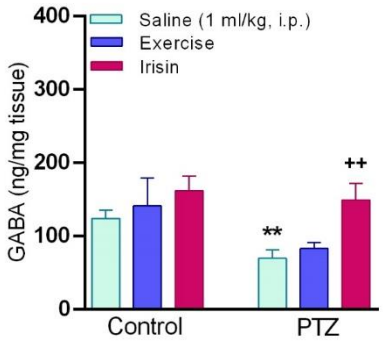

GABA levels
Brain GABA levels of ip Saline or pentylenetetrazole treated saline, exercise, irisin groups. ** p<0.01 compared to saline-treated control group; ++p<0.01 compared to saline-treated PTZ group. Data expressed as Mean±SEM.

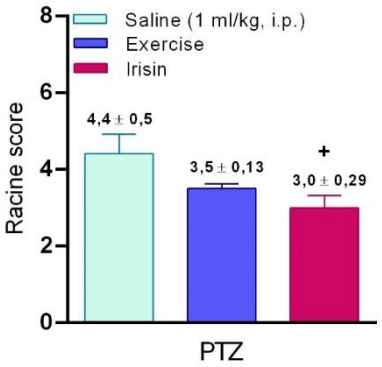

Racine scores
Racine scores of ip Saline or pentylenetetrazole treated saline, exercise, and irisin groups. +p<0.05 compared to saline-treated PTZ group. Data expressed as Mean±SEM.

References

[1] Fisher RS, van Emde Boas W, Blume W, et al. Epileptic seizures and epilepsy: definitions proposed by the International League Against Epilepsy (ILAE) and the International Bureau for Epilepsy (IBE). Epilepsia. 2005;46(4):470-2.

[2] Rabiee F, Lachinani L, Ghaedi S, et al. New insights into the cellular activities of Fndc5/Irisin and its signaling pathways. Cell Biosci. 2020;10:51.

[3] Ergul Erkec O, Algul S, Kara M. Evaluation of ghrelin, nesfatin-1 and irisin levels of serum and brain after acute or chronic pentylenetetrazole administrations in rats using sodium valproate. Neurol Res. 2018;40(11):923-9.

B 06-29

Circulating biomarkers in differentiating stroke from stroke mimics

M. M. Almusined[1], P. Kakkar[1], T. Kakkar[1], L. Makawa[1,2], K. Kain[2], T. Patankar[2], A. Hassan[2], S. Saha[1]

[1] *Discovery and Translational Science Department, Leeds Institute of Cardiovascular and Metabolic Medicine, Faculty of Medicine & Health,University of Leeds, Leeds, UK*

[2] *Leeds Teaching Hospitals NHS Trust, Leeds, UK*

Introduction

Stroke is the 2nd leading cause of death and the 3rd leading cause of disability worldwide. The diagnosis of stroke remains largely clinical, yet widely used stroke scoring systems (e.g., FAST TEST or CINCINNATI STROKE SCALE) do not allow distinction of patients with acute stroke from those with mimics (e.g., migraine, seizures, mass brain lesions). A computed tomography (CT) scan can confirm haemorrhage, but many patients with suspected stroke are subsequently confirmed to have alternative pathologies. *Diffusion-weighted* magnetic resonance imaging (DW-MRI) helps to distinguish between acute stroke and mimic but requires longer scanning time and is insufficiently

sensitive in minor stroke. Recently, the blood biomarkers strategy showed a promising diagnostic method in the research field. This study aims to examine circulating biomarkers in acute stroke patients compared to mimics identified by clinical scoring systems as well as CT and MRI scans.

Methods

In this study 49 patients with acute ischaemic stroke and 17 patients with stroke mimics were recruited. The levels of biomarkers [e.g.,Glial fibrillary acidic protein (GFAP), Neuron-specific enolase (NSE), Neurofilament light chain (NfL), Occludin, Zonula occludens protein (ZO-1) and Claudin-5] in blood obtained from stroke patients and stroke mimics were measured by enzyme-linked immunosorbent assay (ELISA) technique. Estimations of infarct volumes based on CT Alberta Stroke Program Early CT Score (ASPECTS), MRI apparent diffusion coefficient (ADC) values and T2 signal intensity were determined. Statistical analysis of circulating biomarkers was performed using Mann–Whitney U test. Spearman's correlation was used to assess the linear relationships between blood biomarkers and imaging markers.

Results

The results showed a significant difference in circulating GFAP, NfL, Occludin, ZO-1 and Claudin-5 but not NSE in stroke patients compared to mimics. ZO-1, Occludin and NfL are significantly different between ischemic patients with ASPECTS **≤** 7 or ASPECTS **>** 7 and mimic patients. A positive correlation between NSE, NfL and Claudin-5 and volume of infarct in MRI was observed. A positive correlation between GFAP and ZO-1 and ADC values in ischemic patients was observed.

Conclusion

Our data suggest that circulating GFAP, ZO-1, Claudin-5, Occludin and NfL can differentiate between ischaemic and mimic patients. Occludin and ZO-1 can differ significantly between ischaemic and mimic patients even when blood is collected after 2 days. NSE, NfL and Claudin-5 are correlated with the MRI volume of infact size. GFAP and ZO-1 levels are correlated with ADC values in ischaemic patients.

B 06-30

Humanin Attenuates Oxaliplatin-Induced Neuropathic Pain in Male Mice

B. Bilgin[1], M. G. Ersoz[2], F. Bulut[1], M. M. Kelestemur[1], M. Adam[1], S. Canpolat[2], **M. Ozcan**[1]
[1] Firat University, Biophysics, Elazig, Turkey
[2] Firat University, Physiology, Elazig, Turkey

This work was supported by a grant from Turkish Scientific Technical Research Organization (TUBITAK Project No: 119R084).

Introduction

Oxaliplatin (OXA) is a platinum-derived chemotherapeutic drug widely used against cancers, but it causes a serious side effect, painful neuropathy. It has been demonstrated that one of the main factors in the development and maintenance of this OXA-induced painful neuropathy is mitochondrial dysfunction. However, the effects of humanin, the first discovered mitochondrial polypeptide, on OXA-induced neuropathic pain remains unclear as a scientific gap. Our main purpose in the present study was to investigate the effects of humanin, a mitochondrial polypeptide, on pain threshold in mice with OXA-induced neuropathic pain.

Methods

Forty-seven male BALB/c mice were randomly divided into five groups; healthy, OXA (control), OXA + humanin (4 mg/kg, ip), OXA + gabapentin (50 mg/kg, ip), and OXA + humanin (4 mg/kg, ip) + gabapentin (50 mg/kg, ip) (n=7, healthy group; n = 10, other groups). OXA was prepared at a concentration of 2 mg/mL in a 5% dextrose solution according to the weight of each animal and was administered intraperitoneally (ip) at a dose of 2 mg/kg twice a week for 4.5 weeks. Cold allodynia was evaluated with the Cold Plate test as paw withdrawal latency (PWL), while mechanical hyperalgesia was evaluated with the von Frey filament test as the paw withdrawal threshold (PWT).

Results

Compared to the healthy group, the OXA group had significantly lower PWT and PWL values (n=7, p<0.001). Both PWT and PWL values were significantly higher in the OXA+humanin group compared to OXA group (n=10, p<0.05). When the OXA + humanin+ gabapentin group was compared with the OXA + gabapentin group, PWT and PWL values were higher, but only the PWL value was statistically significant (n=10, p<0.05).

Conclusion

These results demonstrate that humanin suppresses OXA-induced cold allodynia and mechanical hyperalgesia, and its combination with gabapentin produces an additional analgesic effect. Humanin can be a promising therapeutic strategy in OXA-induced neuropathic pain.

B 06-31

Modulation of gabazine on Purkinje output of cerebellar brain slices in a model of paroxysmal dystonia.

F. S. Kragelund[1], D. Franz[1], M. Heerdegen[1], A. Lüttig[2], S. Perl[2], A. Richter[2], R. Köhling[1]
[1] University of Rostock, Oscar Langendorff Institute of Physiology, Rostock, Germany
[2] University of Leipzig, Institute of Pharmacology, Pharmacy and Toxicology Faculty of Veterinary Medicine (VMF), Leipzig, Germany

This study was supported by the German Research Foundation (DFG) within the Collaborative Research Centre (SFB 1270/1 ELAINE 299150580). We also thank Tina Sellmann for the surgical support.

Dystonia is a neurological syndrome that alters muscle control for voluntary movement and sustained posture. Although the basal ganglia play a role in dystonia, an abnormal cerebellar function is also involved (Pizoli et al., 2002).

Deep brain stimulation (DBS) is a standard treatment option for drug-refractory dystonia, and the most promising targets are Globus Pallidus internus (GPi) or subthalamic nucleus (STN) (Paap et al., 2020; Spiliotis et al., 2021). The mechanisms of DBS, however, are as yet unclear. In this context, we were interested in the impact of DBS on cerebellar activity, and specifically the role of GABAergic transmission in DBS-induced changes.

We explored this question in a genetic model of primary paroxysmal dystonia (dt^{sz} hamster, 6-8 weeks old) and appropriate controls, bilaterally implanted with bipolar DBS electrodes in the entopeduncular nucleus (homolog to the GPi in humans).

To gauge cerebellar activity, parasagittal cerebellar slices (200 µm thick) were recorded in a high-density microelectrode array (HD-MEA - BioCAM X, 3Brain AG, Wädenswil, Switzerland, 4,096 recording electrodes arranged in a 3.8 mm x 3.8 mm area), perfused with first Krebs solution for 10 minutes, (3 mL/min, at room temperature), and thereafter adding 5uM of Gabazine (Sigma-Aldrich; Merck KGaA, Darmstadt, Germany). Neuronal activity was sampled at 19,753.78 Hz/electrode and analyzed with BrainWave 5 (3Brain AG).

Our preliminary results indicate that blocking the $GABA_A$ receptor with gabazine modulates the Purkinje cell spike firing, with respect to amplitude and frequency differentially between the DBS

and sham-DBS groups. Based on these findings, DBS appears to alter GABA-receptor dependent cerebellar output.

B 06-33

CENTRAL ADMINISTRATION OF CANNABINOID LIGANDS MODULATES ANXIETY-LIKE BEHAVIOR IN OLFACTORY BULBECTOMIZED RAT

M. S. Velikova[1], D. K. Doncheva[1], **R. E. Tashev**[2]
[1] *Medical University of Varna, Physiology and Pathophysiology, Varna, Bulgaria*
[2] *Medical University of Sofia, Physiology and pathophysiology, Sofia, Bulgaria*

Introduction

Accumulating studies reveal that cannabinoid receptor (CBR) signaling plays role in the control of emotional behavior. CBRs have been also implicated in anxiety and depressive disorders, but their role in these states is not well-established (1). There are two types of CBR (CB1 and CB2), the CB1 is expressed predominantly in the brain. The aim of the study was to examine the effects of CB ligands (HU210, CB1/CB2 agonist) and SR141716A (CB1 antagonist) applied i.c.v. on the anxiety-like behavior of rats with olfactory bulbectomy model of depression, using elevated plus-maze (EPM) test.

Methods

Male Wistar rats were anesthetized with Calypsol (50mg/kg, i.p); OBX was performed as described (2). Cannulae were implanted into the right ventricle and HU 210(5μg/1μl), SR141716A(3μg/1μl) or saline(1μl) were injected i.c.v. for 7 days (n=7) as described (3,4). Results were analyzed by one-way ANOVA and post hoc SNK test.

Results

ANOVA showed a significance for “depression” in OBX rats for the number of open arm entries (nOA)($F_{1,23}$=16,05P≤0.001), time spent in open arms (tOA)($F_{1,23}$=111,77 P≤0.001); ratio open/total number of entries (O/T)($F_{1,23}$=26.44P≤0.001).The OBX rats showed an increased anxiety-like behavior demonstrated by decreased nOA(P≤0.001), tOA(P≤0.001),O/T(P≤0.001).There was a significance for “drug” factor in the OBX rats for nOA($F_{2,20}$=30,5 P≤0,001);tOA($F_{2,20}$=57,461P≤0,001);O/T($F_{2,20}$=68,232P≤0,001);number of closed arm entries(nCA)($F_{2,20}$=39,027P≤0,001);time spent in closed arms (tCA)($F_{2,20}$=57,461P≤0,001);total number of entries(Tn)($F_{2,20}$=17,186P≤0,001). HU210 microinjected to OBX rats increased nOA(P≤0.001),tOA(P≤0.001),O/T(P≤0.001);decreased nCA(P≤0.001),tCA(P≤0.001),Tn(P≤0.01);while SR141716A increased nCA(P≤0.05),tCA(P≤0.05) compared to the OBX-controls. ANOVA showed a significance for “drug” in the sham-operated rats for nOA($F_{2,20}$=11,571P≤0,001);tOA($F_{2,20}$=27,358 P<0,001);O/T($F_{2,20}$=71,675P≤0,001);nCA($F_{2,20}$=84,00 P≤0,001);tCA($F_{2,20}$=27,358 P≤0,001);Tn($F_{2,20}$=26,823 P≤0,001). HU210, injected to the sham-controls increased the nOA(P≤0.01); tOA(P≤0.02); O/T(P≤0.001) and decreased nCA(P≤0.002), tCA (P≤0.02); while SR141716A decreased nOA(P≤0.01); tOA (P≤0.001), O/T (P≤0.001); and increased nCA (P≤0.001); tCA(P≤0.001), Tn(P≤0.001) as compared to the saline-treated sham controls (SSC). HU210, injected to OBX rats increased the nOA(P≤0.03), O/T(P≤0.003), decreased nCA(P≤0.003) and Tn(P≤0.05);SR141716A increased nCA(P≤0.001),tCA(P≤0.001),Tn(P≤0.001) and decreased nOA(P≤0.002),tOA(P≤0.001),O/T(P≤0.001) compared to SSC.

Conclusion

The results demonstrated that the activation of CBR decreased the anxiety-like behavior in both sham-operated and OBX rats. The selective CB1 antagonist produced a significant anxiogenic-like effect in these rats. Our data support the suggestions that CB1 receptors are involved in the altered anxiety behavior in OBX rats and that the enhanced CB receptor signaling may be beneficial for the treatment of anxiety.

References

[1] Korem N, Zer-Aviv TM, Ganon-Elazar E, Abush H, Akirav I. Targeting the endocannabinoid system to treat anxiety-related disorders. J Basic Clin Physiol Pharmacol. 2016;27:193–202.
[2] Kelly JP, Wrynn AS, Leonard BE. The olfactory bulbectomized rat as a model of depression: an update. Pharmacol Ther.1997;74(3):299 –316
[3] Pellow S, P Chopin P, File S.E, Briley M Validation of open:closed arm entries in an elevated plus-maze as a measure of anxiety in the rat . J Neurosci Methods 1985; 14(3):149-167
[4] Velikova M, Doncheva D, Tashev R. Subchronic effects of ligands of cannabinoid receptors on learning and memory processes of olfactory bulbectomized rats. Acta Neurobiol Exp.(Wars) 2020;80(3):286-296

B 06-34

Unravelling the cooperative activation of the subunits in P2X2 ion channels

C. Sattler[1], T. Eick[1], S. Hummert[1], C. Unzeitig[1], R. Schmauder[1], A. Schweinitz[1], M. Otte[1], E. Schulz[3], F. Schwede[2], K. Benndorf[1]
[1] *University Hospital Jena, Institute of Physiology II, jena, Germany*
[2] *BIOLOG Life Science Institute GmbH & Co. KG, Bremen, Germany*
[3] *University of Applied Sciences, Falcuty of Electrical Engineering, Schmalkaden, Germany*

Ionotropic purinergic receptors (P2XRs) are expressed in several cell types. They are involved in diverse physiological and pathophysiological processes like pain, inflammation or synaptic transmission. Binding of extracellular ATP at the interphases of two neighbored subunits induces a conformational change of the pore forming transmembrane domains TM2, resulting in a nonspecific cation flux. A central role of the b-14 sheet, which connects the binding pocket with the pore, and in particular the amino acid H319 has been suggested for transmission of the signal within a subunit.
Here we performed global fit strategies to kinetically unravel the activation of the three subunits in rat P2X2 receptors. The strategy is based on four complex and intimately coupled kinetic schemes, sharing the majority but not all parameters, which were fitted to multiple current data sets recorded from wild-type receptors and mutated receptors, sensitized by the mutation H319K, with either ATP or its fluorescent derivative 2-[DY-547P1]-AET-ATP (fATP) as ligand. The extended global fit allowed us to determine 26 rate constants for wild -type P2X2 channels and to gain new insights into the gating mechanism.
Conclusions from our results are: 1. The steep concentration-activation relationship typical for wild-type P2X2 channels is caused by a subunit flip reaction with strong positive cooperativity that overbalances a pronounced but lesser negative cooperativity for the three ATP binding steps. 2. The net probability fluxes in the kinetic scheme are characterized by a marked hysteresis in the activation-deactivation cycle for the third binding step. 3. The facilitated opening in the H319K mutant is caused by a significantly enhanced flip reaction when only one ligand is bound.

B 06-35

Mechanisms underlying remote ischemic conditioning (RIC): potential role against ischemic stroke

I. Mollet[1], J. P. Marto[2], R. Viana-Soares[2], C. Martins[2], M. Angelo-Dias[2], M. Mendonça[2], D. Noronha-Osorio[3], C. Pires[1], A. S. Carvalho[2], H. Gamboa[3], R. Matthiesen[2], L. M. Borrego[2], M. Viana-Baptista[2], **H. L. Vieira**[1]

[1] Universidade Nova de Lisboa, UCIBIO NOVA School of Science and Technology, Caparica, Portugal

[2] Universidade Nova de Lisboa, Nova Medical School, Lisbon, Portugal

[3] Universidade Nova de Lisboa, Physics Depart NOVA School of Science and Technology, Caparica, Portugal

The funding agency that supported the work "Fundação para a Ciência e Tecnologia" (FCT) with 4 projects: Applied Molecular Biosciences Unit-UCIBIO (UID/Multi/04378/2019), iNOVA4Health - Programme in Translational Medicine (UID/Multi/04462/2013), LA/P/0140/2020 of the Associate Laboratory Institute for Health and Bioeconomy and PTDC/MEC-NEU/28750/2017.

Introduction

Stroke is one of the main cause of neurological disability worldwide and the second cause of death in people over 65 years old, resulting in great economic and social burden. Ischemic stroke accounts for 85% of total cases, and the approved therapies are based on re-establishment of blood flow, and do not directly target brain parenchyma. Thus, novel therapies are urgently needed. Preconditioning, or simply conditioning, is a noxious stimulus below damage threshold, which is able to activate endogenous mechanisms of defence and to promote tolerance and cytoprotection. Remote ischemic conditioning (RIC) is the ischemic conditioning of non-vital organs with low-risk (such as arms) that provide protection in another organ, such as the brain. Thus RIC emerges as a potential therapy against ischemic stroke.

Methods and Results

Herein we have explored the underlying mechanisms of RIC, namely what is activated in the arm that responds in the brain. RIC procedure was applied to young and senior healthy volunteers for the assessment of circulating biochemical factors and immune cells at 4 different time points, as well as autonomous nervous system during RIC procedure. Three different hypothesis for inter-organ communication were explored:

(i) The autonomous nervous system is involved in RIC signalling. RIC procedure modulates both parasympathetic and sympathetic autonomic nervous system, which was assessed by heart rate variability, namely the increase on the non-linear parameter SD2 [1].

(ii) Circulating immune cell were analysed at 4 time points following RIC procedure for the characterization of the innate and adaptive circulating immune cell populations [2]

(iii) Circulating humoral factors were identified following RIC procedure in healthy volunteers. Circulating protein pattern was characterized by proteomic analysis (mass spectrometry). Moreover, nitric oxide, biliverdin and carboxyhaemoglobin (COHb) levels were quantified, revealing an increase on COHb levels following RIC.

Finally, functional validation of conditioned human plasma was performed in experimental models for assessing potential cytoprotective properties. Human cell lines were treated with conditioned human plasma for the analysis of different features: neuronal viability, morphology and synaptic formation; neuroinflammation (microglia cells) and blood brain barrier permeability (brain microvascular endothelial cells). Although RIC-induced changes in biochemical composition of human plasma, no improvement on cell function was found induced by conditioned human plasma when compared to human plasma. One can speculate that a more chronic application of RIC is needed for leading to cytoprotection and neuroprotection.

Conclusion

In this work an extensive characterization of RIC inter-organ communication was performed using human samples and healthy volunteers. By disclosing the underlying mechanisms one can better explore the potential use of RIC as therapy.

References

[1] Noronha Osório D, Viana-Soares R, Marto JP, Mendonça MD, Silva HP, Quaresma C, Viana-Baptista M, Gamboa H & Vieira HLA (2019) Autonomic nervous system response to remote ischemic conditioning: Heart rate variability assessment. *BMC Cardiovasc. Disord.***19**.

[2] Mollet I, Martins C, Ângelo-Dias M, Carvalho AS, Aloria K, Matthiesen R, Baptista MV, Borrego LM & Vieira HLA (2022) Pilot study in human healthy volunteers on the mechanisms underlying remote ischemic conditioning (RIC) – Targeting circulating immune cells and immune-related proteins. *J. Neuroimmunol.*, 577847.

B 06-37

ClC-3-associated Cl^-/H^+ exchange is required for neurotransmitter accumulation in adrenal chromaffin granules

J.D. Sierra Marquez, C. Fahlke, R. E. Guzman

Forschungszentrum Jülich GmbH, Institute of Biological Information Processes (IBI-1), Jülich, Germany

This work was supported by a grant from the Deutsche Forschungsgemeinschaft (GU 2042/2-1 to R.E.G).

Introduction

Naturally occurring mutations in ClC-3 or ClC-4 Cl^-/H^+ exchangers lead to neurodevelopmental disorders, with intellectual disability and epilepsy as the main symptoms. Most of the patients show also behavioral and mood disorders such as anxiety, depression, and hyperactivity, conditions that are associated with an imbalance in the monoaminergic system (dopamine and serotonin)[1]. We recently demonstrated that vesicular Cl^-/H^+ exchangers regulate the granular monoamine accumulation process in chromaffin cells, likely by acidifying secretory vesicles via a Cl^- -driven H^+ import. However, CLCs Cl^-/H^+-exchangers have also been proposed to accumulate Cl^- in endosomes harnessing existing pH gradients[2,3]

Methods

We used chromaffin cells from newborn mice, a suitable neuroendocrine and neural cell model, high-resolution membrane cell capacitance, carbon fiber amperometry, and rescue experiments to investigate the importance of CLC chloride/proton transport functions for monoamine accumulation.

Results

In a double mutant (*Dmut*) knock-in/out mouse model (*Clcn3*$^{E281Q/E281Q}$/*Clcn4*$^{-/-}$) that express only a transport deficient ClC-3 and lacks any ClC-3/4-associated Cl^-/H^+ exchange, we observed similar exocytotic responses as in *Clcn3*$^{-/-}$ cells[4]. Moreover, a significant reduction in the vesicle

catecholamine content was observed in the *Dmut* chromaffin granules as compared to the control condition. To assess the importance of stoichiometric Cl^-/H^+-exchangers, we reinserted the WT ClC-3c, the variant mainly found in mature LDCV[4], as well as the E255A ClC-3c, that mediate Cl^- uniport into *DMut* chromaffin cells. Amperometric measurements showed only full rescue of the catecholamine content in the *Dmut*+ WT ClC-3c but not in the *Dmut*+ E255A ClC-3c- demonstrating that coupled Cl^-/H^+-exchange is necessary for proper monoamine accumulation.

Conclusion

We conclude that the ClC-3-associated Cl^-/H^+ exchange regulates the priming process of large dense-core vesicles as well as vesicle monoamine accumulation by contributing to the acidification of these organelles in adrenal chromaffin cells.

References

[1] Dwivedi, D Bhalla, U 2021, 'Physiology and therapeutic potential of SK, H, and M medium Afterhyperpolarization ion channels', *Frontiers in Molecular Neuroscience*, 14:658435.

[2] Novarino, G et al., 2010 'Endosomal chloride-proton exchange rather than chloride conductance is crucial for renal endocytosis', *Science*, 328:1398–1401.

[3] Weinert, S et al., 2020, 'Uncoupling endosomal CLC chloride/proton exchange causes severe neurodegeneration', *The EMBO Journal*, 39(9): e103358

[4] Comini, M *et al.*, 2022, 'CLC Anion/Proton Exchangers Regulate Secretory Vesicle Filling and Granule Exocytosis in Chromaffin Cells', *Journal of Neuroscience*, 42 (15) 3080-3095.

B 06-38

The Regulatory Role of Brain Neuropeptide-S in Locomotor Functions

I. Akçalı, E. Çubukcu, S. Yüksel, **M. Bülbül**, A. Ağar

Akdeniz University, Department of Physiology, Antalya, Turkey

This work was supported by The Scientific and Technological Research Council of Turkey (TUBITAK) within Research Programme-1001 (220S745).

Introduction

The novel brain peptide, neuropeptide-S (NPS) was initially identified as a ligand of the orphan G-protein coupled receptor GPR154, thereafter called neuropeptide-S receptor (NPSR). In mammalian brain, NPS is predominantly produced by a group of cells between locus coeruleus and Barrington's nucleus; whereas, the mRNA of the NPS precursor has been detected in several forebrain structures including the amygdala and hypothalamus (Xu et al., 2007; Xu et al., 2004). In rodents, centrally administered exogenous NPS was demonstrated to increase locomotion (Li et al., 2015), moreover, it was found to improve the parkinsonian dysfunctions by inducing dopamine release and neuronal survival (Bulbul et al., 2019; Didonet et al., 2014). In fact, the role of brain NPS in motor functions remains insufficiently identified. Therefore, the present study was designed to investigate the regulatory role of central endogenous NPS in locomotion.

Methods

For central drug delivery, adult male Sprague-Dawley rats underwent intracerebroventricular (icv) cannulation prior to the experiments. A day after surgery, rats received angiotensin-II (150 ng, icv) and they were returned to the home cages with access to a water bottle. The latency to drink was recorded and rats failed to exhibit drinking behavior within 120 sec were excluded from the study. Following 7-day recovery period, rats were centrally treated with NPSR antagonist ML154 (n=12) or dimethyl sulfoxide as vehicle (n=10) 30 min prior to the motor tests. Motor performance and motor coordination were assessed by rotarod test and measuring the locomotor activity and the state of catalepsy. Following the measurements, coronal frozen brain sections were harvested and the neurochemical profile of NPSR-expressing cells was visualized by double immunofluorescence. Data were expressed in means ± SE; whereas, Student's t-test was used to analyze the differences among the treatments.

Results

Compared with the vehicle-treated rats (3370 ± 313 activity/5 min, n=10) ML-154 significantly reduced the locomotor activity (1572 ± 308 activity/5 min, n=12, p=0.001). In rotarod test, the duration of the activity was found to be significantly lower (70.2 ± 14.5 sec, n=12, p=0.001) in the ML154-treated rats compared with the vehicle-treated counterparts (161.3 ± 24.3 sec, n=10). Compared to the vehicle-injected rats (1.61 ± 0.14 sec, n=10), icv administration of ML154 led to a prominent cataleptic behavior (4.23 ± 0.87 sec, n=12, p=0.001). NPSR was found to be co-expressed with tyrosine hydroxylase and corticotropin releasing factor in neuron of basal forebrain and brainstem.

Conclusion

The present findings revealed that NPS may affect neuronal circuits associated with the regulation of motion in central nervous system. Therefore, NPSR appears to be a potential therapeutic target for the treatment of movement disorders.

References

[1] Bulbul, M., Sinen, O., Ozkan, A., Aslan, M.A., Agar, A., 2019. Central neuropeptide-S treatment improves neurofunctions of 6-OHDA-induced Parkinsonian rats. Experimental neurology 317, 78-86.

[2] Didonet, J.J., Cavalcante, J.C., Souza Lde, S., Costa, M.S., Andre, E., Soares-Rachetti Vde, P., Guerrini, R., Calo, G., Gavioli, E.C., 2014. Neuropeptide S counteracts 6-OHDA-induced motor deficits in mice. Behavioural brain research 266, 29-36.

[3] Li, M.S., Peng, Y.L., Jiang, J.H., Xue, H.X., Wang, P., Zhang, P.J., Han, R.W., Chang, M., Wang, R., 2015. Neuropeptide S Increases locomotion activity through corticotropin-releasing factor receptor 1 in substantia nigra of mice. Peptides 71, 196-201.

[4] Xu, Y.L., Gall, C.M., Jackson, V.R., Civelli, O., Reinscheid, R.K., 2007. Distribution of neuropeptide S receptor mRNA and neurochemical characteristics of neuropeptide S-expressing neurons in the rat brain. The Journal of comparative neurology 500, 84-102.

[5] Xu, Y.L., Reinscheid, R.K., Huitron-Resendiz, S., Clark, S.D., Wang, Z., Lin, S.H., Brucher, F.A., Zeng, J., Ly, N.K., Henriksen, S.J., de Lecea, L., Civelli, O., 2004. Neuropeptide S: a neuropeptide promoting arousal and anxiolytic-like effects. Neuron 43, 487-497.

B 06-39

Intrinsic burst firing in dopamine VTA neurons projecting to medial shell of Nucleus accumbens

T. Ziouziou[1], C. Knowlton[2], C. Canavier[2], J. Roeper[1]

[1] *Goethe University, Institute of Neurophysiology, Frankfurt, Germany*

[2] *Louisiana State University Health Sciences Center, Department of Cell Biology and Anatomy, New Orleans, USA*

This work was supported by the CRC 1080 and the NIH grant R01DA041705 to CCC and JR.

Dopamine midbrain neurons (DA) are intrinsic pacemakers engaged in a variety of neuronal circuits that control voluntary movement, emotion and reward-based learning. Disruptions in the functional activity of DA neurons are believed to be associated with major brain disorders such as schizophrenia or addiction. Investigating the biophysical mechanisms of how electrical activity of specific DA subpopulations is regulated and disturbed, will be crucial to improve our understanding of these afflictions.

The diversity of the mesolimbic DA system is anatomically organized and comprises relevant functional differences in biophysical properties as e.g. varying dynamic range of firing and rebound properties (Lammel et al. 2008; Knowlton, Ziouziou et al. 2021). So far, the characterization of DA neurons has been based on the key assumption that all DA neurons operate as intrinsic pacemaker cells. This implies that high frequency burst firing of DA neurons, often observed in vivo, are exclusively trigged by synaptic inputs. However, by combining retrograde tracing and *in vitro* on-cell, whole-cell and perforated patch-clamp recordings, we recently identified a small subset (< 10%) of medial shell of Nucleus accumbens-projecting (mNAcc) DA VTA neurons that intrinsically generate high-frequency burst discharges. Stimulation of muscarinic receptors by 1 µM Oxotremorine M increased the occurrence of these bursts in mNAcc-projecting DA VTA neurons to about 30% (perforated patch: n = 7/16; on-cell: n = 6/21) but did not induce burst firing in lateral shell of Nucleus accumbens-projecting (lNAcc) DA neurons (perforated patch: n = 0/6; on-cell: n = 0/12). The burst properties of mNAcc DA VTA neurons were reminiscent of recently observed *in vivo* plateau bursting (Otomo et al. 2020) with 2-4 high-frequency spikes and a significant depolarizing shift in action potential thresholds (intraburst frequency: 45.9 ± 28.6 Hz; spikes in bursts: 2.4 ± 0.7; threshold shift between 1st and last intraburst spikes: 4.4 ± 3.8 mV; n = 7, N = 9; mean ± SD).

Since muscarinergic receptor stimulation increased bursting, we further investigated the contribution of downstream targets, in particular the role of M-channel (Kv7) inhibition, for burst generation. We show that Kv7 channel inhibition by 10 µM XE991 was sufficient to induce high-frequency burst discharges in the majority of mNAcc-projecting DA neurons (on-cell: n = 16/18, N = 5; whole-cell: n = 6/6, N = 1). In contrast, in ongoing experiments Kv7 channel inhibition of lNAcc-projecting DA neurons did not lead to bursting (on-cell: n = 0/5, N = 2; perforated patch: n = 0/3, N = 2). Our data might provide a mechanism for the effects of Kv7 modulators on *in vivo* burst firing of DA neurons (Drion et al. 2010). However, to reveal the functional role of ACh-facilitated bursting in mNAcc-targeting DA neurons *in vivo*, we must await projection-specific molecular interventions.

References

[1] Lammel, S., A. Hetzel, O. Hackel, I. Jones, B. Liss, and J. Roeper. "Unique Properties of Mesoprefrontal Neurons within a Dual Mesocorticolimbic Dopamine System." *Neuron* 57, no. 5 (Mar 13 2008): 760-73. https://doi.org/10.1016/j.neuron.2008.01.022. https://www.ncbi.nlm.nih.gov/pubmed/18341995.

[2] Knowlton, C. J*., T. I. Ziouziou*, N. Hammer, J. Roeper, and C. C. Canavier. "Inactivation Mode of Sodium Channels Defines the Different Maximal Firing Rates of Conventional Versus Atypical Midbrain Dopamine Neurons." [In eng]. *PLoS Comput Biol* 17, no. 9 (Sep 2021): e1009371. https://doi.org/10.1371/journal.pcbi.1009371. https://www.ncbi.nlm.nih.gov/pubmed/34534209. *co-first authors

[3] Otomo, K., J. Perkins, A. Kulkarni, S. Stojanovic, J. Roeper, and C. A. Paladini. "In Vivo Patch-Clamp Recordings Reveal Distinct Subthreshold Signatures and Threshold Dynamics of Midbrain Dopamine Neurons." *Nat Commun* 11, no. 1 (Dec 8 2020): 6286. https://doi.org/10.1038/s41467-020-20041-2. https://www.ncbi.nlm.nih.gov/pubmed/33293613.

[4] Drion, G., M. Bonjean, O. Waroux, J. Scuvee-Moreau, J. F. Liegeois, T. J. Sejnowski, R. Sepulchre, and V. Seutin. "M-Type Channels Selectively Control Bursting in Rat Dopaminergic Neurons." *Eur J Neurosci* 31, no. 5 (Mar 2010): 827-35. https://doi.org/10.1111/j.1460-9568.2010.07107.x. https://www.ncbi.nlm.nih.gov/pubmed/20180842.

B 06-40

Theobromine-containing diet enhances learning and memory in senescence-accelerated mouse-prone 8 (SAMP8) mice

E. Sumiyoshi[1,2], K. Matsuzaki[1], N. Sugimoto[1,3], M. Katakura[4], O. Shido[1]

[1] *Shimane University, Department of Environmental Physiology, Izumo, Japan*

[2] *Matsumoto University, Department of Sports and Health Science, Matsumoto, Japan*

[3] *Kanazawa University, Department of Health Sciences, Kanazawa, Japan*

[4] *Josai University, Department of Pharmaceutical Sciences, Sakado, Japan*

This study was funded by grants from the Japan Society for the Promotion of Science (18K17965 & 20K19674).

Introduction

Theobromine is one of the methylxanthine derivatives that are enriched in cacao. Preclinical studies in rodents have shown that long-term oral intake of theobromine improves cognitive function as assessed using a three-lever task, a Y-maze, and a novel object recognition task (NOR). Moreover, we reported that cacao-enriched dark chocolate intake for about 1-month improved brain function in healthy young subjects as assessed by the Stroop color word test and the Digit cancellation test. However, it is unclear whether oral intake of theobromine improves age related cognitive decline. In this study, we examined the effects of theobromine-containing diet on cognitive function in senescence-accelerated mouse-prone 8 (SAMP8) mice.

Methods

This study was conducted in accordance with the Guidelines for Animal Experimentation of Shimane University, compiled from the Guidelines for Animal Experimentation of the Japanese Association for Laboratory Animal Science and the experiments were approved by the Animal Experiment Committee of Shimane University (approval number: IZ30-97). The SAMP8 mice (15-week old) were divided into two groups; a normal diet intake group (P8CN: n = 8) and a TB-containing (0.05%) diet intake group (P8TB: n = 8) for 50 days under the free feeding and drinking water. The SAM-resistant 1 (SAMR1) mice were used as normal aging controls and were a normal diet intake group

(R1CN: n = 8). After theobromine-containing diet intake, cognitive function was assessed using a NOR task. After the NOR task was completed, blood was collected under anesthesia, and the brain (cerebral cortex, hippocampus) were sampled. The brain-derived neurotrophic factor (BDNF) concentrations in the cerebral cortex and hippocampus were quantified by the ELISA method.

Results

Body weight, amount of food intake and amount of water intake did not differ between the P8CN and P8TB groups through the intervention period (all, P>0.17). In the NOR task, short-term memory in the P8TB group was significantly improved compared to that in the P8CN group ($P < 0.05$). Also, BDNF concentrations in the cerebral cortex and hippocampus were significantly increased in the P8TB group compared to the P8CN group ($P < 0.05$). In addition, BDNF concentrations in the cerebral cortex and hippocampus were significantly higher in the R1CN group compared to the P8CN group ($P < 0.05$).

Conclusion

These results suggest that long-term intake of theobromine-containing diet may improve cognitive function even in SAMP8 mice. In the future, we plan to investigate the anti-inflammatory and antioxidant effects of the brain. (COI: No)

B 06-41

TRPV1 expressing neurons in supraoptic nucleus can contribute to osmoregulation via network oscillations

E. Alcin, H. Mörz, R.-D. Treede, W. Greffrath

Heidelberg University, Mannheim Medicine Faculty, Centre for Translational Neuroscience, Mannheim, Germany

EA was supported by a Humboldt Research Fellowship for Postdoctoral Researchers from the Alexander von Humboldt Foundation.

Introduction

The hypothalamic magnocellular neurosecretory cells (MNCs), located in the supraoptic (SON) and paraventricular nucleus (PVN), play a crucial role in the regulation of water and salt balance by secreting oxytocin (OT) and vasopressin (VP) in an osmolality-dependent manner[1]. MNCs react precisely to hypertonic stimulation with membrane depolarization, which is generated by cell shrinkage-induced opening of an N-Terminal-truncated variant of TRPV1 channels[2]. However, a couple of in vitro electrophysiological studies propose a product of TRPV1 gene commits to osmosensory transduction in hypothalamic neurons to regulate VP secretion[2,3] , in an in vivo study, it has been clearly shown that TRPV1 channels are not obligatory for VP secretion and thirst stimulated by hypernatremia[4]. Insight into this information, we aimed to 1) investigate whether OT or VP are colocalized with TRPV1 in the hypothalamic MNCs, 2) test the role of hyperosmolarity (Mannitol), Capsaicin, Glutamate or Potassium on dissociated MNCs from SON and 3) assess the role of Capsaicin, Glutamate or Potassium on brain slices include SON.

Methods

Adult male Sprague-Dawley rats (weighing 150–250 g) were used in all experiments[5].

Immunohistochemistry: For the detection of TRPV1 proteins and either VP or OT, 25 µm hypothalamic coronal sections containing the SON and PVN were processed according to a double-immunofluorescence protocol[5].

Calcium imaging: For measurements of [Ca2+]i, dissociated MNCs were loaded with 1 µM Rhod-2 and Pluronic F-127 for 45-60 min in Tyrode's solution. After washing with Tyrode's solution, cells were mounted on the stage of an inverted microscope in an open bath chamber and superfused by Tyrode's solution (1–3 ml/min) at room temperature (RT)[5].

Preparation and maintenance of brain slices: 300 µM coronal sections were collected and maintained in an incubation chamber at RT for at least 2 h in artificial cerebrospinal fluid (aCSF). A single slice was loaded with Rhod-2 (6 µM) for 60 min in aCSF and was superfused with aCSF at RT (flow rate 2-3 ml/min). Throughout all procedure, aCSF was saturated with carbogen gas (95% O_2, 5% CO_2).

Results

We show that TRPV1 channels are colocalized with OT or VP in SON (Pearson´s coefficient colocalized volume; 0,46 and 0,30 respectively), but not in PVN (Pearson´s coefficient colocalized volume; -0,005 and -0,88 respectively) Fig. 1. Mannitol, Capsaicin, Glutamate or Potassium increased mean intensity value in dissociated MNCs from SON Fig. 2. Capsaicin (36,17±4,08, p<0,01), Glutamate (32,97±2,44, p<0,01) or Potassium (32,14±2,18, p<0,01) administration increased 36 out of 50 cells network oscillations compared with aCSF perfusion (26,47±2,17) in brain slice include SON.

Conclusion

As a conclusion, MNCs in SON express TRPV1 and these non-specific cation channels together with other factors like glutamate receptors can contribute to network activity in SON and hence participate in regulation of water and salt balance.

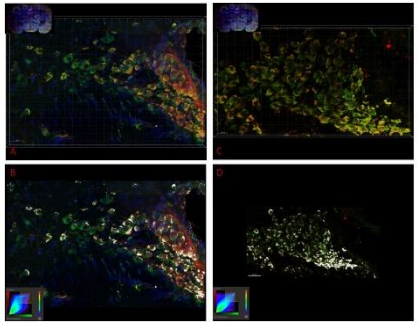

Figure 1
TRPV1 and either oxytocin or vasopressin immunohistochemistry of supraoptic nucleus. A, a merge image (yellow) showing double-labeled TRPV1 immunoreactive cells (green) and oxytocin immunoreactive cells (red). B, colocalization of TRPV1 and oxytocin (white). C, a merge image (yellow) showing double-labeled TRPV1 immunoreactive cells (green) and vasopressin immunoreactive cells (red). D, colocalization of TRPV1 and vasopressin (white).

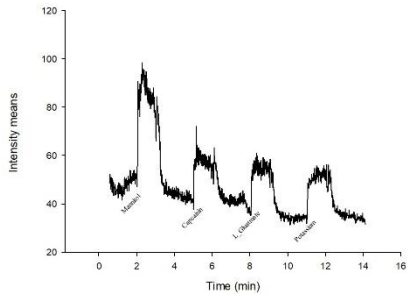

Figure 2
Dissociated hypothalamic magnocellular neurons from supraoptic nucleus. Intensity mean value change after 40 mOsm Mannitol, 10 µM Capsaicin, 200 µM L_Glutamate or 140 mM Potassium administration.

References
1 Mason WT. Supraoptic neurones of rat hypothalamus are osmosensitive. *Nature*. 1980; 287:154-157.
2 Sharif-Naeini R, Witty MF, Seguela P, Bourque CW. An N-terminal variant of Trpv1 channel is required for osmosensory transduction. *NatNeurosci*. 2006;9:93-98.
3 Ciura S, Bourque CW.Transient receptor potential vanilloid 1 is required for intrinsic osmoreception in organum vasculosum lamina terminalis neurons and for normal thirst responses to systemic hyperosmolality. *J Neurosci*. 2006; 26: 9069–9075, 2006.
4 Tucker AB, Stocker SD. Hypernatremia-induced vasopressin secretion is not altered in TRPV1_/_ rats. *Am J Physiol Regul Integr Comp Physiol*. 2016; 311: R451–R456.
5 Greffrath W, Binzen U, Schwarz ST, Saaler-Reinhardt S, Treede RD. Co-expression of heat sensitive vanilloid receptor subtypes in rat dorsal root ganglion neurons. NeuroReport. 2003;17:2251-55.

B 06-42

Effect of High Intensity Interval Exercise on Pain, Disability and Autonomic Balance in Patients with Chronic Low Back Pain

K. S. Al Ghamdi[1], T. Yar[1], S. M. Al Saadi[2], H. M. AlMaawi[3]
[1] *Imam Abdulrahman bin Faisal University, Department of Physiology, College of Medicine, Dammam, Saudi Arabia*
[2] *Imam Abdulrahman bin Faisal University, Department of Physiotherapy, King Fahd University Hospital, Dammam, Saudi Arabia*
[3] *Abu Arish General Hospital, Department of Physiotherapy, Jazan, Saudi Arabia*

The authors wish to acknowledge those who participated in the study and members of the department of physiotherapy at King Fahd University Hospital for their immense cooperation.

Introduction
Chronic low back pain (CLBP) is a clinical condition of large magnitude with great socio-economical effect. In about 90% of patients the cause of CLBP cannot be ascertained and is termed as nonspecific CLBP (NSCLBP). Patients with low back pain often suffer from altered autonomic balance. Dysregulation of autonomic nervous system (ANS) is also implicated to be an underlying cause in the initiation and persistence of chronic muscle pain. Exercises can improve pain, disability and physical fitness. High intensity interval exercise (HIIE) is a newer modality where short bursts of high intensity exercise are interspersed with rest intervals. HIIE might prove more useful and effective for individuals with nonspecific CLBP and could have a better adherence rate in the long run. This study evaluated the efficacy of six weeks HIIE training program on pain, disability and autonomic balance in patients with nonspecific CLBP.
Methods
Ethical approval was obtained from Imam Abdurrahman bin Faisal University. Eighty patients with NSCLBP and mild to moderate disability/pain according to Oswestry Disability Index (ODI) were recruited from King Fahd University Hospital. Patients signed an informed consent form and then they were randomly assigned to one of the two groups: Experimental Group (n= 40) was assigned for HIIE in addition to standard regular physiotherapy, and standard regular physiotherapy group was designated as control group (n=40). Deep breathing test to obtain expiratory to inspiratory ratio (E:I) and orthostatic tolerance test to obtain 30:15 ratio were performed at the beginning of the study to exclude cardiovagal autonomic dysfunction and repeated at the end of the study for comparison. Pre and post intervention assessment included pain intensity through Numerical Rating Scale, disability through ODI and autonomic balance through heart rate variability (HRV, time domain and frequency domain parameters) and baroreflex sensitivity (BRS) at rest and in response to an orthostatic challenge. Data was analyzed using SPSS version 20. Normality of data was tested with Shapiro Wilkinson test Level of significance was set at $p<0.05$.
Results
HIIE intervention with standard physiotherapy for 6 weeks led to a significantly greater improvement in pain and disability compared to standard physiotherapy alone in patients suffering from mild to moderate NSCLBP. The classical autonomic tests were normal for both groups indicating normal cardiovagal regulation. HRV parameters and BRS were also within normal limits and did not show significant changes over the period of intervention in this group of patients. A better reactivity to orthostatic stress and a faster HR recovery in HIIE group after 6 weeks of treatment indicated an improved sympathovagal balance and a faster reactivation of parasympathetic system in HIIE group compared to control.
Conclusion
HIIE can be a useful addition to the exercise regimens in practice for patients with CLBD.

B 06-43

Effect of nutritional status and interventions on spontaneous and hypoxia-evoked carotid sinus nerve activity in rats

J. F. Sacramento, J. P. Cunha-Guimarães, C. S. Prego, S. V. Conde

Universidade Nova de Lisboa, NOVA Medical School|Faculdade de Ciências Médicas, Lisboa, Portugal

Portuguese Foundation for Science and Technology research grant EXPL/MED-NEU/0733/2021 and contract CEEC IND/02428/2018 to Joana F. Sacramento.

Introduction

The carotid bodies (CB), peripheral chemoreceptors classically defined as an O_2 sensors, are also metabolic sensors involved in the regulation of energy and glucose homeostasis [1]. Moreover, CBs dysfunction is key for the development of metabolic diseases, since the resection or electric modulation of the carotid sinus nerve (CSN), the CB sensitive nerve, prevents and reverses dysmetabolic pathological features in prediabetes and type 2 diabetes (T2D) animal models [2-4]. Increased caloric intake is one of the major causes of dysmetabolism, also promoting an increase in the CB and CSN activity [1,2,5]. Aiming to develop selective therapeutic tools to modulate CB-CSN activity to treat diseases associated with overnutrition, as T2D and obesity, we characterized CSN neural activity in rats in different nutritional status and submitted to different nutritional interventions.

Methods

Three groups of male Wistar rats were used: control (normal chow diet, NC), high-fat group (HF, 60% lipid-rich diet, 21 days) and high-fat/high-sucrose group (HFHSu, 60% fat+35% sucrose, 25 weeks). CSN ex vivo recordings in normoxia (20%O_2+5%CO_2) and in response to hypoxia (0%O_2+5%CO_2) were performed in CB-CSN preparation collected from animals in fasting state, ad libitum or after the ingestion of Fortimel, a high protein nutritional supplement (1,46g/2ml). Insulin sensitivity was evaluated through an insulin tolerance test. Spike sorting and clustering were performed, and CSN activity correlated with insulin sensitivity and fasting glycemia. Animals were killed by an intracardiac overdose of pentobarbital sodium (60mg/kg i.p.). Experiments followed the 2010/63/EU European Union Directive and were approved by NOVA Medical School Ethics Committee and Portuguese Authority for Animal Health. Differences between means were calculated using One-Way ANOVA and considered significantly different for $p<0.05$.

Results

CSN activity is characterized by 4 different types of action potentials (AP). In NC animals, basal CSN activity increased by 76 ($p<0.05$) and 80% ($p<0.05$) in postprandial and ad libitum states, respectively, when compared with fasted animals, an effect characterized by an increase in type 2 AP ($p<0.05$) in the postprandial state. Also, hypoxia-evoked CSN response increased by 776 ($p<0.05$) and 361% ($p<0.01$) in postprandial and ad libitum NC animals vs fasted animals, respectively, an effect that is characterized by the increase in type 2 ($p<0.05$) and 3 ($p<0.05$) AP. In ad libitum animals, HF and HFHSu diets increased by 195 and 301% CSN basal activity, respectively, an effect characterized by increased type 2 ($p<0.0001$) and 4 ($p<0.05$) AP, and correlated with insulin resistance but not with fasting glycemia. CSN response to hypoxia was similar between ND and hypercaloric animal models.

Conclusion

Nutritional status and interventions modulate differently CSN neural activity. CSN neural signatures might be a good parameter to distinguish overnutrition states.

References

[1] Conde SV, Sacramento JF, Guarino MP (2010). Carotid body: a metabolic sensor implicated in insulin resistance. Physiol Genomics. 50(3):208-214.

[2] Ribeiro MJ, Sacramento JF, Gonzalez C, Guarino MP, Monteiro EC, Conde SV (2013). Carotid body denervation prevents the development of insulin resistance and hypertension induced by hypercaloric diets. Diabetes. 62(8):2905-2916.

[3] Sacramento JF, Ribeiro MJ, Rodrigues T, Olea E, Melo BF, Guarino MP, Fonseca-Pinto R, Ferreira CR, Coelho J, Obeso A, Seiça R, Matafome P, Conde SV (2017). Functional abolishment of carotid body activity restores insulin action and glucose homeostasis: key roles for visceral adipose tissue and the liver. Diabetologia. 60(1):158-68.

[4] Sacramento JF, Chew DJ, Melo BF, Donegá M, Dopson W, Guarino MP, Robinson A, Prieto-Lloret J, Patel S, Holinski BJ, Ramnarain N, Pikov V, Famm K, Conde SV (2018). Bioelectronic modulation of carotid sinus nerve activity in the rat: a potential therapeutic approach for type 2 diabetes. Diabetologia. 61(3):700-710.

[5] Ribeiro MJ, Sacramento JF, Gallego-Martin T, Olea E, Melo BF, Guarino MP, Yubero S, Obeso A, Conde SV. High fat diet blunts the effects of leptin on ventilation and on carotid body activity. J Physiol. 2018;596(15):3187-3199.

B 06-44

Naringin prevents smokeless tobacco (SLT) induced mitochondrial health degradation, apoptosis in neurons, neurobehavioral pattern and improves systemic toxicity

S. Dey[1], S. Biswas[1], H. Biswas[3], S. C. Biswas[3], R. D. Sharma[2]

[1] *University of Calcutta, Physiology, Kolkata, India*

[2] *Belda College, Physiology, Belda, India*

[3] *CSIR IICB, Neuroscience, kolkata, India*

NTRF research fund to SD and ICMR senior research fellowship to SB

Introduction

The smokeless tobacco (SLT) is a perilous addiction ruining the physiological systems in slow implacable way. The frequency of SLT use in India is about 25%, with high mortality. Absorbable nicotine is higher in SLT than cigarettes and orally absorbed nicotine stays longer in the bloodstream. Some critical components penetrate deep into the cells perturbing the entire cellular metabolic processes enhancing the systemic toxicity and possibly neurodegeneration. Current study was intended to address specific mechanism of SLT-mediated neuronal cell death and its prevention using phytochemical naringin (NG), a flavanone-glycoside.

Methods

To emphasize the systemic distresses, Swiss albino mouse model was developed using a wide range of doses of orally administered SLT. Graded doses of water soluble lyophilized SLT upto 1000mg/kg bw on mouse as well as 0-10mg/ml on differentiated PC12 (rat pheochromocytoma) and SH-SY5Y (human neuroblastoma) cell lines were applied. A plethora of cellular and molecular toxicity parameters were evaluated using cell culture, animal behavior study tools, immunochemistry, flowcytometry and microscopic techniques.

Results
A dose-dependent systemic physiological change, alterations of mouse behavioral patterns and indications of neuronal death was observed upon chewing tobacco treatment. Oral SLT administration reduced the horizontal ambulatory activity and induced anxiolytic function. *In vivo* studies have given certain insights into mechanistic neuronal cell death. Concurrent with the neuronal death pattern, differentiated neuronal cell culture model of PC12 and SH-SY5Y were employed to underpin the SLT induced threats. SLT reduced the oxidative phosphorylation and aerobic glycolysis as determined by the diminution of ATP production and basal respiration. There was breakdown of mitochondrial health and structure with concomitant membrane potential drop along the increasing SLT doses. The involvement of mitochondria and its downstream factors were further confirmed by immune-blot, flowcytometry and microscopic techniques. Hallmark apoptotic signals like leakage of cytochrome *c* was observed after 24hr (6mg/ml) SLT treatment. We observed time dependent increase of t-Bid levels and down-regulation of Bid gave significant protection from cell-death upto 72hr in neurons and NG pretreatment significantly reduced (1.49X) t-Bid expression. Bid authoritatively mediated mitochondrial membrane permeabilization and subsequent cytochrome *c* release leading to apoptosis, neurotoxicity and neurodegeneration. In protective studies, citrus flavonoid NG ameliorated the challenges of SLT mediated systemic stress responses particularly on neuronal cells.
Conclusion
The present study is a comprehensive, in-depth report portraying the fatal effects of SLT identifying some specific clues of neurodegeneration. Another bright side of the work was identification of role of NG against the prevention of SLT mediated perils.

B 06-45
An experimental study of mental activity in healthy individuals using simple and complex sensorimotor reaction times to various visual stimuli
K. Janashia, A. Chikviladze, G. Sanadiradze, A. Ramishvili, N. Tvildiani
David Tvildiani Medical University, Central scientific research laboratory, Tbilisi, Georgia

Introduction
Studies have shown that first-year medical students, experience psychological stress and, in some cases, mental illness due to new environments and stressful study regimes, which negatively affect their ability to study, academic performance, and full participation in life (1, 2).
Methods
An experimental study was conducted on first and next (2-3) year medical students, out of which 17 were males and 21 females. Participants were exposed to two randomized order simulated virtual tasks that differed in their demand levels. Some derivative indices - correct answers in percent (CA%), reaction sustainability (RS), and functional ability level (FAL) of mental activity were calculated based on the simple and complex reaction time measures (SSMRT, CSMRT) (3-5).
Results
No significant difference in mental activity between the two genders in 2-3 year medical students, except for CA% in the males' group (p=0.044) during CSMRT which indicates that males are able to concentrate better; There were significant differences in parameters of SSMRT (FAL p=0.001) and CSMRT (RS p=0.007; FAL p=0.007) between first-year males and females; Significant differences were found also in parameters of SSMRT (RS p=0.012; FAL p=0.016; CA% p=0.001) and CSMRT (RS p=0.009; FAL p=0.013; CA % p= 0.014) between first and next-year medical students in the females' group and significant differences in the males' group only in CA% (p=0.049) of SSRT.
Conclusion
Independent of gender, in 2-3 year medical students the sensorimotor and cognitive abilities are almost the same. The better mental performance parameters in the male group of first-year students can be explained only by the presence of certain stress in the female group, which can be related to the difficulty adapting to new environments and stressful learning regimes of the medical universities. In addition, male students are able to concentrate better compared to females on acute visual stress. Our results contribute to a better understanding of the psychophysiology of mental activity and further demonstrate how a virtual model can be used to investigate acute cognitive stress effects.

References
[1] Guthrie EA, Black D, Shaw CM, Hamilton J, Creed FH, Tomenson B. Psychological stress in medical students: a comparison of two very different university courses. Stress Med. 1998;13:179–84. https://doi.org/10.1002/(SICI)1099-1700(199707)13:3<179::AID-SMI740>3.0.CO;2-E
[2] Taskin C. The visual and auditory reaction time of adolescents with respect to their academic achievements. J Educ Train Stud. 2016; 4(3):202-7. doi:10.11114/jets.v4i3.1374.
[3] Sternberg S, Backus BT. Sequential processes and the shapes of reaction time distributions. Psychological Review. 2015; 122(4), 830–7. doi.org/10.1037/a0039658.
[4] Psychophysiological methods, Method "Simple visual-motor reaction" [Internet].[cited 2022 May 23]. Available from: https://studme.org/101602/ekologiya/psihofiziologicheskie_metodiki.
[5] Bobrova NL. The rationale for the use of complex diagnostic methods for the assessment of a human's psychophysiological state. Bulletin of NTUU "KPI" Informatics, management, and computer engineering. [cited 2022 May 23]. 61:49-53. Available from: https://ela.kpi.ua/bitstream/123456789/16717/1/8.pdf.pdf.

B 06-46
Changes in total choline levels in heart tissues of vagotomized rats.
H. Kazdağlı[1], H. F. Özel[2], E. Barış[3], M. Özbek[4]
[1] *Izmir University of Economics, Elderly Care / Vocational School of Heath Sciences, İzmir, Turkey*
[2] *Manisa Celal Bayar University, Radiology / Vocational School of Heath Sciences, Manisa, Turkey*
[3] *Izmir University of Economics, Department of Pharmacology / Faculty of Medicine, İzmir, Turkey*
[4] *Manisa Celal Bayar University, Department of Physiology / Faculty of Medicine, Manisa, Germany*

Introduction
Several mechanisms are identified for peripheral sympathetic–parasympathetic interactions on cardiac regulation thus understanding the factors affecting main neurotransmitter acetylcholine levels is crucial. Our previous studies showed that different types of vagotomy may affect cardiac function distinctly. This study was designed to evaluate different branches of acute vagotomy that may distinctly affect the levels of acetylcholine levels released from vagus nerve endings which

might be responsible for the contralateral vagus over-activity causing hemodynamic parameters (1).

Methods

The experimental study was approved by the local Ethics Committee for Animal Experimentations. 12-16 weeks old male Wistar rats (288,6 ± 34,23 g, n=40) were used for experiments to eliminate the effect of the menstrual cycle on HRV parameters. Animals were randomly divided into five groups (each n=8): sham, right vagotomy, left vagotomy, bilateral vagotomy, and atropine. During the experimental procedure right, left, or bilateral vagotomy was performed. In the sham-operated group, the right and left vagal nerves were exposed and fixed, but no incision was made. In the Atropine group, vagal innervation was chemically prevented with Atropine Sulfate (5 mg/kg, i.p.). After the experiments rats were sacrificed with urethane (1.5 g/kg, i.p.). Totalcholine/acetylcholine levels in heart tissues of experimental groups were measured by a commercially available kit according to the manufacturer's instructions by spectrophotometer. One-way analysis of variance (ANOVA) with Tukey test for multiple comparison tests was used for statistical analysis. $p<0.05$ was accepted statistically significant.

Results

Total choline/acetylcholine levels were significantly higher only in right vagotomy group compared to sham (10,09 ± 6,964 nM, $p<0.001$) and bilateral vagotomy groups (12,00 ± 3,588 nM, $p<0.01$). The levels were not statistically differs between Atropine-treated group (8,720 ± 1,923 nM), left vagotomy group (10,24 ± 4,951 nM) and in right vagotomy group (22,05 ± 4,494 nM).

Conclusion

Asymmetrical vagal innervation produces change in acetylcholine release in heart tissues. Our data showed that acute right vagotomy significantly increased the total choline levels. Together with our previous findings, this data showed that right vagotomy may induce compensatory hemodynamic recovery through contralateral vagus overactivity along with the enhancement of total choline/acetylcholine levels in heart tissue (2).

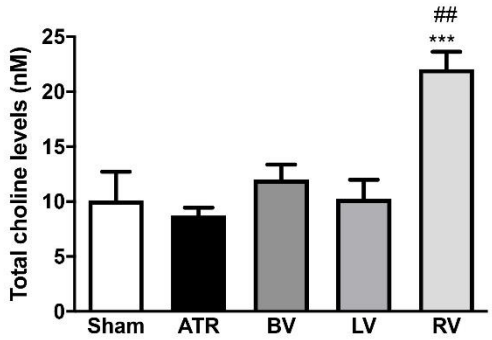

Figure 1
Total choline levels in heart tissues in groups of Sham, Atropine, Bilateral Vagotomy, Left Vagotomy and Right Vagotomy.

References

(1) Chen LN, Zang WJ, Yu XJ, Liu J, Li DL, Kong SS, et al. Compensatory Recovery of Vagal Control of Hemodynamics after Unilateral Vagotomy. Physiol Res [Internet]. 2008 [cited 2022 Mar 12];57:119–32. Available from: www.biomed.cas.cz/physiolres

(2) Kazdagli, Hasan, Hasan Fehmi Ozel, and Mustafa Ozbek. "The Effects of Bilateral and Unilateral Vagotomy on Heart Rate Dynamics." *ACTA PHYSIOLOGICA*. Vol. 234. 111 RIVER ST, HOBOKEN 07030-5774, NJ USA: WILEY, 2022.

B 06-47

An examination of the activity of the ubiquitin-proteasome system during brain ageing and in Parkinson's diseased patients.

D. Wayne, W. G. Carter

University of Nottingham, School of Medicine, Derby, UK

We are grateful to The Neuropsychopharmacology Research Group at the Department of Pharmacology of the University of the Basque Country (UPV/EHU) that supplied the human post-mortem samples used in the ageing brain cohort studies (https://www.ehu.eus/en/web/neuropsicofarmacologia/aurkezpena), and the Parkinson's UK Brain Bank, Imperial College London, that supplied the Parkinson's disease brain tissue and matched control subjects.

Introduction

The global population is rising and so is the number of patients living with neurodegenerative diseases (NDDs). Approximately one million people are affected by NDDs in the UK, and 50 million people worldwide suffer from dementia. The accumulation of intra- or extra-cellular protein deposits is a histopathological hallmark of a number of NDDs. Reduced activity of the ubiquitin-proteasome system (UPS) may be one of the molecular mechanisms that could lead to reduced clearance of potentially toxic protein aggregates. To examine this further, the activity of the UPS was quantified in *post-mortem* tissue in the brains of a cohort of aged individuals (n = 40, age range 23-93 years) and from brain regions of Parkinson's disease (PD) patients (n = 11) and controls (n = 10).

Methods

The activity of theUPS was quantified using a fluorometric assay for the chymotrypsin-like activity of the 20S proteasome. Protein profiling was also performed using denaturing polyacrylamide gel electrophoresis to detect the accumulation of protein aggregates.

Results

UPS activity did not change significantly between samples from the ageing brain cohort or between brain regions from PD patients vs controls ($p > 0.05$). Protein profiling revealed cytoskeletal protein reductions during ageing with reduced α- and β-tubulin expression in brains of individuals of ≥60 years of age, and there were differences in cytoskeletal protein expression between PD brain samples and controls.

Conclusion

Collectively, our results suggest that the ATP-dependent chymotrypsin-like activity of the UPS is stable in the ageing brain and for PD patients, but that molecular changes to the cytoskeleton are present.

B 06-48

Effects of human monoclonal anti-GluN1 autoantibody on NMDA receptor channel function

S. Yang[1], J. R. Heckmann[1], J. Yu-Strzelczyk[1], S. Gao[1], C. Geis[2], **M. Heckmann**[1]

[1] Julius-Maximilians Universität Würzburg, Department of Neurophysiology/ Institute of Physiology, Würzburg, Germany

[2] Jena University Hospital, Department of Neurology/Section of Translational Neuroimmunology, Jena, Germany

Autoantibodies from patients with autoimmune encephalitis are pathogenic and induce typical disease signs upon passive-transfer [1, 2]. Intermediate and long-term antibody effects on synaptic target antigen internalization and on disturbance of synaptic protein function NMDA receptor (NMDAR) have been described [3, 4]. However, direct and acute effects of specific human autoantibodies on ionotropic receptor function are largely unexplored. Here, we use cell-attached single channel recording in HEK cells to investigate the direct effects of specific monoclonal human autoantibody (IgG 003-102) against the GluN1 subunit of the NMDAR. Our preliminary results showed that NMDAR displays high heterogeneity regarding channel open probabilities. IgG 003-102 reduces the simultaneous channel opening of the NMDAR receptor. However, prolonged channel open duration was also observed upon acute antibody exposure. We, therefore, suggest that IgG 003-102 might reduce the mobility of the GluN1 subunit and increase the barrier for the conformational transition of NMDAR. i.e., both channel opening and closing. In addition, the effects of Fab fragments on NMDAR channel functions are under investigation now.

References

[1] Planaguma, J., et al., *Human N-methyl D-aspartate receptor antibodies alter memory and behaviour in mice.* Brain, 2015. **138**(Pt 1): p. 94-109.

[2] Jones, B.E., et al., *Autoimmune receptor encephalitis in mice induced by active immunization with conformationally stabilized holoreceptors.* Sci Transl Med, 2019. **11**(500).

[3] Moscato, E.H., et al., *Acute mechanisms underlying antibody effects in anti-N-methyl-D-aspartate receptor encephalitis.* Ann Neurol, 2014. **76**(1): p. 108-19.

[4] Ladepeche, L., et al., *NMDA Receptor Autoantibodies in Autoimmune Encephalitis Cause a Subunit-Specific Nanoscale Redistribution of NMDA Receptors.* Cell Rep, 2018. **23**(13): p. 3759-3768.

B 06-49

Acetazolamide modulates intracranial pressure directly by its action on the cerebrospinal fluid secretion apparatus

D. Barbuskaite[1], E. K. Oernbo[1], J. H. Wardman[1], T. L. Toft-Bertelsen[1], E. Conti[1], S. N. Andreassen[1], N. Gerkau[2], C. Rose[2], N. MacAulay[1]

[1] University of Copenhagen, Department of Neuroscience, Copenhagen, Denmark

[2] Heinrich-Heine University Düsseldorf, Medical Faculty, Institute of Neurobiology, Düsseldorf, Germany

Introduction

Elevated intracranial pressure (ICP) is observed in many neurological pathologies, e.g. hydrocephalus and stroke. This condition is routinely relieved with neurosurgical approaches, since effective and targeted pharmacological tools are still lacking. The carbonic anhydrase inhibitor, acetazolamide (AZE), may be employed to treat elevated ICP. However, its effectiveness is questioned, its location of action unresolved, and its tolerability low. Here, we determined the efficacy and mode of action of AZE in the rat brain.

Methods

We employed *in vivo* approaches including ICP and cerebrospinal fluid secretion measurements in anaesthetized rats and telemetric monitoring of ICP and blood pressure in awake rats in combination with *ex vivo* choroidal radioisotope flux assays and transcriptomic analysis.

Results

The drug effectively reduced the ICP, irrespective of the mode of drug administration and level of anaesthesia. The effect appeared to occur via a direct action on the choroid plexus and an associated decrease in cerebrospinal fluid secretion, and not indirectly via the systemic action of AZE on renal and vascular processes. Upon a single administration, the reduced ICP endured for approximately 10 h post-AZE delivery with no long-term changes of brain water content or choroidal transporter expression. However, a persistent reduction of ICP was secured with repeated AZE administrations throughout the day.

Conclusion

AZE lowers ICP directly via its ability to reduce the choroid plexus CSF secretion, irrespective of mode of drug administration.

B 06-50

Novel Iboga-derivatives ameliorate nociception, inflammatory and modulate Acute Pain in Mice

S. Dey[1], T. Bhattacharya[1], S. Sinha[2], S. Gupta[2], A. Gupta[2], S. Ghosh[1]

[1] University of Calcutta, Physiology, Kolkata, India

[2] Indian Association for Cultivation of Sciences, Organic Chemistry, kolkata, India

Partial research funding from DSBT, Government of West Bengal and Life Sciences Research Board, Governemnt of India

Introduction

Acute pain mediates certain behavioural impairments leading to neuroinflammatory changes and initiates plasticity events. Existing analgesics regulate pain however at the cost of limited efficacy and side effects. The present study explored efficient and exclusive analgesic effects of Iboga-analogues against acute pain model. To determine the induction of neuroinflammatory changes evoked by formalin; To evaluate the antinociceptive and anti-inflammatory properties of novel ibogaine derivatives; To find any concomitant neuomodulatory effect leading to early plasticity events.

Methods

Male Swiss Albino mice were grouped as **control, formalin treated, formalin+ iboga-alcohol (C1), formalin + iboga-amide (C2), formalin + iboga-methylamide, formalin + 11b (C4).** Pain assessment was done by paw diameter, paw licking and tail immersion test. Open field test (OFT) and elevated plus maze (EPM) were employed to assess locomotor movement and anxiety phenomena. Inflammatory mediators, neurotransmitters and neurotrophic factors were measured from isolated serum, hind paw tissue and spinal L4-L6 segment. One-way ANOVA following Student's t-test were performed. $p<0.05$ was considered as significant.

Results

Increase in paw diameter (**80%**) after formalin injection was significantly reduced in ibogaine-analogue treated groups. Decreased tail flick latency in acute pain was significantly reversed in iboga derivative treated group (**35-40% in C1, C3**). Ibogaine analogues intervention significantly altered the restricted locomotor activity, anxiogenic behaviour in pain (**3.5-4.5x**). Post sacrifice hind paw Substance P, COX-2, p65 nuclear translocation confirmed the inflammatory pain model. Serum IL-6 & TNF-α level were significantly decreased in **C1** treated group **(25% & 30%)**. Pain induced downregulation of GABA and Dopamine **(23% & 13%)** were upregulated in compound treated groups **(33% & 14% in C1)** whereas, elevated SP and Glutamate levels were ameliorated. Fall in BDNF in acute pain was reversed by iboga-analogues whereas, GDNF elevation was further exaggerated as a survival que to the formalin induced noxious stimuli.

Conclusion

The novel Iboga derivatives particularly iboga-alcohol executed effective antinociceptive action and prevented neuroinflammation. The present evidence-based work serves as strong clinical drug development clues.

B 06-52

Release site-based plasticity on millisecond and minute timescales mediated by Unc13A regulatory domains

M. Jusyte[1], N. Blaum[2], M. M.M. Berns[2], J. R.L. Kobbersmed[3], M. A. Böhme[1], **A. M. Walter**[1,2]

[1] Leibniz Forschungsinstitut für Molekulare Pharmakologie, Molecular and Theoretical Neuroscience, Berlin, Germany

[2] University of Copenhagen, Faculty of Health Sciences, Department of Neuroscience, Copenhagen, Denmark

[3] University of Copenhagen, Department of Mathematical Sciences, Copenhagen, Denmark

This work was supported by grants from the Deutsche Forschungsgemeinschaft to A.M.W. (Emmy Noether Programme, Project Number 261020751 and the TRR 186, Project Number 278001972) and the Novo Nordisk Foundation (Young Investigator Award NNF19OC0056047 to A.M.W.).

Introduction

Chemical synaptic transmission relies on the action potential (AP) induced fusion of neurotransmitter containing vesicles at presynaptic release sites and on transmitter detection by postsynaptic receptors. Synaptic plasticity, the change of this transmission, forms the basis of temporal processing, stable information flow, and information storage. The number of synaptic vesicles exceeds that of the release sites by several orders of magnitude, making the sites gatekeepers of synaptic transmission and prime plasticity targets, but whether this is the case and by which mechanisms this may be achieved is largely unknown. The evolutionarily conserved protein Unc13A determines release sites and its local levels change for long-term plasticity. However, on shorter timescales presynaptic plasticity is realized without detectable changes in Unc13A levels, raising the question whether and how available Unc13A undergoes activity-dependent switching to plastically adapt release site participation.

Methods

We here use mathematical modelling and experimental analysis of the *Drosophila melanogaster* neuromuscular junction to explore the contribution of acute Unc13A regulation to release site-based plasticity and its relevance for temporal coding and homeostasis. By combining genetic and pharmacological manipulation with electrophysiology and super-resolution microscopy we find a pivotal role of Unc13A regulatory domains for synaptic plasticity on a timescale of milliseconds and minutes.

Results

Mutation of the conserved Calmodulin binding domain revealed its relevance in Ca^{2+}-dependent release site population, millisecond short-term facilitation, and presynaptic homeostatic potentiation of transmitter release to compensate reduced postsynaptic transmitter sensitivity within minutes. Our data are consistent with impaired plasticity being causing by “maxing out” release site participation and super-resolution imaging revealed a slight redistribution of the catalytically active MUN domain to the plasma membrane which may be responsible for this. Acute activation of the Unc13A regulatory C1 domain by phorbol esters elicited similar effects on wildtype synapse which were occluded by the mutation of the Calmodulin binding domain, indicating that either domain induces a binary release site switch.

Conclusion

Thus, our findings indicate that Unc13A regulatory domains are tuned to integrate a multitude of signals on various timescale to switch release site participation for synaptic plasticity.

B 06-53

Identification of a new secreted Protein 1 (SEP1) specific for ASIC1

S. J. Kuspiel, S. Gründer, D. Wiemuth

RWTH Aachen, Institute of Physiology, Aachen, Germany

Acid-sensing ion channel 1 (ASIC1) is an ionotropic receptor directly activated by extracellular protons. It is a member of the Deg/ENaC family of ion channels and highly abundant in the CNS. ASIC1 plays a role in various physiological and pathophysiological processes e.g. synaptic transmission, long-term potentiation and stroke. ASIC1 is well characterized, the identity and role of possible modulatory binding partners, however. remains elusive. In a recent Knock-out (KO)-controlled proteomics screen we identified possible binding partners, one being highly specific for ASIC1: Secreted Protein 1 (SEP1). We verified direct interaction between SEP1 and ASIC1a using co-immunoprecipitation. Interestingly SEP1 strongly increased current density (4-5 fold, $p<0.001$) in heterologous expression systems without changing the biophysical properties of ASIC1a. We show that SEP1 is secreted and therefore most likely interacts with the extracellular domain of ASIC1a. The specific site of interaction and the mechanism underlying the effect of SEP1 on ASIC1 remain unclear. Currently, we investigate the role of SEP1 in neurons. We conclude that SEP1 may be important in various physiological and pathophysiological processes related to ASIC1a.

B 06-55

Hyposalivation in Streptozotocin-Induced Diabetes: Role of Cholinergic System

O. O. Asafa, J. I. Abeje, B. Bolarinwa, S.-T. T. Shittu, T. J. Lasisi

University of Ibadan, Department of Physiology/ College of Medicine, Ibadan, Nigeria

Introduction

The association between diabetes mellitus and hyposalivation has been well documented. . However, there is a paucity of data on the activity of the cholinergic system in diabetes-induced hyposalivation. This current research aimed to investigate one of the probable underlying mechanisms of diabetes-induced salivary hypofunction in male Wistar rats.

Methods
Institutional Ethical committee guidelines were adhered to. Two weeks after acclimatization, a total of thirty-two (32) male adult Wistar rats (180-250 g) was randomly divided into control (C) and diabetic (D) groups, followed by a subdivision into two equal subgroups (n = 8/subgroup) based on the number of weeks [one (C1, D1) and two (C2, D2) weeks]. Diabetes was induced using a single intraperitoneal dose of streptozotocin (60 mg/kg). Following the confirmation of diabetes, rats were euthanized using ketamine (75 mg/kg, i.p.) and xylazine (0.5 mg/kg, i.m.), followed by the collection of stimulated saliva (using pilocarpine, 10 mg/kg, i.p.) for 10 minutes. Biochemical analysis of the saliva and gland samples was done using standard methods. Histological evaluation of the salivary glands was done using the Phosphotungstic Acid Iron Hematoxylin Special Staining Method (PTAH). Data were presented as mean ± SEM and analyzed using student t-test statistic at p less than 0.05.
Results
There was a significant reduction in the body weight and submandibular glandular weight of the diabetic groups compared with their controls in the first- and two-week periods. The fasting blood sugar levels were significantly higher in the diabetic groups compared with their controls in the first- and two-weeks periods. There was a significant decrease in the salivary flow rate of the diabetic groups compared with their controls. Similarly, there was a significant decrease in the salivary total protein levels of the diabetic groups compared with their controls. However, the salivary lag time was significantly higher in the diabetic groups compared with their controls. There was a significant reduction in the levels of salivary gland acetylcholine in the diabetic groups compared with their controls. Similarly, levels of submandibular total protein and nitric oxide were significantly lower in the diabetic groups compared with their controls. There were no significant differences in the submandibular gland acetylcholinesterase, Na+/K+-ATPase and calcium levels. Histological examination of the glands showed that the density of the myoepithelial cells was significantly lower in the diabetic groups compared with the controls.
Conclusion
These findings showed that the diabetes-induced salivary hyposecretion may be mediated via suppression of acetylcholine production, nitric oxide downregulation, myoepithelial cells repression and total protein reduction in the submandibular salivary gland.

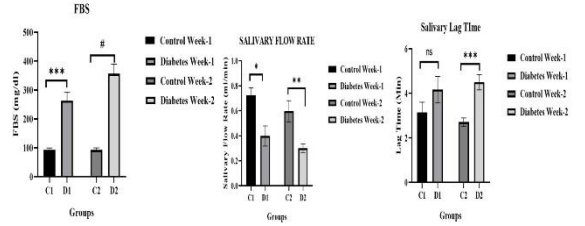

Figure 1
Effects of Streptozotocin-induced diabetes on Fasting Blood Glucose, Salivary Flow Rate and Salivary Lag Time

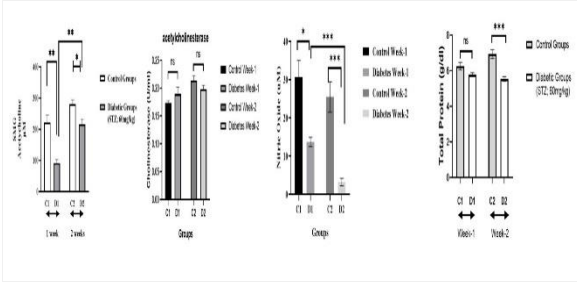

Figure 2
Effects of Streptozotocin-induced diabetes on Submandibular gland Acetycholine, Acetylcholinesterase, Nitric Oxide and Total Protein

---

B 06-56
Secondarybile acids suppressed colonic secretion of the pro-inflammatory cytokine, interleukin-6 in Sprague Dawley rats.
Q. Xiao[1,2], D. O. Malley[1,2]
[1] *University College Cork, Physiology, Cork, Ireland*
[2] *University College Cork, APC Microbiome Ireland, Cork, Ireland*

Dervla O' Malley designed the research study and review the abstract, Qiao Xiao performed the research, analyzed the data, and write the abstract.

Introduction
Cross-barrier signalling from molecules in the intestinal lumen can impact on intestinal secreto-motor activity and gut-to-brain signalling. In addition to facilitating lipid digestion and absorption, hepatic bile acids (BAs) also act as signalling molecules, where their bioactivity is determined by their conjugation status and whether or not they have been microbially modified. The aim of this study was to explore the physiological effects of primary and secondary BAs on colonic function with a focus on the pro-inflammatory cytokine, interleukin-6 (IL-6) and incretin hormone, Glucagon-like peptide-1 (GLP-1).
Methods
Fluorescent immunolabeling was used to investigate expression of G protein-coupled bile acid receptor 1 (GPBAR1, also called TGR5) and IL-6 receptors in colonic tissue from healthy Sprague Dawley rats. The pro-secretory effects of primary and secondary BAs were assessed by measuring basolateral secretion of IL-6 and GLP-1 using an enzyme-linked immunosorbent assay (ELISA). Calcium imaging was used to assess the neurostimulatory effects of primary and secondary BAs on submucosal neurons.
Results
TGR5, GLP-1 and IL-6 receptors are expressed on colonic submucosal neurons. However, exposure of submucosal neurons to both primary and secondary bile acids had no direct stimulatory actions in calcium imaging studies. Moreover, mucosal secretion of GLP-1 was not modified by primary or secondary BAs. Interestingly, secondary (CDCA, LCA, and TLCA) but not primary BAs (CA and DCA) inhibited colonic basolateral secretion of IL-6, which has neurostimulatory actions on sub-mucosal neurons.
Conclusion

BAs do not directly stimulate submucosal neurons, nor do they appear to stimulate mucosal L-cells. However, consistent with previously reported inhibitory actions of BAs in the gut, unconjugated and conjugated secondary BAs inhibited basal colonic secretion of IL-6 when applied to the mucosal side. As IL-6 has neurostimulatory actions on submucosal neurons, this could indirectly modify colonic absorpto-secretory function.

References
[1] Keating N, Mroz MS, Scharl MM, Marsh C, Ferguson G, Hofmann AF, Keely SJ. Physiological concentrations of bile acids down-regulate agonist induced secretion in colonic epithelial cells. J Cell Mol Med. 2009 Aug;13(8B):2293-2303.
[2] Duboc H, Tolstanova G, Yuan PQ, Wu V, Kaji I, Biraud M, Akiba Y, Kaunitz J, Million M, Tache Y, Larauche M. Reduction of epithelial secretion in male rat distal colonic mucosa by bile acid receptor TGR5 agonist, INT-777: role of submucosal neurons. Neurogastroenterol Motil. 2016 Nov;28(11):1663-1676.
[3] Lund ML, Egerod KL, Engelstoft MS, Dmytriyeva O, Theodorsson E, Patel BA, Schwartz TW. Enterochromaffin 5-HT cells - A major target for GLP-1 and gut microbial metabolites. Mol Metab. 2018 May;11:70-83.

B 06-57

The effect of secreted protein 1 (SEP1) on the assembly of ASIC1a

A. Wiesehahn[1,2], S. Gründer[1], G. Schmalzing[2], D. Wiemuth[1]
[1] *RWTH Aachen, Institute of Physiology, Aachen, Germany*
[2] *RWTH Aachen, Institute of Clinical Pharmacology, Aachen, Germany*

Acid-Sensing Ion Channel 1a (ASIC1a) belongs to the degenerin/epithelial Na+ channel superfamily and is expressed in the mammalian nervous system. Activated by local extracellular acidification, ASIC1a plays an important role in synaptic transmission, brain ischemia and inflammation. We identified the potential binding partner (SEP1), which modifies the function of ASIC1a through interaction. By denaturating and native polyacrylamide gel electrophoresis (PAGE), we further investigated the effect of SEP1 on ASIC1a. For this, ASIC1a and SEP1 were expressed in HEK ASIC1 knock-out cells, purified and resolved by SDS-PAGE and high resolution clear native PAGE. We found that SEP1 promoted the assembly of ASIC1a into its trimeric state. This effect seems to be specific to ASIC1a, as it was not observed for the other ASIC subunits. Taken together, our results suggest a role of SEP1 in ASIC1a assembly.

B 06-58

Noradrenergic Regulation of Aerobic Glycolysis and Lipid Droplet Metabolism in Astrocytes

A. Horvat[1,2], T. Smolič[1], P. Tavčar Verdev[1], M. Kreft[3,2], R. Zorec[1,2], **N. Vardjan**[1,2]
[1] *University of Ljubljana, Faculty of Medicine, Institute of Pathophysiology, Laboratory of Neuroendocrinology – Molecular Cell Physiology, Ljubljana, Slovenia*
[2] *Celica Biomedical, Laboratory of Cell Engineering, Ljubljana, Slovenia*
[3] *University of Ljubljana, Biotechnical Faculty, Department of Biology, Ljubljana, Slovenia*

FLII12Pglu-700μδ6 was a gift from Wolf Frommer (Addgene plasmid # 17866; http://n2t.net/addgene:17866; RRID:Addgene_17866) and Laconic was a gift from Luis Felipe Barros (Addgene plasmid # 44238; http://n2t.net/addgene:44238; RRID:Addgene_44238). The authors' work was supported by grants from the Slovenian Research Agency (P3-0310, J3-2523, J3-9266, J3-9255) and COST Action CA18133 (ERNEST).

Introduction

Astrocytes, a subtype of neuroglial cells with key homeostatic brain functions, are ideally anatomically positioned between the blood vessels and neurons to mediate the delivery of D-glucose from the circulation to the energy-consuming neuronal networks. Many studies suggest that neurons rely heavily on the availability of metabolites, such as L-lactate, derived from astrocytes. Astroglial produce L-lactate in aerobic glycolysis, a process during which D-glucose despite the normal oxygen levels is converted to L-lactate, which can act as a brain fuel and/or signal. Aerobic glycolysis in astrocytes is regulated by activation of plasma membrane receptors, such as adrenergic receptors (ARs). Activation of AR increases in astrocytes intracellular Ca^{2+} and cAMP signals, however the extent to which the Ca^{2+} and cAMP signals regulate astroglial glucose mobilisation, aerobic glycolysis and lipid metabolism is not well understood.

Methods

To determine the role of intracellular Ca^{2+} and cAMP in the regulation of astroglial free glucose mobilization and aerobic glycolysis, we performed real-time fluorescence microscopy using glucose and lactate nanosensors and measured the cytosolic concentration of free D-glucose ($[glc]_i$) and L-lactate ($[lac]_i$) in isolated cortical astrocytes upon α-/β-AR activation. We also determin the effect of noradernergic activation on lipid droplet formation by labeling lipid droplets with Nile Red dye.

Results

We have showed by using AR agonists to selectively stimulate intracellular Ca^{2+} or cAMP signals that intracellular Ca^{2+}, but not cAMP, triggers an increase in intracellular $[glc]_i$ and $[lac]_i$ in astrocytes, suggesting Ca^{2+}-mediated glucose uptake and aerobic glycolysis in astrocytes. Astrocytes are glycogen storing cells in the brain. When the glycogen shunt, a process of glycogen remodelling, was inhibited, the increases in $[glc]_i$ and $[lac]_i$ were reduced by ~65 % and ~30 %, respectively, indicating that at least ~30 % of the D-glucose utilization is linked to the glycogen remodelling and aerobic glycolysis. Moreover, an increase in lipid droplet accumulation, typically seen in brain pathologies, was observed in astrocytes upon chronic exposure to endogenous AR agonist noradrenaline, the effects of which were mediated by activation of β- and $α_2$-ARs, but not $α_1$-ARs, implying a role of cAMP, but not Ca^{2+} signals, in the adrenergic regulation of lipid metabolism in astrocytes.

Conclusion

Taken together, an increase in the intracellular Ca^{2+} upon adrenergic activation is the prime mechanism of augmented aerobic glycolysis in astrocytes, while cAMP has only a moderate role, but importantly contributes to regulation of lipid metabolism in astrocytes. The results provide novel information on the signals regulating brain metabolism and open new avenues to explore whether astroglial Ca^{2+} or cAMP signals are dysregulated and contribute to neuropathologies with impaired brain metabolism.

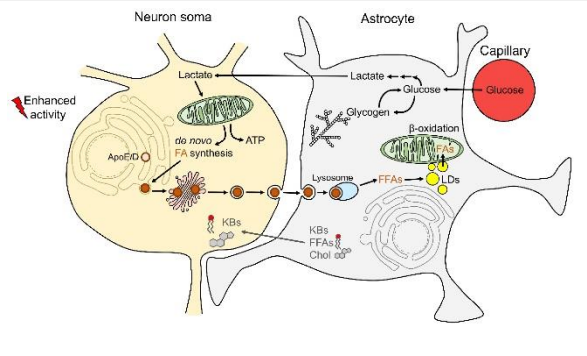

Astrocyte–neuron coupling of L-lactate and lipid metabolism.

References

[1] Horvat A, Muhič M, Smolič T, Begić E, Zorec R, Kreft M, Vardjan N 2021, 'Ca^{2+} as the prime trigger of aerobic glycolysis in astrocytes', *Cell Calcium,* 95:102368.

[2] Smolič T, Tavčar P, Horvat A, Černe U, Halužan Vasle A, Tratnjek L, Kreft ME, Scholz N, Matis M, Petan T, Zorec R, Vardjan N 2021, 'Astrocytes in stress accumulate lipid droplets', *Glia,* 69(6):1540-1562.

B 06-59

Investigation of the Effects of Vitamin E and Selenium-yeast on Cognitive Performance of Wistar rats subject to Prenatal Oxidative Stress

O. M. Ochayi[1,2], B. U. Anyaehie[2], E. Iyare[2]

[1] *Baze University, Abuja/University of Nigeria, Enugu, Department of Physiology, Federal Capital Territory, Nigeria*

[2] *University of Nigeria, Enugu, Department of Physiology, Enugu, Nigeria*

Introduction

Stress during pregnancy is termed prenatal stress (PS), and this stress has adverse effects on dams and pups: PS impairs cognition via the oxidative stress pathway. Animals treated with vitamin E or selenium-yeast showed better tolerance to immobilization stress. Several gaps have been observed in previous studies, ranging from the stress models used, for cognitive assessments, and the absence of effective therapeutic targets to mitigate the adverse effects of prenatal oxidative stress.

Methods

Thirty-five virgin female Wistar rats were mated with males counterpart, and pregnancy was confirmed by the presence of a vagina plug; the first day of pregnancy was tagged day zero (D0), and the rats were randomly divided on day 3 of pregnancy into seven groups (n=5), non-stressed; group 1 (negative control, given 1 mL/kg of distilled water) and six stress groups exposed to 4 h (09:00 – 01:00) of noise using white noise generator connected to a 15 Watt speaker emitting sound at 100 dB placed 30 cm above animal cages for 15 days; group 2 (positive control, given 1 mL/kg/

day of distilled water, orally), group 3 vitamin E (200 mg/kg/day orally), group 4 selenium (0.05 mg/kg), group 5 yeast (50 mg/kg/day, orally), group 6 selenium-yeast (0.4 mg/kg, orally) and group 7 vitamin E (200 mg/kg/day) + selenium-yeast (0.4 mg/kg/day, orally). On pregnancy day 19 novel object recognition test (NORT) and Y-maze were used to evaluate the cognitive performance of the dams and pups on lactation day (LD) 21. The rats were anesthetized with ketamine at 60 mg/kg and sacrificed; tissues were harvested on LD 10 and LD22, blood serum was used for CORT assay and brain tissue for antioxidant enzymes markers, and hippocampus for immunohistochemical staining using GFAP-antibody. Data were expressed in mean (± SEM). And values of $p<0.05$ were considered to be statistically significant. The difference between the mean was ascertained using a one-way analysis of variance (ANOVA). Using Graph pad prism 8.0

Results

The mean CORT concentration significantly ($p< 0.05$) increases in group 2 compared with group 1 and antioxidant-treated groups of PD and pups. The mean discrimination index (DI) significantly ($p<0.05$) decreases in group 2 compared to group 1. However, the mean decrease in DI was attenuated in the antioxidants treated groups. The mean percentage alternation significantly ($p<0.05$) reduced in group 2 compared to group 1, this effect was attenuated in the antioxidants treated groups. The values for SOD, CAT, and GPx significantly ($p<0.05$) reduces and MDA increased in group 2 compared to group 1, Photomicrograph reveals an increase in the proportion of astrocytes activation in group 2 compared with group 1, and the antioxidant groups of the dams and pups.

Conclusion

Prenatal oxidative stress induces cognitive impairment probably as a result of astrocyte activation in PD, and this effect can be reversed with the pre-administration of antioxidants.

References

[1] Azimi, R, Nolan, JM, Prado-Cabrero, A, Roche, W, Coen, R, Power, T, & Mulcahy, R 2022, Omega-3 fatty acid, carotenoid, and vitamin E supplementation improve working memory in older adults: A randomized clinical trial, *Clinical Nutrition*, *41*(2), 405-414.

[2] GNBao, AM, & Swaab, DF 2019, The human hypothalamus in mood disorders: the HPA axis in the center, *IBRO Reports*, *6*, 45-53., Lastname, GN YYYY, 'Article', *Journal*, Edition, Page, Place of publication: publishers

---

B 06-60

Factors influencing the urinary metabolomic analysis in children with autism spectrum disorders

G. Repiska[1], D. Olesova[2], A. Kovac[2], K. Babinska[1], H. Celusakova[1], D. Ostatnikova[1]

[1] *Comenius University in Bratislava, Faculty of Medicine, Institute of Physiology, Bratislava, Slovakia*

[2] *Slovak Academy of Sciences, Institute of Neuroimmunology, Bratislava, Slovakia*

The study was supported by Slovak Research and Development Agency (APVV-15-0045, APVV 15-0085, APVV-20-0070, APVV-20-0139) and Ministry of Education, Science, Research and Sport of the Slovak Republic (VEGA 1/0068/21).

Introduction

The current research in the autism field suggests that the urinary metabolomic analysis could be a

useful tool in clarification of etiopathogenesis and searching for the potential biomarkers for autism spectrum disorders (ASD). ASD is a group of heterogeneous neurodevelopmental disorders, characterized by impairments in communication, reciprocal social interaction and restricted, repetitive behaviors or interests. The multifactorial nature of ASD is one of the reasons there is still no biological marker identified to confirm the diagnosis of ASD. In our study, we aimed to analyze urine samples of children with ASD and controls by targeted metabolomics, verify our results from the pilot study, and test the factors influencing the final results of the analysis.

Methods

The first–morning urines of 70 children with ASD and 60 typically developing controls were analyzed in two sets by quantitative LC–MS/MS metabolomic analysis performed by combining direct injection mass spectrometry with a reverse-phase LC–MS/MS. Data were statistically evaluated and visualized using web-based platform Metaboanalyst v5.0.

Results

In the first set of samples included in our pilot study, we found differences in 3 metabolites – 2 acylcarnitines and glycerophospholipid. However, after subsequent analysis with the second set of samples, we did not confirm previously found differences between children with ASD and healthy developing children. In addition, we were not able to detect all of 185 analyzed analytes in all samples. Thus, we assumed that different factors could influence the results of urinary metabolomics, such as pre-analytical factors – processing and storage of urine samples, but also the inclusion criteria for participant selection – age, gender, behavioral characteristics of ASD and control samples. Our results showed that there are no significant differences between samples stored at -20 ˚C compared to – 80 ˚C but the repeated freezing-thaw cycle may influence the results of urinary metabolomics. On the other hand, the selection of homogenous group of ASD patients in terms of severity of autism, behavioral characteristics, age is crucial in identification of potential biomarkers of ASD. At the same time, gender has no significant effect on the results analysis in our group of samples.

Conclusion

Our results indicate that the urinary metabolomic may show an ASD-specific metabolic pattern and has great potential in ASD research. However, it is necessary to consider the factors influencing the results and examine in o more detail the diagnostic sensitivity and specificity of the markers. Last but not at least, it is necessary to focus also on their relationships with behavioral parameters and common comorbidities such as gastrointestinal symptoms.

B 06-61

Leveraging the Dynamic Multi-site Serotonin/Histamine Relationship as an Indicator for a Human Model of Depression

B. Baumberger, P. Hashemi
Imperial College London, Department of Bioengineering, London, UK

la Caixa "Foundation" (LCF/BQ/EU21/11890065)

Introduction

Histamine is infamous for mediating peripheral inflammation; but histamine is also found in high concentrations in the brain. While it's been known for some time that histamine is a signaling molecule in the brain, histamine dynamics are very difficult to measure and thus several fundamental aspects of the mechanisms that control the extracellular and modulatory behavior of this messenger remain undefined.

Methods

In this work we undertake the first in-depth characterization of *in vivo* histamine dynamics in real time using fast-scan cyclic voltammetry at carbon fiber microelectrodes. We measure electrically evoked histamine in the mouse hypothalamus and find that histamine release is sensitive to pharmacological manipulation at the level of synthesis, packaging, autoreceptor control of release, and metabolism.

Results

We find two breakthrough aspects of histamine modulation. First, there are differences in H_3 receptor regulation of histamine between sexes showing that histamine release in female mice is much more tightly regulated than in male mice under H_3 or inflammatory drug challenge. We hypothesize that this finding may contribute to hormone-mediated neuroprotection mechanisms in female mice. Second, we find that a high dose of a commonly available antihistamine, the H_1 receptor inverse agonist diphenhydramine, rapidly decreases serotonin levels.

Due to the inaccessibility of the human brain, there is a need to find neuroinflammation indicators in the body to characterize the histaminergic system in humans. It has been found that systemic inflammation induces neuroinflammation, but there is a lack of knowledge on the physiological mechanisms that underlie this process.

Conclusion

Therefore, we have designed and are characterizing a skin probe that measures histamine in the reticular dermis to understand how histamine levels change in response to pharmacological distress. By developing a method to measure histamine levels in the skin and comparing the measurements to brain data, we hope to describe how systemic inflammation induces neuroinflammation.

References

[1] Bendorius, M., Po, C., Muller, S. & Jeltsch-David, H. From systemic inflammation to neuroinflammation: The case of neurolupus. *Int. J. Mol. Sci.***19**, (2018).

[2] Al Sulaiman, D. *et al.* Hydrogel-Coated Microneedle Arrays for Minimally Invasive Sampling and Sensing of Specific Circulating Nucleic Acids from Skin Interstitial Fluid. *ACS Nano***13**, 9620–9628 (2019).

[3] Hersey, M., Hashemi, P. & Reagan, L. P. Integrating the monoamine and cytokine hypotheses of depression: Is histamine the missing link? *Eur. J. Neurosci.* 1–17 (2021) doi:10.1111/ejn.15392.

[4] Mandal, A. *et al.* Cell and fluid sampling microneedle patches for monitoring skin-resident immunity. *Sci. Transl. Med.***10**, (2018).

[5] Cabrera-Pastor, A. *et al.* Peripheral inflammation induces neuroinflammation that alters neurotransmission and cognitive and motor function in hepatic encephalopathy: Underlying mechanisms and therapeutic implications. *Acta Physiol.***226**, (2019).

B 06-62

Long-term Ingestion of High Fructose Corn Syrup Decreased Male Rats' Sexual Motivation

G. Zorlu[1], A. Ozgen[2], G. Ozbeg[2], F. Tan[2], Z.D. Oz[2], M.R. Ozdede[2], G.G. Avcu[1], **I. Serhatlioglu**[1]

[1] *Firat University, Faculty of Medicine, Department of Biophysics, Elazig, Turkey*

[2] *Firat University, Faculty of Medicine, Department of Physiology, Elazig, Turkey*

This study was supported by TUBITAK (project#121S092).

Introduction

The consumption of high fructose corn syrup (HFCS) has increased considerably during the past years and is partially responsible for the high incidence of metabolic diseases. The lifestyle during postnatal development can result in altered metabolic programming, thereby impairing the sexual motivation during adulthood. Therefore, the aim of this study was to evaluate the effects of HFCS feeding on male rats sexual motivation.

Methods

Twenty male Sprague-Dawley rats that have sexual experience and weighing between 200 and 250 grams were randomly divided into two groups: the control group (n=10) and the HFCS group (n=10). The control group received drinking water in addition to standard feed, whereas the HFCS group received a 15 % fructose solution (~15 % w/v) instead of drinking water. After eight weeks of HFCS feeding, all rats were subjected to a sexual incentive motivation test. As seen in the figure (fig), sexual motivation test apparatus consists of three parts and measures 100x50x40 cm. Each male test rat was allowed 20 minutes to investigate the three chambers in the first arena after being placed in the central chamber. Scores were recorded for the first pass latency, the time spent in the end zone, and the time spent in the approach zone. The student's t-test was used for statistical analysis.

Results

The rats in the HFCS group had a significant increase in the time spent by the male rat compared to the control group in the Approach zone ($p<0.05$). There was no statistically significant difference in the time spent in the End Zone and the first pass latency. Rats in the HFCS group compared to the control group; It was observed that the female rats significantly decreased the time spent in the Approach zone and End Zone ($p<0.05$).

Conclusion

Long-term consumption of HFCS reduces sexual motivation in adult male rats, according to research. The amount of time spent with the male animal used as a social stimulus increased, however. Our findings suggest that long-term HFCS consumption may result in decreased heterosexual motivation.

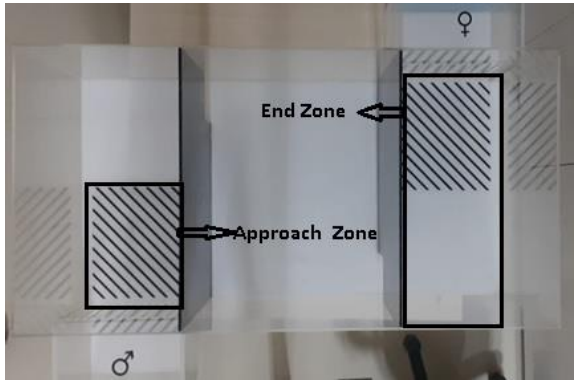

Fig.
Sexual motivation test apparatus

B 06-63

Analysis of gene expression changes in the cerebellum after pallidal deep brain stimulation in the animal model of the dystonic dt^{sz} mutant hamster

A. Bornemann[1], D. Franz[1], N. Engel[1], M. Heerdegen[1], F. Santana Kragelund[1], A. Lüttig[2], S. Perl[2], F. V. Plocksties[3], A. Richter[2], R. Köhling[1]

[1] *University Medical Center Rostock, Oscar Langendorff Institute of Physiology, Rostock, Germany*

[2] *University of Leipzig, Veterinary Faculty, Institute of Pharmacology, Pharmacy and Toxicology, Leipzig, Germany*

[3] *University Rostock, Institute of Applied Microelectronics and Computer Engineering, Rostock, Germany*

This study is supported by the German Research Foundation (DFG) within the Collaborative Research Centre (SFB 1270/1 ELAINE 299150580). We also thank Tina Sellmann for the support at the surgeries.

Abnormal functionality in the basal ganglia plays a considerable role in the pathophysiology of dystonia. However, recent studies considered dystonia more and more a network disorder comprising the cortico-basal ganglia-thalamo-cortical and cerebellar-thalamo-cortical networks (Jinnah et al., 2017). Current theories tend to examine the spatial and temporal coding of activity patterns within the motor circuitry (Gernert et al., 2002; Neumann et al., 2017; Silberstein et al., 2003). Additional to the basal ganglia, the cerebellum is increasingly coming into focus to describe a model for the pathogenesis of dystonia (Prudente et al., 2014). In animal studies, for example, it has been shown that abnormal excitatory activity resulted in generalized dystonia (Pizoli et al., 2002).

For the presented study, we analyzed the cerebellar gene expression in the animal model of the dt^{sz} mutant hamster, which represents the motor phenotype of paroxysmal generalized dystonia

(Richter and Richter, 2014). We designed amplification primers of genes already published to be critical in the cerebellar function. The following table summarizes the investigated genes:

Gene	Name	Function
Grik2	Glutamate ionotropic kainate receptor, subunit 2 (beta 2)	Glutamatergic signaling
Grik5	Glutamate ionotropic kainate receptor, subunit 5 (gamma 2)	Glutamatergic signaling
Gria2	Glutamate ionotropic AMPA receptor, subunit 2	Glutamatergic signaling
Scn8a	Voltage-gated sodium channel, subunit alpha 8	Firing pattern of the Purkinje neurons
Gabra6	$GABA_A$ receptor, subunit alpha 6	GABAergic signaling
Adrb2	Beta 2 – adrenergic receptor	Catecholamine signaling
Gad1	Glutamate decarboxylase 1	GABA synthesis

We were also interested in the effect of the pallidal deep brain stimulation (DBS), effective treatment of generalized or cervical dystonia, on the gene expression. The dt^{sz} mutant hamster was continuously stimulated with a 50 µA current pulse at 130 Hz for 11 days. To facilitate unrestricted movement of the animals with continuous stimulation, we utilized the software defined implantable modular platform, STELLA (Plocksties et al., 2021), implanted in the hamsters' flank. In stereotactic surgery, bipolar electrodes were implanted bilaterally in the entopeduncular nucleus (homolog to the globus pallidus internus in humans) under deep isoflurane anaesthesia. For comparing the gene expression of stimulated and non-stimulated dt^{sz} mutant hamsters, we removed the cerebellum directly after the DBS turned off or after the appropriate period. After tissue processing, gene expression was analysed with the quantitative RT-PCR. On the one hand, our results indicate the effect of pallidal DBS on the cerebellar gene expression and, on the other hand, give information on the pathophysiology of dystonia.

References

[1] Gernert, M., Bennay, M., Fedrowitz, M., Rehders, J.H., and Richter, A. (2002). Altered discharge pattern of basal ganglia output neurons in an animal model of idiopathic dystonia. J. Neurosci. *22*, 7244–7253.

[2] Jinnah, H.A., Neychev, V., and Hess, E.J. (2017). The Anatomical Basis for Dystonia: The Motor Network Model. Tremor Other Hyperkinet. Mov. (N. Y). *7*, 506.

[3] Pizoli, C.E., Jinnah, H.A., Billingsley, M.L., and Hess, E.J. (2002). Abnormal cerebellar signaling induces dystonia in mice. J. Neurosci. *22*, 7825–7833.

[4] Plocksties, F., Kober, M., Niemann, C., Heller, J., Fauser, M., Nüssel, M., Uster, F., Franz, D., Zwar, M., and Lüttig, A. (2021). The software defined implantable modular platform (STELLA) for preclinical deep brain stimulation research in rodents. J. Neural Eng. *18*, 56032.

[5] Richter, F., and Richter, A. (2014). Genetic animal models of dystonia: Common features and diversities. Prog. Neurobiol. *121*, 91–113.

B 06-64

Possible Decreased Autophagy and Increased Mitophagy Process in Sleep Deprivation

A.K. Salihoğlu

Karadeniz Technical University, Department of Physiology, Faculty of Medicine, Trabzon, Turkey

I would like to express my gratitude to my dear supervisor, Prof. Dr. Ahmet AYAR, who has never withheld his scientific and spiritual support.

Introduction

Sleep deprivation (SD) is the condition of not having adequate duration and/or quality of sleep to support good alertness and performance in the daytime. The pathogenesis of SD is not clarified yet and there is no specific treatment. In addition to clinical studies, recent evidence indicates hope from *in silico* analysis. This study aimed to detect possible pathophysiological factors in SD by examining the expression levels of genes, using bioinformatics tools.

Methods

Gene expression levels in the GSE98582 dataset obtained from Gene Expression Omnibus (GEO) database were re-analyzed in the R program for this research. In the dataset, 343 SD and 213 control DNA samples derived from human blood were recruited. Gene set enrichment analyses were performed in Gene Ontology (GO) and ENRICHR tools. Based on Benjamini-Hochberg correction, adjusted *p*-values <0.05 were accepted as significant.

Results

Gene expression levels indicated that autophagy-related proteins-2B,7,13 (ATG 2B,7.13), ectopic P-granules autophagy protein-5 (EPG5), lysosomal associated membrane protein-2 (LAMP2), mechanistic target of rapamycin (MTOR), phosphatidylinositol 3-kinase catalytic subunit type-3 (PIK3C3) [responsible for autophagy] were down-regulated ($p<0.05$); and mitofusin-2 (MFN2), PTEN induced putative kinase-1 (PINK1), microtubule-associated protein-1 light chain-3 beta (MAP1LC3B), optineurin (OPTN), ubiquitin A-52 (UBA52), GABA type-A receptor-associated protein (GABARAP) [responsible for mitophagy] were up-regulated ($p<0.05$) in SD group, compared with the control group.

Conclusion

This study indicates down-regulation in autophagic process and on the contrary, up-regulation in mitophagic process in SD patients. This interesting contradistinction, implicates impaired autophagy and mitophagy, may play a role in the basis of cellular pathophysiology of SD.

B 06-65

Mechanical pain perception characteristics during different satiety levels

T. Gvasalia, I. Kvatchadze

Tbilisi State Medical University, Department of Physiology, Tbilisi, Georgia

Tbilisi State Medical University

Introduction

According to the definition of the International Association for the Study of Pain, pain is subjective and emotional experience related to tissue damage (Treede, 2018, Wiesenfeld-Hallin, 2005). Individual pain perception depends on multiple factors, including metabolic status of the body (Zmarzty et al., 1997).

Our study aims to assess experimental pain induced by irritation during different satiety levels.

Methods

The sample of the study was comprised of volunteer male and female students aged 18-25 (n=50=25+25).). The main selection criterium for participants was their health state; Prior to the start of the study, participants were given information about their rights – they could refuse taking part in the study at any stage. Accordingly, written informed consents were obtained from every participant. All procedures and protocol of the study are approved by Tbilisi State Medical University Biomedical Research Committee. The study was conducted in compliance with all requirements.

Mechanical pain sensitivity was evaluated using computerized algometer - *AlgoMed (Medoc, Ltd, Ramat Yishai, Israel),* delivering mechanical stimuli to the participants; Meanwhile, mechanical pressure threshold, mechanical pain threshold and pain tolerance threshold were determined. A flat probe of algometer was applied to the participant's palm delivering increasing and quantifiable pressure at a rate of 30kPa/sec. The quantitative assessment of the parameters was automatically performed by pressing the remote control button. To prevent sensibilization of skin, sequential stimuli were given with 30sec intervals. For minimazing adaptation, after each episode, probe was displaced.

The experiment was carried during physiologic starvation and 30 minutes after getting meal- in primary, sensory-motor satiety.The data was analysed with Student criteria,statistical reliability was $P<0.05$.

Results

According to data, mechanical pain threshold is higher in primary satiety,than in starvation.During analysis of mechanical pain threshold,primary satiety theshold equaled 350±2,6 kPa and starvation threshold equaled- 297±1,98 kPa.As for individual resistance threshold to mechanical pain,measured value during primary satiety made up 610±3,9 kPa and during physiological starvation 459±2,9kPa (Table).

Conclusion

For further studies it is recommended to analyse individual pain perception during metabolic satiety too.This correlation can be beneficial for managing pain and improving life quality in chronic patients.

References

[1] 1.Treede R.D. The International Association for study of Pain definition of pain: as valid in 2018 as in 1979, but in need of regularly updated foonotes. // Pain Reports, 2018

2.Wiesenfeld-Hallin Z. Sex differences in Pain Perception // Gender Medicine / Vol.2, No.3, 2005

3.Zmarzty SA, Wells AS, Read NW. The influence of food on pain perception in healthy human volunteers. PhysiolBehav. 1997 Jul;62(1):185-91

B 06-66

Evaluation of autonomic function in patients of achalasia diagnosed by high resolution manometry

A. A. Kokkuvayil[1], R. K. Netam[1], A. Roy[1], D.S. Chandran[1], A.K. Jaryal[1], G.K. Makharia[2], R. Parshad[3], K.K. Deepak[1]

[1] All India Institute of Medical Sciences, New Delhi, Department of Physiology, New Delhi, India

[2] All India Institute of Medical Sciences, New Delhi, Department of Gastroenterology and human nutrition, New Delhi, India

[3] All India Institute of Medical Sciences, New Delhi, Departments of Surgical disciplines, New Delhi, India

Departments of Physiology, Department of Surgical disciplines and Department of Gastroenterology and human nutrition of All India Institute of Medical Sciences, New Delhi, India

Introduction

Achalasia is a primary motility disorder of the esophagus characterised by loss of relaxation of lower esophageal sphincter and absence of peristalsis in the esophagus (1). The peristaltic relaxations and contractions are regulated by vagal fibres (2). The present study was designed to study the cardiovascular autonomic functions in patients diagnosed with achalasia.

Methods

This study is a case control study. 30 patients with clinical and radiological sign of achalasia were recruited from the Departments of Surgical disciplines and Gastroenterology and human nutrition. Both males and females were recruited. Subjects less than or equal to 60 years were recruited. A high resolution manometry was performed in patients with clinical and radiological features of achalasia to confirm the diagnosis. Parasympathetic reactivity and sympathetic reactivity were evaluated using-head up tilt test (HUT), deep breathing test (DBT), Valsalva manoeuvre (VM), hand grip test (HGT) and cold pressor test(CPT) and compared with those of 30 healthy controls obtained from laboratory historical data.

Results

We found that parameters for parasympathetic autonomic reactivity such as 30:15 ratio, Valsalva ratio and parameters for sympathetic autonomic reactivity change in diastolic blood pressure during HGT and CPT of achalasia patients were significantly lesser than healthy controls.

Conclusion

Parasympathetic and sympathetic autonomic reactivity of achalasia patients were lesser than healthy controls. Autonomic dysfunction is not restricted to the gastrointestinal tract and systemic or global autonomic dysfuction coud be present in achalasia patients.

References
[1] Vaezi MF, Pandolfino JE, Vela MF. ACG clinical guideline: diagnosis and management of achalasia. Am J Gastroenterol. 2013 Aug;108(8):1238–49
[2] Storr M, Geisler F, Neuhuber WL, Schusdziarra V, Allescher HD. Characterization of vagal input to the rat esophageal muscle. Auton Neurosci . 2001 ;91(1–2):1–9.

B 06-69

The visual perception of wetness: multisensory integration of visual and tactile stimuli varying in stain wetness, chroma and size.

C. Merrick[1], R. Rosati[2], D. Filingeri[3]
[1] *Loughborough University, THERMOSENSELAB, School of Design and Creative Arts, Loughborough, UK*
[2] *Procter and Gamble Service GmbH, Frankfurt am Taunus, Germany*
[3] *University of Southampton, THERMOSENSELAB, Skin Health Research Group, School of Health Science, Southampton, UK*

The present research was conducted in the context of an industry co-funded Ph.D. Loughborough University, The Engineering and Physical Sciences Research Council, and Procter and Gamble Service GmbH provided financial support.

Introduction

A multitude of sensory modalities are involved in humans' experience of wetness, yet we know little of how common haptic interactions are affected by the integration or absence of other sensory cues such as vision. Therefore, we aimed to quantify the effect of physical stain volume, chroma and size on the perception of wetness. An additional aim was to compare wetness perception under different sensory conditions, including visuotactile and visual only interactions.

Methods

Eighteen participants (10 female: 23.0 ± 3.9 years; 22.4 ± 2.1 kg/m^2 body mass index; 8 male: 21.4 ± 3.2 years; 22.4 ± 1.8 kg/m^2 body mass index) visually observed and / or used their index fingerpad to perform controlled dynamic interactions with stimuli varying in physical wetness (0, 2.16x10^{-4} or 3.45x10^{-4} ml mm^{-2}), stain chroma (clear, light, dark) and stain size (1150 or 5000 mm^2). After interaction participants rated wetness perception using a 100 mm visual analogue scale (very dry to very wet) and dichotomous choice paradigm (dry or wet).

Results

During visual only conditions the magnitude of wetness perception increased with physical wetness. Participants were only able to differentiate whether the stimuli was dry or wet, but could not accurately assess the magnitude of wetness in a visual only context. However, during visuotactile conditions the magnitude of physical wetness could also be distinguished, with wetness discrimination improving at lower and higher extremes of physical wetness level. Overall, there was a significant difference between the magnitude estimation of wetness in visual only compared to visuotactile conditions ($F_{1, 17}$ = 20.03, P < 0.001). In both visual only and visuotactile conditions greater stain chroma resulted in increased wetness perception ($F_{2,16}$ = 14.8, P < 0.001; $F_{2,34}$ = 27.5, P < 0.001). In contrast, stain size did not have a significant effect on wetness perception in either visual only ($F_{1, 17}$ = 0.952, P = 0.330) or visuotactile conditions ($F_{1, 17}$ = 3.09, P = 0.079).

Conclusion

The results show that certain visual aspects have an independent influence on wetness perception, as participants perceive wetness differently when interacting with different chromas of saline such that higher intensities result in greater wetness perception. However, there was no significant effect of stain size on wetness perception. While the presence of specific visual cues had an influence on wetness perception in this instance, tactile inputs significantly build on the perceptive abilities of visual only conditions such that visual dominance does not apply to these sensory integrations. This research has identified several factors involved in the visual perception of wetness, contributing to the knowledge of the overall multisensory network of human wetness perception. Findings are relevant for the design of products with wetness management properties and may be furthered in digital contexts such as virtual and augmented realities.

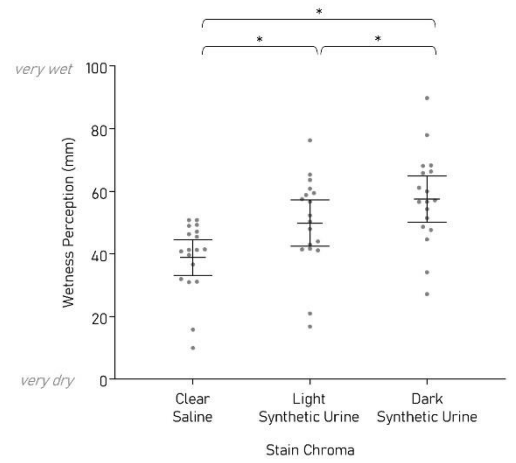

Wetness perception in visuotactile conditions across three different stain chromas.
$\bar{x}$ ± 95 % CIs (n = 18) wetness perception (mm) in visuotactile conditions collapsed over three different stain chromas with significantly different pairings indicated (*).

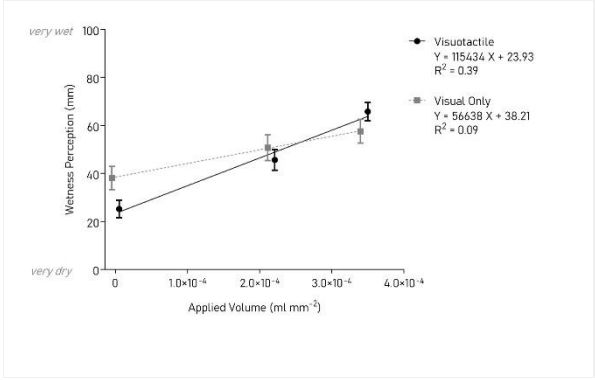

Wetness perception at three different wetness levels under visuotactile and visual only conditions. $\bar{x}$ ± 95 % CIs (n = 18) perceived wetness (mm) plotted at three wetness levels (ml mm^{-2}) under visuotactile and visual only sensory conditions with linear regression equations.

B 06-70

A crosstalk between the central and peripheral immune parameters in an optimized intracerebroventricular streptozotocin induced rat model

R. Ghosh, T. Ghosh

University of Calcutta, Physiology, kolkata, India

This research work was supported by the University Grant Commission - Major Research Project [F. No. 42-532/2013 (SR) dt. 22nd March, 2013]. Debajit Bhowmick [Nanoscience and Nanocentre, University of Calcutta] and Dr. Arijit Ghosh (post doc fellow in the Neurophysiology laboratory) are acknowledged for their assistances in some parts of the work.

Introduction

Induction of neuroinflammation is possible after intracerebroventricular(ICV) injection of streptozotocin(STZ) in experimental animals (Salkovic-Petrisic et al., 2013). This is a well-established procedure which ultimately results in dementia (Hoyer S, 2004). An optimization of the dose of STZ which exhibits pronounced repeatable neuroinflammatory changes is already reported (Ghosh et al., 2020). There is an extensive communication between the central and the systemic immune responses in neurodegeneration. Ongoing neurodegeneration and neuroinflammation leads to efflux of inflammatory mediators across the blood-brain barrier inducing systemic immune reactions and in turn myeloid or lymphocytic cells move into the central nervous system (Britschgi M and Wyss-Corray,2007). It has also been found that signals and immune molecules from AD brains of patients modulate peripheral immune responses. The peripheral immunological pattern is yet to be reported in ICV STZ rat model of dementia.

Methods

In the present study, 30 male albino rats were ICV injected with 3 mg of STZ per kg of bodyweight. Inflammatory markers i.e. TNF-α, IL-1β, ROS and nitrite were quantified in the hippocampus and serum at 3 weeks and 8 weeks. Rat TNF-Flex Set and BD Cytometric Bead Array rat soluble protein master buffer kit (BD Biosciences, USA) was used to assess TNF-α levels and the values was analysed in BD FACS verse instrument using FCAP Array software. Commercial rat IL-1β ELISA Kit (Ray Bio, Norcross, GA) was used for estimation of hippocampal IL-1β levels. ROS and nitrite levels were measured using spectrophotometric and spectroflurometric principles. Memory function was assessed by the radial arm maze test following STZ injection (Mizuno et al., 2000). The institutional animal ethical committee rules and regulations were strictly followed during the experimental procedures (IAEC/IV/Proposal/TKG-04/2015 dated 19.01.2015). All the rats were sacrificed under ether anaesthesia(inhalation) followed by decapitation.

Results

STZ treatment significantly ($p<0.05$) increased neuroinflammatory markers and decreased memory functions at 3 weeks and 8 weeks.The neuroinflammation was also reflectedin the serum inflammatory parameters which has indicated a crosstalk between the central and peripheral immune systems. However, marked changes werenot found between the 3 week and 8-week study. No significant results were obtained in both central and peripheral inflammatory markers in the two time points of the study.

Conclusion

Therefore, induction of neuroinflammation with streptozotocin at the dose of 3mg/kg was able to modulate the peripheral immune parameters significantly in a 3-week study.

References

[1] Britschgi M and Wyss-Corray T. Systemic and acquired immune responses in Alzheimer's disease International Review of Neurobiology.2007; 82:205-233.

[2] Ghosh, R., Sil, S., Gupta, P. *et al*. Optimization of intracerebroventricular streptozotocin dose for the induction of neuroinflammation and memory impairments in rats. *Metab Brain Dis*. 2020; 35: 1279–1286.

[3] Hoyer, S. Causes and consequences of disturbances of cerebral glucose metabolism in sporadic Alzheimer disease: therapeutic implications. Adv. Exp. Med. Biol.2004; 541:135–152.

[4] Mizuno M., Yamada K., Olariu A., Nawa H., Nabeshima T. Involvement of Brain-Derived Neurotrophic Factor in Spatial Memory Formation and Maintenance in a Radial Arm Maze Test in Rats. The Journal of Neuroscience 2000; 20: 7116-7121.

[5] Salkovic-PetrisicM, Knezovic A, Hoyer S, Riederer P. What have we learned from the streptozotocin-induced animal model of sporadic Alzheimer's disease, about the therapeutic strategies in Alzheimer's research. J Neural Transm. 2013; 120: 233–252

B 06-71

Acute muscle pain induced by eccentric muscle contraction facilitates a transient bilateral flexion reflex pattern in the feline spinal cord

E. D. Schomburg[1], H. Steffens[2], P. Dibaj[3], T. Sears[4]

[1] *Goettingen University, Institute of Physiology, Goettingen, Germany*

[2] *Goettingen University, Institute of Physiology, Goettingen, Germany*

[3] *Max Planck Institute for Multidisciplinary Natural Sciences, Department of Neurogenetics, Goettingen, Germany*

[4] *King's College London, Neurorestoration Group,Wolfson CARD, London, UK*

Motivation

Short or longer lasting pain of a limb muscle caused by an acute or a longer lasting myositis promoted a bilateral flexion reflex response to activation of group III/IV afferents in the feline spinal

cord i.e. a pattern distinct from the classic crossed extension reflex (Schomburg et. al. 2015). The aim of the present study was to test whether acute muscle damage and pain induced by eccentric muscle stretch may induce a similar effect.

Methods

All terminal experiments were made on anaemically decapitated (under full volatile anaesthesia), high spinal cats. Using selective chemical activation of group III/IV afferents in the left extensor gastrocnemius-soleus (GS) muscles injection we investigated bilaterally their reflex responses conditioned by unilateral strong eccentric muscle stretch of the GS muscle (stretching the muscle during supramaximal electrical stimulation of the muscle nerve. The reflex activity of the extensor GS and the flexor PBSt were bilaterally recorded by monosynaptic reflex testing.

Results

Short lasting activation of group III and IV muscle afferents by intra-arterial injection of KCL into the gastrocnemius-soleus (GS) muscle, evoked an ipsilateral FRA (flexor reflex afferents) pattern of flexor excitation and extensor inhibition without any clear contralateral effects. This pattern remained also after low spinalisation. Approximately 10 min after strong eccentric contraction of the left GS reflex transmission to the ipsilateral PBSt and GS was facilitated compared to control and a clear facilitation of transmission to the contralateral PBSt was now apparent. This facilitation persisted for up to 1 hour following the eccentric contraction and was by 2 hours absent. Notwithstanding a strong right PBST response to chemical activation of the afferents in the right GS no corresponding crossed facilitation of the left PBST occurred after eccentric contraction of the left GS.

Conclusion

An acute as well as a longer lasting nociceptive input to the spinal cord may influence the outcome of motor activity. Possibly, this has to be considered, if experiments with extensive operative preparation are performed.

Reference: *Schomburg ED et al., 2015. Long lasting activity of nociceptive muscular afferents facilitates bilateral flexion reflex pattern in the feline spinal cord. Neurosci. Res. 95, 51-58*

References

[1] **Reference:** Schomburg ED et al., 2015. Long lasting activity of nociceptive muscular afferents facilitates bilateral flexion reflex pattern in the feline spinal cord. Neurosci. Res. 95, 51-58

B 06-72

On Physiology and Odontology

M. C. Michailov[1], E. Neu[1], M. Joseph[1,2], J. Michel[1,2], D. Siebenhüner[1,2], T. Senn[1], J. Foltinova[1,3], G. Weber[1,4], H. Zoepfl[1,5]

[1] Inst. Umweltmedizin (IUM) c/o ICSD/IAS e.V., POB 340316, 80100 M. (Int.CouncilSci.Develop./Int.Acad.Sci. Berlin-Innsbruck-Muenchen-NewDelhi-Paris-Sofia-Vienna), Muenchen, Germany

[2] Dental Practice, Muenchen, Germany

[3] Univ. Bratislava, Med. Fac., Bratisava, Slovakia

[4] Univ. Luxembourg & Vienna, Fac. Psychology (Dean), Vienna, Austria

[5] Univ. Muenchen, Fac. Psychol. & Ped. (Ex-Inst.-Dir.), Muenchen, Germany

Introduction

Enormous health problems of humanity depends also on odontology. First reports about dental pathophysiology are given [1-5]. In Germany will be discussed about complex pathophysiology of Bert SAKMANN (Nobel-price together with Erwin NEHER) some years ago, because it appeared sepsis, caused by dental-infection. This led to enormous psychic disturbances: “I had a blood-poisoning and was in fever-delusion. I saw myself as dead-person, who lives farther as internet-figure. A frontier-experience” [5]. Actually are given new approaches in this matter.

Methods

Diagnosis by clinical observations and X-rays in dental -practices (n>30 patients).

Treatment by antibiotics, phytotherapy, diet,etc. Lasertherapy of *caries dentium & periodontitis* (Erbium:YAG 2940nm+1064nm/Fotona & diode laser 810nm/ARC) [3,4].

Results

Combined dental therapy prevents pulpitis, i.e. destruction of dental vitality (vascular&neuro-regulation), also tooth-extraction, leading to artificial teeth. In a patient (85years) tooth was eliminated spontaneously, i.e. physiologically, contrary to example of Bert SAKMANN. Patients with conservative and laser therapy – of caries dentium and periodontitis - demonstrate possibility for existence of natural teeth during whole life!

Table: Patients with

a. Caries Dentium: Therapy Effect, n=20 Laser > 1year; n=10 Antibiotics < 6 months

b. Periodontitis: Therapy Effect, n=10 Laser asymptomatic; n=5 Antibiotics asymptomatic

Further analysis will be given by presentation.

Conclusion

Paradigm changes in dentological education&research in context of an integrative physiology supporting biological way of life – diet, sport, etc. is necessary, related to somatopsychic (Yujiro IKEMI) and psychosomatic theories (Thure von UEXKÜLL). During opening ceremony of World-Congr-Psychosomatic-Med Emperor AKIHITO honoured congress by strategical ideas. “Total symptoms of mind and body seeking ways of holistic care ... It is extremely important for patients … my hope contributes … the progress of medical science and people's happiness in the entire world” [1c]. This could support future odontology in context of UNO-AGENDA21 for better health-education-ecology-economy on global level [1a].

Dedications Neu et al. FEPS-2022: Nobel Laureates (ICSD-IAS members supporting ICSD-Projects)

REF: *Michailov,Neu,Joseph et al:*

[1a]-**Philosophy**: FISP-2018-Univ.-Peking, Abs-Book (AB) p.1348-50,1373-4, 1420.

[1b]-**Psychology**: IUPsyS-2020-Prague, Int.J.Psychol. Suppl, abstract-no.5024,5076,5079,6950,6964,7018.

EFPA-2019-Moscow, AB p.1520,1530,1549

[1c]-ICPM-2005 Kobe: J.**Psychosom**.Res, p. 58: 85-86.

[2a]-**Physiology**: IUPS-2022-Peking:Abstract-Book:918,919,934,935.

[2b]-**Pharmacology**: GTPS/DGPT-2022-Bonn, Arch.Pharmacol. 396/S1:S11,S73-74,S75.

[3]-**Pathology**: ESP-**2019-**Nice, Eur.J.Pathol.475/Suppl.1: E-PS-03-023, 17-032&033, 25-066&067;

[4]-**Rad.Res**: IARR-2019-Manchester, Paper-No.658/Po.117, 653/192,654/116,659/124.

[5]-Daily Munich Journal **„tz“**:17.12.18/p.21, 11.02.19/p.13.

B 06-85

Omega-3 supplementation attenuates cardiac autonomic neuropathy in a rat model of type 2 diabetes through BDNF dependent mechanism

S. M. Abd-Elmonem, S. M. Greish, F. Abbas, **Y. M. El-Wazir**
Suez Canal University, Department of Physiology, Faculty of Medicine, Ismailia, Egypt

Introduction

Cardiac autonomic neuropathy (CAN) in diabetes mellitus (DM) is associated with high morbidity and mortality. So far, there is no available definitive treatment for CAN. BDNF depletion may be involved in DM-associated CAN. On the other hand, BDNF level was shown to improve with enhanced dietary supplementation of omega 3 fatty acids (omega). Thus, we investigated the role of BDNF in a DM-CAN rodent model and the potential effect of omega 3 fatty acids in normalizing BDNF and improving CAN.

Methods

Seventy Wistar rats were equally divided into 7 groups **(G)**. **GI**: Normal control (N). **GII:** N+BDNF blocker, where normal rats received intra-peritoneal injection (IP) of Trkb receptor antagonist (K252a) daily at a dose of 50 µg/kg body weight for the first 2 weeks **(1). GIII**: (DM), rats were subjected to STZ-NA induced type II diabetes **(2).GIV**: DM+BDNF group, diabetic rats received human recombinant BDNF at a dose of 0.4 µg /kg/day IV via tail vein for 4 weeks after diabetes confirmation **(3). GV**: DM+Early omega group, omega-3 supplementation, at a dose of 0.5 g/kg/day by oral gavage, was started directly after diabetes confirmation and continued for 8 weeks. **(4).GVI**: DM+Omega+BDNF blocker group, in which BDNF blocker was added daily on 7th and 8th weeks. **GVII**: DM+Late omega group, omega-3 supplementation was initiated after the occurrence of CAN and continued till the 12th week with the same dose as in groups V and VI.

Baroreflex sensitivity was assessed by recording the slope of the bradycardic response to phenylephrine (slope) at the 4th, 8th and 12th weeks using BIOPAC MP150 according to the manual guidelines after anesthesia of rats by thiopental sodium (60 mg/kg) IP **(5)**. All the experimental animals received humane care according to the guidelines of the institutional research ethical committee (3081). One-way ANOVA was used to compare results between the groups.

Results

At the 12th week, the slope was lower than both that of the 4th and 8th weeks (0.47 vs 1.02 & 0.67 respectively*). Blocking BDNF action in normal rats also decreased the slope relative to normal controls (1.2 vs 2.47*). Treatment of the diabetic rats with BDNF elevated the slope compared to the diabetic controls (2.01 vs 1.02*). Early oral supplementation of omega-3 increased the slope compared to **GIII** at the 4th (1.69 vs 1.02*) and 8th weeks (2.1 vs 0.67*). It also restored the normal slope by the 8th week. Late omega supplementation increased the slope compared to diabetic rats at the 12th week (2.01 vs 0.47*). Injection of BDNF blocker in **GVI** decreased the slope at the 8th week compared to the 4th week of the same group (0.8 vs 1.7*) and compared to **GV** group (0.8 vs 2.1*). At the 8th week the bradycardic slope of the **GVII** group was lower than that of **GV** (1.63 vs 2.1*).

Conclusion

Omega-3 supplementation, especially when used early, can be a low-cost intervention for diabetic CAN.

References

[1] Jiménez-Maldonado A, de Álvarez-Buylla E, Montero S, Melnikov V, Castro-Rodríguez E, Gamboa-Domínguez A, Rodríguez-Hernández A, Lemus M & Murguía J (2014). Chronic Exercise Increases Plasma Brain-Derived Neurotrophic Factor Levels, Pancreatic Islet Size, and Insulin Tolerance in a TrkB-Dependent Manner. PLOS ONE 9(12), e115177.

[2] Lin Y, Hsu K, Wu E, Tsai M, Wang C, Chang C & Chang K (2008). Autonomic neuropathy precedes cardiovascular dysfunction in rats with diabetes. Diabetes, 2(38), 110-115.

[3] Hang P, Zhao J, Sun L, Li M, Han Y, Du Z & Li Y (2017). Brain-derived neurotrophic factor attenuates doxorubicin-induced cardiac dysfunction through activating Akt signaling in rats. Journal of cellular and molecular medicine 21(4), 685-696.

[4] Yadav S, Mitha KV, Shenoy MT, Mayannavar S, Ganaraja B. Beneficial effect of Omega-3 polyunsaturated fatty acids on neurosensorial impairments and oxidative status in Streptozotocin induced diabetic rats. Indian J Physiol Pharmacol. 2014 Oct-Dec;58(4):346-53.

[5] Oliveira T, Candeia-Medeiros N, Cavalcante-Araújo P, Melo I Fávaro-Pípi E, Fátima L, Rocha A, Goulart L, Machado U, Campos R & Sabino-Silva R (2016). SGLT1 activity in lung alveolar cells of diabetic rats modulates airway surface liquid glucose concentration and bacterial proliferation. Scientific Reports 6(5), 21-29.

PB 07 | Vascular & Smooth Muscle Physiology

B 07-01

Effects of gestational Sulforaphane supplementation on maternal and offspring vascular function

J. K. Morris[1], P. M. Psefteli[1], P. D. Taylor[2], M. Nandi[3], S. J. Chapple[1]

[1] *King's College London, British Heart Foundation Centre of Excellence, School of Cardiovascular and Metabolic Medicine and Sciences, London, UK*

[2] *King's College London, Department of Women and Children's Health, School of Life Course Sciences, London, UK*

[3] *King's College London, Institute of Pharmaceutical Science, London, UK*

Introduction

Gestational diabetes mellitus (GDM) and maternal obesity account for 10-25% of pregnancies in the UK[1]. They are associated with the development of cardiometabolic complications later in life including hypertension, stroke, or type 2 diabetes[2,3]. Current interventions show limited benefit in reducing these risks, leaving demand for new treatments. Sulforaphane (SFN), an isothiocyanate found in cruciferous vegetables, is an inducer of the Nrf2 antioxidant pathway. SFN has demonstrated the ability to attenuate obesity, diabetes and/or cardiovascular complications in humans and non-pregnant mouse models[4,5]. Using an established model of obese insulin resistant mouse pregnancy, I sought to assess if SFN can ameliorate vascular dysfunction in dams and offspring.

Methods

Wildtype C57BL/6J dams are fed a high fat high sugar (HFHS) diet for ~7 weeks inducing obesity and insulin resistance. Upon mating vehicle (corn oil, Ob) or SFN (ObSFN) were supplemented orally at 2.5mg/kg 6 days a week. Additionally, a delayed intervention began E15.5 (ObSFN-Late), to coincide with the typical period of GDM diagnosis in humans. Dams were terminated on post-natal day 35 and male offspring maintained on HFHS diet were terminated at 15 weeks of age. Second order mesenteric arteries were harvested to assess vascular reactivity *ex vivo* through wire myography in response to Noradrenaline (NA), Acetylcholine (ACh) ± Indomethacin [10^{-9} to 10^{-4} M].

Results

Dams supplemented with continuous and late SFN intervention demonstrated attenuated maximal vasoconstriction compared to vehicle treated dams (%NA 188±7 Ob vs. 129±9 ObSFN or 140±6 ObSFN-Late). Vessels of SFN treated dams preincubated with cyclo-oxygenase (COX) inhibitor, indomethacin, demonstrated enhanced vasodilation vs Ob (%ACh 19±2 Ob vs 45±5 ObSFN or 48±6 ObSFN Late), indicating SFN enhances dilation independently of COX. Surprisingly, preliminary data suggests late SFN intervention augments maximal vasodilation (%ACh 49±2 Ob vs. 79±3 ObSFN-Late). In offspring, trends towards reduced NA-induced constriction in HFHS fed offspring of SFN dams (OS+HFHS) (%NA 129±11 OO+HFHS vs. 99±11 OS+HFHS or 109±16 OSL+HFHS) were observed, however, ACh induced vasodilation was similar between groups (%ACh 50±2 OO+HFHS vs. 63±2 OS+HFHS).

Conclusion

In conclusion, my data demonstrates gestational SFN supplementation exerts vasoprotective effects in dams and to a lesser extent in offspring. SFN-mediated protection was apparent in both continuous and late SFN intervention groups suggesting that even a late intervention is effective for treatment of obese and GDM mothers.

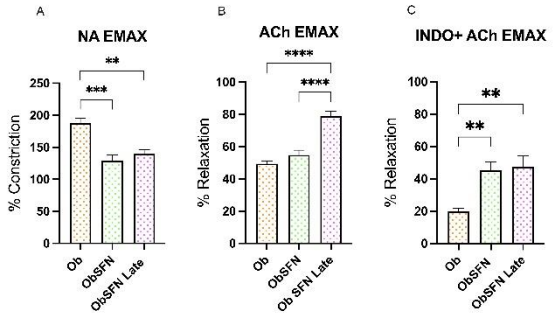

Figure 1: Maternal sulforaphane supplementation improves vascular reactivity in dams Maximal vasoconstriction (%) of Noradrenaline dose response (NA) [10^{-9} to 10^{-4} M] in obese (Ob), Obese sulforaphane (ObSFN) and Obese late Sulforaphane (ObSFN Late) treated dams (A). Maximal vasodilation responses following Acetylcholine dose response (ACh; 10^{-9} to 10^{-4} M) (B) and with vessels preincubated in indomethacin (INDO) (C). Data represent mean±SEM, n=3-7, analysed by 1-way ANOVA, *p<0.05, **p<0.01, ***p<0.001, ****p<0.0001

References

[1] Devlieger R, Benhalima K, Damm P, Van Assche A, Mathieu C, Mahmood T, et al. Maternal obesity in Europe: where do we stand and how to move forward?: A scientific paper commissioned by the European Board and College of Obstetrics and Gynaecology (EBCOG). Eur J Obstet Gynecol Reprod Biol. 2016;201:203-8.

[2] Tam WH, Ma RCW, Ozaki R, Li AM, Chan MHM, Yuen LY, et al. In Utero Exposure to Maternal Hyperglycemia Increases Childhood Cardiometabolic Risk in Offspring. Diabetes Care. 2017;40(5):679-86.

[3] Metzger BE, Lowe LP, Dyer AR, Trimble ER, Chaovarindr U, et al. Hyperglycemia and adverse pregnancy outcomes. N Engl J Med. 2008;358(19):1991-2002.

[4] Axelsson AS, Tubbs E, Mecham B, Chacko S, Nenonen HA, Tang Y, et al. Sulforaphane reduces hepatic glucose production and improves glucose control in patients with type 2 diabetes. Sci Transl Med. 2017;9(394).

[5] Bahadoran Z, Mirmiran P, Hosseinpanah F, Rajab A, Asghari G, Azizi F. Broccoli sprouts powder could improve serum triglyceride and oxidized LDL/LDL-cholesterol ratio in type 2 diabetic patients: a randomized double-blind placebo-controlled clinical trial. Diabetes Res Clin Pract. 2012;96(3):348-54.

B 07-02

Sex differences in human pulmonary microvascular endothelial cells in the conditions of shear stress

D. S. Kostyunina[1], E. Dillon[1], K. D. Rochfort[2], P. M. Cummins[2], **P. McLoughlin**[1]

[1] University College Dublin, Conway Institute of Biomolecular and Biomedical Science, Dublin, Ireland

[2] Dublin City University, School of Biotechnology and National Institute for Cellular Biotechnology, Dublin, Ireland

The author has objected to a publication of the abstract.

B 07-03

Myocardin regulates exon usage in smooth muscle cells through induction of splicing regulatory factors

L. Liu[1,2], D. Kryvokhyzha[3], C. Rippe[1], A. Jacob[4], A. B. Muñoz[1], K. Stenkula[1], O. Hansson[3,5], C. W. Smith[4], S. Fisher[6], K. Swärd[1]

[1] Lund University, Department of Experimental Medical Science, Lund, Sweden

[2] The Sixth Affiliated Hospital of Guangzhou Medical University, Department of Urology, Qingyuan, China

[3] Lund University Diabetes Centre, Department of Clinical Sciences, Lund, Sweden

[4] University of Cambridge, Department of Biochemistry, Cambridge, UK

[5] Helsinki University, Institute for Molecular Medicine Finland (FIMM), Helsinki, Finland

[6] University of Maryland-Baltimore, Department of Medicine (Cardiology) and Physiology and Biophysics, Baltimore, USA

We thank Katarzyna Kawka for invaluable technical support throughout this work. We also thank Malin Svensson at the sequencing facility, and Bengt Uvelius for the human bladder biopsies retrieved in prior studies to generate the bladder SMCs used here.

Introduction

Differentiation of smooth muscle cells (SMCs) depends on the transcriptional co-activator myocardin (*MYOCD*). The role of MYOCD for the SMC program of gene transcription is well established. In contrast, the role of MYOCD in control of SMC-specific alternative exon usage, including exon splicing, has not been explored.

Methods

RNA correlation analyses and an RNA-sequencing experiment were done to detect potential splicing factors regulated by MYOCD. Adenoviral vectors and siRNAs were used for overexpression and knockdown. RT-PCR and western blots were performed for confirming mRNA and protein expression changes. Agarose gel electrophoresis was used together with variant-specific PCR primers to quantify defined splicing events.

Results

We identified four splicing factors (*MBNL1*, *RBPMS*, *RBPMS2*, and *RBFOX2*) that correlate with *MYOCD* across human SMC tissues. Forced expression of MYOCD in human coronary artery SMCs *in vitro* upregulated these splicing factors. For global profiling of transcript diversity, we performed RNA-sequencing after MYOCD transduction. We analyzed alternative transcripts with three different methods. Exon-based analysis identified 1637 features with differential exon usage. For example, usage of 3' exons in *MYLK* that encode telokin increased relative to 5'exons, as did the 17 kDa telokin to 130 kDa MYLK protein ratio. Dedicated event-based analysis identified 239 MYOCD-driven splicing events. Events involving *MBNL1*, *MCAM*, and *ACTN1* were among the most prominent, and this was confirmed using variant-specific PCR analyses. In support of a role for RBPMS and RBFOX2 in MYOCD-driven splicing, we found enrichment of their binding motifs around differentially spliced exons. Moreover, knockdown of either RBPMS or RBFOX2 antagonized splicing events stimulated by MYOCD, including those involving *ACTN1*, *VCL*, and *MBNL1*.

Conclusion

We conclude that MYOCD, via RBPMS and RBFOX2, writes the SMC-specific splicing code as part of the broader program of SMC differentiation.

B 07-04

Dynein coordinates β-adrenoceptor-mediated relaxation in normotensive and hypertensive rat mesenteric arteries

J. van der Horst[1,2], S. Rognant[1], Y. Hellsten[2], C. Aalkjaer[3], T. Jepps[1]

[1] University of Copenhagen, Department of Biomedical Sciences, Copenhagen, Denmark

[2] University of Copenhagen, Department of Nutrition, Exercise and Sports, Copenhagen, Denmark

[3] Aarhus University, Department of Biomedicine, Copenhagen, Denmark

Introduction

The voltage-gated Kv7.4 and Kv7.5 channels contribute to the β-adrenoceptor-mediated vasodilatation. In arteries from hypertensive rats, the Kv7.4 channel is downregulated and function attenuated, contributing to the reduced β-adrenoceptor-mediated vasodilatation in these arteries. Recently, we found that disruption of microtubules (with colchicine), or inhibition of the microtubule motor protein dynein (with ciliobrevin D), increased the membrane levels and function of Kv7.4 channels in smooth muscle cells. The aim of this study was to investigate whether colchicine or ciliobrevin D could improve Kv7.4 function in third-order mesenteric arteries from the spontaneously hypertensive rat (SHR), thereby restoring the β-adrenoceptor-mediated vasodilatation.

Methods & results

Ciliobrevin D enhanced the relaxation to the β-adrenoceptor agonist, isoprenaline, in rat mesenteric arteries both *ex vivo* and *in vivo*. The Kv7 channel blocker, linopirdine, partially inhibited the ciliobrevin D-enhanced isoprenaline response. The β2-adrenoceptor antagonist ICI 118551 (100nM) attenuated the ciliobrevin D-enhanced isoprenaline relaxation, whereas the β1-adrenoceptor antagonist, bisoprolol (10nM) had no effect on the ciliobrevin D-enhanced relaxation. In mesenteric arteries from the SHR, ciliobrevin D and colchicine both improved the isoprenaline-mediated vasorelaxation and relaxation to the Kv7.2-7.5 activator, ML213. With immunostaining, we confirmed that ciliobrevin D enhanced the Kv7.4 membrane abundance in isolated vascular smooth muscle cells. In addition, ciliobrevin D increased the functional contribution of the β2-adrenoceptor to the isoprenaline-mediated relaxation. Immunostaining experiments showed that ciliobrevin D prevented isoprenaline-mediated internalization of the β2-adrenoceptor.

Conclusion

These data show that colchicine and ciliobrevin D can restore β-adrenoceptor-mediated vasodilatation in arteries from the SHR by increasing both the Kv7.4 channel and β2-adrenoceptor contribution.

B 07-05

Human blood vessel maturation is associated with widescale reduction in cytosolic, but not mitochondrial, ribosomal protein abundances

F. Burté, P. Palmowski, J. Taggart, S. C. Robson, M. J. Taggart
Newcastle University, Biosciences Institute, Faculty of Medical Sciences, Newcastle upon Tyne, UK

Supported by the British Maternal and Fetal Medicine Society and Action Medical Research/Borne (GN2807)

Investigation of the mechanisms underlying the development and maturation of human blood vessels is important for understanding disease circumstances and consideration of procedures to minimise dysfunction associated with these. However, the molecular processes involved are difficult to study in healthy human biospecimens. During pregnancy, the placenta is an organ forming de novo and access to biospecimens at different gestational endpoints offers the potential to investigate the molecular processes contributing to physiological blood vessel development and maturation.
Previously, we have reported on proteomic analysis of human chorionic plate placental arteries extracted from organs obtained, following written informed consent (LREC 10/H0906/71), from first (7-12 weeks gestation, n=9) and third (39-40 weeks gestation, n=8) trimesters of normal pregnancy [1]. Homogenised arteries were trypsin digested and peptides analysed in triplicate via liquid chromatography mass spectrometry (LC-MS) using SWATH [2]. In this study, of the 3586 proteins quantified and 1078 differentially expressed between 1st and 3rd trimesters (quantified using ≥5 unique fragment ion intensities per peptide, log(2) transformed and median-corrected before unpaired t-test analysis with multiple corrections FDR<0.01, and magnitude changes >1.5-fold between conditions), we explore if human blood vessel maturation was associated with changes in cytosolic and/or mitochondrial ribosomal protein abundances.
Placental artery maturation was associated with substantial reductions in cytosolic ribosomal proteins. Of 40 proteins of the 60S large ribosomal unit identified, 34 were significantly reduced in 3rd trimester compared to 1st trimester. Of the 40S ribosomal subunit, 26 of the 31 identified proteins were reduced. The three proteins with largest changes were RPL31 (log(2)FC values of 4.1 ± 0.3 in 1st trimester and 0.9 ± 0.4 in 3rd trimester; ~9-fold decrease), RPL34 (log(2)FC 4.7 ± 0.1 versus 2.5 ± 0.1; ~5-fold decrease)and RPS27 (log(2)FC 1.3 ± 0.3 in first trimester and -0.8 ± 0.3; ~4.2-fold decrease). Of note, similar widescale changes were not observed in the mitoribosome. Of the 22 mitochondrial proteins quantified, only three were significantly changed between 1st and 3rd trimester (MRPL21: log(2)FC -1.7 ± 0.2 versus -3.4 ± 0.2, ~3-fold decrease; MRPL55: log(2)FC -2.6 ± 0.2 versus -4.2 ± 0.2, ~3-fold decrease; MRPS25: log(2)FC -4.0 ± 0.2 versus -3.1 ± 0.2, ~2-fold increase).
Our data suggest that the end-stage of human blood vessel maturation is marked by widescale reduction in cytosolic ribosomal protein abundances perhaps indicative of the acquisition of differentiated cell phenotype. Given the reported involvement of some ribosomal proteins in regulating vascular smooth muscle growth and tumourogenesis [3;4], it will be informative in future studies to investigate the dynamic nature of these switches with the examination of biosamples from other gestational timepoints.

References
[1] Palmowski, P, Treumann, A, Watson, R, Taggart,J, Robson, SC, Europe-Finner, N, Taggart, MJ 2019, 'Proteomic signatures of human placental vascular maturation', *Proc Physiol Soc*, 43, PC265
[2] Ludwig, C, Gillet, L, Rosenberg, G, Amon, S, Collins, B, Aebersold, R 2018, 'Data-independent acquisition-based SWATH-MS for quantitative proteomics: a tutorial', *Mol Syst Biol*, 14(8), e8126
[3] Huang, X, Gao, Y, Jiang, B, Zhou, Z, Zhan, A 2016, 'Reference gene selection for quantitative gene expression studies during biological invasions: A test on multiple genes and tissues in a model ascidian Ciona savignyi', *Gene*, 576(1 Pt 1), 79-87
[4] Du, C, Wang, T, Jia, J, Li, J, Xiao, Y, Wang, J, Mao, P, Wang, N, Shi, L, Wang, M, 2022, 'Suppression of RPL34 Inhibits Tumor Cell Proliferation and Promotes Apoptosis in Glioblastoma', *Appl Biochem Biotechnol*, Online ahead of print

---

B 07-06

Dietary antioxidant vitamins intake and systemic vascular function in Bolivian highlanders with chronic mountain sickness

T. Filipponi[1], C. J. Marley[1], J. V. Brugniaux[1,2], S. F. Rimoldi[3], E. Rexhaj[3], L. Pratali[4], C. Salinas Salmòn[5], C. Murillo Jauregui[5], M. Villena[5], C. Sartori[6], U. Scherrer[3,7], D. M. Bailey[1]
[1] *University of South Wales, Neurovascular Research Laboratory, Pontypridd, UK*
[2] *Grenoble Alpes University, HP2 Laboratory, INSERM U1300, Grenoble, France*
[3] *University Hospital, Department of Cardiology and Biomedical Research, Bern, Switzerland*
[4] *Institute of Clinical Physiology, Pisa, Italy*
[5] *Instituto Bolivano de Biologia de Altura, La Paz, Bolivia*
[6] *University Hospital, University of Lausanne, Department of Internal Medicine, Lausanne, Switzerland*
[7] *Universidad de Tarapacá, Facultad de Ciencias, Departamento de Biología, Arica, Chile*

DMB is supported by a Royal Society Wolfson Research Fellow (#WM170007).

Introduction
Chronic mountain sickness (CMS), a high-altitude maladaptive syndrome, is a public health problem experienced primarily by Andean countries (1). Impaired systemic vascular endothelial function subsequent to a free radical-mediated reduction in nitric oxide (NO) bioavailability [oxidative-nitrosative stress (OXNOS)] may contribute to the increased cardiovascular risk observed in CMS patients (CMS+) (2, 3, 4, 5). The observation that antioxidant defences are depressed in CMS+ tentatively suggests that inadequate dietary intake may predispose to vascular dysfunction. Hence, the aim of the study was to investigate the intake of dietary antioxidant vitamins, fruit and vegetable consumption, and systemic vascular function in CMS+ and healthy, well-adapted highlanders (CMS-). We hypothesised that CMS+ will show impaired systemic vascular function subsequent to a low intake of dietary antioxidant vitamins.
Methods
Thirty-three male Bolivian highlanders with CMS (n=20, CMS+; age 58±8 y), without CMS (n=13, CMS-; age 54±7 y), and thirteen British male lowlanders born and bred close to sea level (n=13 controls; 60±7 y) consented to the study. Participants were interviewed to collect a 48-hour structured dietary recall. Dietary data were analysed using NetWISP dietary analysis software (Version 4.0, Tinuviel Software; Anglesey, UK). Systemic vascular function was assessed using flow-mediated dilation (FMD, duplex ultrasound), arterial stiffness (applanation tonometry), the latter

defined by carotid-femoral pulse wave velocity (c-f PWV), augmentation index normalised for a heart rate of 75 beats/minute (AIx@75) and carotid intima-media thickness (cIMT). Data were tested for normality using Shapiro-Wilk *W* tests and analysed using one-way ANOVAs and *post hoc* Bonferroni-adjusted independent samples *t*-tests. Significance level was established at $P<0.05$.

Results

CMS+ patients reported lower intake of vitamin C ($P = 0.003$ vs. CMS-; $P = <0.000$ vs. controls) and carotene ($P = 0.050$ vs. CMS-; $P = 0.058$ vs. controls) due to inadequate consumption of fruit ($P = <0.000$ vs. controls) and vegetables ($P = <0.000$ vs. CMS-; $P = <0.000$ vs. controls). CMS+ exhibited impaired FMD ($P = <0.001$ vs. controls) and greater c-f PWV ($P = <0.001$ vs. controls) and AIx@75 ($P = 0.022$ vs. controls) compared to lowlander controls along with increased cIMT ($P = 0.027$ vs. CMS-) compared to CMS-.

Conclusion

Collectively, these findings demonstrate that CMS+ are characterised by inadequate intake of dietary antioxidant vitamins due to reduced consumption of fruit and vegetables. A corresponding reduction in dietary antioxidant vitamin intake may contribute to systemic OXNOS-mediated impairments in vascular function. Public health programmes need to consider targeted dietary interventions, including nutrition education and dietary modification, that may help improve the overall health of highlanders, especially CMS+ who may be at increased cardiovascular risk.

References

[1] 1. Villafuerte, FC, Corante, N 2016, 'Chronic Mountain Sickness: Clinical Aspects, Etiology, Management, and Treatment', *High Alt Med Biol*, 17, 61-69.

2. Bailey, DM, Brugniaux, JV, *et al.* 2019, 'Exaggerated systemic oxidative-inflammatory-nitrosative stress in chronic mountain sickness is associated with cognitive decline and depression', *J Physiol*, 597, 611-629.

3. Bailey, DM, Rimoldi, SF, *et al.* 2013, 'Oxidative-nitrosative stress and systemic vascular function in highlanders with and without exaggerated hypoxemia', *Chest*, 143, 444-451.

4. Rimoldi, SF, Rexhaj, E, *et al.* 2012, 'Systemic vascular dysfunction in patients with chronic mountain sickness', *Chest*, 141, 139-146.

5. Corante, N, Anza-Ramirez, C, *et al.* 2018, 'Excessive Erythrocytosis and Cardiovascular Risk in Andean Highlanders', *High Alt Med Biol*, 19, 221-231.

B 07-07

CO-releasing molecules relax rat small mesenteric arteries: contribution of Kv7 channels

R. Schubert[1], D. Zhang[2,3], B. Krause[4], H.-G. Schmalz[4], P. Wohlfart[5], B. Yard[2]

[1] *Physiology, Institute of Theoretical Medicine, Faculty of Medicine, University of Augsburg, Augsburg, Germany*

[2] *Department of Nephrology, Endocrinology and Rheumatology, Fifth Medical Department of Medicine, Medical Faculty Mannheim, University of Heidelberg, Mannheim, Germany*

[3] *Department of Nephrology, The Second Hospital of Anhui Medical University, Hefei, China*

[4] *Department of Chemistry, University of Cologne, Cologne, Germany*

[5] *Diabetes Research, Sanofi Aventis Deutschland GmbH, Frankfurt am Main, Germany*

Introduction

Carbon monoxide (CO), a product of endogenous heme oxygenases, is an important signalling molecule. In addition, it is considered a potential therapeutic agent. Recently, several different CO releasing molecules (CORMs) have been synthesized, including enzyme-triggered CORMs (ET-CORMs) allowing a better control over CO release. The HO-1/CO system contributes considerably to the function of the circulatory system, in particular to vasodilation. Thus, CO and CORMs have been shown to relax vessels through activation of soluble guanylate cyclase (sGC) and different types of potassium channels. Effects of CO were observed to be mediated preferentially by calcium-activated potassium channels whereby effects of CORMs were found to be mediated by voltage-dependent potassium channels. However, ET-CORMs have not been studied in this regard so far. Recently, voltage-dependent Kv7 channels have been shown to contribute considerably to the regulation of vascular tone. Therefore, this study tested the hypothesis that vasorelaxation induced by ET-CORMs is mediated by sGC and Kv7 channels.

Methods

The study was performed on rat mesenteric arteries using real-time PCR based on TaqMan microfluidic card technology and isometric myography as well as either acetate-containing (rac-1 and rac-4) or pivalate-containing (rac-8) ET-CORMs. Approval for the use of laboratory animals in this study was granted by a government committee on animal welfare (I-17/17).

Results

Both acetate containing ET-CORMs (rac-1 and rac-4) strongly relaxed the arteries, while we did not observe an effect of the pivalate containing ET-CORM (rac-8). Thus, further experiments focused on rac-4. The rac-4-induced vasorelaxation was not mimicked by byproducts of rac-4 hydrolysis, suggesting that CO is mediating its effect. After pre-treatment of the vessels with the sGC inhibitor ODQ we did not observe any rac-4-induced vasorelaxation. Further, we did also not observe an effect of rac-4 in vessels pre-contracted with a solution containing a high extracellular KCl concentration suggesting the involvement of potassium channels. Several different potassium channels, Kv1, Kv2, Kv3, Kv7, Kv11, Kir2, Kir6, BK and SK, were abundantly expressed in the vessels studied. The role of Kv3, Kv11, and SK channels was not further studied, since no specific inhibitors or no published data suggesting their involvement in GC-mediated vasorelaxation are available. Vessels were pre-contracted by methoxamine in combination with mixtures of potassium-channel blockers composed to leave only one potassium channel (either Kv1, Kv2, Kv7, Kir2, Kir6 or BK channel) available. Vasorelaxation induced by rac-4 was observed only when Kv7 channels remained available. In addition, after pre-treatment of vessels with the Kv7 channel blocker XE991 we did not detect any effect of rac-4.

Conclusion

In summary, the presented results suggest that the effect of the CO-releasing ET-CORM rac-4 is mediated by sGC and Kv7 channels.

B 07-08

LncRNA HIF1α-AS1 is a DNA:DNA:RNA triplex-forming lncRNA in human endothelial cells

M. S. Leisegang[1], J. Kaur Bains[2], S. Seredinski[1], J. A. Oo[1], N. M. Krause[2], C.-C. Kao[3], S. Günther[4], N. Sentürk Cetin[5], T. Warwick[1], C. Cao[1], F. Boos[1], J. Izquierdo Ponce[1], R. Bednarz[1], C. Valasarajan[4], D. Fuhrmann[7], J. Preussner[4], M. Looso[4], S. S. Pullamsetti[4], M. H. Schulz[8], F. Rezende[1], R. Gilsbach[1], B. Pflüger-Müller[1], I. Wittig[1], I. Grummt[5], T. Ribarska[9], I. G. Costa[3], H. Schwalbe[2], R. P. Brandes[1]

[1] Goethe University, Institute for Cardiovascular Physiology, Frankfurt, Germany
[2] Goethe University, Institute for Organic Chemistry and Chemical Biology, Center for Biomolecular Magnetic Resonance (BMRZ), Frankfurt, Germany
[3] RWTH Aachen, Institute for Computational Genomics, Frankfurt, Germany
[4] Max Planck Institute for Heart and Lung Research, Bad Nauheim, Germany
[5] German Cancer Research Center DKFZ-ZMBH, Division of Molecular Biology of the Cell II, Heidelberg, Germany
[6] Justus Liebig University, Department of Internal Medicine, Gießen, Germany
[7] Goethe University, Institute of Biochemistry I, Frankfurt, Germany
[8] Goethe University, Institute for Cardiovascular Regeneration, Frankfurt, Germany
[9] Oslo University Hospital, Oslo, Norway

Introduction

Formation of DNA:DNA:RNA triplex through Hoogsteen base-pairing has been observed in artificial systems, but whether these interactions occur in cells and impact on cellular function is controversial. Moreover, the physiological relevance, the mechanistic mode of action and participating protein complexes of triplex forming lncRNAs are unclear. The long non-coding RNA (lncRNA) HIF1α-AS1 is located antisense to the important Hypoxia-inducible factor 1α gene, but the function is, however, unknown and was identified here.

Methods and Results

To identify functionally important DNA:DNA:RNA triplex-forming lncRNAs in human endothelial cells, we used a combination of bioinformatic techniques, RNA/DNA pulldown and biophysical studies. The lncRNA HIF1α-AS1 was retrieved here as a top hit. Knockdown of the lncRNA in endothelial cells increased their angiogenic capacity. The lncRNA was reduced in endothelial cells isolated from glioblastoma and from lungs of patients with pulmonary arterial hypertension. In contrast, reoxygenation after hypoxia induced HIF1α-AS1. The lncRNA reduced the expression of numerous genes, including EPH Receptor A2 (EPHA2) and Adrenomedullin, through DNA:DNA:RNA triplex formation. Exchange of the triplex forming region of HIF1a-AS1 with other known triplex forming regions by CRISPR Arcitect abolished its effects on gene expression. Protein interaction studies revealed that HIF1α-AS1 interacts with the human silencing hub (HUSH) complex, which contains the epigenetic repressor MPP8. An assay for transposase-accessible chromatin followed by sequencing revealed that HIF1α-AS1 acts as an adapter for the HUSH complex on EPHA2 and Adrenomedullin.

Conclusion

As exemplified here with HIF1α-AS1, DNA:DNA:RNA triplex formation is operative in vascular tissue to limit the angiogenic response and important for trans-acting gene expression control through the recruitment of epigenetic silencer complexes.

B 07-09

Exploring the medium- and longer-term macrovascular effects of e-cigarettes and Nicotine Replacement Therapy in adults making a stop-smoking attempt.

M. Klonizakis[1], E. McIntosh[1], A. Gumber[1], L. Brose[2]

[1] Sheffield Hallam University, Lifestyle, Exercise and Nutrition Improvement (LENI) Research Group, Department of Nursing and Midwifery, Sheffield, UK
[2] King's College London, National Addiction Centre, Institute of Psychiatry, Psychology & Neuroscience, London, UK

We would like to thank our participants for taking part in our study and the Stop Smoking Services in Sheffield for accepting referrals and supporting our participants in our NRT-based group.
The trial was funded by Heart Research UK under a Translational Research Grant (RG2658).

Introduction

Smoking is a major CVD risk factor. This is because it causes endothelial injury and dysfunction in both coronary and peripheral arteries and an increased risk of thrombosis. Therefore, it is no surprise that it remains the second-leading mortality risk factor in the world, mainly due to cancer, lung disease and cardiovascular disease (CVD).Thankfully, smoking cessation offers CVD risk-reduction benefits, which increase as time since cessation increases. Vaping products or electronic cigarettes (e-cigarettes) have been the most popular choice of support for smoking cessation in England, and by 2020 were being used by 27% of smokers making a cessation attempt. Nevertheless, evidence on the effect of e-cigarettes on cardiovascular health of smokers making a quite attempt, remains limited.

Methods

We conducted a single-center, U.K.-based, pragmatic three-arm randomized (1:1:1) controlled trial, which recruited from the community, adult smokers (≥10 cigarettes/day), who were willing to attempt to stop smoking with support.

Exclusion criteria were: i) inability to walk, ii) recent (within 6 months) CVD events or cardiac surgery, iii) insulin-controlled diabetes mellitus, iv) coexisting skin conditions, leg ulcers, vasculitis or deep venous occlusion, v) pregnancy, vi) major surgery scheduled during the study, vii) contraindications /unsuitability for NRT, viii) current daily use of e-cigarettes and ix) current cessation attempt supported by a stop smoking service.

Participants (n=248) were randomized to receive behavioral support with either a) e-cigarettes with 18mg/ml nicotine; b) e-cigarettes without nicotine; c) NRT. Flow Mediated Dilation (%FMD) were recorded at baseline, 3- and 6-months after stopping smoking.

Results

%FMD showed an improvement at 3- and 6-months follow-up, over baseline in all three groups (e.g., β= 2.40, 95% CI: 1.66 to 3.14 $p < 0.0001$ at 3-months over baseline and β= 2.99, 95% CI: 2.22 to 3.77 $p < 0.0001$ at 6-months over baseline). There was no statistically significant difference in %FMD between the intervention groups.

Conclusion

None of the groups (i.e., nicotine-containing and nicotine-free e-cigarettes or NRT) offered superior cardiovascular benefits to the others, although in overall, smokers making a quit attempt experienced positive cardiovascular impact after both a 3- and 6-month period.

B 07-10

3D coronary capillary network is altered in mouse model of heart failure with preserved ejection fraction

N. Nicolas[1], M.-A. Renault[2], E. Roux[1]

[1] *Univ. Bordeaux, Inserm, UMR1034, Biology of Cardiovascular Diseases, Pessac, France*

[2] *Biologie des maladies cardiovasculaires, Inserm U1034, Pessac, France*

Introduction

Heart Failure with preserved Ejection Fraction (HFpEF) is a cardiovascular disease characterized by telediastolic dysfunction. Main risk factors include advanced age (> 67 years old), sex (women being more susceptible to develop the disease), and several comorbidities, particularly obesity and diabetes (1). HFpEF has been shown to be associated with the rarefaction of coronary microvascularisation (2). The aim of our study was to characterize quantitatively the 3D topological reorganization of the coronary microvasculature of the capillary coronary network in a mouse model of HFpEF.

Methods

Experiments were done on 14-week-old female C57BL/Ks leptin receptor-deficient ($Lepr^{db/db}$) mice (n=7), a physiopathological model of HFpEF accumulating human risk factors of HFpEF (3). $Lepr^{db/db}$ mice develop early obesity and type 2 diabetes, and C57BL/Ks mice have increased risks of renal dysfunction. 8-week old male C57BL/6J mice (n=7) were used as normal control, i.e. without any known human risk factor of HFpEF. 3D imaging of the coronary capillary network was done by light-sheet microscopy on iDISCO+ optical cleared hearts after lectin-labeling of the capillaries by retro-orbital injection on anesthetized animals (Isoflurane 3%). Image processing consisted of skeletonization and distance mapping of greyscale segmented images using ImageJ software. Capillary network in the left (LV), and right (RV) ventricles, and septum (S) was characterized by the volume network density, the fractal dimension, the average length (L), diameter (D), and tortuosity (T) of the segments, and (normalized per mm^3 of cardiac tissue) the number of segments and nodes and the total network length. Data are given as mean±SD. Using Graphpad Prism software, data were compared by Student t test, and frequency distribution of L, D, and T was fitted by exponential decay curve (L, T) and Gaussian curve (D) and compared by F test. Differences were significant if $p<0.05$.

Results

Compared to controls, $Lepr^{db/db}$ mice LV showed a significantly reduced volume density (40±6 vs 49±9 %), number of segments (402,000±68,000 vs 518,000±110,000), number of nodes (220,000±39,000 vs 280,000±60,000) and total length (55±1.2 vs 54±1.7 m). LV capillaries were significantly more tortuous than control. Representative images of LV capillaries are represented in figure 1. $Lepr^{db/db}$ mice RV showed a significantly reduced fractal dimension (2.4±0.03 vs 2.4±0.02), number of segments (339,000±24,000 vs 401,000±43,000), number of nodes (180,000±14,000 vs 220,000±25,000) and total length (53±0.6 vs 54±1.3 m). RV capillaries were significantly larger than control. S capillary network was not different from the control.

Conclusion

Our study showed that the LV capillary network presented signs of rarefaction and structural alterations that may contribute to LV dysfunction in HFpEF. It also evidenced specific alterations of the RV capillary network architecture, suggesting possible function impairment.

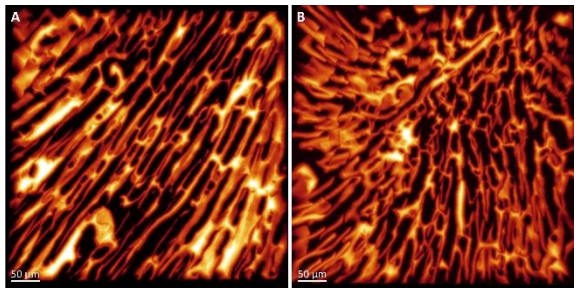

Figure 1. 3D imaging of coronary capillary network. Representative segmented image of the left ventricular coronary capillary network. A: C57BL6/J mouse. B: $Lepr^{db/db}$ mice. The average diameters of each segment are encoded in false colors from red (small diameter) to white (large diameter).

References

[1] Groenewegen A, Rutten FH, Mosterd A, Hoes AW. Epidemiology of heart failure. Eur J Heart Fail. 2020 Aug;22(8):1342–56.

[2] Taqueti VR, Di Carli MF. Coronary Microvascular Disease Pathogenic Mechanisms and Therapeutic Options. Journal of the American College of Cardiology. 2018 Nov;72(21):2625–41.

[3] Valero-Muñoz M, Backman W, Sam F. Murine Models of Heart Failure With Preserved Ejection Fraction. JACC: Basic to Translational Science. 2017 Dec;2(6):770–89.

B 07-11

DDAH1 prevents eNOS inhibition by ADMA in rat small mesenteric arteries

Y.Y.H. Ng[1], F. Leiper[2], J. Leiper[2], K. A. Dora[1], C. J. Garland[1]

[1] *University of Oxford, Department of Pharmacology, Oxford, UK*

[2] *University of Glasgow, Institute of Cardiovascular & Medical Sciences, BHF Glasgow Cardiovascular Research Centre, Glasgow, UK*

This work was supported by the British Heart Foundation PhD Studentship awarded to Y. Y. Hanson Ng.

Endothelial dysfunction involving the loss of nitric oxide (NO) is an early hallmark of cardiovascular disease and is associated with increased abnormal vasoconstriction (vasospasm) and reduced vasorelaxation. Endogenous methylarginines, such as N^G-monomethylarginine (L-NMMA) and asymmetric dimethylarginine (ADMA) inhibit endothelial NO synthase (eNOS), reducing NO bioavailability. Plasma ADMA concentration is a strong independent predictor of cardiovascular disease and mortality. Intracellular ADMA levels are tightly regulated by a family of dimethylarginine dimethylaminohydrolase (DDAH) enzymes. The present study investigated the interaction between DDAH and ADMA in resistance arteries. Third-order mesenteric arteries (160 – 320 µm diameter) from male Wistar rats (210 – 285 g) were studied with wire myography. Arteries were pre-contracted

with phenylephrine (1 – 3 µM), and NO-dependent vasorelaxation was assessed with acetylcholine (ACh; 0.001 – 1 µM) in the presence of inhibitors of endothelium-dependent hyperpolarisation (EDH; apamin (Ap; 100 nM) and NS6180 (NS; 1 µM)). Data are presented as percentage vasorelaxation to 300 nM ACh and values expressed as mean ± SEM of *n* biological replicates unless otherwise stated. Statistical analysis was performed with two-way ANOVA with Tukey's multiple comparisons. After block of EDH, ADMA (300 µM) markedly attenuated ACh-induced NO-dependent vasorelaxation (Control: 99.26 ± 0.20%; Ap, NS, ADMA: 68.35 ± 7.67%; $P < 0.05$ at 0.001 – 1 µM; $n = 7$) and shifted ACh EC_{50} [95% CI] (Control: 5.88 [4.99 – 6.82] nM; Ap, NS, ADMA: 38.18 [18.69 – 72.74] nM; $n = 7$). The addition of a synthetic DDAH1 inhibitor, L-257 (100 µM), was associated with block of vasorelaxation by ADMA (Ap, NS, ADMA, L-257: 28.08 ± 5.30%; $P < 0.05$ at 0.3 – 1 µM versus Ap, NS, ADMA; $n = 6–7$). Exogenous L-arginine (1 mM) reversed this ADMA block of ACh-induced vasorelaxation (Control: 99.57 ± 0.73%; ADMA, L-Arg: 91.72 ± 6.01%; ADMA, L-257, L-Arg: 91.30 ± 7.92%; ns; $n = 7 – 14$). In summary, our data indicate that in rat mesenteric resistance arteries: i) ADMA attenuates NO-dependent vasorelaxation by reducing NO bioavailability; ii) DDAH1 activity can limit the inhibitory effects of ADMA; iii) L-arginine rescues NO-dependent vasorelaxation in the presence of ADMA and L-257, indicating a competitive inhibition.

B 07-12

Epoxyeicosatrienoic acids and prostanoids crosstalk at the receptor and intracellular signaling levels to maintain vascular tone

J. Bezzenberger[1,2], P. F. Malacarne[1,2], M. Lopez[1,2], N. Müller[1,2], T. Warwick[1,2], R. Brandes[1,2], F. Rezende[1,2]

[1] *Goethe University, Institute for Cardiovascular Physiology, Frankfurt, Germany*

[2] *German Center for Cardiovascular Research, Partner site Frankfurt Rhein-Main, Frankfurt, Germany*

Introduction

Arachidonic acid (AA, 20 carbons w-6 PUFA) is a precursor of various vasoactive lipids. The cytochrome P450 monooxygenases (CYP450) such as CYP450 2C and 2J isoenzymes, metabolize AA to epoxyeicosatrienoic acids (EETs) through epoxygenation of any of its four double bounds. Alternatively, AA is metabolized to prostacyclin, prostaglandins or thromboxane by cyclooxygenases. The vascular effects of the later class of lipids is well understood. However, despite over 30 year of research on EETs, their mode of action in the vascular system is still incompletely understood.

Methods

Since all 60 isoforms of CYP450 enzymes depend on the cytochrome P450 reductase enzyme (POR) for their function, we have generated an endothelial-cell-specific, tamoxifen-inducible knockout mouse of POR (ecPOR-/-).

Results

Knockout of POR in endothelial cells resulted in impaired endothelium-dependent relaxation to acetylcholine as determined by isometric tension recordings of isolated mouse aortic rings. Lipid measurements revealed reduced aortic levels of EETs (lipidomics, LC/MS) but increased aortic levels of prostanoids such as thromboxane and prostaglandins after endothelial-specific deletion of POR. The sensitivity to the thromboxane receptor agonist U46619 and prostaglandin E2 (PGE_2), was also increased by deletion of POR. Ex vivo incubation with a non-hydrolyzible EET (14,15-EE-8(Z)-E, EEZE) reverted the increased sensitivity to U46619 in ecPOR-/- to the levels of control mice. EETs had no effect on vascular tone in phenylephrine-preconstricted vessels but dilated vessel contracted with U46619 or PGE_2. As U46619 acts through RhoA-dependent kinase, this system was analyzed. Deletion of POR impacted gene expression of this pathway and inhibition of Rho-GTPase with SAR407899 decreased the sensitivity to U46619.

Conclusion

These data suggest that EETs act as competitive antagonists of prostanoid receptors and that lack of EET production sensitizes to vasoconstriction by the induction of the Rho kinase system.

B 07-14

Treatment with the mitochondria-targeted antioxidant (MitoQ) enhances nitric oxide bioavailability and metabolism in skeletal muscle microvascular endothelial cells derived from hypertensive rats.

C. C. Hansen[1], S. Møller[1], K. A. Wickham[1,2], L. Gliemann[1], Y. Hellsten[1]

[1] *University of Copenhagen, Department of Nutrition, Exercise and Sports, Copenhagen, Denmark*

[2] *Brock University, Environmental Ergonomics Lab, St. Catharines, Canada*

The MitoQ was a gift from Matteo Fiorenza for which we are thankful. The excellent technical support of Karina Olsen and Gemma Kroos is gratefully acknowledged.

Funding

The study was supported by Independent Research Fund Denmark – Medical Sciences (8020-00167B to Y.H), and by a grant from Lundbeck foundation (R289-2018-116 to Y.H.). Lastly by a grant from the Danish ministry of Culture (FPK.2018-0047 to L.G.)

Introduction

Excess formation of reactive oxygen species by mitochondria may decrease nitric oxide bioavailability and cause endothelial dysfunction. This study examined the influence of hypertension and the mitochondria targeted antioxidant MitoQ on mitochondrial respiration, redox potential and nitric oxide formation in rat primary endothelial cells isolated from skeletal muscle.

Methods

Limb skeletal muscle tissue from spontaneously hypertensive rats (SHR) and from Wistar control rats (WR_{con}) was used for isolation of microvascular endothelial cells. The cells were used for analysis of mitochondrial respiration, H_2O_2 and nitric oxide (NO) formation with high resolution respirometry, glycolysis, and the content of related proteins was determined. Measurements were conducted in control conditions and after 7 days of treatment of cells with MitoQ.

Results

The results reveal that, whereas mitochondrial respiration was similar in endothelial cells from SHR and WR_{con}, mitochondrial ROS formation was 109% higher and NOX 2 protein levels were 97% higher in SHR endothelial cells compared to WR_{con} cells (fig. 1). The expression of glutathione peroxidase-1 was 52% lower in SHR than WR_{con} cells. Incubation of cells with MitoQ lowered ROS formation in SHR cells, elevated the expression of superoxide dismutase and increased basal NO formation (fig. 1).

Conclusion

The results reveal spontaneously hypertensive rats presented a higher mitochondrial ROS formation. Furthermore it was demonstrated that redox balance and nitric oxide bioavailability is

markedly improved by treatment of with MitoQ in primary microvascular endothelial cells from skeletal muscle of spontaneously hypertensive rats.

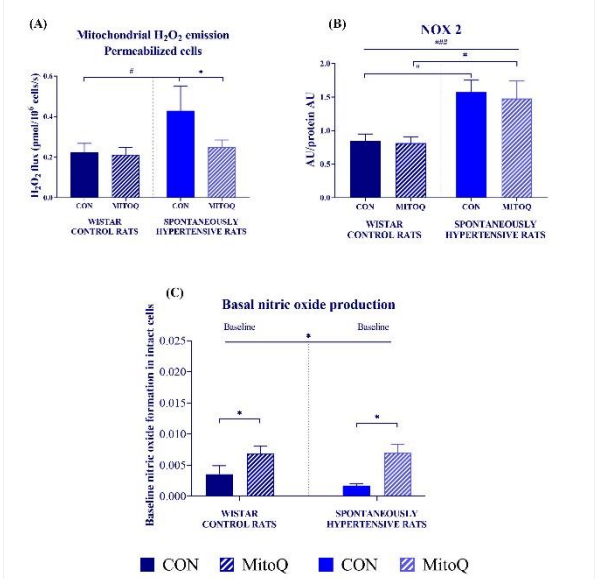

Figure 1. Redox potential including mitochondrial H2O2 emission and nitric oxide formation
(A) mitochondrial H2O2 emission in permeabilized cells at LEAK respiration in Complex I + II (n=8 for CON and n=4 for MitoQ treated cells for spontaneously hypertensive rats and Wistar control rats), (B) NOX2-gp91 protein expression (n=8 in each group), (C) Basal nitric oxide formation in intact cells (n=5 in each group) for endothelial cells from hypertensive and normotensive rats with and without MitoQ * denotes significantly different from CON, p<0.05. # denotes significantly different from Wistar CON, effect of hypertension, p<0.05. ### denotes p<0.001. Data are presented as mean ± SEM

B 07-16

Azithromycin induces autophagy in Vascular Smooth Muscle Cells.

R. Stamatiou[1], E. Kitharidi[1], A. Vasilaki[2], A. Hatziefthimiou[1]
[1] *university of Thessaly, Medical Department, Physiology Laboratory, Larissa, Greece*
[2] *university of Thessaly, Medical Department, Pharmacology Laboratory, Larissa, Greece*

Introduction
Respiratory and vascular inflammation lead to airway/vessel wall remodeling including hyperplasia and/or hypertrophy of smooth muscle cells. Azithromycin, a macrolide antibiotic, is used in low-dose, long-term treatment of chronic respiratory and cardiovascular inflammatory diseases. The aim of the present study was to investigate the effect of azithromycin on vessels, using both rabbit aortic SMC primary cultures (cellular level) and rabbit aortic rings (tissue level).
Methods
Cells and tissues were incubated with azithromycin (1-10μM) in the presence and absence of 10% FBS for 24-72 h. In cell cultures, the effect of azithromycin on autophagy was observed microscopically, in the presence or absence of the autophagy inhibitor 3methyladenine (3MA, 5mM). Cell viability was evaluated with Trypan blue staining. In aortic rings, the azithromycin (10μm) effect was studied after tissue sectioning and with the use of Cresyl Violet and Toluidine Blue stains as well as immunofluorescent localization of the autophagy markers Beclin and LC3.
Results
In vascular smooth muscle cell cultures, cell incubation for 24-72 h with azithromycin (1-10μM), in the presence or absence of 10% FBS, reduces cell number and induces the appearance of autophagic vacuoles (Fig. 1). The presence of 10μM AZM in the culture medium for 48h reduced VSMC number from 150000±12760 to 109400±7439 ($p<0.05$) while its presence for 72h reduced cell number from 154700±15390 to 39060±4688 ($p<0.001$; Fig. 1A). In the presence of 10% FBS, VSMCs proliferated and the effect of AZM on their number became apparent as early as after 24 hours in culture (Fig. 1B). Indicatively, in the presence of 10% FBS, after 24h 10μM AZM reduced cell number from 239100±19160 to 134400±28920 ($p<0.001$), after 48h from 360900±5337 to 243800±2552 ($p<0.001$) and after 72h from 435900±8606 to 315600±7439 ($p<0.001$; Fig. 1B). It is worth noticing, that even in the presence of AZM for 72h, VSMCs maintained their capability to proliferate in 10% FBS supplemented medium ($p<0.001$; Fig. 1B).
This effect was reversed by either azithromycin exclusion from the incubation medium or in the presence of 3MA (5mM). Furthermore, incubation of aortic rings for 24h with azithromycin (0.1 or 10μM) increased Beclin and LC3 immunoreactivity (Fig. 2) and promoted a wavy smooth muscle appearance.
Conclusion
In conclusion azithromycin, induces autophagy in vascular smooth muscles both in the cellular and the tissue level. The observed effect could demonstrate a positive way of azithromycin action beyond its anti-microbial and anti-inflammatory properties.

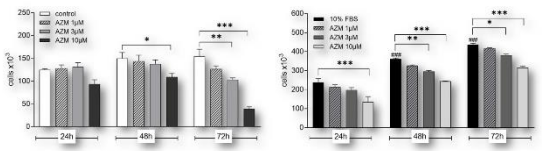

Figure 1. Effect of azithromycin (AZM 1 µM, 3 µM and 10µM) on vascular smooth muscle cell number after 24h, 48h and 72h of incubation, in the absence (A) or presence of 10% FBS (B). Values are presented as means (SE) of 4 independent experiments. *p<0.05, **p<0.01, ***p<0.001, compared to values of the relative control or 10% FBS alone and ###p<0.001, compared to cells incubated in the presence of 10% FBS for 24h.

The effect of AZM in vascular smooth muscle cell viability and proliferation

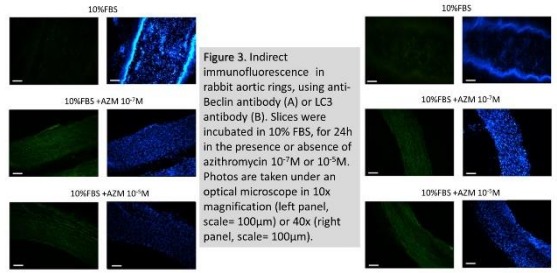

Figure 3. Indirect immunofluorescence in rabbit aortic rings, using anti-Beclin antibody (A) or LC3 antibody (B). Slices were incubated in 10% FBS, for 24h in the presence or absence of azithromycin 10^{-7}M or 10^{-5}M. Photos are taken under an optical microscope in 10x magnification (left panel, scale= 100µm) or 40x (right panel, scale= 100µm).

The induction of autophagy in vascular rings by AZM

B 07-17

Contribution of hypertension to microvascular smooth muscle bioenergetics in rats

C. Tranberg, S. Møller

University of Copenhagen, Department of Nutrition, Exercise and Sports, Copenhagen, Denmark

We thank Karina Olsen (Univ. of Copenhagen) for her technical assistance and expertise. The study is funded by the Independent Research Fund of Denmark - Medical Sciences and Lundbeck Foundation.

Background

We know that macro- and microvascular dysfunction is present in people with essential hypertension. Functional changes such as reduced nitric oxide availability occur in the vascular cells and is most likely due to an inactivation by reactive oxygen species (ROS). The mitochondria have been shown to be dysfunction in cardiovascular diseases, however, it is not known in which cell type, or in which segment of the vascular tree the dysfunction is found in.

Aim

To study the contribution of macro- and microvascular smooth muscle and endothelial cells on cellular metabolism in normo- and hypertensive rats.

Methods

Procedures were approved by the Danish National Animal Experiments Inspectorate. All animals received ad libitum tap water and standard chow. Microvascular cells were harvested from microvasculature found in skeletal muscle biopsies, and macrovascular cells from larger conduit vessels dissected from 13–14-week-old male normotensive Wistar rats and spontaneously hypertensive rats. Once isolated and confluent, mitochondrial respiration and ROS production were measured with high-resolution respirometry (O2k Oroboros) in isolated cells from normotensive (n= 4) and hypertensive (n= 3) male rats.

Results

The pilot study showed that there was no difference in respiration and ROS production between microvascular cells and the larger, conduit vessels (aorta and femoral) in normo- and hypertensive rats. In the microvascular smooth muscle cells, respiration was lower in the hypertensive rats compared to the normotensive, this was significant in the following: Complex I ($p<0.01$), Complex I + II (at physiological and maximal concentration, both $p<0.001$), Complex V/ATP synthase ($p<0.001$), with inhibition of Complex V and maximal respiration without Complex V (both $p<0.001$), and after inhibition of Complex I and Complex III ($p<0.001$). However, no difference was found in respiration between groups in the microvascular endothelial cells.

The ROS production in the microvascular smooth muscle cells was significantly higher in the hypertensive rats, with the inhibition of Complex V ($p<0.01$). In the large, conduit vessels there was a significantly higher ROS production in the hypertensive rats at Complex I ($p<0.001$).

Conclusion

According to the result of the pilot study, the microvascular smooth muscle cells seem to be dysfunctional in hypertensive rats compared with normotensive rats.

B 07-18

Serial block face-scanning electron microscopy and 3D image reconstruction of the murine retinal neurovascular unit.

M. Albargothy[2], E. Troendle[1], D. Steel[2], T. Curtis[1], **M. Taggart**[2]

[1] *Queen's University Belfast, Belfast, UK*

[2] *Newcastle University, NEWCASTLE UPON TYNE, UK*

Supported by the Randerson Foundation, Newcastle University. Northern Ireland Health and Social Care R&D Division (STL/4748/13) and MRC (MC_PC_15026).

The retinal neurovascular unit (NVU) performs a crucial role in matching blood delivery to meet the metabolic demands required of processing light signals for visual sensation. The NVU consists of many cell types including those of the capillary vasculature (endothelium and pericytes), macroglia (Müller glia and astrocytes), microglia and neurons (ganglion cells, bipolar cells, horizontal cells and amacrine cells; Simo et al., 2014). However, the three-dimensional complexity of heterocellular arrangements, certainly at the level of nanometre spatial resolution, remains to be fully characterised. This is important to establish in order to gain a deeper understanding of the possible mechanisms of neurovascular coupling and how these may be altered in diseases such as diabetic retinopathy. In this study, therefore, we have employed serial block face-scanning electron microscopy (SBF-SEM) and computational image reconstruction to obtain new information on the three-dimensional nature of heterocellular arrangements of the murine NVU.

Retinas were obtained from 3 month-old adult C57BL/6 mouse mice (killed by schedule 1 procedures), fixed, stained and embedded for analysis by SBF-SEM (Cocks et al., 2018). Up to 150 serial scanning electron microscopy images (70-100nm section depth; image pixel resolution of 6nm) of four individual capillaries in the superficial plexus were obtained (covering, in transverse cross-section, capillary lengths of 12µm-18µm). Examination of the data in the x-, y- and z-planes was performed with the use of semi-automated computational segmentation of cell features of interest, followed by 3D model reconstruction as required, using Micriscopy Image Browser(MIB v2.1; http://mib.helsinki.fi/), Amira (http://www.fei.com/software/amira-3d-for-life-sciences/) and/or Imaris (https://imaris.oxinst.com/) software. Upon 3D examination, a notable feature of retinal capillaries was the extensive sheath-like coverage by singular pericytes intervoven closely in a mesh-like manner with the basement membrane. Close approach of pericytes (<10nm) to the underlying endothelial cells was evident particularly in the regular appearance of peg-and-socket formations. Extremely thin processes of macroglia, especially Müller cells, typically made close contact to the basement membrane and, occasionally, pericytes. They usually formed a cellular barrier between the capillaries and neuronal cells of the NVU via a tortuous 3D arrangement albeit distances separating each cell membrane featured could be < ~20nm total.
This study presents new data on the nanoscale spatial characteristics in x-, y- and z-planes of hetrocellular and extracellular matrix components of the murine retinal NVU. This provides a platform from which to better inform our understanding of the structure-function relationships involved in the regulation of retinal neurovascular responses to physiological and pathophysiological stimuli.

References
[1] Simó, R., Stitt, A. and Gardner, T., 2014. Neurodegeneration in diabetic retinopathy: does it really matter?. *Diabetologia*, 61(9), pp.1902-1912.
[2] Cocks, E., Taggart, M., Rind, F. and White, K., 2018. A guide to analysis and reconstruction of serial block face scanning electron microscopy data. Journal of Microscopy, 270(2), pp.217-234.

B 07-19

Investigation into the role of omega-3 polyunsaturated fatty acids (ω-3 PUFAs) and their structural analogues on Kv7 channel function and vasodilator mechanism

K. Behnam, G. Cottrell, A. McNeish
University of Reading, Department of Chemistry, Food and Pharmacy, Reading, UK

British Heart Foundation FS/PhD/20/29049

Introduction
A well-known correlation between diet and disease is the relationship between fish consumption and cardiovascular disease prevention. Fish are a great source of cardioprotective ω-3 PUFAs, namely docosahexaenoic acid (DHA) and eicosapentaenoic acid (EPA). One of the effects of ω-3 PUFAs is their ability to evoke vascular relaxation and contribute to the maintenance of healthy blood pressure and vascular function. While their exact mechanism of action is largely unknown, many studies suggest that PUFAs may target specific ion channels in vasculature. Here we demonstrate that relaxations produced by ω-3 PUFAs are Kv7 dependent. We also further characterize the structural properties required to activate these channels.

Methods
Adult male Wistar Kyoto rats were killed by an overdose of isoflurane followed by cervical dislocation and 2 mm segments of aorta were dissected. Wire myography was used to examine the vasodilator activity of various PUFAs. U46619, (TP receptor agonist) was used to elicit a sub-maximal contraction (EC70-95%). Cumulative concentration response curves to PUFAs (100 nM-30 µM) were generated and repeated in the presence of a non-selective Kv7 channel blocker, XE-991. PUFAs were assessed to check the impact of the chain length, degree of saturation, head unit charge and position of the first ω and Δ double bonds on the relaxation. Data was expressed as the mean ± SEM and analysed using two-way ANOVA and Bonferroni post- hoc test (n≥5).
Results
The effects of PUFAs chain lengths were assessed by comparing relaxations to DHA (ω-3, 22:6), EPA (ω-3, 20:5) and stearidonic acid (SDA, ω-3, 18:3), which showed no significant difference between the compounds. Head unit charge was tested using DHA-gly (negative; ω-3, 22:6), DHA-methyl ester (neutral; ω-3, 22:6) and DHA-amine (positive; ω-3, 22:6). The charge is an important property that allows PUFAs to act on the Kv7 channels as DHA-gly was able to cause a significantly larger relaxation than DHA-methyl ester and DHA-amine. Monounsaturated FA, oleic acid (ω-9, 18:1), and a PUFA, SDA, were used to test the importance of FAs' saturation level which showed that they needed to be polyunsaturated to cause relaxation. Lastly, the effects of the position of the first double bond at the ω and Δ positions were measured using docosapentaenoic acid (DPA; ω-3, 20:5) and ω-6 DPA (ω-6, 20:5), respectively. The results from these experiments indicated that the position of the Δ double bond is one of the key features required for the relaxation within the aorta.
Conclusion
These results suggest that PUFAs cause relaxation of the aorta via Kv7 channels. Key structural properties appear to contribute to the responses observed, including a polyunsaturated aliphatic chain, negative head charge and position of the first Δ double bond. Future work will aim to confirm the subtypes of the Kv7 channels on which PUFAs act within the aorta, well as their expression and localisation within the tissue.

B 07-20

A2B agonists as vasorelaxants in pulmonary arteries

J. Lewandowski[1], D. Wenzel[1,2]
[1] *Ruhr-University Bochum, Department of Systems Physiology, Bochum, Germany*
[2] *University of Bonn, Institute of Physiology I, Bonn, Germany*

Introduction
G protein-coupled receptors (GPCRs) are important regulators of pulmonary blood pressure. The adenosine A2B receptor is a GPCR that can activate G_s, $G_{q/11}$, G_i and $G_{12/13}$ and was found to be upregulated in humans suffering from pulmonary hypertension (PH). In addition, adenosine levels are elevated under hypoxic conditions and adenosine is known to be involved in the regulation of vascular tone as well as smooth muscle cell growth, both pathophysiological characteristics of PH. Therefore, we were interested in the role of adenosine/A2B signaling in pulmonary arteries.
Methods
The effect of adenosine, A2B receptor agonists and antagonists on tone regulation of mouse large pulmonary arteries (PAs) was analyzed in isometric force measurements in a wire-myograph. Because small intrapulmonary arteries determine pulmonary vascular resistance and are therefore of pathophysiological relevance, we then also examined adenosine signaling in functional lung slices.

Results
In isometric force measurements, preincubation of mouse PAs with adenosine or the A2B specific agonist BAY 60-6583 (BAY) reduced a subsequent vascular tone increase by the vasoconstrictor 5-HT as demonstrated by a right shift of 5-HT dose response curves (EC_{50} Ade: -6.5 ± 0.02 (n=7) vs EC_{50} DMSO: -7.0 ± 0.03 (n=7), p<0.001; EC_{50} BAY: -6.5 ± 0.05 (n=7) vs EC_{50} DMSO: -6.9 ± 0.05 (n=7), p<0.001 (Two-way ANOVA)). These effects could be abrogated by additional preincubation with the A2B specific antagonist PSB-603 (PSB) (EC_{50} PSB+BAY: -6.5 ± 0.08 (n=7) vs EC_{50} DMSO: -6.6 ± 0.02 (n=7), p>0.05 (Two-way ANOVA)). In addition, single dose application of BAY after 5-HT-induced contraction caused a pronounced vasorelaxation in PAs (BAY: 21.0 ± 3.5% (n=8) vs DMSO: -0.6 ± 2.7% (n=8), p<0.001 (unpaired student's t-test)). Similar to the results in large PAs, adenosine caused a vasorelaxation in small intrapulmonary arteries of functional lung slices that was even stronger when BAY was applied (Ade: 36.3 ± 2.8% (n=7) vs DMSO: 7.6 ± 2.5% (n=10), p<0.01; BAY: 74.1 ± 10.4% (n=5) vs DMSO: 7.6 ± 2.5% (n=10), p<0.001 (One-way ANOVA)). Moreover, our experiments demonstrate a dose-dependent effect in response to different BAY concentrations (10^{-7}M: 0.8 ± 2.8%, p>0.05; 10^{-6}M: 12.1 ± 2.5%, p<0.01; 10^{-5}M: 33.5 ± 3.5%, p<0.001; 10^{-4}M: 49.6 ± 2.6%, p<0.001 compared to solvent control (Two-way ANOVA)) in functional lung slices.
Conclusion
These results reveal that adenosine and A2B agonists induce a prominent vasorelaxation in large and small PAs. Further experiments are required to determine the underlying signaling pathway and potential therapeutic effects of A2B activation in PH.

B 07-21
Sphingosine-1-phosphate receptor 2 activates gastrointestinal smooth muscle cell contraction via signaling pathways shared with prostaglandin E2
A. Evers, T. Noack, V. Wendel, R. Patejdl
Rostock University Medical Center, Oscar Langendorff Institute of Physiology, Rostock, Germany

Background & Motivation: Sphingosine-1-phosphate (S1P) signaling is involved in a plethora of physiological processes like cell migration, differentiation and contraction. Synthetic S1P-analogues are used as immunomodulators in multiple sclerosis and chronic inflammatory bowel disease. The prodrug FTY720 induces contractions of isolated rat gastric fundus which are mediated via the S1P-receptor 2 ($S1PR_2$)[1]. The cell-type specific expression of this receptor and the mechanisms underlying its activation are yet unknown.
The aim of this study was to elucidate the actions and cellular targets of intrinsically active S1P-analogue FTY720-P in isolated gastric fundus muscle from rats and mice.
Methods: Animals were anesthetized with ether (rats) or isoflurane (mice) and decapitated. Circular smooth muscle strips were excised and transferred to organ baths for isometric force recording or fixated for immunofluorescence staining. Following reference contractions evoked by high-K^+, FTY720-P induced effects and their modulation by preincubation with calcium channel blockers and responses to receptor antagonists were studied and quantified as % of the initial high-K^+-response. Indomethacin was used to exclude possible interactions between endogenous prostaglandins and FTY720-P.

To investigate their localization, double stains were made with antibodies labeling the $S1PR_2$-receptors and the cell-type specific markers c-kit (interstitial cells of Cajal, ICC), b-tubulin (neurons) and Iba1 (macrophages).
Results: The contractile actions of FTY720 could be prevented by blocking its endogenous activation by S1P-kinase using ABC294640. Exogenous application of FTY720-P induced similar concentration dependent increases in muscle tone in rats and mice (rats: 10µmol/L: 16.3%±11.8%, p<.001, n=25). Inhibiting the L-type calcium channels by nifedipine cancelled the FTY720-P effect almost completely whereas inhibiting the $S1PR_2$ by 1µmol/L JTE013 lead to a decrease of the FTY720-P effect (rat: 10µmol/L FTY720-P after JTE013: 5.6%±1,4%, p=.002, n=9). The application of the stable prostaglandin-E2-analogue $dmPGE_2$ lead to the annulment of FTY720-P effect: 10µmol/L FTY720-P after $5*10^{-10}$ mol/L $dmPGE_2$: -1,7%±6,4%, p<.001, n=14. Immunofluorescence of murine muscle strips revealed that $S1PR_2$ was expressed exclusively in smooth muscle cells (SMC).
Discussion: $S1PR_2$-receptors are expressed in rodent gastric fundus SMC and may contribute to the control gastric tone and filling. Both sphingosine- and prostaglandin pathways have been described to inhibit potassium channels, thereby subsequently activating voltage-dependent calcium channels [2–4]. We assume that this common pathway of both FTY720-P and prostaglandins may give rise to interactions between the S1P and the prostaglandins on the level of gastrointestinal motility.

References
[1] Kraft M, Zettl UK, Noack T, Patejdl R. The sphingosine analog fingolimod (FTY 720) enhances tone and contractility of rat gastric fundus smooth muscle. Neurogastroenterol Motil 30. Oktober 2018
[2] Ren J., The actions of prostaglandin E2 on potassium currents in rat tail artery vascular smooth muscle cells: regulation by protein kinase A and protein kinase C. Journal of Pharmacology and Experimental Therapeutics, April 1996.
[3] Coussin F, Scott RH, Nixon GF. Sphingosine 1-phosphate induces CREB activation in rat cerebral artery via a protein kinase C-mediated inhibition of voltage-gated K+ channels. Biochemical Pharmacology. November 2003;66(9):1861–70.
[4] Chang WT, Liu PY, Wu SN. Actions of FTY720 (Fingolimod), a Sphingosine-1-Phosphate Receptor Modulator, on Delayed-Rectifier K+ Current and Intermediate-Conductance Ca2+-Activated K+ Channel in Jurkat T-Lymphocytes. Molecules. 2. Oktober 2020;25(19):4525.

B 07-22
Evaluation of *in vitro* activities of guanine based purines in rat uterus
M.G. Zizzo[1,2], A. Cicio[1], R. Serio[1]
[1] *University of Palermo, Biological, Chemical and Pharmaceutical Sciences and Technologies (STEBICEF), Palermo, Italy*
[2] *University of Palermo, ATen Center, palermo, Italy*

Introduction: Recently, guanine-based purines have been shown to act not only as metabolic agents, but also as extracellular signaling molecules in nervous and muscular preparations, suggesting that guanine-based purines, as the well know adenine-based purinergic family, could

play a role in the modulation of the smooth muscle contractility. The goal of this study was to investigate the effects of guanine-based purines on spontaneous and pharmacologically –induced uterine contractions and the possible mechanism(s) of action.

Methods: Uterine horns from virgin Wistar rats were dissected out and isometric force was measured *in vitro* in strips of longitudinal myometrium. The effects of guanosine and guanine on the spontaneous uterine contractions were observed. Then the guanine based purine response was evaluated in uterine strips contracted by KCl (60mM) or oxytocin (5 nM).

Results: After establishing regular phasic contractions, cumulative application of guanosine (10 μM -3 mM), significantly inhibited spontaneous uterine contractility. Guanine (10 μM -3 mM) had no effects. The inhibitive effect of guanosine on the contraction of uterine smooth muscle in rats was blocked by NBTI, nucleoside uptake inhibitor, but it was not influenced by adenosine based receptor antagonist, by inhibitors of guanylate or adenylate cyclase or by potassium channel blockers. Guanosine was able to inhibit the external calcium (Ca^{2+}) influx-induced contraction, but it had no effect on the contraction induced by high-KCl solution. In addition, Guanosine significantly reduced the contraction induced by oxytocin, also in the absence of external Ca^{2+} entry.

Conclusions: Our data demonstrate a potent and consistent tocolytic effect of guanosine in rat myometrium both on spontaneous and oxytocin-induced contractions subsequently to its intracellular intake. Guanosine-inhibitory effects seem to involve the blockade of extracellular Ca^{2+} influx and modulation of intracellular Ca^{2+} release from the intracellular store. However, guanosine does not interact with L-type voltage gated calcium channel. K^+ channels or with cAMP or cGMP pathways. Although further studies are needed to identify the intracellular mechanism/s activated by guanosine, we feel that guanosine could be investigated as promising drug effective in the treatment of uterine spasmodic disorders.

B 07-23

Supplementation of n-3 polyunsaturated fatty acids, selenium, vitamin E and lutein in a form of functional food improves flow mediated dilation of brachial artery in patients with chronic coronary artery disease

A. Stupin[1,2], Z. Breškić Ćurić[2,3], K. Selthofer-Relatić[4,5], A.M. Masle[2,6], A. Kibel[1,5], B. Juranić[2,5], **I. Drenjančević**[1,2]

[1] *Faculty of Medicine Josip Juraj Strossmayer University of Osijek, Department of Physiology and Immunology, Osijek, Croatia*

[2] *Josip Juraj Strossmayer University of Osijek, Scientific Center of Excellence for Personalized Health Care, Osijek, Croatia*

[3] *General Hospital Vinkovci, Department of Internal Medicine, Vinkovci, Croatia*

[4] *Department of Internal Medicine, Faculty of Medicine Josip Juraj Strossmayer University of Osijek, Osijek, Croatia*

[5] *Department for Cardiovascular Disease, Osijek University Hospital, Osijek, Croatia*

[6] *Department of Rheumatology, Clinical Immunology and Allergology, Osijek University Hospital, Osijek, Croatia*

This study was funded by European Structural and Investment Funds to Science Centre of Excellence for Personalized Health Care, the Josip Juraj Strossmayer University of Osijek, Scientific Unit for Research, Production and Medical Testing of Functional Food, # KK.01.1.1.01.0010.

Introduction

Coronary artery disease (CAD), the most common type of heart disease and the leading cause of death in developed countries, is clinically manifested with established endothelial dysfunction (ED), which presents one of the earliest symptoms underlying various cardiovascular diseases (CVDs). It has been extensively reported that flow-mediated dilation (FMD) of the brachial artery in response to post-occlusive reactive hyperemia, assessed with ultrasounds, is impaired in patients with CAD, reflecting both local and systemic ED. Increased oxidative stress levels has been identified as a key pathophysiological mechanism mediating the development of ED. Thus, this study aimed to assess the effect of supplementation of cardiovascular protective and antioxidant nutrients (e.g. polyunsaturated fatty acids (n-3 PUFA), selenium, vitamin E and lutein) in a form of functional food on brachial artery FMD in patients with chronic stable CAD.

Methods

Thirty patients with diagnosed chronic stable CAD (9 women and 21 men) were instructed to eat three hard boiled hen eggs per day during study protocol that lasted for 21 days (total of 63 eggs). Subjects were divided in experimental NUTRI4 group (15 subjects) which consumed n-3 polyunsaturated fatty acids (n-3 PUFAs), selenium, vitamin E and lutein enriched hen eggs (1050 mg of n-3 PUFA/day, 0.06 mg of selenium/day, 3.29 mg of vitamin E/day, and 1.85 mg of lutein/per day), and in control group (15 subjects) which consumed regular hen eggs produced on the same farm (249 mg of n-3 PUFA per day, 0.05 mg of selenium/day, 1.79 mg of vitamin E/day, and 0.33 mg of lutein/per day). Brachial artery FMD (following 5-minute vascular occlusion) and nitroglycerin (NTG) dilation (following 400 mcg of NTG sublingual administration) were assessed using ultrasound and appropriate vascular probe (GE Healthcare Vivid iQ R2). Obtained images were analyzed by Brachial Analyzer for Research v.6 software (Medical Imaging Applications, USA).

Results

Brachial artery FMD significantly increased in NUTRI4 group following respective dietary intervention (FMD % of dilation before 6.84 ± 3.60 vs. after 9.14 ± 4.79, P=0.015), while it remained unchanged in controls (FMD % of dilation before 9.67 ± 3.60 vs. after 9.89 ± 3.26, P=0.850). Brachial artery NTG dilation did not significantly change in both NUTRI4 (NTG % of dilation before 13.70 ± 7.19 vs. after 12.38 ± 6.12, P=0.502) and Control group (NTG % of dilation before 14.42 ± 6.40 vs. after 14.46 ± 5.95, P=0.985) following respective dietary protocol.

Conclusion

Supplementation of n-3 PUFA, selenium, vitamin E and lutein in a form of functional food improves brachial artery FMD (endothelium dependent vasodilation), but not NTG dilation (endothelium-independent) in chronic CAD patients, potentially by providing more favorable lipid and antioxidant milieu.

B 07-24

Uncovering the mechanisms responsible for intravenous paracetamol-induced hypotension:NAPQI formation by the endothelial cells in the vascular wall

J. Dannesboe, J. Bastrup, T. A. Jepps, C. L. Hawkins

University of Copenhagen, Department of Biomedical Sciences, Copenhagen, Denmark

Introduction

Intravenous Acetaminophen (APAP) is used commonly in the intensive care unit or post-surgery for its analgesic effect. Intravenous administration of APAP is well documented to cause severe transient hypotension. The mechanism underlying these hemodynamic changes is still not clear, but the APAP metabolite N-acetyl-p-benzoquinone-imine (NAPQI) can directly and indirectly activate

voltage-gated Kv7 channels in vascular smooth muscle cells promoting a vasodilation. APAP metabolism to NAPQI requires cytochrome p450 enzymes. These enzymes are abundant in the liver, where oral APAP is metabolized, but are also present in the endothelial cells of the vascular wall.

Methods

Human Coronary Artery Endothelial Cells (HCAEC) and HEK293 cells were treated APAP (0 – 50 mM) or APAP metabolites to see the effect on viability and thiol concentration levels. The formation of APAP-adducts and cytochrome P450 expression and location was investigated by mass spectrometry, immunocytochemistry and immunohistochemistry of HCAEC and rat mesenteric arteries (rMA), respectively.

Results

APAP decreased HCAEC viability and thiol levels in a concentration dependent manner. The cytochrome P450 inhibitor Ketoconazole partially rescued the drop in viability and thiol levels. When cells are treated with NAPQI it decreases viability and thiol levels similarly to APAP and can partially recover the thiol levels after 24 h. Immunocytochemistry and immunohistochemistry showed that APAP-adducts are formed when treating HCAEC with APAP. Mass spectrometry revealed that CYP20A1 was one of the only cytochrome P450 enzymes both expressed in rMA and HCAEC and confirmed by immunocytochemistry and immunohistochemistry making it a strong potential candidate for being involved in APAP metabolism.

Conclusion

The decreased thiol levels suggest that HCAECs can metabolize APAP to NAPQI. CYP20A1 is a potential candidate endothelial P450 enzyme involved the metabolism of APAP. By improving our understanding of the metabolism of IV APAP, we might be able to prevent the iatrogenic hypotension.

B 07-25

Human Neuropsin (hOPN5) as a new tool to control gastric contractility

D. L. Zipf[1], M. Vogt[1], R. Patejdl[2], T. Bruegmann[1]

[1] *University Medical Center Göttingen, Institute for Cardiovascular Physiology, Göttingen, Germany*

[2] *Rostock University Medical Center, Oscar-Langendorff-Institute of Physiology, Rostock, Germany*

Gastroparesis is a burdensome disease characterized by impaired gastric emptying in absence of a physical obstruction, which is most often caused by dysfunctional coordination of smooth muscle cells (SMC) contraction due to loss of function of interstitial cells of Cajal and enteric nervous system. Unfortunately, there is currently no treatment that can effectively restore gastric emptying.

We have recently demonstrated direct optogenetic stimulation of SMC using the unselective cation channel Channelrhodopsin 2, allowing selective depolarization with high spatio-temporal resolution and thereby control gastric contractility and motility.

Herein, we explore direct optogenetic stimulation of SMC with human Neuropsin (OPN5). Human OPN5 is highly selective for G_q-proteins and can be activated by UV light (385 nm). We used a transgenic mouse model expressing human OPN5 in fusion with eYFP controlled by the chicken-β-actin-promotor. Macroscopic pictures of explanted stomachs showed clear eYFP signals in both longitudinal and circular muscle layers. Immunohistochemistry staining of cryosections revealed eYFP signals within smooth muscle actin positive SMC, which could not be found within enteric neurons or ICC, therein proving that OPN5 expression is restricted to SMC in the stomach. After single cell dissociation, we found eYFP expression in 38 ± 4% (n = 4) of SMC. To prove the function and characterize the efficiency, we performed isometric force measurements of antral smooth muscle strips, comparing UV light effects with the responses to electrical field stimulation (EFS), global depolarization by 60 mM K^+ and muscarinic receptor activation by 10 µM Carbachol. UV light (1.8 mW/mm^2, 5 s) induced 1.5 ± 0.2 mN (N = 5, n = 20) corresponding to ~72% of the force induced by electrical field stimulation and ~36% of the force induced by global depolarization with high K^+. Wiltype mice did not react to UV light but responded similarly to all other stimuli. When applying 1 µM TTX, a significant decrease was observed in EFS response ($p = 0.0089$, paired t-test, N = 2, n = 8) but not in UV light mediated response, further proving direct stimulation of SMC. To evaluate the role of electrical coupling via gap junctions for G_q-protein mediated activation spread within SMC layers, we investigated the effects of 30 µM Carbenoxolone on UV light mediated activation. The application of Carbenoxolone was abolishing the spontaneous activity of antral strips, which could not be observed for UV light stimulation.

In conclusion, we were able to demonstrate OPN5 ability to facilitate antral contractions in mouse stomachs by direct stimulation of SMC making it an exciting new option for optogenetic control of smooth muscle contraction. Although ChR2 mediated membrane depolarization was able to generate stronger contractions before, OPN5, being a human protein, is less likely to trigger immune responses and therefore a possible candidate for future treatment of gastroparesis.

B 07-26

Tubulin acetylation has an endothelial-dependent bimodal effect on vasorelaxations and is implicated in hypertension

A. M. Mozzicato, J. A. Bastrup, T. A. Jepps

Copenhagen University, Department of Biomedical Sciences, Copenhagen, Denmark

Introduction

Post-translational modifications (PTMs), such as acetylation, have been shown to contribute to the onset of various diseases, due to their ability to manipulate protein function, localization, and signaling pathways. PTMs affect the dynamic integrity of the microtubule network, with acetylation of the α-tubulin Lys40 site being linked to enhanced microtubule stabilization. Therefore, the aim of this study was to assess α-tubulin acetylation in the hypertensive model, as it relates to spontaneous hypertensive rat (SHR) vasorelaxation.

Methods

Vascular smooth muscle cells (VSMCs) were isolated from the mesenteric arteries of Wistar Kyoto (WKY), SHR, and control rats. To mimic increased acetylation, control VSMCs were subsequently treated with the histone deacetylase (HDAC)-6 inhibitor, tubacin. Isolated VSMCs were stained with α-tubulin and acetylated tubulin antibodies.Acetylation of the vessels was assessed by using Western Blot (WB) analysis to gauge acetylated tubulin and α-tubulin levels. Arteries were treated with tubacin and the eNOS inhibitor, L-NAME, which prevents nitric oxide release from the endothelium.

Results

Isolated VSMCs from SHR and WKY arteries showed an increase in the colocalization of acetylated tubulin with α-tubulin (P=0.03). Similarly, tubacin-treated VSMCs indicated an increase in this colocalization of acetylated tubulin (P=0.003). This was confirmed using WBs, to indicate an increase in acetylation of tubacin-treated arteries (P=0.009). Using wire myography, we were able to show that treatment of arteries with tubacin produced an endothelium-dependent bimodal effect

on the isoprenaline relaxation. Tubacin enhanced the isoprenaline-mediated relaxation when the endothelium was intact, but attenuated the relaxation in vessels treated with L-NAME (P<0.01).

Conclusion

HDAC-6 inhibitors, such as tubacin, are suggested as novel treatments for hypertension. Our findings show that HDAC-6 inhibition can improve vasorelaxations when the endothelium is intact, through a nitric oxide-dependent mechanism. Importantly, we also show that increased tubulin acetylation in vascular smooth muscle might be a hallmark feature of hypertension, contributing to reduced vasorelaxation in vascular beds with endothelial dysfunction. Thus, use of HDAC-6 inhibitors in humans with vascular disease needs to be carefully considered and monitored in future studies.

B 07-27

Ouabain potentiates the arterial contraction in an agonist-dependent manner.

D. Nielsen, V. V. Matchkov

Aarhus University, Department of Biomedicine, Aarhus, Denmark

Introduction

The Na,K-ATPase is a known regulator of numerous cellular functions, including dynamic regulation of ion concentrations and downstream signaling. Inhibition of the Na,K-ATPase with ouabain potentiates vascular contraction and this has been suggested mediated via elevation of intracellular Ca^{2+} and sensitization of contractile machinery to Ca^{2+} (1). The large conductance Ca^{2+}-activated K^{+}-channels (BK) co-localize with the Na,K-ATPase and regulate vascular tone via membrane potential control of Ca^{2+} influx (2). We aim here to examine a potential agonist-dependence pro-contractile action of ouabain, and an effect of simultaneous inhibition of both the Na,K-ATPase and the BK channels.

Methods

Rat mesenteric small artery segments were used for assessment of isometric force development to agonist stimulation with either thromboxane A2 analog, U46619, or methoxamine, Mtx. The effects of preincubation with either 10 µM ouabain, or 100 nM iberiotoxin (IbTx), or both on the contractile concentration-response curves were compared to matching time-controls with vessels from the same rat. The concentration-response curves were fitted to a four-parameter, nonlinear regression curves and derived parameters were compared with an extra sum-of-squares F test. Data are presented as means ± standard error of the means and P < 0.05 were considered significant.

Results

Ouabain significantly potentiated agonist-induced contraction during U46619 stimulation (n=4; Fig. 1) but not Mtx stimulation (n=7; Fig. 2). Inhibition of the BK channels with IbTx potentiated contraction in response to both U46619 (n=4) and Mtx stimulation (n=7). However, a combination of IbTx and ouabain had an additive effect only for U46619 concentration-response curve, while for Mtx-induced contraction, there was no difference between IbTx effect alone and in the presence of both IbTx and ouabain.

Conclusion

The data suggest that micromolar ouabain potentiates agonist-induced contraction of small mesenteric rat arteries in agonist-dependent manner, with no significant effect for Mtx contraction. The ouabain-dependent potentiation of U46619-induced contraction is additive to the pro-contractile action of the BK channel inhibition.

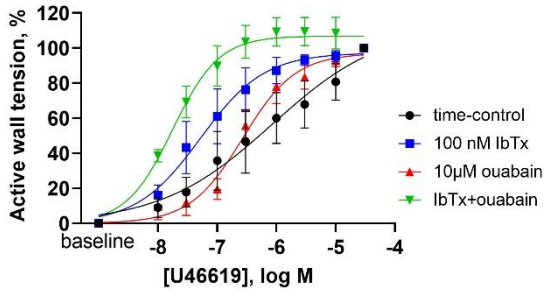

Figure 1.
The additive potentiating effect of both ouabain and iberiotoxin (IbTx) on U46619 concentration-response curve. The simultaneous recording of active wall tension changes (n=4). Mesenteric small arteries from the same rat were incubated with either 10 µM ouabain, or 100nM IbTx, or both, and compared to time-control. The curves were compared with an extra sum-of-squares F test and significant difference between time-control and ouabain (P<0.05), or IbTx (P<0.001), or both (P<0.001) was found.

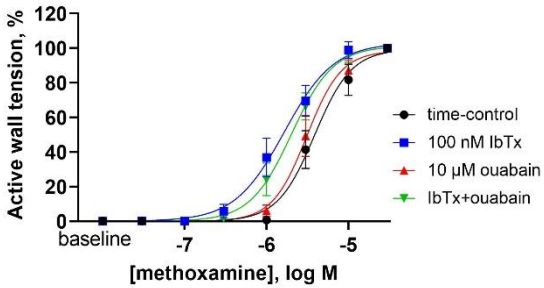

Figure 2. Iberiotoxin (IbTx), but not ouabain, potentiated mesenteric artery contraction to methoxamine (n=7). The simultaneous recording of active wall tension changes of arteries from the same rat, incubated with either 10 µM ouabain, or 100nM IbTx, or both. The curves were compared with an extra sum-of-squares F test and significant difference between time-control and IbTx ($P<0.001$), or both ($P<0.001$) was found.

References

[1] Bouzinova EV, Hangaard L, Staehr C, Mazur A, Ferreira A, Chibalin AV, Sandow SL, Xie Z, Aalkjaer C, and Matchkov VV. 2018. The alpha2 isoform Na,K-ATPase modulates contraction of rat mesenteric small artery via cSrc-dependent Ca(2+) sensitization. *Acta Physiol (Oxf)* 224: e13059.

[2] Jaggar JH, Porter VA, Lederer WJ, and Nelson MT. 2000. Calcium sparks in smooth muscle. *Am J Physiol* 278: C235-C256.

B 07-28

Mechanisms underlying synthesis and release of ET-1 in rat resistance arteries

K. M.R.M. Banecki, C. J. Garland, K. A. Dora

University of Oxford, Department of Pharmacology, Oxford, UK

This research was supported by a British Heart Foundation PhD Studentship awarded to Katherine M. R. M. Banecki.

Since its discovery, the potent vasoconstrictor peptide, endothelin-1 (ET-1) has been the subject of much research regarding its roles in various pathologies. Remarkably, there are still significant gaps in our knowledge regarding the mechanisms of storage and release of ET-1. Isolated rat pulmonary, mesenteric and coronary arteries were mounted in a wire myograph to record tension, and the same arteries were fixed and processed for en face immunohistochemistry. We show that in these arteries, basal expression of ET-1 in endothelial cells (ECs) is low; in mesenteric arteries, the percentage of ECs expressing ET-1 in arteries is 5 ± 2 % (n = 8), in pulmonary 7 ± 3 % (n = 9) and in coronary 19 ± 7 % (n = 8). Importantly, the formation and release of ET-1 in mesenteric arteries could be rapidly stimulated by the PAR1 thrombin receptor agonist TFLLR (5 µM), such that 29 ± 8 % of cells (n = 9) expressed ET-1 within 5 mins ($p = 0.033$, one way ANOVA with multiple comparisons using Tukey correction). To assess any paracrine actions, the subsequent release of ET-1 was assessed against TFLLR-mediated tone. The non-selective ET receptor antagonist bosentan (blocks both ET_A and ET_B receptors, 10 µM) reduced contraction to TFLLR such that at 10 and 20 mins incubation, it reduced from 6.9 ± 0.3 and 5.9 ± 0.3 mN/mm to 5.2 ± 0.5 and 4.3 ± 0.5 mN/mm, respectively ($p = 0.0232$ and $p = 0.0195$ respectively, two way ANOVA with multiple comparisons using Šidák correction). Nitric oxide (NO) is thought to inhibit ET-1 expression, yet L-NAME, a NO synthase inhibitor (100 µM), did not alter vasoconstriction to TFLLR ($p > 0.05$, mixed-effects analysis with multiple comparisons using Šidák correction). TFLLR enhancement of ET-1 expression was not observed in either the pulmonary or coronary arteries. The ability of thrombin receptor stimulation to increase expression and release of ET-1 in some but not all arteries is an important consideration in identifying the mechanisms operating in health and disease, and is the subject of ongoing investigation.

B 07-29

Investigation of the effect of paracetamol on spontaneous bladder detrusor smooth muscle contractions in female rats

Z. Ercan[1], E. Kacar[1], I. Serhatlioglu[1], M. G. Hekim[1], F. Tan[2]

[1] *Firat University, Elazig, Turkey*

[2] *Osmaniye Korkut Ata University, Osmaniye, Turkey*

Introduction

Paracetamol is a widely used pharmacological agent as an analgesic and antipyretic. The effectiveness of paracetamol, which is also widely used in urinary system diseases, on bladder contraction is unknown. The aim of this study was to investigate the effects of paracetamol on contractile activity of the isolated urinary bladder smooth muscle.

Methods

In the study Wistar-albino intact female rats were used (n=7). Urinary bladder strips (2 mm× 10 mm) were mounted in 5 mL organ baths containing with krebs solution at 37°C and pH 7.4, constantly bubbled with 95% oxygen-5% carbon dioxide. The area under the curves (AUC) and peak to peak (p-p) of isometric contractions of strips were measured. After the regulation period, paracetamol was added non-cumulatively at 1000µM and 2000µM concentrations. The AUC and p-p values were standardized as a % change before and after the application. The data was statistically analyzed using the SPSS 22.0 program with paired t test.

Results

Paracetamol caused a statistically significant decrease in the AUC and p-p values of spontaneous bladder contractions at 1000 µM and 2000 µM doses ($p<0.05$).

Conclusion

The results indicated that paracetamol had a significant inhibitory effect on urinary bladder smooth muscle contractions in vitro. This effect of paracetamol should be considered when used in clinical conditions where bladder contractile activity changes (overactive bladder, neurogenic bladder, etc.). This study may be a guide for its use in the treatment of bladder pathology in the future.

B 07-30

Salt-inducible kinase 3 (SIK3) regulates smooth muscle specific genes

C. Rippe, L. Liu, K. Swärd

Lund University, Department of Experimental Medical Science, Lund, Sweden

This work was supported by the Crafoord Foundation (20210920).

Introduction

Salt-inducible kinase 3 (SIK3) is one of three members of a family of kinases related to AMPK. These kinases regulate several metabolic and proliferative pathways (1). Correlation analyses have show that SIK3 is positively correlated with smooth muscle specific genes and that SIK3 is the isoform with highest expression in smooth muscle. The most well-known substrates of SIKs are class II histone deacetylases (HDAC) and cAMP-regulated transcriptional coactivators (CRTC). SIKs regulate the subcellular localization of these substrates by promoting cytoplasmic retention. Class II HDACs act on myocyte enhancer factor 2 (MEF2) in the nucleus and inhibits the transcription of genes (2). We propose that SIK3 can modulate the phenotype of smooth muscle cells by indirect regulation (derepression) of MEF2, which induces smooth muscle genes.

Methods

Human coronary artery smooth muscle cells (HCASMC) were transduced with ad-CMV-null, -MEF2A, or -SIK3. First we assessed if SIK3 overexpression induced smooth muscle specific genes. Then, an RNAseq was performed to assess the overlap in expression between SIK3 and MEF2A. A SIK inhibitor (HG 9-91-01) as well as a virus overexpressing a SIK3-mutand which lacks kinase activity was used to investigate the if gene expression is dependent on the kinase activity. We assessed mRNA and protein expression using western blot and qPCR respectively.

Results

We found that SIK3 upregulated a set of smooth muscle specific genes and that SIK3 and MEF2 showed a significant overlap of genes that were regulated in a similar manner, suggesting that MEF2 is involved in SIK3-mediated gene regulation. To study if the effects of SIK3 are mediated via phosphorylation of HDACs, we inhibited SIK by HG 9-91-01. However, we did not find a signifcant reduction in pHDAC or total HDAC7. When assessing the effect of the SIK3-kinase dead mutant, most of the genes that we studied did not seem to be dependent on the kinase activity.

Conclusion

We conclude that both SIK3 and MEF2A can regulate genes involved in the contractile phenotype of vascular smooth muscle, however, we cannot confirm a direct regulation through class II HDACs. Further studies are needed to shed light on the regulatory pathways of SIK3 in vascular smooth muscle cells.

References

[1] Darling NJ, Cohen P. Nuts and bolts of the salt-inducible kinases (SIKs). Biochem J. 2021;478(7):1377-97

[2] Lu J, McKinsey TA, Nicol RL, Olson EN. Signal-dependent activation of the MEF2 transcription factor by dissociation from histone deacetylases. Proc Natl Acad Sci U S A. 2000;97(8):4070-5

B 07-31

Doxorubicin mediated impairment of vascular tone and recovery by NRF2 antioxidant pathway activator CDDO.

A. Verma, P. Sharma, R. D. Rainbow

University of Liverpool, Department of Cardiovascular & Metabolic Medicine, Liverpool, UK

Anthracyclines are a class of anticancer agents widely employed in the treatment of solid organ tumours and haematological malignancies, with doxorubicin (DOX) considered most efficacious (1). While extensive research has highlighted DOX-induced cardiotoxicity, insight into vascular toxicity remains more elusive. Recent evidence suggests anthracyclines can mediate endothelial dysfunction and arterial stiffening, both during and after treatment (2, 3). Doxorubicin was recently shown to reduce phenylephrine mediated contraction, induce ex-vivo vascular stiffness, and impair endothelium-dependent relaxation (4). Hence, further insight into the changes in vascular function mediated by DOX is important as the vasculature is the primary tissue exposed to its toxic effects culminating in progressive vascular dysfunction, an antecedent to the development of future cardiovascular disease.

Methods

Briefly, male Wistar animals were culled, and mesenteric arteries removed for use on a Wire-Myograph following culture at 16°C in PSS (48h) and treatment with 1 μM DOX (24 h). 2nd order vessels were mounted from Wistar animals and held at a tension equivalent to a pressure of 90 mmHg.

Results

Contractile responses to Angiotensin II were reduced compared to untreated vessels ($p<0.01$) and restored in vessels co-treated with CDDO-me. Contractile responses in DOX treated vessels to cumulative concentrations of phenylephrine, UTP and endothelin I were attenuated and rescued by DOX/CDDO-me co-treatments. Dilatation by P1075, a potent K_{ATP} channel activator expressed as percentage of peak constrictor remained unchanged in DOX and DOX/CDDO-me co-treatments. Contractile desensitization was assessed for UTP using 5 min pulse of EC_{50} concentration of UTP, 5 mins washout, desensitising maximal concentration for 5 mins, wash and a final re-application of EC_{50} concentration of UTP for 5 mins. Desensitization was expressed by measuring the second response as a percentage of the first, a lower percentage representing more desensitization ($REC_{50(2)}/REC_{50(1)}$). Both, DOX ($p<0.01$ vs. untreated) and DOX/CDDO-me ($p<0.01$ vs. untreated) abrogated contractile desensitization. All data from 24 vessels from 4 animals were compared using one-way ANOVA (with Bonferroni's post-hoc test).

Conclusions

The results demonstrate that DOX attenuates contractile response and desensitization, with DOX/CDDO-me mediating contractile recovery in response to agents of known vasoconstriction and abrogated desensitization. Additionally, neither DOX nor DOX/CDDO-me mediated relaxation of tone, suggesting the effects of DOX at least in part for vasodilation may be driven through mechanisms other than those governed by potassium channels. These data are indicative that the deviation in vascular tone observed may be driven through the well cited pro-oxidant activity of DOX and the potential effect the potent activator of the NRF2 antioxidant pathway, CDDO may have in mediating recovery of vascular function.

References
[1] THORN, C. F., OSHIRO, C., MARSH, S., HERNANDEZ-BOUSSARD, T., MCLEOD, H., KLEIN, T. E. & ALTMAN, R. B. 201 Doxorubicin pathways: pharmacodynamics and adverse effects. *Pharmacogenetics and genomics,* 21, 440-446.
[2] HE, H., WANG, L., QIAO, Y., ZHOU, Q., LI, H., CHEN, S., YIN, D., HUANG, Q. & HE, M. 2020. Doxorubicin Induces Endotheliotoxicity and Mitochondrial Dysfunction via ROS/eNOS/NO Pathway. *Frontiers in Pharmacology,* 10.
[3] PARR, S. K., LIANG, J., SCHADLER, K. L., GILCHRIST, S. C., STEELE, C. C. & ADE, C. J. 2020. Anticancer Therapy–Related Increases in Arterial Stiffness: A Systematic Review and Meta‐Analysis. *Journal of the American Heart Association,* 9, e015598.
[4] BOSMAN, M., FAVERE, K., NEUTEL, C. H. G., JACOBS, G., DE MEYER, G. R. Y., MARTINET, W., VAN CRAENENBROECK, E. M. & GUNS, P. D. F. 2021a. Doxorubicin induces arterial stiffness: A comprehensive in vivo and ex vivo evaluation of vascular toxicity in mice. *Toxicol Lett,* 346, 23-33.

B 07-32

Identification of differentially expressed genes and functional activity of ion channels and receptors in rat vascular tissues

F. M. Alanazi[1,2], P. Sharma[1], R. D. Rainbow[1]
[1] *University of Liverpool, Department of Cardiovascular and Metabolic Medicine/Institute of Life Course and Medical Sciences, Liverpool, UK*
[2] *University of Tabuk, Department of Biology/Faculty of Science, Tabuk, Saudi Arabia*

I would like to thank and express my gratitude to my supervisors, Dr. Richard Rainbow and Dr. Parveen Sharma for their support, suggestion and guidance during experimental works.
I would also like to thank Tabuk University in the Kingdom of Saudi Arabia for funding this project and for granting me this scholarship.

Introduction

The vascular response to vasoconstrictors, dilators and pharmacological modulators is not equivalent in all vascular beds [4]. Smooth muscle cells (SMCs) are distinguished by their ion channels and receptors, which play an important role in regulating blood flow and vessel diameter [1,5]. Ion channels and receptors play a key role in the physiological function of arteries [3], but their expression profiles remain unclear [2]. This study aimed to assess the hypothesis that the expression profiles of ion channels and receptors differ according to the vascular bed. To specifically address this in a model system, the contractile response to uridine-5′-triphosphate (UTP) was investigated in arteries of various diameters in the rat mesentery.

Methods

Thoracic and abdominal aortic, 1st and 2nd order pulmonary and 1st to 4th order mesenteric arteries were dissected from Wistar rats. The vessels were used to perform deep RNA sequencing (next-generation sequencing) to determine gene expression profiles. A bioinformatics approach was then used to analyse the functional interactions. To confirm altered expression profiles, the effect of UTP on vessel tension was tested using a wire myograph.

Results

16814 differences in gene expression were identified between the vascular beds. The heat map revealed patterns of differential expression, while distance matrices indicated patterns of expression. In a principal component analysis plot, the first and second components for gene counts explained approximately 54 % of the total variance. The gene networks created from protein-protein interaction data presented biological processes that are affected by specific variations in gene expression. Furthermore, the concentration responses for UTP in different orders of arteries illustrated substantial differences in artery sensitivity based on the size of the vessels, which is confirmed by transcriptomics changes in P2X and P2Y receptors.

Conclusion

Our study demonstrated the physiological heterogeneity of vascular tissues between arterial beds, as reflected by our transcriptomic analysis. This finding may have significant implications for developing new treatments for vascular diseases. The study also established that arteries have a heterogeneous contractile phenotype throughout the vascular bed and that properties vary with artery size.

References
[1] Alexander, M.R. and Owens, G.K., 2012. Epigenetic control of smooth muscle cell differentiation and phenotypic switching in vascular development and disease. *Annual review of physiology, 74,* pp.13-40.
[2] Boerman, E.M., Sen, S., Shaw, R.L., Joshi, T. and Segal, S.S., 2018. Gene expression profiles of ion channels and receptors in mouse resistance arteries: Effects of cell type, vascular bed, and age. *Microcirculation, 25*(4), p.e12452.
[3] Dogan, M.F., Yildiz, O., Arslan, S.O. and Ulusoy, K.G., 2019. Potassium channels in vascular smooth muscle: a pathophysiological and pharmacological perspective. *Fundamental & clinical pharmacology, 33*(5), pp.504-523.
[4] Gitterman, D.P. and Evans, R.J., 2000. Properties of P2X and P2Y receptors are dependent on artery diameter in the rat mesenteric bed. *British journal of pharmacology, 131*(8), pp.1561-1568.
[5] Rensen, S.S.M., Doevendans, P.A.F.M. and Van Eys, G.J.J.M., 2007. Regulation and characteristics of vascular smooth muscle cell phenotypic diversity. *Netherlands Heart Journal, 15*(3), pp.100-108.

B 07-33

Venous Pulse Wave Velocity is affected by the magnitude of the Pulse Wave

L. Ermini[1], T. Sechi[2], G. E. Preston[2], S. Roatta[1]
[1] *University of Turin, Department of Neuroscience, Integrative Physiology Lab, Torino, Italy*
[2] *Polytechnic of Turin, Department of Electronics and Telecommunications, Torino, Italy*

Introduction

Venous Pulse Wave Velocity (vPWV) has been recently reconsidered as a possible marker of total blood volume changes thanks to the development of a non-invasive methodology adequate for human applications (1–3). However, unlike arteries, no reliable Pulse Waves (PWs) are present in the venous flow, making their exogenous generation necessary (e.g., by a rapid compression of the limb extremity). However, the PWV is generally dependent also on the magnitude of the perturbation and, more precisely, on the ratio among the local increment of pressure and volume (i.e., dP/dV), as theoretically stated by the Bramwell-Hill equation (4). Aim of this study is to experimentally

investigate the influence exerted by the magnitude of the elicited venous PW on the vPWV measurement, as a possible confounding factor.

Methods

vPWV was measured on the upper limb of 9 healthy volunteers (5M, age 22-32 yrs.) while they were lying supine, after 15 minutes of rest. Three different compression levels (100, 200, 300 mmHg of 1-s duration), in a randomized order, were delivered at the wrist by means of a pneumatic cuff. Eight compressions were delivered 15-s apart for each level. The passage of PW was proximally detected at the level of the basilic vein by Doppler ultrasound and vPWV computed as cuff to US-probe distance, divided by the pulse transit time (see Figure 1). The peak frequency of the Doppler shift was used as an indication of the vPW amplitude.

Results

Overall, the compression level did not have a significant effect on vPWV ($p=0.06$), as assessed by a Repeated Measures ANOVA (RM-ANOVA), while it did have on the peak frequency of the Doppler shift ($p<0.01$). However, increasing the compression extent from 100 to 300 mmHg induced an increase in vPWV of 9 ± 8 % ($p<0.05$, RM-ANOVA with Bonferroni adjustment for multiple comparisons) accompanied by an increase in the peak frequency of the Doppler shift of 52 ± 29 % ($p<0.01$, RM-ANOVA with Bonferroni adjustment for multiple comparisons). A visual representation of the whole results is given in Figure 2. Finally, the average Pearson correlation coefficient (computed after proper Fisher z-transformation) between vPWV and peak frequency values of each generated PW was 0.60 ± 0.41 ($p<0.01$, Wilcoxon signed-rank test).

Conclusion

In accordance with the Bramwell-Hill equation, we showed that the magnitude of the exogenously generated venous PWs, varied across a wide range, significantly affects their propagation velocity, although the observed changes in vPWV were on average moderate. The results suggest that the delivery of the compressive stimulus should be carefully implemented and monitored. Further studies are needed to elucidate whether monitoring the frequency peak of the Doppler shift can help to control for this confounding factor while measuring vPWV.

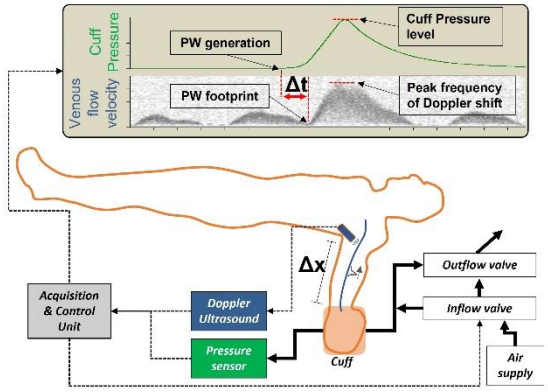

Figure 1
Experimental set-up for venous Pulse Wave Velocity (vPWV) measurement, which is computed as the ratio among the PW travelled distance (Δx) and the PW transit time (Δt). Further details are available elsewhere (1,2).

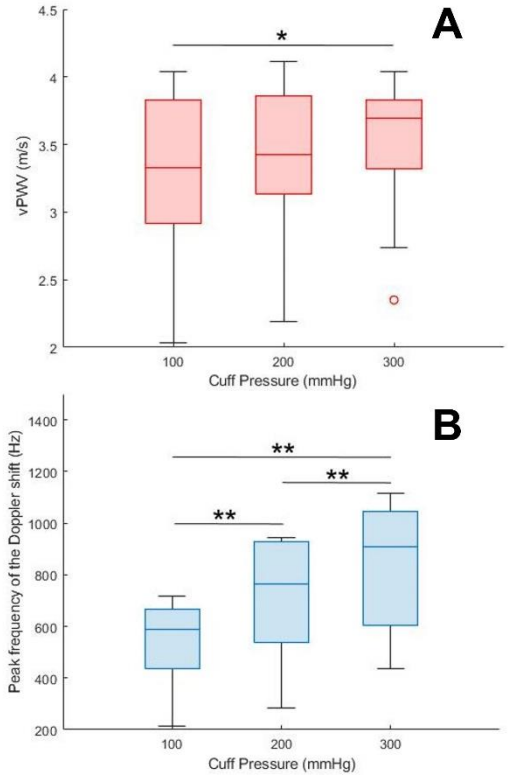

Figure 2
A) Distributions of the average venous Pulse Wave Velocity (vPWV) values for three different Cuff Pressure levels.
B) Distributions of the average Peak frequency of the Doppler shift values, related to the elicited Pulse Wave, for three different Cuff Pressure levels. The horizontal line within the colored boxes represents the median, while the vertical black bars represent the lower and upper quartiles. Asterisks indicate statistically significant differences, assessed by Repeated Measures ANOVA with Bonferroni adjustment for multiple comparisons: *p<0.05, **p<0.01.

References

1 Ermini L, Chiarello NE, De Benedictis C, Ferraresi C, Roatta S. 2021, "Venous Pulse Wave Velocity variation in response to a simulated fluid challenge in healthy subjects", *Biomedical Signal Processing and Control*, 63(1):102177, England: Elsevier

2 Ermini L, Ferraresi C, De Benedictis C, Roatta S 2020, "Objective Assessment of Venous Pulse Wave Velocity in Healthy Humans", *Ultrasound in Medicine & Biology*, 46(3):849–854, England: Elsevier

3 Barbagini A, Ermini L, Pertusio R, Ferraresi C, Roatta S 2022, "A Portable Device for the Measurement of Venous Pulse Wave Velocity", *Applied Sciences*, 12(4):2173, Switzerland: MDPI

4 Boutouyrie P, Briet M, Vermeersch S, Pannier B 2009, "Assessment of pulse wave velocity", *Artery Research*, 3(1):3–8, England: Atlantis Press

B 07-34

Salt Sensitivity is not Moderated by Duration of HAART Use Among Normotensive and Hypertensive HIV Patients in a Tertiary Hospital in Lagos

S. O. Elias[1], S. B. Ajisegiri[1], S. A. Bamiro[1], G. A. Umoren[1], A. A. Akinbami[2,3]

[1] *Lagos State University College of Medicine, Department of Physiology, Lagos, Nigeria*

[2] *Lagos State University College of Medicine, Department of Haematology, Lagos, Nigeria*

[3] *Lagos State University Teaching Hospital, Department of Haematology and Blood Transfusion, Lagos, Nigeria*

The authors appreciate all the patients who participated in the study.

Introduction

Salt sensitivity, the propensity to respond with significant changes in blood pressure in response to dietary salt change, has been reported among NT and HT Nigerians.[1] Regardless of blood pressure status, salt sensitivity worsens mortality especially among blacks.[2] Exposure to HAART has been reported to increase blood pressure after 5 years.[3] This study was designed to determine the effect of exposure to highly active antiretroviral therapy (HAART) on salt sensitivity among normotensive (NT) and hypertensive (HT) HIV patients in a tertiary hospital in Lagos.

Methods

Ethical approval was obtained from Lagos State University Teaching Hospital, Ikeja. Forty-four participants who had been on HAART for at least 6 months were recruited and divided equally into Group I (NT) and Group II (HT) after giving informed consent. All experiments were performed in accordance with the Helsinki Declaration. After measuring baseline parameters, blood pressure (BP), plasma and urine electrolytes were measured. Salt taste threshold (STT) was thereafter determined by having participants taste increasing concentrations (15 mmol/L to105 mmol/L) of freshly prepared NaCl solution; they were blinded to the identity and concentration of the preparations. Participants were divided into Low Salt Taster (LST), if their taste threshold was <60mmol/L and High Salt Tasters (HST) if >60mmol/L.[4] Statistical analysis was carried out using unpaired Student t test and two-way Analysis of variance (ANOVA) followed by Tukey's post-hoc test. Statistical significance was accepted at $P < 0.05$ level.

Results

Low Salt Tasters were higher among NT (73%) vs 46% among HT while High Salt Tasters were more among HST (55%) vs 27% among NT. The SBP and DBP in hypertensive LST were significantly higher ($P<0.0001$) compared to normotensive LST. Similarly, SBP and DBP were higher among hypertensive HST ($P<0.0003$) than normotensive HST. Plasma and urine sodium concentration in NT and HT LST and HST were not significantly different. Irrespective of duration, mean SBP and DBP among HT participants were significantly higher ($P< 0.003$; $P<0.0012$) than that of NT participants. Among both groups, SBP and DBP increased significantly from the 4-6y of exposure to HAART followed by a significant dip ($P<0.05$) in SBP and DBP at 7-9y duration HT, followed by further increase with increased duration. However, among the NT, DBP reduced significantly at 13-15y of exposure followed by a very significant increase in those with >15y of exposure. Plasma and urine electrolytes for NT and HT HIV participants were similar and within normal ranges throughout the different durations of HAART use.

Conclusion

The effect of HAART on blood pressure was significant from 4-6y of exposure although duration of exposure did not seem to affect salt sensitivity among the participants.

References

[1] Elias SO, Jaja SI, Sofola OA. J. 2014, 'Vascular Reactivity and Salt sensitivity in Normotensive and Hypertensive Adult Nigerian', *J Afr. Ass. Physiol. Sci*. 2:95-103

[2] Weinberger MH. 'Salt sensitivity is associated with an increased mortality in both normal and hypertensive humans', *J Clin Hypertens (Greenwich)*. 2002; 4(4):274-276

[3] Baekken M, Sandvik L, Oektedalen O. 2008, 'Hypertension in an urban HIV- positive population compared with the general population: influence of combination antiretroviral therapy', *J Hypertens*, 26:2126-2133

[4] Nikam LH 2015, 'Salt Taste Threshold and its Relation to Blood Pressure in Normotensive Offspring of Hypertensive Parents amongst Indian Adolescents', *Indian Journal of Physiology and Pharmacology*, 59:34-40

B 07-35

Antidiabetic Omarigliptin Dilates Rabbit Aorta by Activating Kv Channels and the SERCA Pump

R. Heo, M. Kang, W.S. Park

Kangwon National University, Department of Physiology/ College of Medicine, Chuncheon, South Korea

This work was supported by the National Research Foundation of Korea (NRF) grant funded by the Korea government (2021-R1F1A1045544, 2021-R1A4A1031574, 2020-R1F1A1052124)

Introduction

We investigated the vasodilatory effect of omarigliptin, an oral antidiabetic drug in the dipeptidyl peptidase-4 inhibitor class, and its related mechanisms using phenylephrine (Phe)-induced pre-contracted aortic rings.

Methods

Arterial tone measurement was performed in aortic smooth muscle cells.

Results

Omarigliptin dilated aortic rings pre-constricted with Phe in a dose-dependent manner. Pretreatment with the voltage-dependent K^+ channel inhibitor 4-aminopyridine significantly attenuated the vasodilatory effect of omarigliptin, whereas pretreatment with the inwardly rectifying K^+ channel inhibitor Ba^{2+}, ATP-sensitive K^+ channel inhibitor glibenclamide, and large-conductance Ca^{2+}-activated K^+ channel inhibitor paxilline did not alter its vasodilation. Pretreatment with the sarco/endoplasmic reticulum Ca^{2+}-ATPase (SERCA) pump inhibitors thapsigargin and cyclopiazonic acid significantly reduced the vasodilatory effect of omarigliptin. Neither cAMP/PKA-related signaling pathway inhibitors nor cGMP/PKG-related signaling pathway inhibitors modulated the vasodilatory effect of omarigliptin. Removal of endothelium did not diminish the vasodilatory effect of omarigliptin. Furthermore, pretreatment with the nitric oxide synthase inhibitor L-NAME or small-conductance Ca^{2+}-activated K^+ channelinhibitor apamin, together with the intermediate-conductance Ca^{2+}-activated K^+ channel inhibitor TRAM-34, did not influence the vasodilatory effect of omarigliptin.

Conclusion

Omarigliptin induced vasodilation in rabbit aortic smooth muscle by activating voltage-dependent K^+ channels and the SERCA pump independently of other K^+ channels, cAMP/PKA- and cGMP/PKG-related signaling pathways, and the endothelium.

B 07-36

Changes in the ion channels expression profile in murine macrophages from a metabolic syndrome model

P. Cidad, D. A. Peraza, S. Moreno-Estar, E. Alonso, J. R. López-López, M.T. Pérez-García
Universidad de Valladolid, Departamento de Bioquímica y Biología Molecular y Fisiología, Universidad de Valladolid; Unidad de Excelencia, Instituto de Biología y Genética Molecular (IBGM), CSIC, Valladolid, Spain Valladolid, Spain, Valladolid, Spain

Supported by grants PID2020-118517RB-I00 and VA172P20 and by a postdoctoral (DAPP) and predoctoral (SME) contracts of the Junta de Castilla y León.

Atherosclerotic cardiovascular disease is the leading cause of mortality worldwide in spite of progress in risk factors prevention and in medical treatments. A major reason for this trend is the ongoing epidemic of obesity-induced insulin resistance and type 2 diabetes (T2DM). T2DM is associated with an increased prevalence of vascular disease, with more aggressive forms of disease and worse outcomes after revascularization. Under T2DM conditions, chronic inflammatory signaling in the vasculature sustains endothelial dysfunction, leukocyte infiltration, and a pro-thrombotic environment. This low-grade metabolic inflammation appears to be triggered by the recruitment and activation of macrophages, which upon metabolic dysfunction switch to a metabolic-disease-specific phenotype (MMe) different from the classical M1 phenotype observed during infection (1).

We have previously found that Kv1.3 blockers inhibit smooth muscle cell proliferation, representing a novel target against restenosis. Moreover, systemic application of Kv1.3 blockers also ameliorates metabolic dysfunction in a T2DM mice model (2), acting on other yet unidentified cells different from vascular smooth muscle. In light of the importance of the macrophage in the pathogenesis of atherosclerosis in diabetes, we propose to explore the functional changes in macrophages metabolic phenotype (MMe), which could contribute to the increasing risk of vascular complications in T2DM, with a focus on ion channel remodeling upon metabolic dysfunction.

To generate a model with metabolic syndrome and T2DM, hypertensive (BPH) mice were fed on a high fat diet (HFD) for 12 weeks. Mice were anesthetized by isoflurane inhalation (5% O2 at 2.5 Lmin-1) and sacrificed by cervical dislocation following the EC guiding principles regarding the care and use of animals (Directive 2010/63/UE). We used bone marrow derived macrophages (BMDM) isolated both from male and female mice to evaluate possible gender-related differences, both under control and HFD conditions. We measured the mRNA expression levels of common macrophages markers (TNFα, IL10, CD36, iNOS). We characterized the expression profile of ion channels (Kv1.3, Kv1.5, Kir2.1, KCa3.1, P2RX1, P2RX1) and their functional contribution by electrophysiological studies, using kinetic and pharmacological tools to dissect the components of the currents.

A larger population of BMDM from HFD mice expressed CD36 marker, indicating a phenotypic change towards a metabolic phenotype. We found gender-related differences in ion channel expression. Compared to male, female BMDM from HFD mice showed changes in the relative contribution of Kv1.3 and KCa3.1 to outward K+ currents. Also, a decreased amplitude of the P2X1 component in female BMDM was observed both in control and in HFD.

Altogether, these changes in ion channel profile could contribute to define the metabolic-specific phenotype of macrophages that associates with the increase vascular risk in T2DM.

References

[1] Kratz, M, et al., 2014. Metabolic dysfunction drives a mechanistically distinct proinflammatory phenotype in adipose tissue macrophages. Cell Metabolism, 20(4), 614–625.

[2] Arévalo-Martínez M, et al., 2021. miR-126 contributes to the epigenetic signature of diabetic vascular smooth muscle and enhances antirestenosis effects of Kv1.3 blockers. Molecular Metabolism, 53:101306.

B 07-37

Pentosan polysulfate, an aggrecanase inhibitor modulates arterial stiffness in spontaneously hypertensive rats

A. Klosinska[1], K. Siew[2], T. Luo[3], N. Figg[1], S. Cleary[1], I. Sharif[4], C. Williams[4], I. Wilkinson[1], M. Sutcliffe[3], K. O'Shaughnessy[1], **Y. Yasmin**[1]
[1] University of Cambridge, Department of Medicine, Cambridge, UK
[2] University College London, Department of Renal Medicine, London, UK
[3] University of Cambridge, Department of Engineering, Cambridge, UK
[4] Covance CRS Limited, Department of Clinical Pharmacology, Huntingdon, UK

We acknowledge support by the National Institute for Health Research, Cambridge Biomedical Research Centre Award and all the staff involved at covance for their time.

Introduction

Arterial stiffness is an independent predictor of all-cause and cardiovascular mortality in many populations. Our recent research showed that loss of aggrecan integrity associates with age-related arterial stiffening in humans[1], and others have shown that inhibition of ADAMTS or aggrecanase enzymes, known to degrade aggrecan protein, improves cardiac function in an aortic banding rat model of heart failure[2].

Currently, there are no drug treatments that specifically target arterial stiffening in humans. However, we hypothesise that the ADAMTS inhibitor, Pentosan Polysulfate (PPS), used for treating interstitial cystitis in humans (Elmiron; oral capsule) and osteoarthritis in a veterinary setting (Cartrophen; injectable solution), represents an attractive candidate molecule that can be repurposed as a first-in-class drug treatment for age-related arterial stiffening.

Methods

To test this we performed an *in vivo* pharmacological experiment using 15wk old spontaneous hypertensive male rats (SHR) that were administered either PPS or vehicle control (n=7 per group) subcutaneously 3 times per week for 4 weeks. Animals were sacrificed on day 28, and fully intact aortae including other tissues (blood, cartilage, brain, etc.) were harvested and fixed in either RNALater or formaldehyde or frozen and stored at -80C for further investigations. Arterial wall thickness, stress-strain and failures stress biomechanical measurement were recorded, and tensile elasticity was calculated *ex vivo* as young's elastic modulus.

Results

Preliminary analysis showed that PPS significantly reduced the aortic wall thickening normally

associated with arterial stiffening in hypertension (Vehicle 225±6µm vs 204±6µm, p=0.0143). PPS also decreased aortic stiffening significantly at supraphysiological pressures in treated rats, and treated rats had a higher failure stress relative to vehicle controls.

Conclusion

This proof-of-principle study demonstrated that an aggrecanase inhibitor pentosan polysulfate can modulate aortic stiffness markers in SHR rats, but the short treatment period may not be adequate to reveal clinically significant differences. Further longitudinal studies are therefore, needed to establish if longer exposure to PPS can reduce aortic stiffness at clinically significant levels in older animals.

References

[1] Yasmin et al. The matrix proteins aggrecan and fibulin-1 play a key role in determining aortic stiffness. *Sci Rep. 2018 Jun 4;**8**(1):8550. doi: 10.1038/s41598-018-25851-5*.

[2] Vistnes M. et al. Penstisan polysulfate decreases myocardial expression of the extracellular matrixenzyme ADAMTS4 and improves cardiac function in vivo rates subjected to pressure overload by aortoc banding. *PLOS One 2014: **9**, e8923. doi: 10.1371/journal.pone.0089621*.

B 07-38

Effects of interferon gamma on endothelial barrier function are modulated by priming for the classical signaling pathway

M. Aslam

Justus Liebig University, Experimental Cardiology, Giessen, Germany

Introduction

Increased vascular permeability is a surrogate marker for the development of atherosclerotic lesions. During the progression of atherosclerosis, the expression of several cytokines, including interferon gamma (IFN-γ), is upregulated. The role of IFN-γ in the development and progression of atherosclerosis is a matter of debate due to evidence for both pro- and anti-atherogenic actions. While endothelial cell (EC) activation and loss of endothelial integrity is one of the major factors contributing to the progression of atherosclerosis, little is known about the effects of IFN-γ on EC barrier function and related signaling.

Methods

The study was carried out using cultured human umbilical vein ECs. Endothelial barrier function was determined by measuring the flux of albumen through EC monolayers cultured on filter membranes. Gene expression was measured by qPCR-based assays. Actin cytoskeleton remodeling was analyzed immunocytochemistry.

Results

Chronic treatment of confluent EC monolayers with IFN-γ (10 ng/mL) for 48 h attenuated thrombin-induced EC hyperpermeability, actin cytoskeleton remodeling, and loss of cell-cell junctions (n=5; $p<0.05$ for all further parameters). Thrombin induced a robust activation of RhoA, Rho kinase, and phosphorylation of myosin light chain (MLC; a marker of EC contractile activation), responses that were significantly attenuated by pre-treatment of EC monolayers with IFN-γ. Likewise, adhesion of freshly isolated human monocytes was significantly reduced on EC monolayers pre-treated with IFN-γ. When ECs were primed towards the classical IFN-γ/stat1 signaling pathway by short-term pre-treatment with PDGF (10 ng/mL; 3 h), all IFN-γ-mediated protective effects on endothelial barrier function, contractile activation, and cell-cell junction formation were surprisingly lost. In addition, IFN-γ transformed the PDGF-primed endothelial monolayers into the inflammatory state, resulting in increased adhesion of non-activated monocytes.

Conclusion

The present study demonstrates that the effects of IFN-γ on EC monolayers depend on the basal state of the ECs. In non-primed ECs, IFN-γ exerts EC barrier-protective effects, whereas in ECs primed for the classical pathway, IFN-γ has barrier-disruptive and pro-inflammatory effects.

B 07-39

Prediction of Physiologically RelevantRNA:DNA:DNA Triple Helix Formation Using Sequencing Data

T. Warwick[1,4], S. Seredinski[1,4], N. M. Krause[3], J. Kaur Bains[3], L. Althaus[5,6], J. A. Oo[1,4], A. Bonetti[7], A. Dueck[5,6], S. Engelhardt[5,6], H. Schwalbe[3], M. S. Leisegang[1,4], M. H. Schulz[2,4], R. P. Brandes[1,4]

[1] *Goethe University, Institute for Cardiovascular Physiology, Frankfurt, Germany*

[2] *Goethe University, Institute of Cardiovascular Regeneration, Frankfurt, Germany*

[3] *Goethe University, Institute of Organic Chemistry and Chemical Biology, Frankfurt, Germany*

[4] *Deutsches Zentrum für Herz-Kreislaufforschung (DZHK), Partner site Frankfurt Rhein-Main, Frankfurt, Germany*

[5] *Technical University Munich, Institute of Pharmacology and Toxicology, Munich, Germany*

[6] *Deutsches Zentrum für Herz-Kreislaufforschung (DZHK), Partner site Munich Heart Alliance, Munich, Germany*

[7] *AstraZeneca, Translational Genomics, Gothenburg, Sweden*

Introduction

The roles of RNA in epigenetics are numerous and important. Understanding the mechanisms by which RNA affects the epigenome is of great importance for physiology, basic research and RNA therapeutics alike[1]. One such mechanism is the formation of RNA:DNA:DNA triple helical structures at genomic regulatory elements, and subsequent modulation of gene expression and other epigenetic processes giving rise to downstream physiological consequences. Prediction of RNA:DNA:DNA interactions has previously relied on base-pairing rules established in artificial cell free, aqueous systems. However, novel sequencing methodologies capturing RNA-DNA interactions in a genome-wide manner provide input for improved predictive models.

Hypothesis

We hypothesised that by using triplexDNA-sequencing and triplexRNA-sequencing[2] as input to machine learning algorithms, the rules governing the formation of RNA:DNA:DNA triple helices could be learned and applied in the prediction of physiologically relevant RNA-DNA interactions.

Methods

Sequences underpinning triple helix formation in DNA and RNA were identified from sequencing data. These were used as input to an expectation-maximisation algorithm, which returned multiple probabilistic models linking DNA and RNA nucleotides. These models were then applied in a local alignment tool, *TriplexAligner*.

Results

TriplexAligner outperformed previously published predictive tools in accurate recall of genome-wide RNA-DNA interactions identified by either RADICL-sequencing[3] or RedC[4]. In particular, *TriplexAligner* performed best in prediction of *trans* RNA-DNA interactions. Using *TriplexAligner*, published RNA:DNA:DNA triple helix interactions with physiological consequences could also be

predicted. Amongst these were interactions involving the non-coding transcripts *HOTAIR*, *NEAT1*, and *SARRAH*[5]. Alignments arising from the novel models were validated biophysically using circular dichroism spectroscopy, electrophoretic mobility shift assays, and melting analysis.

Conclusion

RNA:DNA:DNA triple helix formation in cellular contexts is more complex than canonical methods suggested. Predictive models learned from genome-wide sequencing data predict RNA-DNA interactions more accurately than previous methods. This is of vital importance to the elucidation of RNA regulatory mechanisms responsible for changes in molecular physiology, as well as screening of potential RNA therapeutics.

References

[1] Oo, James A., Ralf P. Brandes, and Matthias S. Leisegang. "Long non-coding RNAs: novel regulators of cellular physiology and function." *Pflügers Archiv-European Journal of Physiology* (2021): 1-14.

[2] Sentürk Cetin, Nevcin, et al. "Isolation and genome-wide characterization of cellular DNA: RNA triplex structures." *Nucleic acids research* 47.5 (2019): 2306-2321.

[3] Bonetti, Alessandro, et al. "RADICL-seq identifies general and cell type–specific principles of genome-wide RNA-chromatin interactions." *Nature communications* 11.1 (2020): 1-14.

[4] Gavrilov, Alexey A., et al. "Studying RNA–DNA interactome by Red-C identifies noncoding RNAs associated with various chromatin types and reveals transcription dynamics." *Nucleic acids research* 48.12 (2020): 6699-6714.

[5] Trembinski, D. Julia, et al. "Aging-regulated anti-apoptotic long non-coding RNA Sarrah augments recovery from acute myocardial infarction." *Nature communications* 11.1 (2020): 1-14.

B 07-40

What are we learning from vascular physiology using Optoacoustic imaging?

T. F. Granja, S. F. Andrade, **L. M. Rodrigues**

Universidade Lusófona de Humanidades e Tecnologias, CBIOS Res Center Biosciences & Health Technoilogies, Lisbon, Portugal

This work is funded by national funds through FCT - Foundation for Science and Technology, I.P., under the UIDB/04567/2020 and UIDP/ 04567/2020 projects. Sergio Andrade is funded by Foundation for Science and Technology (FCT) Scientific Employment Stimulus contract with the reference number CEEC/CBIOS/NUT/2018.

Introduction

Recent research and developments in the field of functional imaging indicate it to be an useful path for relevant exploration of vascular physiology and pathophysiology [1]. Multi-spectral optoacoustic tomography (MSOT)offers an interesting potential for real-time assessment of *in vivo* vascular function. Following previous studies[2,3] we studied the vascular effects of a Post-Occlusive Reactive Hyperemia (PORH) maneuver in the forearm of healthy women of different ages using MSOT.

Methods

This exploratory study selected six healthy women divided by age in group I (GI),26.5 ± 5.0 years old and group II (GII), 49.0 ± 6.3 years old, after informed written consent. The protocol was previously approved by the institutional ethical committee (CE.ECTS/P10.21). The PORH was obtained in one forearm after occlusion of the brachial artery (the same side) with a cuff inflated (200 mmHg) for 1 minute. Recordings were obtained with an MSOT instrument (iThera Medical, Germany) at 900 nm for HbO_2, and 760nm for Hb The signal evolution of these chromophores was followed continuously during rest, occlusion, and post-occlusion until full recovery. Statistical analysis was performed in Graphpad Prism version 9 and a 5% significance level was applied.

Results

MSOT videos were reconstructed to quantify HbO_2 and Hb within our defined 15mm^3 volume regions of interest (ROI). From these, the mean saturation of oxygen (mSO_2) and total Hb (HbT) could be calculated. Unlike the classical POHR decay obtained with laser Doppler flowmetry usinga single measurement point, occlusion evokes chromophore increase in larger vessels due to stasis. After pressure release, perfusion is resumed and velocity and recovery times calculated. Our results indicate that both recovery and reoxygenation times are longer in the older participants.

Conclusion

MSOT offers a different functional approach to vascular study. The depth and extension (spatial resolution) obtained with this instrument contrasts with the limited single-point measurements provided by laser Doppler flowmetry or by photopletysmography. As shown with this exploratory PORH maneuver, this possibility to test vascular performance and involved adaptive mechanisms in real-time opens a wide area of applications with clinical interest that should be explored.

References

[1] Guerraty, M., Bhargava, A., Senarathna, J., Mendelson, A. A. & Pathak, A. P. Advances in translational imaging of the microcirculation. Microcirculation. 28 (3), e12683, doi:10.1111/micc.12683, (2021)

[2] Wang, L. V. & Yao, J. A practical guide to photoacoustic tomography in the life sciences. Nat Methods. 13 (8), 627-638, doi:10.1038/nmeth.3925, (2016).

[3] Granja, T., Andrade, S. & Rodrigues, L. Optoaccoustic Tomography – good news for microcirculatory research: Tomografia Optoacústica – boas notícias para a investigação microcirculatória. Biomedical and Biopharmaceutical Research. 18 1-13, doi:10.19277/bbr.18.269, (2022).

B 07-41

Impaired Soluble Guanylyl Cyclase in Aging Mouse Mesenteric Arteries

F. B. Lichtenberger, C. Zhong, M. Xu, C. Erdogan, P. B. Persson, A. Patzak, P. H. Khedkar

Charité – Universitätsmedizin Berlin, Institute for Translational Physiology, Berlin, Germany

A.P. and P.B.P. were funded by DFG for 1368, and SFB 1365

Introduction

With age, arterial functionality changes, including increased vasoconstriction and decreased vasorelaxation, affecting blood flow and organ function, leading to cardiovascular disease. The age-related decrease in endothelium-dependent vasodilation is not necessarily associated with structural

changes in the arterial wall. NO is the primary dilatation mediator in many vascular beds, such as mesentery and kidney.
The role of the endothelial compartment has been widely investigated, whereas knowledge about NO-induced signalling in aged vascular smooth muscle cells (VSMC) is still very limited.

Methods

We analysed the vessel function of mesenteric arteries of juvenile (~13 weeks) and aged (~40 weeks) male mice (C57BL/6) with a wire myograph. A direct cGMP ELISA kit was used to measure the cGMP concentration in isolated mesenteric arteries. mRNA expression of sGC subunits and PDE isoforms were analysed by qPCR. Van Gieson staining was used to compare arterial dimension of juvenile and aged aorta and mesenteric arteries.

Results

Aged vessels in comparison to juvenile vessels showed a reduced Acetylcholine (Ach)-induced relaxation. Bolus application of vasorelaxans such as NO donor sodium nitroprusside (SNP) as well as soluble guanylyl cyclase (sGC) activation by runcaciguat caused slower responses in aged vessels. This was accompanied by lower cGMP concentrations and a weaker response to the PDE5 inhibitor (sildenafil) in aged vessels. The mRNA expression of the α1 and α2 subunits of sGC as well as PDE5 mRNA was higher in juvenile animals. Beside differences in function and gene expression, no histological changes in mesenteric arteries and aortas was observed between groups.

Conclusion

Altered NO signalling in VSM can already be seen in mice at an early age, even in the absence of histopathological changes. Decreased sGC activity hallmarks aged vessel dysfunction.

References

[1] Zhong, C.; Xu, M.; Boral, S.; Summer, H.; Lichtenberger, F.-B.; Erdogan, C.; Gollasch, M.; Golz, S.; Persson, P.B.; Schleifenbaum, J.; et al., Age Impairs Soluble Guanylyl Cyclase Function in Mouse Mesenteric Arteries. Int. J. Mol. Sci. 2021, 22, 11412.

[2] Wennysia, I.C.; Zhao, L.; Schomber, T.; Braun, D.; Golz, S.; Summer, H.; Benardeau, A.; Lai, E.Y.; Lichtenberger, F.B.; Schubert, R.; et al. Role of soluble guanylyl cyclase in renal afferent and efferent arterioles. Am. J. Physiol. Renal. Physiol.2021, 320, F193–F202.

B 07-42

Human vascular endothelial cells display vessel type-specific inflammatory profiles and response to EGF

V. Dubourg, B. Schreier, G. Schwerdt, M. Kopf, S. Mildenberger, M. Gekle
Martin-Luther University Halle, Julius Bernstein Institute of Physiology, Halle (Saale), Germany

Endothelial cells (EC) constitute the inner layer of blood vessels and are key players in vascular homeostasis and inflammation. Usually considered uniform in experimental settings, EC can however originate from structurally and functionally different vessels, suggesting inherent differences in between cells from various vessels and different responsiveness to external stimuli.
Here we performed a deep transcriptomic analysis to compare human aortic endothelial cells (HAoEC) and coronary endothelial cells (HCAEC), combining RNA-sequencing and functional analysis. Additionally, we subjected these cells to stimulation with Epidermal Growth Factor (EGF), a well-described vascular active substance, in order to compare their reactivity.

Our analysis revealed that HAoEC and HCAEC had different transcriptomic footprints and that their differentially expressed genes were partly found enriched in pathways related to inflammation (based on Gene Ontology Enrichment analysis), suggesting distinct inflammatory profiles in aortic and coronary arteries.
Additionally, the activation of these cells by EGF appeared to trigger both a general and a cell-type specific effect, not only quantitatively (number of regulated genes) but also qualitatively (putatively affected cellular functions). Indeed, further analysis (based on QIAGEN Ingenuity Pathway Analysis) suggested that the EGF-induced changes in gene expression associate with vasculature-related functions for both cells types. However, EGF also appeared to potentially enhance the intrinsic differences in inflammatory profiles, by specifically increasing a HCAEC-driven leukocyte attraction, while downregulating the expression of adhesion molecules and chemoattractants in HAoEC.
Finally, we selected inflammation markers in order to confirm experimentally some of the hereinabove bioinformatics predictions. We thus observed that HAoEC and HCAEC displayed different basal expression levels for cytokines (IL-8 and MCP-1) and adhesion molecules (VCAM1 and ICAM1), that were additionally regulated by EGF in a cell type-dependent manner.
Taken together, our study highlights that, although they are both vascular endothelial cells, HAoEC and HCAEC are distinguishable, especially regarding inflammation regulation, what may be particularly relevant for vascular maintenance but also dysfunction.

B 07-43

Imaging microvascular dynamics at a sub-millisecond scale.

A. G. Olmos, **D. Postnov**
Aarhus University, Center of Functionally Integrative Neuroscience, Department of Clinical Medicine, Aarhus, Denmark

Structural and functional abnormalities in the microvasculature (vessels ≲100μm in diameter) are associated with leading causes of disability worldwide[1], including hypertension, stroke, diabetes, and dementia. Furthermore, these abnormalities precede noticeable changes in blood pressure or sugar levels making monitoring them pivotal in early diagnostics[2]. Some critical biomarkers, such as small arteries' stiffness and local hemodynamic resistance, can theoretically be measured non-invasively by characterizing the pulse wave propagation through the microvasculature. In practice, however, conventional tools cannot accurately capture the pressure wave propagating through the small vessels due to spatial and/or temporal resolution limitations. Because of these limitations, assessment of stiffness and pulse waveform characteristics remain primarily available in large arteries and aorta.

To resolve this problem, we have developed High-Speed Laser Speckle Contrast Imaging[3,4] (HS-LSCI) – the first optical technique to allow full-field blood flow imaging at >5000 frames per second. In HS-LSCI we utilize a high-speed camera (6000 frames per second at 1024x1024 pixels, Photron Nova s6, USA) and an optimized optical system to record laser speckle fluctuations over a large field of view while maintaining laser radiation below the maximum permissible exposure level. Recorded intensity passes through several layers of contrast analysis and segmentation to produce low-noise high-framerate blood flow index images, which are then used for further biomarkers extraction.
We demonstrate HS-LSCI's ability to image propagation of the cardiac pulse wave in the microcirculation by using it to image brain perfusion in an anaesthetized mouse (C57BL/6J, 3 months old, 2% isoflurane, chronically implanted cranial window). We use the captured blood flow

data to estimate the pulse wave velocity, stiffness, pulsatility and resistivity indexes (see Fig 1 for examples of measured biomarkers). Furthermore, we demonstrate that HS-LSCI provides more than ten times improved sensitivity to the blood flow changes in small arteries compared to the conventional laser speckle contrast imaging (LSCI). Overall, we conclude that HS-LSCI provides new, invaluable information for vascular research and has the potential to become the first tool to monitor microcirculatory stiffness in animal models and humans.

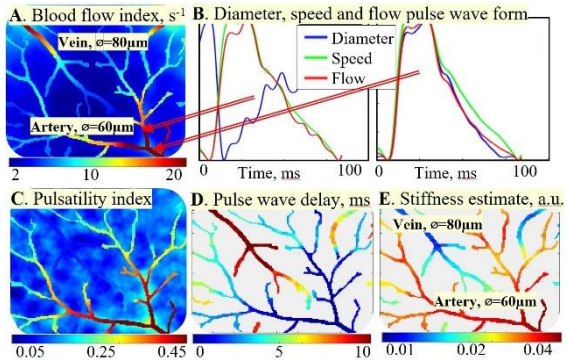

Figure 1. Exemplary biomarkers measured with HS-LSCI. **A** - Quantitative blood flow index (s-1). **B** - Diameter and flow changes during a single cardiac cycle in parent-daughter small artery branches. **C** – Corresponding pulsatility index. **D** and **E** - Pulse wave delay relative to the pulse onset in the artery and corresponding stiffness estimate.

References

[1] Levy BI, Schiffrin EL, Mourad JJ, Agostini D, Vicaut E, Safar ME, Struijker-Boudier HA. Impaired tissue perfusion: a pathology common to hypertension, obesity, and diabetes mellitus. Circulation. 2008 Aug 26;118(9):968-76..

[2] Buus NH, Mathiassen ON, Fenger-Grøn M, Præstholm MN, Sihm I, Thybo NK, Schroeder AP, Thygesen K, Aalkjær C, Pedersen OL, Mulvany MJ. Small artery structure during antihypertensive therapy is an independent predictor of cardiovascular events in essential hypertension. Journal of hypertension. 2013 Apr 1;31(4):791-7

[3] Olmos AG, Postnov DD. High-speed laser speckle contrast imaging. Patent pending, application number EP 22173808. 2022

[4] Postnov DD, Tang J, Erdener SE, Kılıç K, Boas DA. Dynamic light scattering imaging. Science advances. 2020 Nov 6;6(45):eabc4628

B 07-44

Changes in arterial stiffness measures CAVI (cardio-ankle vascular index) and kCAVI (knee CAVI) induced by head-down and head-up tilt

B. Czippelová[1,2], Z. Turianiková[1,2], D. Švec[2], M. Javorka[2]

[1] *Comenius University, Jessenius Faculty of Medicine in Martin, Biomedical Centre Martin, Martin, Slovakia*

[2] *Comenius University, Jessenius Faculty of Medicine in Martin, Department of Physiology, Martin, Slovakia*

Supported by grants VEGA 1/0200/19, 1/0283/21

Introduction

Cardio-ankle vascular index (CAVI) is a measure non-invasively estimating arterial stiffness from aortic arch to distal arteries of the lower extremities. CAVI reflects not only the structural changes in the vessel wall, related to the atherosclerotic process, but also the functional stiffness – i.e. arterial tone modulated by sympathetic activity. An alternative index kCAVI, measured from heart to knee, covers smaller part of the peripheral circulation able to react to changes in autonomic nervous system. The aim of our study was to evaluate the effect of changes in systemic vascular resistance (SVR) modulated by sympathetic activity elicited by head-down tilt (-10°) and head-up tilt of two inclinations (20°, 40°) on parameters CAVI and kCAVI.

Methods

In our study we examined 16 volunteers (4 females, age 21.8 ± 1.8 y).CAVI and kCAVI were measured using VaSera VS1500 device. SVR was assessed using the formula: SVR=80*(mean MBP/mean CO), where MBP is mean blood pressure measured on beat-to-beat basis (Finometer) and CO is cardiac output measured using impedance cardiography (Itamar Medical). Median values of 300 heart beats of MBP and CO were used for the calculation of SVR. All parameters were measured in supine position, in head-down tilt position (-10°) and two head-up tilt positions (20°, 40°). ANOVA with Post Hoc test for repeated measures with Bonfferoni correction was used for statistical analysis.

Results

Compared to the supine position, CAVI as well as SVR were significantly higher at both angles of HUT($CAVI_S$ = 5.81 ± 0.54, $CAVI_{20}$ = 6.75 ± 0.53, $CAVI_{40}$ = 7.76 ± 0.93; SVR_S = 1041.1 ± 170.9, SVR_{20} = 1176.7 ± 216.3, SVR_{40} = 1214.7 ± 209.1). Stiffness index kCAVI was significantly higher than kCAVI in supine position only in 40° head-up tilt ($kCAVI_S$ = 5.61 ± 0.54, $kCAVI_{20}$ = 5.99 ± 0.44, $kCAVI_{40}$ = 6.76 ± 0.99). Head-down tilt did not provoke significant changes in the monitored parameters. See Fig.1.

Conclusion

The results of our study suggest that CAVI is sensitive to changes in systemic vascular resistance provoked by head-up tilt. Alternative stiffness index kCAVI, measured form heart to knee, seems to be less sensitive to changes in systemic vascular resistance, because stronger stimulus (HUT in 40°) was needed to elicit significant changes in kCAVI. In addition, from our results we can hypotetize that in addition to peripheral vasomotor activity (affecting the diameter of the peripheral arteries), sympathetic activity also affects the arterial stiffness of the aorta and femoral arteries, which can be documented by increased kCAVI in 40° HUT.

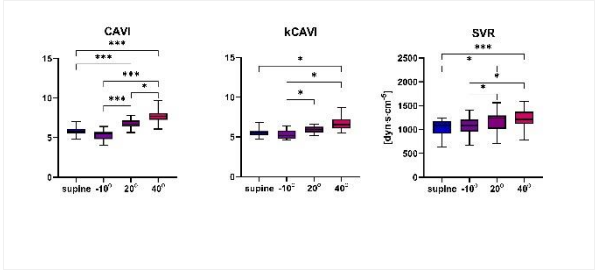

Fig.1
Cardio-ankle vascular index (CAVI), knee CAVI (kCAVI), systemic vascular resistance (SVR) in supine position, -10° HDT, 20° HUT, 40° HUT, * p < 0.05, *** p < 0.001

B 07-46

Bosentan Effects on Selected Erythrocyte and Plasma Parameters in Monocrotaline Model of Pulmonary Arterial Hypertension

T. Jasenovec[1], D. Radosinska[2], M. Kollarova[1], N. Vrbjar[3], P. Balis[3], S. Trubacova[4], L. Paulis[4], L. Tothova[5], J. Radosinska[1,3]

[1] *Comenius University in Bratislava, Faculty of Medicine, Institute of Physiology, Bratislava, Slovakia*

[2] *Comenius University in Bratislava, Faculty of Medicine, Institute of Immunology, Bratislava, Slovakia*

[3] *Slovak Academy of Sciences, Centre of experimental medicine, Bratislava, Slovakia*

[4] *Comenius University in Bratislava, Faculty of Medicine, Institute of Pathophysiology, Bratislava, Slovakia*

[5] *Comenius University in Bratislava, Faculty of Medicine, Institute of Molecular Biomedicine, Bratislava, Slovakia*

This study was supported by the Scientific Grant Agency of the Ministry of Education, Science, Research and Sport of the Slovak Republic - grant No. VEGA 1/0193/21 and 2/0153/21, grant from Slovak Research and Developing Agency - APVV -18-0287 and grant from The Austrian Research Promotion Agency - FFG 872313.

Introduction

Pulmonary arterial hypertension (PAH) is a rare, but serious disease with poor prognosis. To elucidate its pathogenesis, monocrotaline (MCT) model was developed. After injection, MCT is bound to erythrocytes. In the oxygen-rich environment of pulmonary precapillary arterioles and capillaries, MCT is released and causes endothelial cell damage, leading to vascular remodeling and PAH development. Several parameters of erythrocytes, including their deformability, aggregability and nitric oxide production are worsened in patients with PAH. However, changes in erythrocyte parameters have not yet been fully described in the MCT model of PAH. Bosentan is an available medicament used in treatment of PAH. Therefore, we focused on erythrocyte parameters, oxidative stress parameters and components of renin-angiotensin-aldosterone system in the MCT-induced PAH as well as possible effects of bosentan treatment.

Methods

We used 12-week-old male Wistar rats (n = 30) divided into 3 groups: control, MCT-treated (60 mg/kg), and MCT- and bosentan-treated (300 mg/kg/day) rats. Four weeks after MCT administration, rats were subjected to 2.5-3 % isoflurane inhalation-induced anesthesia and the blood was drawn. Erythrocyte deformability was determined by the filtration method and erythrocyte nitric oxide production using DAF-2 DA fluorescence probe. Parameters of oxidative stress in plasma, erythrocyte osmotic resistance and Na,K-ATPase kinetics were measured spectrophotometrically/spectrofluorometrically. The angiotensin peptide and aldosterone concentrations were determined by liquid chromatography-tandem mass spectroscopy.

Results

We confirmed PAH development after MCT administration. It also resulted in decreased hematocrit, increased V_{max} and decreased K_{Na} kinetic parameters of erythrocyte Na,K-ATPase. An activation of the alternative pathway of renin-angiotensin system (increased Ang I, Ang 1-7, and Ang 1-5 without changes in Ang II level) and down-regulation of aldosterone was also observed. Bosentan treatment improved erythrocyte deformability, decreased AOPP and fructosamine levels as well as increased GSH/GSSG ratio.

Conclusion

Our findings do not completely match the findings in patients with PAH reporting an increase in Ang II, increased oxidative stress and deterioration in erythrocyte deformability. MCT administration impaired Na^+ binding properties of erythrocyte Na,K-ATPase, which probably led to a compensatory increase in the number of active enzyme molecules. Bosentan treatment enhanced erythrocyte deformability, which may contribute to the improvement of hemodynamics in PAH. This effect is most likely due to the antioxidant effect of bosentan, as several markers of oxidative stress improved. To obtain more comparable erythrocyte parameters to human PAH, adjustments to used model might be appropriate (e.g. different age of animal, MCT dosage, experiment duration).

B 07-47

Prorenin can affect vascular tone by modulating the intracellular pH of vascular smooth muscle cells.

S. Rognant[1], H. A.T. Pritchard[2], A. Greenstein[2], C. Aalkjaer[3], T. A.Q. Jepps[1]

[1] *University of Copenhagen, Vascular Biology Group, Department of Biomedical Sciences, Copenhagen, Denmark*

[2] *University of Manchester, Division of Cardiovascular Sciences, Faculty of Biology, Medicine and Health, Manchester, UK*

[3] *Aarhus University, Department of Biomedicine, Aarhus, Denmark*

The levels of plasma prorenin, the precursor of renin, have been shown to be elevated in stroke prone SHR animals compared to WKY[1]. The C-terminal fragment of the prorenin receptor ((P)RR) is an accessory protein of the vacuolar H^+-ATPase[2,3], which is involved in intracellular compartmental acidification and cellular pH homeostasis. In vascular smooth muscle cells (VSMCs), an elevation of external pH by 0.1 increases the frequency of Ca^{2+} sparks originating from the ryanodine receptors (RyR_2), which cause vasorelaxation. Furthermore, a 0.2 pH increase can shift Ca^{2+} sparks to Ca^{2+} waves, which elicit vasoconstriction[4]. The overall aim of this study is to investigate the effect of prorenin on vascular tone and its potential involvement in hypertension. We hypothesized that an increase in intracellular pH following binding of prorenin to its receptor could

increase Ca^{2+} sparks, and further alkalynisation could lead to Ca^{2+} waves thereby shifting prorenin from a vasodilator to a vasoconstrictor.
We performed proximity ligation assay on rat mesenteric artery VSMCs to study the co-localization between the (P)RR and RyR_2. We used rat mesenteric arteries and pressure myography to investigate the effect of prorenin on the lumen diameter and calcium imaging to detect live changes of $[Ca^{2+}]_i$.
We show that the (P)RR and the RyR_2 are within a distance of 40 nm in VSMCs. The frequency and amplitude of STOCs are attenuated in VSMCs when incubated with 10 nM prorenin. Finally the pressure myography revealed that 1 nM prorenin can induce a constriction, which was correlated with a higher Ca^{2+} spark duration, as well as a raise in rise and decay time.

References
1 Ichihara A, Kaneshiro Y, Takemitsu T, et al. Nonproteolytic activation of prorenin contributes to development of cardiac fibrosis in genetic hypertension. *Hypertension*. 2006;47(5):894-900. doi:10.1161/01.HYP.0000215838.48170.0b
2 Jurgen Ludwig, Stefan Kerscher, Ulrich Brandt, Kathy Pfeiffer FG, David K. Apps and HS. Identification and Characterization of a Novel 9.2-kDa Membrane Sector-associated Protein of Vacuolar Proton-ATPase from Chromaffin Granules* | Elsevier Enhanced Reader. *J Biol Chem*. Published online 1998. Accessed April 22, 2021.9
3 Nguyen G, Delarue F, Burcklé C, Bouzhir L, Giller T, Sraer J-D. Pivotal role of the renin/prorenin receptor in angiotensin II production and cellular responses to renin. *J Clin Invest*. 2002;109(11):1417-1427. doi:10.1172/jci14276
4 Heppner TJ, Bonev AD, Fernando Santana L, Nelson MT. Alkaline pH shifts Ca2+ sparks to Ca2+ waves in smooth muscle cells of pressurized cerebral arteries. *Am J Physiol - Hear Circ Physiol*. 2002;283(6 52-6)

B 07-48

Impact of Lactic Acidosis on Human Aortic Smooth Muscle Cells in Septic Milieu

P. Terpe[1,2], A. Leimert[2], M. Bucher[2], M. Gekle[1], S. Ruhs[2]
[1] *Martin Luther University Halle-Wittenberg, Julius Bernstein Institute of Physiology, Halle (Saale), Germany*
[2] *University Clinic Halle, University Clinic for Anesthesiology and Surgical Intensive Care, Halle (Saale), Germany*

Introduction
Sepsis, a life-threatening organ dysfunction, is characterized by (i) altered metabolism, which leads to a lactic acidosis with high serum lactate levels and (ii) vasodilation-mediated hypotension. The vasculature of septic patients shows a strongly reduced reactivity to vasopressor substances, which leads to vasodilation and hypotension followed by a high mortality rate. The underlying mechanisms are not well understood. In our study, we investigate the influence of lactic acid (LA)-induced acidosis on primary human aortic smooth muscle cells (HAoSMCs). We compare the effect of LA-induced acidosis with the effect of acidosis per se-induced by hydrochloric acid (HCl - pH 6.8) - as well as to the respective control (pH 7.4; NaLactate - pH 7.4).

Methods
HAoSMCs were cultured under the following conditions for 48 h: (i) Control - pH 7.4; (ii) HCl - pH 6.8; (iii) LA - pH 6.8 and (iv) NaLactate - pH 7.4. Subsequently, treatment-related metabolic changes (intracellular pH measurement, ATP production, glucose consumption, mitochondrial oxidative phosphorylation (OXPHOS)), alterations of the transcriptome (next generation sequencing (NGS), GO Term enrichment), and phenotypic changes (vascular calcification, vascular senescence) were analysed.
Results
Both forms of acidic treatment led to a similar and sustained intracellular acidification. The glucose consumption (glycolytic rate) was strongly reduced by acidic treatment whereby the effect was greater for LA than for HCl treatment. The ATP-dependent oxygen consumption rate of the mitochondria showed no differences between the treatment groups, as revealed by the seahorse measurement. The relative contribution of glycolysis and oxidative phosphorylation to ATP production changed under acidosis. Under control conditions, ATP was mainly generated by glycolysis, whereas under acidic conditions the relative contribution of OXPHOS increased. Cellular ATP levels were maintained at control levels under single acidic conditions, but were reduced in LA-induced acidosis. The metabolic changes induced by acidic treatments were accompanied by changes of the cellular transcriptome. Acidic treatment induced pathways involved in vascular calcification (VC), which is most pronounced in LA treatment. This was confirmed by enhanced activity of alkaline phosphatase (ALP), vascular senescence and a reduced rate of DNA synthesis.
Conclusion
In summary, acid treatment of HAoSMCs leads to rapid intracellular acidification and changes in cellular metabolism, transcriptome and vascular phenotype, which in turn leads to vascular calcification. In general, LA-induced acidosis shows a stronger effect than HCl-induced acidosis. The LA-induced metabolic and phenotypic changes in HAoSMCs may be partly responsible for the vascular hyporeactivity against vasoconstrictor agents that occurs in sepsis.

B 07-51

Blockade of voltage-dependent K^+ channels by benztropine, a muscarinic acetylcholine receptor inhibitor, in coronary arterial smooth muscle cells

M. Kang, R. Heo, W.S. Park
Kangwon National University, Department of Physiology/ College of Medicine, Chuncheon, South Korea

This work was supported by the National Research Foundation of Korea (NRF) grant funded by the Korea government (2021-R1F1A1045544, 2021-R1A4A1031574).

Introduction
Benztropine is an inhibitor of the acetylcholine muscarinic receptor and is FDA-approved as an adjunctive therapy for all forms of parkinsonism. In this study, We investigated the effect of the acetylcholine muscarinic receptorinhibitor benztropine on voltage-dependent K^+ (Kv) channels in rabbit coronary arterial smooth muscle cells.
Methods
Whole-cell patch-clamp technique was performed in native coronary arterial smooth muscle cells.
Results
Benztropine inhibited Kv currents in a concentration-dependent manner, with an apparent IC_{50} value

of 6.11 ± 0.80 µM and Hill coefficient of 0.62 ± 0.03. Benztropine shifted the steady-state activation curves toward a more positive potential, and the steady-state inactivation curves toward a more negative potential, suggesting that benztropine inhibited Kv channels by affecting the channel voltage sensor. Train pulse (1 or 2 Hz)-induced Kv currents were effectively reduced by the benztropine treatment. Furthermore, recovery time constants of Kv current inactivation increased significantly in response to benztropine. These results suggest that benztropine inhibited vascular Kv channels in a use (state)-dependent manner. The inhibitory effect of benztropine was canceled by pretreatment with the Kv 1.5 inhibitor, but there was no obvious change after pretreatment with Kv 2.1 or Kv7 inhibitors.

Conclusion

Benztropine inhibited the Kv current in a concentration- and use (state)-dependent manner. Inhibition of the Kv channels by benztropine primarily involved the Kv1.5 subtype.

B 07-52

Protocol Optimisation for a Fluorescent Nitric Oxide Indicator in Rat Mesenteric Arteries *Ex Vivo*

L. Wallis, L. Donovan, A. Johnston, C. Garland, K. Dora

University of Oxford, Department of Pharmacology, Oxford, UK

Endothelial cell (EC) dysfunction is an early hallmark of cardiovascular disease, associated with reduced bioavailability of nitric oxide (NO) and raised vasoreactivity. Despite this, the current techniques do not appear to reliably measure NO synthesis in intact arteries. Here, we optimise a novel protocol to extend the use of DAR-4M AM, a sensitive cell-trappable NO dye, into living cells of rat small mesenteric arteries. By using confocal fluorescence microscopy, we found that in cell-free chambers, Krebs buffer containing Cu_2FL2E (1 µM FL2E and 2 µM Cu^{2+}), or DAR-4M AM (5 µM, Cu^{2+}-free), the addition of the NO-donor molecule, S-nitroso-N-acetylpenicillamine (SNAP, 10 µM) caused a time-dependent and significant increase in fluorescence compared to baseline. This was further enhanced by the addition of 1 µM and 10 µM Cu^{2+}, for each dye respectively (by increasing NO-availability from SNAP). To assess biological relevance, wire myography showed that 10 µM SNAP fully reversed contraction to phenylephrine in rat mesenteric arteries. However, in the same system, >2 µM Cu^{2+} caused vascular smooth muscle (VSM) and EC dysfunction in mesenteric arteries. Next, using confocal microscopy and pressure myography, we showed that both Cu_2FL2E and DAR-4M AM could be loaded into arterial cells, and each also labelled the elastin. The role of this elastin label was assessed by co-loading Alexa Fluor 633 hydrazide (AF-633, 1 µM). However, despite many types of approaches, we were unable to measure increases in fluorescence to either ACh (1 µM) or SNAP (10 µM) when cells were loaded with Cu_2FL2E. Instead, we turned our attention to DAR-4M. Increases in the ratio of DAR-4M and AF-633 were visualised in pressurised, isolated rat mesenteric arteries stimulated with the EC-dependent agonist ACh (1 µM) or SNAP (10 µM). The addition of either drug evoked an accumulating, time-dependent (and by 20 mins) significant increase in fluorescence in both EC and VSM above baseline. This response did not require the addition of Cu^{2+}, thus simplifying the protocol and more reducing the possibility of cellular damage. These experiments will be repeated in the presence of L-NAME, an NO synthase inhibitor, to further consolidate the link between DAR-4M T fluorescence and NO production. Moving forward, these preliminary data will facilitate the advance of our understanding of vascular function, and potentially elucidate the basal vs. stimulated NO release conundrum.

B 07-53

Mechanical Pulsemeter

T. Braun

Dr. Braun, Praxisklink, Facharzt für Innere und Allgemeinmedizin, Sportmedizin, Notfallmedizin, Rötz, Germany

I thank all my teachers of medicine in the past, who inspired my for this work, I thank all my patients, who had been very patient with me, I thank my father and grandfather, who tought me the manual skills I needed for this new developement and last, but not least my family for their patience and support.

Introduction

The subjective perception of the radial pulse is common in medicine. However, the mechanical upward and downward movement of the arterial wall (pulse beat) is not measureable neither objective nor precise in terms of time. Alternatively, only photoplethysmographic and sonographic examinations are currently done, or experimentally since 2012 light microscopic examinations are also possible. The goal was to make the pulse beat precisely measurable. There were three main problems to be solved: In daily medical practice, the radial pulse is palpated with different finger pressures. A precise fixation of a device on the forearm is problematic due to the different layers of tissue. It must be possible to record the pulse beat in real time in an exactly measurable and reproducible manner.

Methods

The touching finger was the model for the measuring device to be developed. After years of work, a structure for the mechanical pulsemeter turned out to be suitable. The pulse beat of the radial artery was recorded by converting the up and down movement of the arterial wall to the rotational movement of the axis of a microdynamo. Depending on the direction of rotation and the speed of rotation, it generates voltages of between (+/-) 0.05 and 0.5 mV, which can be recorded with an accuracy of fractions of a second. This rotational movement is achieved by means of a lever construction whose fulcrum is the axis of the microdynamo. A probe is placed near the pivot point and placed on the palpable radial artery. Constant, defined pressure on the artery is mediated via the lever. This can be done with attached weights or spring balancers. With stronger pressure, the probe sinks further and the lever changes its position; therefore the pivot point is height-adjustable. The precise fixation of the mechanical pulse meter takes place in dorsiflexion of the hand, whereby the forearm is placed on a padded splint. The device is fixed over the flexor tendons using circular retaining straps. The special shape of its base plate helps to largely avoid pressure on the radial artery, that is examined.

Results

The evaluation of the mechanical pulsemeter was carried out on voluntary patients after their expressed approval. 52 pers. (10 - 82 y., mean 55 y. 30 f., 20 m.) have been examined so far. At rest, constant, reproducible curves resulted, which on the one hand varied individually from patient to patient, but on the other hand showed constant characteristics and remained stable for minutes. Pulse rate, time points of fastest, maximum and minimum arterial expansion could be recorded. Arrhythmias and other individual chances could be recorded and provisionally interpreted.

Conclusion

The mapping of the pulse beat in real time opens many new possibilities. The data can be related to others from ECG, skin resistance, photoplethysmography or blood pressure. Additional information about the cardiovascular system is possible and findings by palpation can be evaluated.

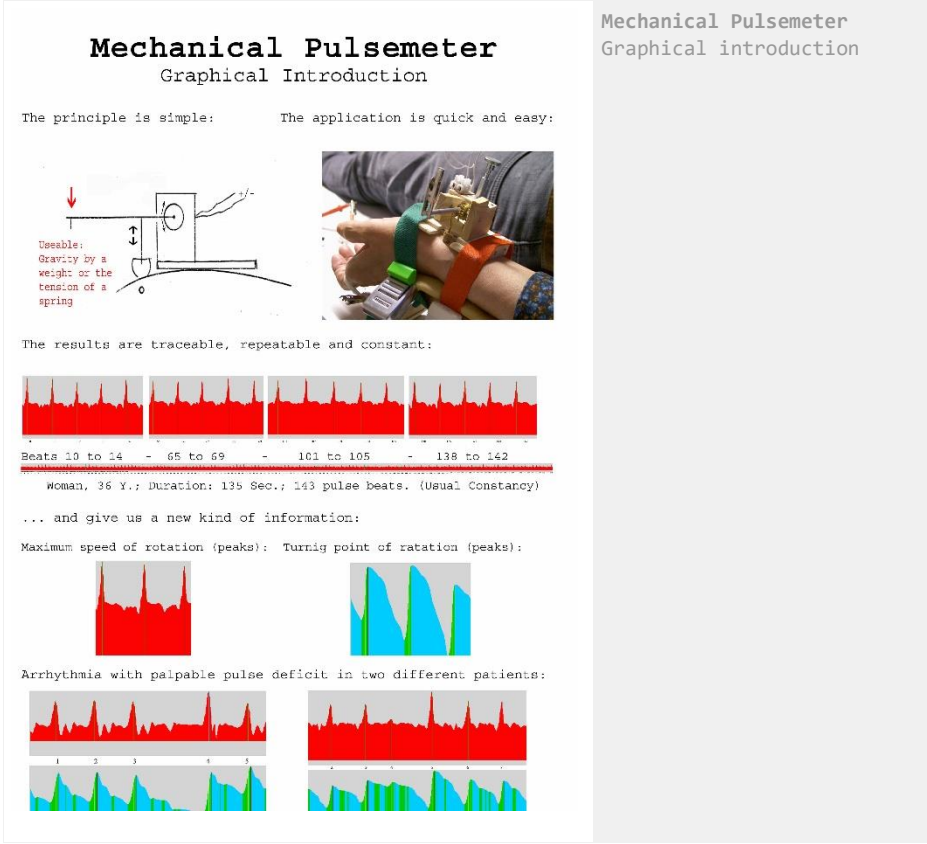

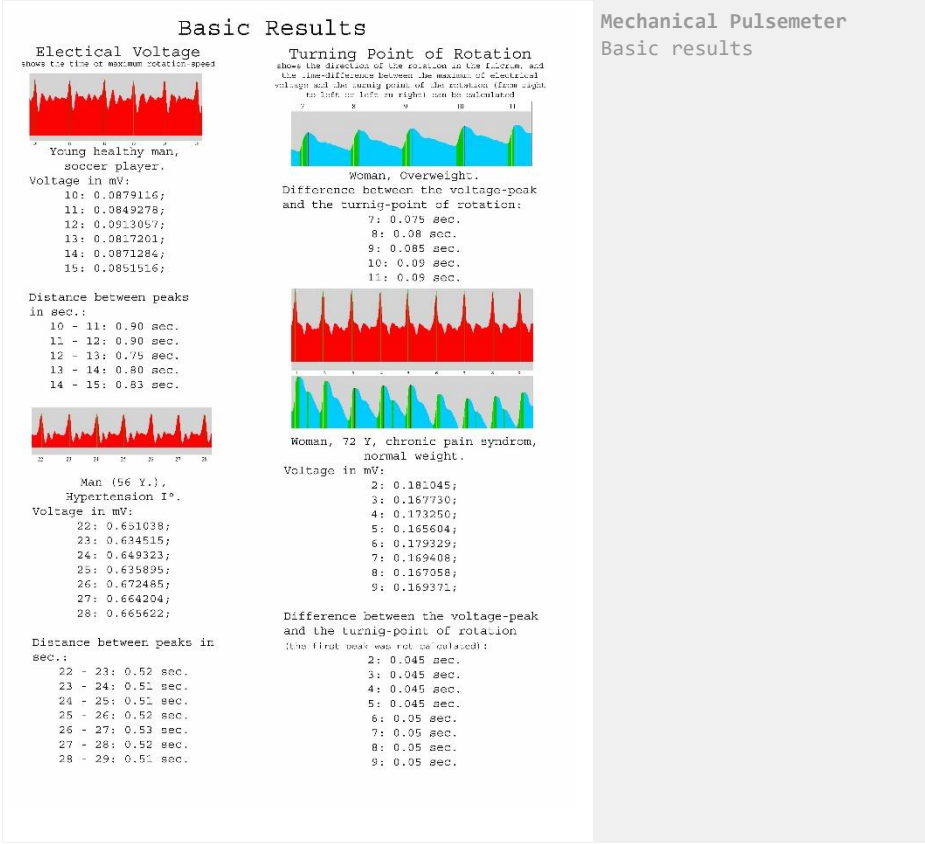

References

[1] Moran JF. Pulse. In: Walker HK, Hall WD, Hurst JW. 1990. Clinical Methods: The History, Physical, and Laboratory Examinations. 3rd edition. Boston: Butterworths. Chapter 17. Available from: https://www.ncbi.nlm.nih.gov/books/NBK278/

[2] Ghasemzadeh, N., & Zafari, A. M. 2011. A brief journey into the history of the arterial pulse. *Cardiology research and practice*, *2011*, 164832. https://doi.org/10.4061/2011/164832

[3] Wu H., Rubinstein M., Shih E., Guttag J., Durand F., Freeman W. 2012. Eulerian Video Magnification for Revealing Subtle Changes in the World. SIGGRAPH 2012. Available from: http://people.csail.mit.edu/mrub/papers/vidmag.pdf (last accessed 13. May 2022)

[4] Jeleazcov C., Krajinovic L., Münster T., Birkholz T., Fried R., Schüttler J., Fechner J. 2010.
Precision and accuracy of a new device (CNAP™) for continuous non-invasive arterial pressure monitoring: assessment during general anaesthesia. British Journal of Anaesthesia, Volume 105, ISSUE 3, pp. 264-272.

B 07-54

Identification of proteins associated with global and specific RNA:DNA:DNA triplexes

S. Haydar[1,3], S. Seredinski[1,3], I. Wittig[1,2], M. S. Leisegang[1,3], R. P. Brandes[1,3]

[1] *Goethe University, Institue for Cardiovascular Physiology, Frankfurt, Germany*

[2] *Goethe University, Functional Proteomics, Institute for Cardiovascular Physiology, Frankfurt, Germany*

[3] *Partner site RheinMain, German Center of Cardiovascular Research (DZHK), Frankfurt, Germany*

Background

Long non-coding RNAs (lncRNAs) play essential roles for epigenetics and gene transcription. Interaction of lncRNAs with DNA occur mainly through RNA:DNA duplex (R-loop) or RNA:DNA:DNA triplex formation. Importantly, recent research highlighted the importance of triplexes for the cardiovascular system, but unlike R-loops, triplex-associated proteins are not known and were identified here.

Methods and results

To identify triplex-associated proteins, several techniques were established. An all-to-all approach was developed to map globally all triplex-proximal proteins in intact endothelial nuclei using quantitative mass spectrometry. This approach, called RADICL-MS (RNA And DNA Interacting Complexes Ligated and mass spectrometry) allowed the identification of proteins associated with all RNase H-resistant triplex structures in the cell. To identify proteins interacting with specific triplexes, such as the *MEG3-TGFBR1* triplex, IDAP (Isolation of DNA Associated Proteins) was used. Here, synthetic labeled lncRNA oligos mimicking the triplex-forming region of lncRNA *MEG3* were used in combination with the corresponding *TGFBR1*-DNA target site cloned in a plasmid-based system in endothelial cells. These two approaches led to the identification of proteins involved in pre-RNA processing, DNA/RNA unwinding and repair, chromatin organization and transcriptional regulation.

Conclusion

IDAP and RADICL-MS are useful tools to identify critical triplex-associated proteins. Nuclear proteins such as helicases, histones and components of the transcriptional machinery potentially act in the assembly and disassembly of triplexes to maintain and participate dynamic remodeling of chromatin.

B 07-55

Impact of elevation of NaCl concentrations in cell culture medium on Human Aortic Endothelial Cells

N. Kozina[1,2], N. Kolobaric[1,2], I. Drenjancevic[1,2]

[1] *Josip Juraj Strossmayer University of Osijek, Department of Physiology and Immunology, Osijek, Croatia*

[2] *Josip Juraj Strossmayer University of Osijek, Scientific Center of Excellence for Personalized Health Care, Osijek, Croatia*

This study was supported under the Faculty of Medicine Osijek Institutional grant IP1-MEFOS - 2019 (PI I. Drenjančević), IP1-MEFOS-2020 (PI I. Drenjančević) IP3-MEFOS- 2021 project (PI I. Drenjančević) and by European Structural and Investment Funds through a grant to the Croatian National Science Center of Excellence for Personalized Health Care, Josip Juraj Strossmayer University of Osijek # KK.01.1.1.01.0010.

Introduction

Cardiovascular diseases (CVDs) are a leading health problem worldwide. High blood pressure is one of the main risk factors for their development and blood pressure levels are closely associated with salt intake. The plasma sodium concentration in population generally varies between 134 and 148 mmol/l. The aim of this study was to assess the effects of elevation of NaCl concentrations in cell culture media on oxidative stress and survival of human aortic endothelial cells (HAEC).

Methods

HAEC cells (from Innoprot; Barcelona, Spain) were grown at 37℃, 5% CO_2 in Endothelial Cell Basal Medium (Medium 200) supplemented with low serum growth supplement (LSGS). The osmolality of this medium (Control medium) was 270 mosmol/kg (133 mmol/l sodium). High NaCl medium was prepared by adding NaCl to the total osmolality of 320 mosmol/kg (158 mmol/l), 350 mosmol/kg (173 mmol/l) and 380 mosmol/kg (188 mmol/l). To elevate NaCl, control medium was replaced by the high NaCl medium. The experiments were performed on cells at about 80% confluence. For all experiments, cells were used at passage P5.

MTT test: The cells were seeded in 96 well plate. After 24 h, 48h and 72h 10 µL of MTT stock solution was added into each well and the plate was placed in an incubator for 4 h to produce formazan crystals. After incubation, 100 µL of MTT solvent was added to dissolve created formazan crystals and microplate was read at 595nm.

Intracellular Reactive Oxygen Species (ROS) Production by Human Aortic Endothelial Cells (HAEC): Cells were seeded in T-25 flasks. The samples were collected after 72-hour exposure to two concentrations (320 mosmol/kg and 350 mosmol/kg) of NaCl. The cells were washed in 1x phosphate-buffered saline (PBS) and prepared for staining protocol. Dihydroethidium (DHE) was used to determine the level of $O2^{\cdot-}$ in HAECs. The cells were resuspended in 100 µL of 1x PBS and incubated with DHE (10 µM final concentration) for 30 min at +4 °C. Following the incubation period, samples were rinsed and resuspended in 350 µL of 1x PBS and analysed. After initial readings, 50 µL of 1 mM phorbol 12-myristate 13-acetate (PMA) was added to each sample to stimulate ROS production. After a 15-minute incubation, the samples were read again on the cytometer. FACS Canto II flow cytometer (BD Bioscience; 488 excitation laser and 530/30 BP analysis filter) was used for the assessment of intracellular ROS production. Data analysis and visualization were performed using Flow Logic software (Inivai Technologies, Mentone, Australia).

Results

The cell viability was significantly reduced after 24h at 350 mosmol/kg and 380 mosmol/kg concentrations of NaCl, while after 48h and 72h viability was reduced at 320 mosmol/kg, 350

mosmol/kg and 380 mosmol/kg concentrations. The level of O2·− was significantly increased in both experimental groups.

Conclusion

Increased NaCl concentration significantly reduces cell viability and increases cellular oxidative stress.

B 07-56

Effect of Functionally Enriched Eggs Consumption in patients with chronic coronary artery disease on vascular inflammation promotors

Z. Mihaljevic[1,2], A. Stupin[1,2], Z. Breskic Curic[2,3], M. Mihalj[2,4], N. Kolobaric[1,2], P. Susnjara[1,2], I. Jukic[1,2], A. Lukinac[2,5], M. Stupin[2,6], A. Kibel[2,6], K. Selthofer-Relatić[2,7], I. Drenjancevic[1,2]

[1] Faculty of Medicine Josip Juraj Strossmayer University of Osijek, Institute and Department of Physiology and Immunology, Osijek, Croatia

[2] Josip Juraj Strossmayer University of Osijek, Scientific Centre of Excellence for Personalized Health Care, Osijek, Croatia

[3] General Hospital Vinkovci, Department of Internal medicine, Vinkovci, Croatia

[4] Clinical Hospital Center Osijek, Department of Dermatology and Venerology, Osijek, Croatia

[5] Clinical Hospital Center Osijek, Department of Rheumatology, Clinical Immunology and Allergology, Osijek, Croatia

[6] Clinical Hospital Center Osijek, Department of Heart and Vascular Diseases, Osijek, Croatia

[7] Faculty of Medicine Josip Juraj Strossmayer University of Osijek, Department of Pathophysiology, Osijek, Croatia

The study was supported by European Structural and Investment Funds through a grant to the Croatian National Science Center of Excellence for Personalized Health Care, Josip Juraj Strossmayer University of Osijek # KK.01.1.1.01.0010.

Activation of endothelial TGF-β signaling may be an important driver of atherogenesis and plays a key role in the induction of vessel wall inflammation and the development and progression of atherosclerosis. Previously, our studies on the consumption of n-3 polyunsaturated fatty acids (n-3 PUFAs) enriched eggs have shown a beneficial effect, by changing the free fatty acid profile to a more favorable lower n6/n3 ratio, lowering total cholesterol and LDL-cholesterol levels in cardiovascular patients with no adverse effects of daily eggs' consumption. The aim of this study was to determine the effect of eggs enriched with n-3 PUFAs, vitamin E, selenium and lutein on the serum levels of pro-inflammatory cytokines. A randomized, double-blind, controlled, interventional study (Clinical Trials ID: NCT04564690) was conducted on patients with chronic coronary syndrome (diagnosed according to ESC guidelines for the diagnosis and management of chronic coronary syndromes, 2019) who consumed 3 hen eggs per day for 3 weeks. Control patients consumed ordinary: n3-PUFAs (438 mg/day), lutein (110 mg/day), selenium (0.181 mg/day) and vitamin E (595 mg mg/day) hen eggs and Nutri4 group patients consumed enriched hen eggs: n3-PUFAs (1026 mg/day), lutein (616 mg/day), selenium (0.191 mg/day) and vitamin E (1098 mg mg/day). All patients used statins and other standard drug therapy for CAD (ACE inhibitors, beta-blockers, antiplatelet drugs), and some of them used ezetimibe depending on their lipid profile. Written informed consent was obtained from each subject. The study protocol and procedures conformed with the standards set by the latest revision of the Declaration of Helsinki and were approved by the Ethical Committee of Osijek University Hospital. Serum levels of TGF-β, C3a, IFN-gamma, IL-6, IL-10, IL-17A(CTLA-8), IL-23, MCP-1 (CCL2) and TNF-alpha were measured with ThermoFisher Scientific ProcartaPlex antibody-based magnetic bead reagent kits and panels for multiplex protein quantitation using the Luminex 200 instrument platform. Quantitation was performed using ProcartaPlex Analysis Application and expressed as concentration in pg/ml, (sample N=9-10 per group). For group comparisons an OneWayANOVA test was used. Within-group comparisons were performed using paired t-test or Wilcoxon test, statistical significance was set as P <0.05. The results showed significantly decreased levels of TGF-β and lL-17A after consuming Nutri4 eggs compared to values prior eggs' consumption and consumption of ordinary eggs. These results suggest that the consumption of n-3 PUFAs enriched eggs can decrease proinflammatory cytokines and contribute to their beneficial effects on the cardiovascular system.

B 07-57

Dilatation of descending vasa recta regulated by NO-sGC-cGMP pathway after hypoxia/re-oxygenation

M. Xu, F. B. Lichtenberger, C. Erdogan, P. B. Persson, A. Patzak, P. H. Khedkar

Charité – Universitätsmedizin Berlin, Institute of Translational Physiology, Berlin, Germany

A.P. and P.B.P. were funded by DFG For 1368, and SFB 1365

Purpose

Acute kidney injury (AKI) goes along with impaired renal medullary blood flow. Hypoxia is involved in the pathogenesis of renal damage and can influence the function of renal microvessels. Dilating these vessels improves renal medullary flow, and this may be renoprotective. Here, we characterize the NO-sGC-cGMP signaling pathway in descending vasa recta (DVR), and test potential vasodilators after hypoxia/re-oxygenation.

Methods

Rat DVR) were isolated and perfused under isobaric conditions. A hypoxia chamber was used to provide the hypoxia (0.1% oxygen) environment.

Results

Sildenafil, a PDE5 inhibitor (10^{-6} mol/l), induced vasodilatation in angiotensin II (Ang II, 10^{-6} mol/l)-pre-constricted vessels. In L-NAME (10^{-4} mol/l) pre-treated and Ang II (10^{-6} mol/l) pre-constricted vessels, BAY 60-2770, an sGC activator (10^{-6} mol/l), dilated vessels NO-independently. The application of Ang II (10^{-12} to 10^{-6} mol/l) showed a stronger constriction effect in vessels after hypoxia/re-oxygenation. Sildenafil failed to dilate the vessels after hypoxia/re-oxygenation. SNP, an NO donor (10^{-3} mol/l), and BAY 60-2770 both induced dilatation in DVR, while BAY 60-2770 dilated DVR faster than SNP under these conditions.

Conclusion

The results emphasize the role of the NO-sGC-cGMP signaling pathway in regulating the tone of renal medullary micro-vessels. The sGC activator BAY 60-2770seems to be the best choice to restore renal blood flow after hypoxia/re-oxygenation compared to SNP as well as sildenafil.

PB 08 | Cardiac Physiology

B 08-01

Targeted disruption of PDE4 and phospholamban interaction in rabbit cardiomyocytes

J. Ling[1,2], G. Borland[2], S. Dobi[3], C. Blair[2], G. Smith[2], G. Baillie[2], N. Macquaide[1]

[1] *Glasgow Caledonian University, Biological and Biomedical Sciences, Glasgow, UK*

[2] *University of Glasgow, Institute of Cardiovascular & Medical Sciences, Glasgow, UK*

[3] *Labcorp Drug Development, Electrophysiology, Cambridge, UK*

This project is funded by British Heart Foundation (PG/17/26/32881).

Introduction

Phosphodiesterases (PDE) regulate local cellular cAMP levels and are targeted to many cellular proteins which are PKA substrates. Phospholamban (PLB) phosphorylation is known to be regulated by PDE3A and a previously unknown PDE4 isoform which we identify here as PDE4D5. PDE3 and 4 inhibition has failed to produce useful inotropic actions and was shown to worsen survival in heart failure patients. This may be due to the action of PDEs on multiple cellular targets. Targeting PDE4D5 could have an inotropic action through its action on PLB without the deleterious effects on other proteins.

Methods

Magnetic beads were used to pull down proteins attached to PLB. The samples were then processed by mass spectrometry to identify proteins associating with the SERCA/PLB complex. An array of peptides 25 amino acids long spanning PDE4D5 was prepared and homogenate from rabbit left ventricle was applied. SERCA antibody was added to show the regions on the PDE4D5 where interaction with the SERCA complex occurred. Peptides designed to disrupt (Drp-P) the SERCA-PDE4 interaction and scrambled control (Scram-P) were synthesised. Adult rabbit myocytes were incubated with 10uM Drp-P or scram-P. Cells were fixed and proximity ligation assay (PLA) was used to quantify SERCA-PDE4 interactions. Rabbits were given a myocardial infarction (MI) by left coronary artery ligation. Rabbit myocytes were electrically stimulated, and images of contraction were recorded. Contraction parameters were quantified using a custom ImageJ macro.

Results

PDE4D5 was identified through mass spectrometry of lysates from PLB pulldown and verified via western blot. PLA assays in Drp-P incubated myocytes showed a 74% reduction in SERCA-PDE4D5 interactions relative to scram control (N=3, $P<0.01$ T-test). Contractility was increased in Drp-P incubated cells versus scram control (N=3, $P<0.05$ T-test).

Conclusion

In conclusion, PDE4D5 is responsible for regulating SERCA activity via modulation of PLB phosphorylation. Targeted disruption of PDE4D5-SERCA complex interaction is a promising inotropic therapy in MI.

B 08-02

The Effect of Chronic Humanin Administration on Apoptosis and Inflammation in STZ-Induced Cardiac Dysfunction in Mouse Model

F. Bulut[1], B. Bilgin[1], M. G. Hekim[2], M. M. Kelestemur[1], M. Adam[1], A. Ozgen[2], **M. Ozcan**[1]

[1] *Firat University, Biophysics, Elazig, Turkey*

[2] *Firat University, Physiology, Elazig, Turkey*

This work was supported by a grant from Turkish Scientific Technical Research Organization (TUBITAK Project No: 119R084).

Introduction

Long-term cardiovascular complications and especially coronary heart disease are the principal causes of morbidity and mortality among diabetic patients. In diabetes, increased apoptosis and inflammation raises the incidence of atherosclerosis and cardiovascular diseases. Humanin is a mitochondrial-derived peptide, comprises of 24 amino acids. Humanin is known to have a protective role in many studies such as ischemia-reperfusion injury, cardiomyopathy and cardiac dysfunction. However, the effect of chronic humanin administration on apoptosis and inflammation in streptozotocin (STZ)-induced cardiac dysfunction in mouse model is not fully known. In the present study, we investigated the effects of chronic humanin administration against STZ-induced cardiac dysfunction in diabetic mice.

Methods

Thirty adult mice were randomly selected for this study. The mice were divided into three groups (10 mice in each group): the control group (saline), the STZ group (diabetic control) and the STZ+Humanin group (treated with 4 mg/kg humanin), . Mice were administered humanin daily for 15 days intraperitoneally. The left ventricle was taken and subjected to the necessary enzymatic processes. by ELISA method, caspase 3, caspase 9, IL-1β, IL-6 and IL-10 were measured from the obtained tissue homogenate.

Results

The administration of chronic humanin decreased caspase 3 and caspase 9 levels in left ventricle of diabetic animals. In addition, while humanin decreased IL-1β level and IL-6 level, it did not change IL-10 level left ventricle of diabetic animals.

Conclusion

In conclusion, based on the above findings, we conclude that humanin possesses protective effects against STZ-induced cardiac dysfunction through decrease the proinflammation levels and inhibiting the apoptotic signaling pathway.

B 08-03

Mitochondrial metabolic remodeling in myocardium of patients with early contractile dysfunction

J. Marinovic[1], F. Runjic[2], C. Bulat[3], M. Cavar[4], L. Frankovic[5], Z. Marovic[3], **M. Ljubkovic**[1]

[1] *University of Split School of Medicine, Physiology, Split, Croatia*

[2] *University Hospital Split, Cardiology, Split, Croatia*

[3] *University Hospital Split, Cardiac Surgery, Split, Croatia*

[4] *University Hospital Split, Radiology, Split, Croatia*

[5] *University of Split School of Medicine, Laboratory for Cancer Research, Split, Croatia*

We would like to thank medical personnel of Department of Cardiac Surgery at University Hospital in Split for their help with collection of patient data and biopsy samples. Funding for this work was granted by the Croatian Science Foundation (6153 to M. LJ.).

Introduction

Chronic heart failure (CHF) is associated with remodeling of cardiac energy metabolism; however, human studies have been largely limited to its final phases - the end-stage CHF (1-4). In the current study, we examined mitochondrial function in myocardium of patients undergoing coronary artery bypass graft surgery (CABG) and being at various levels of cardiac contractile spectrum. Our aim was to investigate if alterations in mitochondrial ability to oxidize substrate are present even before the end-stage contractile failure ensues.

Methods

Samples of left ventricular myocardium from forty patients undergoing CABG were obtained by subepicardial needle biopsy. All patients had left ventricular ejection fraction (LVEF) higher than >40%. Mitochondrial oxidation of carbohydrate and fatty acid metabolites (pyruvate and palmitoyl-carnitine, respectively), as well as maximal respiratory capacity were assessed measuring oxygen consumption rate in saponin-permeabilized myocardial fibers. Expression of key factors influencing mitochondrial oxidative function (respiratory complexes, beta-oxidation enzymes, mitofusin-2 and PGC-1α) was assessed by immunoblotting. Accumulation of ceramide was evaluated by immunofluorescence. Univariable and multivariable linear regression analysis was used for testing the association between ejection fraction and mitochondrial respiration under different conditions. Pearson correlation analysis was used to assess potential relations between EF and other parameters.

Results

LVEF was positively associated with mitochondrial respiratory capacity, but not with rate of oxidation of individual substrates (Figure 1A-C) and this relationship persisted after adjusting for age, sex, body mass index and diabetes status (β=0.11; P=0.03). Citrate synthase activity (indicator of mitochondrial content) did not associate with LVEF (Figure 1D). LVEF was positively correlated with mitochondrial biogenesis and remodeling factors (PGC-1a and mitofusin-2), as well as with expression of key β-oxidation enzymes (VLCAD and HADHA; Figure 1E-H). Moreover, LVEF was negatively associated myocardial accumulation of ceramide (Figure 1I).

Conclusion

Our study shows that relationship between cardiac contractility and mitochondrial functional capacity exists even in patients with normal-to-moderately decreased cardiac systolic function. Also, it suggests that reduced capacity for fatty acid oxidation and increased accumulation of toxic ceramide is present in the early phases of cardiac systolic decline.

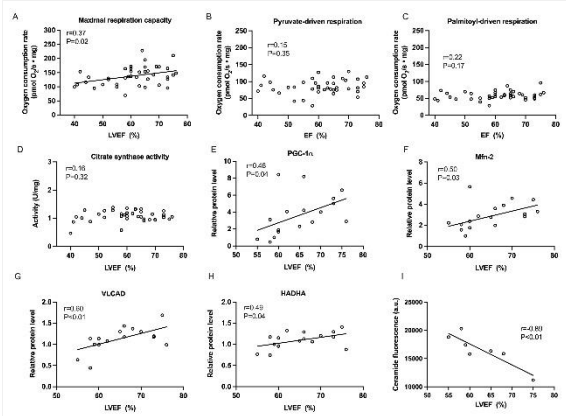

Cardiac systolic function of patients is related with their mitochondrial respiratory function
Shown are correlations between left ventricular ejection fraction (LVEF) and the following: mitochondrial respiratory capacity (A); pyruvate- and palmitoyl-driven mitochondrial respiration (B-C, respectively); citrate synthase activity (D); expression of PGC-1a, Mfn-2, VLCAD and HADHA (E-H, respectively); and ceramide accumulation (I).

References

[1] Sabbah HN, Gupta RC, Singh-Gupta V, Zhang K, Lanfear DE, 2018, Abnormalities of Mitochondrial Dynamics in the Failing Heart: Normalization Following Long-Term Therapy with Elamipretide, *Cardiovasc Drugs Ther,* 32(4):319–28.

[2] Lemieux H, Semsroth S, Antretter H, Höfer D, Gnaiger E 2011, Mitochondrial respiratory control and early defects of oxidative phosphorylation in the failing human heart. *The International Journal of Biochemistry & Cell Biology,* 43(12):1729–38.

[3] Scheiber D, Jelenik T, Zweck E, Horn P, Schultheiss H-P, Lassner D, et al, 2019, High-resolution respirometry in human endomyocardial biopsies shows reduced ventricular oxidative capacity related to heart failure. *Exp Mol Med.* 51(2):1–10.

[4] Stride N, Larsen S, Hey-Mogensen M, Sander K, Lund JT, Gustafsson F, et al, 2013, Decreased mitochondrial oxidative phosphorylation capacity in the human heart with left ventricular systolic dysfunction, *European Journal of Heart Failure*, 15(2):150–7.

B 08-04

Subcellular control of cAMP microdomain signaling in cardiomyocytes using targeted optogenetics

B. Mansuroglu, P. Sasse
University Hospital Bonn, Department of Physiology 1, Bonn, Germany

Funded by Deutsche Forschungsgemeinschaft (DFG, German Research Foundation, (313904155/SA1785/7-1, 380524518/SA1785/9-1, 214362475 / GRK1873/3)Plasmids provided by Prof. Peter Hegemann and Dr. Yinth Andrea Bernal Sierra (Humboldt University Berlin)

In cardiomyocytes cAMP/PKA-dependent phosphorylation of L-type Ca^{2+} channels (LTCC) and Ryanodine receptors type 2 (RyR2) increases contractile force but due to the close vicinity of both proteins, it is unclear if their cAMP/PKA microdomains are functionally separated or cross-talking. To investigate differences from selective phosphorylation we aim to generate LTCC and RyR2 cAMP microdomains by light using a novel optogenetic approach of subcellular targeting the photo-activated adenylate cyclase from *Turneriella parva* (TpPAC). TpPAC was targeted together with EYFP or mCitrine to the RyR2 by fusion with the high affinity protein FKBP12.6 and to the LTCC ß subunit by fusing with a specific nanobody (nb.F3). TpPAC-EYFP served as control for global cytosolic cAMP generation.
Intact TpPAC light-dependent cAMP generation by fusion proteins was shown in HEK293 cells co-expressing the cAMP-sensitive GloSensor in which blue light elevated cAMP levels in a light dose-dependent manner.
After expression in neonatal mouse cardiomyocytes TpPAC-EYFP showed homogeneous distribution. TpPAC-mCitrine-FKBP12.6 localized near z-discs indicating RyR2 targeting and nb.F3-TpPAC-EYFP showed some cell membrane targeting but also aggregates and both targeted TpPAC show some background cytosolic expression. Brief blue light flashes resulted in transient acceleration of spontaneous beating frequency by all constructs in a light dose-dependent manner. Production of cAMP globally in the cytosol or locally at the RyR2 by brief light pulses of 250 ms results in a long-lasting constant plateau (> 50 s) of elevated beating rate effect. In contrast, the effect of cAMP generation locally at the LTCC declined after its peak without a clear plateau but with a longer lasting small cAMP effect. Ca^{2+} imaging of electrically (0.75-1 Hz) paced cardiomyocytes with the red shifted dye Cal630 showed light-induced increase of Ca^{2+} transient height with all three constructs. Interestingly, local generation of cAMP at the RyR2 also result in increase of diastolic Ca^{2+} levels, which was significantly higher than after localized LTCC or global cytosolic cAMP generation.
Altogether the kinetic differences point towards light-induced generation of a “large” cAMP pool in the cytosol and the RyR2 microdomain and a high PDE expression or activation mechanism in the LTCC microdomain. Furthermore, the higher increase of diastolic Ca^{2+} by cAMP in RyR2 microdomains is highlighting PKA-dependent Ca^{2+} leak from the sarcoplasmic reticulum and might be important to understand cardiac arrhythmia mechanisms.

B 08-05

Does imipramine cause detubulation of adult rat ventricular cardiomyocytes resulting in contractile failure and a phenotype akin to drug-induced heart failure?

L. R. McGuinness[1], M. Mahaut-Smith[2], R. D. Rainbow[1]
[1] *University of Liverpool, Department of Cardiovascular and Metabolic Medicine/Institute of Life Course and Medical Sciences, Liverpool, UK*
[2] *University of Leicester, Department of Molecular & Cell Biology, Leicester, UK*

Introduction
Heart failure constitutes insufficient cardiac output that fails to meet systemic metabolic demands, arising from impaired heart muscle. Altered calcium handling underpins cardiac muscle inefficiency, with a decline in calcium transients observed in failing hearts with reduced ejection fraction (1). T-tubules are key structures involved in efficient contractile function within cardiomyocytes by propagating action potentials to facilitate synchronous calcium release from sarcoplasmic reticulum stores, resulting in immediate interaction with sarcomere units to generate effective contractile force, suggesting that disruption to the T-tubule network would produce a phenotype akin to the failing heart, based on calcium dysregulation (2). Recent evidence suggests the anti-depressant imipramine can act as a detubulating agent through interaction with T-tubules to breakdown their integrity and lose functionality (3). The research presented aimed to establish the functional impact imipramine has on freshly isolated cardiomyocytes and their contractile behaviour.
Methods
Cardiomyocytes were isolated from adult male Wistar rats and perfused with either normal Tyrode’s solution to act as control conditions or imipramine (30, 100 or 300 µM) at 32±2°C, with 1 Hz electric field stimulation to induce contraction. Contractile force generated by the cardiomyocytes was determined by measuring the length of contracting cardiomyocytes using an edge detection system, whilst corresponding intracellular calcium changes under both control and imipramine conditions were determined using fluo-4 AM dye loaded into cardiomyocytes (emissions collected >512 nm upon excitation at 480 nm). To visualise the effects of imipramine on T-tubules, staining of the cardiomyocytes was achieved using the fluorescent membrane probe FM 1-43, alongside control images of cardiomyocytes that had not undergone imipramine treatment.
Results
At the lowest concentration observed, imipramine resulted in reduced contractile behaviour across the cardiomyocytes, with many losing contractile ability all together (mean AUC ***$p<0.001$). Such observations were synonymous with blunted and inhomogeneous calcium transients (mean AUC **$p<0.01$), whilst staining of the T-tubule network showed a clear disruption to these organised membrane invaginations, confirming that T-tubule disturbances explain the irregularities in calcium signalling observed.
Conclusion
These data suggest inefficient intracellular calcium signalling underpins the dysfunctional contractile activity observed, which can further be attributed to disrupted T-tubules. Imipramine is suspected to interfere with the T-tubule network via PI(4,5)P2, causing a breakdown of its integrity (4). This hinders the T-tubules ability to facilitate contraction, resulting in reduced contractility that effectively mimics heart failure *in-vitro* and may provide insight into the clinical manifestation of pathophysiological heart failure.

References
[1] Gwathmey JK, Copelas L, MacKinnon R, Schoen FJ, Feldman MD, Grossman W, et al. Abnormal intracellular calcium handling in myocardium from patients with end-stage heart failure. Circ Res. 1987;61(1):70-6
[2] Vermij SH, Abriel H, Kucera JP. A fundamental evaluation of the electrical properties and function of cardiac transverse tubules. Biochim Biophys Acta Mol Cell Res. 2020;1867(3):11850
[3] Osman S, Taylor KA, Allcock N, Rainbow RD, Mahaut-Smith MP. Detachment of surface membrane invagination systems by cationic amphiphilic drugs. Sci Rep. 2016;6:18536.
[4] Wu T, Baumgart T. BIN1 membrane curvature sensing and generation show autoinhibition regulated by downstream ligands and PI(4,5)P2. Biochemistry. 2014;53(46):7297-309.

B 08-06

Establishing a new cardiac toxicity screening method using pig myocardial slices

R. Shi[1], M. Reichardt[1], D. Fiegle[2], T. Czajka[3], Z. Sun[4], T. Salditt[3], T. Seidel[2], A. Dendorfer[4], T. Bruegmann[1]

[1] *University Medical Center Göttingen, Institute for Cardiovascular Physiology, Göttingen, Germany*

[2] *Friedrich-Alexander-University Erlangen-Nürnberg, Institute of Cellular and Molecular Physiology, Erlangen-Nürnberg, Germany*

[3] *University of Göttingen, Institute for X-ray Physics, Göttingen, Germany*

[4] *Hospital of the University Munich, Walter-Brendel-Centre of Experimental Medicine, Munich, Germany*

Cardiotoxicity screening is crucial in drug development to reduce risks to patients and economic losses. Different in-vitro approaches have been developed, but they are still lacking normal tissue composition and physiological load. Herein, we explore biomimetic cultivation (BMC) of myocardial slices from healthy pigs as a new cardiotoxicity screening approach.

Pig left-ventricular samples were cut into 300 µm thick slices. X-Ray diffraction analysis revealed an average lateral spacing of actin and myosin filaments of ~ 45 nm. After mounting into the BMC chambers, slices were pre-stretched by 1.5 mN. The twitch force was recorded during electrical stimulation to determine the force-frequency relationship (FFR), the frequency dependence of contraction duration, the effective refractory period (ERP), and the pacing threshold.

Slices generated 2.4 ± 1.4 mN twitch force at 1 Hz electrical pacing, showed a positive FFR, and a shortening of contraction duration with increased pacing rates. The addition of 300 µM lidocaine, a selective blocker of Na^+ channels, increased the pacing threshold by ~300%. The L-type Ca^{2+} channel activator Bay K8644 (300 nM) increased the twitch force to 295 ± 195% (n = 7), while the Ca^{2+} channel blocker nifedipine (100 nM) decreased the force to 21 ± 5.6% (n = 9). The hERG K^+ channel blocker dofetilide (3 nM) prolonged the ERP and contraction duration to 220 ± 36% and 161 ± 4 % (n = 5), respectively. The ß-adrenergic and potassium channel inhibitor sotalol (10 µM) prolonged the ERP from ~400 ms to ~600 ms, and addition of JNJ 303 (1 µM) further prolonged the ERP to ~850ms, suggesting that the I_{ks} current could be detected after blocking I_{kr}. Late sodium currents could be provoked by 100 nM dofetilide after 12 h treatment, but not by moxifloxacin (100 µM) and were identified by the inhibitory action of ranolazine (10 µM).

To validate our new approach for cardiotoxicity screening, we tested five drug candidates selected from the CiPA list as well as acetylsalicylic acid, PBS, and DMSO as controls in a blinded test. The Na^+ channel blocker disopyramide increased the pacing threshold by ~200%. ERP and contraction duration were prolonged after applying the I_{Kr} blockers. The L-type Ca^{2+} channel blocker Bepridil decreased the contraction force and increased the diastolic force, presumably by blocking NCX. Thus, we were able to detect all arrhythmic drugs and their specific effects on cardiac electrophysiology.

In conclusion, we established a new approach for cardiotoxicity assessment and demonstrate its efficiency. Importantly, this approach uses pig myocardium, which is of high relevance for humans and can be upscaled to medium throughput screening due to the large number of slices that can be obtained from one heart. Thus, we suggest that our approach can reduce animal numbers and improve the predictive value and efficiency of preclinical cardiotoxicity screening.

B 08-07

A Novel Neonatal Cardiac Injury Model Reveals Early Postnatal Regenerative Capacity, and a Compensatory Role for the non-Injured Right Heart in Mouse.

T. Hu[1], M. Hesse[1], M. Malek Mohammadi[1], E. Carls[1,2], M. Schiffer[1,2], B.K. Fleischmann[1]

[1] *University of Bonn, Institute of Physiology I, Medical Faculty, Bonn, Germany*

[2] *University Hospital Bonn, Department of Cardiac Surgery, Bonn, Germany*

The neonatal mouse heart has an increased regenerative capacity after injury. However, the extent of this regenerative potential is under debate partially due to the technical limitations of current injury models. To investigate the full capacity of neonatal heart regeneration, we developed a highly reproducible neonatal ischemic injury model for the left ventricle by cauterization of the stem of the left coronary artery.

Our histological analysis of hearts after cauterization at postnatal day 1 (P1) demonstrated that this model consistently reproduced large lesions in the left ventricle at 2 days post-surgery (dps). By analyzing cell cycle activity and authentic cell division in cardiomyocytes after the injury using transgenic mouse models, we showed that cardiomyocytes underwent both increased proliferation and binucleation to compensate for the loss of myocardium. In addition, P1 injured hearts were able to form new arteries in the left ventricle, which could be an important factor affecting initial cellular viability and proliferation of cardiomyocytes. Furthermore, longitudinal echocardiography examination for P1 infarcted mice showed that the regeneration process progressed from an initially severely impaired left ventricular function at 1dps to relatively healthy hearts with only moderately reduced function in adulthood. Interestingly, we also found that the regenerative capacity was largely lost when inducing the injury as early as P3. These mice had substantially lower survival rates in comparison to P1 mice and no signs of cardiac regeneration. In addition, transcriptome analysis performed shortly after injury revealed for P1 injured hearts increased proliferation rates and angiogenesis especially in the right ventricle, attributing a potentially important compensatory mechanism to the uninjured part of the heart. Taken together, our neonatal myocardial infarction model demonstrated a prominent regenerative capacity in P1 hearts, which is associated with proliferation of cardiomyocytes, neo-arteriogenesis and compensatory growth.

B 08-08

Does cell-type specific silencing of MAO-B interfere with the development of right ventricle (RV) hypertrophy or RV failure in pulmonary hypertension?

P. Brosinsky[1], J. Heger[1], A. Sydykov[2], R. Schulz[1]

[1] *Justus-Liebig-University, Institute of Physiology, Giessen, Germany*

[2] *Justus-Liebig-University, Excellence Cluster Cardio-Pulmonary System, Giessen, Germany*

Pulmonary arterial hypertension (PAH) causes the development of compensatory right ventricular (RV) hypertrophy and - if severe and prolonged - may lead to RV failure. An increased production of reactive oxygen species (ROS) from mitochondria is involved in the development of RV hypertrophy and failure; however, the proteins involved in ROS generation still have to be identified. Monoamine oxidases (MAO), located at the outer mitochondrial membrane, can degrade neurotransmitters leading to increased ROS production and indeed, inhibition of monoamine oxidase B (MAO-B) decreases ROS production.

Therefore, we analysed heart-specific, inducible MAO-B-knockout mice undergoing PAH by „*pulmonary artery banding*" (PAB). Echocardiography was used to determine RV geometry and function in vivo and in isolated mitochondria, ROS production and respiration was measured.

Our data showed a significant decrease of ROS molecules for MAO-B-KO mice during a treatment of PEA (Phenethylamin, a common MAO-B substrate), suggesting a successful deletion of MAO-B. Additionally, the right ventricules of MAO-B-KO mice seem to be unaffected in response to PAB surgery. Echocardiography analysis revealed significant differences of functional parameters in the two control groups.

	RVID (mm)		*RVWT (mm)*		*TAPSE (mm)*	
	SHAM	*PAB*	*SHAM*	*PAB*	*SHAM*	*PAB*
C57BL6/J	1,18	1.69**	0,28	0.48**	1,36	0.78**
MAO-B$^{fl/fl}$	1,23	1.85**	0,28	0.59**	1,25	0.79**
Myh6-MCreM_x_MAO-B$^{fl/fl}$	1,19	1.24	0,25	0.29	1,33	1.15

RVID (right ventricular internal diameter), RVWT (right ventricular wall thickness), TAPSE (tricuspid annular plane systolic excursion), C57BL6/J (SHAM n= 4, PAB n=4); MAO-B$^{fl/fl}$ (SHAM n= 4, PAB n=5); Myh6-MCreM_x_MAO-B$^{fl/fl}$ (SHAM n= 5, PAB n=6), **p<0.01

In conclusion, MAO-B-KO mice seem to be protected from RV dilatation and functional impairment compared to the control groups.

B 08-09

Identification of target genes in human bicuspid aortic valve stenosis (bAVS)

A. Brandtner[1], A. Brückner[1], S. Rieck[1], W. Röll[2], F. Bakhtiary[2], D. Wenzel[3,1], B.K. Fleischmann[1]

[1] *University of Bonn, Institute of Physiology I, Medical Faculty, Bonn, Germany*

[2] *University Hospital Bonn, Department of Cardiac Surgery, Bonn, Germany*

[3] *Ruhr-University Bochum, Department of Systems Physiology, Bochum, Germany*

Introduction

Aortic valve stenosis (AVS) is a prevalent disease characterized by a sclerotic aortic valve and known to increase the risk of death from cardiovascular disease by 50%. Until today, there is no curative therapeutic approach for AVS. In particular bicuspid AVS (bAVS) is of interest because the hereditary malformation of leaflet fusion predisposes to AVS development at relatively young age and bAVS is often associated with aortic aneurysm formation indicating that the underlying molecular mechanism of bAVS may be critical for vascular disease more in general.

Methods

We therefore isolated RNA from human bicuspid aortic valves obtained from the department of cardiac surgery at the University Hospital Bonn and investigated gene expression by RNA-seq analysis. In addition, also cell biological characterization by qPCR and immunostainings combined with high resolution microscopy was performed. As controls, valves from patients with aortic insufficiency were used.

Results

By using RNA-seq and differential gene expression analysis we could identify Serpine1 and Apelin as interesting targets that were found to be strongly upregulated (adjusted p-value < 0.001; log2FC > 2) in bAVS. Interestingly, both genes are known to have important roles in the maintenance of cardiac contractility and also in cardiac tissue remodeling, atherosclerosis and progression of fibrosis. Upregulation of these genes in bAVS was confirmed by qPCR and immunostainings demonstrating pronounced Serpine1 and Apelin protein expression in valve interstitial cells (VICs) of bAVS.

Conclusion

Thus, we have identified Serpine1 and Apelin as interesting targets in the pathophysiology of bAVS. Their contribution to valve pathophysiology will be further investigated by overexpression and downregulation of these genes in VICs and valvular endothelial cells (VECs) in vitro.

B 08-10

Developmental Hypoxia Increases Susceptibility to Cardiac Ventricular Arrhythmias in Adult Offspring

M. C. Lock[1], K. L. Smith[1], Y. Niu[2], O. V. Patey[2], S. G. Ford[2], A. W. Trafford[1], D. A. Giussani[2], G. L. Galli[1]

[1] *The University of Manchester, Division of Cardiovascular Sciences, Manchester, UK*

[2] *University of Cambridge, Department of Physiology, Development and Neuroscience, Cambridge, UK*

Supported by the British Heart Foundation. Thank you to Dr. Yatong Li from MappingLab for expert advice on optical mapping experiments.

Introduction

Chronic fetal hypoxia, a common complication of pregnancy, increases susceptibility to systolic and diastolic dysfunction in the adult offspring (Giussani. *Circulation***144(17)**:1429-1443, 2021). However, whether developmental hypoxia programmes a pro-arrhythmogenic risk is completely unknown. Recent evidence suggests that cardiac myocytes from adult offspring of hypoxic pregnancy have abnormal calcium cycling and adrenergic hypersensitivity (Lock et al. *Reprod Sci* 28:87A, 2021). These properties increase the risk of arrhythmia in many models of cardiac disease. Therefore, we investigated whether hypoxic pregnancy increases the propensity to develop arrhythmic events in adult progeny in rats.

Methods

Time-mated female Wistar rats were randomly assigned to Normoxia (21% O_2) or Hypoxia (13% O_2). Chronic hypoxia was induced via an isobaric hypoxia chamber between gestational day 6-20 (Term=23d). Offspring were culled to 4 males and 4 females at birth. At 4 months of age, 1 male

and 1 female offspring per litter was humanely killed (CO_2 inhalation). Optical mapping was performed on Langendorff perfused hearts with an oxygenated KH solution. Hearts were loaded with intracellular calcium indicator (Rhod-2) and voltage sensitive dye (RH237) for simultaneous measurements of calcium transients and membrane potential across the left ventricle. Following dye infusion the left ventricle was burst paced from the apex at increasing frequencies (10-20hz) to induce arrhythmias before and after treatment with 100nmol Isoprenaline.

Results

Hearts from hypoxic pregnancies become arrhythmic at an earlier stage of the burst protocol than Normoxic animals. Hypoxia also increased the duration of the action potential compared to Normoxic animals after bust pacing (10hz paced APD90; Figure 1B). Females seem relatively more protected than males against arrhythmia. Combined, the data show abnormal calcium handling in offspring of hypoxic pregnancy resulting in increased arrhythmic events.

Conclusion

These data support the developmental programming of an increased risk of cardiac arrhythmia in adult offspring of hypoxic pregnancy. Prolonged action potentials as seen in the hypoxic hearts are a common feature associated with cardiac disease and in line with the 'second hit' phenomenon. The mechanism is yet unknown; but is likely to be related to the known change in calcium handling in hypoxic hearts along with an increased susceptibility to adrenergic stimulation.

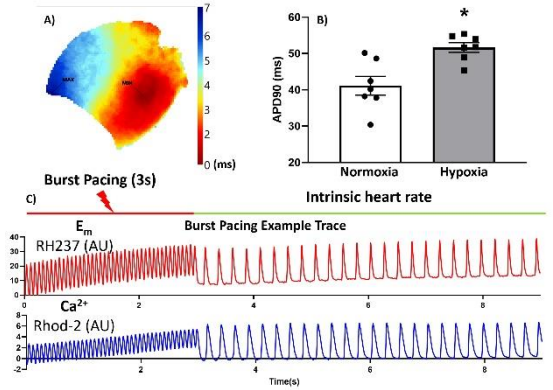

Figure 1: Burst pacing results in increased incidence of arrhythmia in hearts isolated from offspring of hypoxic pregnancies. A) Example active time map of epicardial membrane potential (RH237) of the left ventricle (ms); B) Action potential duration (APD90) was prolonged in hearts from hypoxic pregnancies ($P<0.05$, t test); C) Example burst pacing membrane potential (RH237) and calcium transients (Rhod-2) from the left ventricle with a return to sinus rhythm.

Figure 1.

B 08-11

Altered biophysical properties of atrial sodium channels increase flecainide effectiveness

D. M. Johnson[1,2], S. O'Brien[1], A. Holmes[1], C. O'Shea[1], S. N. Kabir[1], M. O'Reilly[1,3], A. Avezzu[4], J. Reyat[1], A. Hall[5,6], C. Apicella[1], P. Ellinor[5,6], S. Niederer[4], N. Tucker[6,7], L. Fabritz[1,8], P. Kirchhof[1,8], D. Pavlovic[1]

[1] *University of Birmingham, Institute of Cardiovascular Sciences, Birmingham, UK*
[2] *The Open University, School of Life, Health and Chemical Sciences, Milton Keynes, UK*
[3] *Amsterdam UMC, Amsterdam, Netherlands*
[4] *King's College London, London, UK*
[5] *Massachusetts General Hospital, Boston, USA*
[6] *The Broad Institute of MIT and Harvard, Boston, USA*
[7] *Masonic Medical Research Institue, Utica, USA*
[8] *University Heart and Vascular Center, Hamburg, Germany*

Funding Statement :
Wellcome trust (109604/Z/15/Z, 221650/Z/20/Z); BHF (PG/17/55/33087,RG/17/15/33106,FS/19/12/34204, FS/19/16/34169,PG/17/30/32961, AA/18/2/34218, FS/13/43/30324), EU (633196), Leducq Foundation, AHA (18SFRN34110082)

Introduction

Atrial fibrillation (AF) affects over 1% of the population and is a leading cause of stroke and heart failure in the elderly. Sodium channel blockade is a common treatment for AF. A feared side effect of inhibitors of the cardiac voltage-gated sodium current (I_{Na}), such a flecainide, however, is ventricular arrhythmia. We investigated the biophysical reasons for the relative safety of sodium channel blockers.

Methods

Whole cell patch clamping was performed to measure I_{Na} and action potentials (APs). Optical mapping of the LA and LV was performed in the intact mouse heart using voltage dye Di-4- ANEPPS and analysed using ElectroMap (1). LA and LV I_{Na} data were used to model changes in AP morphology using a modified mathematical model of the ventricular cardiomyocyte (2). Expression of NaV1.5, NaVβ2 and NaVβ4 was measured by Western blotting and SCN5A, SCN4B and SCN2B by RNAseq analysis in matched mouse and non-failing human LA and LV.

Results

At physiological holding potentials (-75mV), LA peak I_{Na} current density was significantly reduced compared to LV. Western blotting data demonstrate that this is not due to reduced atrial NaV1.5/SCN5A expression in either mouse or human. AP recordings revealed LA cells exhibit reduced upstroke velocity (238.6±27.7vs304.2±27.9mV/ms, p=0.0018) compared to the LV (n=23-40/5 cells/mice). Modelling studies confirmed these findings. At all holding potentials, 1μM flecainide inhibited I_{Na} to a larger extent in the LA compared to LV cells (**Figure 1**). Furthermore, flecainide decreased AP upstroke velocity to a higher degree in LA (47.9±18.8%) when compared to LV cells (18.6±9.8%, p=0.04, n=4 mice). Optical mapping demonstrated reduced conduction velocity in the LA (24.4±2.7cm/s) compared to LV (36.1±6.2cm/s, p=0.03, n=5). Flecainide significantly decreased conduction velocity in the LA (-40.4±7.2%, p<0.05 vs time control), but not LV.

Conclusion

Significant differences exist in the biophysical properties of sodium channels in the LA and LV, and their response to flecainide. The reduced effectiveness of flecainide in the LV can explain the relative safety of sodium channel blocker therapy.

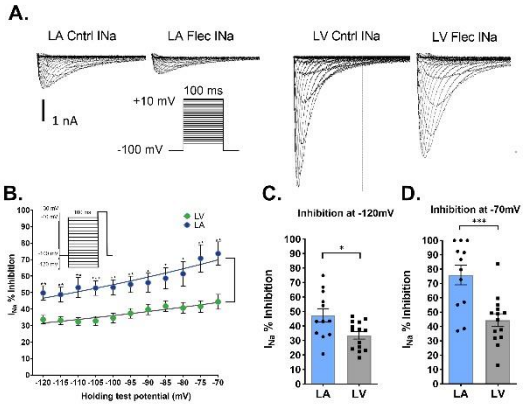

Flecainide inhibits atrial INa to a larger extent than ventricular INa

Figure 1

A) Representative raw I_{Na} traces from left atrial (LA) and left ventricular (LV) cardiomyocytes with and without flecainide.

B) % inhibition of I_{Na} in left atrial (LA) and left ventricular (LV) cardiomyocytes from a variety of holding potentials, when stimulating I_{Na} by a voltage step to -30 mV (n = 11/6 cells/mice).

C) LA and LV I_{Na} inhibition by flecainide from a holding potential of -120 mV.

D) LA and LV I_{Na} inhibition from a holding potential of -70 mV.

n = 12/6 cells/mice for LA and 14/4 for LV.

References

[1] O'Shea C, Holmes AP, Yu TY, Winter J, Wells SP, Correia J, et al. ElectroMap: High-throughput open-source software for analysis and mapping of cardiac electrophysiology. Sci Rep. 2019 Feb 4;9(1):1389.

[2] Pandit, S. V., Clark, R. B., Giles, W. R., & Demir, S. S. (2001). A mathematical model of action potential heterogeneity in adult rat left ventricular myocytes. *Biophysical journal*, *81*(6), 3029–3051. https://doi.org/10.1016/S0006-3495(01)75943-7

B 08-12

Cobalt-mediated contractile dysfunction in adult rat hearts and consequent effects on cardiomyocyte calcium transients

S. MacMillan[1], **Z. O. Olatunji**[2], Z. Y. Bosakhar[1], G. MacKenzie[1], M. H. Grant[3], R. Tate[1], N. Macquaide[2], S. Currie[1]

[1] *University of Strathclyde, Strathclyde Institute of Pharmacy and Biomedical Sciences, Glasgow, UK*

[2] *Glasgow Caledonian University, Department of Biological and Biomedical Sciences, Glasgow, UK*

[3] *University of Strathclyde, Department of Biomedical Engineering, Glasgow, UK*

Introduction

Exposure to circulating cobalt levels in patients with metal-on-metal hip replacements has been implicated in the development of cardiac hypertrophy and heart failure, yet the specific underlying causative mechanism(s) are unknown.

Methods

We have used a rat model to examine both chronic and acute effects of cobalt chloride ($CoCl_2$) on cardiac parameters at both whole organ and cellular levels. For chronic effects, experimental adult male rats (180-220g) received daily intraperitoneal (IP) injections of either vehicle (n≤10) or 1mg/kg $CoCl_2$ (n≤14) for 28 days. Heart function was assessed post-treatment using echocardiography and the cobalt content in whole blood, heart tissue and cardiac myocytes (CM) measured by ICP-MS. Rats were anaesthetised via IP injection with 0.1µg/kg Dolethal containing 0.1µl heparin sodium and upon loss of reflex, hearts removed for processing. CM were isolated from both experimental and naïve rat hearts to assess both the chronic (28 day) and acute effects of cobalt on intracellular calcium handling studied using live single cell confocal microscopy. Naïve CM were treated with 1, 10 and 100µM $CoCl_2$ for 5min, 1h and 24h.

Results

Rats treated with $CoCl_2$ for 28 days showed normal weight gain over the experimental period (vehicle: 59.6±4%, n=10; $CoCl_2$: 55.9±2.3%, n=14) with no changes in heart weight (vehicle: 1.3±0.2g, n=5; $CoCl_2$: 1.3±0.1g, n=6) but evidence of impaired contractility (% fractional shortening; vehicle: 61.5±3.5%, n=10; $CoCl_2$: 53.6±1.4%, n=14; $p<0.05$, student's t-test). Cobalt levels were significantly increased in whole blood (vehicle: 3.9±1.1µg/l, n=7; $CoCl_2$: 53.7±2.3µg/l, n=9; $p<0.0001$, student's t-test), heart tissue (vehicle: 13.3±3.2ng/g, n=4; $CoCl_2$: 81.7±10.6ng/g, n=4; $p<0.001$, student's t-test) and CM (vehicle: 0.4±0.1µg/l, n=4; $CoCl_2$: 2±0.4µg/l, n=4; $p<0.01$, student's t-test). Ca^{2+} transients measured in CM from chronic cobalt-treated rats showed a significant reduction in Ca^{2+}amplitude compared to controls (vehicle: 1.27±0.08; N=2 rats, n=32 cells; $CoCl_2$: 1.05±0.04; N=6 rats, n=133 cells; $p<0.05$, unpaired t-test). Similarly, a concentration and time-dependent reduction was observed in the Ca^{2+}transient amplitude and first transients for acute cobalt treatments of naïve cells after 5min (N=4 rats; control - 2.30±0.13, n=33; 1µM - 1.95±0.09, n=36; 10µM - 1.75±0.10, n=38; 100µM - 1.37±0.07, n=31), after 1h (N=4; control - 1.55±0.09, n=25; 1µM - 1.61±0.09, n=31; 10µM - 0.81±0.06, n=22, or after 24h (N=2; control - 1.46±0.12, n=6; 1µM - 1.48±0.11, n=5; 10µM - 1.18±0.11, n=10; $P<0.0001$, one-way ANOVA). Importantly, $CoCl_2$ (100µM) treatment for >1h consistently resulted in deterioration of CM viability.

Conclusion

Taken together, these results suggest that $CoCl_2$ has a negative chronic inotropic effect on the heart. These effects are associated with reduced Ca^{2+} release in isolated myocytes exposed to $CoCl_2$ acutely and chronically. Future work will focus on the cellular mechanisms involved.

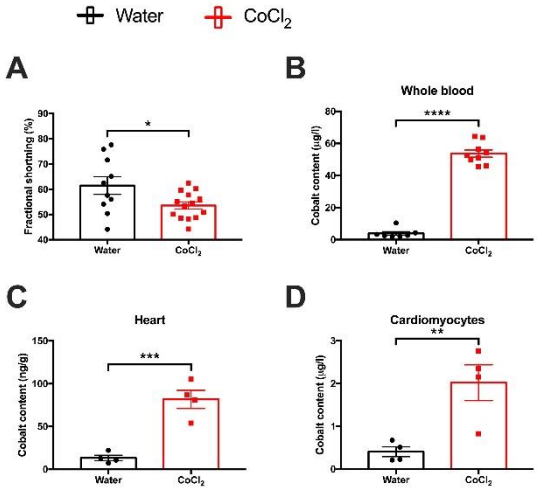

Fig 1. Chronic exposure to cobalt reduces % FS and increases metal content in blood, heart, and CM. Bars and dots show means±SEM of (A) percentage fractional shortening measured by echocardiography, and (B-D) cobalt content in (B) whole blood, (C) heart tissue, and (D) isolated cardiomyocytes measured by ICP-MS from rats which received daily intraperitoneal injections of vehicle (n≤10) or 1mg/kg $CoCl_2$ (n≤14) for 28 days. FS = fractional shortening, CM = cardiac myocytes. *=p<0.05, **=p<0.01, ***=p<0.001, ****=p<0.0001, significance tested by student's t-test.

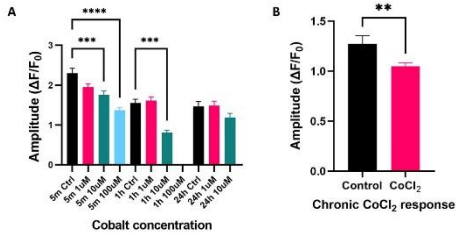

Fig 2. CoCl2 treatment reduces Ca2+ transient amplitude in cardiac myocytes. Bar charts show mean±SEM of amplitude of transient ($\Delta F/F_0$) from isolated cardiac myocytes treated (A) acutely with 0-100mM $CoCl_2$ for up to 24h and (B) chronically via daily intraperitoneal injections in rats for 28 days. **=p<0.01, ***=p<0.001, ****=p<0.0001, significance tested by two-way ANOVA for (A) and unpaired t-test for (B).

B 08-13

An automated unbiased algorithmic pipeline to analyze single-channel recordings and to investigate cooperative interactions between sodium channels

Z. Selimi[1], J.-S. Rougier[2], H. Abriel[2], **J. P. Kucera**[1]

[1] *University of Bern, Department of Physiology, Bern, Switzerland*

[2] *University of Bern, Institute of Biochemistry and Molecular Medicine, Bern, Switzerland*

Introduction

The function of cardiac voltage gated sodium (Na^+) channels ($Na_V1.5$) is central in the pathogenesis of arrhythmias as these channels are crucial for myocardial electrical excitation. Recently, based on single-channel recordings of Na^+ channel pairs, a new paradigm was proposed in which Na^+ channels interact and exhibit coupled gating [1]. Yet, single-channel recordings are corrupted by noise, baseline drift and capacitance artefacts. The most common procedures for removing these fluctuations and identifying conductive states rely on manual procedures, which are biased and may lead to inaccurate data interpretation. To address this issue, we developed an automated pipeline to separate the true signal from the capacitance artefact and baseline drift, and to idealize the single-channel currents. This permitted an unbiased assessment of potential interactions between Na^+ channels.

Methods and Results

Cell-attached patch clamp experiments were performed in HEK293 cells transiently expressing wild-type human $Na_V1.5$ channels. Currents from 2-4 channels were recorded upon a voltage step to –

40 or –60 mV. First, the individual sweeps were detrended by linear optimization using a library of exponential functions with different time constants [2]. Then, the de-drifted signal was digitally filtered. Subsequently, the baseline was offset by subtracting the peak of a Gaussian function that was fit through the histogram of samples that did not correspond to channel openings. The novel idea behind the next step is that the average of the idealized currents identified by thresholds between current levels must reconstruct at best the ensemble average current. Assuming identical single channel currents, the thresholds were set at the midpoints between current levels and the mean square residual with respect to the ensemble average current was computed. The thresholds were then adjusted automatically using nonlinear optimization to minimize this residual. This procedure was repeated under the assumption of different numbers of channels. The best possible fit was reached when this number corresponded to the true number of channels in the patch. Thus, the counting of open channels at any given time during the voltage step protocol was unbiased. To explore any potential interaction between the channels, the distribution of these counts was compared (chi-square test) to the binomial distribution expected for independent channels. The interaction was quantified by computing the difference in Shannon's entropy between these distributions. In 6 patches investigated so far, our analysis indicates that the interaction between Na^+ channels is not significant or only very weak, in contrast to what was published by others [1].

Conclusion

Our pipeline allows an unbiased analysis of single-channel currents and will be important for further studies in which we will examine whether interactions between Na^+ channels can be potentiated by auxiliary proteins.

References

[1] Clatot J, Hoshi M, Wan X, Liu H, Jain A, Shinlapawittayatorn K, Marionneau C, Ficker E, Ha T, Deschenes I. 2017. Voltage-gated sodium channels assemble and gate as dimers. *Nat Commun* 8:2077.

[2] Kang P W, Chakouri N, Diaz J, Tomaselli G F, Yue D T, Ben-Johny M. 2021. Elementary mechanisms of calmodulin regulation of $Na_v1.5$ producing divergent arrhythmogenic phenotypes. *Proc. Natl Acad. Sci. USA* 118, e2025085118.

B 08-14

Connexin 43 overexpression in cardiomyocytes or myofibroblasts of healthy and infarcted hearts - characterization of an inducible Cx43 mouse model

P. Niemann[1], M. Schiffer[1,2], E. Carls[2], C. Geisen[1,2], M. Hesse[1], M. Malek Mohammadi[1], W. Röll[2], B.K. Fleischmann[1]

[1] *University of Bonn, Institute of Physiology I, Medical Faculty, Bonn, Germany*

[2] *University Hospital Bonn, Department of Cardiac Surgery, Bonn, Germany*

The author has objected to a publication of the abstract.

B 08-15

Simultaneous sympatholytic parasympathomimetic effects of centrally acting antiadrenergic drugs dose-dependently reduce the complexity of RR-interval variability.

M. Turcani, E. Ghadhanfar

Kuwait University, Physiology, Faculty of Medicine, Kuwait, Kuwait

Introduction

Antiadrenergic therapy with β-blockers prolongs the survival of heart failure (HF) patients. However, moxonidine, a centrally acting sympatholytic drug, increased mortality when used to reduce sympathetic overactivity in HF patients (1). Centrally acting sympatholytic drugs, in contrast to β-blockers, not only inhibit sympathetic activity but also exhibit parasympathomimetic effects. We hypothesized that a combination of sympatholytic and parasympathomimetic activity might reduce the complexity of RR-interval variability (RRIV). It was shown that reduced fractal complexity of RRIV is associated with elevated mortality (2).

Methods

Telemetric transmitters (HD-S11, Data Sciences, USA) were implanted into anesthetized (120 $mg.kg^{-1}$ ketamine & 6 $mg.kg^{-1}$ xylazine i.p.) eight 12-week old male Wistar rats. Implants allowed noninvasive monitoring of aortic pressure, ECG, core body temperature, and locomotor activity. The fractal complexity in the RRI time series was estimated with the detrended fluctuation analysis. Short-term (α1) and long-term (α2) fractal scaling exponents were calculated according to Peng (3). Six increasing doses of central sympatholytics moxonidine and clonidine (0 – 12.15 µmol.kg-1) and the β-blocker metoprolol (0 – 291.1 µmol.kg-1) were applied s.c.

Results

Moxonidine (imidazoline I1 & α2-adrenergic receptor agonist) dose-dependently reduced the α1 fractal exponent (Fig 1A), suggesting a gradual loss of coordination in the cardiac autonomic regulation. At the highest dose, RRIV became uncorrelated (α1 = 0.53 (0.12), $p<0.001$ by the Tukey HSD after the multivariate (Wilks) repeated measure 2-way ANOVA by time and dose. Data are means & S.D. in brackets). Similarly, clonidine (α2-adrenergic receptor agonist) also shifted the α1 exponent (Fig. 1B) toward the uncorrelated chaotic white noise (α1 = 0.55(0.1)). However, metoprolol (β1-adrenergic receptor blocker) did not affect the optimal (1/f noise) short-term correlation in the RR-interval time series (α1 = 1.02(0.08)). An increase in the high-frequency power of RRIV after moxonidine could explain a 30% of α1 diminution. The largest decline in the α2 exponent indicated that clonidine exhibited the most potent sympatholytic effect (Fig. 2B). Even the low doses shifted the α2 exponent of 1.41(0.14), which reflects a rigid, tightly controlled regulatory system, toward the white noise (0.66(0.16)). In contrast, metoprolol attenuated the Brownian

component of RRIV (Fig. 2C) and brought the long-term α2 exponent to ideal complexity characterized by α2 = 1.06 (0.07). Moxonidine affected the α2 exponent only at the highest concentration (Fig. 2A), reducing it to 1.04(0.09).

Conclusion

Higher doses of central sympatholytics are causing a loss of complexity of RR-interval time series, which might reflect a reduction in adaptive capacity of the cardiac autonomic regulation and could be related to the increased mortality in the MOXCON trial (1).

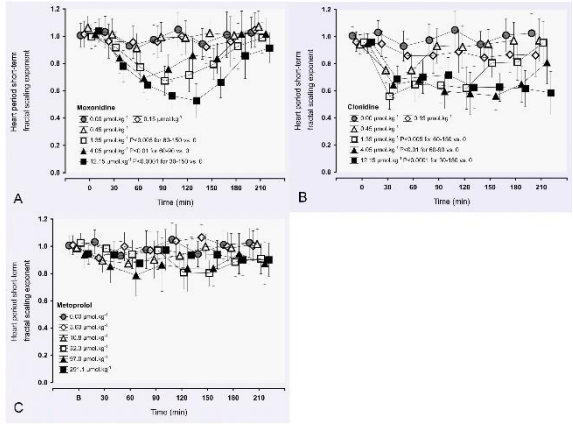

Fig. 1. Effect of antiadrenergic drugs on the short-term fractal scaling exponent α1.
Panel A: Higher doses of moxonidine reduced α1 exponent (a surrogate measure of the cardiac vagal activity), suggesting a parasympathomimetic effect. At 12.15 µmol.kg^{-1}, the heart period variability became uncorrelated. Panel B: Clonidine affected the fractal complexity of RR-interval time series similarly to moxonidine but was effective at lower doses. Panel C: Metoprolol showed no statistically significant effect on α1 exponent, consistent with its absence of a parasympathomimetic effect.

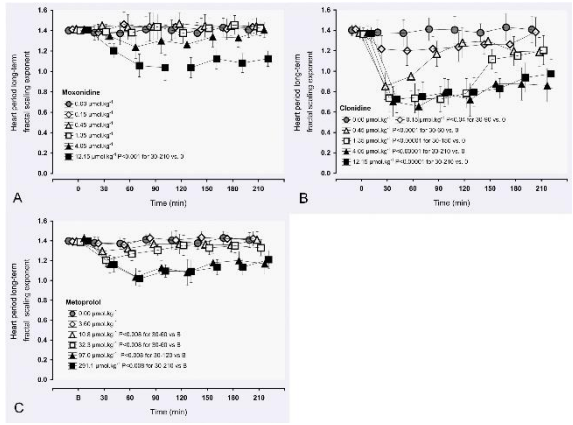

Fig. 2. Effect of antiadrenergic drugs on the long-term fractal scaling exponent α2.
Panel A: Only the highest dose of moxonidine reduced α2 exponent, a surrogate index of the cardiac sympathetic activity. This might indicate a limited sympatholytic effect of moxonidine on the heart. Panel B: All clonidine doses shifted α2 exponent from the rigid Brown noise to the ideal fractal complexity of 1/f noise. The shift was approximately equal with all doses. Panel C: Effect of metoprolol on α2 exponent was close to moxonidine, confirming its cardiac sympatholytic action. Based on α2 exponent shifts, the cardiac sympatholytic effect of metoprolol was weaker than that of clonidine.

References

[1] Cohn JN, Pfeffer MA, Rouleau J, Sharpe N, Swedberg K, Straub M, Iltse C, Wright TJ, MOXCON Investigators 2003, 'Adverse mortality effect of central sympathetic inhibition with sustained-release moxonidine in patients with heart failure (MOXCON)', *Clinical Trial Eur J Heart Fail* 5, 659-67, doi: 10.1016/s1388-9842(03)00163-6

[2] Sen, J, McGill, D 2018, 'Fractal analysis of heart rate variability as a predictor of mortality: a systematic review and meta-analysis', *Chaos* 28, 072101, doi: 10. 1063/1.5038818

[3] Peng, CK, Havlin, S, Stanley, HE, Goldberger, AL 1995, 'Quantification of scaling exponents and crossover phenomena in nonstationary heartbeat time series', *Chaos* 5, 82-87, doi: 10.1063/1.166 141

B 08-16

Effect of adrenaline on serum mid-regional pro-atrial natriuretic peptide and central blood volume

C. Sejersen[1], J. Bjerre-Bastos[2,3], J. P. Gøtze[4,5], H. B. Nielsen[6,7], A. R. Bihlet[3], N. H. Secher[1]

[1] *Rigshospitalet, Department of Anaesthesia, Copenhagen, Denmark*

[2] *University of Copenhagen, Department of Biomedical Sciences, Copenhagen, Denmark*

[3] *NBCD A/S, Herlev, Denmark*

[4] *Rigshospitalet, Department of Clinical Biochemistry, Copenhagen, Denmark*

[5] *Rigshospitalet, Department of Biomedical Sciences, Copenhagen, Denmark*

[6] *Zealand University Hospital Roskilde, Department of Anaesthesia, Roskilde, Denmark*

[7] *University of Copenhagen, Department of Nutrition, Exercise and Sports, Copenhagen, Germany*

Atrial natriuretic peptide (ANP) has vasodilatory, natriuretic, and diuretic properties and is secreted in response to atrial wall distension and thereby provides an indirect evaluation of central blood volume (CBV). Adrenaline possesses chronotropic and inotropic effects which increases stroke volume (SV) and cardiac output (CO) with the increase in SV by adrenaline infusion does not seem to be the result of increased venous return to the heart. The present study evaluated the serum mid-regional proANP$_{(53\text{-}90)}$ (MR-proANP), a stable ANP variant, response to adrenaline infusion with simultaneous recording of CBV by thoracic electrical admittance (TEA) and haemodynamic variables by pulse-contour analysis during four 5-min intervals with graded infusion of adrenaline. Adrenaline infusion increased heart rate (33 ± 18%), SV (6 ± 13%) and thereby CO (42 ± 23%, all $P < 0.05$). The increase in CO did, however, not result from an increase in CBV as TEA remained stable (-3 ± 17%, $P = 0.230$). Serum MR-proANP concentrations increased (26 ± 25%; $P < 0.001$) by adrenaline infusion and remained elevated 60 min thereafter. Thus, as CBV remained similar serum MR-proANP is not only influenced by CBV but also responds to the chronotropic and inotropic state of the heart by adrenaline infusion or adrenaline may directly induce release of ANP variants from the myocytes.

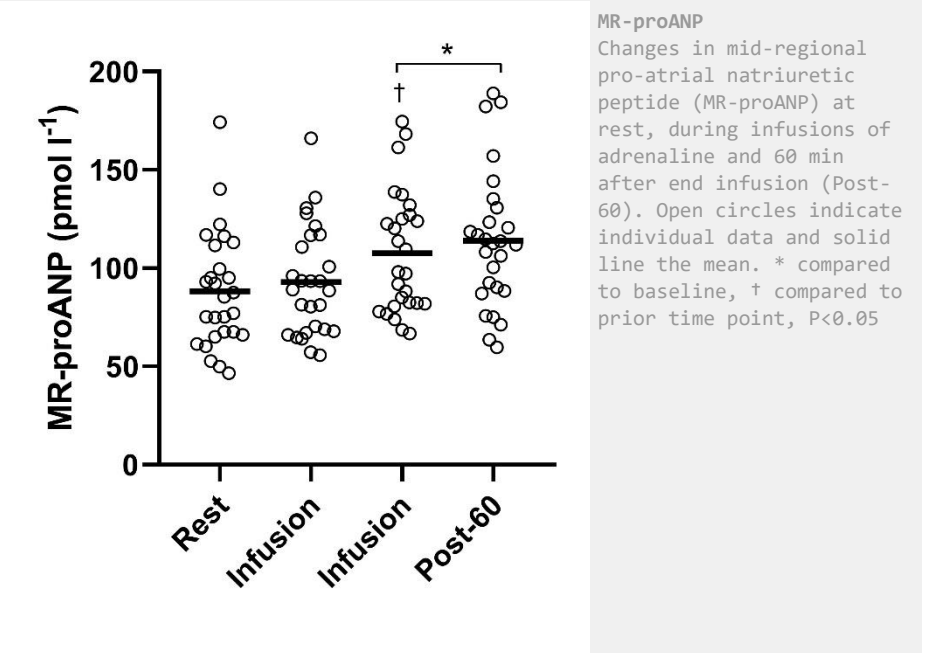

MR-proANP
Changes in mid-regional pro-atrial natriuretic peptide (MR-proANP) at rest, during infusions of adrenaline and 60 min after end infusion (Post-60). Open circles indicate individual data and solid line the mean. * compared to baseline, † compared to prior time point, $P<0.05$

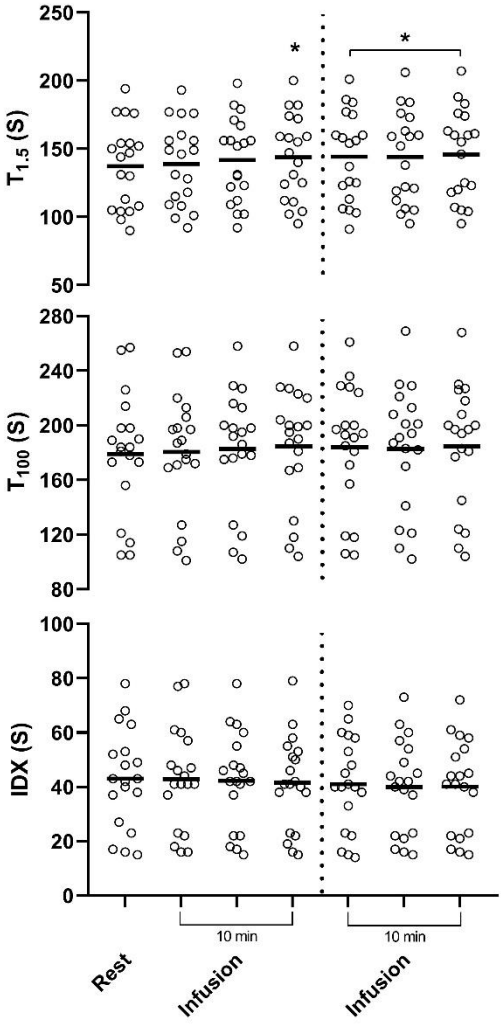

Thoracic electrical admittance
Change in thoracic electrical admittance at 1.5 (T1.5) and 100 kHz (T100) at rest and during the four infusions of adrenaline depicted in 5 min segments with the dotted line indicating separation between intervals for blood sample collection. IDX is the difference between T1.5 and T100 to indicate changes in regional intracellular water. Open circles indicate individual data and solid line the mean. * compared to baseline, $P<0.05$.

B 08-17

Unravelling the role of acidic organelles in Goat Atrial Fibrillation

T. Ayagama[1], R. A. Capel[1], P. Charles[2], D. A. Priestman[1], D. Aston[3], S. J. Bose[1], G. Berridge[2], A. Galione[1], R. Fischer[2], A. Cribbs[4], L. Heather[5], B. Boland[6], H. Kramer[7], F. M. Platt[1], U. Schotten[8], S. Verheule[8], R. A. Burton[1]

[1] *University of Oxford, Department of Pharmacology, Oxford, UK*
[2] *University of Oxford, Target Discovery Institute, Nuffield Department of Medicine, Oxford, UK*
[3] *Royal Papworth Hospital NHS Foundation Trust, Department of Anaesthesia and Critical Care, Cambridge, UK*
[4] *University of Oxford, Department of Medical Sciences, John Radcliffe Hospital, Oxford, UK*
[5] *University of Oxford, Department of Physiology, Anatomy and Genetics, Oxford, UK*
[6] *University College Cork, Department of Pharmacology and Therapeutics, Cork, Ireland*
[7] *University of Cambridge, MRC Laboratory of Molecular Biology, Cambridge, UK*
[8] *University of Maastricht, School for Cardiovascular Diseases, Faculty of Health, Medicine and Life Sciences, Maastricht, Netherlands*

This work is supported by Sir Henry Dale Wellcome Trust and Royal Society Fellowship (109371/Z/15/Z; to R.A.B.B.). This project was supported by a British Heart Foundation Project Grant (PG/18/4/33521).T.A. received funding from the Returners Carers Fund (PI R.A.B.B.), Medical Science Division, University of Oxford.

Introduction

Lysosomes have traditionally been thought of as cellular waste processing organelles and are now known to be an active component of functional atrial signals(1). Lysosome number and dysfunction has been characterised in several cardiac conditions(2), however, their role in atrial fibrillation (AF) is yet to be defined. Here we focus on unravelling molecular alterations in acidic organelles in atrial tissue using a fractionation protocol(3) followed by multi-omics analysis.

Methods

The goat study was carried out in accordance with the principles of the Basel Declaration and regulations of European directive 2010/63/EU. The local ethical board for animal experimentation of the Maastricht University approved the protocol. AF was induced and maintained in goats (C. hircus) for 6 months, followed by an open chest sacrifice experiment (N=3 AF and N=3 sham controls). We adapted our recently published endolysosome (EL) isolation-fractionation method (3) to study the EL proteins in the AF goat model. Label-free quantitative MS/MS mass spectrometric (QExec LumosTM mass spectrometer) and transcriptomic (RNASeq) analyses of peptides and mRNA were performed on the EL and whole tissue lysate (TL) to identify statistically significant changes in proteins and genes. Mass spectrometric data were analysed using Progenesis QI (WatersTM Cooperation, version 4.2) and Perseus (version 1.5.2.4) to identify proteins. Volcano plots were generated using normalised intensities with a two-way Student's t-test, and proteins significantly different between AF and Sham goat models of each TL and EL sample identified. The PANTHER Overrepresentation Test was performed for the highest abundant EL proteins using the panther-gene ontology database (Panther–GO). The functional network interactions were mapped using KEGG, Reactome (version 77) and String analysis (version 11.5).

Results

Out of 2104 proteins, 340 proteins in TL and 148 in EL were significantly altered in AF. Some significantly regulated proteins, such as Ras-related protein 11 (RAB11), were validated with Western blotting. In addition, TL highlighted mitochondrial oxidative-phosphorylation OXPHOS, and

AMPK pathway protein upregulation, indicating a potential increased ATP energy demand in AF. EL fractions showed enrichment for EL specific proteins, including Lysosomal alpha-glucosidase (GAA), Ras-related protein Rab-7a (Rab7a), Clathrin light chain B (CLTB), vacuolar protein-sorting-associated protein 25 (VPS25) and T-complex protein 1 subunit beta (CCT2). Upregulation of protein processing suggests increased vesicular trafficking, potentially related to increased metabolic energy demand. In addition, the downregulation of autophago-lysosome fusion proteins such as dynein, dynactin and dynamin indicates a possible disruption in the cellular degradation of macromolecules.

Conclusion

The data presented provides evidence to support the role of the lysosome as an important organelle in AF pathology.

References

[1] Collins TP, Bayliss R, Churchill GC, Galione A, Terrar DA. NAADP influences excitation-contraction coupling by releasing calcium from lysosomes in atrial myocytes. Cell Calcium. 2011;50(5):449-58.

[2] Chi C, Riching AS, Song K. Lysosomal Abnormalities in Cardiovascular Disease. Int J Mol Sci. 2020;21(3):811

[3] Ayagama T, Bose SJ, Capel RA, Priestman DA, Berridge G, Fischer R, et al. A modified density gradient proteomic-based method to analyze endolysosomal proteins in cardiac tissue. iScience. 2021;24(9):102949.

B 08-18

Human BIN1 isoforms grow, maintain, and regenerate excitation–contraction couplons in adult rat and human induced pluripotent stem cell-derived cardiomyocytes

J. Guo[1], Q. Tian[1], M. Barth[1], W. Xian[1], S. Ruppenthal[1], H.-J. Schaefers[2], Z. Chen[3,4], A. Moretti[3,4], K.-L. Laugwitz[3,4], P. Lipp[1]

[1] Saarland University, Centre for Molecular Signaling, Homburg, Germany

[2] Saarland University Medical Center, Department of Thoracic and Cardiovascular Surgery, Homburg, Germany

[3] Technische Universität München, Department of Medicine, Klinikum rechts der Isar, Munich, Germany

[4] German Centre for Cardiovascular Research, Partner site Munich Heart Alliance, Munich, Germany

Excitation-contraction (EC) coupling is one of the main mechanisms that regulate the function of ventricular cardiomyocytes. Structurally, EC coupling relies on the membrane invagination—transverse tubular system (T-tubules) which enables the fast activation of ryanodine receptor 2 (RyR2) in the sarcoplasmic reticulum by the calcium entry from the L-type calcium channel (LTCC) in the sarcolemma. The bridging integrator 1 (BIN1) is one of the main proteins that regulate the biogenesis of T-tubules. Its expression and function in human cardiomyocytes are not fully elucidated, which is investigated in the present study. We firstly analyzed the expression pattern of BIN1 splicing variants using the total RNA samples of heart tissue from healthy human donors (purchased from BioChain). Through PCR and sanger sequencing we identified five different BIN1 splicing variants (6, 8, 9, 10, and 13), which are not completely the same with those identified in the mouse heart (Hong, TingTing. et al. 2014) and rat heart (Li, Lin-Lin, et al. 2020). It is also inconsistent with the previous finding that BIN1 isoforms with the phosphoinositide binding motif (PI) (8 and 13) were exclusively expressed in the skeletal muscles (Lee, Eunkyung, et al.2002). Overexpression of these BIN1 isoforms in HEK cells demonstrated that the PI-containing isoforms have stronger capacity to generate tubules. We further characterized the effects of these isoforms in cultured rat ventricular cardiomyocytes and human induced pluripotent stem cell-derived cardiomyocytes (hiPSC-CMs) via adenoviral gene transfer, immunostaining and confocal microscopic imaging of calcium using either the calcium dye (Fluo-4) or calcium biosensor (Junctin-GCaMP6). To analyze the EC couplons in cardiomyoyctes, a previously published analysis method CaCLEAN was applied (Tian, Qinghai, et al. 2017). We found that all these BIN1 isoforms can maintain the T-tubules as well as the EC coupling of cultured ventricular myocytes at different degrees. Particularly, BIN1 isoforms with PI domain (8 and 13) brought out the most significant effects. When overexpressed in the hiPSC-CMs, isoform 8 and 13 generated abundant tubules with which LTCCs or RyR2s were colocalized. Further analysis of the calcium release by CaLCLEAN revealed that there were functional EC couplons formed around the newly induced tubules. As a result, the EC coupling of hiPSC-CMs was significantly improved compared with those without BIN1 expression. Based on these results we conclude that BIN1 isoforms, especially those with PI motif, play essential roles in the maintenance, regeneration, and de novo biogenesis of T-tubules in cardiomyocytes. These newly tubules can trigger the build-up of EC couplons which further enhance the efficiency of calcium handling. *The work was funded in parts by the DFB/SFB894 and DFB/SFB TR 152.*

References

Hong, TingTing, et al. "Cardiac BIN1 folds T-tubule membrane, controlling ion flux and limiting arrhythmia." Nature medicine 20.6 (2014): 624-632.

Lee, Eunkyung, et al. "Amphiphysin 2 (Bin1) and T-tubule biogenesis in muscle." Science 297.5584 (2002): 1193-1196.

Li, Lin-Lin, et al. "Nanobar array assay revealed complementary roles of BIN1 splice isoforms in cardiac T-tubule morphogenesis." Nano letters 20.9 (2020): 6387-6395.

Tian, Qinghai, et al. "An adaptation of astronomical image processing enables characterization and functional 3D mapping of individual sites of excitation-contraction coupling in rat cardiac muscle." Elife 6 (2017): e30425.

B 08-19

Titin properties in diabetic and non-diabetic mouse and human hearts after myocardial infarction

J. P. Hoffmeister[1], M. Isic[1], S. Kötter[1], M. Thielmann[3], P. Kleinbongard[2], J. Schmitt[4], **M. Krüger**[1]

[1] Heinrich-Heine University Düsseldorf, Medical Faculty, Institute of Cardiovascular Physiology, Düsseldorf, Germany

[2] University of Essen Medical School, Institute of Pathophysiology, Essen, Germany

[3] University of Essen Medical School, Department of Thoracic and Cardiovascular Surgery, Essen, Germany

[4] Heinrich-Heine University Düsseldorf, Medical Faculty, Institute of Pharmacology and Clinical Pharmacology, Düsseldorf, Germany

We thank Sabine Bongardt and Jelena Löblein for excellent technical assistance and Wolfgang Ristau for management of the clinical data.

Introduction

The study aims at the mechanistic understanding of sarcomere dysfunction in the remote myocardium (RM) after ischemia/reperfusion (I/R) and the exacerbating effects of type-2 diabetes mellitus (T2DM). Both disease entities have been shown to affect titin-based cardiomyocyte stiffness in mouse models. Here, we perform a first exploratory study on biopsies from diabetic and non-diabetic patients with and without recent myocardial infarction (max. 21 days after I/R) to test the translatability of our previous results from mouse heart.

Method

Samples were taken from RM of diabetic leptin-receptor deficient (db/db) mice and heterozygous littermates (db/+) 24h and of wildtype BL/6J mice 21 days after experimental ischemia/reperfusion (I/R, 60 min by transient ligation of coronary arteries in a closed-chest surgical model, anesthesia: intraperitoneal injection of ketamine (60 mg/kg) and xylazine (10 mg/kg)), or sham operation (sham). Data were compared to biopsies taken from right atrial tissue during bypass surgery. Samples were immediately frozen in liquid nitrogen. Cardiomyocytes were mechanically isolated from the frozen tissue and titin isoform composition, titin and troponin I (cTnI) phosphorylation were tested by SDS-PAGE and Western blot analysis using phosphosite-directed antibodies.

Result

In db/+ mice 24h after I/R titin phosphorylation at S11878 (pS11878) was significantly increased to 153±14%, and increased cardiomyocyte passive tension (PT). In db/db mice titin pS11878 was increased to 135±12%, and pS12022 to 197±21% compared to db/+, and increased cardiomyocyte PT at baseline. cTnI phosphorylation was reduced in db/db hearts at baseline, indicating increased myofilament Ca^{2+}-sensitivity. No further increase was observed in pS11878, pS12022 and PT 24h after I/R. Instead, pS4010 levels in db/db increased to 147±16% (P<0.05). Titin isoform composition was preserved among groups. In wild-type mice 21d after I/R the increase in cardiomyocytes PT was partially reversed, but pS11878 remained increased (169±23% of sham). Preliminary results (n=4-6 per group) from human biopsies indicate that titin isoform expression remains unchanged by T2DM and I/R, but we observed increased levels of the titin degradation band T2 in a subset of T2DM ± I/R, compared to non-diabetic hearts. Titin phosphorylation was not significantly changed, but requires further analyses due to large variability in the data sets. cTnI phosphorylation is significantly reduced by 27±4 % in diabetic human biopsies ± I/R (P<0.05).

Conclusion

Data from mouse hearts suggest complex modification of sarcomere function to adapt RM to high mechanical stress acutely after I/R, but also in the long term. The acute adaptation fails in diabetic hearts. First data from human biopsies indicate similarities to mouse hearts, but further analyses, considering treatment and comorbidities of the human patients are required.

B 08-20

Twenty-four hours preservation of hearts prior to cardiomyocyte isolation to reduce the number of experimental animals

B. Pfeilschifter, T. Seidel, T. Volk

Friedrich-Alexander-Universität Erlangen-Nürnberg, Institute for Physiology II, Erlangen, Germany

Introduction

The isolation of cardiac myocytes from adult animals represents an important technique in basic cardiovascular research and is without alternative for many research questions. However, to obtain cardiomyocytes, the heart must be removed, so that the donor animal is sacrificed. For this reason, the yield should be as large as possible. Nevertheless, animal models, especially transgenic mice, are frequently and possibly unnecessarily replicated because it is believed that cardiomyocytes must be isolated and investigated immediately after heart collection to avoid unacceptable qualitative and functional limitations. In this project, we investigate if hearts from laboratory animals can be preserved for at least 24h prior to myocyte isolation without affecting subsequent experiments.

Methods

Adult mice were killed by cervical dislocation after analgesia with isoflurane. Hearts were excised and used for enzymatic cardiomyocyte isolation either immediately (control) or after conservation for 24h at 4°C. After cell isolation, action potentials and K+ currents were measured using the whole-cell patch-clamp technique.

Results

Action potential (AP) recordings unveiled no significant differences in resting membrane potential (-81.4 vs. -80.6 mV), overshoot (36.2 vs. 30.9 mV) and AP duration at 90% repolarization (APD90) (71.1 vs. 62.7 ms, n = 23/22 cells in control/conservation group, respectively). Other measures of APD (APD20, APD50 and APD at 0 mV) did not differ either, indicating preserved AP shape in conserved hearts. Maximum upstroke velocity of the AP was higher with 170.5±15.1 V/s in the control group compared to 137.3 ± 11.1 V/s after conservation (p=0.09). However, when APs were initiated from the same holding potential of VPip = -85 mV, upstroke velocity was similar in both groups (196.9±14.1 vs. 188.2±15.1 V/s). This suggests, that the fast Na+ current was not affected by conservation. The current density of the transient outward potassium current (Ito), the main repolarizing current of the mouse AP, was similar both groups (40.3±2.7 vs. 41.8±4.1 pApF-1 at VPip = 60 mV; n = 29/20). Moreover, the inwardly rectifying K+ current (KIR) was also similar in myocytes from control and conserved hearts (5.23±0.5 vs. 6.33±0.3 pApF-1 at VPip = -120 mV, n=16/7).

Conclusion

We show that important cellular electrophysiological characteristics, such as resting membrane potential, AP shape and duration and potassium currents are only marginally affected by cold storage of the heart for 24h. We suggest that the presented method will allow for transport of excised hearts over long distances, making the replication of transgenic lines and disease models obsolete in many cases. Due to its simplicity, the method would also permit multiple use of animals sacrificed for non-cardiac studies.

B 08-21

Why the heart of coelacanth fish necessitates a major revision of the ancestral heart of terrestrial vertebrates

B. Jensen[1], H. Lauridsen[2]

[1] *Amsterdam UMC, Department of Medical Biology, Amsterdam, Netherlands*

[2] *Aarhus University, Department of Clinical Medicine, Aarhus, Denmark*

Introduction

The heart of the first land-living vertebrates, tetrapods, is inferred by comparing present-day lungfish and amphibians. These groups belong to lobe-finned fish as do the rare coelacanths. Few coelacanth hearts have been studied and it has been concluded they are exceedingly primitive because of a linear chamber topology. Until now, the coelacanth heart has been omitted from inferences of the ancestral tetrapod heart.

Methods

Using MRI, CT, and 3D-modelling, we assessed the morphology of in-situ hearts of two coelacanths, 13 specimens from all three major groups of amphibians, five specimens from all three major groups of lungfish, nine ray-finned fish, 22 cartilaginous fish, two lampreys, and two hagfish.

Results

The coelacanth heart is long mostly due to an elongate outflow tract, but this setting resembles that of fellow ray-finned non-teleost fish. The cardiac chambers have a substantial left-right symmetry as in other bony fish, while the coelacanth sinus venosus and atrium are positioned relatively caudally. Nonetheless, the coelacanth heart is much different from the hearts of cartilaginous fish, lampreys, and hagfish, and it is not primitive. We then assessed 20 gross morphological characters in amphibians, lungfishes, and coelacanths. Nine were shared by all groups. Five were shared by amphibians and lungfishes only, such as a lung vein connecting to the left atrium and an atrial septum. Six were shared by amphibians and coelacanth, such as a valved atrioventricular junction (lungfishes have a 'plug') and absent ventricular septum.

Conclusion

We conclude the ancestral tetrapod heart likely had a lungfish-like atrium and a coelacanth-like ventricle.

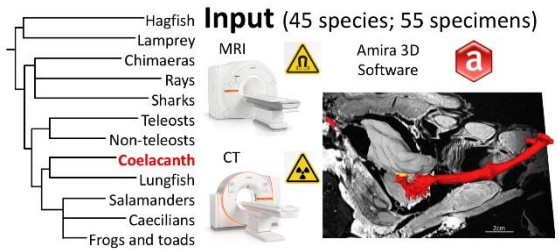

Overview of the study

Figure 1. We imaged the heart in-situ of 45 species of fish and amphibians, the phylogenetic relation of which is shown on the left, using either MRI or CT scanning followed by 3D remodeling. This allowed us 1) to assess whether the heart of coelacanths is primitive as previously claimed - it is not - and 2) to infer the primitive state of the heart of the first land-living vertebrates which, our analyses show, likely comprised a lungfish-like atrium and a coelacanth-like ventricle.

B 08-23

Properties of late calcium sparks in murine ventricular myocytes in the presence of pharmacological inotropes

O. Hood, G. Toerien-Howie, H. Davies, E. D. Fowler

Cardiff University, School of Biosciences, Cardiff, UK

This work was supported by a Physiological Society Research Springboard Studentship to OH,Cardiff University Seedcorn award and BHF IBSRF (FS/IBSRF/21/25071) to EDF.

Introduction

Arrhythmias are a major cause of sudden cardiac death (SCD). Calcium dysregulation is key to pathological electrophysiology, via the Na/Ca exchange mechanism. Late calcium sparks (LCS) were recently shown to occur during the Ca transient decay in normal rabbit ventricular myocytes (Fowler et al. 2018), and LCS frequency was increased in myocytes from rabbits with heart failure (Fowler et al. 2020). Association with early afterdepolarisations was observed, implying the importance of LCS in disease. Mouse is the most commonly used mammalian model organism due to its genetic tractability, however little is known regarding the properties of LCS in murine ventricular

myocytes, which may be important for interpreting arrhythmias in this species (Guo et al. 2012; Fowler et al. 2020). This work aims to characterise LCS properties in mouse ventricular myocytes under both basal conditions and in the presence of cardiac inotropes.

Methods

All procedures accorded with current EU/UK legislation. Wildtype C57BL/6 mouse hearts were removed, and immediately perfused via the aorta with physiological saline on a Langendorff apparatus. Individual ventricular myocytes were isolated by gentle shaking following perfusion with a solution containing collagenase. All experiments were performed at 22°C. External Ca was gradually raised from 0.05-1mM, and myocytes were loaded with Fluo-4-AM (Ca indicator). Following electrical field stimulation at 1Hz using a pair of Pt electrodes, Ca release was monitored using an inverted confocal laser scanning microscope (Zeiss LSM880) in line scanning mode at 1kHz with 488nm excitation and emission collected at >500nm. LCS were detected using an automated algorithm in background-subtracted recordings (Fowler et al. 2018). Data were collected from 20 cells from 4 mice. Statistical tests performed were paired T-tests, and normality was checked using Shapiro-Wilk tests. Data are presented as mean ± SEM.

Results

Under basal conditions diastolic Ca spark frequency in mouse myocytes was 4.3±0.8 /s/100µm, with an average amplitude of 0.51±0.03 F/F_0 and full width at half-max of 2.3±0.1 µm. Under basal conditions, the frequency of LCS in mouse myocytes was greater 7.7±1.4 LCS/s/100µm (P=0.04 vs diastolic Ca sparks) but the mean amplitude was similar to diastolic Ca sparks. Isoproterenol (100nM) approximately doubled the frequency of diastolic Ca sparks (P=0.02) and caused a 4-fold increase in LCS frequency (P=0.001) but did not affect amplitude.

Conclusions

Further research into other inotropic stimuli is underway to produce a comprehensive understanding of their effect on LCS frequency and properties in murine cells. This will help the mechanistic understanding of arrhythmogenesis in model organisms to improve the development of potential treatments for SCD.

References

[1] Fowler, E. D., Kong, C. H. T., Hancox, J. C. & Cannell, M. B. Late Ca2+ sparks and ripples during the systolic Ca2+ transient in heart muscle cells short communication. Circ. Res. 122, 473–478 (2018).

[2] Fowler, E. D. et al. Arrhythmogenic late Ca 2+ sparks in failing heart cells and their control by action potential configuration. Proc. Natl. Acad. Sci. 117, 2687–2692 (2020).

[3] Guo, T. et al. CaMKIIδC slows [Ca]i decline in cardiac myocytes by promoting Ca sparks. Biophys. J. 102, 2461–2470 (2012).

B 08-24

The effect of estradiol, 17β-E2, on the human and animal cardiac Kv7.1/KCNE1 channels

V. A. Linhart[1], L.-M. Erlandsson[1], A. Halili[1], J. E. Nikesjö[1], K. E. Odening[2], S. I. Liin[1]

[1] *Linköping University, Department of Biomedical and Clinical Sciences, Linköping, Sweden*

[2] *University of Bern, Department of Cardiology, Bern, Switzerland*

Introduction

The cardiac voltage-gated potassium channel Kv7.1/KCNE1 has an important role in the ventricular cardiac action potential, where it contributes to the repolarization phase. Inherited mutations in genes encoding for this channel, and compounds that inhibit channel function, have been functionally linked to the arrythmia Long QT syndrome (LQTS). To aid in arrhythmia risk assessment, it is therefore important to find which compounds inhibit the Kv7.1/KCNE1 channel and, thus, lead to higher risk of suffering from LQTS symptoms, such as arrhythmia and sudden cardiac death. The steroid hormone estradiol (17β-E2) has been implicated with prolonging the QT interval and increasing the risk for women with congenital or acquired LQTS when compared to men. However, little is known about the mechanistic basis of modulation of the Kv7.1/KCNE1 channel by 17β-E2.

Methods

We used the two-electrode voltage clamp technique to study the effect of 17β-E2 on the Kv7.1/KCNE1 channel expressed in *Xenopus* oocytes.

Results

We find that 10µM of 17β-E2 inhibits the maximum conductance of Kv7.1/KCNE1 channel by roughly 60% (SEM) and that the effect requires the KCNE1 subunit. Moreover, we find that LQTS-associated mutations in KCNE1 tune the 17β-E2 effect.

As the KCNE1 subunit varies between animal species, we tested the 17β–E2 effect on the Kv7.1/KCNE1 channel of rabbit, guineapig and zebrafish and compared it to the effect seen in the human channel. The rabbit Kv7.1/KCNE1 channel shows pronounced 17β–E2-induced reduction in maximum conductance compared to the human Kv7.1/KCNE1 channel (for 10µM the maximum conductance was decreased by roughly 95%).

Conclusion

Altogether, this study increases our understanding of the mechanistic basis for 17β-E2 inhibition of Kv7.1/KCNE1 and demonstrates mutation and species dependent responses to 17β-E2. It suggests the combined burden of LQTS mutations and 17β-E2 influence may induce the LQTS phenotype.

B 08-25

Impact of acute carnosine and beta-alanine supplementation on genes related to carnosine metabolism in rat cardiomyocytes

J. V. Creighton[1], K. J. Elliott-Sale[1,3], M. D. Turner[2], C. L. Doig[2], C. Sale[1,3]

[1] *Nottingham Trent University, Musculoskeletal Physiology Research Group, Sport, Health and Performance Enhancement (SHAPE) Research Centre, School of Science and Technology, Nottingham, UK*

[2] *Nottingham Trent University, Centre for Diabetes, Chronic Diseases and Ageing, School of Science and Technology, Nottingham, UK*

[3] *Manchester Metropolitan University, Department of Sport and Exercise Sciences, Institute of Sport, Manchester, UK*

Thanks to Nottingham Trent University and Natural Alternatives International for funding this project.

Introduction

Carnosine is a pleiotropic histidine-containing dipeptide synthesised from beta-alanine and L-histidine, which can be obtained from the diet. Carnosine is suggested to have putative roles in intracellular pH buffering, calcium handling and oxidative stress in cardiac tissue. Carnosine content in tissue is regulated through carnosine synthesis, carnosine hydrolysis, and the activity of transaminase enzymes, in addition to amino acid and non-specific peptide transporters. It remains unclear as to whether carnosine can accumulate in the cardiac tissue with exogenous beta-alanine

(the rate-limiting precursor of carnosine synthesis) provision. This study mapped the expression of genes related to carnosine synthesis enzymes and transporters in cardiomyocyte cells in response to acute carnosine or beta-alanine supplementation. Changes in gene expression may reveal mechanisms by which beta-alanine or carnosine availability influence carnosine homeostasis.

Methods

Differentiated H9c2 cells (rat ventricular cardiomyocytes) were exposed to 0.1, 0.5, 1, 5 or 10 mM of carnosine or beta-alanine for 4-hours (n = 3 - 5). Gene expression was measured using real-time qPCR. The fold change in expression of the genes of interest were calculated using the delta-delta Ct method against the reference gene 18S. Data were analysed by one-way ANOVA.

Results

Cardiomyocyte cells expressed the following genes of interest: carnosine synthesis (*CARNS1*), carnosine hydrolysis (*CNDP1, CNDP2*), beta-alanine transporter (*TAU-T*), amino acid transporter (*PAT1*), non-specific peptide transporters (*PEPT1, PEPT2, PHT1*, *PHT2*) and transaminase (*GABA-T*). The beta-alanine transaminase *AGXT2* was not expressed in cardiomyocyte cells. Carnosine supplementation had no effect on the expression of these genes ($p>0.05$). Beta-alanine supplementation significantly decreased the expression of *TAU-T* at 0.5 mM (62%↓, $p<0.05$), 1 mM (54%↓, $p<0.05$) and 10 mM (59%↓, $p<0.05$), with no significance at 0.1 mM (50%↓, $p>0.05$) and 5 mM (12%↓, $p>0.05$). *PHT1* expression was significantly decreased at all beta-alanine concentrations (35 – 66%↓, $p<0.05$) except 5 mM (48%↓, $p>0.05$).

Conclusion

Cardiomyocytes express genes of the enzymes and transporters needed to uptake and utilise carnosine and beta-alanine. The reduced mRNA expression of the transporter *TAU-T* suggests potential competition between both beta-alanine and taurine for *TAU-T* and suggests this solute carrier protein could play a role in beta-alanine metabolism. Importantly, *CARNS1* expression did not change with supplementation, indicating increases in intracellular carnosine may not be dependent upon carnosine synthesis and instead may shift towards dependence on the transportation of beta-alanine into cells.

B 08-26

Monoamine oxidase A-mediated effects of serotonin on rat heart

J. Knittel, R. Schreckenberg, J. Heger, K.-D. Schlüter
Justus Liebig University, Department of Physiology, Gießen, Germany

Introduction: Monoamine oxidases (MAOs) are proteins of the outer mitochondrial membrane, which produce reactive oxygen species (ROS) by metabolizing biogenic amines. Two isoforms, MAO-A and MAO-B, have been identified with MAO-A being the predominant isoform in rat heart. Its upregulation under pathophysiological conditions, such as hypertension, adverse cardiac remodelling, and consecutive heart failure, implies an important role for MAO-A in disease progression. However, data on the effects of MAO-A-mediated metabolism on cardiomyocytes are limited.

Methods: Adult ventricular rat cardiomyocytes (ARVC) were isolated from Wistar-Hannover rats (WHR) as described previously [1,2]. Cells were stimulated with the MAO-A substrate serotonin directly or 20 hours prior to the measurement and the contractility upon electrical stimulation was assessed. Additionally, we photometrically quantified the hydrogen peroxide generation of isolated heart mitochondria in presence of serotonin [3]. The expression of genes related to the serotonin metabolism were analysed by qPCR in heart tissue from WHR or spontaneous hypertensive rats (SHR) of different ages.

Results: Long-term stimulation of AVRC with 100 µM serotonin led to a decrease of 55 % in relative cell shortening (SEM 0,46, $p<0,0001$, n=54, one-way ANOVA), while lower concentrations showed no significant effects. In presence of the specific MAO-A inhibitor clorgyline, concentrations of up to 100 µM serotonin were tolerated without significant loss of contractile function. In contrast, short-term stimulation experiments demonstrated a decrease of 14 % in cell shortening at concentrations of 1 µM serotonin (SEM 0,36, $p=0,0036$, n=81, one-way ANOVA), which persisted with the addition of clorgyline. Hydrogen peroxide generation was increased by 59 % in presence of 100 µM serotonin in isolated cardiac mitochondria (SEM 0,07, $p=0,0017$, n=4, one-way ANOVA) but was completely reversed by the addition of clorgyline. Gene analysis revealed an age-dependent increase in MAO-A expression in both WHR and SHR with SHR showing a significant increase at earlier ages. The expression of the serotonin transporter (SERT) decreased equally with age in WHR and SHR, whereas catalase expression showed no age-dependent alterations. The expression of aldehyde dehydrogenase-2 decreased significantly in older WHR but remained at a similar level in SHR.

Conclusion: Serotonin leads to MAO-A-mediated cellular dysfunction in AVRC. Short-term effects, however, occurred independent of MAO-A inhibition. Besides hypertension, ageing promotes an increase in the expression of MAO-A. The age-dependent downregulation of the serotonin transporter could thus represent a protective mechanism to reduce serotonin-mediated ROS generation. Our results implicate MAO-A as a potential therapeutic target, but further research on MAO-A inhibition in in-vivo models is needed.

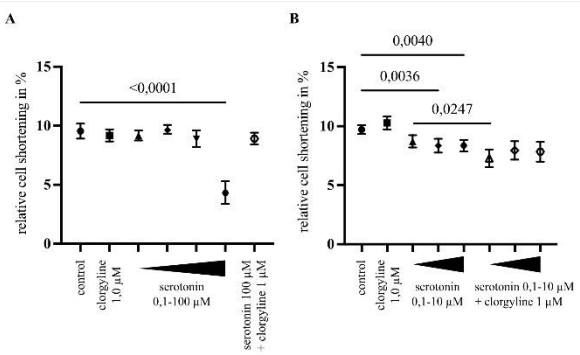

Relative cell shortening of ARVC

The contractility of ARVC was assessed upon electrical stimulation. Serotonin was added in different concentrations **(A)** 20 hours or **(B)** directly prior to the measurement. Long-term stimulation with 100 µM serotonin led to a significant reduction which was completely abolished by clorgyline. Short-term stimulation resulted in a decreased cell shortening already at concentrations of 1 µM serotonin which persisted in presence of clorgyline. Mean values and 95 % confidence intervals are given. P-values were calculated by using one-way ANOVA with Tukey correction.

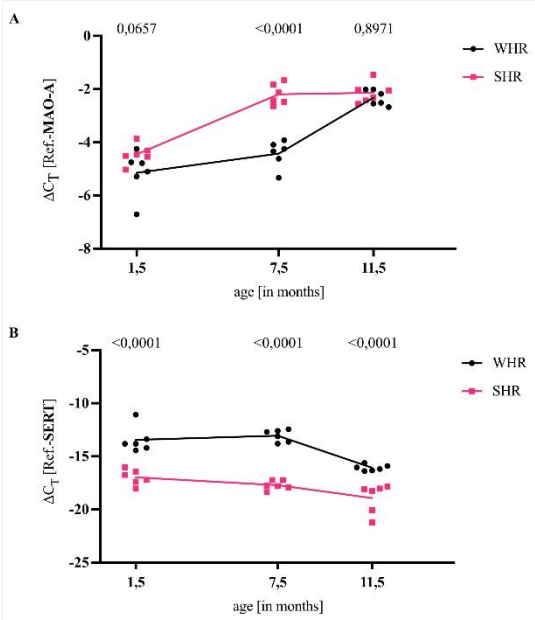

Age-dependent gene expression of MAO-A and SERT in rat heart

(A) The expression of MAO-A in SHR was significantly increased at the age of 7,5 months ($\Delta\Delta C_T$ 2,2, SEM 0,29, $p<0,0001$). An age-dependent increase could be observed in both WHR and SHR. **(B)** The expression of SERT was significantly lower in SHR irrespective of age. However, an age-dependent downregulation occurred in both WHR and SHR. ΔC_T values are presented for the different ages (1,5, 7,5 and 11,5 months) and their mean values are linked. WHR and SHR were compared at each timepoint using two-way ANOVA with Sidak correction (n=6).

References

[1] Nippert, F., Schreckenberg, R. and Schlüter, K.-D., 2017, 'Isolation and Cultivation of Adult Rat Cardiomyocytes', *Journal of Visualized Experiments*, 128, e56634

[2] Schlüter, K.-D., Schreiber, D., 2005, 'Adult Ventricular Cardiomyocytes', *Basic Cell Culture Protocols*, 290, 305-314, Humana Press

[3] Grivennikova, --V. G., Kareyeva, A. V. and Vinogradov, A. D., 2018, 'Oxygen-dependence of mitochondrial ROS production as detected by Amplex Red assay', *Redox biology*, 17, 192-199

B 08-27

THE CARDIOPROTECTIVE ROLE OF IKS POTENTIATION AGANIST ISCHAEMIC INJURY

A. I. Alnaimi[1,2], S. Brennan[1], R. Rainbow[1], P. Sharma[1]

[1] *University of Liverpool, Department of Cardiovascular and Metabolic Medicine/Institute of Life Course and Medical Sciences, Liverpool, UK*

[2] *University of Imam Abdulrahman Bin Faisal, Department of Cardiac Technology/Institute of Applied Medical Sciences, Dammam, Saudi Arabia*

My utmost acknowledgement very rightfully belongs to Dr Richard Rainbow and Dr Sean Brennan. I would also like to extend my gratitude to the Saudi government, which funded my project, and to the University of Imam Abdulrahman Bin Faisal University for being an integral part of funding the project.

Introduction

In the UK alone there are around 86,000 heart attacks each year with around 52,000 of these being the most serious ST-segment elevation myocardial infarctions (STEMI) (1). Ischaemia occurs in a response to the lack of oxygen supply into downstream tissue beyond the blockage area of coronary artery. The intrinsic cardioprotective pathways within the heart, activated by ischaemic preconditioning, have been effective at reducing infarct size in pre-clinical models, however have not successfully translated to efficacy in humans (2,3). In most cardioprotective phenotypes, there is a reduction in electrical excitability leading to a reduction in the Ca^{2+} accumulation during each systolic interval reducing energy consumption required to restore Ca^{2+} homeostasis. Here, we demonstrate cardioprotection against ischaemia via pharmacological manipulation of the slowly activating K^+ (IKs) current in order to directly mimic the changes seen in electrical activity in cardioprotection.

Methods

Adult male Wister rats (300-400 g) were killed by cervical dislocation. Whole-cell patch clamp electrophysiology to measure action potentials and *ex vivo* Langendorff whole heart coronary ligation experiments as a model of myocardial infarction. Specific pharmacological inhibitors and activators were used to modulate channel activity in each experimental protocol.

Results

The selective IKs blocker JNJ303 prolonged the cardiac action potential duration, albite insignificantly (n = 6, P=0.27) and increased infarct size following ischaemia (n = 5, P=0.0005). However, selective potentiation of ventricular IKs using ML277 shortened the cardiac action potential duration (n = 8, P=0.024) and decreased the infarct size in the whole heart (n = 5, P<0.0001). These data suggest an important role of ventricular IKs in cardioprotection against ischemia.

Conclusion

Potentiation of the IKs current in cardiomyocytes may be cardioprotective by shortening the cardiac action potential, reducing intracellular calcium loading and thus preserving cellular ATP. This could be clinically used as a novel pharmacological cardioprotection against myocardial ischaemia.

References

[1] BHF, B. H. F. 2021. *Heart Statistics* [Online]. Available: https://www.bhf.org.uk/what-we-do/our-research/heart-statistics [Accessed May 22, 2022.

[2] Murry, C., Jennings, R. & Reimer, K. 1986. Preconditioning with ischemia: A delay of lethal cell injury in ischemic myocardium Circulation. 1986; 74: 1124–36 doi: 10.1161/01. *CIR*, 74(1124.

[3] Kitakaze, M. 2010. How to mediate cardioprotection in ischemic hearts—accumulated evidence of basic research should translate to clinical medicine. *Cardiovascular drugs and therapy*, 24(3), pp 217-223.

B 08-28

Quantification of autophagosome/lysosome fusion in cardiomyocytes and brains of biallelic SPRED2-KO mice reveals a defect in autophagy.

D. Hepbasli, S. Gredy, A. Niedermeier, K. Schuh

University of Wuerzburg, Institute of Physiology I, Wuerzburg, Germany

Dysfunction of autophagy has been associated with cardiac arrhythmias and cardiomyopathies, mainly because failure of the system leads to intracellular depositions. One important signaling cascade controlling myocardial cell homeostasis and important steps of autophagy, is the ERK-MAPK pathway [1]. SPRED2 is an important inhibitor of this pathway and plays a role in a variety of processes, e.g. in cardiovascular organ development and brain development. SPRED2 also interacts with LC3, which is essential for autophagy to occur. LC3-II, which is present in all autophagic vacuoles, is the most commonly used protein to determine autophagic flux [2]. Biallelic SPRED2-KO mice develop impaired autophagy, heart failure, and a shortened lifespan. SPRED2 is an essential regulator of cardiac autophagy, and its absence leads to cardiac dysfunction and life-threatening arrhythmias [3]. The objective of this study was to verify if SPRED2 influences the fusion process of autophagosomes with lysosomes and thus disrupts autophagy.

To prove our hypothesis, we crossed SPRED2-KO mice with transgenic CAG-RFP-EGFP-LC3 mice (JaxMice, strain 027139), which express double-labeled LC3 ubiquitously. This allows both quantification of autophagosomes, characterized by double EGFP/RFP fluorescence and quantification of lysosomes, characterized by disappearance of EGFP fluorescence due to low pH in lysosomes [4].

Using structured illumination microscopy, we revealed that in cardiomyocytes not only the number of sites of lysosome fusion was reduced in SPRED2-KO mice, but also that the double fluorescence signal was decreased, indicating a reduced autophagic activity (Fig. 1a). We also observed that in WT cardiomyocytes more acid-insensitive RFP signal remained (Fig. 1b), which can be explained by the lower pH after fusion with lysosomes. To investigate the influence of SPRED2 on autophagy in other organs, we measured the expression of tagged LC3 in SPRED2-KO brain slices using a confocal microscope. In the hippocampus, we observed an increased signal of EGFP in SPRED-KO mice. This difference was evident in both the average size of the signal (Fig. 1c) as well as the number of EGFP signals (Fig. 1d). These data indicate that the fusion of autophagosomes and lysosomes is disturbed in SPRED2-KO mice.

Our findings demonstrate that SPRED2 is involved in fusion or transport of autophagosomes and lysosomes, and that autophagy is disrupted in mice lacking SPRED2. With the decreased fusion of lysosomes intracellular recycling gets interrupted, which may lead to substrate overload in the cell. Recently, the first humans carrying mutations in the SPRED2 gene have been identified [5]. To diagnose and treat such very rare diseases in the future, investigation of such molecular and physiological functions of SPRED2 is indispensable.

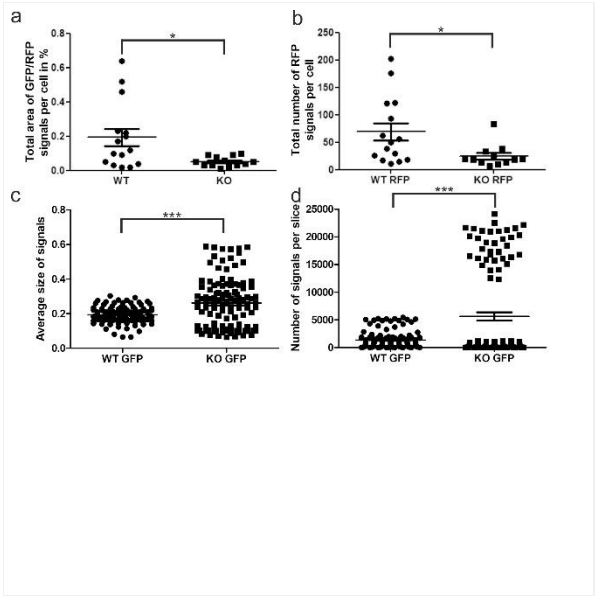

Altered autophagic activity in SPRED2-KO mice. a)Combined total area of GFP/RFP signals in isolated cardiomyocytes of WT and SPRED2-KO (p= 0,0159, WT n= 15, KO n= 13). b) Total number of RFP signals per isolated cardiomyocyte of WT and SPRED2-KO (p= 0,0238, WT n= 15, KO n= 12). c) Average relative size of GFP signals in hippocampus of WT and SPRED2-KO (p= 0,0001, WT n= 12, KO= 12). d) Number of individual signals of GFP in hippocampus of WT and SPRED2-KO (p= 0,0001, WT n= 12, KO= 12).

References

[1] Corcelle, E., et al., 2007, '*Control of the autophagy maturation step by the MAPK ERK and p38: lessons from environmental carcinogens.*' Autophagy, **3**(1): p. 57-9.

[2] Klionsky, D.J., et al., 2016, '*Guidelines for the use and interpretation of assays for monitoring autophagy (3rd edition).*' Autophagy, **12**(1): p. 1-222.

[3] Ullrich, M., et al., 2019, '*SPRED2 deficiency elicits cardiac arrhythmias and premature death via impaired autophagy.*' J Mol Cell Cardiol, **129**: p. 13-26.

[4] Li, L., et al., 2014, '*New autophagy reporter mice reveal dynamics of proximal tubular autophagy.*' J Am Soc Nephrol, **25**(2): p. 305-15.

[5] Motta, M., et al., 2021, '*SPRED2 loss-of-function causes a recessive Noonan syndrome-like phenotype.*' Am J Hum Genet, **108**(11): p. 2112-2129.

B 08-29

The biphasic modulation of calcium leak by calsequestrin-2

H. A.E.C. Cruz, E. T. Sibbles, **M. L. Munro**

University of Otago, Physiology and HeartOtago, Dunedin, New Zealand

This work was supported by a Health Research Council of New Zealand Emerging Researcher First Grant (20-265 to MLM) and a Heart Foundation of New Zealand Research Fellowship (1784 to MLM).

Introduction

A transient increase in intracellular calcium is critical for enabling the contraction of cardiac myocytes. The bulk of this calcium originates from the internal store, the sarcoplasmic reticulum (SR), and is released via the ryanodine receptor (RyR2). This physiological calcium release is tightly regulated on a beat-to-beat basis in the healthy heart; however, calcium leak through RyR2 can occur in pathological settings and is linked with the development of arrhythmias. Atrial fibrillation (AF) is the most common form of arrhythmia and is associated with increased calcium leak activity [1]. The propensity for RyR2 to exhibit calcium leak can be modulated by calsequestrin-2 (CSQ2), an intra-SR calcium buffering protein which interacts with RyR2 [2]. While the majority of studies to date suggest that CSQ2 reduces RyR2 calcium leak, both overexpression and knockdown of CSQ2 result in arrhythmogenic calcium handling [3,4]. An increased expression of RyR2 relative to CSQ2 has been identified in AF patients, compared to non-AF patients [5]. However, how changes in the expression ratio of these two proteins influences RyR2 calcium leak has not been investigated and may represent a mechanism to target for novel anti-arrhythmic therapies. Therefore, we investigated the effect of altering the CSQ2:RyR2 expression ratio on calcium leak activity.

Methods

HEK293 cells stably expressing RyR2 tagged with GFP (RyR2-GFP) were used for this study. RyR2-GFP cells were transfected with CSQ2 tagged with mCherry or a mock control and subjected to single-cell calcium imaging using Fura-2-AM to measure calcium leak activity. The relative intensity of GFP and mCherry fluorescence was measured and used as an indicator of RyR2 and CSQ2 expression, respectively. Cells were grouped into low, medium or high CSQ2:RyR2 expression based on mCherry:GFP fluorescence. The percentage of cells exhibiting calcium leak (propensity) and the frequency of calcium leak events were determined and compared between groups.

Results

Overall, CSQ2 expression reduced the propensity and frequency of RyR2-mediated calcium leak events compared to control. When analysed according to CSQ2:RyR2 expression levels, a biphasic effect was observed. Low CSQ2:RyR2 expression increased both the propensity and frequency of calcium leak compared to control, while medium and high CSQ2:RyR2 produced a progressive reduction in calcium leak activity.

Conclusion

Together, these findings reveal a complex relationship between CSQ2 and RyR2 calcium leak activity which may have implications in arrhythmic settings.

References

[1] Dobrev D, Wehrens XHT. (2017). Calcium-mediated cellular triggered activity in atrial fibrillation. J Physiol. 595(12):4001-8.

[2] Györke I, Hester N, Jones LR, Györke S. (2004). The Role of Calsequestrin, Triadin, and Junctin in Conferring Cardiac Ryanodine Receptor Responsiveness to Luminal Calcium. Biophys J. 86(4):2121-8.

[3] Chopra N, Kannankeril PJ, Yang T, Hlaing T, Holinstat I, Ettensohn K, Pfeifer K, Akin B, Jones LR, Franzini-Armstrong C, Knollmann BC (2007). Modest reductions of cardiac calsequestrin increase sarcoplasmic reticulum Ca 2+ leak independent of luminal Ca2+ and trigger ventricular arrhythmias in mice. Circ Res. 101(6):617–626.
[4] Knollmann BC, Knollmann-Ritschel BE, Weissman NJ, Jones LR, Morad M. (2000). Remodelling of ionic currents in hypertrophied and failing hearts of transgenic mice overexpressing calsequestrin. J Physiol 525(Pt 2):483–498.
[5] Voigt N, Heijman J, Wang Q, Chiang DY, Li N, Karck M, et al. (2014). Cellular and Molecular Mechanisms of Atrial Arrhythmogenesis in Patients with Paroxysmal Atrial Fibrillation. Circulation. 129(2):145-56.

B 08-30

Functional consequences of bulbus arteriosus remodeling in farmed Atlantic salmon

S. Kavaliauskiene[1], O. Stødle[1], V. Becker[1], M. A. Vindas[2], M. Frisk[1], I. B. Johansen[2]
[1] *University of Oslo and Oslo University Hospital Ullevå, Institute for Experimental Medical Research, Oslo, Norway*
[2] *Norwegian University of Life Sciences, Faculty of Veterinary Medicine, Department of Preclinical Sciences and Pathology, Ås, Norway*

Introduction
The salmonid heart is well known for its plasticity and ability to adapt to varying demands in association with environmental challenges such as water salinity and temperature changes. During temperature acclimation, the ventricle undergoes hypertrophic remodeling to adjust to colder temperatures and atrophic remodeling under chronic warming. However, little is known about the remodeling occurring in the bulbus arteriosus (the ventricular outflow tract) upon temperature change. This non-contractile and elastic chamber serves to protect the gill capillaries from high systolic blood pressure and is key for proper cardiac function and blood circulation.
Results
In the current study, we examined the effects of elevated temperature in Atlantic salmon (*Salmo salar* L.) reared at 6-7 ℃ (cold) and 10-13℃ (warm) during the freshwater stage. We observed that relative bulbus size was increased in warm-reared individuals compared to those reared at cold temperature. Next, we examined *in vivo* bulbus function with an ultrasound system (Vivid iq, GE Healthcare) fitted with a pediatric cardiac probe (12S) in anesthetized fish (75mg/L tricaine methanesulfonate through gill irrigation). Fish were euthanized by a blow to the head and *ex vivo* pressure-volume measurements were performed on excised bulbi. These experiments showed that the large bulbi from warm-reared individuals are less compliant and elastic than those from fish raised at cold temperature. In addition, echocardiographic examination of the ventricle suggested mild diastolic dysfunction in the warm acclimated group.
Conclusion
Collectively, our results indicate that hearts from salmon raised at modestly elevated temperatures during the early life stages have reduced ability to adjust blood pressure in the gill capillaries, suggestive of warm acclimation leading to decreased cardiac function. Thus, our results highlight that further temperature elevation due to climate changes may have adverse effects on Atlantic salmon.

B 08-31

Autonomic activity and hemodynamic parameters in relation to the clinical severity of sickle cell anaemia (SCA) among adults

A. M. Hassan[1], M. A. Osman[1], L. A. Kaddam[1,2]
[1] *ALNeelain University, Departement of Physiology Faculty of Medicine, khartoum, Sudan*
[2] *king AbdulaAziz University, Departement of Physiology Faculty of Medicine, Rabigh, Saudi Arabia*

We would like to acknowledge Dr. Areej Alsir and Dr. Awab Omer, Physiology Department Alneelain University for their kind help in data collection.

Introduction
Autonomic Nervous System had been recently speculated as a contributor to Sickle Cell Anaemia pathophysiology. Autonomic Nervous System (ANS) had been recently speculated as a contributor in Sickle Cell Anaemia pathophysiology. Autonomic dysfunction in SCA can be involved in pain crises, vaso-occlusive crises and sudden death. Cardiovascular complications are major cause of morbidity and mortality in SCA, This study evaluated the relationships between autonomic activity, hemodynamic parameters, and the clinical severity of sickle cell anaemia among adult cases
Methods
A cross-sectional hospital-based study, conducted in a referral hematology clinic, Military Hospital, Khartoum, Sudan; including thirty-five cases diagnosed with sickle cell anaemia and twenty-five healthy adults as a comparative group. A standardized data collection tool was used to collect background variables and laboratory measurements. Autonomic activity and hemodynamic parameters were evaluated by studying Heart Rate Variability and Pulse Wave Analysis respectively. A multiple linear regression model was constructed to predict the impact of autonomic and hemodynamic dysfunction on the clinical severity of SCA. All tests used were considered as statistically significant when $p < 0.05$
Results
Total Power was lower among cases, while High Frequency Maximum was significantly higher ($p < 0.001$) among sickle cell anaemia cases. Augmentation Pressure, Augmentation Index and Aortic Pulse Pressure were also significantly higher ($p = 0.002$, 0.012 and 0.013 respectively) among SCA cases. Autonomic activity and hemodynamic parameters statistically significantly ($p < 0.001$) predicted the clinical severity of sickle cell anaemia. The global autonomic activity was impaired among sickle cell anaemia cases
Conclusion
The overall autonomic nervous supply (sympathetic and parasympathetic) was impaired among SCA patients. Higher levels of augmentation pressure, augmentation index and aortic pulse pressure and lower level of brachial diastolic blood pressure were recorded among SCA patients, these results indicated increased mortality risk. The clinical severity was significantly predictable using a regression model involving heart rate variability measures, pulse wave analysis and TWBC, reflecting the significant impact of autonomic nervous system and haemodynamic factors on sickle cell anaemia morbidity and mortality.
References
[1] Philip Manma Kolo, E.O.S., Timothy O. Olanrewaju, Ademola E. Fawibe, Ayodele Soladoye. Cardiac autonomic dysfunction in sickle cell anaemia and its correlation with qt parameters. Niger Med J 2013; 54:382-85.
[2] Haywood, L.J. Cardiovascular function and dysfunction in sickle cell anemia. J NATL MED ASSOC 2009; 101:24-33.

[3] Tünzale Bayramoğlu1, O.A., Kamil Nas, Miklós Illyes, Ferenc Molnar, Emel Gürkan, et al. Arterial stiffness and pulse wave reflection in young adult heterozygous sickle cell carriers. Turk J Haematol. 2013; 30:379–386.
[4] Babiker AO, Kaddam LA. Risk factors of metabolic syndrome among adult Sudanese sickle cell anemia patients. BMC hematology. 2018 Dec;18(1):1-7.

B 08-32

Wavelength-dependent light transmission through the heart wall and transmural coupling and their consequences for optogenetic pacing and defibrillation

J. D. Stockhausen, J. S. Langen, P. Sasse
University of Bonn, Physiology, Faculty of Medicine, Bonn, Germany

This work was supported by the German Research Foundation [313904155/SA1785/7-1, 380524518/SA1785/9-1] and the BONFOR Program, Medical Faculty, University of Bonn

The expression of the light gated ion channel channelrhodopsin2 (ChR2) in cardiomyocytes of mouse hearts enables optogenetic pacing (1) as well as defibrillation to terminate ventricular tachycardia by epicardial illumination (2) with a novel mechanism of endocardial conduction block (3). Therefore, light transmission, epi- to endocardial cell coupling and the extent of light-induced transmural depolarization are important parameters to predict the effectiveness of optogenetic pacing and defibrillation in hearts larger than mouse hearts.
To investigate light transmission of myocardial tissue and the influence of blood, 300 µm thick slices from mouse hearts without blood and with clotted blood in the capillaries were cut with a vibratome (N=6 hearts; n=11-13 slices). Light of defined wavelengths (350-800 nm, 5 nm steps, 2 nm bandwidth) was generated by a monochromator, focused on left ventricular parts and transmission was measured with an integrating sphere. Extinction was calculated according to Lambert-Beer´s law and was high <450 nm and between 530 and 570 nm, reflecting haemoglobin and myoglobin absorption (4). Comparison of values with and without blood and blood extinction allowed to estimate the highest contribution of blood to total light attenuation of 17,8% (at 550 nm) and a blood volume relative to wall volume of 3%. Light transmission of slices with different thickness (200-400µm; N=3; n= 6-10) could be fitted as monoexponential decay (R^2>0.9) with decay constants depending on the wavelength (3.08 μm^{-1} for 460 nm and 1.01 μm^{-1} for 670 nm) reflecting the higher transmission of red light (50% transmission of 460 nm at 225 µm and of 670 nm at 685 µm).
To investigate the consequences of light attenuation in the heart for optogenetic depolarization, pacing thresholds of single isolated cardiomyocytes (n=18 cells) were compared to those of Langendorff-perfused ChR2 hearts (N=10). Interestingly, successful pacing of the whole heart required 2.5-fold higher light intensity than for single cell pacing (460 nm; heart: 27.7±8.6 $\mu W/mm^2$ N=10; cells: 11.2±4.1 $\mu W/mm^2$, n=18). Thus, it seems that deeper, less illuminated layers counteract epicardial depolarization, similar to the concept of electrical coupling preventing ventricular extra beats.
Finally, sharp microelectrode recording was used to measure depolarization of resting membrane potential by epicardial illumination (460 nm) at calibrated depths in the ventricular wall. This value decreased at larger depths but not as fast as light attenuation. For instance, at a depth of 225 µm with only 50% of light remaining, light-induced depolarization was ~85% of the epicardial value and 50% depolarization was found at a depth of 605 µm. Thus, although light is attenuated at deeper layers, the electrical coupling from above increases depolarization and thereby helps conduction block for successful defibrillation.
(values: mean±s.e.m, N=hearts, n=cells or slices)

References

[1] Bruegmann T, Malan D, Hesse M, Beiert T, Fuegemann CJ, Fleischmann BK, et al. Optogenetic control of heart muscle in vitro and in vivo. Nat Methods. 2010;7(11):897–900.
[2] Bruegmann T, Boyle PM, Vogt CC, Karathanos T V., Arevalo HJ, Fleischmann BK, et al. Optogenetic defibrillation terminates ventricular arrhythmia in mouse hearts and human simulations. J Clin Invest. 2016;126(10):3894–904.
[3] Sasse P, Funken M, Beiert T, Bruegmann T. Optogenetic termination of cardiac arrhythmia: Mechanistic enlightenment and therapeutic application? Front Physiol. 2019;10(JUN).
[4] Arakaki LSL, Burns DH, Kushmerick MJ. Accurate myoglobin oxygen saturation by optical spectroscopy measured in blood-perfused rat muscle. Appl Spectrosc. 2007;61(9):978–85.

B 08-34

Cardioprotective adaptation in a state of reduced oxygen utilization and dichloroacetate modulation: Heart mitochondrial protein regulation.

M. Ferko[1], I. Waczulikova[2], T. Ravingerova[1], I. Talian[3], N. Andelova[1]
[1] *Centre of Experimental Medicine, Slovak Academy of Sciences, Institute for Heart Research, Bratislava, Slovakia*
[2] *Comenius University, Department of Nuclear Physics & Biophysics, Faculty of Mathematics, Physics and Informatics, Bratislava, Slovakia*
[3] *Safarik University, Department of Medical and Clinical Biophysics, Faculty of Medicine, Kosice, Slovakia*

This study was supported by APVV 15-0119, APVV 19-0540; VEGA 2/0121/18, VEGA 2/0141/18, VEGA 1/0016/20, VEGA 1/0775/21.

Introduction

Oxygen metabolism disorders present a high risk, which often leading to organ dysfunction. In particular, the myocardium is characterized by increased energy requirements under conditions of pathological load. For monitoring of energy deficiency under conditions of reduced oxygen utilization, an experimental model of acute streptoztocin (STZ)-induced diabetes mellitus (D) has been proposed. Due to the fact that mitochondria play a vital role in oxygen metabolism, it is necessary to evaluate their performance with respect to diseases that are characterized by increased energy requirements, such as D [1].
We aimed to expand knowledge about key signaling pathways linked to the regulation of respiratory chain, mPTP opening and ROS signaling in the conditions of D treated with a metabolic modulator dichloroacetate (DCA).

Methods

Male Wistar rats (n=24) aged 12-15 weeks and weighing 323±28 g were used for our experiments. The acute 8-day D model induced by single dose of STZ (65 mg/kg i.p.) was exposed to DCA

administered to animals (150 mg/kg and 75 mg/kg i.p.) 60 minutes and 15 minutes before heart excision. The experiment was performed on intraperitoneally anesthetized animals (thiopental, 50-60 mg/kg of body weight applied with heparin 500 IU). Prior to the heart extraction, the animals were stabilized for 30 minutes. Isolated rat heart mitochondria were used for quantitative label-free LC-MS/MS proteomic analysis.

Results

Proteomic analyzes revealed a significant protein stimulation of respiratory chain complex I and II (both $p < 0.0001$) in the D group compared with the healthy control group. In diabetic animals treated with DCA, we observed a significant decrease in protein expressions for complex II ($p < 0.001$) and complex IV ($p < 0.05$). We demonstrated significantly ($p < 0.001$) upregulated protein amine oxidase [flavin-containing] A (AOFA) in D mitochondria, indicating oxidative damage. DCA in diabetic animals (D+DCA) downregulated AOFA ($p < 0.05$) and stimulated thioredoxin-dependent peroxide reductase ($p < 0.05$), a protein with antioxidant function. D condition was associated with mitochondrial resistance to calcium-overload through mPTP regulation, despite of increased ($p < 0.05$) protein level of voltage-dependent anion-selective protein (VDAC1). In contrast, D+DCA condition influenced ROS levels and downregulated ($p < 0.05$) VDAC1 and ($p < 0.05$) VDAC3 when compared to D alone.

Conclusion

Stimulation of mitochondrial respiratory chain and mPTP complex proteins is involved in endogenous compensatory mechanisms leading to the maintenance of myocardial function under increased energy load conditions. Characterization of the combined effect of D+DCA showing that DCA acted as an effector of calcium uptake regulation and ROS production. Overall, the achieved results expanded the available knowledge about mitochondrial signaling pathways in the rat heart that can lead to cardioprotection during reduced oxygen utilization induced by D.

References

[1] Andelova N, Waczulikova I, Talian I, Sykora M, Ferko M. mPTP Proteins Regulated by Streptozotocin-Induced Diabetes Mellitus Are Effectively Involved in the Processes of Maintaining Myocardial Metabolic Adaptation. Int J Mol Sci. 2020 Apr 9;21(7):2622. doi: 10.3390/ijms21072622

B 08-35

The effects of *Senecio nutans* hydro-alcoholic extract on intracellular calcium handling and contractility in sheep ventricular myocytes.

M. A. Jones[1], A. Foster[1], J. Palacios[2], D. J. Greensmith[1]

[1] *University of Salford, Biomedical Rresearch Centre, School of Science, Engineering and Environment, Salford, UK*

[2] *Universidad Arturo Prat, Laboratorio de Bioquímica Aplicada, Facultad de Ciencias de la Salud, Iquique, Chile*

We gratefully acknowledge Professor Andrew Trafford and Dr Katherine Dibb (University of Manchester, UK) for providing the sheep cells used in our experiments.

Introduction

The plant *Senecio nutans* SCh. Bip is widely used by the Andean communities of northern Chile to treat diseases including gastrointestinal disorders and altitude sickness. Recent evidence suggests it may be of value in modern medicine as an anti-hypertensive. For example, Paredes *et al.* (2016) show *S. nutans* to produce vasodilation via Ca^{2+} and nitric oxide-dependent mechanisms. Furthermore, Cifuentes *et al*. (2016) demonstrate negatively inotropic effects in the heart, though the cellular mechanisms were not elucidated. To address this, we measured the effects of *S. nutans* hydro-alcoholic extracts on cardiac intracellular calcium handling and contractility.

Methods

Sheep ventricular myocytes were isolated enzymatically in accordance with the Animals (Scientific Procedures) Act, UK, 1986, Directive 2010/63/EU of the European Parliament and local ethical review boards. Cells were loaded with Fura-2 (0.1 µM) then field stimulated at 0.5Hz and excited sequentially at 340 nm and 380 nm (200 Hz). Changes of cytoplasmic Ca^{2+} were inferred from the ratio of light emitted at 340:380 nm, calibrated using custom-written software. Sarcomere length was measured simultaneously using a Myocam-S CCD camera and SarcLen acquisition module (Ion Optix, USA). Changes to Sarcoplasmic reticulum (SR) Ca^{2+} content were estimated by rapid application of caffeine (10 mM). Analysis of variance was used for statistical analysis with significance taken as $p<0.05$.

Results

1µg/ml (the measured IC_{50}) *S. nutans* rapidly (10-20s) decreased the $[Ca^{2+}]_i$ transient amplitude and sarcomere shorting by 40 ± 4% ($n=24$, $p<0.001$) and 49 ± 4% ($n=24$, $p<0.001$) respectively. The effect on $[Ca^{2+}]_i$ partially reversed upon washout while that on contractility reversed fully. The amplitude of the caffeine evoked $[Ca^{2+}]_i$ transient was reduced by 24 ± 4% ($n=13$, $p<0.001$), progressing to a 41 ± 6% decrease ($n=13$, $p<0.001$) during washout, indicating respective decreases in SR Ca^{2+} content. The rate of decay of the systolic Ca^{2+} transient (k_{sys}) represents the combined activity of SERCA and NCX and was reduced by 17 ± 4% ($n=24$, $p=0.002$). The rate of decay of the caffeine-evoked Ca transient (k_{caff}) represents NCX alone and was increased by 17 ± 4 % ($n = 13$, $p=0.04$). Subtraction of k_{caff} from k_{sys} indicates SERCA activity (k_{SERCA}), which was decreased by 21 ± 8 % ($n = 13$, $p=0.02$). During washout, $-k_{SERCA}$recovered while the increase of k_{NCX} progressed to 41 ± 7 % ($n = 13$, $p<0.001$).

Conclusion

These findings suggest *S. nutans* decreases SERCA activity and increases NCX activity, which reduces SR Ca^{2+} content. This accounted for a reduction in the calcium transient amplitude thus contractility. Though further investigations are required to measure the effect of *S. nutans* on the other sub-cellular Ca^{2+} handling mechanisms, the changes to global Ca^{2+} and contractility dynamics provide a cellular basis for the previously reported negatively inotropic effects.

References

[1] Cifuentes, F., Paredes, A., Palacios, J., Muñoz, F., Carvajal, L., Nwokocha, C. R., & Morales, G. (2016). Hypotensive and antihypertensive effects of a hydroalcoholic extract from Senecio nutans Sch. Bip. (Compositae) in mice: Chronotropic and negative inotropic effect, a nifedipine-like action. *J Ethnopharmacol, 179*, 367-374. https://doi.org/10.1016/j.jep.2015.12.048

[2] Paredes, A., Palacios, J., Quispe, C., Nwokocha, C. R., Morales, G., Kuzmicic, J., & Cifuentes, F. (2016). Hydroalcoholic extract and pure compounds from Senecio nutans Sch. Bip (Compositae) induce vasodilation in rat aorta through endothelium-dependent and independent mechanisms. *J Ethnopharmacol, 192*, 99-107. https://doi.org/10.1016/j.jep.2016.07.008

B 08-36

Cardiovascular effects of physical activity in two different doses of Doxorubicin

F. Machado[2], Â. Amaro-Leal[1,2], A. I. Afonso[2], I. Rocha[1,2], V. Geraldes[1,2]

[1] *Faculdade de Medicina da Universidade de Lisboa, Lisbon, Portugal*

[2] *Centro Cardiovascular da Universidade de Lisboa, Lisbon, Portugal*

The authors gratefully acknowledge the financial support of Fundação para a Ciência e Tecnologia (FCT), through the TRACKING3C project (Ref: PTDC/MEC-CAR/31626/2017).
Vera Geraldes acknowledge the post-doctoral fellowship given by the Fundação para a Ciência e Tecnologia (FCT) (Ref: SFRH/BPD/119315/2016) and Ana I. Afonso for her PhD scholarship (2020.09352.BD).

Cancer incidence has increased exponentially in the last century. Although the amazing drug advances, traditional chemotherapy regimens, particularly anthracyclines, continue to play a key role in breast cancer treatment. However, these improvements are accompanied by systemic adverse effects, particularly cardiovascular toxicity.
To clarify Doxorubicin (DOX) action on the cardiovascular system upon cumulative treatment, we used a healthy animal model to determine the extension of doxorubicin effects due to two therapeutic doses and the exercise training (ET) effectiveness on cardiovascular parameters.
For that, female *Wistar* rats, with 12 weeks of age, were DOX-treated for 4 weeks: DOX 8 (n=7), a cumulative dose of 8 mg/kg (2 mg/kg/week), DOX 16 (n=6), a cumulative dose of 16 mg/kg (4 mg/kg/week). Two other groups were made with the same doses of DOX but with an ET program implemented (DOX 8 + ET and DOX 16 + ET). The ET protocol consisted of a 25 cm/sec treadmill exercise for 30 min, 5 times/week. At the end of the protocol, animals were anaesthetized and blood pressure (BP), electrocardiogram, heart rate (HR) and respiratory frequency (RF) were recorded.
Our results showed that a cumulative dose of 16 mg/kg triggered hypotension: a significant decrease in mean BP (DOX 16: 90 ± 10; CTL: 128 ± 2 mmHg, $p<0.0012$), systolic BP (DOX 16: 103 ± 10; CTL: 153 ± 4 mmHg, $p<0.0002$) and diastolic BP (DOX 16: 80 ± 10; CTL: 108 ± 3 mmHg, $p<0.0224$), as well as in HR (DOX 16: 288 ± 22; CTL: 379 ± 51 bpm, $p<0.003$), compared to the CTL group.[VLPG1] [FDCM2] There was also a significative hypopnea in the DOX 8 group compared to CTL group (DOX 8: 37 ± 6; CTL: 54 ± 3 cpm[VLPG3] [FDCM4] , $p<0.0389$). During DOX treatment, the ET protocol counteracts some of the adverse effects induced by DOX, normalizing the mean BP (DOX 8: 119 ± 7; DOX 8 + ET: 142 ± 4 mmHg, $p<0.0122$), systolic BP (DOX 8: 139 ± 8; DOX 8+ ET: 168 ± 5 mmHg, $p<0.0076$), diastolic BP (DOX 8: 102 ± 3; DOX 8 + ET: 124 ± 5 mmHg, $p<0.0309$), HR (DOX 8: 367 ± 14; DOX 8 + ET: 405 ± 5 mmHg, $p<0.0164$) and RF (DOX 8: 37 ± 6; DOX 8 + ET: 63 ± 4 mmHg, $p<0.0027$). In the DOX16 group, the ET protocol was not able to revert the adverse physiological changes.
These findings suggest that the DOX effects on physiological parameters are different according to the cumulative dosage, with the highest dosage causing the most serious effects. Although ET has an evident beneficial effect on the cardiovascular system during DOX therapy in both dosages, a more noticeable effect was observed at the lowest dose. It may be necessary to perform ET in the DOX16 group for a longer period to observe its protective effect or this ET protocol is not able to avoid the side effects of higher cumulative doses of DOXO. Although complementary data is still needed, the present data showed that ET has an evident beneficial effect to counteract the adverse effects of anthracycline therapies.

B 08-38

Load-dependent Control of T-tubule Development and Maintenance in Sheep

O. Manfra[1,2], S. Louey[3,4], S. S. Jonker[3,4], H. Perdreau-Dahl[1,2], M. Frisk[1,2], G. D. Giraud[3,4], K. L. Thornburg[3,4], W. E. Louch[1,2]

[1] *Oslo University Hospital and University of Oslo, Institute for Experimental Medical Research, Oslo, Norway*

[2] *University of Oslo, K.G. Jebsen Centre for Cardiac Research, Oslo, Norway*

[3] *Oregon Health and Science University, Center for Developmental Health, Knight Cardiovascular Institute, Portland, USA*

[4] *Oregon Health and Science University, Department of Physiology and Pharmacology, Portland, USA*

[5] *Veterans Affairs Portland Health Care System Portland, Portland, USA*

Contraction of the heart is a tightly controlled process, initiated at subcellular elements called dyads. Within these structures, Ca^{2+} release channels known as ryanodine receptors (RyRs) in the sarcoplasmatic reticulum (SR) are located within close proximity to L-type Ca^{2+} channels (LTTCs) and the Na^{+}-Ca^{2+} exchanger (NCX) in the adjacent sarcolemma (T-tubules). This arrangement is believed to allow efficient triggering of Ca^{2+} induced Ca^{2+} release. However, despite decades of investigation, the precise organization and function of these structures remains unclear. Even less clear is how dyads are assembled in developing heart, knowledge that is key for generating mature cardiomyocytes from stem cells for tissue engineering.
In this project, we examined dyadic formation in unprecedented detail, using a large mammalian model, such as sheep (Ovis aries). Employing advanced imaging methods (Fast Airyscan, Zeiss LSM 880), we demonstrate that the t-tubule density and dyadic assembly proceed gradually during the fetal sheep development, from 93 days of gestational age, with term being 145days, until the post-natal stage. Furthermore, we examined the effect of load on the t-tubules and dyads development. We used two different interventions on the fetal sheep heart to alter the fetal arterial pressure. The first animal model used three different protein-infusion conditions: a) Infusion of sheep plasma to increase systolic load of the fetal heart(1), b) Infusions of the angiotensin converting enzyme inhibitor, enalaprilat, to reduce the fetal systolic load(2), c) Infusions of lactated Ringer's solution, as control condition to measure the effect of normal cardiac load. In addition, increased systolic load effect on the fetal heart was studied using a second animal model, where a variable inflatable occluder is placed on the post ductal aorta to pressure-load the heart. In order to perform fetal surgery, anesthesia on ewes was induced via an intravenous mixture of diazepam (10mg) and ketamine (400mg), and maintained using 1-2% isoflurane in a carrier gas mixture of 70:30 oxygen and nitrous oxide while mechanically ventilated (1). At the conclusion of each study, pregnant ewes and lambs were euthanized using an intravenous overdose of pentobarbital sodium (SomnaSol) (3, 4).Here, we report that increasing systolic load by infusing plasma or occlusion of the post-ductal aorta accelerates hypertrophy and t-tubule growth. Conversely, reducing fetal systolic load with enalaprilat infusion significantly slows t-tubule development, and decreases cardiomyocyte size. Load-dependent modulation of substructure maturation was linked to altered expression patterns of the t-tubule regulatory proteins JPH2, amphiphysin-2 (Bin1) and other Bin-1 partners. Interestingly, altered t-tubule densities did not relate to changes in dyadic junctions, indicating that distinct signals are responsible for maturation of the SR.

References
[1] Giraud GD, Faber JJ, Jonker SS, Davis L, Anderson DF. Effects of intravascular infusions of plasma on placental and systemic blood flow in fetal sheep. American journal of physiology Heart and circulatory physiology. 2006;291(6):H2884-8.
[2] O'Tierney PF, Anderson DF, Faber JJ, Louey S, Thornburg KL, Giraud GD. Reduced systolic pressure load decreases cell-cycle activity in the fetal sheep heart. American journal of physiology Regulatory, integrative and comparative physiology. 2010;299(2):R573-8.
[3] Jonker SS, Faber JJ, Anderson DF, Thornburg KL, Louey S, Giraud GD. Sequential growth of fetal sheep cardiac myocytes in response to simultaneous arterial and venous hypertension. American journal of physiology Regulatory, integrative and comparative physiology. 2007;292(2):R913-9.
[4] Thornburg K, Jonker S, O'Tierney P, Chattergoon N, Louey S, Faber J, et al. Regulation of the cardiomyocyte population in the developing heart. Progress in biophysics and molecular biology. 2011;106(1):289-99.

B 08-40

Role of inward rectifier current downregulation in heart failure and arrhythmogenesis predicted by a novel computational model of rat ventricular electrophysiology

H. J. Stevenson-Cocks[1,2], M. A. Colman[2], E. White[2], A. P. Benson[2]
[1] *Newcastle University, School of Biomedical, Nutritional and Sport Sciences, Newcastle upon Tyne, UK*
[2] *University of Leeds, School of Biomedical Sciences, Leeds, UK*

Disruption to normal excitation-contraction coupling processes in the heart can result in arrhythmias which are potentially fatal; however, the underlying mechanisms are complex, dynamic, and multi-scale in nature, thus are difficult to experimentally dissect. Computational investigations, however, allow researchers to gain quantitative and mechanistic insight into pro-arrhythmic phenomena. Despite common use of the rat as an animal model of cardiovascular disease, existing computational models of rat ventricular electrophysiology are unable to account for stochastic subcellular calcium dynamics, which are known to trigger arrhythmias. We therefore developed a new computational model by coupling a recent rat electrophysiology model [1] with a novel model of stochastic spatio-temporal Ca^{2+} cycling [2], and extensively validated the model against a wealth of experimental data. The new model was utilised to explore how reductions in inward rectifier current (I_{K1}) observed in heart failure (HF) in our lab [3] influenced pro-arrhythmic spontaneous Ca^{2+} release events.
The new model reproduced rate-dependent changes in action potential, electrophysiological and Ca^{2+} handling characteristics from the literature across a range of cycle lengths (80-1000 ms), under both control and beta-adrenergic stimulation conditions (simulated application of isoprenaline, ISO). A simulated 50% reduction in I_{K1} (HF), in line with experiments (3), led to a 31% prolongation in action potential duration (APD) from 39 to 51 ms and a rise in sarcoplasmic reticulum calcium levels ($[Ca^{2+}]_{SR}$). In ISO simulations, APD prolongation was also observed and $[Ca^{2+}]_{SR}$ was augmented from 500 to 900 μM (HF vs HF+ISO). In both control+ISO and HF+ISO conditions, spontaneous Ca^{2+} release was observed but was higher in magnitude (94 vs 100 nM), involved a higher proportion of open ryanodine receptors and occurred sooner after cessation of pacing (1085 vs 1287 ms) under I_{K1} remodelling.
Utilising spontaneous Ca^{2+} release functions in the model (in which $[Ca^{2+}]_{SR}$ and initiation of spontaneous release were fixed), we also found that, independent of Ca^{2+} load, I_{K1} remodelling led to an increased magnitude of delayed afterdepolarisations compared to control and resulted in triggered activity in HF but not control simulations (at high and low $[Ca^{2+}]_{SR}$), despite an increased spontaneous calcium release magnitude and more depolarised membrane in control simulations. Together these results suggest that HF-associated electrophysiological remodelling promotes and alters the dynamics of spontaneous release events and, in combination with a destabilised membrane, leads to pro-arrhythmic triggered activity, with implications for tissue-level arrhythmogenesis.

References
[1] Gattoni S, Roe AT, Frisk M, Louch WE, Nieder SA, Smith NP (2016). The calcium-frequency response in the rat ventricular myocyte: an experimental and modelling study. *Journal of Physiology*, 594(15), 4193-4224.
[2] Colman MA (2019). Arrhythmia mechanisms and spontaneous calcium release: Bi-directional coupling between re-entrant and focal excitation.*PLoS Computational Biology*, 15, e1007260.
[3] Benoist D, Stones R, Drinkhill M, Bernus O, White E (2011). Arrhythmogenic substrate in hearts of rats with monocrotaline-induced pulmonary hypertension and right ventricular hypertrophy. *American Journal of Physiology - Heart and Circulatory Physiology*, 300, H2230-H2237.

B 08-41

Analysis of cadiomyocytes derived from human induced pluripotent stem cells carrying a myopathy- causing BAG3^{P209L} mutation

I. Rißе[1], M. Peitz[2], B. K. Fleischmann[1], M. Hesse[1]
[1] *University of Bonn, Institute of Physiology I, Medical Faculty, Bonn, Germany*
[2] *University of Bonn, Core Facility Cell Programming, Bonn, Germany*

Mechanical strain in striated muscle inevitably leads to an increase of damaged proteins that need to be replaced to maintain protein homeostasis. As a member of the chaperone-associated selected autophagy (CASA) complex, the co-chaperone BAG3 contributes to protein homeostasis by autophagic degradation of damaged proteins. A heterozygous amino acid substitution at position 209 of the BAG3 protein impairs this function and causes severe skeletal muscle dystrophy and restrictive cardiomyopathy, reducing the life expectancy of patients to an average of 20 years. In a humanized mouse model for this disease we were able to show that BAG3^{P209L} is more prone to aggregation and sequesters BAG3^{WT} into the insoluble pool, depleting functional BAG3. This leads to an impairment of CASA and accumulation of damaged proteins, causing sarcomere disintegration and muscular dystrophy.
To investigate this in the human system and to understand the full spectrum of BAG3-related muscular disease, we have generated an isogenic series of heterozygous as well as homozygous genome-edited human induced pluripotent cell (iPSC) lines with the BAG3^{P209L} mutation. We could successfully generate beating cardiomyocytes from the BAG3^{P209L} homozygous and heterozygous

cell lines, as well as from controls. So far, we could not observe any obvious differences between the cardiomyocytes of the three cell lines. Current efforts are directed at analyzing changes in the protein quality control system by performing biochemical and immunofluorescence analyses and to apply mechanical stress by electrostimulation. In addition, we will also focus on the integrity of sarcomeres and Z-disks after pharmacological inhibition of autophagy or the proteasome. Thus, we hope that the hiPSC lines will provide better insight into the disease pathomechanisms and hence enable to design strategies for the development of new experimental therapies for $BAG3^{P209L}$-related myofibrillar myopathy.

B 08-42

Heterogeneity of aortic endothelial cells in healthy C57BL/6 mice

A. Brückner[1], A. Brandtner[1], S. Rieck[1], B.K. Fleischmann[1], D. Wenzel[1,2]

[1] *University of Bonn, Institute of Physiology I, Medical Faculty, Bonn, Germany*

[2] *Ruhr-University Bochum, Department of Systems Physiology, Bochum, Germany*

The author has objected to a publication of the abstract.

B 08-43

Alteration of MiRNAs profiling on experimental model of chronic anthracycline-induced cardiomyopathy

M. Adamcova[1], H. Kovarikova[2], I. Baranova[2], O. Popelova-Lencova[3], P. Kollarova-Brazdova[3], Y. Mazurova[4], M. Sterba[3]

[1] *Charles University, Faculty of Medicine, Department of Physiology, Hradec Králové, Czech Republic*

[2] *Charles University, Faculty of Medicine, Department of Clinical Biochemistry and Diagnostics University Hospital, Hradec Králové, Czech Republic*

[3] *Charles University, Faculty of Medicine, Department of Pharmacology, Hradec Králové, Czech Republic*

[4] *Charles University, Faculty of Medicine, Department of Histology and Embryology, Hradec Králové, Czech Republic*

This work was supported by the Project InoMed CZ.02.1.01/0.0/0.0/18 069/0010046 co-funded by the ERDF.carc

Introduction

MicroRNAs are small, non-coding RNA molecules involved in regulation and fine-tuning of gene expression. The present study aims to determine changes in miRNAs on the well-established experimental model of chronic anthracycline (ANT) cardiotoxicity at two distinct stages of cardiotoxicity development.

Methods

Cardiotoxicity was induced in rabbits treated with daunorubicin (DAU, 3 mg/kg, weekly; for 5 and 10 weeks) and compared with the control (saline in the same schedule). The 1st analysis was done after the five DAU cycles (cumulative dose ~250 mg/m^2) when we found first signs of cardiotoxicity, i.e., significantly increased levels of plasma cardiac troponin T (cTnT 0.018±0.003 µg/L vs. 0.006±0.001 µg/L; p< 0.001), but yet without any change in LV systolic function. The 2nd analysis was performed after the ten DAU cycles (cumulative dose ~500 mg/m^2) which induced significant LV systolic dysfunction (FS 41.2 ± 0.4 % vs 29.0 ± 2.9 %; p<0.001 and dP/dt_{max} 8714 ± 275vs 5341 ± 499 mm Hg; p<0.001) and typical histopathological hallmarks of chronic ANT cardiotoxicity.

Results

Based on results obtained from TaqMan® Advanced miRNA Human A and B Cards we selected 32 miRNAs for confirmation by Real-time PCR with specific assays (TaqMan® Advanced miRNA Assay systems). After 5 weeks, 10 miRNAs were significantly up-regulated: miR-let-7f-2-3p (p<0.05), miR-20b-5p (p<0.05), miR-21-3p (p<0.05), miR-21-5p (p<0.05), miR-34a-3p (p<0.001), miR-34a-5p (p<0.001), miR-34c-5p (p<0.01), miR-142-3p (p<0.05), miR-155-5p (p<0.001) with dominant change in miR-1298-5p (29-fold change, p<0.01) . miR-34a-5p and miR-21 were related to p53-mediated DNA damage signalling. After 10 weeks only miR-504-3p (p<0.01) was significantly down-regulated and 11 of miRNAs were significantly up-regulated: miR-21-3p (p<0.01), miR-21-5p (p<0.001), miR-34a-3p (p<0.01), miR-34a-5p (p<0.001), miR-34c-5p (p<0.001), miR-142-3p (p<0.01), miR-155-5p (p<0.001), miR-223 (p<0.001), miR-433-3p (p<0.05), miR-1298-5p (p<0.001) with the dominant change in 34a-5p (76-fold change). Most of miRNAs measured after 10 weeks of the treatment very significantly positively correlated with cTnT and negatively with parameters of systolic dysfunction (LVFS and dP/dt_{max}). The best correlation has been achieved between miR-21-5p and LVFS and dP/dt_{max}, respectively and (-0.959; p<0.001, resp. -0.890; p<0.001) and miR-223-3p (-0.911; p<0.001; resp.- 0.803; p<0.001), which are probably involved in the alteration of cross-bridge cycling and fibrosis.

Conclusion

To our knowledge, this is the first study describing the changes of miRNAs profile in chronic ANT cardiotoxicity with precisely defined stages of cardiomyopathy development.

B 08-45

Effects of choline and CDP-choline on heart rate variability and total choline levels in rats.

H. Kazdağlı[1], S. Alpay[2], E. Barış[3], H. F. Özel[4]

[1] *Izmir University of Economics, Elderly Care / Vocational School of Heath Sciences, İzmir, Turkey*

[2] *Manisa Celal Bayar University, Department of Physiology / Faculty of Medicine, Manisa, Turkey*

[3] *Izmir University of Economics, Department of Pharmacology / Faculty of Medicine, İzmir, Turkey*

[4] *Manisa Celal Bayar University, Radiology / Vocational School of Heath Sciences, Manisa, Turkey*

Introduction

Heart rate variability (HRV) is a measure of the variation of the time distance between two consecutive heartbeats which reflects autonomic nervous system function along with the relative contributions of sympathetic and parasympathetic nervous systems (PNS) (1). Choline and CDP-choline modulate autonomic functions by increasing acetylcholine synthesis and cholinergic neurotransmissions (2). This study aims to evaluate the possible effects of cholinergic system-acting drugs; choline and CDP-choline on HRV parameters.

Methods

The experimental study was approved by the local Ethics Committee for Animal Experimentations and experiments have been carried out in accordance with the Declaration of Helsinki. 12-16 weeks old Wistar male rats were anesthetized with Ketamine (75 mg/kg) and Xylazine (10 mg/kg) combination and randomized into three groups (each n=8): 1. Control (1 ml Saline), 2. Choline (100

mg/kg), 3. CDP-choline (400 mg/kg). 0.9% Saline, Choline, and CDP-choline were applied intraperitoneally. After the drug administration, electrocardiography (ECG) recordings were obtained for 45 minutes. After detecting R waves with the Pan-Tompkins algorithm, the tachogram of RR intervals was generated and frequency domain HRV analyses were performed. After the ECG recordings animals were sacrificed with cervical dislocation. Total choline/acetylcholine levels in blood and heart tissues of experimental groups were measured by a commercially available kit according to the manufacturer's instructions by spectrophotometer (3). One-way analysis of variance (ANOVA) with Tukey test for multiple comparison tests was used for statistical analysis. $p<0.05$ was accepted significant.

Results

Power of high frequency (HF) and total power (TP) was significantly increased in both choline and CDP-choline groups within 15 minutes. Heart rate, Power of low frequency (LF) significantly decreased in the choline treated group whereas the power of very low frequency (VLF) significantly decreased in the CDP-choline treated group. LF/HF ratio significantly decreased by the choline treatment within 15 minutes whereas significant changes were obtained for CDP-choline within 45 minutes (Fig 1). Total choline/acetylcholine levels significantly increased in serum and heart tissues of choline and CDP-choline treated animals compared to control (Fig 2). The level was significantly higher in the choline group compared to both CDP-choline and the control groups.

Conclusion

Our HRV analysis results suggested parasympathomimetic activation by choline and CDP-choline treatments by increasing HF and TP and decreasing LF/HF. Parallelly, increased total choline/acetylcholine levels in both serum and heart tissues also showed increased parasympathomimetic activation. Furthermore, our data suggest a more rapid response on HRV parameters by choline treatment compared to CDP-choline which is supported by the significant difference in total choline acetylcholine levels in tissues.

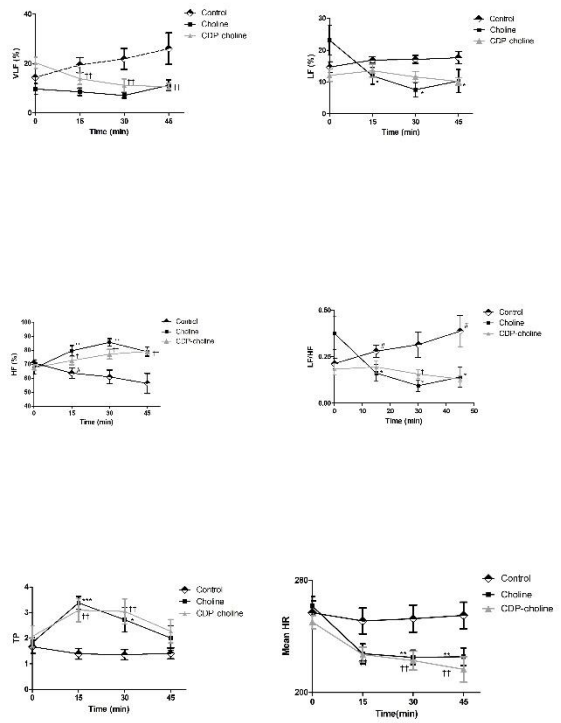

Figure 1
HRV parameters in control, choline and CPD-choline groups.

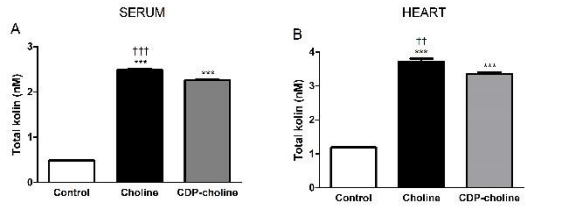

Figure 2
Total choline levels in control, choline and CPD-choline groups in serum and heart tissues.

References

(1) Shaffer F and Ginsberg JP (2017) An Overview of Heart Rate Variability Metrics and Norms. Front. Public Health 5:258. doi: 10.3389/fpubh.2017.00258

(2) Cansev M, Ilcol YO, Yilmaz MS, Hamurtekin E, Ulus IH. (2008) Choline, CDP-choline or phosphocholine increases plasma glucagon in rats: involvement of the peripheral autonomic nervous system. Eur J Pharmacol. 589(1-3):315-22.
(3) Wurtman R.J., Cansev M., Ulus I.H. (2009) Choline and Its Products Acetylcholine and Phosphatidylcholine. In: Lajtha A., Tettamanti G., Goracci G. (eds) Handbook of Neurochemistry and Molecular Neurobiology. Springer, Boston, MA.

B 08-46

Characterisation of carotid body mitochondrial function in healthy and heart failure sheep.

A. Swiderska, M. Obeidat, G. W. Madders, A. S. Whitley, G. L.J. Galli, A. W. Trafford
The University of Manchester, Division of Cardiovascular Sciences, Manchester, UK

Authors would like to thank the British Heart Foundation for funding this project.

Carotid bodies (CBs) are the main peripheral oxygen sensors implicated in the progression of many diseases, including heart failure (HF) [1]. In HF, CB function is enhanced and contributes to the sympathetic overdrive [2]. While CBs are an attractive target for future therapies, therapeutic development has been limited due to a lack of full understanding of the CB oxygen sensing mechanism in health and HF. Previous reports showed that elevated reactive oxygen species (ROS) contribute to altering the oxygen chemotransduction cascade in HF [3]. However, the effects on CB mitochondrial function have not been investigated. Investigating mitochondrial function is important as it has been hypothesised that the unusually low oxygen affinity of cytochrome c oxidase (complex IV) and mitochondrial ROS (mitoROS) may play an important role in the CB oxygen sensing mechanism [4]. However, these assumptions have not been validated by measurements of electron transport chain (ETC) function and mitoROS production in the CB. This study therefore sought to describe the ETC function, mitoROS production and oxygen affinity of complex IV in control and HF CB.

Tissue homogenates were prepared using CB and left ventricle from control and tachypaced HF sheep [5]. High-resolution respirometry was used to measure mitochondrial oxygen consumption and H_2O_2 production by using substrate-uncoupler-inhibitor titration protocols (normalised to citrate synthase activity), as well as the kinetics of mitochondrial oxygen affinity. A citrate synthase assay was used to estimate mitochondrial content in each homogenate sample. Additionally, the protein abundance of mitochondrial complexes per total protein was measured by Western blot.

CB mitochondria have a low aerobic capacity and a high complex IV oxygen affinity compared to the heart. H_2O_2 production rate was comparable between tissues. Mitochondrial oxygen consumption was statistically increased during leak respiration with complex I substates in HF CBs. Surprisingly, the rate of H_2O_2 production was comparable between control and HF CB. Furthermore, oxygen affinity of CB complex IV was not affected by HF. Protein abundance of mitochondrial complexes and citrate synthase activity in control and HF CBs remained unchanged.

These results suggest that the CB mitochondrial function is altered in HF. An increase in leak respiration indicate that mitochondria are less efficient at producing ATP. The lack of an increase in H_2O_2 production rate by CB mitochondria suggests that the increase in ROS levels observed in HF CBs may originate from non-mitochondrial sources. Provided that there was no change in complex IV oxygen affinity, there is a potential that the oxygen sensing mechanism was affected by extra-mitochondrial factors. However, these studies will have to be repeated in intact isolated glomus (sensory) cells to ensure that results were not influenced by the presence of other cell populations in the homogenate preparation.

References
[1] Paton JFR, Sobotka PA, Fudim M, Engleman ZJ, Hart ECJ, et al. 'The carotid body as a therapeutic target for the treatment of sympathetically mediated diseases'. *Hypertension*. 2013 Jan;61(1):5-13
[2] Marcus NJ, Del Rio R, Schultz EP, Xia XH, Schultz HD. 'Carotid body denervation improves autonomic and cardiac function and attenuates disordered breathing in congestive heart failure'. *J Physiol*. 2014 Jan 15;592(2):391-408.
[3] Li YL, Gao L, Zucker IH, Schultz HD. 'NADPH oxidase-derived superoxide anion mediates angiotensin enhanced carotid body chemoreceptor sensitivity in heart failure rabbits'. *Cardiovasc Res*. 2007 Aug 1;75(3):546-54.
[4] Holmes AP, Ray CJ, Coney AM, Kumar P. 'Is carotid body physiological O2 sensitivity determined by a unique mitochondrial phenotype?' *Front Physiol*. 2018 May, 9, 562.
[5] Briston SJ, Caldwell JL, Horn MA, Clarke JD, Richards MA, et al. 'Impaired beta-adrenergic responsiveness accentuates dysfunctional excitation-contraction coupling in an ovine model of tachypacing-induced heart failure.' *J Physiol*. 2011 Mar 15;589(Pt 6):1367-82.

B 08-47

Cardiovascular effects of vitamin C on chloroquine induced cardiovascular dysfunction

E. E.W. Nabofa, D. C. Obi
Babcock University, Physiology, ilishan-Remo, Nigeria

I would like to acknowledge the faculties and staffs of the department of Physiology, Babcock University, Nigeria for their cooperation during the course of this study.

Introduction

Due to COVID19, two most commonly used drugs that are affordable and available off the counter in West Africa include Chloroquine (CQ) and Vitamin C. The World Health Organization has warned against the unorthodox use of CQ because of its possible cardiotoxic side effects. Thus modeling chloroquine cardiovascular dysfunction was of interest and how vitamin C affects cardiovascular function in this model was determined.

Methods

Male adults albino Wister rats (32) weighing between 180-200 g were randomly divided into four groups (n=7). Animal experimentation lasted for 7 days. Group 1 animals served as control group and were untreated. Group 2-4 animals were orally administered with CQ (970mg/Kg) on day 1. Groups 3 and 4 were daily administered with vitamin C 200 and 1000 mg/kg respectively. Cardiovascular, biochemical, histological and molecular parameters were determined at the end of the study.

Results

Chloroquine altered cardiovascular function evident by elevated blood pressure, cardiac arrhythmia, increased cardiac oxidative stress, alter cardiac histo-architecture and increased CnTI expression. Vitamins C especially at the higher dose of 1000 mg/Kg significantly mitigated these alterations which was associated with altered HDAC3 expressions when compared with control.

Conclusion
Vitamin C especially at high dose mitigated chloroquine induced cardiac dysfunction which involved the modulation of HDAC3/CnTI signaling pathway.

References
[1] Nnodim, Johnkennedy,Ujowundu Cosmus Onyekachi , Udujih Hellen Ifeoma , Okorie Hope , Nwobodo Emmanuel Ikechukwu , Nwadike Constance Nnedimma 2012, 'Hepatocellular enzyme activities and protein level following administration of vitamins during Chloroquine induced hepatoxicity in wistar rats', *Indian J. Innovations Dev.*, Vol. 1, No. 4: Indian Society for Education and Environment ,
[2] Trivedi CM, Lu MM, Wang Q, Epstein JA. Transgenic overexpression of Hdac3 in the heart produces increased postnatal cardiac myocyte proliferation but does not induce hypertrophy. J Biol Chem. 2008;283(39):26484–26489.

B 08-49
Use of echocardiography for non-invasive assessment of cardiac morphology and function in Atlantic salmon

V. Becker[1], S. Kavaliauskiene[1], I. B. Johansen[2], I. Sjaastad[1], W. E. Louch[1], M. Frisk[1]
[1] *University of Oslo and Oslo University Hospital Ullevå, Institute for Experimental Medical Research, Oslo, Norway*
[2] *Faculty of Veterinary Medicine, Department of Preclinical Sciences and Pathology, Oslo, Norway*

Introduction
Non-lethal tools for examination of cardiac morphology and function in fish are scarce, and current methodologies are generally invasive, time consuming, and stationary. Echocardiography has previously been examined as a non-invasive, quick and transportable alternative, but the presence of spongious myocardium in most species has hindered its usability. However, technical improvements during the last decade have enabled more refined functional assessment, and hold promising potential for application in fish.
Methods
We examined the application of echocardiography in 22 Atlantic salmon (*Salmo salar L.*), anaesthetized using tricaine methanesulfonate (MS-222) through gill irrigation at a dose of 0.75mg/L. The size of the fish ranged from 345-2800 grams and 31-62 cm and was kept at a water temperature of 10℃. To facilitate versatility and transportability, a compact system (Vivid iq,GE Healthcare) was employed using two different probes; a linear (12L, 5-13 MHz) and Phased Array dedicated cardiac probe (12S, 4-12 MHz). Several protocols and projections were tested and intra- and inter-variation were assessed. Accuracy of cardiac dimension measurements was verified by comparison with excised hearts.
Results
We observed that measurements of cardiac dimensions (ventricle, atrium and bulbus) were equally robust using both probes, as evidenced by low variability and high accuracy. However, the cardiac probe was favourable for capturing detailed functional parameters, such as ejection fraction, fractional shortening, strain, and strain rates. As with morphological measures, functional assessment was found to be precise and reproducible regarding both systolic and diastolic function.
Conclusion
In conclusion, we have demonstrated that echocardiography is a powerful, non-invasive tool that enables reliable and reproducible assessment of cardiac structure and function in fish. Importantly, the transportability and versatility of the system tested enables cardiac assessment in otherwise inaccessible locations.

B 08-50
Deep Learning based peripheral blood pressure estimation using parameters derived from impedance-cardiography

T. L. Bothe, A. Patzak, N. Pilz
Charité - Universitätsmedizin Berlin, corporate member of Freie Universität Berlin and Humboldt-Universität zu Berlin, Institute of Translational Physiology, Berlin, Germany

Objective
Continuous, non-invasive blood pressure (BP) measurement devices are a current, noteworthy trend in hypertension research. Most current devices are based on pulse-wave-velocity or pulse-wave-analysis, showing varying measurement accuracy. This study wants to explore the possibility of a Deep Learning enhanced BP model derived from physiological parameters detected via impedance-cardiography. A proof of concept system for peripheral BP determination could lead the way for future impedance-cardiography-based systems for central BP estimation.
Methods
We simultaneously measured cuff-based BP data (Ontrak, Spacelabs Healthcare) and a set of physiological parameters (CardioScreen 1000, medis.GmbH) during rest, psychological and physical stress in 71 young and healthy adults. Psychological stress was induced by an adapted version of the Trier Social Stress Test. Physical stress was applied via a double-peak stress profile on a 45° angled bike ergometer. Multiple models based on conventional machine learning and Deep Learning architectures for BP estimation were trained. All models were validated via a k-fold validation scheme, in-line with best practice guidelines for machine learning applications.
Results
BP models derived from impedance-cardiography systems correlate with systolic ($p < 0.001$) and diastolic ($p < 0.001$) cuff-based BP levels. Deep Learning architectures retrieve mean deviations below 3 mmHg with limits of agreement of ± 15 mmHg for both systolic and diastolic values. Parameters indicating changes in contractility (e.g., pre-ejection period, acceleration index) and sympathetic tone (e.g., heart rate) showed the highest predictive power, especially for systolic BP.
Conclusion
Deep Learning BP estimation models based on physiological parameters measured by impedance-cardiography provide exceptional and robust peripheral BP estimation accuracy in a laboratory setting. These systems could lead the way to a broad application of cuff-less, continuous BP measurement devices and possibly enable ambulatory, non-invasive and precise estimation of central BP.

B 08-52

Different autonomic self-regulation in healthy males causes different sensitive reactions to high geomagnetic activity

A. Ramishvili[1], K. Janashia[1], L. Tvildiani[1], G. Ramishvili[2]

[1] *David Tvildiani Medical University, Central scientific research laboratory, Tbilisi, Georgia*

[2] *Ilia State University, Solar physics group, School of Natural Sciences and Medicine, Tbilisi, Georgia*

Introduction

We tested the hypothesis of whether different self-regulation of the autonomic nervous system (ANS) in healthy males' reacted differently to high geomagnetic activity (GMA), causing specific sensitive reactions (1-3).

Methods

In total, 51 healthy volunteers, aged 18 to 24 years participated in the observational study, out of which 27 were volunteers with an initial heart rate - of HR<80 and 24 with HR>80. The ANS response to GMA has been measured via heart rate variability (HRV) (4) in the different phases of geomagnetic storms (GMSs).

Results

In the case of initial higher vagal tone (HR<80) (5), changes were found to indicate a significant intensification of both parts of ANS as sympathetic as well as parasympathetic – SP, PP (increased HR p=0.006, high-frequency band of cardiointervals in percent - HF% p=0.03 and reduced Standard Deviation Normal to Normal R-R interval - SDNN p=0.008). In the case of initial (HR>80), changes indicate a significant enhancement of SP (reduced SDNN p=0.047). In both cases (HR<80, HR>80) changes indicate a pronounced stress level on days after the main phase of GMSs, the delay is one day.

Conclusion

High GMA is a sufficient environmental factor for healthy males, causing an intensification of both parts of the ANS as a stress reaction, especially in the restoration phase of storms. This period is needed for the human organism to achieve an optimal adaptive reaction. However, the different self-regulation of the ANS results in different dynamics in its variation depending on the individual's character of resting ANS states; the volunteers with initial higher vagal tone are more adaptable to the impact of different phases on GMS.

References

[1] Alabdulgader A, McCraty R, Atkinson M, Dobyns Y, Vainoras A, et al. Long-Term Study of Heart Rate Variability Responses to Changes in the Solar and Geomagnetic Environment. Scientific Reports. 2018; 8:2663. doi:10.1038/s41598-018-20932-x.

[2] Cornelissen G, Halberg F, Breus T, Syitkina E, Baevsky R, et al. Non-photic solar associations of heart rate variability and myocardial infarction. Atmosphere and Solar terrestrial physics. 2002; 64:707-20.

[3] Otsuka K, Cornelissen G, Weydahl A, Holmeslet B, Hansen T, et al. Geomagnetic disturbance associated with decrease in heart rate variability in a subarctic area. Biomed. Pharmacother. 2001; 55, (suppl S1):51-6. doi:10.1016/s0753-3322(01)90005-8.

[4] Malik M, Bigger JT, Camm AJ, Kleiger RE, Malliani A, et al. Heart rate variability. Standards of measurement, physiological interpretation, and clinical use. Task Force of the European Society of Cardiology and the North American Society of Pacing and Electrophysiology. Eur Heart J. 1996; 17(3):354-81. https://doi.org/10.1093/oxfordjournals.eurheartj.a014868.

[5] Thayer JF, Yamamoto SS, Brosschot J. F, et al. The relationship of autonomic imbalance, heart rate variability and cardiovascular disease risk factors. Int J Cardiol. 2010; 141(2):122-31. doi: 10.1016/j.ijcard.2009.09.543.

B 08-53

Relationship between serum metabolites and cardiac autonomic modulation in apparently healthy individuals: a metabolomics approach

E. F. Signini[1], A. Castro[2], P. Rehder-Santos[1], J. C. Milan-Mattos[1], V. Minatel[1], C. B.F. Pantoni[1], A. Porta[3,4], A. G. Ferreira[2], R. V. Oliveira[2], A. M. Catai[1]

[1] *Federal University of São Carlos, Physiotherapy Department, São Carlos, Brazil*

[2] *Federal University of São Carlos, Chemistry Department, São Carlos, Brazil*

[3] *University of Milan, Department of Biomedical Sciences for Health, Milan, Italy*

[4] *Vascular Anesthesia and Intensive Care, Policlinico San Donato, San Donato Milanese, Department of Cardiothoracic, Milan, Italy*

The authors thank São Paulo Research Foundation (FAPESP) (grant number: 2018/25082-3, 2016/22215-7, 2010/52070-4) and Coordination for the Improvement of Higher Education Personnel (CAPES) (grant number: 23028.007721/2013-41 and Finance Code 001) for the financial support.

Introduction

Metabolism and autonomic nervous system (ANS) activity are closely integrated (1). Despite the emergence of metabolomics and cardiac autonomic modulation (CAM) analyses to assess these components, the relationship between them is still unclear (2,3). The study of a large number of serum metabolites, as well as the use of advanced techniques for analyzing CAM, may help to clarify this relationship and contribute to the interpretation of clinical outcomes. The objective was to investigate the relationship between metabolism and ANS through metabolomics and CAM in apparently healthy individuals.

Methods

70 apparently healthy eutrophic subjects (39 men and 31 women) aged 20 to 40 years underwent blood serum collection in the morning after 12h of fasting. The measurement of serum levels of metabolites was performed using the hydrogen nuclear magnetic resonance technique (Bruker, AVANCE III, 600MHz). In the afternoon, they underwent 15 minutes of cardiovascular data collection in the supine position for the CAM assessment by univariate symbolic analysis (SA) and spectral analysis (SpA) over heart periods. SA and SpA were calculated based on 256 consecutive values of the heart period, determined as the temporal distance between two R-R intervals of electrocardiogram (ADinstruments, BioAmp FE132). The following relative indices were used: no variation (0V%), one variation (1V%), two like variations (2LV%), and two unlike variations (2UV%) for the SA and normalized low frequency (LF%) and normalized high frequency (HF%) for the SpA. The cardiac sympathetic modulation (CSM) and cardiac parasympathetic modulation (CPM) were assessed by 0V% and LF%, and by 2LV%, 2UV%, and HF%, respectively. The Pearson or

Spearman correlations were performed between metabolites and CAM variables considering all individuals and for each sex, using Munro's proposal and $p < 0.05$.

Results

47 metabolites were identified. Metabolites with statistical significance, represented almost exclusively by amino acids, showed a direct relationship with CSM ($0.238 \leq r \leq 0.413$) and an inverse relationship with CPM ($-0.521 \leq r \leq -0.236$) considering all individuals and for each sex. The methionine was highlighted for exclusively presenting low and moderate correlations with indices related to CSM and CPM considering males (0V%: $r = 0.372$, $p = 0.020$; 1V%: $r = 0.374$, $p = 0.019$; 2LV%: $r = -0.506$, $p = 0.001$; 2UV%: $r = -0.340$, $p = 0.034$) and female (0V%: $r = 0.380$, $p = 0.035$; 2UV%: $r = -0.450$, $p = 0.011$), as well as without distinction of sex (0V%: $r = 0.413$, $p < 0.001$; 1V%: $r = 0.238$, $p = 0.047$; 2LV%: $r = -0.383$, $p = 0.001$; 2UV%: $r = -0.380$, $p = 0.001$; LF%: $r = 0.248$, $p = 0.038$; HF%: $r = -0.262$, $p = 0.028$).

Conclusion

High levels of serum amino acids during fasting are related to worse CPM indices in apparently healthy subjects. Furthermore, the serum level of methionine is likely to be related to impairments in CAM regardless of sex.

References

(1) Hyun U, Sohn JW. Autonomic control of energy balance and glucose homeostasis. Exp Mol Med. 2022;54(4):370–6

(2) Nicholson JK, Lindon JC. Systems biology: Metabonomics. Nature. 2008;455(7216):1054–6

(3) Porta A, Marchi A, Bari V, Heusser K, Tank J, Jordan J, et al. Conditional symbolic analysis detects nonlinear influences of respiration on cardiovascular control in humans. Philos Trans A Math Phys Eng Sci. 2015;373(2034)

B 08-56

Exploring the effect Titin Truncating Variants have on Atrial Fibrillation

M. J. Cumberland[1], N. Sontayananon[2], A. Holmes[1], B. Rodriguez[3], P. Kirchhof[1], C. Denning[4], B. Davies[5], K. Gehmlich[1]

[1] University of Birmingham, Institute of Cardiovascular Sciences, Birmingham, UK

[2] University of Oxford, Department of Medical Sciences, John Radcliffe Hospital, Oxford, UK

[3] University of Oxford, Department of Computer Science, Oxford, UK

[4] University of Nottingham, Biodiscovery Institute, Nottingham, UK

[5] University of Oxford, Transgenic Core, Oxford, UK

National Centre for the Replacement, Refinement and Reduction of Animals in Research/British Heart Foundation studentship NC/T001747/1

Introduction

Titin truncating variants (TTNtvs) are the predominant genetic cause of dilated cardiomyopathy, accounting for nearly 1 in 7 cases (Roberts et al., 2015). Further to this genomics studies have recently provided a robust link between the presence of TTNtvs and the development of atrial fibrillation. The pathogenic mechanism behind TTNtv associated atrial fibrillation is unknown.

Materials and Methods

A titin truncating variant previously identified in a cohort of 11 probands at risk of early onset atrial fibrillation was edited into an induced pluripotent stem cell line using CRISPR-Cas9 (Hoorntje et al., 2018). The cells were differentiated into atrial iPSC-cardiomyocytes (iPSC-CM) to explore the impact of the variant on sarcomere organisation, cellular transcription, and electrophysiology.

Results

Atrial iPSC-CM carrying a heterozygous titin truncating variant constructed functional and undisrupted sarcomeres. The cells carrying a TTNtv showed no significant difference in intracellular electrophysiology but demonstrated an upregulation of cardiac stress markers.

Discussion

The exact mechanism behind the link between titin truncating variants and atrial fibrillation is unclear and likely subtle. Normal intracellular electrophysiology and upregulation of cardiac stress markers implies that the pathogenicity behind the variants is likely associated with structural rather than electrical remodelling.

References

[1] Roberts, A.M., Ware, J.S., Herman, D.S., Schafer, S., Baksi, J., Bick, A.G., Buchan, R.J., Walsh, R., John, S., Wilkinson, S. and Mazzarotto, F., 2015. Integrated allelic, transcriptional, and phenomic dissection of the cardiac effects of titin truncations in health and disease. *Science translational medicine*, *7*(270), pp.270ra6-270ra6.

[2] Hoorntje, E.T., van Spaendonck-Zwarts, K.Y., Te Rijdt, W.P., Boven, L., Vink, A., van der Smagt, J.J., Asselbergs, F.W., van Wijngaarden, J., Hennekam, E.A., Pinto, Y.M. and Deprez, R.H.L., 2018. The first titin (c. 59926+ 1G> A) founder mutation associated with dilated cardiomyopathy. *European journal of heart failure*, *20*(4), p.803.

B 08-57

T-tubule loss in rat and human cardiomyocytes aggravates the effects of reduced SERCA activity on Ca^{2+} release

D. J. Fiegle, T. Volk, T. Seidel

Friedrich-Alexander-Universität Erlangen-Nürnberg, Institute of Cellular and Molecular Physiology, Erlangen, Germany

We would like to thank Prof. Michael Weyand and PD Dr. Christian Heim from the Department of Cardiac Surgery, Friedrich-Alexander-Universität Erlangen-Nürnberg and University Hospital Erlangen, Germany and Prof. Hendrik Milting from the Erich & Hanna Klessmann Institute, Clinic for Thoracic and Cardiovascular Surgery, Heart and Diabetes Centre NRW, Ruhr-University Bochum, Bad Oeynhausen, Germany for the procurement of myocardial tissue samples and excellent collaboration.

Introduction

Impaired cardiomyocyte Ca^{2+} release is a characteristic of heart failure. Although the loss of the transverse tubular system (t-system) and downregulation of the sarco/endoplasmic reticulum Ca^{2+} ATPase (SERCA) are accepted determinants of disturbed Ca^{2+} release, their interdependence is

insufficiently studied.[1,2] Therefore, we investigated how SERCA inhibition modulates the effect of t-system density on Ca^{2+} release.

Methods

Left-ventricular cardiomyocytes were obtained by enzymatic isolation from human failing heart samples after written informed consent, and from adult rats after narcosis (thiopental i.p., 100mg/kg) and cervical dislocation.[3] We stained membranes with Di8-ANEPPS and used Fluo4 AM as Ca^{2+} indicator for simultaneous analysis of the t-system and Ca^{2+} release by confocal line scanning. Rat cells were kept in culture for two days to induce t-system variability.[4] Human cells were imaged immediately after isolation. We compared Ca^{2+} release activation time (t_a) before (CTRL) and after partial SERCA inhibition by thapsigargin (TPSG). Pixel-wise analysis of the three-dimensional t-system distance (ΔTT) and t_a along the scanned line was performed in each cell.

Results

Using the 25th percentile of mean ΔTT as threshold (0.54µm), rat myocytes were divided into high and low t-system density. In the high t-system density group, TPSG-treated cells showed longer t_a than CTRL cells (35.9±4.8ms vs 85.2±21.4ms, p=0.05, n=12/6 cells, N=6/6 animals). As expected, in the group with low t-system density, CTRL cells revealed greater t_a than high t-system cells (51.1±7.8ms). Importantly, TPSG-treated cell displayed a much more pronounced increase in t_a (141±22.2ms, p<0.001, n=31/21 cells, N=5/5 animals). Using the same approach and a threshold of 0.85µm, we investigated human myocytes from failing hearts. In the high t-system density group we found no significant difference of t_a between CTRL (94±16ms) and TPSG (83.9±10.3ms, p=0.59, n=18/16 cells, N=12 patients). However, in the low t-system group, TPSG-treated cells exhibited a more than doubled t_a (102±7.4ms vs 227±50.1ms, p<0.05, n=57/45 cells, N=12). The treatment of human cells with isoproterenol had opposite effects. To avoid any bias from thresholding, a linear mixed-effects model was used to pixel-wise analyze the dependency of t_a on ΔTT within each recorded cell. The model revealed significantly steeper relationships in TSPG-treated human cells than in CTRL (CTRL 25.8±6.4 vs 49.0±6.4ms/µm, p<0.001).

Conclusion

We found significant interaction between SERCA activity and t-system density in rat and human cardiomyocytes, implicating that reduced SERCA activity and t-system loss mutually aggravate their effects on Ca^{2+} release. These results enlighten the mechanisms behind the pronounced contractile dysfunction in failing hearts, where diminished SERCA activity and t-system loss typically coincide, and will help to interpret results from animal and in-vitro models of cardiac disease.

References

[1] Swift, F., Franzini-Armstrong, C., Øyehaug, L., Enger, U. H., Andersson, K. B., Christensen, G., Sejersted, O. M., & Louch, W. E. (2012). Extreme sarcoplasmic reticulum volume loss and compensatory T-tubule remodeling after Serca2 knockout. *Proceedings of the National Academy of Sciences of the United States of America*, *109*(10), 3997–4001.

[2] Celestino-Montes, A., Pérez-Treviño, P., Sandoval-Herrera, M. D., Gómez-Víquez, N. L., & Altamirano, J. (2021). Relative role of T-tubules disruption and decreased SERCA2 on contractile dynamics of isolated rat ventricular myocytes. *Life sciences*, *264*, 118700.

[3] Fiegle, D. J., Volk, T., & Seidel, T. (2020). Isolation of Human Ventricular Cardiomyocytes from Vibratome-Cut Myocardial Slices. *Journal of visualized experiments : JoVE*, (159), 10.3791/61167.

[4] Seidel, T., Fiegle, D. J., Baur, T. J., Ritzer, A., Nay, S., Heim, C., Weyand, M., Milting, H., Oakley, R. H., Cidlowski, J. A., & Volk, T. (2019). Glucocorticoids preserve the t-tubular system in ventricular cardiomyocytes by upregulation of autophagic flux. *Basic research in cardiology*, *114*(6), 47.

PB 09 | Blood Physiology, Oxygen, Stem cells, Regeneration, Molecular Aging

B 09-01

The role ofthe hypoxia-inducible factor-2alpha in focal cerebral ischemia

V. von Oepen, J. Fandrey, T. Leu

University of Duisburg-Essen, Department of Physiology, Essen, Germany

Stroke is one of the major reasons for death and disability. Insufficient blood flow in stroke interferes the brain from proper oxygenation, leading to the stabilization of hypoxia-inducible factors (HIFs). To determine the role of HIFs in stroke, particularly HIF-2α, we use an *in vivo* mouse model called tMCAO (transient middle cerebral artery occlusion) and an *in vitro* model with human SH-SY5Y cells.

On both, *Hif-2α* deficient and wild type mice, tMCAO was performed for two hours and protein and RNA samples were collected of ischemic and control brains. To simulate stroke in SY5Y cell culture, oxygen-glucose-deprivation (OGD) experiments were performed under almost anoxic conditions (0.2% oxygen) and without glucose. RNA and Protein samples were taken hourly for up to 4 hours, following 1 or 24 hours of reperfusion. Prior to reperfusion, either Roxadustat or a selective HIF-2α inhibitor (PT-2358) were administered. First results show a significant increased expression of HIF-2α regulated neurotrophic factors such as *Nrg1*, *NeuroD1* and *GDNF* already after one hour of OGD, while the inhibition of HIF-2α during reperfusion leads to significantly less cell death.

Our preliminary results lead us to the conclusion that HIF-2α might influence the outcome after ischemia and reperfusion in a time-dependent manner. In future experiments we want to figure out the effects of HIF-2α during stroke and after reperfusion by analyzing more HIF-2α target genes via qPCR, as well as getting more insights of the HIF-2α regulation by Western Blot analysis, to better understand the cellular response to ischemia and reperfusion, which may help to provide therapeutically approaches for a better outcome after stroke.

B 09-02

Contact with albumin-derived perfluorocarbon-based artificial oxygen carriers (A −AOCs) does not activate primary human macrophages (PHM)

L. Tchuendem[1], K. Ferenz[1,2]

[1] *University of Duisburg-Essen, University Hospital Essen, Institute of Physiology, Essen, Germany*

[2] *CeNIDE, University of Duisburg-Essen, Duisburg, Germany*

Artificial oxygen carriers (AOCs) are applied directly into the body through an intravenous injection. In the body, the first cells that are in contact with AOCs are endothelial cells and immune cells. Thus, primary human macrophages (PHM) will be exposed to albumin-derived perfluorocarbon-based artificial oxygen carriers (A−AOCs). Activation of PHM was investigated by using the human monocytic cell line Tohoku Hospital Pediatrics-1 (THP-1) after differentiation to PHM with phorbol12-myristate13-acetate (PMA).
Cytotoxicity of A-AOCs was checked with lactate dehydrogenase (LDH) assay. PHM ($1x10^4$cells/well, 10 ng/ml PMA for 72 h + 24 h resting without PMA) were treated with medium +/- 17-2% of A-AOCs for 4 h. To analyze the influence of A−AOCs on cell adhesion, we checked for intracellular adhesion molecule−1 (ICAM-1) expression in PHM using western blot. For western blot analysis, PHM were treated with medium, LPS (1 µg/ml) or 10-2% of A-AOCs at 21% O_2 for 24 h. To confirm the non-activation of PHM by A−AOCs, we measured cytokine release (IL−1β and TNF−α) in PHM ($5x10^5$cells/ml, 10 ng/ml PMA for 72 h + 24 h resting without PMA) by ELISA and quantified the mRNA expression of selected immunologically relevant genes by qPCR after treatment with medium, LPS (1 µg/ml) or 10-2% of A-AOCs at 21% O_2 for 24 h. To investigate the uptake of A-AOC by PHM ($5x10^5$cells/ml) were labelled with TRITC-Concanavalin A (100 µg/ml) for 30 min and subsequently incubated with 4% of FITC-labelled-A-AOCs (1mg/ml) for 30 min or 2 h & visualized at 580 nm and 519 nm with a fluorescence microscope.
LDH assay revealed toxicity only for LPS & positive control. In addition, ICAM-1 expression (associated with pro-inflammatory conditions) increased in LPS-treated control cells but not in A−AOCs treated cells. Furthermore, fluorescence microscopy showed uptake of A−AOCs by PHM already after 30 min, which further increased after 2 h of incubation. The non-activation of PHM was confirmed by very low cytokine release as well as low RNA expression of the selected immunologically relevant genes after 24 h incubation with A−AOCs. Taken together, our results demonstrate that, although PHM engulf A−AOCs, PHM tolerate our A−AOCs very well and are not activated in the presence of A−AOCs.

B 09-03

Modeling oxygen transport in humans with altered hemoglobin-oxygen affinity

T. K. Roy[1], J. Shepherd[3], P. Dominelli[4], J. Herrick[2], J. Hoyer[2], K. Webb[1], M. Joyner[1], T. Secomb[5]
[1] *Mayo Clinic, Dept of Anesthesiology, Rochester, USA*
[2] *Mayo Clinic, Dept of Laboratory Medicine and Pathology, Rochester, USA*
[3] *Medical College of Wisconsin, Dept of Anesthesiology, Milwaukee, USA*
[4] *University of Waterloo, Dept of Kinesiology and Health Sciences, Waterloo, Canada*
[5] *University of Arizona, Dept of Physiology, Tucson, USA*

Supported by National Institutes of Health R35 HL139854 and U01 HL133362.

The shape of the oxyhemoglobin dissociation curve is a major determinant of oxygen transport under resting and exercise conditions. The affinity of hemoglobin for oxygen (Hb-O_2 affinity) can be characterized by its P_{50} value, defined as the oxygen tension at which it is 50% saturated. Rare hemoglobin (Hb) variants in humans result from mutations that can alter Hb affinity, and the extents to which these mutations affect levels of hemoglobin and oxygen transport remain unknown. As an example, patients with high Hb-O_2 affinity are often seen to have a high Hb concentration, perhaps reflecting a compensatory polycythemia due to impaired oxygen extraction. The purpose of this study was thus to examine the relationship between Hb-O_2 affinity (as measured by P_{50}), hemoglobin concentration [Hb], and oxygen transport. To accomplish this, we developed a mathematical model for oxygen uptake and utilization under resting and exercise conditions accounting for alterations in P_{50} and [Hb]. All study procedures were approved by the Mayo Clinic Institutional Review board (16-007719) and were in accordance with the Declaration of Helsinki. A database of rare human Hb variants was used to correlate P_{50} (mmHg) with [Hb] (g/dL) and yielded an approximately linear relationship ($[Hb] = -0.3135 \times P_{50} + 23.636$; $r = -0.82$, $P < 0.0001$) demonstrating an increase in [Hb] with increasing Hb-O_2 affinity (lower P_{50}) [1]. A mathematical model incorporating this relationship was used to simulate oxygen transport in subjects with normal (P_{50} = 26 mmHg), increased (13 mmHg), and decreased affinity (39 mmHg) Hb variants. Oxygen uptake in the lung was modeled using a single compartment model, and oxygen utilization in the tissue was modeled using the Fick principle. Separate sets of calculations were performed for rest and exercise, assuming corresponding values of oxygen demand and cardiac output. The results indicate that increased Hb-O_2 affinity variants compensate for enhanced oxyhemoglobin binding with higher values of [Hb] to maintain oxygen transport under exercise conditions, but that low values of Hb-O_2 affinity lead to unsustainable levels of oxygen extraction at the assumed values of cardiac output. In conclusion, the combined effects of altered Hb-O_2 affinity and the associated changes in [Hb] values must be considered when assessing the impact of Hb variants on oxygen uptake and utilization in exercise and in pathophysiological states.

References

[1] Shepherd JRA et al., 2019, 'Modelling the relationships between haemoglobin oxygen affinity and the oxygen cascade in humans', *J Physiol* 597.16, pp 4193–4202.

B 09-04

The metabolism of peripheral blood mononuclear cells of patients suffering from hereditary haemorrhagic telangiectasia is reduced and can be modulated by hypoxia inducible factor-1alpha stabilization

Y. Schild, J. Bosserhoff, J. Fandrey, A. Wrobeln
University of Duisburg-Essen, Institute of Physiology, Essen, Germany

Hereditary haemorrhagic telangiectasia (HHT) is a rare disease with an estimated prevalence of 1 in 5000 people. The disease is caused by mutations of genes within the transforming growth factor beta (TGF-β) pathway superfamily. The altered TGF-β signalling impacts angiogenesis, resulting in malformations of blood vessels which can lead to life threatening bleedings[1].
Furthermore, an impaired TGF-β signalling alters development and function of the immune system. Over the past decade several scientific papers were published that indicate a connection between HHT and an immune deficiency. The observation that sepsis is the leading cause of death for HHT patients underlines the need to investigate the altered immune response in HHT patients[2]. So far, little is known about the underlaying molecular processes which lead to an immune deficiency in HHT patients.
We are interested in the immune modulatory capacity of the hypoxia inducible factor (HIF). This transcription factor could be a link between the altered TGF-β signalling in HHT patients and their immune deficiency as there is crosstalk between TGF-β with hypoxia signalling[3]. Additionally, HIF

plays a pivotal role in the regulation of inflammation. Our group previously showed significant reduction of HIF-1α, regarding gene expression and protein abundance, in leukocytes of HHT patients[4]. HIF-1 induces, among others, gene expression of glycolytic enzymes. Glycolysis is crucial for the activation, function and/or differentiation of different immune cells. In this regard, glycolysis drives the differentiation of macrophages towards the proinflammatory M1 phenotype, dendritic cells relay on glycolysis for their maturation and proinflammatory T cell subsets require a glycolytic switch for their activation and differentiation[5]. Hence, we speculated that glycolysis is reduced in HHT-leukocytes in a HIF dependant manner and that glycolysis could be enhanced by Roxadustat, an HIF-α stabilizing drug.
Here we showed that mRNA levels of glycolytic enzymes are significantly reduced in HHT-peripheral blood mononuclear cells (PBMCs) compared to non-HHT-PBMCs. Furthermore, we investigated the metabolic profiles of PBMCs in HHT patients, using the *Seahorse extracellular flux analyser*. Glycolysis and oxidative phosphorylation were significantly reduced in resting PBMCs of HHT patients compared to non-HHT-PBMCs. However, the glycolysis rate could be restored by HIF-1α stabilisation via Roxadustat administration to a level comparable to non-HHT controls, whilst the oxidative phosphorylation was only mildly reduced.
The loss of HIF-1α in HHT-PBMCs causes metabolic impairment and thereby may explain the altered immune response of HHT patients. The restauration of the glycolytic rate due to Roxadustat treatment might have a beneficial effect on the immune response. However, PBMCs encompass a multitude of immune cells and the effect of Roxadustat must be investigated on each cell type individually.

References

[1] Faughnan, M. E.; Palda, V. A.; Garcia-Tsao, G.; Geisthoff, U. W.; McDonald, J.; Proctor, D. D. et al. (201): International guidelines for the diagnosis and management of hereditary haemorrhagic telangiectasia. In: *Journal of medical genetics* 48 (2), S. 73–87. DOI: 0.1136/jmg.2009.069013.
[2] Droege, Freya; Thangavelu, Kruthika; Stuck, Boris A.; Stang, Andreas; Lang, Stephan; Geisthoff, Urban (208): Life expectancy and comorbidities in patients with hereditary hemorrhagic telangiectasia. In: *Vascular medicine (London, England)* 23 (4), S. 377–383. DOI: 0.1177/1358863X18767761.
[3] McMahon, Stephanie; Charbonneau, Martine; Grandmont, Sebastien; Richard, Darren E.; Dubois, Claire M. (2006): Transforming growth factor beta induces hypoxia-inducible factor-1 stabilization through selective inhibition of PHD2 expression. In: *The Journal of biological chemistry* 28 (34), S. 24171–24181. DOI: 10.1074/jbc.M604507200.
[4] Wrobeln, Anna; Leu, Tristan; Jablonska, Jadwiga; Geisthoff, Urban; Lang, Stephan; Fandrey, Joachim; Droege, Freya (2022): Altered hypoxia inducible factor regulation in hereditary haemorrhagic telangiectasia. In: *Scientific reports* 12 (1), S. 5877. DOI: 10.1038/s41598-022-09759-9
[5] Chen, Jing-Yue; Zhou, Ji-Kai; Pan, Wei (2021): Immunometabolism: Towards a Better Understanding the Mechanism of Parasitic Infection and Immunity. In: *Frontiers in immunology* 12, S. 661241. DOI: 10.3389/fimmu.2021.661241

B 09-06

Establishment of an *in vitro* platform to test the effect of trans-resveratrol loaded artificial oxygen carriers on reperfusion injury in HL-1 cells

O. Karaman[1,2], J. K. Hausherr[1], M. Kirsch[2], K. B. Ferenz[1,3]
[1] *University Hospital Essen, University of Duisburg-Essen, Institute of Physiology, Essen, Germany*
[2] *University Hospital Essen, University of Duisburg-Essen, Institute of Physiological Chemistry, Essen, Germany*
[3] *University of Duisburg-Essen, Center for Nanointegration Duisburg-Essen, Duisburg, Germany*

The clinical procedure of organ transplantation is inevitably associated with the process of ischemia reperfusion injury (IRI), where damage to the organ occurs during times of hypoxia and is aggravated by reestablishment of the blood flow. Damage caused by IRI during organ transplantation is still considered one of the main factors for a higher incidence of acute and chronic graft rejection[1]. Cessation of the blood flow and the resulting ischemic period lead to alterations of cellular metabolism, signal pathways and gene expression, which lay the foundation for harmful inflammatory and oxidative processes during reperfusion. Perfusion systems suitable for different organs emerged in the clinics are utilizing erythrocytes to prevent the manifestation of a prolonged ischemia. Unfortunately, these systems rely on blood donations, which already represent a scarce resource. Our albumin derived artificial oxygen carriers (A-AOC) are able to physically dissolve and deliver physiological levels of oxygen due to their perfluorocarbon core. Therefore, A-AOCs are capable of supplying organs with oxygen during storage in order to prevent IRI and can be utilized as a replacement for erythrocytes.
The potential of A-AOCs to reduce IRI was assessed in an ischemia reperfusion cell model utilizing murine HL-1 cells. Within the scope of these experiments, a special cell culture setup, which is utilizing transwell inserts, was successfully established. A-AOCs tend to sediment in a static environment and form a layer on adherent cells, which leads to undesired cell stress and falsification of results. The use of transwell inserts prevents this phenomenon, as they allow a spatial separation of cells and A-AOCs. Cells were exposed to 3h 0.1% O_2 in hypoxic chamber and were then transferred to a normoxic incubator to initiate reperfusion for 1h. During the simulated ischemia cells were treated with oxygenated A-AOCs (100% O_2 at 0.5 bar). Every 30 minutes A-AOCs were replaced by freshly oxygenated particles. The occurring cell damage and apoptosis rate during the experimental process will be evaluated by detection of lactate dehydrogenase release, western blots for cleaved caspase 3 and GSH/GSSG ratio. To supplement potentially beneficial effects of A-AOCs, the oxygen carriers will be additionally loaded with the antioxidative compound trans-resveratrol (RESLOCs: resveratrol loaded oxygen carrier) to enhance suppression of oxidative damage during reperfusion.
Preliminary results in cell culture and *ex vivo* perfusion systems generated in the group already demonstrate the ability of A-AOCs to provide cells with oxygen and sustain physiological functions[2]. Hence, a reduction of cellular damage and overall improvement of cell viability is expected in cells treated with A-AOCs in this grave IRI setup. These beneficial effects of the oxygen carrier should also occur in cells exposed to RESLOCs, but in a more pronounced way, especially in regards to oxidative stress.

References
[1] LChatterjee, Shampa, and Aron B. Fisher. "The role of ischemia-reperfusion injury in graft rejection." *Immunobiology of Organ Transplantation*. Springer, Boston, MA, 2004. 545-572.
[2] Wrobeln, Anna, et al. "Functionality of albumin-derived perfluorocarbon-based artificial oxygen carriers in the Langendorff-heart." *Artificial cells, nanomedicine, and biotechnology* 45.4 (2017): 723-730.

B 09-07

Human leukocytes in inflammatory hypoxia

T. Schönberger[1], B. Tebbe[2], M. Jakobs[3], O. Witzke[4], M. Schedlowski[3], J. Fandrey[1]
[1] *University of Duisburg-Essen, Institute of Physiology, Essen, Germany*
[2] *University Hospital Essen, Department of Nephrology, Essen, Germany*
[3] *University of Duisburg-Essen, Institute of Medical Psychology and Behavioral Immunobiology, Essen, Germany*
[4] *University Hospital Essen, Clinic for Infectious Diseases, Essen, Germany*

We would like to thank Prof. Dr. Peter Horn and the team of the Institute for Transfusion Medicine of the University Hospital Essen for supply and preparation of buffy coats for PBMC isolation.

Introduction

In inflammatory conditions, leukocytes are challenged with a high variety of different environments and oxygen concentrations. Within short time, leukocytes need to adapt to different conditions to fight pathogens and maintain physiological health. Hypoxia significantly affects leukocyte function and controls the innate and adaptive immune response mainly through transcriptional gene regulation via the hypoxia-inducible factors (HIFs)[1,2]. The HIF effects and interplay with inflammatory responses on cellular level are still under investigation. We aim to gain a deeper understanding of the cellular adaption processes of circulating human leukocytes challenged with inflammation and hypoxia.

Methods

We studied acute immune response in healthy male subjects using an experimental human endotoxemia model. 30 volunteers received an intravenous injection of 0.4 ng/kg lipopolysaccharide (LPS) as inflammatory stimulus prior or after exposure to hypoxia (10.5% normobaric oxygen) for four hours. Standard determination of clinical blood parameters and oxygen saturation was complemented by analysis of cell populations regarding surface marker expression via flow cytometry and gene expression patterns via qRT-PCR. In addition, we studied LPS treated Peripheral Blood Mononuclear Cells (PBMC) under different oxygen conditions in combination with LPS treatment, regarding HIF protein accumulation (Western Blotting), gene expression and surface marker expression.

Results

We could show, that the combination of *in vivo* hypoxia and LPS administration led to differently altered gene expression patterns of HIF and target genes depending on the immune cell subset (neutrophils, monocytes, T cells). Further, we observed an altered inflammatory response in PBMCs upon hypoxic pretreatment.

Conclusion

The adaption of circulating leukocytes during inflammation and hypoxia are highly interdigitated. Revealing this interplay and the possible priming effects in immune cells could give rise to new treatment options for patients fighting against infection and inflammation.

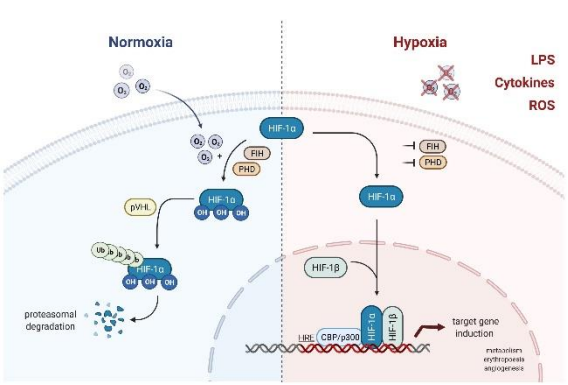

Hypoxia-inducible factor pathway
Under normoxic conditions, the hypoxia-inducible factor (HIF-1) α-subunit gets hydroxylased by Prolyl-hydroxylases (PHD) and the Factor-inhibiting HIF (FIH), recognized by the von-Hippel-Lindau (pVHL) E3 ligase complex, ubiquitinated and finally degradated by the proteasome (left part). Under hypoxic or inflammatory conditions PHD and FIH are inhibited and HIF-1α can accumulate and translocate into the nucleus where it dimerizes with the HIF-1β-subunit and induces transcription of target genes (left part).

References
1 Semenza, G. L. 2001. 'HIF-1, O2, and the 3 PHDs: how animal cells signal hypoxia to the nucleus.' *Cell, 107*(1), 1-3.
2 Watts, E. R., Walmsley, S. R., 2019, 'Inflammation and Hypoxia: HIF and PHD Isoform Selectivity', *Trends in Molecular Medicine*, Volume 25, Issue 1, Pages 33-46

B 09-08

Synthesis and characterization of perfluorocarbon-based albumin nanoparticles for practical application

F. Nocke[1], M. Penzel[1], M. A. Schroer[2], K. B. Ferenz[3,4]

[1] *University Hospital Essen, Institute of Physiological Chemistry, Essen, Germany*

[2] *University of Duisburg-Essen, Nanoparticle Process Technology (NPPT), Department of Mechanical Engineering, Essen, Germany*

[3] *University Hospital Essen, Institute of Physiology, Essen, Germany*

[4] *University of Duisburg-Essen, CeNIDE, Essen, Germany*

Perfluorocarbons (PFCs) are a well-known representative of artificial blood substitutes. The major advantages of perfluorocarbons over hemoglobin are high gas solubility, chemical and biological inertness, low viscosity, and a higher fluidity. Since they are lipophobic and hydrophobic, they require an emulsifier in aqueous media to produce a stable emulsion.[1-3] In this study, a new stable emulsion of perfluorodecalin (PFD) and albumin (albumin-derived artificial oxygen carrier, A-AOC) was developed and analyzed. The albumin-perfluorocarbon mixture was premixed with an Ultra-Turrax and subsequently emulsified in a microfluidizer with a pressure gradient. Particle shape and size information have been determined by ultra-small X-ray scattering (USAXS) measurements. Emulsifier concentration on the particle surface was measured photometrically using bromocresol green (BCG). To determine the effect of a transport on the emulsion, samples were analyzed before and after transport with dynamic light scattering and the sample temperature was logged with a temperature tracker during the entire duration of the transport. In addition, the compatibility of nanoparticles with the commercially available ex vivo organ perfusion medium “STEEN Solution” was evaluated by measuring the oxygen capacity directly after synthesis and after 14 days of storage. A respirometer was used for this purpose.

The USAXS-data indicate that the particles have an overall spherical shape and exhibit a bimodal volume distribution as shown in Figure 1. The emulsifier concentration on the particle surface is 18.38 g/L, which is 2 times greater than for the comparable organ life fluid particles.[4] A three-day transport resulted in significant growth of the emulsion, although the temperature inside the transport vessel remained at refrigerator-like temperatures the whole time. STEEN Solution can be used as a perfusion medium with the A-AOCs. After storage for 14 days, the oxygen capacity did not decrease. The oxygen carriers were still functional.

In summary, the new stable emulsion contains particles in nanometer range with spherical shape. Moreover, synthesis is compatible with STEEN Solution and a transport over three days destabilized the emulsion only slightly.

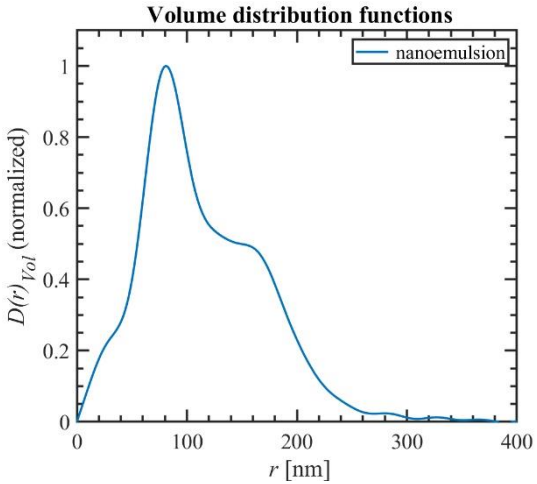

Figure 1: Particle size distribution function of the A-AOCs measured with USAXS
The figure shows the particle size distribution of the A-AOC. The particle radius is smaller than 400 nm.

References

[1] Riess, J.G., 2006, *‘Perfluorocarbon-based oxygen delivery’*, Artificial cells, blood substitutes, and biotechnology, 34(6), p. 567-580.

[2] Ferenz, K.B., Steinbicker, A.U., 2019, *‘Artificial oxygen carriers—past, present, and future—a review of the most innovative and clinically relevant concepts’*, Journal of Pharmacology and Experimental Therapeutics,, 369(2), p. 300-310.

[3] Wrobeln, A., et al., 2017, ‘Functionality of albumin-derived perfluorocarbon-based artificial oxygen carriers in the Langendorff-heart’, Artificial cells, nanomedicine and biotechnology, 45(4), p. 723-730.

[4] Arnolds, O., Cantore, M., Ferenz, K.B., Haferkamp, S., Jägers, J., Kirsch, M., Metzger, J., Nocke, F., Pütz, S., Schauerte, C., Stoll, R., 2021, ‘Zusammensetzung enthaltend künstliche Sauerstoffträger zur Verhinderung von Organschäden in Transplantationsorganen’, DE102021211272.2.

B 09-09

Alterations in Neutrophil Counts Change LDL Levels

M. Sevim[1], T. Altınoluk[1], M. M. Kahraman[1], T. Akgün[1], A. Şahin[2], H. N. Özekici[3], A. Fil[3], B. Yıldız[3], B. Yücetürk[3], E. N. Lale[3], B. Yeğen[1], A. Yıldırım[1]

[1] *Marmara University, School of Medicine, Physiology Department, İstanbul, Turkey*

[2] *Marmara University, Genetic and Metabolic Diseases Research and Implementation Centre, İstanbul, Turkey*

[3] *Marmara University, School of Medicine, İstanbul, Turkey*

Our work was supported by The Scientific and Technological Research Council of Turkey (TUBITAK) 1002 project no 220S681, TUBITAK 2214-A project no 1059B142000347 and 2247-C Trainee Researcher Fellowship Program (STAR) project no 1199B472116456.

It is well-known that blood neutrophil count varies significantly in many diseases. Although the effects of neutrophils have been examined in almost all terms of inflammation, and the impact of metabolic changes on neutrophil count is well defined, how the changes in the neutrophil count would affect the lipid metabolism was not investigated. Thus, the aim was to evaluate the impact of changes in neutrophil number on blood cholesterol levels.

To establish neutropenia and neutrophilia, two different types of recombinant G-CSF (filgrastim: Neupogen®, 0.15ml(5µg), intraperitoneal [i.p.], lenograstim: Granocyte®, 0.15ml(5µg), i.p.) and anti-neutrophil serum (ANS, (Ly-6G, clone 1A8), 0.15ml, i.p.) was subcutaneously injected into both young C57BL/6 male (n=12) and female (n=12) mice. Then blood and liver samples were collected to further investigation after the application of ketamine hydrochloride (100mg/kg, i.p.) and xylazine (7.5mg/kg, i.p.) anaesthesia. While any significant changes in neutrophil numbers increased the total blood cholesterol levels in male mice, an increased total blood cholesterol level (p=0.0339) was only occurred with increasing the neutrophil count (p=0.006) in female mice. Moreover, it was demonstrated that the elevation in total cholesterol level in male mice was associated with LDL (p=0.0008), but not HDL.

To assess the possible underlying mechanism of the relationship between neutrophil count and LDL levels, blood IL-17, G-CSF and liver HMG-CoA reductase enzyme activity were examined in male mice (n=4-6). To further evaluate the impact of sexes, blood samples were collected from the male (n=12) and female (n=13) human subjects at two different time points (at menstruation and late follicular phase in females and at similar time intervals in males).

There was a significant correlation between total cholesterol and LDL and neutrophils only in female mice (p=0.0113, p=0.0242 respectively), but not in males. In consistence with mice data, it was demonstrated in female subjects that when estrogen levels were significantly increased during the menstrual cycle (p=0.0091), the neutrophil numbers were significantly decreased (p=0.0034), and the cholesterol levels were significantly increased (p=0.0325). And while there were no significant differences in G-CSF levels, a significant increase in IL-17 was observed only in ANS-given mice (p=0.0486), and there was a significant decrease in HMG-CoA Reductase activity in both ANS- (p=0.006) and filgrastim-injected mice (p=0.0096) when compared to the control group.

Taken together, it was demonstrated that any significant changes in neutrophil count directly affect LDL levels. Further, this interaction was observed during the menstrual cycle with fluctuating estrogen levels. And this effect was most likely not due to the interaction of neutrophils and liver but probably related to phagocytosis of neutrophils.

B 09-10

Adding a time resolution to single-cell RNA-seq data with DynaSCOPE™

M. Seker, B. Gargouri, W. Zhu, N. Fang

Singleron Biotechnologies GmbH, Cologne, Germany

Introduction

Current single-cell RNA-sequencing methods provide a snapshot of the experimental setup. For the investigation of trajectories from single-cell data, several bioinformatical methods have been developed but experimental data is lacking.

Methods and Results

This is overcome with the DynaSCOPE™ kit from Singleron that builds on the existing GEXSCOPE® single-cell RNA-seq workflow. By chemical labelling of nascent mRNA, newly-transcribed and pre-existing RNAs are discriminated in single cells, adding a time stamp to single-cell RNA-seq experiments.

Conclusion

The accurate measurement of freshly synthesized and long-lasting mRNA might help to understand immediate regulatory dynamics in tissue developmental, environmental changes, drug treatments and infection mechanisms from an experimental and bioinformatical perspectives.

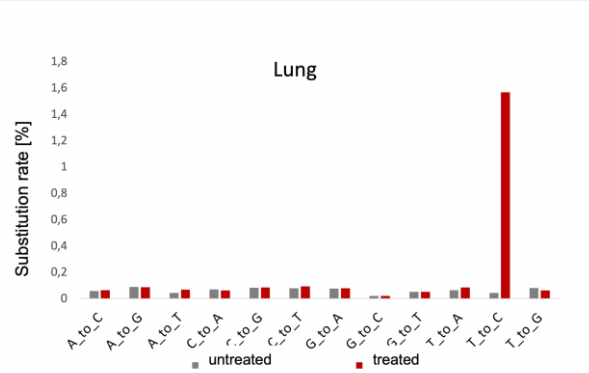

DynaSCOPE™ - Metabolic labeling of RNA
Specificity of the T-to-C substitution rate of DynaSCOPE™. Murine lung cells were left untreated or treated with S4U for 2 hours and the substitution rate for all nucleotides were measured.

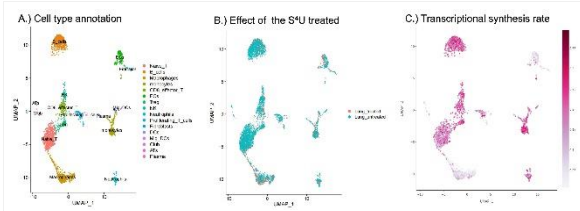

DynaSCOPE™ - RNA synthesis rate
UMAP plot of a murine lung sample from the normal GEXSCOPE® single-cell RNA-seq workflow (untreated) or with the metabolic mRNA labelling of DynaSCOPE™ (treated). The UMAP plot on the left shows the cell type annotation of each cluster (A). The plot in the middle is the same UMAP but coloured by the treatment (B), while the UMAP plot on the right (C) shows the transcriptional synthesis rate (nascent transcripts / all transcripts).

B 09-11

The effect of isoleucine preconditioning on neuroprotection via HIF-1α signaling after oxygen-glucose deprivation insult

X. Yao, J. Fandrey, T. Leu
University of Duisburg-Essen, Institute of Physiology, Essen, Germany

Introduction

Isoleucine is an essential branched-chain amino acid, which can significantly increase glucose uptake [1]. Although its role in protein synthesis and nutrition is already known, our knowledge about its regulation of neuronal cells after the onset of ischemic stroke is limited. Most acute ischemic stroke patients show a positive test for hyperglycemia [2]. Furthermore, hyperglycemia impairs hypoxia-dependent protection of hypoxia -inducible factor-1α (HIF-1α) against proteasomal degradation[3]. Downstream of HIF-1α, the relocation of P53 to the nucleus after cellular stress is promoting the inhibition of malignant cells growth [4]. In addition, relocalization of mitochondria is dependent on HIF-1α during long term hypoxia in tumor cells [5].
In this study, the neuroprotection of proper isoleucine preconditioning should be validated and be connected to the stabilization of the HIF-1α protein. Besides, the relation between the evidence of increased level of HIF-1α and the promotion of nuclear P53 should be investigated. Moreover, it is important to investigate whether pretreatment with isoleucine contributes the amount and redistribution of mitochondria.

Hypothesis

We hypothesize that isoleucine preconditioning exerts neuroprotective effect on neuron via HIF-1α through regulating the amount/location of mitochondria and nuclear P53 dependent cell apoptosis.

Research Design

To first confirm the neuroprotection of proper isoleucine preconditioning, different concentrations of isoleucine will be given to cells for different time periods before oxygen-glucose deprivation (OGD) insult. Cell viability will be measured by cell counting kit-8 assay and LDH release assay.
After establishing an efficient isoleucine precondition, HIF-1α protein and its target genes will be measured after isoleucine preconditioning. Protein will be detected by western blotting. Target genes will be detected via qPCR.
By generating a HIF-1α knockout cell line constructed by a lentivirus- based CRISPR/Cas9 system, nuclear P53 will be measured to see if it is regulated by the level of HIF-1α. Protein will be detected by western blotting. Somatic mitochondria will be detected by immunofluorescence staining.
To test the effect of nuclear P53 and to evaluate the effect of mitochondria on injured cells, MDMM2, P53 nuclear transporter,and CHCHD4, a regulator of mitochondria localization, will be investigated as increased somatic mitochondria are accompanied by the accumulation of nuclear reactive oxygen species (ROS). ROS will be detected by immunofluorescence staining. Protein will be detected by western blotting.

References

[1] Catrina, SB, et al. 2004 Hyperglycemia regulates hypoxia-inducible factor-1alpha protein stability and function. Diabetes 53(12):3226-32.
[2] Doi, M, et al. 2005 Isoleucine, a blood glucose-lowering amino acid, increases glucose uptake in rat skeletal muscle in the absence of increases in AMP-activated protein kinase activity. The Journal of nutrition 135(9):2103-8.
[3] Li, WA, et al. 2013 Hyperglycemia in stroke and possible treatments. Neurological research 35(5):479-91.
[4] Mandal, A, and CM Drerup 2019 Axonal Transport and Mitochondrial Function in Neurons. Frontiers in cellular neuroscience 13:373.
[5] O'Brate, A, and P Giannakakou 2003 The importance of p53 location: nuclear or cytoplasmic zip code? Drug resistance updates : reviews and commentaries in antimicrobial and anticancer chemotherapy 6(6):313-22.

B 09-12

Soluble epoxide hydrolase is required in mediating resolution of inflammation

X. Li[1], S. Kempf[1], F. Delgado Lagos[1], J. Hu[1], I. Fleming[1]
[1] *Goethe University Frankfurt, Institute for Vascular Signalling, Centre for Molecular Medicine, Frankfurt, Germany*
[2] *Clinic of the Goethe-University, Institute of Biochemistry I, Frankfurt, Germany*

This work was supported by the Deutsche Forschungsgemeinschaft (Research Training Group "Resolution of inflammation (GRK 2336)" and the CardioPulmonary Institute, EXC 2026, Project ID: 390649896).

Background

Polyunsaturated fatty acids (PUFAs) play essential roles in mediating inflammation and its resolution. PUFA metabolites generated by the cytochrome P450 (CYP) - soluble epoxide hydrolase

(sEH) axis are known to regulate macrophage activation/polarization but little is known about their role in the resolution of inflammation.

Methods

Monocytes were isolated from murine bone marrow or human peripheral blood and differentiated to naïve macrophages (M0). Thereafter cells were polarized using LPS and IFNγ (M1), IL-4 (M2a), or TGFβ1 (M2c). Gene expression was analyzed by RNA sequencing, RT-qPCR and Western blotting. Phagocytosis of zymosan and oxo-LDL were also assessed in vitro. Zymosan-induced peritonitis combined with immune cell profiling was used to evaluate the resolution of inflammation in vivo.

Results

The expression of sEH was comparable in M0, M1 and M2a macrophages but markedly elevated in M2c polarized cells. The increase in sEH expression elicited by TGF-β relied on the TGFβ receptor ALK5 and the phosphorylation of SMAD2, which was able to bind to the sEH promoter. In macrophages lacking sEH, M2c polarization was incomplete and characterized by lower levels of pro-resolving phagocytosis associated receptors (Tlr2 and Mrc1), as well as higher levels of the pro-inflammatory markers; Nlrp3, IL-1β and TNFα. Fitting with the failure to upregulate phagocytosis associated receptors, the uptake of zymosan and ox-LDL was less efficient in M2c macrophages from $sEH^{-/-}$ mice. The latter animals also demonstrated a retarded resolution of inflammation (zymosan-induced peritonitis) in vivo with fewer resident macrophages and recruited macrophages. PUFA profile analysis indicated decreased sEH substrates e.g., 11, 12-EET, as well as increased sEH products e.g., 11, 12-DHET, indicating an increased sEH activity in M2c macrophages. At the molecular level, 11,12-EET contributed to impaired M2c macrophage polarization by activating its associated receptor.

Conclusions

Taken together, our data indicates that sEH expression is required for the effective M2c polarization of macrophages and thus the resolution of inflammation.